Landolt-Börnstein
Numerical Data and Functional Relationships in Science and Technology
New Series / Editor in Chief: W. Martienssen

Group IV: Physical Chemistry
Volume 19

Thermodynamic Properties of Inorganic Materials
compiled by SGTE

Subvolume B
Binary Systems
Phase Diagrams, Phase Transition Data,
Integral and Partial Quantities of Alloys

Part 1
Elements and Binary Systems from Ag-Al to Au-Tl

Editor
Lehrstuhl für Werkstoffchemie,
Rheinisch-Westfälische Technische Hochschule Aachen

Authors
Scientific Group Thermodata Europe (SGTE)

Springer

ISSN 1615-2018 (Physical Chemistry)

ISBN 3-540-65327-9 Springer-Verlag Berlin Heidelberg New York

Library of Congress Cataloging in Publication Data
Zahlenwerte und Funktionen aus Naturwissenschaften und Technik, Neue Serie
Editor in Chief: W. Martienssen
Vol. IV/19B1: Editor: Lehrstuhl für Werkstoffchemie, Rheinisch-Westfälische Technische Hochschule Aachen
At head of title: Landolt-Börnstein. Added t.p.: Numerical data and functional relationships in science and technology.
Tables chiefly in English.
Intended to supersede the Physikalisch-chemische Tabellen by H. Landolt and R. Börnstein of which the 6th ed. began publication in 1950 under title: Zahlenwerte und Funktionen aus Physik, Chemie, Astronomie, Geophysik und Technik.
Vols. published after v. 1 of group I have imprint: Berlin, New York, Springer-Verlag
Includes bibliographies.
1. Physics--Tables. 2. Chemistry--Tables. 3. Engineering--Tables.
I. Börnstein, R. (Richard), 1852-1913. II. Landolt, H. (Hans), 1831-1910.
III. Physikalisch-chemische Tabellen. IV. Title: Numerical data and functional relationships in science and technology.
QC61.23 502'.12 62-53136

Springer-Verlag Berlin Heidelberg New York
a member of BertelsmannSpringer Science+Business Media GmbH

Printed in Germany

Cover layout: Erich Kirchner, Heidelberg
Typesetting: Authors and Redaktion Landolt-Börnstein, Darmstadt
Printing and Binding: WB-Druck, Rieden/Allgäu

SPIN: 10655491 63/3020 - 5 4 3 2 1 0 – Printed on acid-free paper

Editors

P. Franke and D. Neuschütz
Lehrstuhl für Werkstoffchemie
Rheinisch-Westfälische Technische Hochschule Aachen
D-52056 Aachen, Germany
http://www.mch.rwth-aachen.de/

Authors

Scientific Group Thermodata Europe (SGTE)
Chairman: A.T. Disdale
Grenoble Campus
1001 Avenue Centrale, BP 66
F-38402 Saint Martin d'Hères, France
http://www.sgte.org/

Member Organisations of SGTE:

The present series of books is the result of a collective work carried out during many years by many individuals. Since a complete list of all contributors is an impossible task, only a contact person is mentioned under each member organisation.

AEA Technology plc
Materials and Chemical Process Assessment
P.K. Mason
220, Harwell Laboratory, Didcot, Oxfordshire, United Kingdom, OX11 0QJ
http://www.aeat.co.uk/mcpa/

GTT Technologies
Gesellschaft für Technische Thermochemie und -physik mbH
K. Hack
Kaiserstraße 100
D-52134 Herzogenrath, Germany
http://www.gtt-technologies.de/

Institut National Polytechnique de Grenoble
Laboratoire de Thermodynamique et Physico-Chimie Métallurgiques
C. Bernard
F-38402 Saint Martin d'Hères, France
http://www.inpg.fr/ltpcm/

IRSID
Department of Physical Chemistry and Surfaces
J. Lehmann
Voie Romaine - BP 30320
F-57283 Maizières-lès-Metz, France

Max-Planck-Institut für Metallforschung und
Institut für Nichtmetallische Anorganische Materialen der Universität Stuttgart
Pulvermetallurgisches Laboratorium
O.B. Fabrichnaya
Heisenbergstraße 5
D-70569 Stuttgart, Germany
http://www.mpi-stuttgart.mpg.de/

National Physical Laboratory
NPL Materials Centre
A.T. Dinsdale
Queens Road, Teddington, Middlesex, United Kingdom, TW11 0LW
http://www.npl.co.uk/mtdata/mts.html

Rheinisch-Westfälische Technische Hochschule Aachen
Lehrstuhl für Werkstoffchemie
E. Münstermann
D-52056 Aachen, Germany
http://www.mch.rwth-aachen.de/

Royal Institute of Technology
Department of Materials Science and Engineering
J. Ågren
S-10044 Stockholm, Sweden
http://www.met.kth.se/tc/

Thermo-Calc Software AB
B. Sundman
Björnnägen 21
S-11347 Stockholm, Sweden
http://www.thermocalc.se/

THERMODATA
B. Cheynet
Grenoble Campus
1001 Avenue Centrale, BP 66
F-38402 Saint Martin d'Hères, France
http://thermodata.online.fr/

The Spencer Group
P.J. Spencer
P.O. Box 393
Trumansburg, New York 14886, USA
http://www.spencergroupintl.com/

Université Paris-Sud XI
Faculté de Pharmacie
Laboratoire de Chimie Physique Minérale et Bioinorganique, EA 401
Y. Feutelais
5 rue J.B. Clément
F-92296 Châtenay-Malabry, France
http://www.u-psud.fr/

The reviews in the present volume of selected binary systems have been prepared by:

P.-Y.Chevalier, A.T. Dinsdale, N. Dupin, O.B. Fabrichnaya, Y. Feutelais, P. Franke, K. Hack, U.R. Kattner, B. Legendre, H.L. Lukas, P.J. Spencer and B. Sundman.

In preparing the data for publication in this series, the editors have been assisted particularly by:

A.T. Dinsdale (Data Manager for Elements), I. Ansara† (Data Manager for Pure Substances), B. Sundman (Data Manager for Solutions), S.G. Fries (Solution Database Coordinator) and A. Hovmark (SGTEbin software).

Landolt-Börnstein

Editorial Office
Gagernstr. 8, D-64283 Darmstadt, Germany
fax: +49 (6151) 171760
e-mail: lb@springer.de

Internet
http://www.landolt-boernstein.com

Helpdesk
e-mail: helpdesk-em@springer.de

Dedication to Ibrahim Ansara

This series of volumes, presenting thermodynamic properties of binary alloys, is dedicated to the memory of Ibrahim Ansara – better known to his friends as Himo. Himo was a member of SGTE from the time of its origin as a CNRS research project in 1967, through the time of its constitution as a European, non-profit-making company under French law in 1979, until his sudden, unexpected death in 2001.

Through all those years, Himo missed scarcely a single SGTE meeting and his continual cheerfulness and enthusiasm, as well as his scientific understanding, were an inspiration to his colleagues both in their joint work of SGTE database development as well as in their individual research projects in their home laboratories. He was a friend to everyone in SGTE, and it is the spirit of friendship and warmth that he promoted that has been largely responsible for the continued close collaboration and achievements of this diverse international group as a whole.

It is very appropriate to dedicate the Landolt-Börnstein handbooks on binary alloy systems to Himo. In the preparation of the previous volumes on pure substances, Himo made substantial contributions both as database manager and as advisor. The present series of volumes on binary alloys has benefited considerably from his contributions to the review and selection of available assessments during the initial stages of the work. It is a sad coincidence that it was during a meeting to prepare the first of these volumes that Himo died.

Philip Spencer

Preface

Thermodynamic data, in conjunction with appropriate software for calculation of complex chemical equilibria, are finding wide application in many areas of materials design and development. In particular, the last 25 years have seen enormous advances in the thermodynamic modelling of alloy solution phases, whereby a knowledge of the underlying crystallographic structure of each phase is fundamental to a reliable representation of the thermodynamic properties and phase equilibria of a particular system of interest. With the aid of thermodynamic calculations, considerable time and costs can and are being saved in producing a material of the required composition and phase constitution required for a particular application.

SGTE has been at the forefront in providing critically assessed thermodynamic data for alloy systems and has provided guidelines for the modelling of alloy phases of different types. Major advantages of the SGTE data are their self-consistency, the fact that they are produced with careful attention to a well-defined quality procedure and that the expertise of SGTE members in various areas of inorganic chemistry and materials science allows review of the numbers by highly qualified scientists in the fields concerned.

Following the publication of a first set of four volumes of SGTE compiled thermodynamic properties of inorganic substances, which dealt with pure substances (Subvolume A), this second set of four volumes presents selected thermodynamic data for binary alloy systems (Subvolume B). The possibility to continue to ternary and multi-component systems is also foreseen. The data in the latter would be so presented as to correspond to potential application themes (steels, light alloys, nickel-base alloys, etc.). The fundamental equations used in evaluating the data are given in the introduction to the volumes and the models used in representing the data are also described.

Each book in this binary alloys series is accompanied by a CD, which allows computer calculation of a range of solution properties for selected temperature and phase composition ranges for the systems presented in that particular volume. Graphical representations, including the calculated phase diagram for each system, are also possible. Information on more comprehensive software, allowing complex equilibrium calculations involving both pure substances and solution phases of different types (e.g. slags, salt systems, aqueous solutions, etc.), can be obtained from SGTE members. A list of the SGTE membership is presented in the cover pages of this volume.

Very many scientists, in addition to those currently participating in SGTE activities, have contributed to the development of the SGTE databases. Their names have become too numerous to list and we respectfully ask them to accept this acknowledgement of their efforts. However, special recognition is given here to the late Himo Ansara, who was SGTE Pure Substances Database manager from the beginning and who made major contributions to these binary alloy volumes. His dedicated work and friendship were an inspiration to all of his colleagues. We remember him with deep affection and gratitude.

Dr. P.J. Spencer
Chairman of SGTE, 1992 – 2002

Ithaca, April 2002

Content

IV/19 Thermodynamic Properties of Inorganic Materials

Subvolume B Binary Systems

Phase Diagrams, Phase Transition Data,
Integral and Partial Quantities of Alloys

Part 1 Elements and Binary Systems from Ag-Al to Au-Tl

Introduction **XIV**

Assessment and selection procedures . . . XIV
Thermodynamic Modelling . . . XVI
Description of the Tables and Diagrams . . . XX
Description of the Software . . . XXII
References . . . XXVI

SGTE Data for Pure Elements **1**

Stable and Metastable Phase Data . . . 1
Standard Element Reference . . . 2
References . . . 2
SGTE Pure Element Transition Data . . . 3
Diagrams of Gibbs Energies and Heat Capacities . . . 6

Binary Systems **32**

Ag – Al . . . 33
Ag – Au . . . 38
Ag – Bi . . . 42
Ag – Ge . . . 45
Ag – In . . . 49
Ag – Ir . . . 53
Ag – Mg . . . 56
Ag – Os . . . 61
Ag – Pb . . . 64
Ag – Pd . . . 67
Ag – Pt . . . 71
Ag – Rh . . . 75
Ag – Ru . . . 78
Ag – Sb . . . 81
Ag – Si . . . 84
Ag – Sn . . . 88
Ag – Ti . . . 92
Ag – Tl . . . 95
Ag – Zn . . . 98
Ag – Zr . . . 103
Al – As . . . 106
Al – Au . . . 109
Al – B . . . 112
Al – Bi . . . 116
Al – C . . . 119
Al – Ca . . . 122

Al – Ce . . . 125
Al – Co . . . 129
Al – Cr . . . 134
Al – Cu . . . 139
Al – Fe . . . 143
Al – Ga . . . 148
Al – Ge . . . 151
Al – In . . . 154
Al – Li . . . 157
Al – Mg . . . 160
Al – Mn . . . 164
Al – Mo . . . 170
Al – N . . . 173
Al – Nb . . . 175
Al – Nd . . . 178
Al – Ni . . . 182
Al – O . . . 188
Al – P . . . 190
Al – Pb . . . 192
Al – Sb . . . 195
Al – Si . . . 198
Al – Ta . . . 201
Al – Ti . . . 205
Al – V . . . 210
Al – W . . . 214
Al – Y . . . 217
Al – Zn . . . 221
Al – Zr . . . 225
As – Au . . . 229
As – Cu . . . 232
As – Fe . . . 235
As – Ga . . . 238
As – Ge . . . 242
As – In . . . 246
As – P . . . 250
As – Sb . . . 254
Au – Bi . . . 259
Au – C . . . 262
Au – Cr . . . 264
Au – Cu . . . 268
Au – Ge . . . 273
Au – In . . . 276
Au – Pb . . . 280
Au – Pd . . . 283
Au – Rh . . . 287
Au – Ru . . . 290
Au – Sb . . . 293
Au – Si . . . 296
Au – Te . . . 299
Au – Tl . . . 302

CD-ROM: Software for the calculation of phase diagrams and thermodynamic data of binary systems

Introduction

The first 4 volumes of this series, under the general heading Thermodynamic Properties of Inorganic Materials, presents SGTE-compiled thermodynamic data for pure substances, including the elements in their stable states. The series now continues with a further 4 volumes of SGTE selected and compiled data – this time for binary alloy systems. For thermodynamic calculations involving alloy solution phases, Gibbs energies of the pure elements in different stable and metastable states are required. Such data have been compiled on behalf of SGTE by Dinsdale [91Din] and have recently been updated [02Din]. The values have found wide use internationally as the basis for thermodynamic assessments of higher order systems.

As with the pure element values, the binary alloy descriptions contained in the present 4-volume series are not only complete in themselves, but also extend the basis for thermodynamic assessments and calculations relating to multicomponent alloys.

Members of SGTE have played a principle role in promoting the concept of "computational thermochemistry" as a time and cost-saving basis for guiding materials development and processing in many different areas of technology. At the same time, through organisation of workshops and participation in CODATA Task Groups, SGTE members have contributed significantly to the broader international effort to unify thermodynamic data and assessment methods.

The SGTE data can be obtained via members and their agents world-wide for use with commercially available software developed by some of the members, to enable users to undertake calculations of complex chemical equilibria efficiently and reliably.

The SGTE Member organisations are:

France:
– Institut National Polytechnique (LTPCM), Grenoble
– Association THERMODATA, Grenoble
– IRSID, Maizières-lès-Metz
– Université de Paris-Sud (EA 401)

Germany:
– Rheinisch-Westfälische Technische Hochschule (MCh), Aachen
– GTT-Technologies, Herzogenrath
– MPI für Metallforschung (PML), Stuttgart

Sweden:
– Royal Institute of Technology (MSE), Stockholm
– Thermo-Calc Software AB, Stockholm

United Kingdom:
– National Physical Laboratory (MATC), Teddington
– AEA Technology plc, Harwell

USA:
– The Spencer Group

Assessment and selection procedures

The assessments of the binary alloy systems presented in this 4-volume series have all been made using the so-called "CALPHAD method" [98Sau]. This method results in an optimised parametric description of the Gibbs energies of the phases of the system when taking into account the crystallographic structure of the phases and all the experimental thermodynamic and phase boundary data available. The thermodynamic parameters provide a consistent analytical description of the phase diagram, chemical potentials, enthalpies of mixing, heat capacities, etc.

As an example, the relations between the Gibbs energy curves and the phase diagram for the Bi-Sn system are demonstrated in Figs. 1 and 2, respectively. In Fig. 1 the Gibbs energy curves for the phases in the Bi-Sn system are given as a function of the mole fraction of Sn, x_{Sn}, at $T = 450$ K. At fixed pressure, temperature and composition, the equilibrium of the system is determined by the state with the lowest Gibbs energy. All equilibrium states are located on the convex hull of the set of G-curves which is constructed by applying double-tangents to the curves. The tangent points denote the boundaries between one- and two-phase regions. In Fig. 2, these points are marked on the selected isotherm of $T = 450$ K. If this construction is repeated for other temperatures the complete phase diagram of the system is obtained.

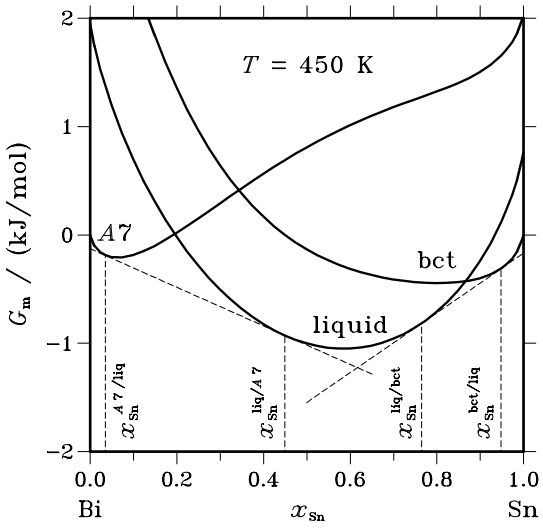

Fig. 1. Gibbs energy functions for the phases in the Bi-Sn system at 450 K.

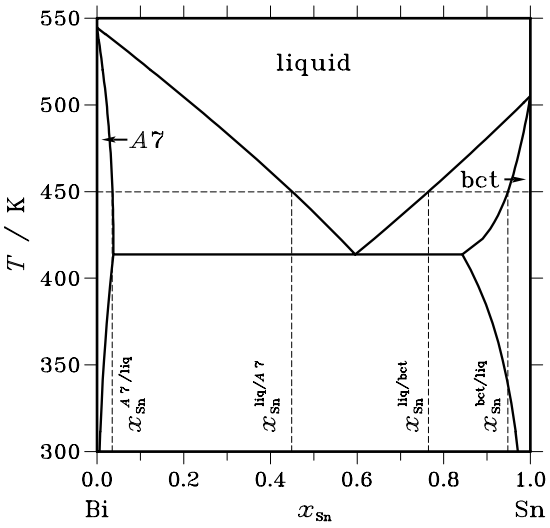

Fig. 2. Phase diagram for the system Bi-Sn.

If several published assessments are available for a particular system, selection has been made following an analysis of how well the available experimental data are reproduced by the description. Compatibility of the modelling used with respect to assembly of a data set for higher order systems has also been taken into account.

There are many different phases present in binary systems and, in order to combine their thermodynamic descriptions in higher order systems, it is important to know their crystal structures as well as the solubilities of alloyed elements in them. In these volumes, the naming of phases has been carried out as consistently as possible so as to facilitate identification of the same phase appearing in different binary systems.

The main characteristics of each system are presented in individual reports which generally include

- the calculated phase diagram
- an abstract summarising the main features of the system
- a summary of the various stable and metastable phases defined in the system together with crystallographic information, the phase name used in the database and the thermodynamic model used, including the occupation of the sublattices
- a table of the invariant reactions
- tables and diagrams with integral quantities
- tables and diagrams with partial quantities
- plots of calculated thermodynamic functions

Criteria for selection of binary alloy assessments

In order to qualify for selection, the following information was reviewed:
- phase diagram
- thermodynamic information
- documentation
- models used for solution phases
- models used for stoichiometric phases
- feasibility of extrapolation
- compatibility with SGTE unary data

Thermodynamic Modelling

Elements

The Gibbs energy of the pure element i, ${}^\circ G_i^\phi(T)$, referred to the enthalpy for its stable state ϕ at 298.15 K, ${}^\circ H_i^\phi(298.15\ \mathrm{K})$, is denoted by GHSER$_i$. This quantity is described as a function of temperature by the following equation:

$$\begin{aligned} \mathrm{GHSER}_i &= {}^\circ G_i^\phi(T) - {}^\circ H_i^\phi(298.15\ \mathrm{K}) \\ &= a + b\,T + c\,T\cdot \ln T + d\,T^2 + e\,T^3 + f\,T^{-1} + g\,T^7 + h\,T^{-9} \end{aligned} \quad (1)$$

A number of temperature ranges may be used. The first and second derivatives of this quantity with respect to temperature are related to the absolute entropy and heat capacity of the compound at the same temperature. Experimental values for heat capacities can thus be directly used in the optimisation and will be related to the coefficients c, d, e, f, g and h.

For elements which have a magnetic ordering, e.g. Co, Cr, Fe, Ni and Mn, the term GHSER is referred to a para-magnetic state. An additional term is thus added to the molar Gibbs energy of the magnetic phase. For elements as well as for solutions, this term is equal to:

$$G^{\mathrm{mag}} = RT\ln(\beta+1)f(\tau) \quad (2)$$

where τ is T/T^* , T^* being the critical temperature for magnetic ordering (Curie temperature T_C for ferromagnetic materials or the Néel temperature T_N for antiferromagnetic materials), and β the average magnetic moment per atom of the alloy expressed in Bohr magnetons.

The function $f(\tau)$ is given as:

$$\begin{aligned} \tau <= 1 \quad &: \quad f(\tau) = 1 - [79\tau^{-1}/140p + (474/497)(1/p-1)(\tau^3/6 + \tau^9/135 + \tau^{15}/600)]/A \\ \tau > 1 \quad &: \quad f(\tau) = -[\tau^{-5}/10 + \tau^{-15}/315 + \tau^{-25}/1500]/A \end{aligned}$$

with $A = 518/1125 + (11692/15975)(1/p-1)$.

These equations were derived by Hillert *et al.* [78Hil] from an expression of the magnetic heat capacity $C_\mathrm{P}^{\mathrm{mag}}$ described by Inden [81Ind].

The value of p depends on the crystal structure. For example, p is equal to 0.28 for fcc and hcp metals and 0.40 for bcc metals [81Ind]. For anti-ferromagnetic alloys the T^* and β are modelled as negative and they are divided by an *anti-ferromagnetic factor* of -1 for bcc and -3 for fcc and hcp before the values are used in equation (2).

For each element, equation (1) is taken from the SGTE unary database. These data have been published previously as the SGTE data for the pure elements by Dinsdale [91Din, 02Din].

The function GHSER$_i$ is also often used to express the thermodynamic functions of metastable structures φ, different from the stable structure of the pure element. The expression ${}^\circ G_i^\varphi(T) - {}^\circ H_i^\phi(298.15\ \mathrm{K})$ is

equivalent to ${}^{\circ}G_i^{\varphi}(T) - {}^{\circ}G_i^{\phi}(T) + \mathrm{GHSER}_i$. The term ${}^{\circ}G_i^{\varphi}(T) - {}^{\circ}G_i^{\phi}(T)$ is often called the lattice stability of element *i* in phase φ.

Binary compounds

The Gibbs energy of the compound $\mathrm{A_aB_b}$ may be expressed as:

$$G_{\mathrm{A_aB_b}}(T) - \mathrm{a}\ {}^{\circ}H_{\mathrm{A}}^{\phi}(298.15\ \mathrm{K}) - \mathrm{b}\ {}^{\circ}H_{\mathrm{B}}^{\phi}(298.15\ \mathrm{K}) = f(T) \tag{3}$$

where a and b are stoichiometric numbers. The expression for $f(T)$ is identical to that given by equation (1).

Equation (3) can be transformed by applying equation (1) for each component

$$\begin{aligned} f(T) &= G_{\mathrm{A_aB_b}}(T) - \mathrm{a}\ {}^{\circ}G_{\mathrm{A}}^{\phi}(T) - \mathrm{b}\ {}^{\circ}G_{\mathrm{B}}^{\phi}(T) + \mathrm{a\ GHSER_A} + \mathrm{b\ GHSER_B} \\ &= \Delta_{\mathrm{f}}G_{\mathrm{A_aB_b}}(T) + \mathrm{a\ GHSER_A} + \mathrm{b\ GHSER_B} \end{aligned} \tag{4}$$

The term $\Delta_{\mathrm{f}}G_{\mathrm{A_aB_b}}(T)$ is the Gibbs energy of formation of the compound referred to the stable elements at temperature T. It can often be taken as a linear function of T.

Gaseous species

An expression identical to equation (1) may be used to describe the Gibbs energy of the gaseous species with the additional $RT\ln(P/P_0)$ term, where P is the total pressure and P_0 the reference pressure, usually 0.1 MPa. The species in the gas phase are assumed to form an ideal solution. The reference state for each vapour species is taken to be the pure components at 0.1 MPa pressure. The thermodynamic properties of the gas species are normally obtained from vapour pressure measurements coupled to spectroscopic data. Data for gaseous substances are covered in more detail in subvolume (A) for pure substances.

Many species, i.e. molecules, may exist in the gas phase and each has a Gibbs energy of formation. The equilibrium within a gas for a given composition at a given temperature and pressure is calculated by minimising the Gibbs energy varying the fraction of the species. As the Gibbs energy is used as the modelling function in most solution databases it is not possible to calculate the critical point for gas/liquid. The models used for the different liquids are also not compatible with the ideal model for the gas.

Condensed phases

The condensed phases can be divided into three groups.

1: Substitutional solutions

For the substitutional solution ϕ, the molar Gibbs energy is expressed as follows:

$$G_{\mathrm{m}}^{\phi} = G_{\mathrm{m}}^{\phi,\mathrm{srf}} + G_{\mathrm{m}}^{\phi,\mathrm{id}} + G_{\mathrm{m}}^{\phi,\mathrm{E}} \tag{5}$$

with

$$G_{\mathrm{m}}^{\phi,\mathrm{srf}} = \sum_i x_i\ {}^{o}G^{\phi} \tag{6}$$

$$G_{\mathrm{m}}^{\phi,\mathrm{id}} = R\,T \sum_i x_i \ln x_i \tag{7}$$

x_i is the molar fraction of component i with $\sum_i x_i = 1$. The term $G_{\mathrm{m}}^{\phi,\mathrm{srf}}$ is the Gibbs energy of the phase relative to the reference state for the components and $G_{\mathrm{m}}^{\phi,\mathrm{id}}$ is the contribution of ideal mixing entropy.

The Redlich - Kister equation [48Red], a power series expansion, is used to express the excess Gibbs energy, $G_{\rm m}^{\phi,{\rm E}}$, for the interaction between the two elements i and j as follows:

$$G_{\rm m}^{\phi,{\rm E}} = x_i x_j \sum_{\nu=0} {}^{\nu}L_{ij}^{\phi} (x_i - x_j)^{\nu} \tag{8}$$

The model parameter ${}^{\nu}L_{ij}^{\phi}$ can be temperature dependent.

If experimental information for ternary solutions is available then an extra term can be added to equation (8). For a ternary system A–B–C, this term is equal to:

$$x_{\rm A} x_{\rm B} x_{\rm C} L_{\rm ABC} \tag{9}$$

The liquid is in most cases treated as a substitutional solution. For liquids with very strong short range order the associate model [78Som] or the ionic liquid model [85Hil] has sometimes been used.

For magnetic alloys, the composition dependence of T^* and β are expressed by:

$$T^*(x) = \sum_i x_i \, {}^{\circ}T_i^* + T^{*,{\rm E}} \tag{10}$$

$$\beta(x) = \sum_i x_i \, {}^{\circ}\beta_i + \beta^{\rm E} \tag{11}$$

where $T^{*,{\rm E}}$ and $\beta^{\rm E}$ are both represented by an expression similar to equation (8).

2: Ordered Phases

The use of the sublattice model, developed by Hillert and Staffansson [70Hil] based on Temkin's model for ionic solutions [45Tem] and extended by Sundman and Ågren [81Sun], allows a variety of solution phases to be treated, for example interstitial solutions, intermediate phases, carbides etc. All of these represent an ordering of the constituents on different sublattices.

As non-stoichiometric phases are formed by several sublattices, they can be schematically described as follows:

$$({\rm A}, {\rm B}, ...)_p ({\rm A}, {\rm B}, ...)_q ...$$

where the constituents A, B, ... can be atoms, vacancies, molecules or ions on the different sublattices .... p, q, ... are the number of sites. If $p + q + ... = 1$, then the thermodynamic quantities are referred to one mole of sites. Most often p and q are selected to be the smallest set of integers.

For each sublattice s, the site fraction of the species i, y_i^s, is equal to

$$y_i^s = \frac{n_i^s}{\sum_j n_j^s} = \frac{n_i^s}{n^s} \qquad \text{with} \qquad \sum_i y_i^s = 1 \qquad \text{and} \qquad \sum_s n^s = n \tag{12}$$

where n_i^s is the number of species i in sublattice s, n^s the number of sites in sublattice s, and n the total number of sites. n^s is related to n by $n^s = n \cdot p/(p + q + ...)$. The number of sublattices and the species occupying them, is generally obtained from crystallographical information. The mole fraction of an element is obtained by

$$x_i = \frac{\sum_s n^s y_i^s}{\sum_s n^s (1 - y_{\rm Va}^s)} \tag{13}$$

where $y_{\rm Va}^s$ is the fraction of vacant sites on sublattice s.
This model also describes stoichiometric phases, in which case the sublattices are occupied only by a single species, and substitutional phases which have a single lattice.

The molar Gibbs energy for a phase ϕ expressed by the sublattice model is equal to

$$G_{\rm m}^{\phi} = G_{\rm m}^{\phi,{\rm srf}} + G_{\rm m}^{\phi,{\rm id}} + G_{\rm m}^{\phi,{\rm E}} \tag{14}$$

As an example, a two sublattice phase with two elements A and B in each of the sublattices is considered. Denoting the sublattices with primes at the symbols, the surface of reference for the Gibbs energy is

$$G^{\rm srf} = y_{\rm A}^{'} y_{\rm A}^{''} \, {}^{o}G_{\rm A:A} + y_{\rm A}^{'} y_{\rm B}^{''} \, {}^{o}G_{\rm A:B} + y_{\rm B}^{'} y_{\rm A}^{''} \, {}^{o}G_{\rm B:A} + y_{\rm B}^{'} y_{\rm B}^{''} \, {}^{o}G_{\rm B:B} \tag{15}$$

The terms ${}^{o}G_{\rm A:A}$ and ${}^{o}G_{\rm B:B}$ represent the Gibbs energies of the phase ϕ for the constituent elements A and B. The colon separates the different sublattices. The terms ${}^{o}G_{\rm A:B}$ and ${}^{o}G_{\rm B:A}$ represent the Gibbs energies of the stoichiometric compounds $\rm A_pB_q$ and $\rm B_pA_q$, which may be stable or metastable. ${}^{o}G_{\rm A:A}$, ${}^{o}G_{\rm B:B}$, ${}^{o}G_{\rm A:B}$ and ${}^{o}G_{\rm B:A}$ are numerically given by equations (3) and (1).

The term $G_{\rm m}^{\rm id}$ is related to the molar configurational entropy and is equal to:

$$G_{\rm m}^{\rm id} = R\,T[p(y_{\rm A}^{'} \ln y_{\rm A}^{'} + y_{\rm B}^{'} \ln y_{\rm B}^{'}) + q(y_{\rm A}^{''} \ln y_{\rm A}^{''} + y_{\rm B}^{''} \ln y_{\rm B}^{''})] \tag{16}$$

Finally, the excess Gibbs energy $G_{\rm m}^{\rm E}$ is equal to

$$\begin{aligned} G_{\rm m}^{\rm E} = {} & y_{\rm A}^{'} y_{\rm B}^{'} [y_{\rm A}^{''} L_{\rm A,B:A} + y_{\rm B}^{''} L_{\rm A,B:B}] \\ & + y_{\rm A}^{''} y_{\rm B}^{''} [y_{\rm A}^{'} L_{\rm A:A,B} + y_{\rm B}^{'} L_{\rm B:A,B}] \\ & + y_{\rm A}^{'} y_{\rm B}^{'} y_{\rm A}^{''} y_{\rm B}^{''} L_{\rm A,B:A,B} \end{aligned} \tag{17}$$

The terms $L_{i,j:i}$ and $L_{i:i,j}$ represent the interaction parameters between the atoms on one sublattice for a given occupancy of the other, and can be described by a Redlich - Kister polynomial, as follows:

$$L_{i,j:i} = \sum_{\nu=0} (y_i^{'} - y_j^{'})^{\nu} \, {}^{\nu}L_{i,j:i} \tag{18}$$

The parameters ${}^{\nu}L_{i,j:i}$ can be temperature dependent. The term $L_{i,j:i,j}$ is known as the reciprocal parameter which may be related to the exchange reaction of A and B between the sublattices. It is usually assumed to be composition independent but may depend on temperature.

The above equations can easily be extended to ternary and higher order systems.

3: Phases with order-disorder transformation

Phases with order-disorder transformation, like $A2/B2$ and $A1/L1_2$ can also be described with the sublattice method although this disregards any explicit short range order contributions. A single Gibbs energy function may be used to describe the thermodynamic properties of both the ordered and disordered phases as follows:

$$G_{\rm m} = G_{\rm m}^{\rm dis}(x_i) + \Delta G_{\rm m}^{\rm ord}(y_i^s) \tag{19}$$

where $G_{\rm m}^{\rm dis}(x_i)$ is the molar Gibbs energy of the disordered phase, given by equation (5) and $\Delta G_{\rm m}^{\rm ord}(y_i^s)$ is the ordering energy given by:

$$\Delta G_{\rm m}^{\rm ord} = G_{\rm m}^{\rm subl}(y_i^s) - G_{\rm m}^{\rm subl}(y_i^s = x_i) \tag{20}$$

where $G_{\rm m}^{\rm subl}(y_i^s)$ is given by equation (14). This must be calculated twice, once with the original site fractions y_i^s and once with these site fractions replaced by the mole fractions. If the phase is disordered the site fractions and mole fractions are equal and thus $\Delta G_{\rm m}^{\rm ord}$ equal to zero.

To ensure stability of the disordered phase, the first differential of $G_{\rm m}^{\rm subl}$ with respect to any variation in the site occupancy must be zero at the disordered state. This enforces some relations between the parameters in $G_{\rm m}^{\rm subl}$ as is discussed in [88Ans].

Description of the Tables and Diagrams

The diagrams and tables which are presented for the binary systems provide an overview of the major thermodynamic properties and the mixing behaviour of these systems. Depending on the nature of the respective system, the number and the type of the presented diagrams and tables varies. For all systems, a calculated phase diagram, a short abstract and a table listing the condensed phases are provided. Additional tables and diagrams present data for invariant reactions, integral and partial quantities of the liquid and solid phases, and standard reaction quantities of intermetallic compounds in the system.

The following list gives on overview of the quantities in the tables and diagrams and their designations. The definition of these quantities is provided in the following paragraphs.

Symbol	Unit	Quantity
a_{A}		thermodynamic activity of the component A in a liquid or solid solution
$\Delta_{\mathrm{f}} C_P^{\circ}$	J mol^{-1} K^{-1}	change of the molar heat capacity at constant pressure upon formation of a compound
ΔC_P	J mol^{-1} K^{-1}	change of the molar heat capacity at constant pressure upon formation of a liquid or solid solution
ΔG_{m}	J mol^{-1}	integral Gibbs energy of a liquid or solid solution
$G_{\mathrm{m}}^{\mathrm{E}}$	J mol^{-1}	integral excess Gibbs energy of a liquid or solid solution
ΔG_{A}	J mol^{-1}	partial Gibbs energy of the component A in a liquid or solid solution
$G_{\mathrm{A}}^{\mathrm{E}}$	J mol^{-1}	partial excess Gibbs energy of the component A in a liquid or solid solution
$\Delta_{\mathrm{f}} G^{\circ}$	J mol^{-1}	standard Gibbs energy of formation of a compound
ΔH_{m}	J mol^{-1}	integral enthalpy of a liquid or solid solution
ΔH_{A}	J mol^{-1}	partial enthalpy of the component A in a liquid or solid solution
$\Delta_{\mathrm{f}} H^{\circ}$	J mol^{-1}	standard enthalpy of formation of a compound
$\Delta_{\mathrm{r}} H$	J mol^{-1}	enthalpy of reaction per mole of atoms
p_{i}	Pa	partial pressure of species i
ΔS_{m}	J mol^{-1} K^{-1}	integral entropy of a liquid or solid solution
$S_{\mathrm{m}}^{\mathrm{E}}$	J mol^{-1} K^{-1}	integral excess entropy of a liquid or solid solution
ΔS_{A}	J mol^{-1} K^{-1}	partial entropy of the component A in a liquid or solid solution
$S_{\mathrm{A}}^{\mathrm{E}}$	J mol^{-1} K^{-1}	partial excess entropy of the component A in a liquid or solid solution
$\Delta_{\mathrm{f}} S^{\circ}$	J mol^{-1} K^{-1}	standard entropy of formation of a compound
T	K	thermodynamic temperature
T_{C}	K	Curie temperature
x_{A}		mole fraction of component A in an alloy or compound
γ_{A}		activity coefficient of the component A in a liquid or solid solution

The first diagram shows the phase diagram of the system. The single-phase fields and the compounds are marked with labels which are used in the tables to refer to the respective phases. All boundaries between phases which transform into each other by first-order transformations are drawn with solid lines. Second-order phase transformations and magnetic transformations are denoted by dashed and dotted lines, respectively.

The table “phases, structures and models”, contains crystallographic data and information on the thermodynamic model in the database. The designations of the phases according to Strukturbericht, prototype, Pearson symbol and the space group have been collected from various sources, including the original publication of the assessment and the reference books of Pearson [85Vil], Massalski [90Mas] and Smithells [92Bra]. The SGTE name is used by the accompanying software on the CD-ROM. The last column of this table denotes how the sublattices of the crystals have been mapped into a thermodynamic model. The species which dissolve in a common sublattice are enclosed in parentheses. The indices denote the stoi-

chiometric coefficients of the respective sublattices. If a sublattice is occupied by a single species only, the parentheses have been omitted. Vacancies are denoted by a box (□).

The table of "invariant reactions" provides detailed data for the invariant equilibria and special transition points shown in the phase diagram. For each of these reactions the temperature and the phase compositions are provided. The compositions of the participating phases are listed in the same sequence as given by the symbolic equation. The last column gives the reaction enthalpy on cooling for one mole of atoms according to the respective transformation.

The thermodynamic quantities for the liquid and solid solutions are provided by a set of three tables which are denoted by a suffix a–c after the Roman number. The first of these tables lists the integral quantities as well as the change of the molar heat capacity. The other two tables give the partial quantities for the respective two components.

The integral and partial quantities can often be obtained easily from experiments. Partial molar quantities are used to describe the thermodynamic behaviour of the individual components. In a binary system, the partial molar Gibbs energy G_{A} of component A can be calculated from the molar Gibbs energy, G_{m}, at constant temperature and pressure by the well-known relation:

$$G_{\mathrm{A}} = G_{\mathrm{m}} + (1 - x_{\mathrm{A}})(\partial G_{\mathrm{m}}/\partial x_{\mathrm{A}})_{P,T} \tag{21}$$

G_{A} is also known as the chemical potential of component A and denoted by the symbol μ_{A}. Similar relations hold for the partial molar enthalpy, H_{A}, and the partial molar entropy, S_{A}.

Partial quantities provide the difference between the values of thermodynamic functions of a component in a solution and the corresponding values for the pure components. Thus, the partial Gibbs energy ΔG_{A} of component A is calculated from G_{A} in the solution and G°_{A} in the pure substance by:

$$\Delta G_{\mathrm{A}} = G_{\mathrm{A}} - G^{\circ}_{\mathrm{A}} \tag{22}$$

Usually, the values of the pure components are given for their most stable modification at the respective temperature and pressure. But in order to avoid ambiguities the reference states for each component are given at the tables. The quantities ΔH_{A} and ΔS_{A} are defined accordingly.

The thermodynamic activity a_{A} of a component A is closely related to the partial Gibbs energy by:

$$a_{\mathrm{A}} = \exp(\Delta G_{\mathrm{A}}/RT) \tag{23}$$

Therefore, the activity is 1 for pure components in the chosen reference state.

The integral Gibbs energy, ΔG_{m} is equal to the difference between the Gibbs energy of one mole of a solution G_{m} and the sum of the molar Gibbs energies of the pure components G°_{i} at the same temperature and pressure. For a binary system the integral Gibbs energy is:

$$\Delta G_{\mathrm{m}} = G_{\mathrm{m}} - x_{\mathrm{A}} G^{\circ}_{\mathrm{A}} - x_{\mathrm{B}} G^{\circ}_{\mathrm{B}} \tag{24}$$

If the reference state of the components is the same phase as the mixture, ΔG_{m} is also called the Gibbs energy of mixing. If the reference state of at least one component is different from the phase of the mixture then ΔG_{m} contains the difference in Gibbs energies for the pure components between two phases. In these cases ΔG_{m} is called the Gibbs energy of formation of the mixture. The quantities ΔH_{m} and ΔS_{m} are defined accordingly.

The excess quantities describe the deviation of the mixture from the ideal mixing behaviour. The molar excess Gibbs energy, $G^{\mathrm{E}}_{\mathrm{m}}$, is given by the difference of the integral Gibbs energy and the Gibbs energy of mixing for an ideal mixture:

$$G^{\mathrm{E}}_{\mathrm{m}} = \Delta G_{\mathrm{m}} - G^{\mathrm{id}}_{\mathrm{m}} \tag{25}$$

In case of a a simple substitutional solution, $G_{\mathrm{m}}^{\mathrm{id}}$ is given by equation (7) and for solid solutions with several sublattices an expression similar to equation (16) applies.

The partial excess quantities can be derived from the integral excess functions by relations similar to those between partial and integral quantities. Thus, analogous to equation (21), the partial excess Gibbs energy of component A is given by:

$$G_{\mathrm{A}}^{\mathrm{E}} = G_{\mathrm{m}}^{\mathrm{E}} + (1 - x_{\mathrm{A}})(\partial G_{\mathrm{m}}^{E}/\partial x_{\mathrm{A}})_{P,T} \tag{26}$$

Since the heat of mixing is zero for an ideal mixture, the excess enthalpy is identical to the heat of mixing and the partial excess enthalpy of a component is equal to its partial enthalpy. Therefore, the partial excess entropy can be calculated from the partial excess Gibbs energy by a temperature derivative or by the difference from the partial enthalpy:

$$S_{\mathrm{A}}^{\mathrm{E}} = -(\partial G_{\mathrm{A}}^{\mathrm{E}}/\partial T)_{P,x_{\mathrm{A}}} = (\Delta H_{\mathrm{A}} - G_{\mathrm{A}}^{\mathrm{E}})/T \tag{27}$$

The activity coefficient is related to the partial excess Gibbs energy by an expression analogous to equation (23):

$$\gamma_{\mathrm{A}} = \exp(G_{\mathrm{A}}^{\mathrm{E}}/RT) \tag{28}$$

For the case of simple substitutional solutions the activity of a component A is related to its mole fraction by: $a_A = \gamma_A x_A$.

The preceding equations describe the thermodynamic behaviour of a single phase. In an unconstrained equilibrium between two phases each component has the same chemical potential and the same activity in each phase and the integral quantities are linear functions of the composition in a two-phase region. In the diagrams, the functions are drawn with dashed lines in these regions.

Special considerations apply to stoichiometric compounds. Here, the partial quantities cannot be defined by the expression given in equation (21) because the composition cannot be varied. Instead, the chemical potentials are defined by the equilibrium with the next adjacent stable phase.

The table of “standard reaction quantities” provides the Gibbs energy, the enthalpy, and the entropy of formation for the given compounds from the pure elements in their most stable state at 298.15 K and 0.1 MPa. Phosphorus deviates from this rule since here the white modification is conventionally chosen as a reference state instead of the more stable red form. All values in this table are given for the reaction of a total amount of 1 mole of atoms.

Description of the Software

The software provided with the volumes can calculate the printed phase diagrams but it also has some additional capabilities.

Phase Names

The phase names are the same as used in the volumes. If the phase has a miscibility gap or could appear as both ordered and disordered in the same system, a ”COMPOSITION SET” number is appended to the name after a hash sign. For example LIQUID and LIQUID#2 may appear as phase names if there is a miscibility gap in the liquid phase. Normally the composition set 1 is not identified explicitly. As both phases are thermodynamically identical the assignment of a specific composition set number is arbitrary. For ordering in the Au-Cu system for example there are four different composition sets for the FCC phase.

Diagram Selection

The two basic windows for SGTEbin are shown in Fig. 3. In the text area of the base window references for data and other key textual information may appear. For the selection of a system press any two of the elements highlighted in bold print. The four buttons at the bottom of the window will become available. Four basic types of diagrams can be generated by use of specific buttons. These are,

- the phase diagram,
- the Gibbs energy curves for all phases as a function of composition at a specific temperature
- the activity curves of the two elements as a function of composition at a specific temperature
- a plot of the phase fractions as a function of the temperature for a given composition

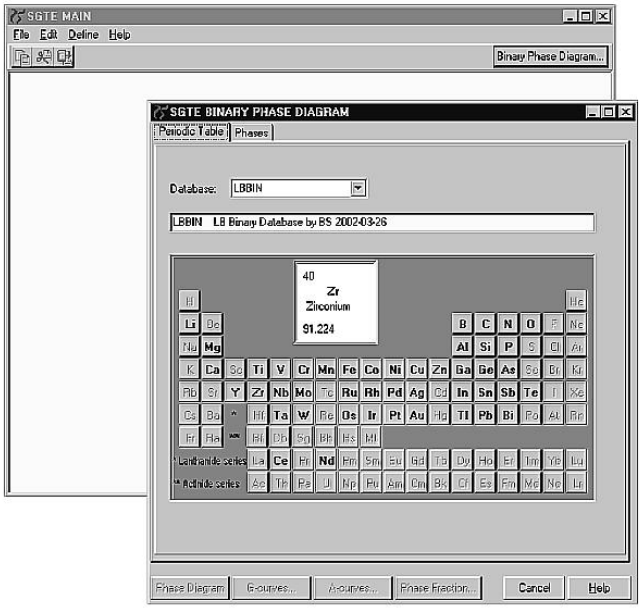

Fig. 3. Base window and periodic chart window.

The basic diagrams are obtained by just selecting two elements and the specific button. From these four calculations an infinite number of modified diagrams can be generated. Some of these will be discussed below.
In addition to selecting the two elements one can also select the set of phases. The folder tagged ”PHASE” gives the default selection of stable phases for the selected system. By changing this selection various metastable diagrams can be calculated.

Phase Diagram

This button will generate a standard temperature - composition phase diagram with the axes in mole fractions and degrees Celsius, see the example in Fig. 4a and 4b. Magnifications and phase labels can be obtained using specific buttons in the graphical window. The REDEFINE button provides a menu, which will allow a change of the axes as shown in Fig. 5. Fig. 6 is equivalent to Fig. 4 but now plotted with activity and temperature in Celsius as axes variables.

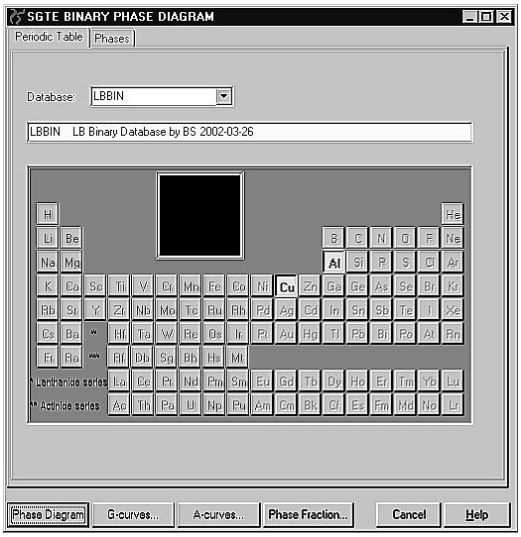

Fig. 4a. The periodic chart window shows the selected elements in red. Note that the buttons in the lower area are activated.

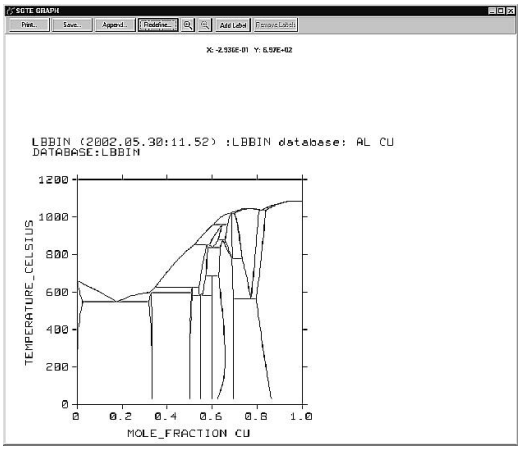

Fig. 4b. A binary phase diagram, here Al-Cu.

There are a number of different possible choices for the axis variable, some will be more sensible than others for a particular phase diagram. You may find it instructive to try a few on your own.

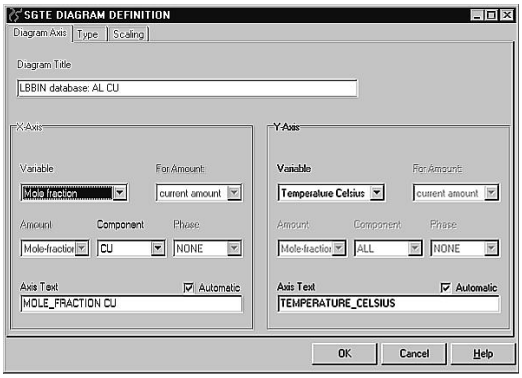

Fig. 5. The REDEFINE window for Al-Cu.

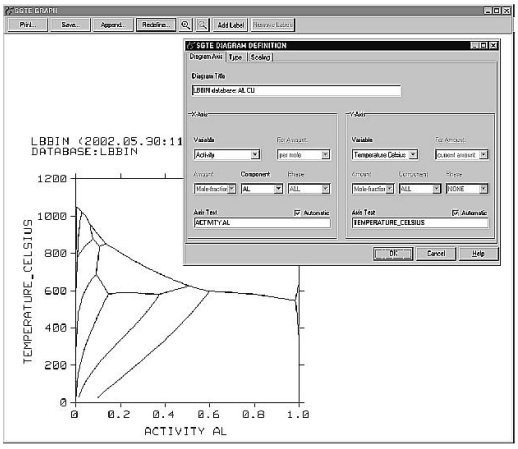

Fig. 6. The calculated Al-Cu system using the activity of Al and the Celsius temperature as axis variables.

G-Curves

In this diagram the Gibbs energies for each phase will be plotted vs composition at a given temperature. This diagram is related to the phase diagram in that the stable combination of phases is given by the lowest Gibbs energy at each composition. An example is given in Fig. 7. The number listed to the right of the diagram identifies each curve. Some phases have limited ranges of existence and stoichiometric phases appear with a small + sign. It is possible to change the axis to plot any integral quantity such as the enthalpy or entropy of the phases. In most cases the default for the reference phase for each element is the stable phase at 298.15 K.

A-Curves

In this diagram the activities of the two elements are plotted vs composition at a given temperature as shown in Fig. 8. The horizontal lines represent two-phase equilibria. It may be useful to change the activity axis to a logarithmic scale in the REDEFINE window or to plot the chemical potential instead. In most cases the default for the reference phase for each element is the stable phase at 298.15 K.

Note the difference between A-CURVES and G-CURVES. In the latter all phases are calculated for their range of composition. In the A-CURVES diagram the phases are included only where they are stable.

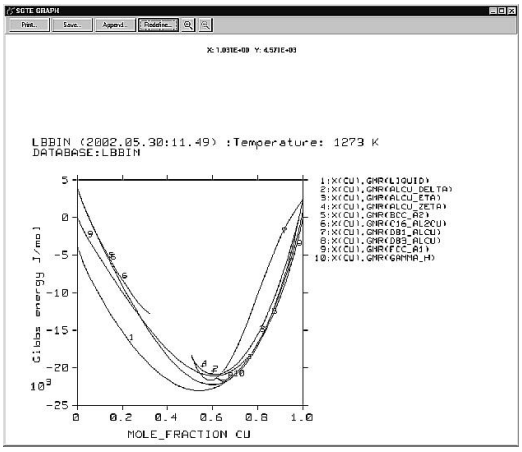

Fig. 7. The diagram calculated by pressing the G curves button. The Gibbs energy curves are shown for all phases of the Al-Cu system at 1273 K.

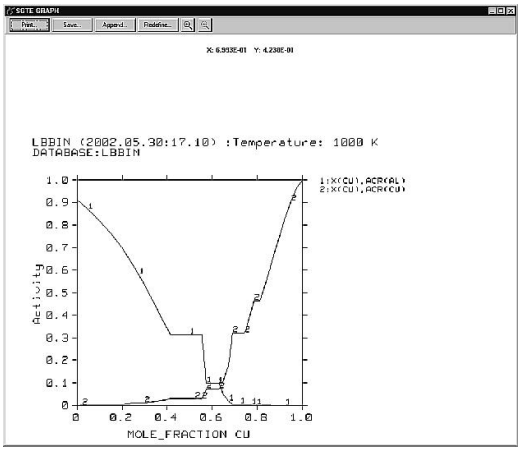

Fig. 8. The diagram calculated by pressing the A curves button. The component activities in the system Al-Cu are shown at 1000 K.

Phase Fraction

This diagram gives the amount of the stable phases as a function of temperature for a given composition as shown in Fig. 9. The amount is given as mass fraction of phase. If one is interested to know how the amount of the phases varies with composition for a given temperature one can use the A-CURVES button and then change the axis with REDEFINE.

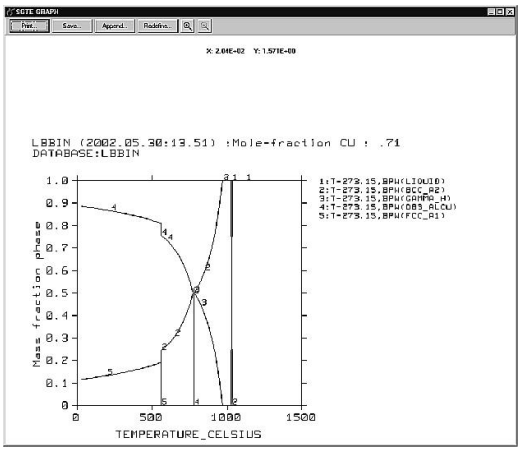

Fig. 9. The diagram calculated by pressing the phase fraction button. The curves show the amount of phase as function of the temperature at a given composition; the mole-fraction of copper is set to 0.71.

Features and Errors

Unfortunately all software has errors. If you find a problem with the software please provide details by sending an email to info@thermocalc.se. Please provide the minimum number of actions needed to reproduce the error. If you would like to suggest an additional feature send an email to the same address. One known problem may occur in the calculation of metastable phase diagrams where there may be a miscibility gap.

References

[45Tem] M. Temkin: Acta Phys. Chim. **20** (1945) 411–420.
[48Red] O. Redlich, A. Kister: Ind. Eng. Chem. **40** (1948) 345–348.
[70Hil] M. Hillert, L.-I. Staffanson: Acta Chem. Scand. **24** (1970) 3618–3626.
[78Hil] M. Hillert, M. Jarl: Calphad **2** (1978) 227–238.
[78Som] F. Sommer: Calphad **2** (1978) 319–324.
[81Ind] G. Inden: Physica **103B** (1981) 82–100.
[81Sun] B. Sundman, J. Ågren: J. Phys. Chem. Solids **42** (1981) 297–301.
[85Hil] M. Hillert, B. Jansson, B. Sundman, Ågren: Metall. Trans. A **16A** (1985) 261–266.
[85Vil] P. Villars, L.D. Calvert: "Pearson's Handbook of Crystallographic Data for Intermetallic Phases", Vol. 1–3, ASM, Metals Park, Ohio, USA, 1985.
[88Ans] I. Ansara, P. Willemin, B. Sundman: Acta metall. **36** (1988) 977–982.
[90Mas] T.B. Massalski, H. Okamoto, P.R. Subramanian, L. Kacprzak: "Binary Alloy Phase Diagrams", 2nd ed., ASM International, Materials Park, Ohio, USA, 1990.
[91Din] A.T. Dinsdale: Calphad **15** (1991) 317–425.
[92Bra] E.A. Brandes, G.B. Brook (eds.): "Smithells Metals Reference Book", 7th ed., Butterworth-Heinemann Ltd., Oxford, 1992.
[97Ans] I. Ansara, N. Dupin, H.L. Lukas, B. Sundman: J. Alloys Compd. **247** (1997) 20–30.
[98Sau] N. Saunders, A.P. Miodownik: "CALPHAD Calculation of Phase Diagrams", Elsevier Science Ltd., Oxford, 1998.
[02Din] A.T. Dinsdale: to be published (2002).

SGTE Data for Pure Elements

A.T. Dinsdale

The data for each phase of each element are presented graphically in terms of the variation with temperature of the heat capacity of the various phases and the difference in Gibbs energy between each phase and the reference phase for the element (ie lattice stability).

The SGTE element data were first presented in September 1989 [89Din] but published in revised form in 1991 [91Din1, 91Din2, 93Din] partially to conform to the 1990 International Temperature Scale [90Pre, 91Rus]. The data have been revised and enhanced since then. Over the last few years these element data have formed the basis of a number of assessments of binary, ternary and higher order systems which have appeared in the open literature.

Stable and Metastable Phase Data

In order to model the thermodynamic properties of binary or multicomponent systems data for each element are required for each phase in which it can form or dissolve. The data for the stable phases are, on the whole, well defined although serious anomalies still exist requiring further experimental study. Data are also required for these phases for temperatures outside their range of stability and this is generally much more of a problem. The traditional CALPHAD approach [70Kau] is to use the enthalpy and entropy of transition to extrapolate the Gibbs energy difference but to neglect any effects due to a difference in heat capacity between the phases. These differences, however, can often be substantial.

The extrapolation of the experimental heat capacity data across a solid state transformation is generally fairly straightforward. The extrapolation of data above and below the fusion temperature is more complicated. If the liquid heat capacity data are extrapolated from above the fusion temperature to lower temperatures there is the possibility that for certain temperatures the liquid phase would have a lower entropy than the solid phases. This is unreasonable and would be prevented in practice by the occurrence of the so-called glass transition, which is thought to take place at about 0.25 of the fusion temperature. A similar problem could occur with the extrapolation of the solid phase data to temperatures well above the melting point where under certain circumstances the solid could be predicted to become stable again.

These problems need to be avoided and SGTE adopted an interim solution for many elements in which the heat capacity of the liquid phase approaches that of the most stable solid phase for temperatures below the melting point [87And]. In a similar way above the melting temperature the heat capacity of the solid phases approaches that of the liquid phase. This has led to the introduction of terms in T^7 and T^{-9} into expressions for the Gibbs energy and removes the possibility of phases becoming incorrectly stable at high or low temperatures. An alternative method was also used for a number of elements to obtain a smoother extrapolation of the heat capacities of the solid and liquid phases.

The definition of data for phases which, for a given element, are metastable present even more of a problem and it has been common to assess these "lattice stabilities", ie expressions for the difference in Gibbs energy between one phase and another, from the critical assessment of data for many binary systems. Many of the initial set of lattice stabilities used were derived by Kaufman (see for example [70Kau, 77Kau, 78Kau]). SGTE sponsored the definition of new values for the Gibbs energies of transformation [86Sau, 88Sau] by considering more recent experimental data for stable phase transformations, taking account of the observed correlation between the entropy of fusion and temperature of fusion and better theoretical prediction of the enthalpy difference between two structures for a given element at 0 K. More recent theoretical studies have indicated that some elements in certain phases may be mechanically unstable for particular ranges of temperature and pressure [95Chan]. The SGTE unary data published in 1991 provided, according to the consensus of SGTE members the most reliable data for the elements. These recommended data have

changed since then as new information became available from experimental studies and improved theoretical methods and to reflect other currently accepted data.

More recently SGTE has also been at the forefront of the development of more scientific approaches to the extrapolation of heat capacities through use of Einstein or Debye equations [95Chas] for crystalline phases and a two state model for the liquid phase [95Ågr, 00Tol]. In due course these will lead to a completely new set of unary data and form the basis for new and improved thermodynamic databases.

Standard Element Reference

The data for each phase are stored in the form of Gibbs energies relative to the "Standard Element Reference" ie the enthalpies of the pure elements in their defined reference phase at 298.15 K (denoted as $G - H_{\mathrm{SER}}$). This reference phase is normally the phase stable at 10^5 Pa and 298.15 K. The exception to this rule is phosphorus for which, by convention, the white form is chosen as the reference phase because the more stable red form is difficult to characterise. This form of data is very convenient to use since all data in a database stored relative to this reference state are interconsistent and can be combined for the calculation of chemical and metallurgical equilibria. Furthermore each dataset contains all the thermodynamic information of interest for a particular phase and does not include any anomalous behaviour in a reference phase. All other thermodynamic functions can be calculated directly from one or more derivatives of the Gibbs energy expression. The concept of $G - H_{\mathrm{SER}}$ can be best understood by noting that a Gibbs energy can be subdivided into its enthalpy and entropy contributions. The entropy of an element in a phase has an absolute value. The enthalpy, on the other hand, and therefore the Gibbs energy, has no absolute value, and a reference state needs to be defined. The most obvious reference state for the enthalpy is that of the element in its reference phase at 298.15 K. This is the reference state used for tabulation of the enthalpy of formation at 298.15 K. Combination of the enthalpy defined in this way with the absolute entropy gives $G - H_{\mathrm{SER}}$.

The remainder of this section on unary data falls into two parts. The first part is a summary of the transition data between the stable phases for all elements for which SGTE has solid and liquid data. All thermodynamic data refer to units of J mol^{-1}. This is similar to the information presented in the Massalski compilation of binary alloy phase diagrams [91Din2] but is updated. The standard entropies at 298.15 K for certain key elements are compatible with the CODATA key values [89Cox] and all temperatures quoted refer to the ITS-90 temperature scale [90Pre, 91Rus]. These include eight of the fixed points on the temperature scale.

The table includes for each element a number of important properties. After the atomic weight is given the difference in enthalpy between 298.15 and 0 K and the standard entropy at 298.15 K of the element in the defined reference phase. The final five columns relate to the temperature, change in enthalpy, change in entropy and change in heat capacity associated with any condensed phase transformation occurring within the element on heating. A number of rows are provided for elements which undergo solid state phase transformations eg Mn. The final row for a given element is associated with melting.

The second part shows the variation of heat capacity of the various phases as a function of temperature and also the difference in Gibbs energy between a given phase and the element reference phase.

References

[70Kau] L. Kaufman, H. Bernstein: "Computer Calculations of Phase Diagrams", Academic Press, New York and London, 1970.

[77Kau] L. Kaufman: Calphad **1** (1977) 7–89.

[78Kau] L. Kaufman, H. Nesor: Calphad **2** (1978) 55–80 and 81–108.

[86Sau] N. Saunders, A.P. Miodownik: "Metastable Lattice Stabilities for the Elements", University of Surrey Report, 1986.

[87And] J.-O. Andersson, A. Fernandez Guillermet, P. Gustafson, M. Hillert, B. Jansson, B. Jönsson, B. Sundman, J. Ågren: Calphad **11** (1987) 93–98.
[88Sau] N. Saunders, A.P. Miodownik, A.T. Dinsdale: Calphad **12** (1988) 351–74.
[89Cox] J.D. Cox, D.D. Wagman, V.A. Medvedev: "CODATA Key Values for Thermodynamics", Hemisphere Publ. Corp., New York NY, USA, 1989.
[89Din] A.T. Dinsdale: "SGTE Data for Pure Elements", NPL Report DMA(A)195, September 1989.
[90Pre] H. Preston-Thomas: Metrologia, **27** (1990) 3–10.
[91Din1] A.T. Dinsdale: Calphad **15** (1991) 317–425.
[91Din2] A.T. Dinsdale: "SGTE Pure Element Transition Data", published within the 3 volume compilation "Binary Alloy Phase Diagrams", 2nd ed., ASM Int., T.B. Massalski, ed., 1991.
[91Rus] R.L. Rusby, R.P. Hudson, M. Durieux, J.F. Schooley, P.M. Steur, C.A. Swenson: Metrologia **28** (1991) 9–18.
[93Din] A.T. Dinsdale: J. Chim. Phys. **90** (1993) 189–200.
[95Ågr] J. Ågren, B. Cheynet, M. Clavaguera-Mora, K. Hack, J. Hertz, F. Sommer, U. Kattner: Calphad **19** (1995) 449–480.
[95Chan] Y.A. Chang, C. Colinet, M. Hillert, Z. Moser, J.M. Sanchez, N. Saunders, R.E. Watson, A. Kussmaul: Calphad **19** (1995) 481–498.
[95Chas] M.W. Chase, I. Ansara, A.T. Dinsdale, G. Eriksson, G. Grimvall, L. Höglund, H. Yokokawa: Calphad **19** (1995) 437–447.
[00Tol] O. Tolochko, J. Ågren: J. Phase Equil. **21** (2000) 19–24.

SGTE Pure Element Transition Data

	Atomic weight	$H_{298} - H_0$ [J/mol]	S_{298} [J/(mol·K)]	Phase	$T_{\rm trs}$ [K]	$\Delta_{\rm trs}H$ [J/mol]	$\Delta_{\rm trs}S$ [J/(mol·K)]	$\Delta_{\rm trs}C_P$ [J/(mol·K)]
Ag	107.8682	5745.	42.55	FCC_A1	1234.93	11296.80	9.1477	1.5402
Al	26.98154	4540.	28.30	FCC_A1	933.47	10711.04	11.4744	−2.2046
Am	243.	6407.00	55.3960	DHCP	1041.98	870.09	0.8350	−2.7810
				FCC_A1	1350.00	5862.06	4.3422	1.2898
				BCC_A2	1449.00	14393.0	9.9330	2.092
As	74.922	5117.032	35.6895	RHO_A7	1090.00	24442.9	22.4247	0.0
Au	196.9665	6016.592	47.4884	FCC_A1	1337.33	12552.0	9.3859	0.0
B	10.81	1222.0	5.9	BET	2348.00	50200.00	21.3799	0.8362
Ba	137.33	6910.0	62.50	BCC_A2	1000.00	7120.0	7.120	−4.3450
Be	9.01218	1950.0	9.50	HCP_A3	1527.00	6849.0	4.4853	−1.8915
				BCC_A2	1560.00	7895.0	5.0609	−1.2123
Bi	208.9804	6426.624	56.735	RHO_A7	544.55	11296.80	20.7452	0.6522
C	12.011	1054.0	5.7423	HEX_A9	4765.3	117369.0	24.6300	0.0
Ca	40.08	5736.0	41.588	FCC_A1	716.00	928.85	1.2972	−1.2336
				BCC_A2	1115.00	8539.54	7.6588	−8.2257
Cd	112.41	6247.	51.80	HCP_A3	594.219	6192.32	10.4209	0.1666
Ce	140.12	7280.16	69.454	FCC_A1	1000.00	2991.60	2.9916	−0.1337
				BCC_A2	1072.00	5460.12	5.0934	0.0836
Co	58.9332	4765.567	30.0400	HCP_A3	694.99	427.59	0.6153	0.000
				FCC_A1	1768.00	16200.01	9.1629	0.8962

	Atomic weight	$H_{298} - H_0$ [J/mol]	S_{298} [J/(mol·K)]	Phase	T_{trs} [K]	$\Delta_{\mathrm{trs}}H$ [J/mol]	$\Delta_{\mathrm{trs}}S$ [J/(mol·K)]	$\Delta_{\mathrm{trs}}C_P$ [J/(mol·K)]
Cr	51.996	4050.0	23.5429	BCC_A2	2180.0	21004.00	9.6349	−10.7118
Cs	132.9054	7711.000	85.23	BCC_A2	301.59	2096.00	6.9498	0.1128
Cu	63.546	5004.	33.15	FCC_A1	1357.77	13263.28	9.7684	1.5391
Dy	162.50	8865.896	74.9559	HCP_A3	1654.15	4591.74	2.7759	4.1866
				BCC_A2	1685.11	11350.52	6.7358	−0.2929
Er	167.26	7392.2912	73.17816	HCP_A3	1802.00	19903.29	11.0451	−4.6468
Eu	151.96	8004.0	80.79304	BCC_A2	1095.00	9213.17	8.4139	−2.9731
Fe	55.847	4489.0	27.2797	BCC_A2	1184.81	1012.86	0.8549	−7.6812
				FCC_A1	1667.47	825.78	0.4952	2.1829
				BCC_A2	1810.94	13806.84	7.6241	4.6526
Ga	69.72	5572.0	40.7271	ORT	302.91	5589.81	18.4534	2.2766
Gd	157.25	9087.648	68.0894	HCP_A3	1508.15	3518.67	2.3331	−0.3127
				BCC_A2	1586.15	9668.04	6.0953	−0.4529
Ge	72.59	4636.	31.09	DIA_A4	1211.40	36944.72	30.4975	−1.1370
Hf	178.49	5845.0	43.56	HCP_A3	2016.00	5860.29	2.9069	−6.6207
				BCC_A2	2506.00	27196.00	10.8524	5.5559
Hg	200.59	9342.	75.90	LIQUID	234.321	2295.34	9.7957	−0.0066
Ho	164.9304	7995.624	75.0191	HCP_A3	1747.00	15926.61	9.1165	−9.7986
In	114.82	6610.0	57.65	TET_A6	429.75	3283.0	7.6393	0.0148
Ir	192.22	5267.656	35.5054	FCC_A1	2719.00	41124.00	15.1247	12.0550
K	39.0983	7088.	64.68	BCC_A2	336.53	2320.86	6.8964	0.0576
La	138.9055	6665.112	56.9024	DHCP	550.00	364.01	0.6618	−0.5686
				FCC_A1	1134.00	3121.26	2.7524	4.5150
				BCC_A2	1193.00	6196.50	5.1941	−5.2300
Li	6.941	4632.00	29.12	BCC_A2	453.60	2999.93	6.6136	0.6362
Lu	174.967	6388.968	50.9611	HCP_A3	1936.00	18648.09	9.6323	−0.0103
Mg	24.305	4998.0	32.671	HCP_A3	923.00	8476.78	9.1839	2.0821
Mn	54.9380	4995.696	32.2206	CBCC_A12	980.00	2253.55	2.2995	−1.5482
				CUB_A13	1360.00	2165.73	1.5925	0.1264
				FCC_A1	1411.00	1908.30	1.3524	3.2651
				BCC_A2	1519.00	12908.94	8.4983	1.7204
Mo	95.94	4589.0	28.56	BCC_A2	2896.00	37479.85	12.9419	−10.5181
Na	22.98977	6460.	51.3000	BCC_A2	370.87	2597.01	7.0025	0.3018
Nb	92.9064	5220.0	36.27	BCC_A2	2750.00	30000.0	10.9091	0.5560
Nd	144.24	7133.72	71.0862	DHCP	1128.00	3029.22	2.6855	−1.435
				BCC_A2	1289.00	7142.09	5.5408	4.2258
Ni	58.69	4787.0	29.7955	FCC_A1	1728.30	17479.82	10.1142	4.248
Np	237.0482	6606.536	50.4590	ORTHO	555.02	4699.92	8.4680	−5.0491
				TETRAG	855.95	3000.12	3.5050	−2.9291
				BCC_A2	916.84	3198.57	3.4887	8.995
Os	190.2		32.6352	HCP_A3	3306.00	57855.00	17.5000	13.8379
P	30.97376	5360.0	41.09	WHITE	317.30	659.0	2.0769	1.9793
Pa	231.0359	6439.176	51.882	BCT_Aa	1443.10	6639.79	4.6011	−2.0962
				BCC_A2	1844.78	12341.18	6.6898	7.5305
Pb	207.2	6870.	64.80	FCC_A1	600.612	4773.94	7.9485	1.1867
Pd	106.42	5468.488	37.8234	FCC_A1	1828.00	16736.00	9.1554	4.5325
Pr	140.9077	7418.232	73.9313	DHCP	1068.00	3167.29	2.9656	−3.5564
				BCC_A2	1204.00	6886.86	5.7200	4.5187

	Atomic weight	$H_{298} - H_0$ [J/mol]	S_{298} [J/(mol·K)]	Phase	$T_{\rm trs}$ [K]	$\Delta_{\rm trs}H$ [J/mol]	$\Delta_{\rm trs}S$ [J/(mol·K)]	$\Delta_{\rm trs}C_P$ [J/(mol·K)]
Pt	195.08	5723.712	41.6308	FCC_A1	2041.50	22175.00	10.8621	−0.8317
Pu	244.	6902.0	54.4610		397.61	3706.00	9.3206	−3.3379
					487.90	478.00	0.9797	−0.5630
					593.06	713.02	1.2023	−0.7521
				FCC_A1	736.40	83.35	0.1132	−0.8764
				TET_A6	755.67	1841.06	2.4363	−1.8400
				BCC_A2	913.00	2824.03	3.0931	8.4470
Rb	85.4678	7489.	76.78	BCC_A2	312.46	2192.42	7.0166	−0.5631
Re	186.207	5333.	36.4820	HCP_A3	3458.00	34075.04	9.8540	9.9322
Rh	102.9055	(4920.384)	31.5557	FCC_A1	2237.00	26593.50	11.8880	1.3593
Ru	101.07	4602.4	28.6144	HCP_A3	2607.00	38589.03	14.8021	0.8342
S	32.06	4412.0	32.07	ORTHO	368.30	401.00	1.0888	0.5358
				MONOCL	388.36	1721.00	4.4315	6.5224
Sb	121.75	5870.152	45.5219	RHO_A7	903.78	19874.00	21.9899	0.4002
Sc	44.9559	5217.448	34.6435	HCP_A3	1608.00	4008.27	2.4927	4.1361
				BCC_A2	1814.00	14095.90	7.7706	0.000
Se	78.96	5514.512	41.9655	HEX_A8	494.00	6694.40	13.5514	3.8536
Si	28.0855	3217.	18.81	DIA_A4	1687.00	50208.00	29.7617	−2.0264
Sm	150.36	7573.04	69.4962	RHO_C19	1190.00	3112.90	2.6159	−1.3808
				BCC_A2	1345.00	8619.04	6.4082	3.2635
Sn	118.69	6323.	51.18	BCT_A5	505.078	7029.12	13.9169	−1.0252
Sr	87.62	6568.	55.694	FCC_A1	820.00	836.80	1.0205	−2.3609
				BCC_A2	1050.00	7431.00	7.0771	8.7110
Ta	180.9479	5681.872	41.4718	BCC_A2	3290.00	36568.17	11.1149	−2.6340
Tb	158.9254	9426.552	73.3037	HCP_A3	1562.00	4380.65	2.8045	−0.3402
				BCC_A2	1632.00	10150.38	6.2196	0.000
Tc	98.		32.9856	HCP_A3	2430.01	33291.19	13.7000	8.3218
Te	127.60	6080.	49.221	HEX_A8	722.66	17376.00	24.0445	16.1903
Th	232.0381	6350.	51.8	FCC_A1	1633.20	3597.01	2.2024	−5.7949
				BCC_A2	2022.99	13807.13	6.8251	6.0679
Ti	47.88	4824.	30.72	HCP_A3	1155.00	4169.98	3.6104	−5.0307
				BCC_A2	1941.00	14146.00	7.2880	8.4656
Tl	204.383	6831.97	64.2997	HCP_A3	507.00	359.82	0.7097	2.0997
				BCC_A2	577.00	4142.16	7.1788	−2.3901
Tm	168.9342	7397.312	74.01496	HCP_A3	1818.00	16840.60	9.2633	3.8918
U	238.0289	6364.	50.20	ORT_A20	942.00	2790.73	2.9625	−5.111
				TET	1049.00	4757.18	4.5350	−4.644
				BCC_A2	1408.00	9142.04	6.4930	10.3764
V	50.9415	4507.0	30.89	BCC_A2	2183.00	21500.0	9.8488	2.3597
W	183.85	4970.0	32.6176	BCC_A2	3694.90	52313.66	14.1583	0.2900
Y	88.9059	5983.457	44.7875	HCP_A3	1751.15	4886.19	2.7903	−3.5825
				BCC_A2	1795.15	11394.22	6.3472	7.9486
Yb	173.04	6711.136	59.8312	FCC_A1	1033.00	1748.91	1.6930	4.059
				BCC_A2	1097.00	7656.72	6.9797	0.6695
Zn	65.38	5657.	41.63	HCP_ZN	692.68	7322.00	10.5705	1.6653
Zr	91.22	5566.27	39.1809	HCP_A3	1138.97	4106.54	3.6054	−6.3115
				BCC_A2	2127.85	20997.77	9.8681	6.0320

Ag (Silver)

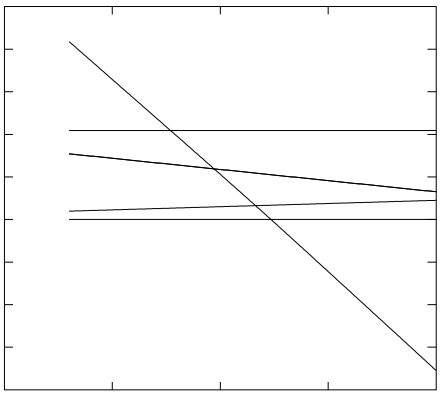

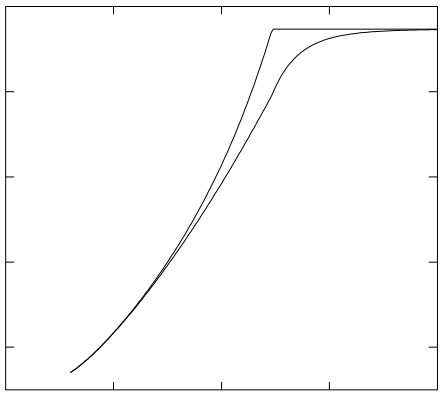

Al (Aluminium)

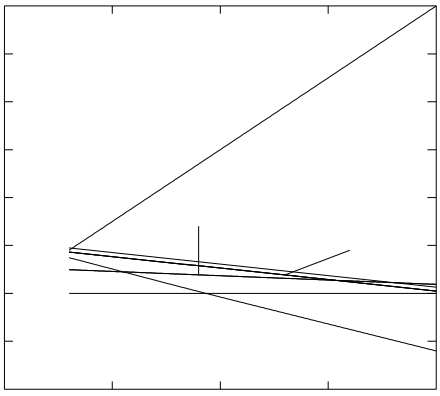

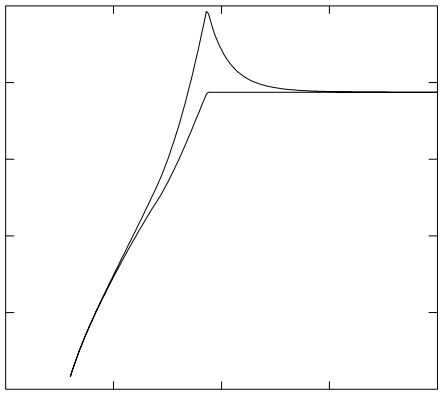

Am (Americium)

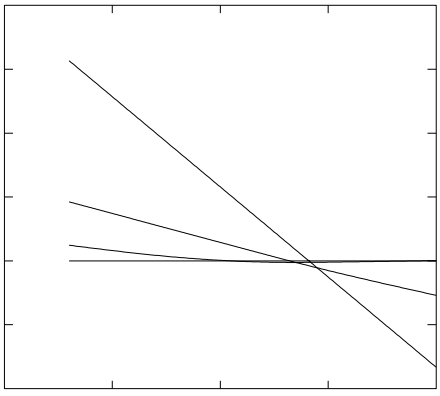

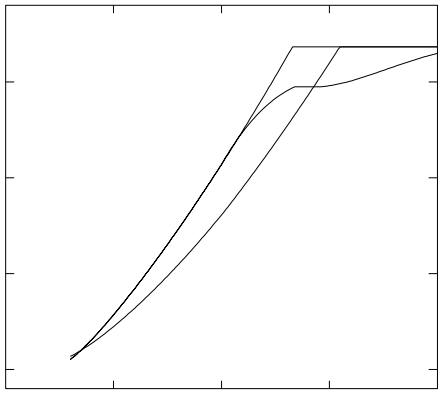

As (Arsenic)

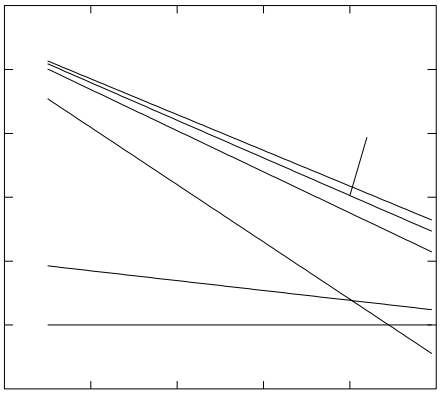

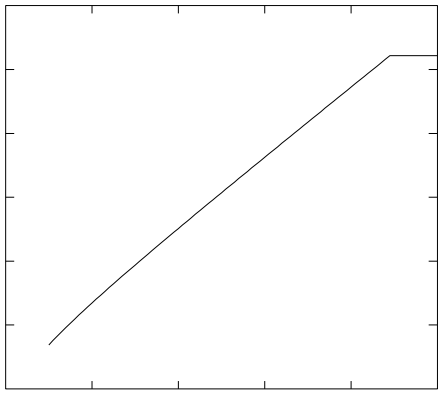

Au (Gold)

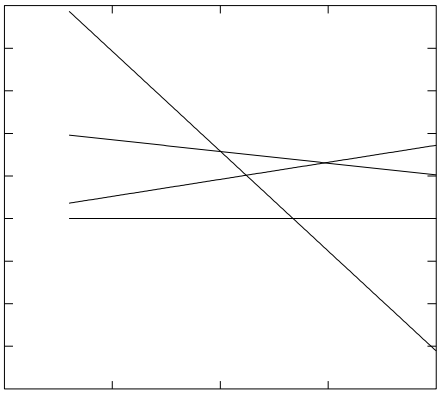

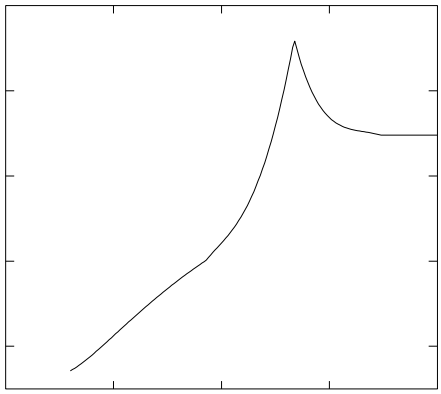

B (Boron)

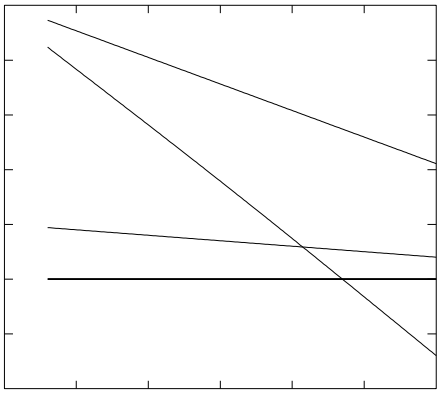

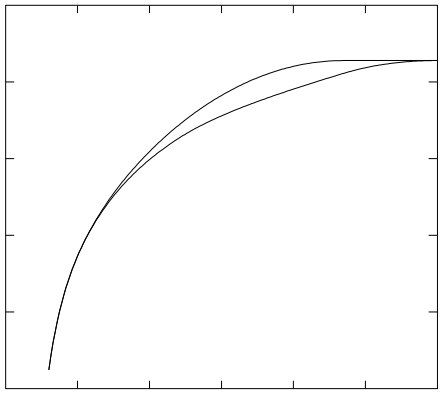

Ba (Barium)

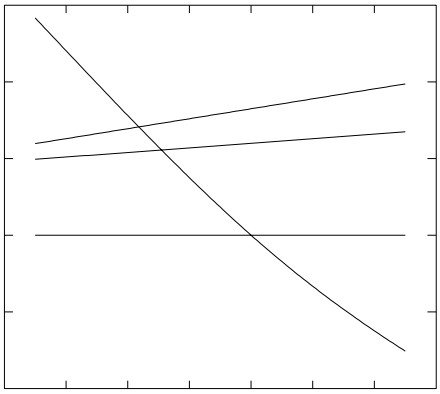

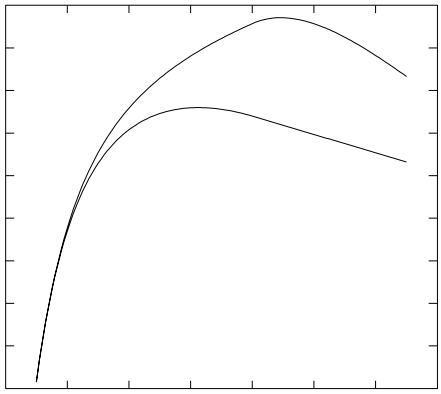

Be (Beryllium)

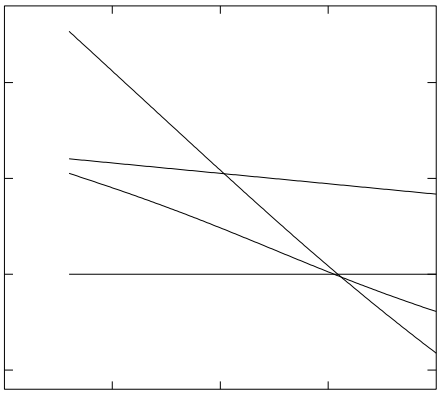

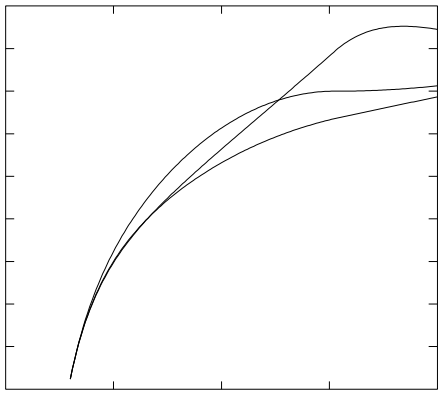

Bi (Bismuth)

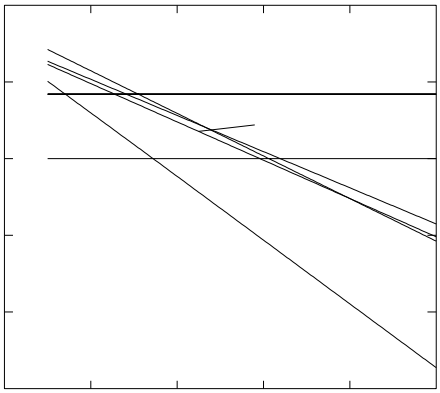

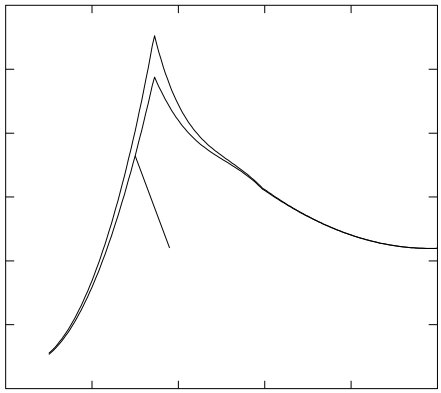

C (Carbon)

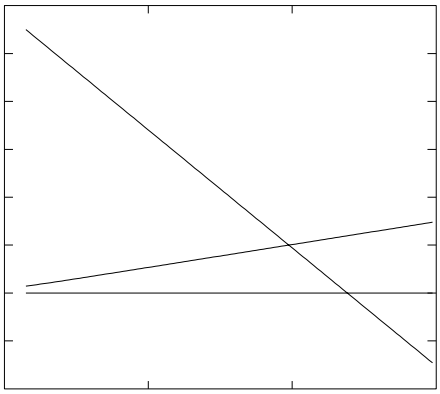

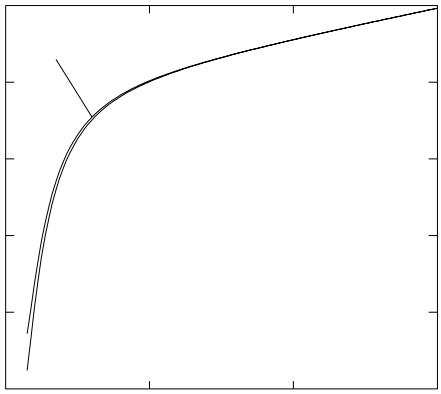

Ca (Calcium)

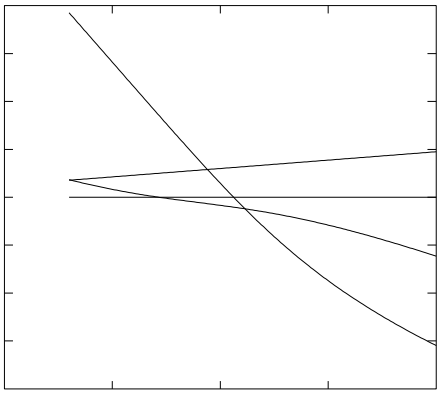

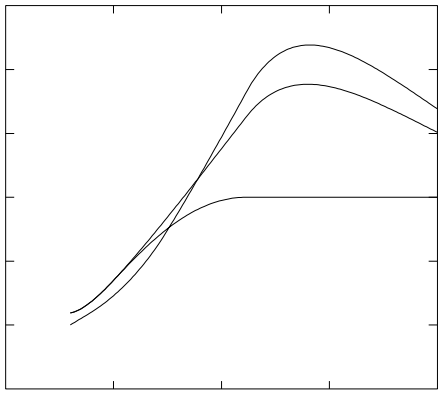

Cd (Cadmium)

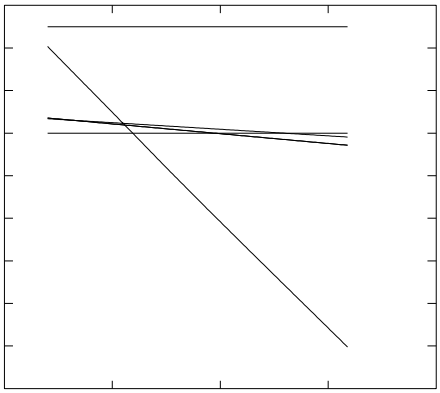

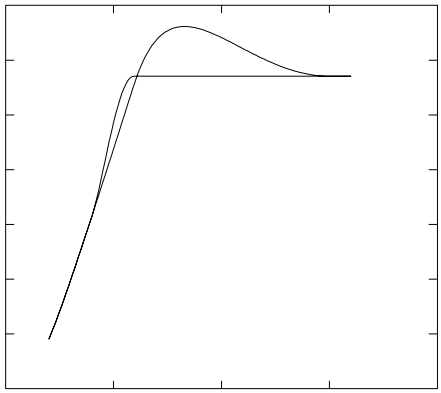

Ce (Cerium)

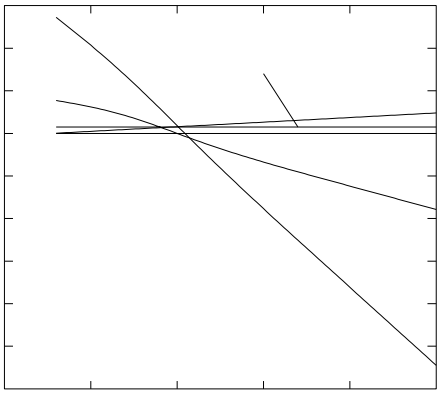

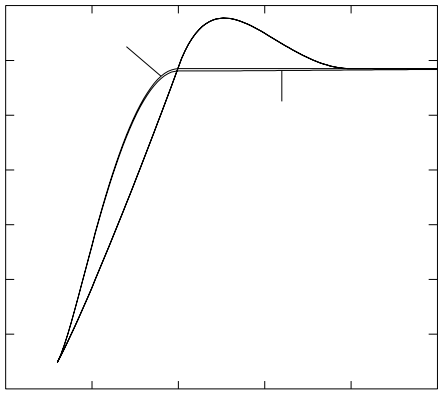

Co (Cobalt)

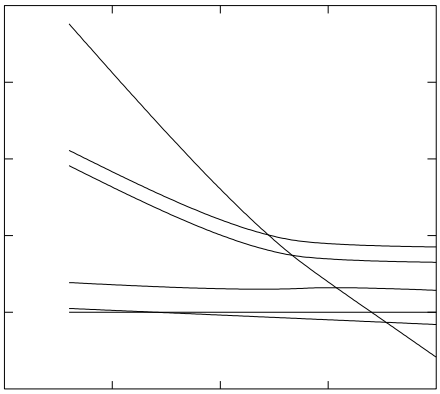

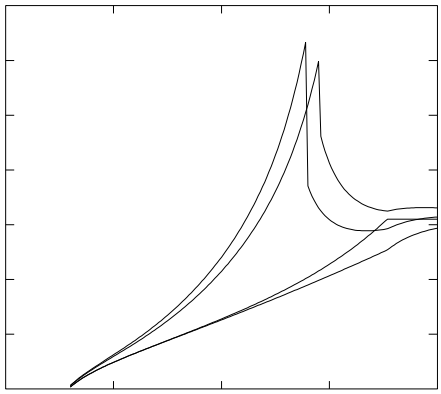

Cr (Chromium)

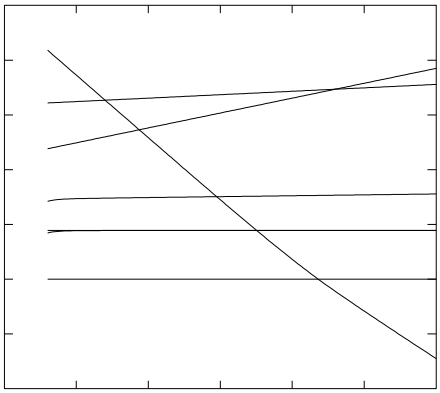

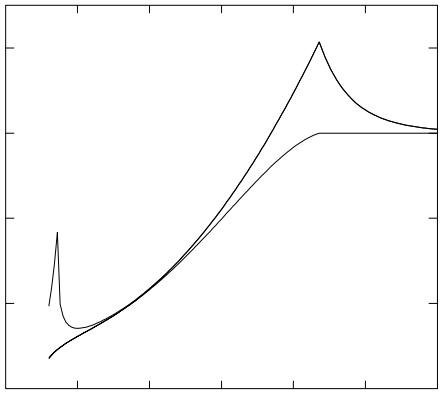

Cs (Caesium)

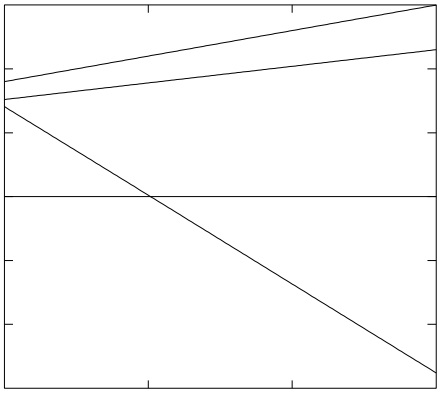

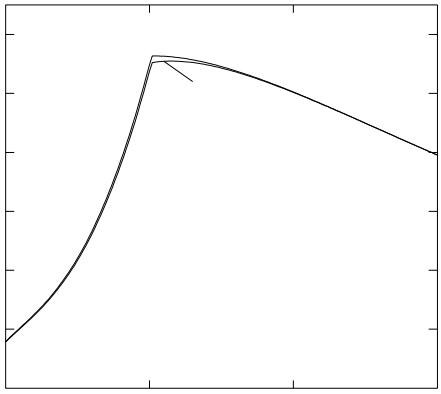

Cu (Copper)

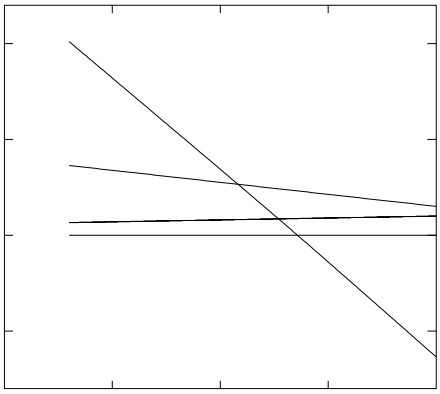

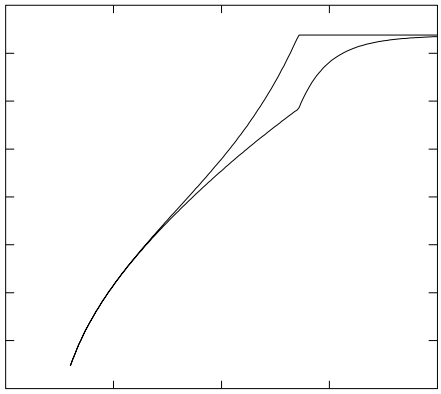

Dy (Dysprosium)

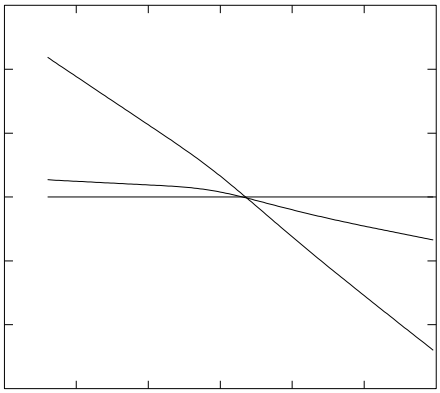

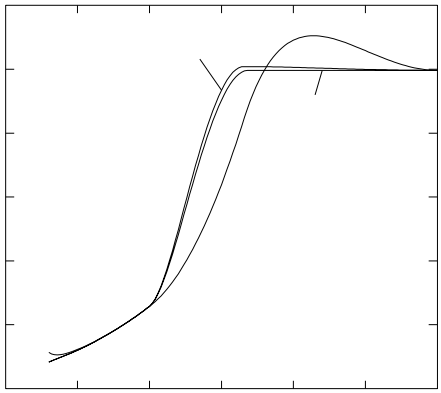

Er (Erbium)

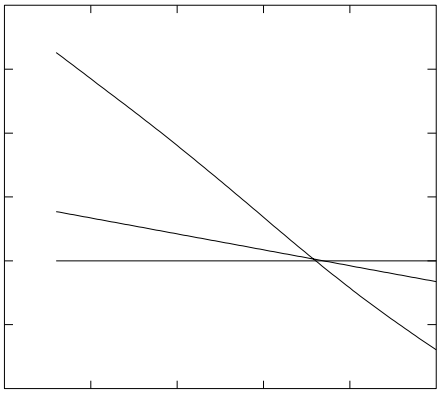

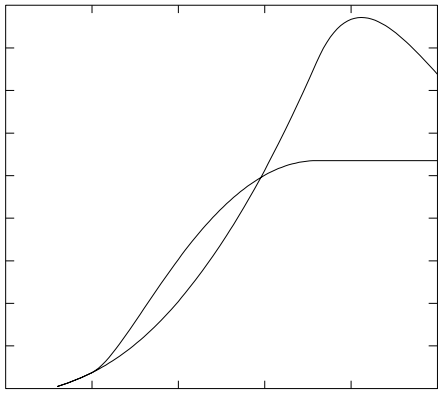

Eu (Europium)

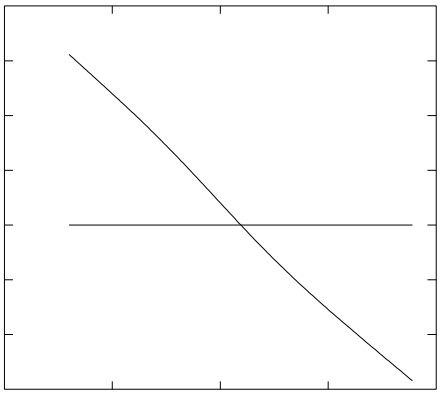

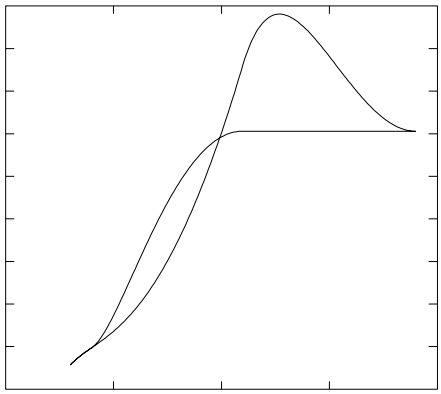

Fe (Iron)

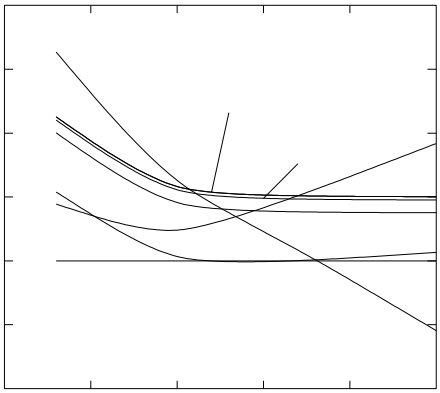

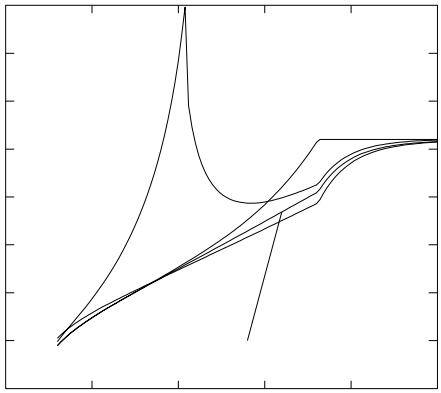

Ga (Gallium)

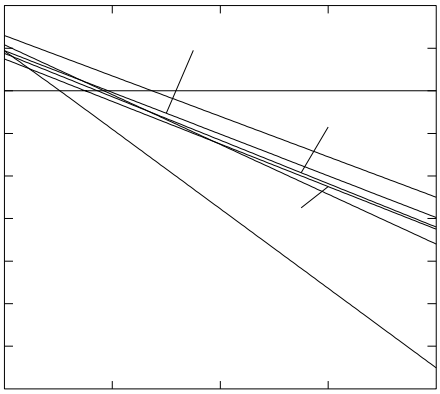

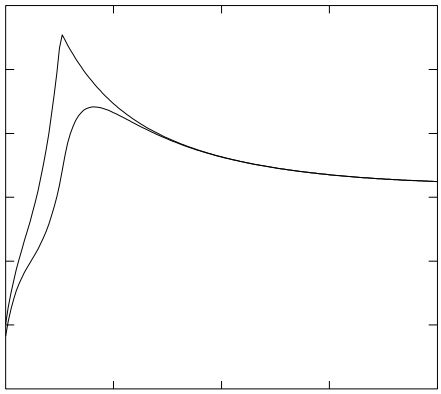

Gd (Gadolinium)

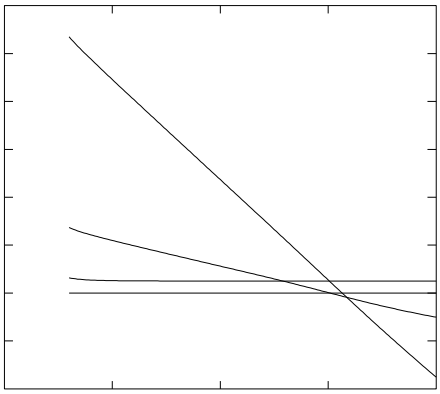

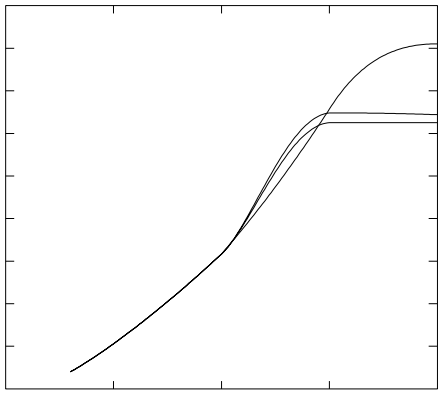

Ge (Germanium)

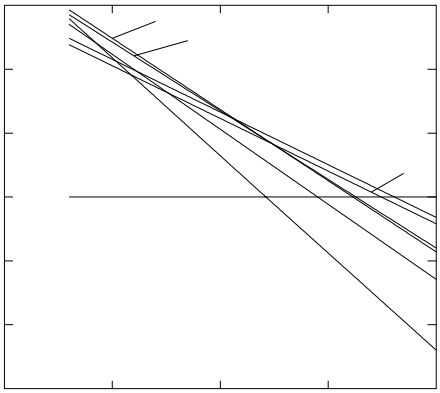

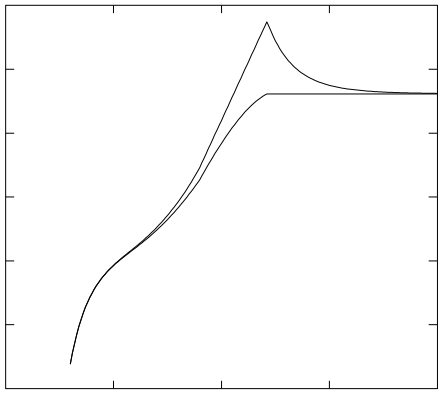

Hf (Hafnium)

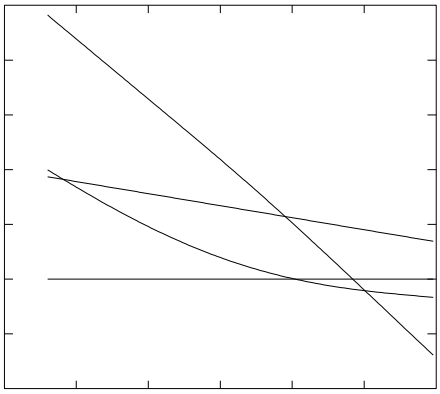

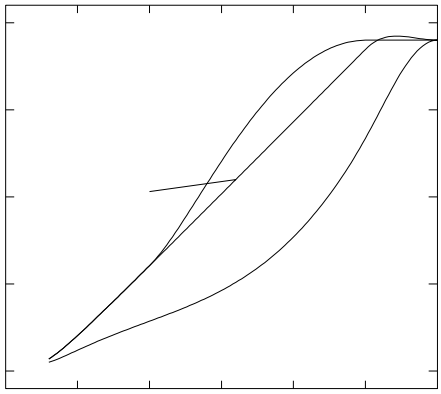

Hg (Mercury)

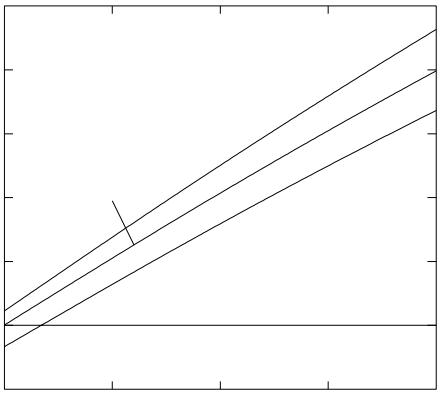

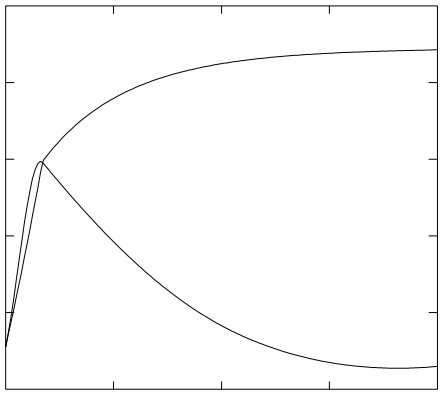

Ho (Holmium)

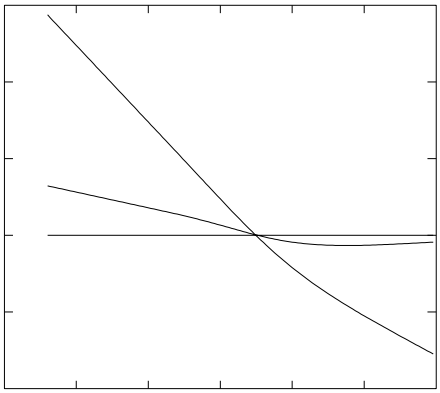

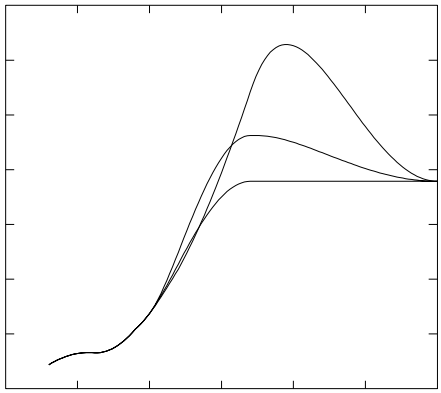

In (Indium)

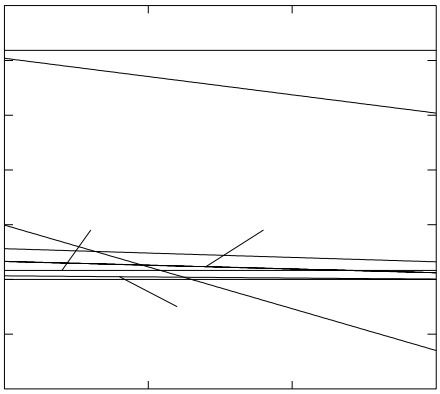

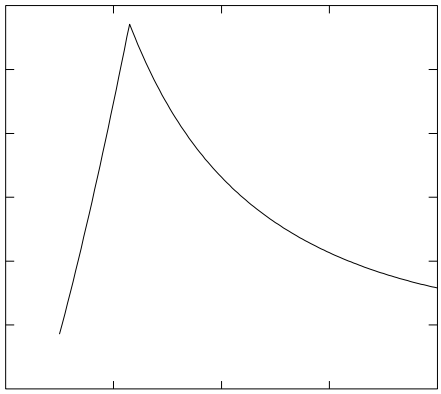

Ir (Iridium)

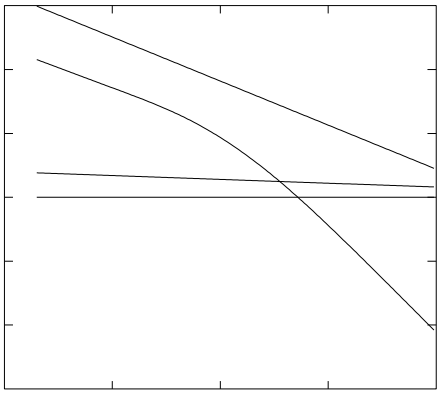

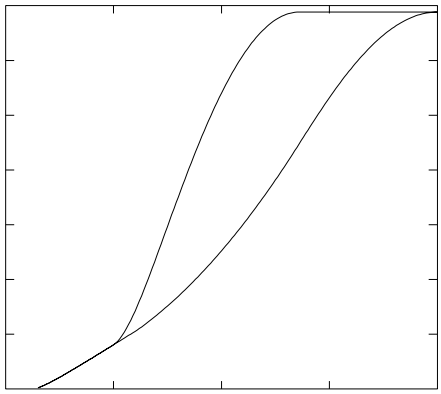

K (Potassium)

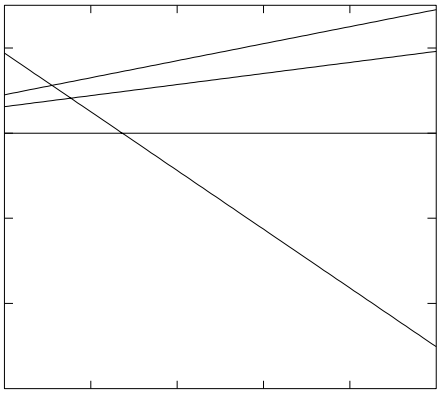

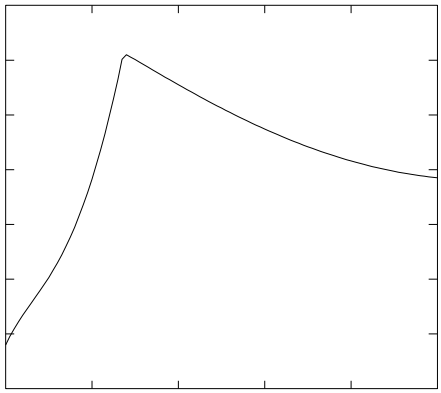

La (Lanthanum)

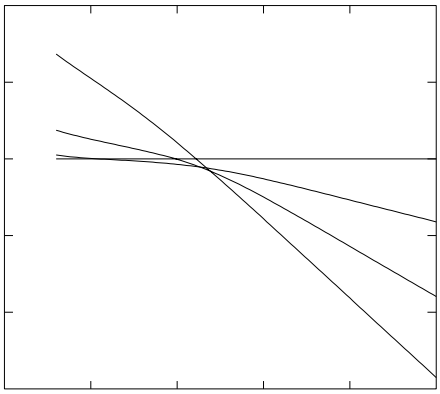

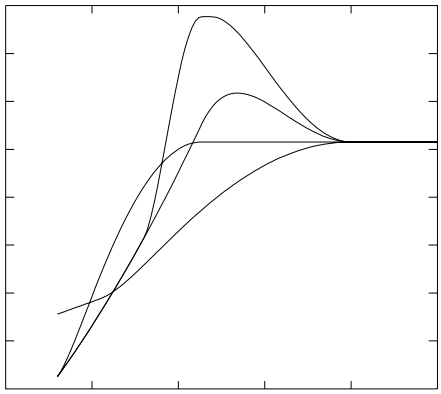

Li (Lithium)

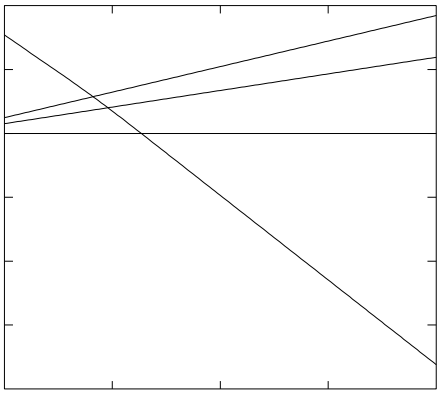

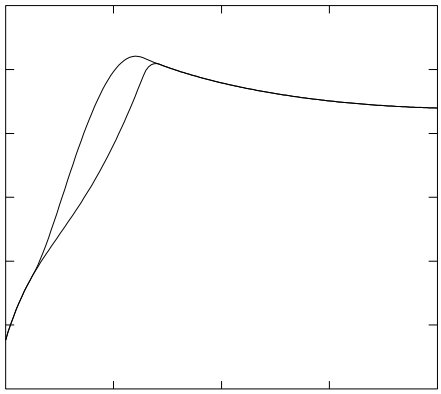

Lu (Lutetium)

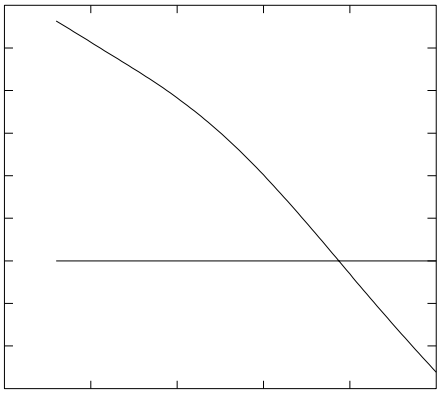

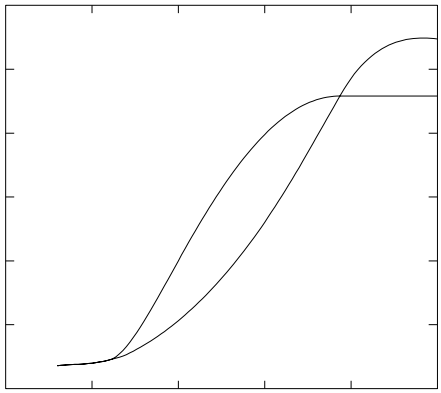

Mg (Magnesium)

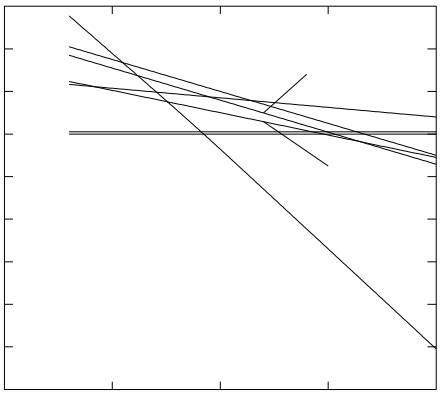

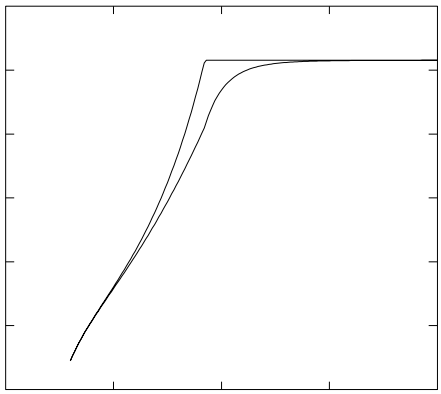

Mn (Manganese)

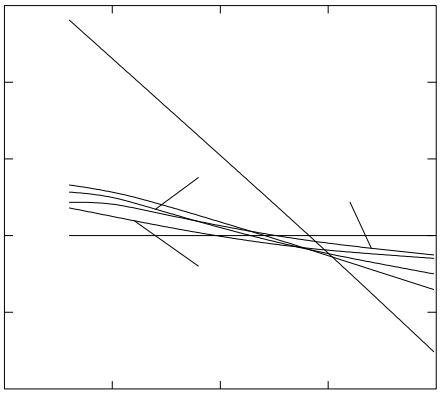

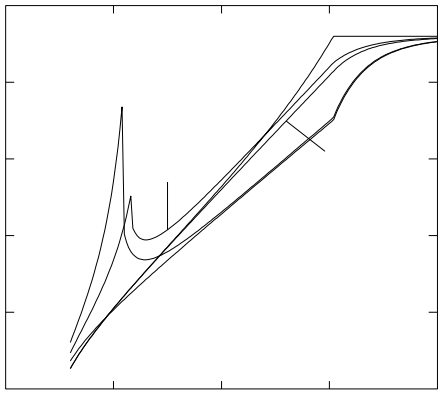

Mo (Molybdenum)

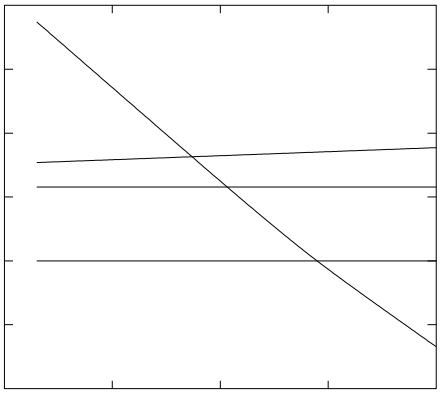

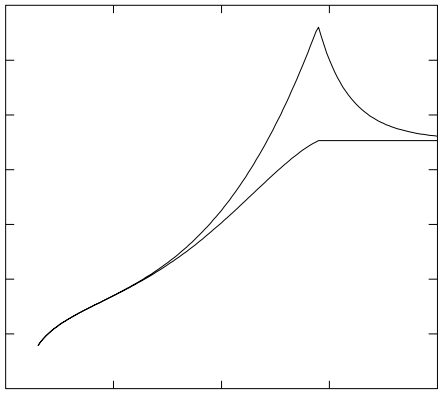

N (Nitrogen)

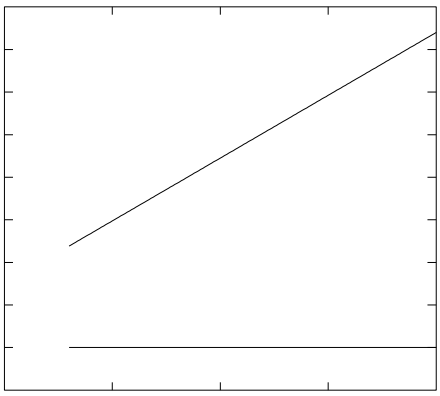

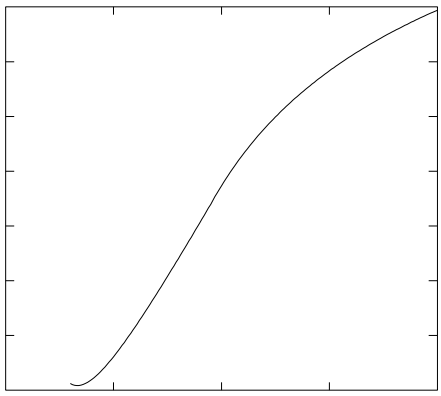

Na (Sodium)

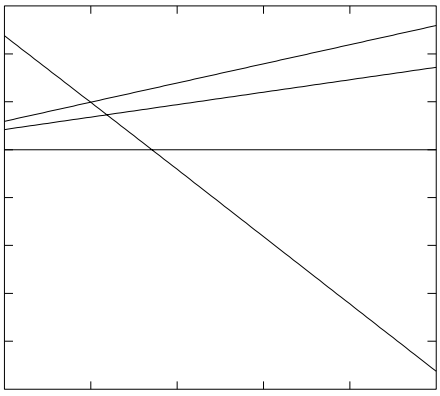

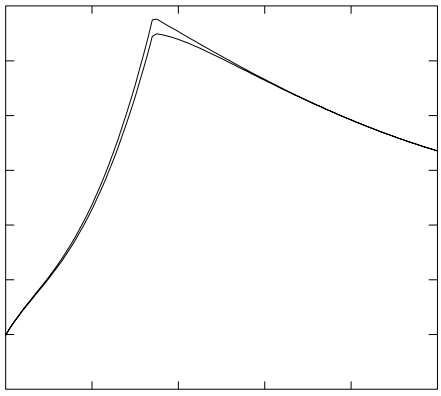

Nb (Niobium)

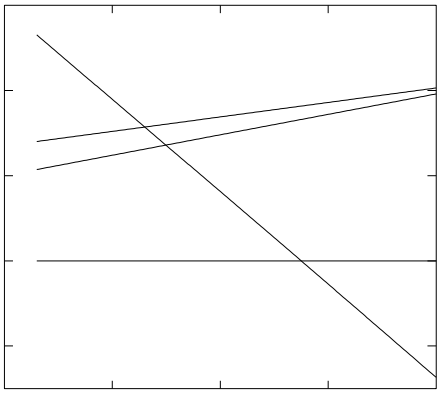

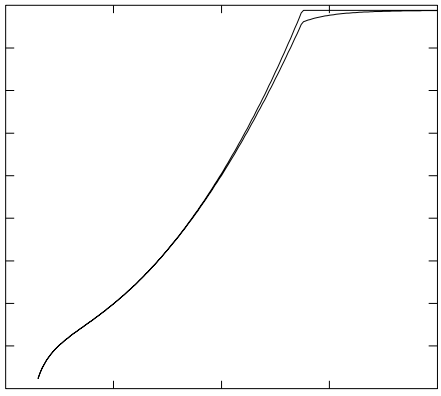

Nd (Neodymium)

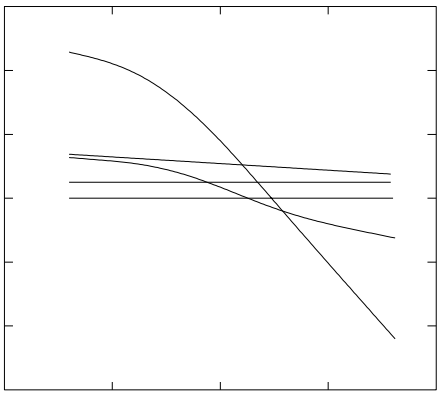

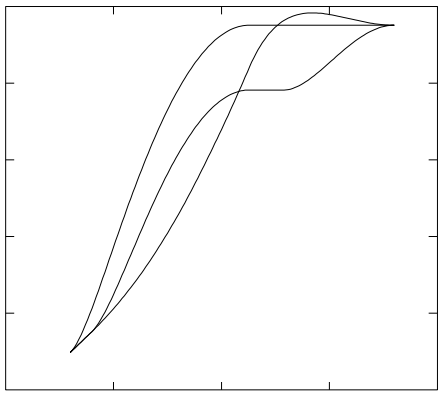

Ni (Nickel)

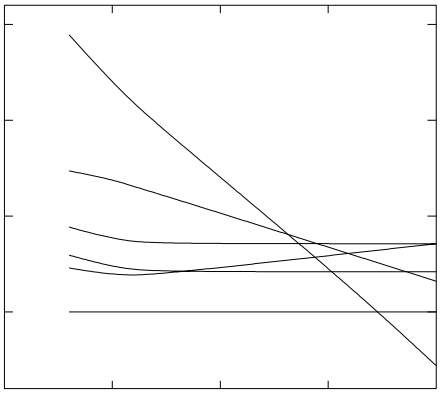

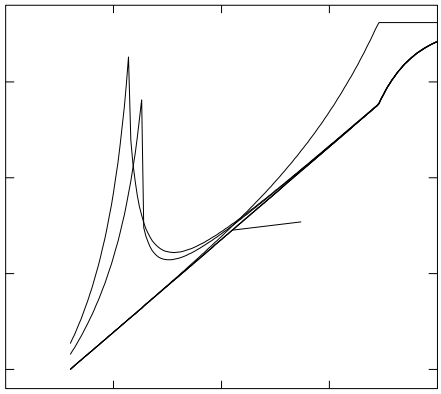

Np (Neptunium)

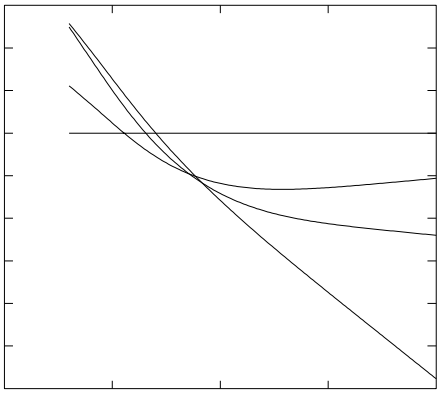

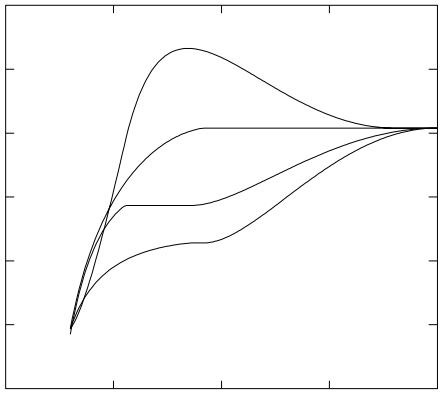

O (Oxygen)

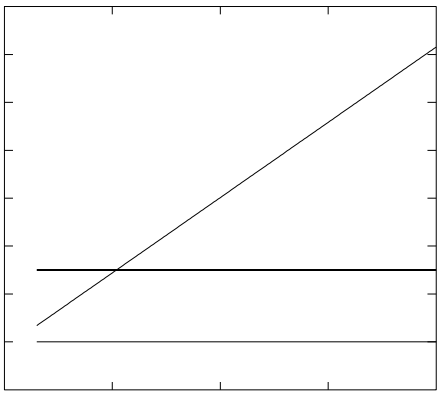

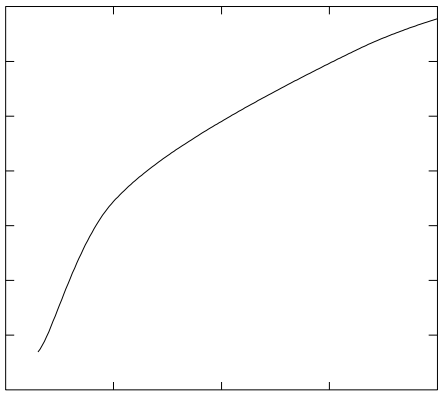

Os (Osmium)

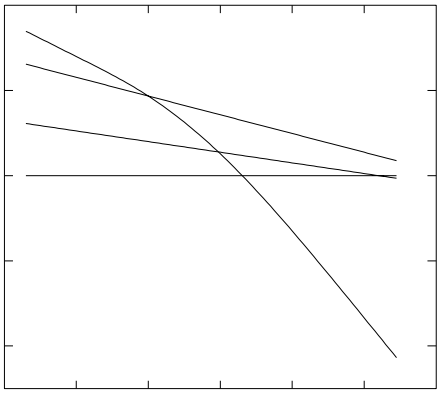

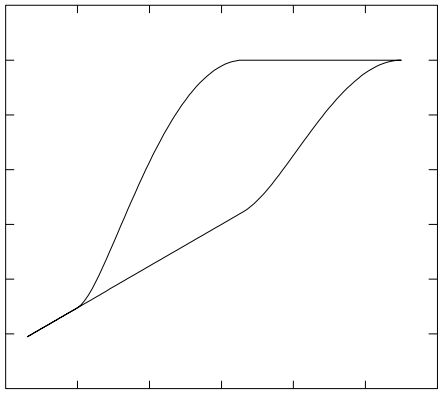

P (Phosphorus)

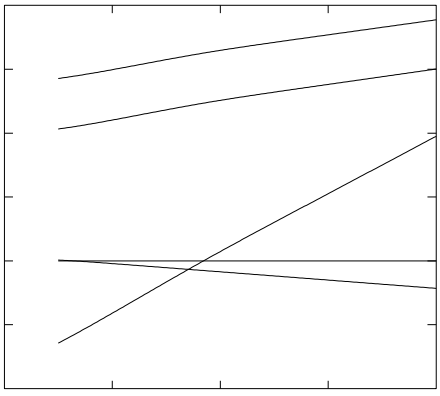

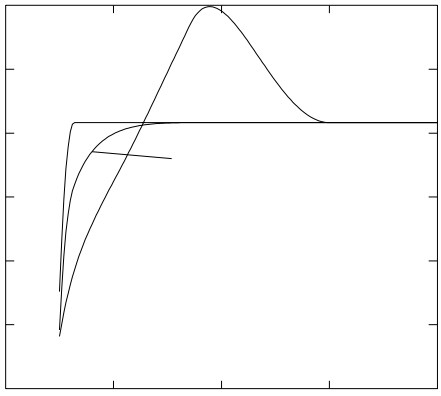

Pa (Protactinium)

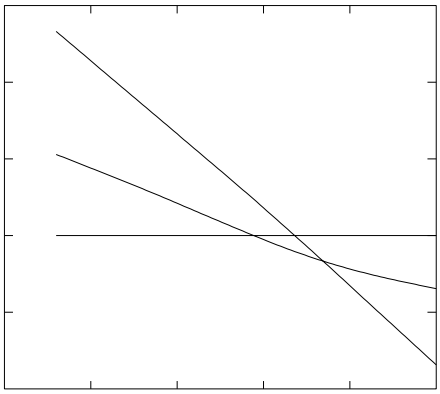

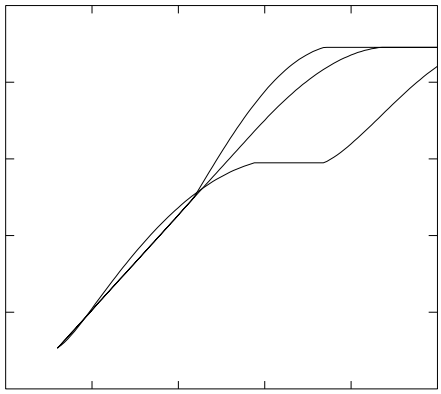

Pb (Lead)

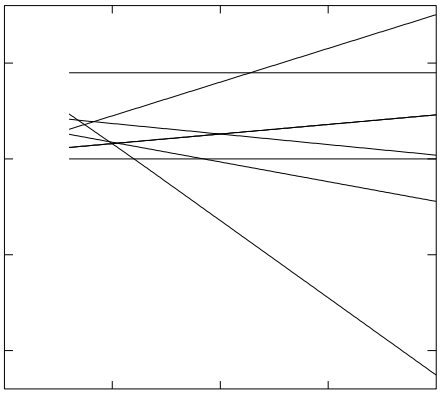

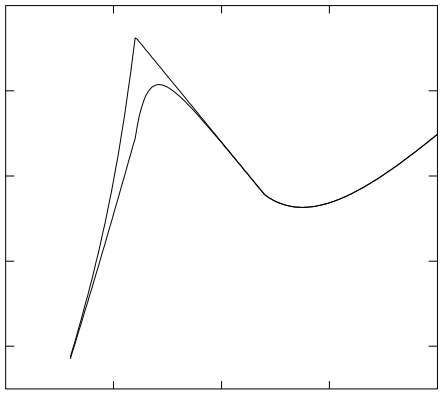

Pd (Palladium)

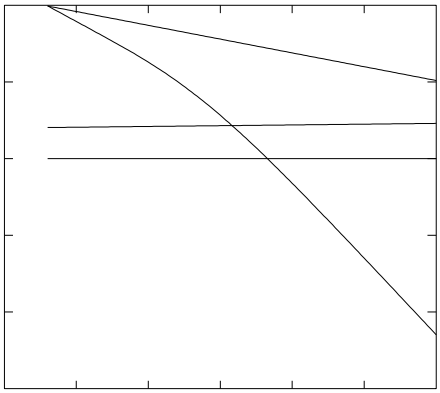

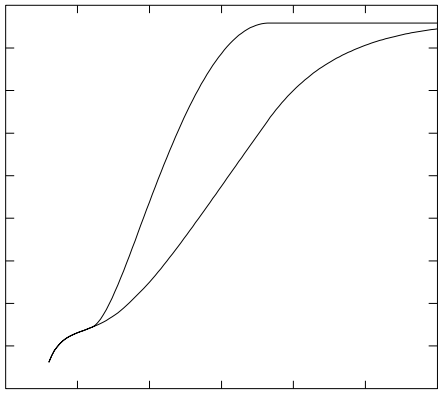

Pr (Praseodymium)

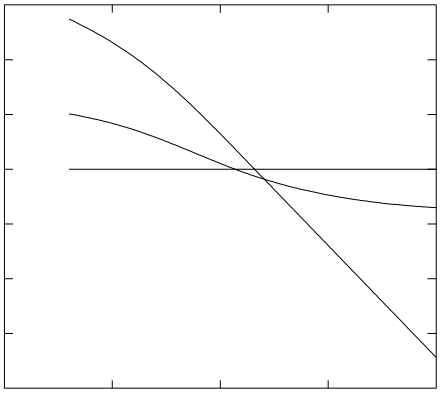

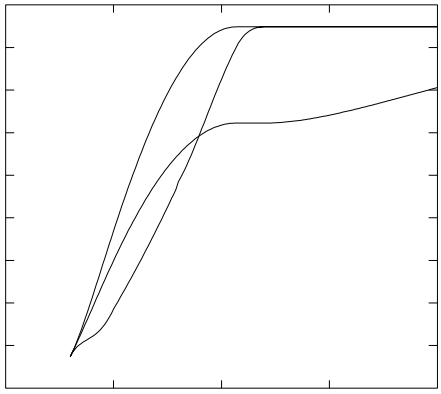

Pt (Platinum)

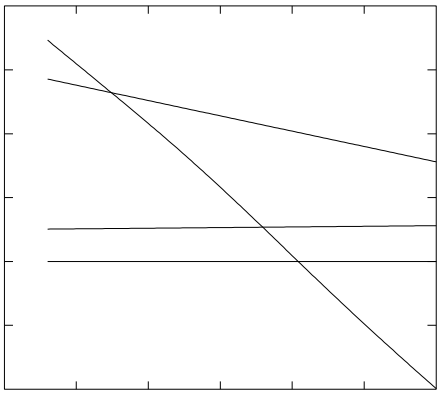

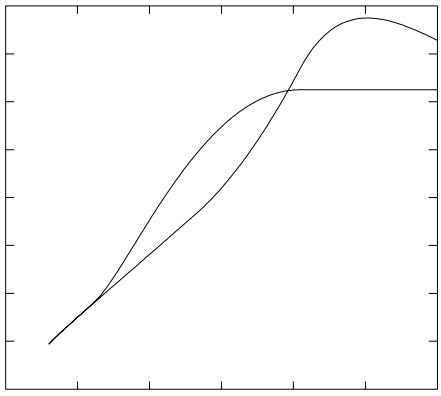

Pu (Plutonium)

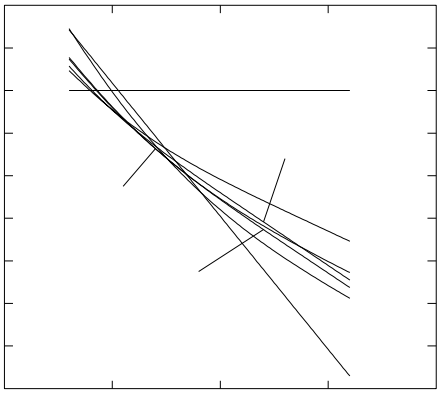

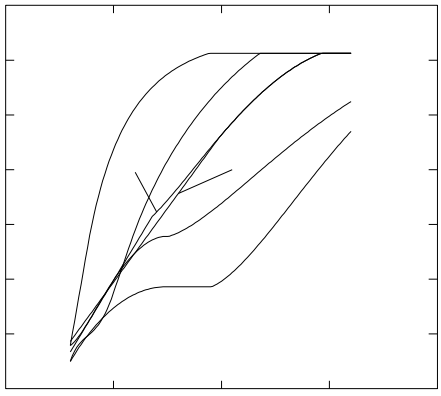

Rb (Rubidium)

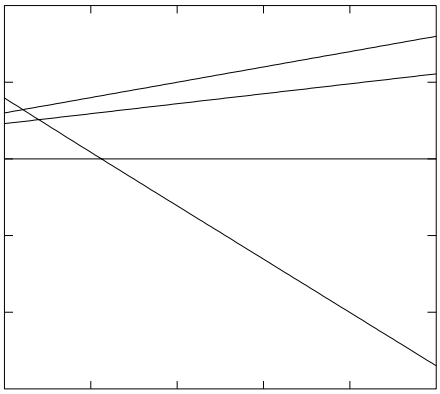

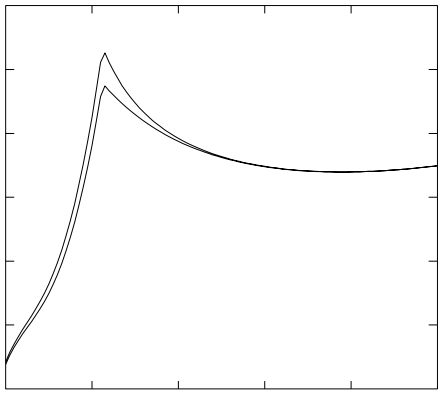

Re (Rhenium)

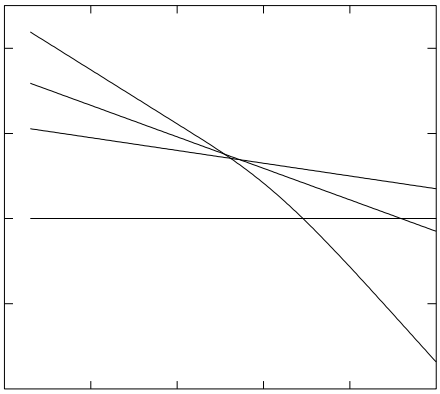

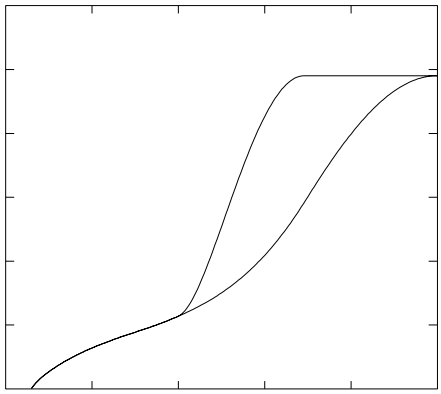

Rh (Rhodium)

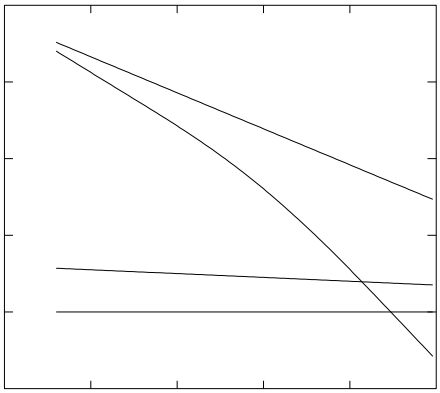

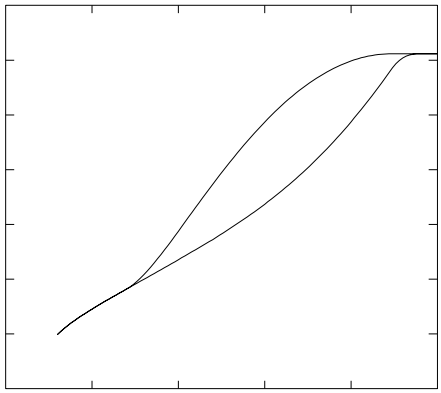

Ru (Ruthenium)

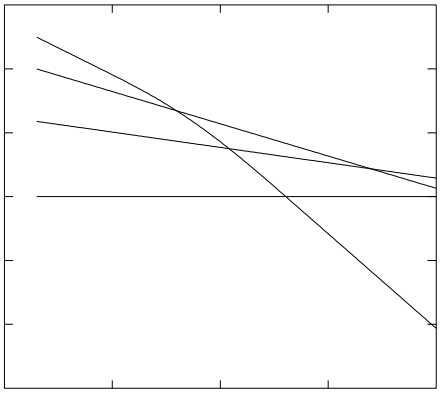

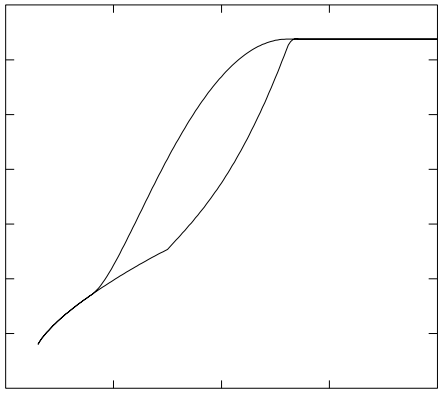

S (Sulphur)

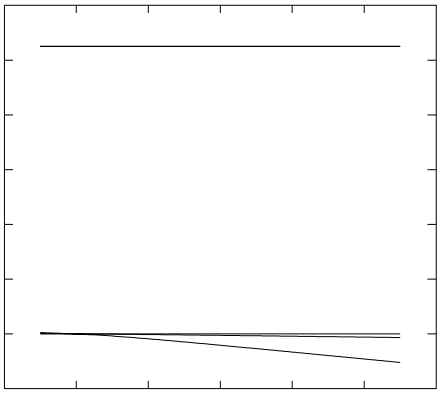

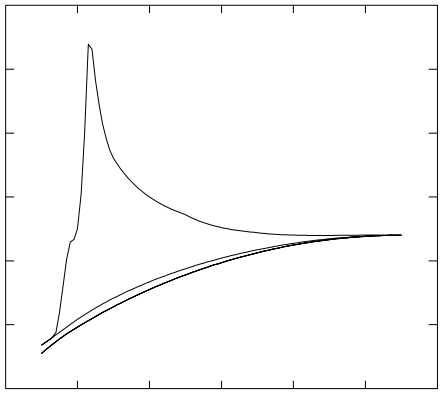

Sb (Antimony)

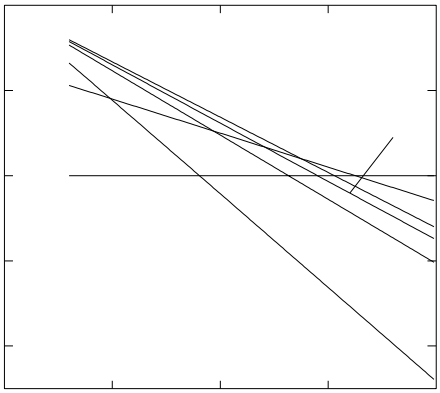

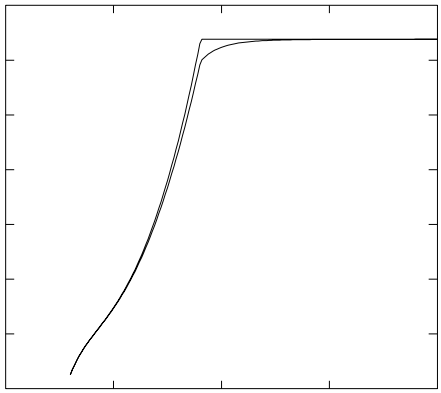

Sc (Scandium)

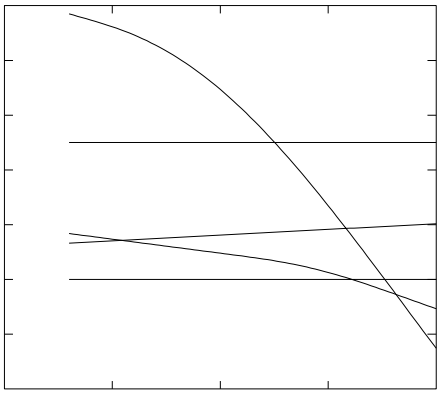

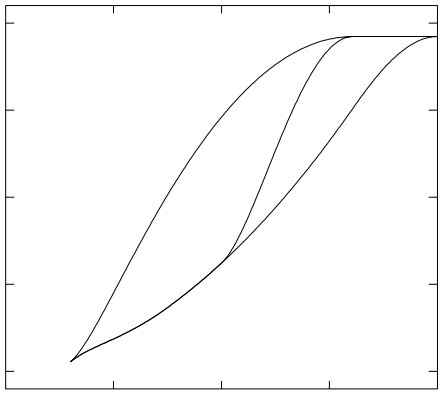

Se (Selenium)

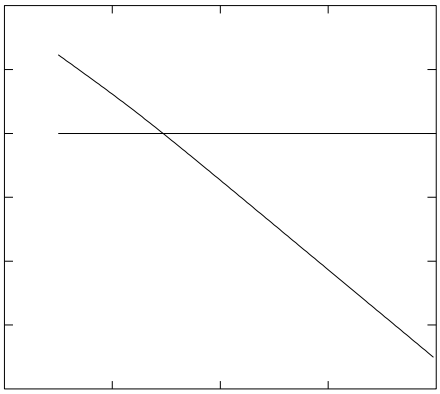

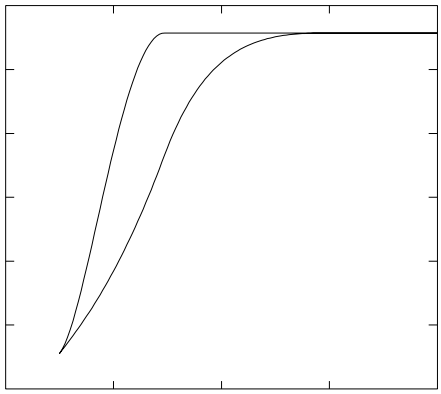

Si (Silicon)

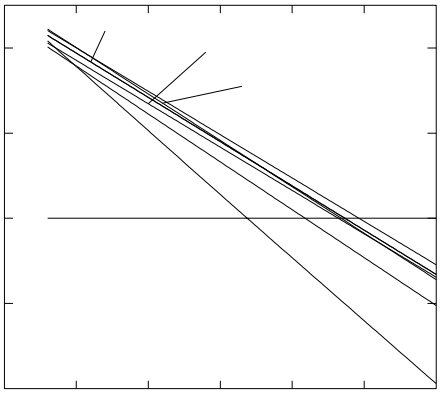

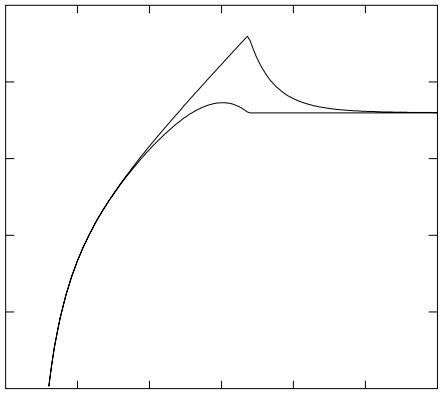

Sm (Samarium)

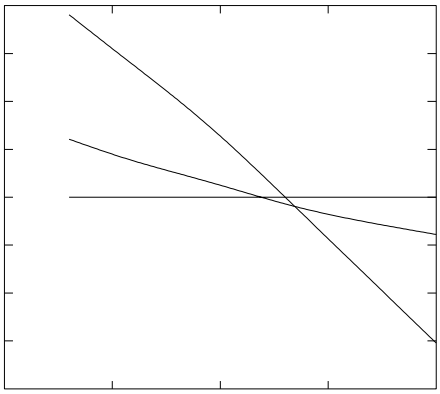

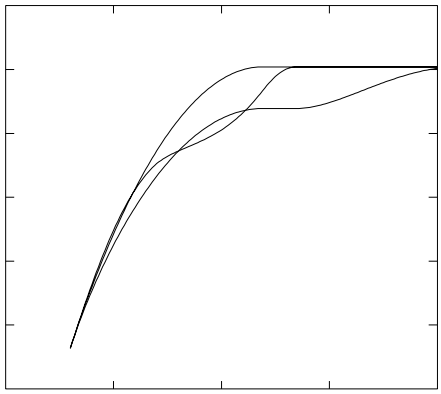

Sn (Tin)

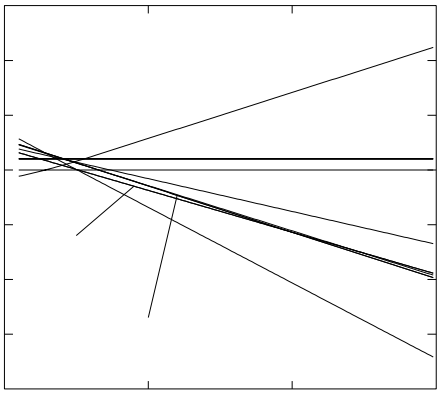

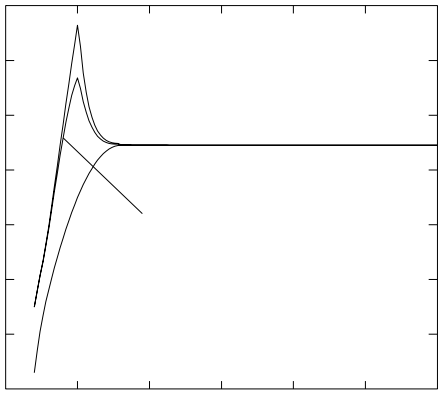

Sr (Strontium)

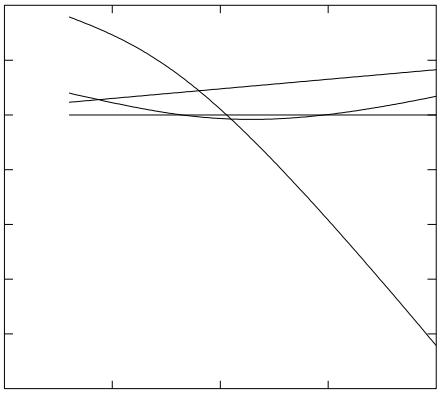

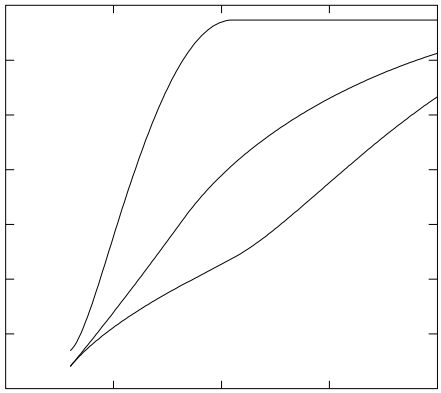

Ta (Tantalum)

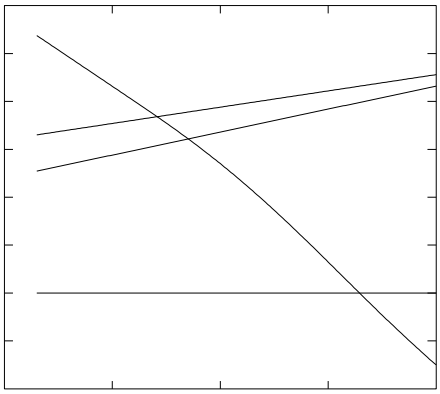

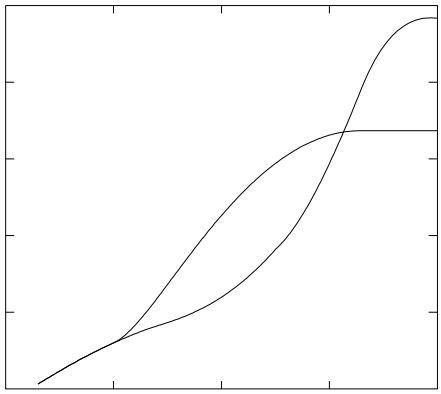

Tb (Terbium)

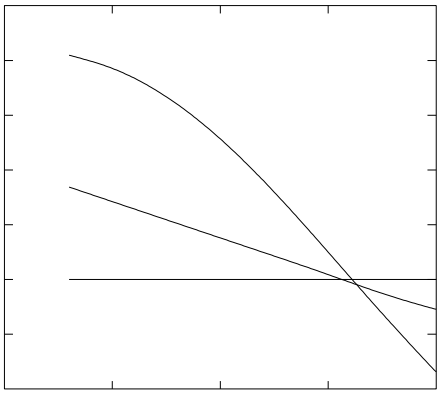

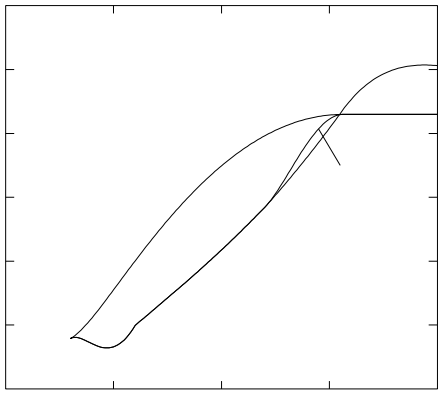

Tc (Technetium)

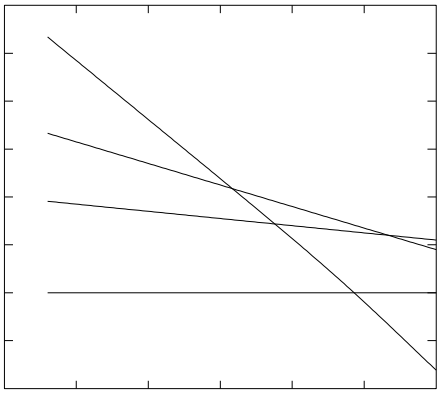

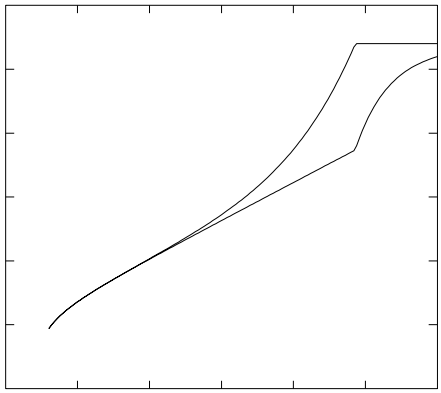

Te (Tellurium)

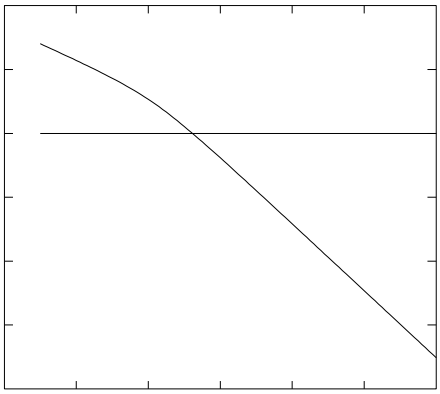

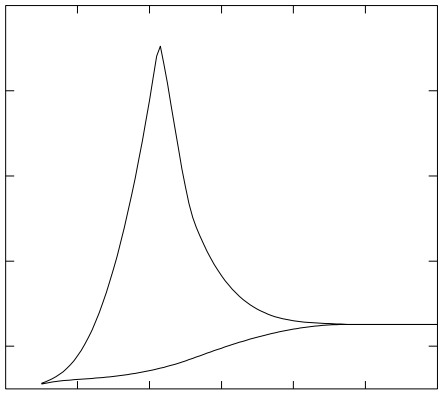

Th (Thorium)

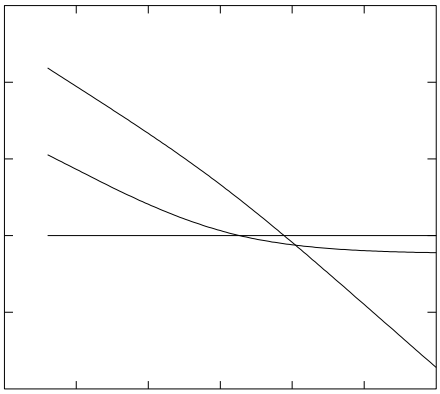

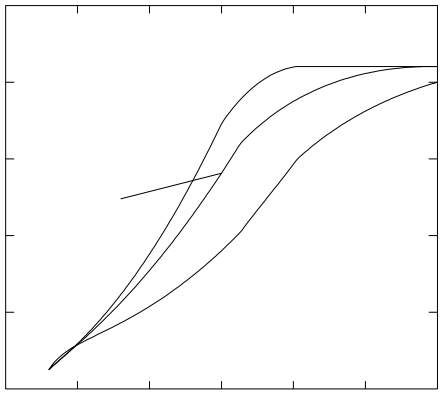

Ti (Titanium)

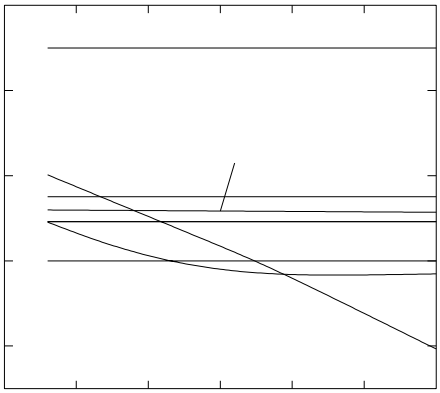

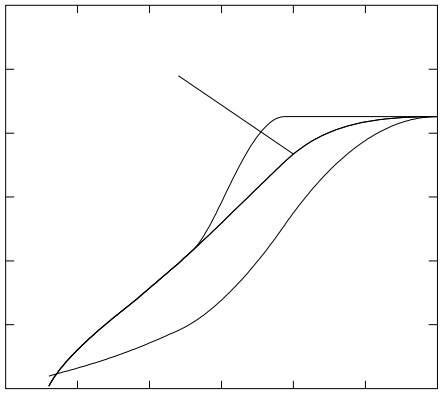

Tl (Thallium)

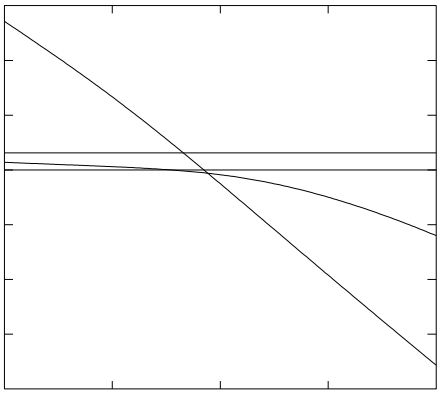

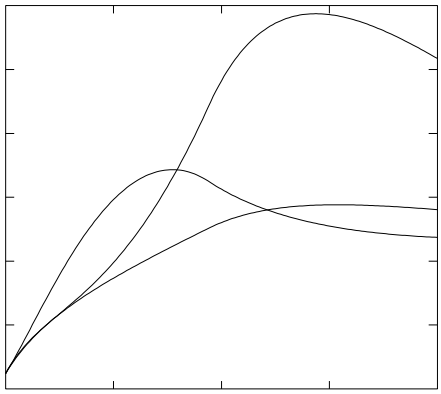

Tm (Thulium)

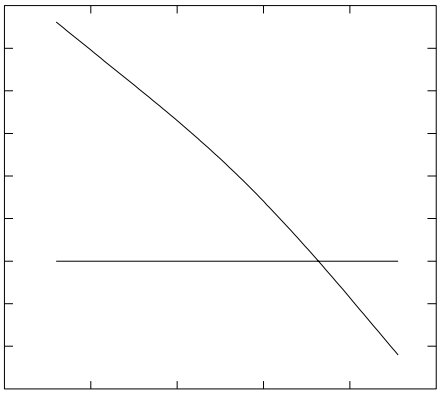

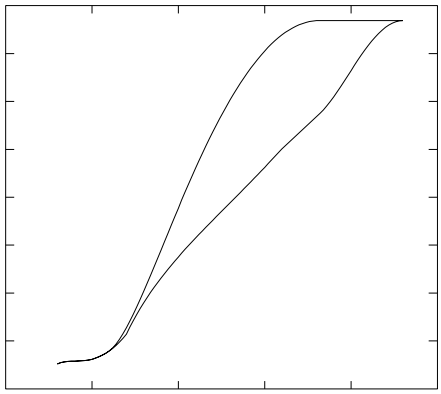

U (Uranium)

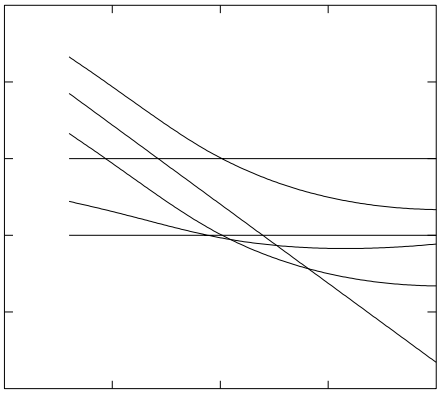

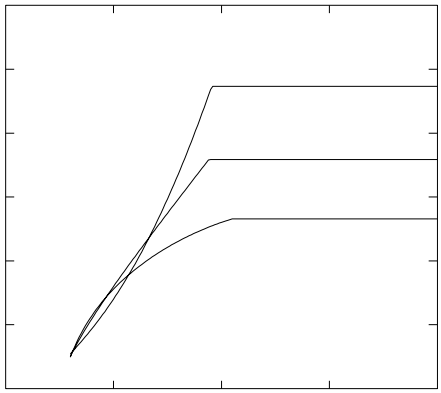

V (Vanadium)

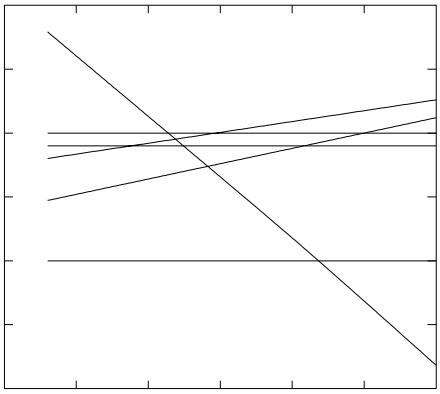

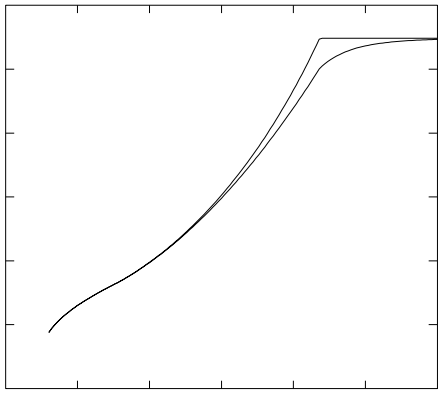

W (Tungsten)

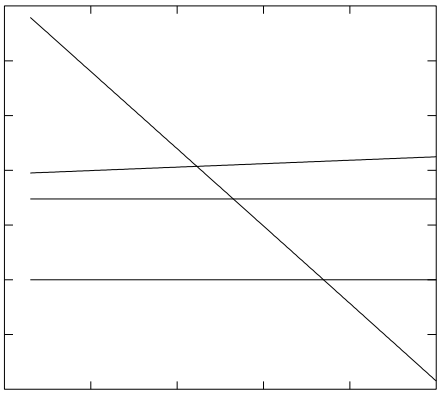

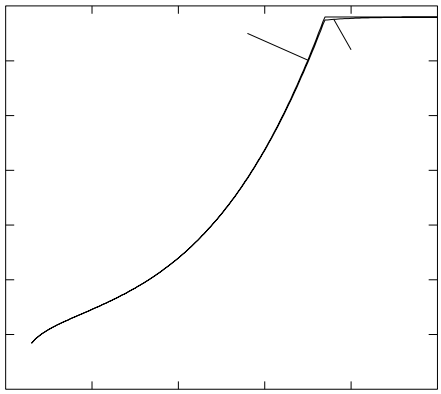

Y (Yttrium)

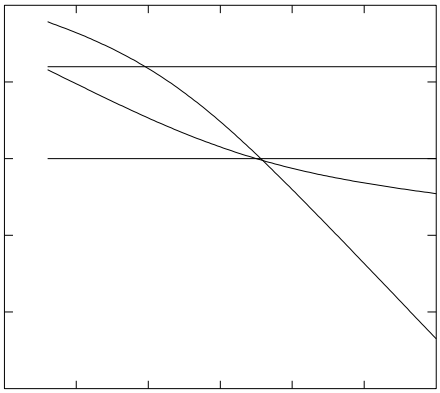

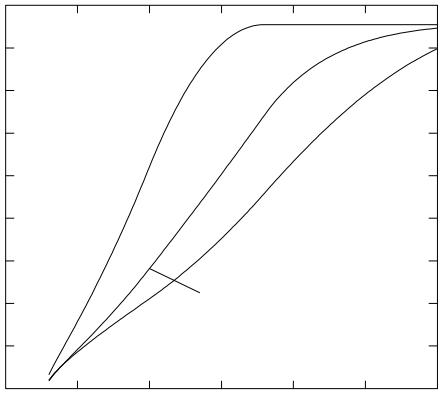

Yb (Ytterbium)

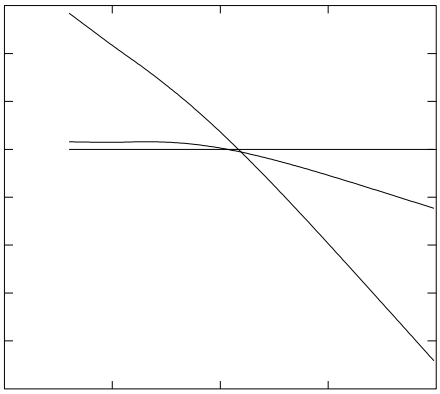

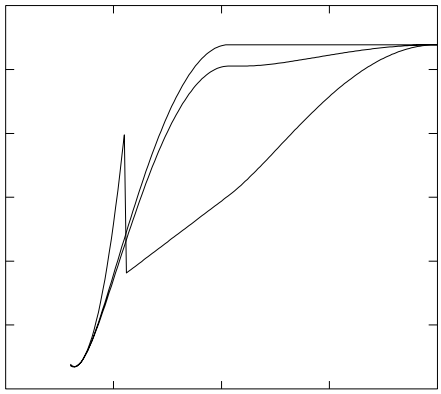

Zn (Zinc)

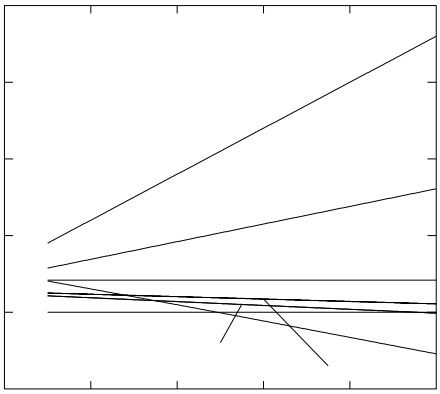

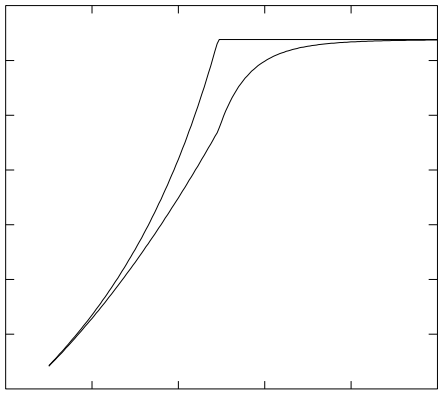

Zr (Zirconium)

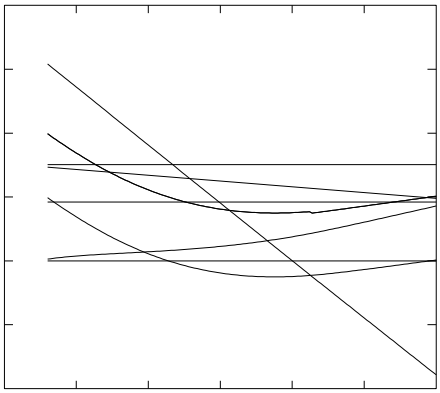

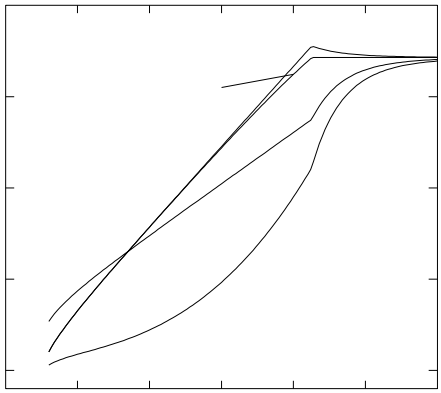

Binary Systems from Ag-Al to Au-Tl

Ag – Al (Silver – Aluminium)

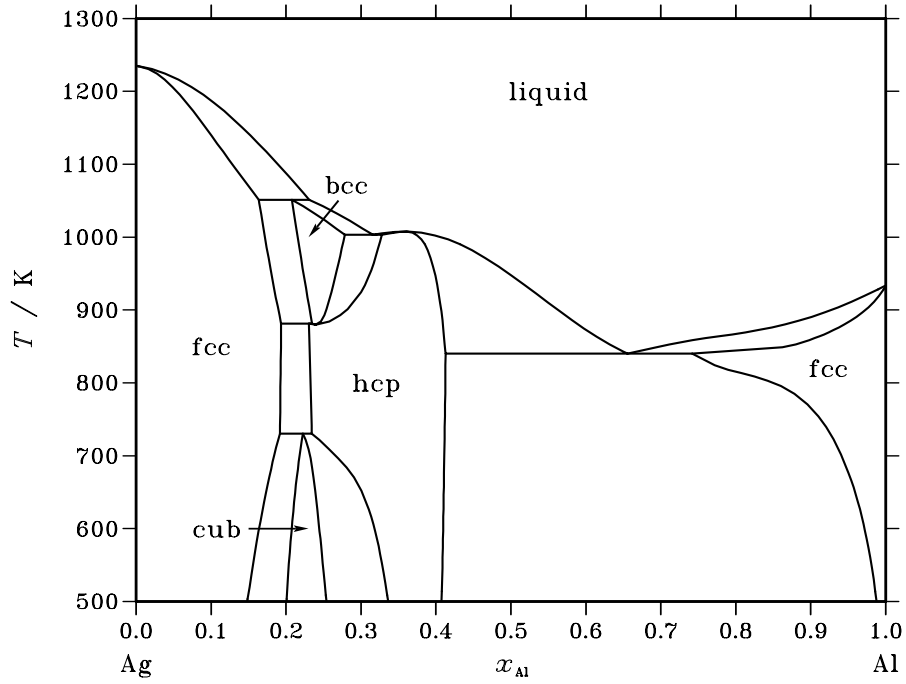

Fig. 1. Calculated phase diagram for the system Ag-Al.

Small quantities of Ag are often added to aluminium alloys to improve their high temperature mechanical properties. The critically assessed dataset for this system adopted by SGTE is from Lim et al. [95Lim] which is based on an earlier assessment of Spencer and Kubaschewski [87Spe]. The system is characterised by complete mixing in the liquid phase and substantial solid solution in each of the crystalline elements. There are also solid solution ranges for the bcc, hcp and cubic $A13$ structures. In addition to phase diagram studies the data of Lim were based upon experimental activity and enthalpy of mixing measurements in both the liquid and crystalline phases. The agreement between the critically assessed data and the experimental values is reasonable.

Table I. Phases, structures and models.

Phase	Struktur-bericht	Prototype	Pearson symbol	Space group	SGTE name	Model
liquid					LIQUID	$(Ag,Al)_1$
fcc	$A1$	Cu	$cF4$	$Fm\overline{3}m$	FCC_A1	$(Ag,Al)_1$
bcc	$A2$	W	$cI2$	$Im\overline{3}m$	BCC_A2	$(Ag,Al)_1$
cub	$A13$	βMn	$cP20$	$P4_132$	CUB_A13	$(Ag,Al)_1$
hcp	$A3$	Mg	$hP2$	$P6_3/mmc$	HCP_A3	$(Ag,Al)_1$

Table II. Invariant reactions.

Reaction	Type	T / K	Compositions / x_{Al}			$\Delta_{\mathrm{r}}H$ / (J/mol)
fcc + liquid ⇌ bcc	peritectic	1051.2	0.164	0.231	0.208	−5233
liquid ⇌ hcp	congruent	1007.6	0.359	0.359		−10626
liquid ⇌ bcc + hcp	eutectic	1003.2	0.316	0.279	0.328	−9890
fcc + bcc ⇌ hcp	peritectoid	881.4	0.193	0.235	0.230	−1089
bcc ⇌ hcp	congruent	880.0	0.239	0.239		−1244
liquid ⇌ hcp + fcc	eutectic	840.0	0.656	0.413	0.742	−10332
fcc + hcp ⇌ cub	peritectoid	730.6	0.192	0.234	0.223	−853

Table IIIa. Integral quantities for the liquid phase at 1300 K.

x_{Al}	ΔG_{m} [J/mol]	ΔH_{m} [J/mol]	ΔS_{m} [J/(mol·K)]	$G_{\mathrm{m}}^{\mathrm{E}}$ [J/mol]	$S_{\mathrm{m}}^{\mathrm{E}}$ [J/(mol·K)]	ΔC_p [J/(mol·K)]
0.000	0	0	0.000	0	0.000	0.000
0.100	−6888	−2762	3.174	−3374	0.471	0.000
0.200	−11228	−4540	5.144	−5819	0.984	0.000
0.300	−13729	−5202	6.559	−7126	1.480	0.000
0.400	−14615	−4866	7.499	−7341	1.904	0.000
0.500	−14177	−3825	7.963	−6685	2.200	0.000
0.600	−12746	−2460	7.912	−5472	2.316	0.000
0.700	−10629	−1163	7.282	−4026	2.202	0.000
0.800	−8012	−251	5.970	−2603	1.809	0.000
0.900	−4818	113	3.793	−1305	1.090	0.000
1.000	0	0	0.000	0	0.000	0.000

Reference states: Ag(liquid), Al(liquid)

Table IIIb. Partial quantities for Ag in the liquid phase at 1300 K.

x_{Ag}	ΔG_{Ag} [J/mol]	ΔH_{Ag} [J/mol]	ΔS_{Ag} [J/(mol·K)]	$G_{\mathrm{Ag}}^{\mathrm{E}}$ [J/mol]	$S_{\mathrm{Ag}}^{\mathrm{E}}$ [J/(mol·K)]	a_{Ag}	γ_{Ag}
1.000	0	0	0.000	0	0.000	1.000	1.000
0.900	−1543	−444	0.845	−404	−0.031	0.867	0.963
0.800	−4457	−2103	1.811	−2045	−0.045	0.662	0.828
0.700	−8773	−4824	3.038	−4918	0.072	0.444	0.634
0.600	−13933	−7855	4.675	−8412	0.428	0.276	0.459
0.500	−19130	−10175	6.888	−11638	1.125	0.170	0.341
0.400	−23658	−10817	9.878	−13754	2.259	0.112	0.280
0.300	−27308	−9196	13.932	−14295	3.922	0.080	0.266
0.200	−30889	−5436	19.579	−13493	6.198	0.057	0.287
0.100	−37498	−694	28.311	−12610	9.166	0.031	0.311
0.000	$-\infty$	2510	∞	−14260	12.900	0.000	0.267

Reference state: Ag(liquid)

Table IIIc. Partial quantities for Al in the liquid phase at 1300 K.

x_{Al}	ΔG_{Al} [J/mol]	ΔH_{Al} [J/mol]	ΔS_{Al} [J/(mol·K)]	G^E_{Al} [J/mol]	S^E_{Al} [J/(mol·K)]	a_{Al}	γ_{Al}
0.000	$-\infty$	−31290	∞	−36880	4.300	0.000	0.033
0.100	−54991	−23620	24.131	−30103	4.986	0.006	0.062
0.200	−38310	−14288	18.479	−20914	5.097	0.029	0.144
0.300	−25291	−6083	14.775	−12278	4.765	0.096	0.321
0.400	−15639	−383	11.736	−5735	4.117	0.235	0.588
0.500	−9225	2525	9.038	−1733	3.275	0.426	0.852
0.600	−5472	3111	6.602	50	2.355	0.603	1.005
0.700	−3481	2280	4.431	374	1.466	0.725	1.035
0.800	−2293	1045	2.567	119	0.712	0.809	1.011
0.900	−1187	202	1.069	−48	0.193	0.896	0.996
1.000	0	0	0.000	0	0.000	1.000	1.000

Reference state: Al(liquid)

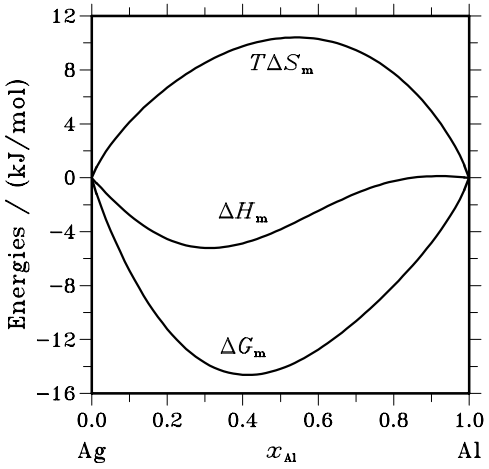

Fig. 2. Integral quantities of the liquid phase at T=1300 K.

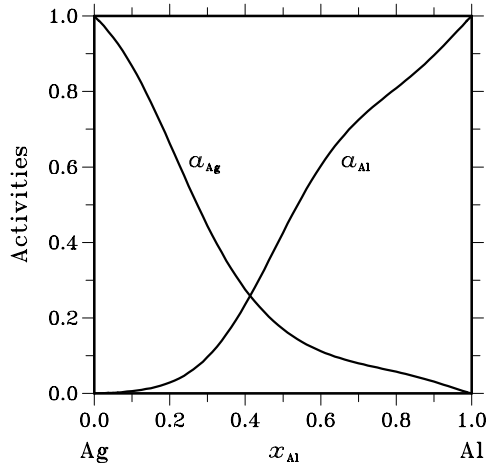

Fig. 3. Activities in the liquid phase at T=1300 K.

Table IVa. Integral quantities for the stable phases at 820 K.

Phase	x_{Al}	ΔG_{m} [J/mol]	ΔH_{m} [J/mol]	ΔS_{m} [J/(mol·K)]	$G_{\mathrm{m}}^{\mathrm{E}}$ [J/mol]	$S_{\mathrm{m}}^{\mathrm{E}}$ [J/(mol·K)]	ΔC_p [J/(mol·K)]
fcc	0.000	0	0	0.000	0	0.000	0.000
	0.050	−2977	−1397	1.926	−1623	0.276	0.000
	0.100	−5060	−2415	3.225	−2843	0.522	0.000
	0.150	−6589	−3101	4.254	−3707	0.740	0.000
	0.193	−7541	−3458	4.979	−4198	0.903	0.000
hcp	0.232	−8275	−3748	5.521	−4582	1.018	0.000
	0.250	−8601	−3914	5.716	−4767	1.041	0.000
	0.300	−9408	−4373	6.140	−5243	1.061	0.000
	0.350	−10038	−4780	6.412	−5624	1.029	0.000
	0.400	−10114	−4741	6.553	−5526	0.958	0.000
	0.413	−9960	−4572	6.571	−5338	0.935	0.000
fcc	0.783	−4029	341	5.330	−466	0.984	0.000
	0.800	−3762	410	5.089	−351	0.928	0.000
	0.850	−2955	533	4.254	−73	0.740	0.000
	0.900	−2128	517	3.225	89	0.522	0.000
	0.950	−1236	344	1.926	118	0.275	0.000
	1.000	0	0	0.000	0	0.000	0.000

Reference states: Ag(fcc), Al(fcc)

Table IVb. Partial quantities for Ag in the stable phases at 820 K.

Phase	x_{Ag}	ΔG_{Ag} [J/mol]	ΔH_{Ag} [J/mol]	ΔS_{Ag} [J/(mol·K)]	$G_{\mathrm{Ag}}^{\mathrm{E}}$ [J/mol]	$S_{\mathrm{Ag}}^{\mathrm{E}}$ [J/(mol·K)]	a_{Ag}	γ_{Ag}
fcc	1.000	0	0	0.000	0	0.000	1.000	1.000
	0.950	−559	−198	0.441	−210	0.015	0.921	0.970
	0.900	−1493	−727	0.934	−775	0.058	0.803	0.893
	0.850	−2712	−1497	1.482	−1604	0.131	0.672	0.790
	0.807	−3921	−2284	1.997	−2461	0.216	0.563	0.697
hcp	0.768	−3921	−1573	2.864	−2122	0.670	0.563	0.733
	0.750	−4254	−1647	3.179	−2292	0.788	0.536	0.714
	0.700	−4926	−1584	4.075	−2494	1.109	0.486	0.694
	0.650	−6878	−2789	4.987	−3941	1.405	0.365	0.561
	0.600	−13575	−8740	5.896	−10092	1.649	0.137	0.228
	0.587	−16562	−11540	6.124	−12933	1.699	0.088	0.150
fcc	0.217	−16562	−3216	16.275	−6134	3.559	0.088	0.407
	0.200	−16605	−2588	17.094	−5632	3.712	0.088	0.438
	0.150	−16790	−419	19.964	−3855	4.191	0.085	0.568
	0.100	−17371	2181	23.843	−1672	4.698	0.078	0.783
	0.050	−19508	5209	30.143	917	5.234	0.057	1.144
	0.000	$-\infty$	8660	∞	3904	5.800	0.000	1.773

Reference state: Ag(fcc)

Table IVc. Partial quantities for Al in the stable phases at 820 K.

Phase	x_{Al}	ΔG_{Al} [J/mol]	ΔH_{Al} [J/mol]	ΔS_{Al} [J/(mol·K)]	G^{E}_{Al} [J/mol]	S^{E}_{Al} [J/(mol·K)]	a_{Al}	γ_{Al}
fcc	0.000	$-\infty$	−32060	∞	−36816	5.800	0.000	0.005
	0.050	−48908	−24191	30.142	−28483	5.234	0.001	0.015
	0.100	−37161	−17609	23.843	−21462	4.698	0.004	0.043
	0.150	−28558	−12187	19.964	−15623	4.191	0.015	0.101
	0.193	−22693	−8372	17.465	−11471	3.779	0.036	0.186
hcp	0.232	−22693	−10950	14.321	−12730	2.171	0.036	0.155
	0.250	−21642	−10714	13.326	−12190	1.800	0.042	0.167
	0.300	−19866	−10880	10.958	−11657	0.947	0.054	0.181
	0.350	−15907	−8479	9.058	−8749	0.330	0.097	0.277
	0.400	−4924	1258	7.539	1323	−0.079	0.486	1.214
	0.413	−563	5346	7.206	5471	−0.153	0.921	2.231
fcc	0.783	−563	1325	2.303	1102	0.272	0.921	1.175
	0.800	−552	1160	2.087	970	0.232	0.922	1.153
	0.850	−513	702	1.482	595	0.131	0.927	1.091
	0.900	−434	332	0.934	284	0.058	0.938	1.043
	0.950	−274	87	0.441	76	0.014	0.961	1.011
	1.000	0	0	0.000	0	0.000	1.000	1.000

Reference state: Al(fcc)

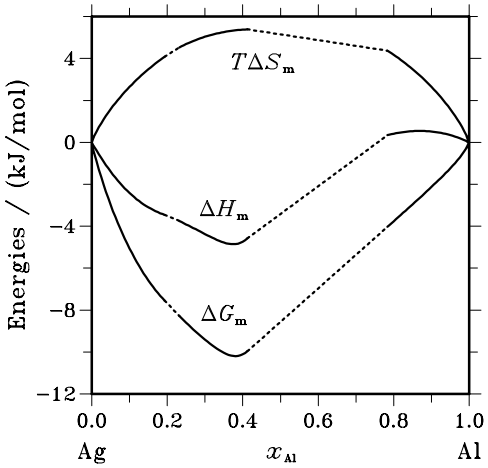

Fig. 4. Integral quantities of the stable phases at T=820 K.

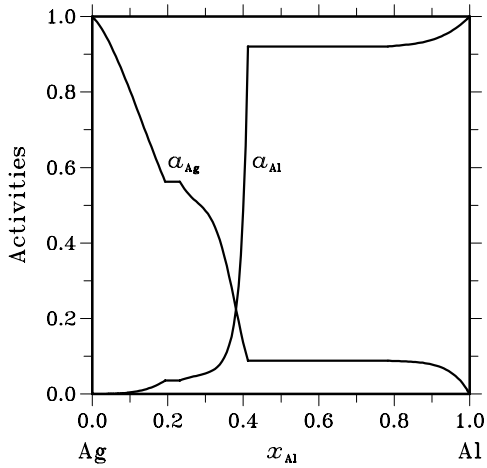

Fig. 5. Activities in the stable phases at T=820 K.

References

[87Spe] P.J. Spencer, O. Kubaschewski: Monatsh. Chem. **118** (1987) 155–167.
[95Lim] S.S. Lim, P.L. Rossiter, J.W. Tibbals: Calphad **19** (1995) 131–142.

Ag – Au (Silver – Gold)

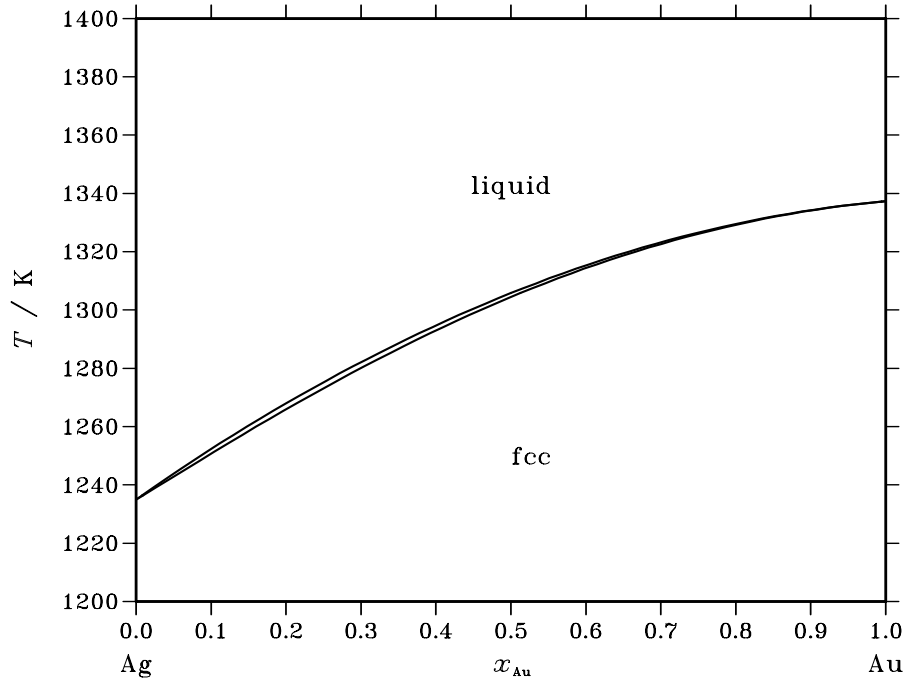

Fig. 1. Calculated phase diagram for the system Ag-Au.

Both Au and Ag are noble metals used in jewellery and electronic applications. Both elements crystallise in the fcc structure and form a continuous series of solutions both in the liquid and crystalline phases. The composition range where the two phases are in equilibrium is very small. The critical assessment of data for this system selected by SGTE was published by Hassam et al. [88Has] based on the phase diagram and activities in the fcc phase compiled by Hultgren et al. supplemented by more recent experimental thermodynamic properties of the liquid phase.

Table I. Phases, structures and models.

Phase	Struktur-bericht	Prototype	Pearson symbol	Space group	SGTE name	Model
liquid					LIQUID	$(Ag,Au)_1$
fcc	$A1$	Cu	$cF4$	$Fm\overline{3}m$	FCC_A1	$(Ag,Au)_1$

Table IIa. Integral quantities for the liquid phase at 1350 K.

x_{Au}	ΔG_{m} [J/mol]	ΔH_{m} [J/mol]	ΔS_{m} [J/(mol·K)]	$G_{\mathrm{m}}^{\mathrm{E}}$ [J/mol]	$S_{\mathrm{m}}^{\mathrm{E}}$ [J/(mol·K)]	ΔC_p [J/(mol·K)]
0.000	0	0	0.000	0	0.000	0.000
0.100	−4987	−1476	2.600	−1338	−0.103	0.000
0.200	−7995	−2624	3.978	−2378	−0.182	0.000
0.300	−9978	−3444	4.840	−3121	−0.239	0.000
0.400	−11121	−3936	5.322	−3567	−0.274	0.000
0.500	−11496	−4101	5.478	−3716	−0.285	0.000
0.600	−11121	−3936	5.322	−3567	−0.274	0.000
0.700	−9978	−3444	4.840	−3121	−0.239	0.000
0.800	−7995	−2624	3.978	−2378	−0.182	0.000
0.900	−4987	−1476	2.600	−1338	−0.103	0.000
1.000	0	0	0.000	0	0.000	0.000

Reference states: Ag(liquid), Au(liquid)

Table IIb. Partial quantities for Ag in the liquid phase at 1350 K.

x_{Ag}	ΔG_{Ag} [J/mol]	ΔH_{Ag} [J/mol]	ΔS_{Ag} [J/(mol·K)]	$G_{\mathrm{Ag}}^{\mathrm{E}}$ [J/mol]	$S_{\mathrm{Ag}}^{\mathrm{E}}$ [J/(mol·K)]	a_{Ag}	γ_{Ag}
1.000	0	0	0.000	0	0.000	1.000	1.000
0.900	−1331	−164	0.865	−149	−0.011	0.888	0.987
0.800	−3099	−656	1.810	−595	−0.046	0.759	0.948
0.700	−5341	−1476	2.863	−1338	−0.103	0.621	0.888
0.600	−8112	−2624	4.065	−2378	−0.182	0.485	0.809
0.500	−11496	−4101	5.478	−3716	−0.285	0.359	0.718
0.400	−15636	−5905	7.208	−5351	−0.410	0.248	0.621
0.300	−20797	−8037	9.452	−7283	−0.559	0.157	0.523
0.200	−27578	−10497	12.652	−9512	−0.730	0.086	0.429
0.100	−37885	−13286	18.222	−12039	−0.923	0.034	0.342
0.000	$-\infty$	−16402	∞	−14863	−1.140	0.000	0.266

Reference state: Ag(liquid)

Table IIc. Partial quantities for Au in the liquid phase at 1350 K.

x_{Au}	ΔG_{Au} [J/mol]	ΔH_{Au} [J/mol]	ΔS_{Au} [J/(mol·K)]	$G_{\mathrm{Au}}^{\mathrm{E}}$ [J/mol]	$S_{\mathrm{Au}}^{\mathrm{E}}$ [J/(mol·K)]	a_{Au}	γ_{Au}
0.000	$-\infty$	−16402	∞	−14863	−1.140	0.000	0.266
0.100	−37885	−13286	18.222	−12039	−0.923	0.034	0.342
0.200	−27578	−10497	12.652	−9512	−0.730	0.086	0.429
0.300	−20797	−8037	9.452	−7283	−0.559	0.157	0.523
0.400	−15636	−5905	7.208	−5351	−0.410	0.248	0.621
0.500	−11496	−4101	5.478	−3716	−0.285	0.359	0.718
0.600	−8112	−2624	4.065	−2378	−0.182	0.485	0.809
0.700	−5341	−1476	2.863	−1338	−0.103	0.621	0.888
0.800	−3099	−656	1.810	−595	−0.046	0.759	0.948
0.900	−1331	−164	0.865	−149	−0.011	0.888	0.987
1.000	0	0	0.000	0	0.000	1.000	1.000

Reference state: Au(liquid)

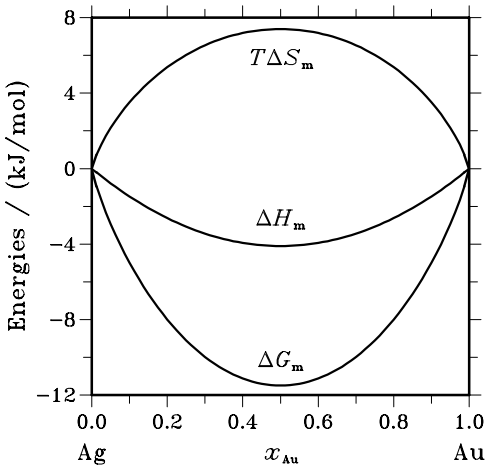

Fig. 2. Integral quantities of the liquid phase at T=1350 K.

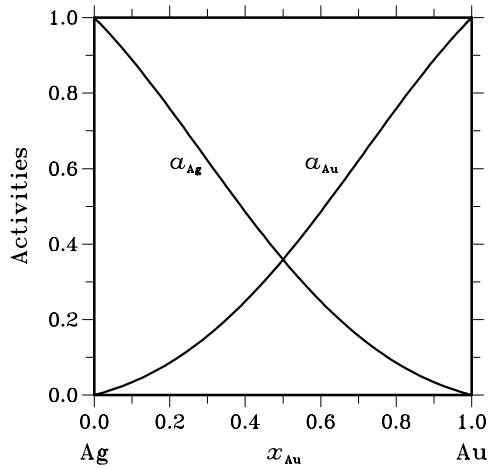

Fig. 3. Activities in the liquid phase at T=1350 K.

Table IIIa. Integral quantities for the stable phases at 1200 K.

Phase	x_{Au}	ΔG_m [J/mol]	ΔH_m [J/mol]	ΔS_m [J/(mol·K)]	G_m^E [J/mol]	S_m^E [J/(mol·K)]	ΔC_p [J/(mol·K)]
fcc	0.000	0	0	0.000	0	0.000	0.000
	0.100	−4647	−1404	2.703	−1404	0.000	0.000
	0.200	−7489	−2496	4.161	−2496	0.000	0.000
	0.300	−9371	−3276	5.079	−3276	0.000	0.000
	0.400	−10459	−3744	5.596	−3744	0.000	0.000
	0.500	−10816	−3900	5.763	−3900	0.000	0.000
	0.600	−10459	−3744	5.596	−3744	0.000	0.000
	0.700	−9371	−3276	5.079	−3276	0.000	0.000
	0.800	−7489	−2496	4.161	−2496	0.000	0.000
	0.900	−4647	−1404	2.703	−1404	0.000	0.000
	1.000	0	0	0.000	0	0.000	0.000

Reference states: Ag(fcc), Au(fcc)

Table IIIb. Partial quantities for Ag in the stable phases at 1200 K.

Phase	x_{Ag}	ΔG_{Ag} [J/mol]	ΔH_{Ag} [J/mol]	ΔS_{Ag} [J/(mol·K)]	G_{Ag}^E [J/mol]	S_{Ag}^E [J/(mol·K)]	a_{Ag}	γ_{Ag}
fcc	1.000	0	0	0.000	0	0.000	1.000	1.000
	0.900	−1207	−156	0.876	−156	0.000	0.886	0.984
	0.800	−2850	−624	1.855	−624	0.000	0.752	0.939
	0.700	−4963	−1404	2.966	−1404	0.000	0.608	0.869
	0.600	−7593	−2496	4.247	−2496	0.000	0.467	0.779
	0.500	−10816	−3900	5.763	−3900	0.000	0.338	0.676
	0.400	−14758	−5616	7.619	−5616	0.000	0.228	0.570
	0.300	−19656	−7644	10.010	−7644	0.000	0.139	0.465
	0.200	−26041	−9983	13.382	−9983	0.000	0.074	0.368
	0.100	−35609	−12635	19.145	−12635	0.000	0.028	0.282
	0.000	$-\infty$	−15599	∞	−15599	0.000	0.000	0.209

Reference state: Ag(fcc)

Table IIIc. Partial quantities for Au in the stable phases at 1200 K.

Phase	x_{Au}	ΔG_{Au} [J/mol]	ΔH_{Au} [J/mol]	ΔS_{Au} [J/(mol·K)]	G^{E}_{Au} [J/mol]	S^{E}_{Au} [J/(mol·K)]	a_{Au}	γ_{Au}
fcc	0.000	$-\infty$	−15599	∞	−15599	0.000	0.000	0.209
	0.100	−35609	−12635	19.145	−12635	0.000	0.028	0.282
	0.200	−26041	−9983	13.382	−9983	0.000	0.074	0.368
	0.300	−19656	−7644	10.010	−7644	0.000	0.139	0.465
	0.400	−14758	−5616	7.619	−5616	0.000	0.228	0.570
	0.500	−10816	−3900	5.763	−3900	0.000	0.338	0.676
	0.600	−7593	−2496	4.247	−2496	0.000	0.467	0.779
	0.700	−4963	−1404	2.966	−1404	0.000	0.608	0.869
	0.800	−2850	−624	1.855	−624	0.000	0.752	0.939
	0.900	−1207	−156	0.876	−156	0.000	0.886	0.984
	1.000	0	0	0.000	0	0.000	1.000	1.000

Reference state: Au(fcc)

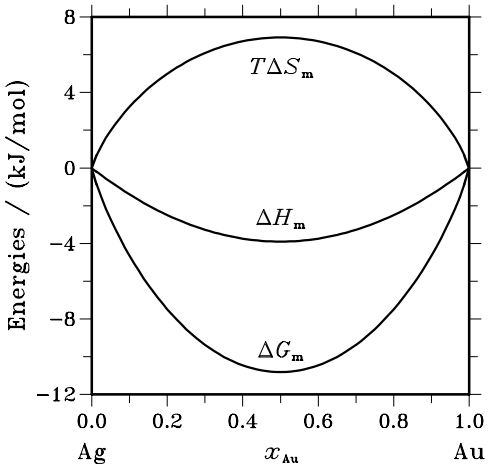

Fig. 4. Integral quantities of the stable phases at T=1200 K.

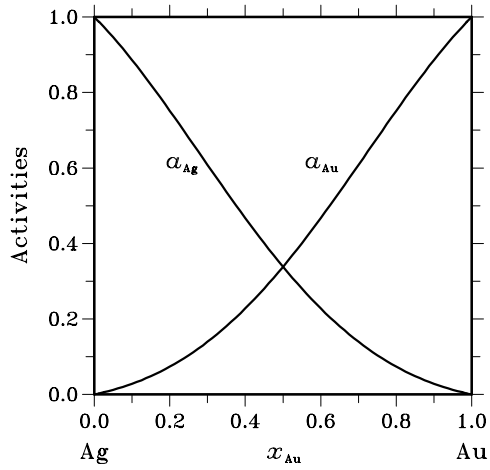

Fig. 5. Activities in the stable phases at T=1200 K.

References

[88Has] S. Hassam, M. Gambino, M. Gaune-Escard, J.P. Bros, J. Ågren: Metall. Trans. A **19A** (1988) 409–416.

Ag – Bi (Silver – Bismuth)

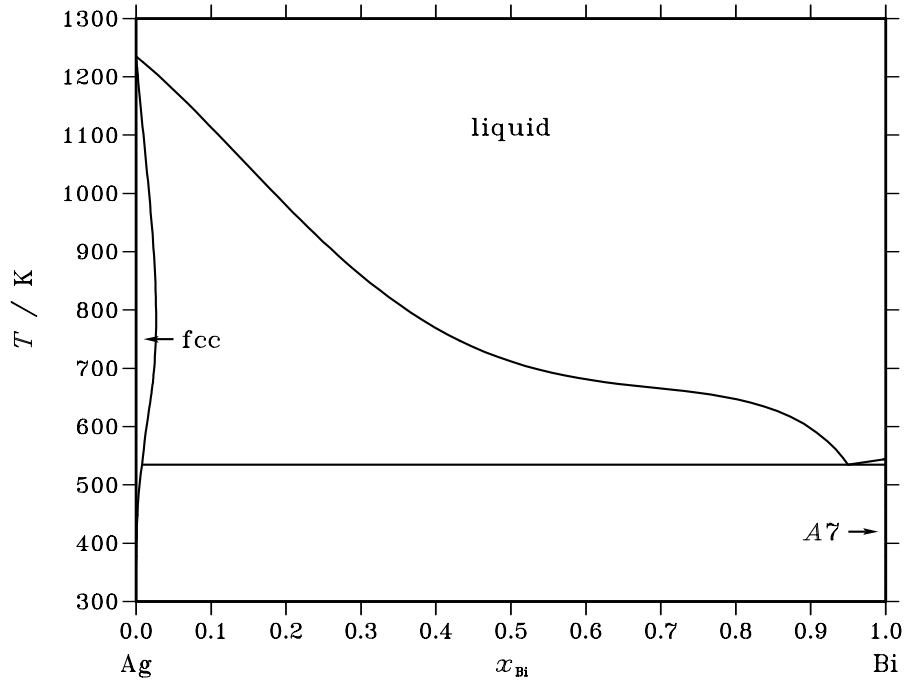

Fig. 1. Calculated phase diagram for the system Ag-Bi.

The silver-bismuth system is part of the commonly used solder system Pb-Sn-Ag-Bi-Sb-Zn. Therefore, this system has been studied in many experimental investigations. Detailed reviews of experimental data are given in [80Ell, 93Kar]. The thermodynamic parameters have been assessed several times [76Zim1, 76Zim2, 93Kar, 94Kat, 98Luk, 99Ass]. The description of [98Luk] is accepted here because it has been tested in multicomponent systems. This thermodynamic description is an update of that of Zimmermann et al. [76Zim2] in order to make it compatible with the SGTE unary descriptions of [01Din].
The Ag-Bi system is a simple nearly degenerate eutectic system. The fcc solid solution has a retrograde solidus with a maximum solubility of about 2.5 at.% Bi. The solid solubility of Bi in fcc-Ag has been determined by thermoelectric power measurements, from lattice parameter data and by electron probe microanalysis. The solid solubility of Ag in solid Bi is negligible and it has not been measured systematically. The enthalpy of mixing of liquid Ag-Bi alloys has been measured by calorimetry. The activities of Ag and Bi in the liquid have been determined by EMF and vapour pressure measurements. All phases are modelled by the substitutional solution model. The calculated thermodynamic quantities and the phase diagram agree well with the experimental data.

Table I. Phases, structures and models.

Phase	Struktur-bericht	Prototype	Pearson symbol	Space group	SGTE name	Model
liquid					LIQUID	$(Ag,Bi)_1$
fcc	$A1$	Cu	$cF4$	$Fm\overline{3}m$	FCC_A1	$(Ag,Bi)_1$
$A7$	$A7$	αAs	$hR2$	$R\overline{3}m$	RHOMBOHEDRAL_A7	Bi_1

Table II. Invariant reactions.

Reaction	Type	T / K	Compositions / x_{Bi}			$\Delta_{\mathrm{r}}H$ / (J/mol)
liquid $\rightleftharpoons$ fcc + $A7$	eutectic	535.0	0.950	0.008	1.000	−11694

Table IIIa. Integral quantities for the liquid phase at 1300 K.

x_{Bi}	ΔG_{m} [J/mol]	ΔH_{m} [J/mol]	ΔS_{m} [J/(mol·K)]	$G_{\mathrm{m}}^{\mathrm{E}}$ [J/mol]	$S_{\mathrm{m}}^{\mathrm{E}}$ [J/(mol·K)]	ΔC_p [J/(mol·K)]
0.000	0	0	0.000	0	0.000	0.000
0.100	−4177	428	3.542	−663	0.840	0.537
0.200	−6334	1074	5.698	−925	1.538	0.955
0.300	−7497	1768	7.127	−894	2.048	1.254
0.400	−7945	2372	7.936	−670	2.340	1.433
0.500	−7839	2775	8.165	−347	2.402	1.492
0.600	−7285	2898	7.833	−10	2.237	1.433
0.700	−6342	2689	6.947	261	1.868	1.254
0.800	−5014	2127	5.493	395	1.332	0.955
0.900	−3187	1218	3.388	327	0.685	0.537
1.000	0	0	0.000	0	0.000	0.000

Reference states: Ag(liquid), Bi(liquid)

Table IIIb. Partial quantities for Ag in the liquid phase at 1300 K.

x_{Ag}	ΔG_{Ag} [J/mol]	ΔH_{Ag} [J/mol]	ΔS_{Ag} [J/(mol·K)]	$G_{\mathrm{Ag}}^{\mathrm{E}}$ [J/mol]	$S_{\mathrm{Ag}}^{\mathrm{E}}$ [J/(mol·K)]	a_{Ag}	γ_{Ag}
1.000	0	0	0.000	0	0.000	1.000	1.000
0.900	−1358	−139	0.937	−219	0.061	0.882	0.980
0.800	−3141	−317	2.172	−729	0.317	0.748	0.935
0.700	−5181	−241	3.799	−1325	0.834	0.619	0.885
0.600	−7346	293	5.877	−1825	1.629	0.507	0.845
0.500	−9559	1404	8.433	−2066	2.670	0.413	0.826
0.400	−11814	3120	11.487	−1910	3.869	0.335	0.838
0.300	−14250	5381	15.101	−1237	5.091	0.268	0.892
0.200	−17346	8042	19.529	50	6.148	0.201	1.005
0.100	−22864	10866	25.946	2025	6.801	0.121	1.206
0.000	$-\infty$	13532	∞	4742	6.761	0.000	1.551

Reference state: Ag(liquid)

Table IIIc. Partial quantities for Bi in the liquid phase at 1300 K.

x_{Bi}	ΔG_{Bi} [J/mol]	ΔH_{Bi} [J/mol]	ΔS_{Bi} [J/(mol·K)]	G^E_{Bi} [J/mol]	S^E_{Bi} [J/(mol·K)]	a_{Bi}	γ_{Bi}
0.000	$-\infty$	2561	∞	−9014	8.904	0.000	0.434
0.100	−29549	5534	26.987	−4661	7.842	0.065	0.650
0.200	−19107	6638	19.804	−1711	6.422	0.171	0.854
0.300	−12902	6456	14.891	112	4.881	0.303	1.010
0.400	−8842	5489	11.024	1062	3.406	0.441	1.103
0.500	−6119	4147	7.897	1373	2.134	0.568	1.135
0.600	−4265	2751	5.397	1256	1.150	0.674	1.123
0.700	−2952	1536	3.452	903	0.487	0.761	1.087
0.800	−1930	648	1.984	482	0.128	0.836	1.046
0.900	−1000	146	0.882	139	0.006	0.912	1.013
1.000	0	0	0.000	0	0.000	1.000	1.000

Reference state: Bi(liquid)

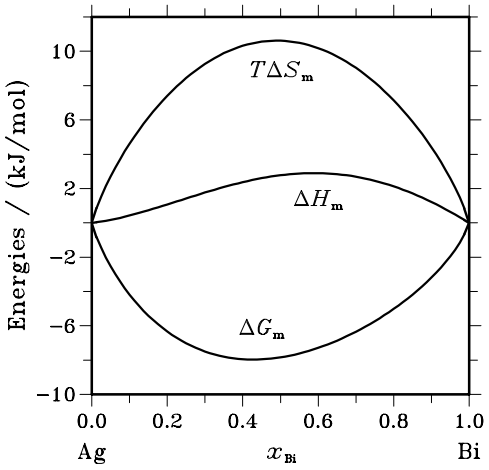

Fig. 2. Integral quantities of the liquid phase at T=1300 K.

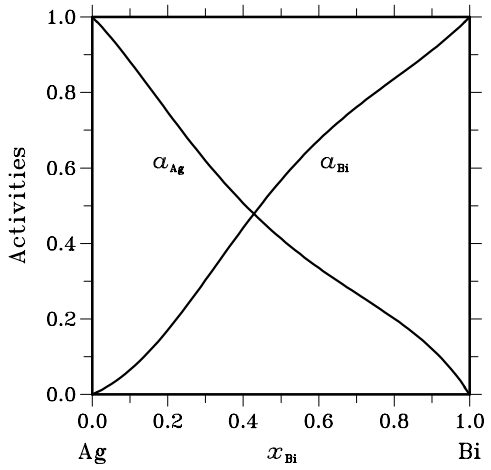

Fig. 3. Activities in the liquid phase at T=1300 K.

References

[76Zim1] B. Zimmermann, Ph. D. Thesis, Universität Stuttgart, Stuttgart, 1976.
[76Zim2] B. Zimmermann, E.-T. Henig, H.L. Lukas: Z. Metallkd. **67** (1976) 815–820.
[80Ell] R.P. Elliot, F.A. Shunk: Bull. Alloy Phase Diagrams **1** (1980) 62–64.
[93Kar] I. Karakaya, W.T. Thompson: J. Phase Equilibria **14** (1993) 525–530.
[94Kat] U.R. Kattner, W.J. Boettinger: J. Electron. Mater. **23** (1994) 603–610.
[98Luk] H.L. Lukas: unpublished optimization 1998.
[99Ass] J. Assal, B. Hallstedt, L.J. Gauckler: J. Amer. Ceram. Soc. **82** (1999) 711–715.

Ag – Ge (Silver – Germanium)

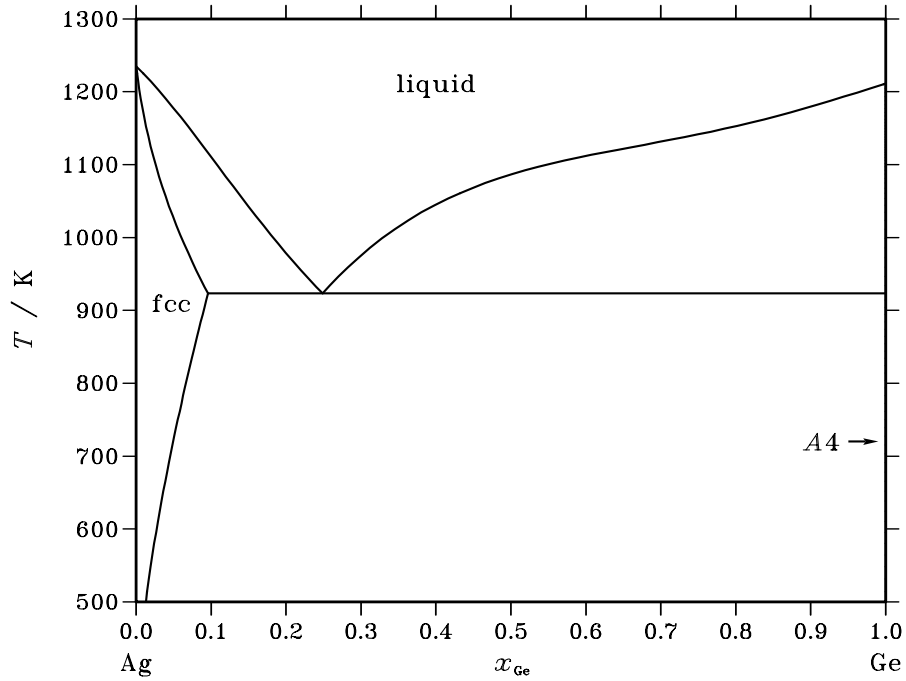

Fig. 1. Calculated phase diagram for the system Ag-Ge.

The Ag-Ge system has been critically assessed by Chevalier [88Che]. A review of the literature concerning the Ag-Ge system has been published by [80Ell]. The phase diagram is rather simple and of eutectic type, with a complete mutual solubility in the liquid state, a limited solid solubility of germanium in the silver rich terminal solid solution, and a negligible solid solubility of silver in pure crystalline germanium; there are no compounds in the system and the liquid and the fcc-phase has been modelled as a simple substitutional solution.

The liquidus curve has been investigated by thermal analysis [29Bri, 36Mau, 75Pre]. The solid solubility of Ge in Ag has been studied by conventional techniques by [29Bri, 36Mau, 40Owe, 40Hum, 50Now]. The calculated eutectic temperature, and composition are very close to the mean experimental values. The maximum solubility of germanium in the silver rich fcc solid solution, is in complete agreement with the experimental results of [75Pre], considered to be the most accurate work. The solubility of silver in germanium is so small that solid Ge has been modelled as a pure phase.

The calculated enthalpy of mixing of the liquid phase is in agreement with the calorimetric measurements [68Cas, 69Cas, 68Wit]. The calculated partial Gibbs energy of elements in the liquid phase is in good agreement with emf measurements [71Bat], and mass spectrometry measurements [79Mar]. It is difficult to reconcile the calculated chemical potential of germanium in the fcc solid solution with experiments on gas-solid equilibria [74Jac].

Table I. Phases, structures and models.

Phase	Struktur-bericht	Prototype	Pearson symbol	Space group	SGTE name	Model
liquid					LIQUID	$(Ag,Ge)_1$
fcc	$A1$	Cu	$cF4$	$Fm\overline{3}m$	FCC_A1	$(Ag,Ge)_1$
$A4$	$A4$	C(diamond)	$cF8$	$Fd\overline{3}m$	DIAMOND_A4	Ge_1

Table II. Invariant reactions.

Reaction	Type	T / K	Compositions / x_{Ge}			$\Delta_{\mathrm{r}}H$ / (J/mol)
liquid $\rightleftharpoons$ fcc + $A4$	eutectic	923.3	0.249	0.096	1.000	−15302

Table IIIa. Integral quantities for the liquid phase at 1300 K.

x_{Ge}	ΔG_{m} [J/mol]	ΔH_{m} [J/mol]	ΔS_{m} [J/(mol·K)]	$G_{\mathrm{m}}^{\mathrm{E}}$ [J/mol]	$S_{\mathrm{m}}^{\mathrm{E}}$ [J/(mol·K)]	ΔC_p [J/(mol·K)]
0.000	0	0	0.000	0	0.000	0.000
0.100	−4383	−716	2.820	−869	0.117	0.000
0.200	−6514	−454	4.661	−1105	0.501	0.000
0.300	−7547	346	6.072	−944	0.993	0.000
0.400	−7856	1319	7.058	−582	1.462	0.000
0.500	−7664	2177	7.570	−172	1.807	0.000
0.600	−7104	2708	7.548	170	1.952	0.000
0.700	−6231	2777	6.929	371	1.850	0.000
0.800	−5010	2324	5.642	399	1.481	0.000
0.900	−3255	1367	3.555	259	0.853	0.000
1.000	0	0	0.000	0	0.000	0.000

Reference states: Ag(liquid), Ge(liquid)

Table IIIb. Partial quantities for Ag in the liquid phase at 1300 K.

x_{Ag}	ΔG_{Ag} [J/mol]	ΔH_{Ag} [J/mol]	ΔS_{Ag} [J/(mol·K)]	$G_{\mathrm{Ag}}^{\mathrm{E}}$ [J/mol]	$S_{\mathrm{Ag}}^{\mathrm{E}}$ [J/(mol·K)]	a_{Ag}	γ_{Ag}
1.000	0	0	0.000	0	0.000	1.000	1.000
0.900	−1498	−569	0.714	−359	−0.162	0.871	0.967
0.800	−3513	−1650	1.433	−1101	−0.422	0.723	0.903
0.700	−5672	−2477	2.458	−1816	−0.508	0.592	0.845
0.600	−7737	−2509	4.021	−2215	−0.226	0.489	0.815
0.500	−9622	−1440	6.294	−2130	0.531	0.411	0.821
0.400	−11418	812	9.408	−1514	1.789	0.348	0.869
0.300	−13457	4097	13.503	−443	3.492	0.288	0.960
0.200	−16511	8036	18.882	886	5.501	0.217	1.085
0.100	−22734	12023	26.736	2155	7.591	0.122	1.221
0.000	$-\infty$	15221	∞	2924	9.459	0.000	1.311

Reference state: Ag(liquid)

Table IIIc. Partial quantities for Ge in the liquid phase at 1300 K.

x_{Ge}	ΔG_{Ge} [J/mol]	ΔH_{Ge} [J/mol]	ΔS_{Ge} [J/(mol·K)]	$G^{\mathrm{E}}_{\mathrm{Ge}}$ [J/mol]	$S^{\mathrm{E}}_{\mathrm{Ge}}$ [J/(mol·K)]	a_{Ge}	γ_{Ge}
0.000	$-\infty$	−13715	∞	−12737	−0.752	0.000	0.308
0.100	−30345	−2040	21.774	−5457	2.629	0.060	0.604
0.200	−18515	4333	17.575	−1119	4.194	0.180	0.902
0.300	−11922	6932	14.504	1091	4.493	0.332	1.106
0.400	−8035	7062	11.613	1869	3.995	0.475	1.189
0.500	−5707	5794	8.847	1786	3.083	0.590	1.180
0.600	−4228	3972	6.308	1293	2.061	0.676	1.127
0.700	−3135	2211	4.112	721	1.146	0.748	1.069
0.800	−2135	896	2.332	277	0.476	0.821	1.026
0.900	−1091	183	0.980	48	0.104	0.904	1.004
1.000	0	0	0.000	0	0.000	1.000	1.000

Reference state: Ge(liquid)

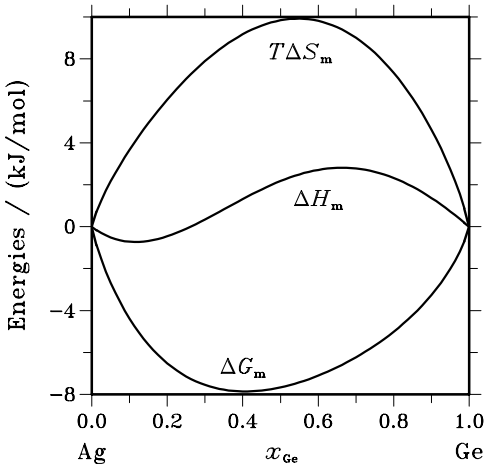

Fig. 2. Integral quantities of the liquid phase at T=1300 K.

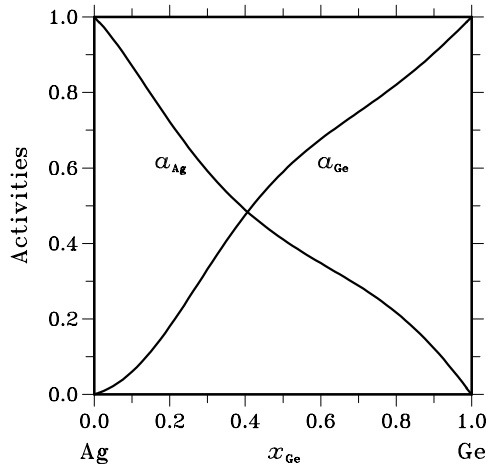

Fig. 3. Activities in the liquid phase at T=1300 K.

References

[29Bri] T.R. Briggs, R.O. McDuffie, L.H. Willisford: J. Phys. Chem. **33** (1929) 1080–1096.
[36Mau] H. Maucher: Forschungsarb. Metallk. Röntgenmetallogr., N° 20 (1936) 1–32.
[40Hum] W. Hume-Rothery, G.V. Raynor, P.W. Reynolds, H.K. Packer: J. Inst. Metals **66** (1940) 209–239.
[40Owe] E.A. Owen, V.W. Rowlands: J. Inst. Metals **66** (1940) 361–378.
[50Now] H. Nowotny, K. Bachmayer: Monatsh. Chem. **81** (1950) 669–678.
[68Cas] R. Castanet, M. Laffitte: C.R. Acad. Sci. Paris, Ser. C **267** (1968) 204–206.
[68Wit] F.E. Wittig: private communication (1968).
[69Cas] R. Castanet, Y. Claire, M. Laffitte: J. Chim. Phys. Phys.-Chim. Biol. **66** (1969) 1276–1285.
[71Bat] G.I. Batalin, E.A. Beloborodova, V.A. Stukalo: Russ. J. Phys. Chem. **45** (1971) 1533.
[71Pre] B. Predel, D.W. Stein: Z. Naturforsch. **26A** (1971) 722.
[74Jac] K.T. Jacob, C.B. Alcock, J.C. Chan: Acta Metall. **22** (1974) 545–551.
[75Pre] B. Predel, H. Bankstahl: J. Less-Common Met. **43** (1975) 191–203.
[79Mar] L. Martin-Garin, C. Chatillon, M. Allibert: J. Less-Common Met. **63** (1979) 9–23.
[80Ell] R.P. Elliott, F.A. Shunk: Bull. Alloy Phase Diagrams **1** (1980) 47–51.
[88Che] P.-Y. Chevalier: Thermochim. Acta **130** (1988) 25–32.

Ag – In (Silver – Indium)

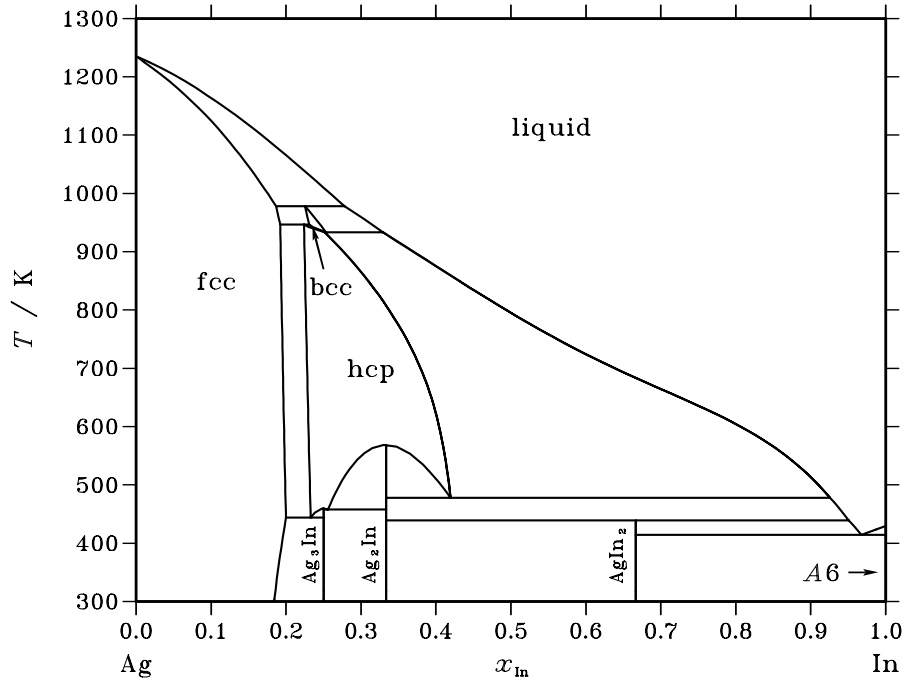

Fig. 1. Calculated phase diagram for the system Ag-In.

The Ag-In system has been critically assessed by Chevalier and Fischer [01Che], and is of interest for nuclear safety applications. The phase diagram as compiled by Moffatt [81Mof] presents a complete mutual solubility in the liquid state, limited solid solubility of indium in the silver rich terminal solid solution, and negligible solid solubility of silver in pure indium. There are two intermediate solid solutions, bcc with a very narrow temperature and composition range, and hcp with a larger existence range, which could transform into a different structure (ζ') below 473 K. Three intermediate compounds have been identified: Ag_3In, Ag_2In_{1-x} with a limited nonstoichiometry range and $AgIn_2$, strictly stoichiometric. All solution phases have been described with a simple substitutional model and the three compounds have been considered as stoichiometric.

The calculated liquidus is in good agreement with experimental data in the silver-rich domain by [34Hum, 37Hum], and in an extended composition range by [35Wei, 70Cam]. The calculated solidus and solid-solid phase transitions are in better agreement with [35Wei] than with [70Cam], which disagree on the hcp limits. The temperatures of the invariant reactions including the bcc phase are in agreement with the works of [35Wei, 70Cam, 91Hor]; the temperatures of the three invariant reactions in the indium rich-region agree with [70Cam, 91Hor]. The $Ag_2In \leftrightarrow$ hcp temperature is well represented, as the upper temperature of Ag_3In (460 K). However, the (ζ') phase below 473 K is replaced by a two-phase region Ag_3In + Ag_2In below 458 K.

The calculated mixing enthalpy of the liquid phase is within the range of data measured by Kleppa [56Kle] at 723 K, Nozaki et al. [66Noz] at 1100 K, Castanet et al. [70Cas] at 743 K and 1280 K, Béja [66Bej] at 1028 K and Qi et al. [89Qi] at 1300 K.

The partial Gibbs energies of silver and indium are in good agreement with the experimental results of [89Qi, 69Alc] at 1300 K. The partial Gibbs energies of indium are in good agreement with experimental results of [63Prz, 72Pre] at 1000 K, and [81Kam] at 1050 K and 1250 K. The partial Gibbs energy of indium in fcc solid solutions is in good agreement with the measurements of [73Jac] at 900 K and [73Mas] at 1000 K. Enthalpies of formation of fcc and hcp solid solutions have been determined by [61Orr] at 317 K and [56Kle] at 723 K. The thermodynamic data of the compounds have been estimated.

Table I. Phases, structures and models.

Phase	Struktur-bericht	Prototype	Pearson symbol	Space group	SGTE name	Model
liquid					LIQUID	$(Ag,In)_1$
fcc	$A1$	Cu	$cF4$	$Fm\overline{3}m$	FCC_A1	$(Ag,In)_1$
Ag_3In	$A3$	Mg	$hP2$	$P6_3/mmc$	AG3IN1	Ag_3In_1
bcc	$A2$	CsCl	$cP2$	$Pm3m$	BCC_A2	$(Ag,In)_1$
hcp	$A3$	Mg	$hP2$	$P6_3/mmc$	HCP_A3	$(Ag,In)_1$
Ag_2In_1	$D0_3$	$AlFe_3$	$cF16$	$Fm\overline{3}m$	D03_AG2IN1	Ag_2In_1
$AgIn_2$	$C16$	Al_2Cu	$tI12$	$I4/mcm$	C16_AG1IN2	Ag_1In_2
$A6$	$A6$	In	$tI2$	$I4/mmm$	TETRAGONAL_A6	In_1

Table II. Invariant reactions.

Reaction	Type	T / K	Compositions / x_{In}			$\Delta_r H$ / (J/mol)
fcc + liquid ⇌ bcc	peritectic	977.8	0.187	0.278	0.225	−2588
fcc + bcc ⇌ hcp	peritectoid	946.7	0.192	0.231	0.224	−1102
bcc ⇌ hcp + liquid	eutectoid	933.3	0.253	0.252	0.329	−1177
hcp ⇌ Ag_2In	congruent	568.6	0.333	0.333		−1952
hcp ⇌ Ag_2In + liquid	eutectoid	477.7	0.420	0.333	0.926	−1221
hcp ⇌ Ag_3In	congruent	460.2	0.250	0.250		−592
hcp ⇌ Ag_3In + Ag_2In	eutectoid	458.2	0.256	0.250	0.333	−663
hcp ⇌ fcc + Ag_3In	eutectoid	443.8	0.233	0.200	0.250	−393
Ag_2In + liquid ⇌ $AgIn_2$	peritectic	439.2	0.333	0.950	0.667	−2548
liquid ⇌ $AgIn_2$ + $A6$	eutectic	414.6	0.967	0.667	1.000	−3731

Table IIIa. Integral quantities for the liquid phase at 1300 K.

x_{In}	ΔG_{m} [J/mol]	ΔH_{m} [J/mol]	ΔS_{m} [J/(mol·K)]	$G_{\mathrm{m}}^{\mathrm{E}}$ [J/mol]	$S_{\mathrm{m}}^{\mathrm{E}}$ [J/(mol·K)]	ΔC_p [J/(mol·K)]
0.000	0	0	0.000	0	0.000	0.000
0.100	−7006	−3035	3.055	−3493	0.352	0.000
0.200	−10754	−4531	4.786	−5345	0.626	0.000
0.300	−12605	−4935	5.900	−6002	0.821	0.000
0.400	−13116	−4621	6.535	−5841	0.939	0.000
0.500	−12660	−3897	6.741	−5168	0.978	0.000
0.600	−11494	−2999	6.535	−4220	0.939	0.000
0.700	−9768	−2097	5.900	−3165	0.821	0.000
0.800	−7511	−1288	4.786	−2102	0.626	0.000
0.900	−4574	−603	3.055	−1060	0.352	0.000
1.000	0	0	0.000	0	0.000	0.000

Reference states: Ag(liquid), In(liquid)

Table IIIb. Partial quantities for Ag in the liquid phase at 1300 K.

x_{Ag}	ΔG_{Ag} [J/mol]	ΔH_{Ag} [J/mol]	ΔS_{Ag} [J/(mol·K)]	G^E_{Ag} [J/mol]	S^E_{Ag} [J/(mol·K)]	a_{Ag}	γ_{Ag}
1.000	0	0	0.000	0	0.000	1.000	1.000
0.900	−2039	−849	0.915	−900	0.039	0.828	0.920
0.800	−5384	−2769	2.012	−2972	0.156	0.608	0.760
0.700	−9284	−4971	3.318	−5429	0.352	0.424	0.605
0.600	−13213	−6878	4.873	−7692	0.626	0.295	0.491
0.500	−16883	−8119	6.741	−9390	0.978	0.210	0.419
0.400	−20266	−8531	9.027	−10362	1.408	0.153	0.383
0.300	−23665	−8160	11.927	−10652	1.917	0.112	0.373
0.200	−27909	−7258	15.885	−10513	2.503	0.076	0.378
0.100	−35296	−6288	22.313	−10407	3.168	0.038	0.382
0.000	−∞	−5919	∞	−11004	3.912	0.000	0.361

Reference state: Ag(liquid)

Table IIIc. Partial quantities for In in the liquid phase at 1300 K.

x_{In}	ΔG_{In} [J/mol]	ΔH_{In} [J/mol]	ΔS_{In} [J/(mol·K)]	G^E_{In} [J/mol]	S^E_{In} [J/(mol·K)]	a_{In}	γ_{In}
0.000	−∞	−39700	∞	−44785	3.912	0.000	0.016
0.100	−51713	−22706	22.313	−26825	3.168	0.008	0.084
0.200	−32233	−11582	15.885	−14837	2.503	0.051	0.253
0.300	−20355	−4849	11.927	−7341	1.917	0.152	0.507
0.400	−12969	−1234	9.027	−3065	1.408	0.301	0.753
0.500	−8437	326	6.741	−945	0.978	0.458	0.916
0.600	−5646	689	4.873	−125	0.626	0.593	0.989
0.700	−3812	501	3.318	44	0.352	0.703	1.004
0.800	−2411	204	2.012	1	0.156	0.800	1.000
0.900	−1161	29	0.915	−22	0.039	0.898	0.998
1.000	0	0	0.000	0	0.000	1.000	1.000

Reference state: In(liquid)

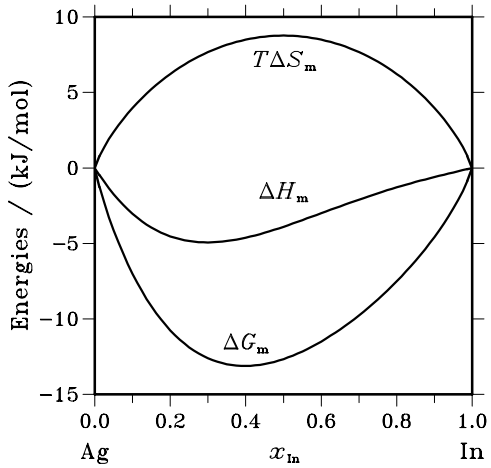

Fig. 2. Integral quantities of the liquid phase at T=1300 K.

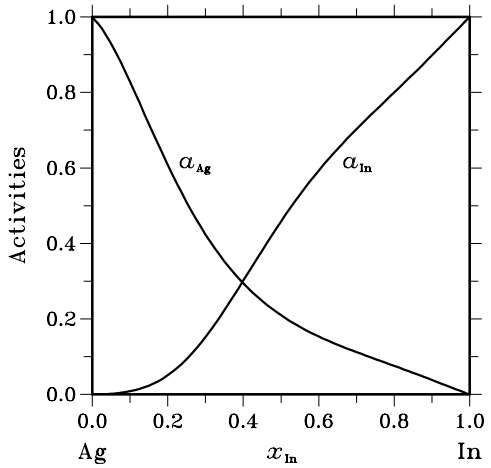

Fig. 3. Activities in the liquid phase at T=1300 K.

Table IV. Standard reaction quantities at 298.15 K for the compounds per mole of atoms.

Compound	x_{In}	$\Delta_{\mathrm{f}}G^{\circ}$ / (J/mol)	$\Delta_{\mathrm{f}}H^{\circ}$ / (J/mol)	$\Delta_{\mathrm{f}}S^{\circ}$ / (J/(mol·K))	$\Delta_{\mathrm{f}}C_P^{\circ}$ / (J/(mol·K))
Ag_3In_1	0.250	−6695	−5817	2.944	0.000
Ag_2In_1	0.333	−7471	−7047	1.424	0.000
Ag_1In_2	0.667	−3966	−3966	0.000	0.000

References

[34Hum] W. Hume-Rothery, G.W. Mabbott, M. Channel-Evans: Phil. Trans. Royal Soc. (London) **A233** (1934) 1–97.

[35Wei] F. Weibke, H. Eggers: Z. Anorg. Chem. **222** (1935) 145–160.

[37Hum] W. Hume-Rothery, P.W. Reynolds: Phil. Trans. Royal Soc. (London) **A160** (1937) 282–303.

[56Kle] O.J. Kleppa: J. Phys. Chem. **60** (1956) 846–852.

[61Orr] R.L. Orr, R. Hultgren: J. Phys. Chem. **65** (1961) 378-380.

[63Prz] E. Przezdziecka-Mycielska, J. Terpilowski, K. Strozecka: Arch. Hutnictwa **8** (1963) 85–102.

[66Bej] R. Béja: reported by [66Noz].

[66Noz] T. Nozaki, M. Shimoji, K. Niwa: Trans. Jpn. Inst. Met. **30** (1966) 7-10.

[67Sny] H.J. Snyder: Trans. AIME **239** (1967) 1385–1391.

[69Alc] C.B. Alcock, R. Sridhar, R.C. Svedberg: Acta Metall. **17** (1969) 839–844.

[70Cam] A.N. Campbell, R. Wagemann, R.B. Ferguson: Can. J. Chem. **48** (1970) 1703–1715.

[70Cas] R. Castanet, Y. Claire, M. Laffitte: J. Chim. Phys. Phys.-Chim. Biol. **67** (1970) 789–793.

[72Pre] B. Predel, U. Schallner: Z. Metallkd. **63** (1972) 341–347.

[73Jac] K.T. Jacob, C.B. Alcock: Metall. Trans. **4** (1973) 2483–2484.

[73Mas] D.B. Masson, S.S. Pradhan: Metall. Trans. **4** (1973) 991–995.

[81Kam] K. Kameda, Y.Yoshida, S. Sakairi: J. Jpn. Inst. Met. **45** (1981) 614–620.

[81Mof] W.G. Moffatt: The Handbook of Binary Phase Diagrams, General Electric, Genium Publishing Corporation, 1981.

[89Qi] G. Qi, M. Hino, T. Azakami: Mater. Trans. JIM **30** (1989) 575–582.

[91Hor] P.J. Horrocks: Ph.D. Thesis, Univ. Manchester, 1991.

[01Che] P.-Y. Chevalier, E. Fischer: unpublished assessment, 2001.

Ag – Ir (Silver – Iridium)

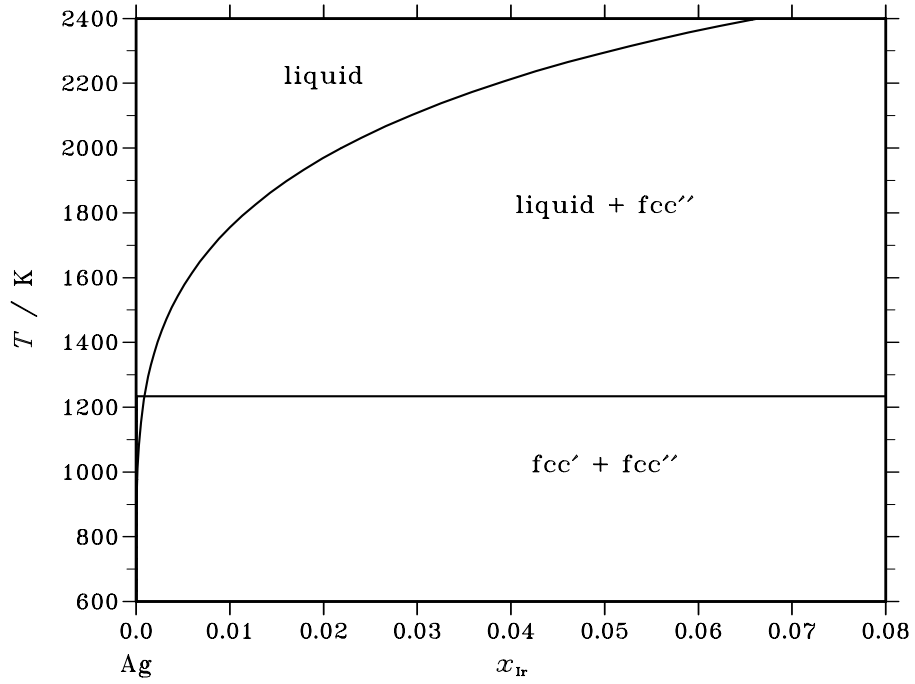

Fig. 1. Calculated partial phase diagram for the system Ag-Ir.

Experimental information for this system is very scarce. In the recommended description [86Kar] for this system, a simple substitutional model has been used to represent the properties of mixing of the liquid and fcc phases using the solubility curve for Ir in liquid Ag and the approximate eutectic temperature of 1234 K, as reported by [86Kar], as a guide in deriving the thermodynamic parameters. Because of the uncertainty of available experimental values, and because the gas phase becomes stable at temperatures a little higher, the description is best used for temperatures below ca. 2300 K.

Table I. Phases, structures and models.

Phase	Struktur-bericht	Prototype	Pearson symbol	Space group	SGTE name	Model
liquid					LIQUID	$(Ag,Ir)_1$
fcc	$A1$	Cu	$cF4$	$Fm\overline{3}m$	FCC_A1	$(Ag,Ir)_1$

Table II. Invariant reactions.

Reaction	Type	T / K	Compositions / x_{Ir}			$\Delta_r H$ / (J/mol)
liquid $\rightleftharpoons$ fcc′ + fcc″	eutectic	1234.2	0.001	0.000	1.000	−11357

Table IIIa. Integral quantities for the liquid phase at 2000 K.

x_{Ir}	ΔG_{m} [J/mol]	ΔH_{m} [J/mol]	ΔS_{m} [J/(mol·K)]	$G_{\mathrm{m}}^{\mathrm{E}}$ [J/mol]	$S_{\mathrm{m}}^{\mathrm{E}}$ [J/(mol·K)]	ΔC_p [J/(mol·K)]
0.000	0	0	0.000	0	0.000	0.000
0.005	−195	434	0.315	328	0.053	0.072
0.010	−278	865	0.572	653	0.106	0.144
0.015	−319	1294	0.806	976	0.159	0.216
0.020	−334	1720	1.027	1296	0.212	0.288
0.022	−335	1881	1.108	1417	0.232	0.315

Reference states: Ag(liquid), Ir(fcc)

Table IIIb. Partial quantities for Ag in the liquid phase at 2000 K.

x_{Ag}	ΔG_{Ag} [J/mol]	ΔH_{Ag} [J/mol]	ΔS_{Ag} [J/(mol·K)]	$G_{\mathrm{Ag}}^{\mathrm{E}}$ [J/mol]	$S_{\mathrm{Ag}}^{\mathrm{E}}$ [J/(mol·K)]	a_{Ag}	γ_{Ag}
1.000	0	0	0.000	0	0.000	1.000	1.000
0.995	−82	1	0.042	1	0.000	0.995	1.000
0.990	−162	5	0.084	5	0.000	0.990	1.000
0.985	−239	12	0.126	12	0.000	0.986	1.001
0.980	−314	22	0.168	22	0.000	0.981	1.001
0.978	−342	26	0.184	26	0.000	0.980	1.002

Reference state: Ag(liquid)

Table IIIc. Partial quantities for Ir in the liquid phase at 2000 K.

x_{Ir}	ΔG_{Ir} [J/mol]	ΔH_{Ir} [J/mol]	ΔS_{Ir} [J/(mol·K)]	$G_{\mathrm{Ir}}^{\mathrm{E}}$ [J/mol]	$S_{\mathrm{Ir}}^{\mathrm{E}}$ [J/(mol·K)]	a_{Ir}	γ_{Ir}
0.000	$-\infty$	87066	∞	65879	10.594	0.000	52.546
0.005	−22763	86529	54.646	65342	10.594	0.254	50.877
0.010	−11772	85995	48.883	64808	10.594	0.493	49.267
0.015	−5562	85463	45.512	64275	10.594	0.716	47.715
0.020	−1308	84932	43.120	63745	10.594	0.924	46.219
0.022	−1	84732	42.366	63545	10.594	1.000	45.664

Reference state: Ir(fcc)

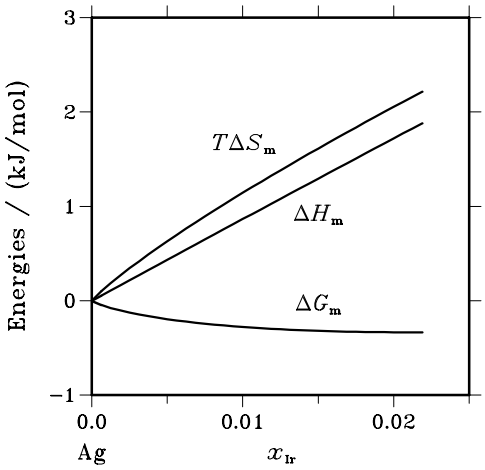

Fig. 2. Integral quantities of the liquid phase at T=2000 K.

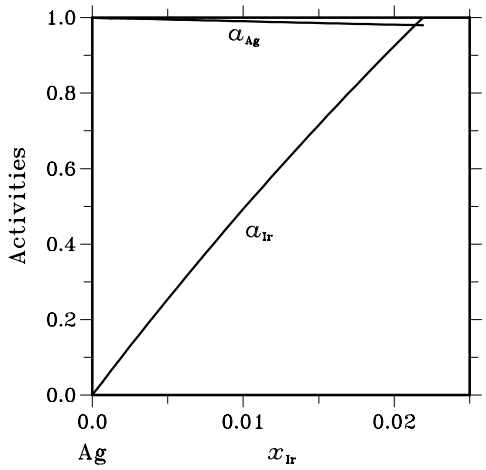

Fig. 3. Activities in the liquid phase at T=2000 K.

References

[86Kar] I. Karakaya, W.T. Thompson: Bull. Alloy Phase Diagrams **7** (1987) 359–360.

Ag – Mg (Silver – Magnesium)

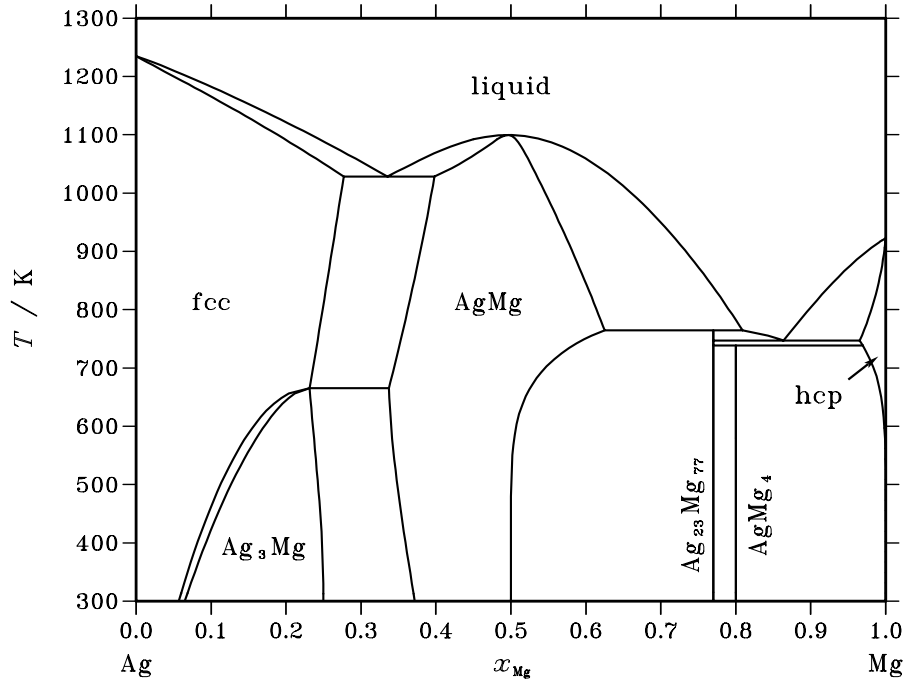

Fig. 1. Calculated phase diagram for the system Ag-Mg.

Small additions of Ag can be used to improve the precipitation-hardening process in Al-Cu-Mg alloys. The thermodynamic description of [97Lim] has been selected, because it updates a previous assessment [84Nay] and it provides new experimental data for the thermodynamic description of the compounds $Ag_{23}Mg_{77}$ and $AgMg_4$.

The liquid, fcc and hcp phases are modelled as simple substitutional solutions whereas Ag_3Mg and AgMg are described as ordered solution phases with $L1_2$ and $B2$ structure, respectively. The compound $Ag_{23}Mg_{77}$ represents the high-temperature (ε') and the low-temperature (ε) modification of a phase with narrow composition range, but due to the lack of data they are not distinguished in the description.

The calculated phase diagram is in acceptable agreement with literature data for the liquidus throughout the whole composition range. The solidus curves next to the terminal fcc and hcp phases are also well reproduced. The two-phase region fcc/AgMg and the field of the Ag_3Mg phase exhibit lager deviations from experimental data. The calculated heats of formation for the liquid, fcc, Ag_3Mg and AgMg phases reveal also certain deviations from experimental data. However, the authors have refrained from using more parameters especially for the ordered phases in order to facilitate extrapolations to higher-order systems.

Table I. Phases, structures and models.

Phase	Struktur-bericht	Prototype	Pearson symbol	Space group	SGTE name	Model
liquid					LIQUID	$(Ag,Mg)_1$
fcc	$A1$	Cu	$cF4$	$Fm\overline{3}m$	FCC_L102	$(Ag,Mg)_1$
Ag_3Mg	$L1_2$	$AuCu_3$	$cP4$	$Pm\overline{3}m$	FCC_L102	$4(Ag,Mg)_1$
AgMg	$B2$	CsCl	$cP2$	$Pm3m$	BCC_B2	$2(Ag,Mg)_1$
$Ag_{23}Mg_{77}$	···	···	cF^*	···	AGMG3	$Ag_{23}Mg_{77}$
$AgMg_4$	···	···	hP^*	···	AGMG4	Ag_1Mg_4
hcp	$A3$	Mg	$hP2$	$P6_3/mmc$	HCP_A3	$(Ag,Mg)_1$

Table II. Invariant reactions.

Reaction	Type	T / K	Compositions / x_{Mg}			$\Delta_{\mathrm{r}}H$ / (J/mol)
liquid ⇌ AgMg	congruent	1099.6	0.496	0.496		−18861
liquid ⇌ fcc + AgMg	eutectic	1028.4	0.335	0.277	0.398	−16114
AgMg + liquid ⇌ $Ag_{23}Mg_{77}$	peritectic	764.5	0.625	0.809	0.770	−21652
liquid ⇌ $Ag_{23}Mg_{77}$ + hcp	eutectic	747.0	0.864	0.770	0.965	−15806
$Ag_{23}Mg_{77}$ + hcp ⇌ $AgMg_4$	peritectoid	738.3	0.770	0.969	0.800	−1160
fcc + AgMg ⇌ Ag_3Mg	peritectoid	665.1	0.232	0.337	0.232	−2097

Table IIIa. Integral quantities for the liquid phase at 1323 K.

x_{Mg}	ΔG_{m} [J/mol]	ΔH_{m} [J/mol]	ΔS_{m} [J/(mol·K)]	$G^{\mathrm{E}}_{\mathrm{m}}$ [J/mol]	$S^{\mathrm{E}}_{\mathrm{m}}$ [J/(mol·K)]	ΔC_p [J/(mol·K)]
0.000	0	0	0.000	0	0.000	0.000
0.100	−10346	−4336	4.543	−6770	1.840	0.000
0.200	−17413	−7581	7.432	−11909	3.271	0.000
0.300	−22183	−9783	9.373	−15464	4.294	0.000
0.400	−24886	−10990	10.503	−17483	4.907	0.000
0.500	−25637	−11250	10.875	−18013	5.112	0.000
0.600	−24505	−10610	10.503	−17102	4.907	0.000
0.700	−21517	−9117	9.373	−14797	4.294	0.000
0.800	−16652	−6819	7.432	−11147	3.271	0.000
0.900	−9775	−3764	4.543	−6199	1.840	0.000
1.000	0	0	0.000	0	0.000	0.000

Reference states: Ag(liquid), Mg(liquid)

Table IIIb. Partial quantities for Ag in the liquid phase at 1323 K.

x_{Ag}	ΔG_{Ag} [J/mol]	ΔH_{Ag} [J/mol]	ΔS_{Ag} [J/(mol·K)]	$G^{\mathrm{E}}_{\mathrm{Ag}}$ [J/mol]	$S^{\mathrm{E}}_{\mathrm{Ag}}$ [J/(mol·K)]	a_{Ag}	γ_{Ag}
1.000	0	0	0.000	0	0.000	1.000	1.000
0.900	−1983	−553	1.080	−824	0.204	0.835	0.928
0.800	−5686	−2149	2.673	−3231	0.818	0.596	0.745
0.700	−11051	−4693	4.806	−7127	1.840	0.366	0.523
0.600	−18036	−8088	7.519	−12417	3.271	0.194	0.323
0.500	−26629	−12242	10.875	−19004	5.112	0.089	0.178
0.400	−36874	−17057	14.979	−26795	7.361	0.035	0.088
0.300	−48937	−22439	20.029	−35693	10.019	0.012	0.039
0.200	−63309	−28292	26.467	−45605	13.086	0.003	0.016
0.100	−81762	−34522	35.706	−56433	16.561	0.001	0.006
0.000	$-\infty$	−41034	∞	−68084	20.446	0.000	0.002

Reference state: Ag(liquid)

Table IIIc. Partial quantities for Mg in the liquid phase at 1323 K.

x_{Mg}	ΔG_{Mg} [J/mol]	ΔH_{Mg} [J/mol]	ΔS_{Mg} [J/(mol·K)]	$G^{\mathrm{E}}_{\mathrm{Mg}}$ [J/mol]	$S^{\mathrm{E}}_{\mathrm{Mg}}$ [J/(mol·K)]	a_{Mg}	γ_{Mg}
0.000	$-\infty$	−48967	∞	−76017	20.446	0.000	0.001
0.100	−85617	−38378	35.706	−60289	16.561	0.000	0.004
0.200	−64324	−29308	26.467	−46620	13.086	0.003	0.014
0.300	−48160	−21661	20.029	−34916	10.019	0.013	0.042
0.400	−35161	−15343	14.979	−25081	7.361	0.041	0.102
0.500	−24646	−10258	10.875	−17021	5.112	0.106	0.213
0.600	−16259	−6312	7.519	−10640	3.271	0.228	0.380
0.700	−9765	−3407	4.806	−5842	1.840	0.412	0.588
0.800	−4988	−1451	2.673	−2533	0.818	0.635	0.794
0.900	−1776	−347	1.080	−617	0.204	0.851	0.945
1.000	0	0	0.000	0	0.000	1.000	1.000

Reference state: Mg(liquid)

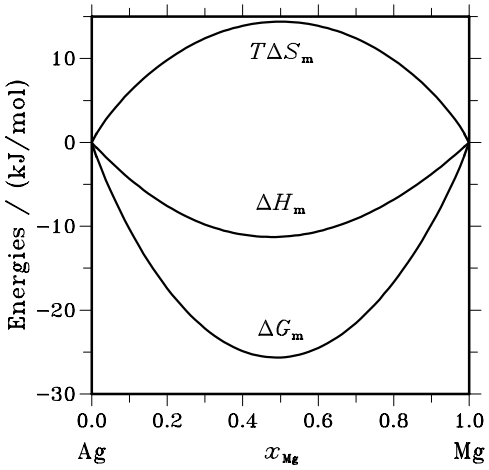

Fig. 2. Integral quantities of the liquid phase at T=1323 K.

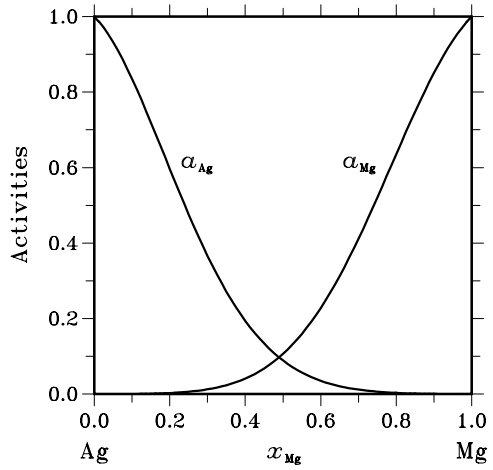

Fig. 3. Activities in the liquid phase at T=1323 K.

Table IVa. Integral quantities for the stable phases at 773 K.

Phase	x_{Mg}	ΔG_{m} [J/mol]	ΔH_{m} [J/mol]	ΔS_{m} [J/(mol·K)]	$G_{\mathrm{m}}^{\mathrm{E}}$ [J/mol]	$S_{\mathrm{m}}^{\mathrm{E}}$ [J/(mol·K)]	ΔC_p [J/(mol·K)]
fcc	0.000	0	0	0.000	0	0.000	0.000
	0.100	−8634	−7143	1.929	−6545	−0.774	0.000
	0.200	−14155	−11691	3.189	−10939	−0.972	0.000
	0.245	−15872	−12994	3.722	−12290	−0.911	0.000
AgMg	0.358	−19552	−18018	1.985	−17618	−0.517	0.139
	0.400	−20824	−19012	2.344	−19207	0.252	0.099
	0.500	−22537	−20653	2.438	−22428	2.296	0.753
	0.600	−19257	−14330	6.374	−17641	4.283	0.099
	0.622	−18311	−12900	7.000	−16511	4.672	0.117
liquid	0.805	−10442	2130	16.264	−7269	12.159	0.596
	0.880	−6771	4177	14.162	−4412	11.111	0.643
hcp	0.974	−1647	−575	1.386	−861	0.369	0.000
	1.000	0	0	0.000	0	0.000	0.000

Reference states: Ag(fcc), Mg(hcp)

Table IVb. Partial quantities for Ag in the stable phases at 773 K.

Phase	x_{Ag}	ΔG_{Ag} [J/mol]	ΔH_{Ag} [J/mol]	ΔS_{Ag} [J/(mol·K)]	$G_{\mathrm{Ag}}^{\mathrm{E}}$ [J/mol]	$S_{\mathrm{Ag}}^{\mathrm{E}}$ [J/(mol·K)]	a_{Ag}	γ_{Ag}
fcc	1.000	0	0	0.000	0	0.000	1.000	1.000
	0.900	−1793	−1357	0.564	−1116	−0.312	0.757	0.841
	0.800	−5572	−4954	0.799	−4138	−1.056	0.420	0.525
	0.755	−7815	−7133	0.882	−6006	−1.459	0.296	0.393
AgMg	0.642	−7815	−8785	−1.255	−3709	−6.567	0.296	0.562
	0.600	−10044	−10554	−0.659	−4831	−7.404	0.210	0.472
	0.500	−26639	−32852	−8.037	−26530	−8.179	0.016	0.016
	0.400	−43930	−52739	−11.396	−47708	−6.508	0.001	0.001
	0.378	−45170	−52356	−9.297	−47950	−5.700	0.001	0.001
liquid	0.195	−45170	−17548	35.733	−34669	22.149	0.001	0.005
	0.120	−54958	−22212	42.363	−41334	24.738	0.000	0.002
hcp	0.026	−54958	−21136	43.755	−31621	13.565	0.000	0.007
	0.000	$-\infty$	−22318	∞	−33395	14.330	0.000	0.006

Reference state: Ag(fcc)

Table IVc. Partial quantities for Mg in the stable phases at 773 K.

Phase	x_{Mg}	ΔG_{Mg} [J/mol]	ΔH_{Mg} [J/mol]	ΔS_{Mg} [J/(mol·K)]	$G^{\mathrm{E}}_{\mathrm{Mg}}$ [J/mol]	$S^{\mathrm{E}}_{\mathrm{Mg}}$ [J/(mol·K)]	a_{Mg}	γ_{Mg}
fcc	0.000	$-\infty$	−85600	∞	−77019	−11.100	0.000	0.000
	0.100	−70202	−59216	14.213	−55403	−4.932	0.000	0.000
	0.200	−48489	−38636	12.746	−38145	−0.636	0.001	0.003
	0.245	−40645	−31017	12.455	−31616	0.774	0.002	0.007
AgMg	0.358	−40645	−34610	7.807	−42615	10.356	0.002	0.001
	0.400	−36993	−31700	6.847	−40771	11.735	0.003	0.002
	0.500	−18435	−8453	12.913	−18326	12.771	0.057	0.058
	0.600	−2809	11276	18.221	2405	11.477	0.646	1.454
	0.622	−2019	11034	16.886	2559	10.963	0.730	1.489
liquid	0.805	−2019	6902	11.541	−623	9.736	0.730	0.908
	0.880	−196	7777	10.315	626	9.251	0.970	1.102
hcp	0.974	−196	−16	0.233	−24	0.010	0.970	0.996
	1.000	0	0	0.000	0	0.000	1.000	1.000

Reference state: Mg(hcp)

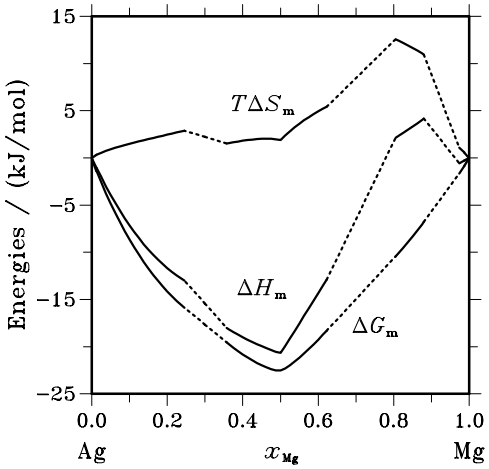

Fig. 4. Integral quantities of the stable phases at T=773 K.

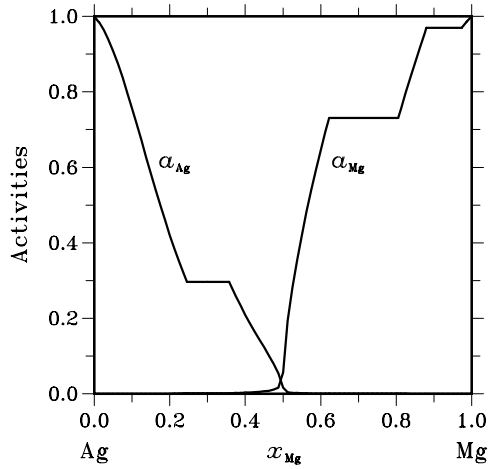

Fig. 5. Activities in the stable phases at T=773 K.

Table V. Standard reaction quantities at 298.15 K for the compounds per mole of atoms.

Compound	x_{Mg}	$\Delta_{\mathrm{f}}G^{\circ}$ / (J/mol)	$\Delta_{\mathrm{f}}H^{\circ}$ / (J/mol)	$\Delta_{\mathrm{f}}S^{\circ}$ / (J/(mol·K))	$\Delta_{\mathrm{f}}C^{\circ}_{P}$ / (J/(mol·K))
$Ag_{23}Mg_{77}$	0.770	−18396	−22600	−14.100	0.000
Ag_1Mg_4	0.800	−16489	−20458	−13.313	0.000

References

[84Nay] A.A. Nayeb-Hashemi, J.B. Clark: Bull. Alloy Phase Diagrams **5** (1984) 348–358.
[97Lim] M. Lim, J.E. Tibballs, P.L. Rossiter: Z. Metallkd. **88** (1997) 162–169.

Ag – Os (Silver – Osmium)

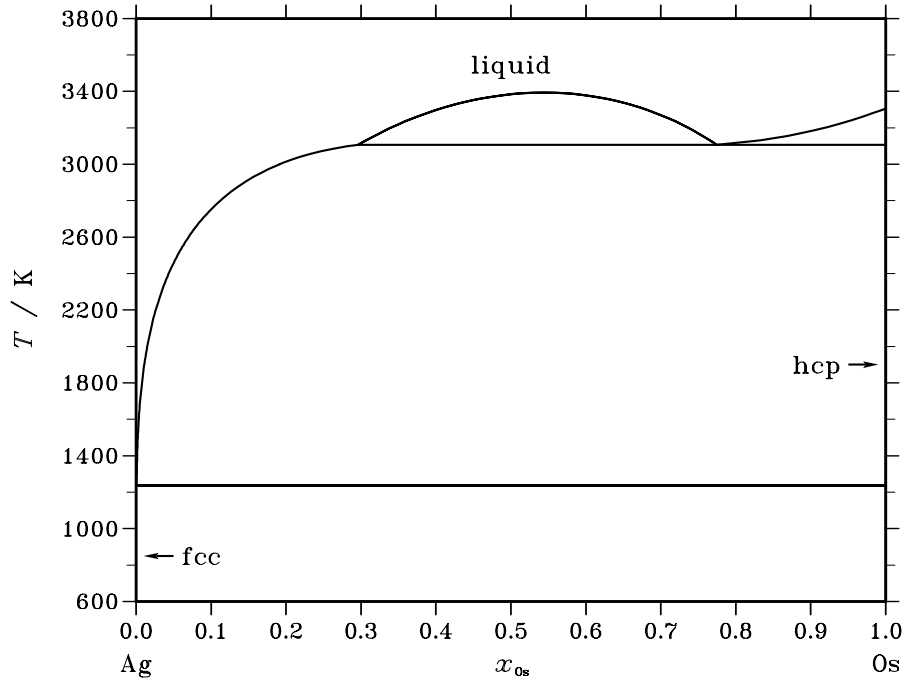

Fig. 1. Calculated phase diagram for the system Ag-Os.

The description presented here for the Ag-Os system is based on the very limited phase diagram information given by [Massalski, 86Kar]. As such, a large uncertainty is associated with the tabulated values. At normal pressure, the condensed phases are no longer stable at temperatures above ca. 2450 K. This should be borne in mind when viewing the tables and figures. The phase diagram presented here (which has been calculated by elimination of the gas phase) results from fitting the solubility of Os in Ag-rich alloys to experimental data. Although the present description relates to all compositions and temperatures, it is best used for Os contents below ∼10 at.% and temperatures below ∼2500 K.

Table I. Phases, structures and models.

Phase	Struktur-bericht	Prototype	Pearson symbol	Space group	SGTE name	Model
liquid					LIQUID	$(Ag,Os)_1$
fcc	$A1$	Cu	$cF4$	$Fm\overline{3}m$	FCC_A1	$(Ag,Os)_1$
hcp	$A3$	Mg	$hP2$	$P6_3/mmc$	HCP_A3	$(Ag,Os)_1$

Table II. Invariant reactions.

Reaction	Type	T / K	Compositions / x_{Os}			$\Delta_r H$ / (J/mol)
liquid ⇌ liquid′ + liquid″	critical	3392.0	0.544	0.544	0.544	0
liquid″ ⇌ liquid′ + hcp	eutectic	3107.1	0.774	0.296	1.000	−43851
liquid′ ⇌ fcc + hcp	eutectic	1234.6	0.000	0.000	1.000	−11333

Table IIIa. Integral quantities for the liquid phase at 2000 K.

x_{Os}	ΔG_{m} [J/mol]	ΔH_{m} [J/mol]	ΔS_{m} [J/(mol·K)]	$G_{\mathrm{m}}^{\mathrm{E}}$ [J/mol]	$S_{\mathrm{m}}^{\mathrm{E}}$ [J/(mol·K)]	ΔC_p [J/(mol·K)]
0.000	0	0	0.000	0	0.000	0.000
0.005	−168	465	0.317	355	0.055	0.048
0.010	−223	928	0.575	708	0.110	0.095
0.015	−236	1380	0.808	1053	0.164	0.142

Reference states: Ag(liquid), Os(hcp)

Table IIIb. Partial quantities for Ag in the liquid phase at 2000 K.

x_{Ag}	ΔG_{Ag} [J/mol]	ΔH_{Ag} [J/mol]	ΔS_{Ag} [J/(mol·K)]	$G_{\mathrm{Ag}}^{\mathrm{E}}$ [J/mol]	$S_{\mathrm{Ag}}^{\mathrm{E}}$ [J/(mol·K)]	a_{Ag}	γ_{Ag}
1.000	0	0	0.000	0	0.000	1.000	1.000
0.995	−82	1	0.042	1	0.000	0.995	1.000
0.990	−163	5	0.084	5	0.000	0.990	1.000
0.985	−240	10	0.125	10	0.000	0.986	1.001

Reference state: Ag(liquid)

Table IIIc. Partial quantities for Os in the liquid phase at 2000 K.

x_{Os}	ΔG_{Os} [J/mol]	ΔH_{Os} [J/mol]	ΔS_{Os} [J/(mol·K)]	$G_{\mathrm{Os}}^{\mathrm{E}}$ [J/mol]	$S_{\mathrm{Os}}^{\mathrm{E}}$ [J/(mol·K)]	a_{Os}	γ_{Os}
0.000	$-\infty$	93269	∞	71298	10.985	0.000	72.791
0.005	−17265	92811	55.038	70841	10.985	0.354	70.814
0.010	−6196	92354	49.275	70384	10.985	0.689	68.896
0.015	0	91907	45.954	69937	10.985	1.000	67.068

Reference state: Os(hcp)

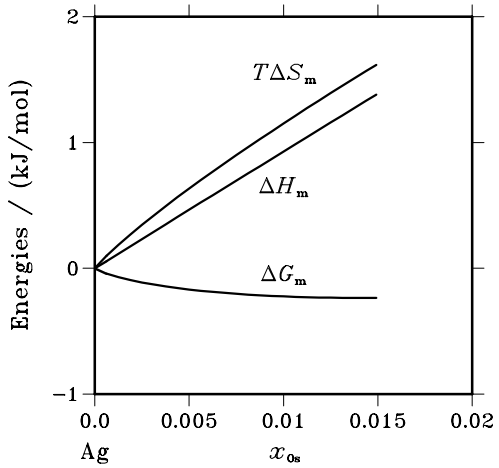

Fig. 2. Integral quantities of the liquid phase at T=2000 K.

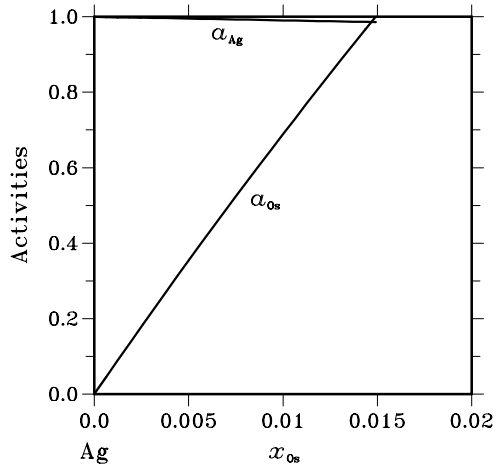

Fig. 3. Activities in the liquid phase at T=2000 K.

References

[86Kar] I. Karakaya, W.T. Thompson: Bull. Alloy Phase Diagrams **7** (1987) 360–362.

Ag – Pb (Silver – Lead)

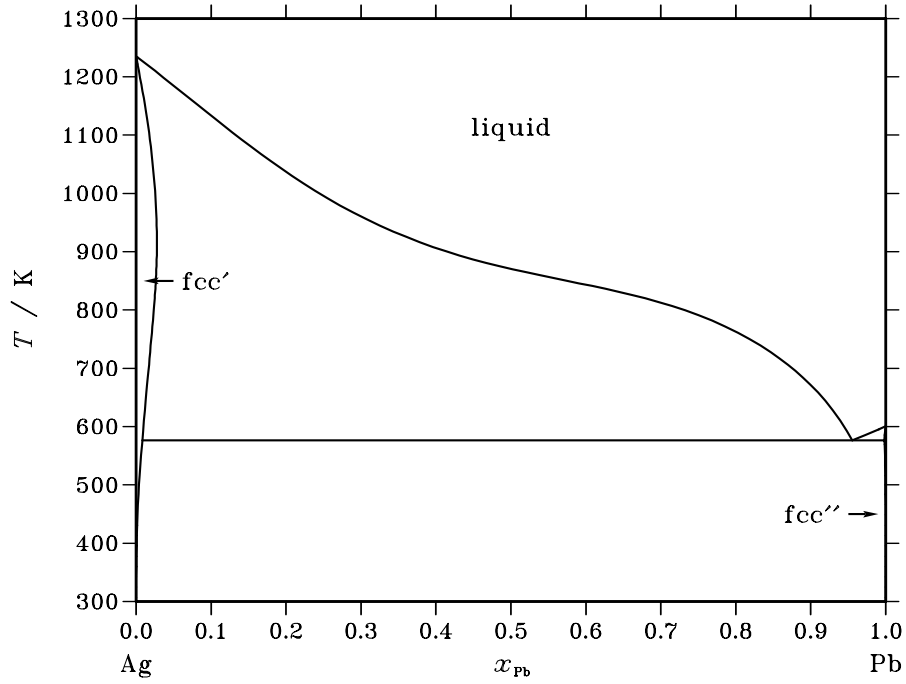

Fig. 1. Calculated phase diagram for the system Ag-Pb.

The silver-lead system is part of the commonly used solder system Pb-Sn-Ag-Bi-Sb-Zn. Therefore, the Ag-Pb system has been studied experimentally many times. A detailed review of experimental data is presented in [80Ell]. The thermodynamic parameters for the Ag-Pb system have been assessed several times [76Zim, 81Ash, 86Hay, 87Kar, 94Lee, 98Roe, 00Luk]. The assessment of [00Luk] has been accepted here. It is based on the same experimental data as [76Zim] and additionally includes a very precise determination of the liquidus for Pb-rich compositions [79Esd].
The system is characterised by a continuous solution of the elements in the liquid phase and a wide miscibility gap in the solid state. The solubility of Pb in fcc-Ag has been determined by thermoelectric power measurements, micrographically and by lattice parameter data. The solubility of Ag in solid Pb is derived from diffusion measurements, thermo-resistometric investigations, electrical resistivity and lattice parameter measurements. In liquid Ag-Pb alloys, the enthalpy of mixing has been measured calorimetrically and the activities of Pb and Ag have been derived from EMF and vapour pressure measurements. All phases are modelled by the substitutional solution model. The calculated thermodynamic quantities and the phase diagram are in good agreement with the experimental data.

Table I. Phases, structures and models.

Phase	Struktur-bericht	Prototype	Pearson symbol	Space group	SGTE name	Model
liquid					LIQUID	$(Ag,Pb)_1$
fcc	$A1$	Cu	$cF4$	$Fm\overline{3}m$	FCC_A1	$(Ag,Pb)_1$

Table II. Invariant reactions.

Reaction	Type	T / K	Compositions / x_{Pb}			$\Delta_{\mathrm{r}}H$ / (J/mol)
liquid $\rightleftharpoons$ fcc′ + fcc″	eutectic	576.4	0.955	0.008	0.998	−5434

Table IIIa. Integral quantities for the liquid phase at 1300 K.

x_{Pb}	ΔG_{m} [J/mol]	ΔH_{m} [J/mol]	ΔS_{m} [J/(mol·K)]	$G^{\mathrm{E}}_{\mathrm{m}}$ [J/mol]	$S^{\mathrm{E}}_{\mathrm{m}}$ [J/(mol·K)]	ΔC_p [J/(mol·K)]
0.000	0	0	0.000	0	0.000	0.000
0.100	−3295	1149	3.419	219	0.716	0.698
0.200	−4834	2127	5.354	575	1.194	1.242
0.300	−5653	2901	6.580	950	1.501	1.630
0.400	−6021	3440	7.278	1253	1.682	1.863
0.500	−6069	3713	7.525	1423	1.761	1.940
0.600	−5851	3689	7.338	1424	1.742	1.863
0.700	−5355	3337	6.686	1248	1.607	1.630
0.800	−4493	2625	5.476	916	1.315	1.242
0.900	−3039	1523	3.510	475	0.807	0.698
1.000	0	0	0.000	0	0.000	0.000

Reference states: Ag(liquid), Pb(liquid)

Table IIIb. Partial quantities for Ag in the liquid phase at 1300 K.

x_{Ag}	ΔG_{Ag} [J/mol]	ΔH_{Ag} [J/mol]	ΔS_{Ag} [J/(mol·K)]	$G^{\mathrm{E}}_{\mathrm{Ag}}$ [J/mol]	$S^{\mathrm{E}}_{\mathrm{Ag}}$ [J/(mol·K)]	a_{Ag}	γ_{Ag}
1.000	0	0	0.000	0	0.000	1.000	1.000
0.900	−1229	81	1.008	−90	0.132	0.893	0.992
0.800	−2603	365	2.283	−191	0.428	0.786	0.983
0.700	−3962	916	3.752	−106	0.786	0.693	0.990
0.600	−5247	1794	5.417	274	1.170	0.615	1.026
0.500	−6513	3064	7.367	979	1.604	0.547	1.095
0.400	−7949	4787	9.796	1955	2.178	0.479	1.198
0.300	−9948	7024	13.055	3066	3.045	0.398	1.328
0.200	−13305	9838	17.802	4091	4.421	0.292	1.460
0.100	−20160	13290	25.730	4729	6.585	0.155	1.549
0.000	$-\infty$	17441	∞	4594	9.883	0.000	1.530

Reference state: Ag(liquid)

Table IIIc. Partial quantities for Pb in the liquid phase at 1300 K.

x_{Pb}	ΔG_{Pb} [J/mol]	ΔH_{Pb} [J/mol]	ΔS_{Pb} [J/(mol·K)]	$G^{\mathrm{E}}_{\mathrm{Pb}}$ [J/mol]	$S^{\mathrm{E}}_{\mathrm{Pb}}$ [J/(mol·K)]	a_{Pb}	γ_{Pb}
0.000	$-\infty$	12251	∞	1043	8.621	0.000	1.101
0.100	−21885	10767	25.117	3003	5.972	0.132	1.320
0.200	−13760	9173	17.641	3637	4.259	0.280	1.400
0.300	−9600	7533	13.179	3414	3.168	0.411	1.371
0.400	−7182	5908	10.069	2722	2.450	0.515	1.286
0.500	−5625	4362	7.682	1867	1.919	0.594	1.189
0.600	−4452	2957	5.699	1069	1.452	0.662	1.104
0.700	−3386	1756	3.956	469	0.990	0.731	1.044
0.800	−2290	822	2.394	122	0.539	0.809	1.011
0.900	−1137	216	1.041	2	0.165	0.900	1.000
1.000	0	0	0.000	0	0.000	1.000	1.000

Reference state: Pb(liquid)

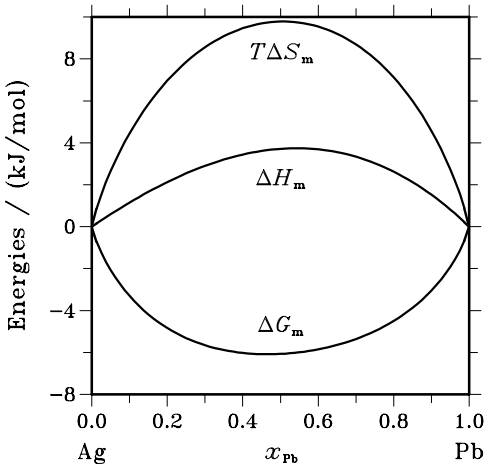

Fig. 2. Integral quantities of the liquid phase at T=1300 K.

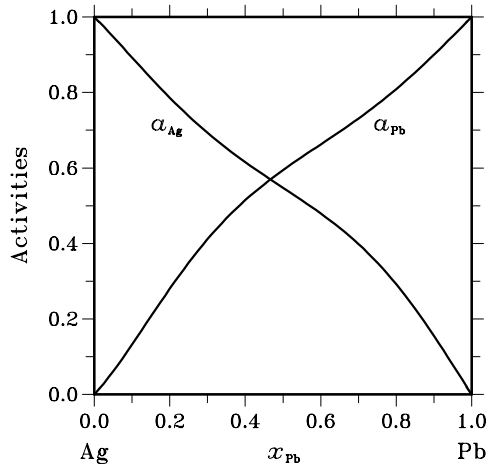

Fig. 3. Activities in the liquid phase at T=1300 K.

References

[76Zim] B. Zimmermann: Ph.D. Thesis, Universität Stuttgart, Stuttgart, 1976.
[79Esd] J.D. Esdaile, N.G. Siviour: Met. Trans. **10A** (1979) 382–384.
[80Ell] R.P. Elliot, F.A. Shunk: Bull. Alloy Phase Diagrams **1** (1980) 56–59.
[81Ash] S. Ashtakala, A.D. Pelton, C.W. Bale: Bull. Alloy Phase Diagrams **2** (1981) 81–83.
[86Hay] F.H. Hayes, H.L. Lukas, G. Effenberg, G. Petzow: Z. Metallkd. **77** (1986) 749–754.
[87Kar] I. Karakaya, W.T. Thompson: Bull. Alloy Phase Diagrams **8** (1987) 326–334.
[94Lee] B.-Z. Lee, C.-S. Oh, D.N. Lee: J. Alloys Comp. **215** (1994) 293–301.
[98Roe] F. Roemermann, R. Blachnik: J. Alloys Comp. **280** (1998) 147–157.
[00Luk] H.L. Lukas: unpublished optimization, 2000.

Ag – Pd (Silver – Palladium)

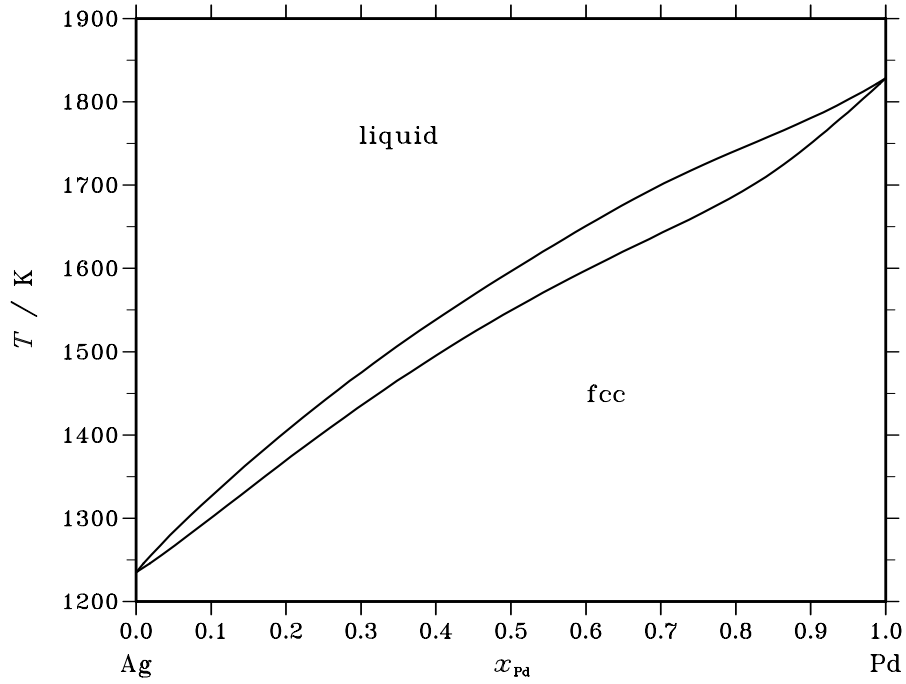

Fig. 1. Calculated phase diagram for the system Ag-Pd.

Alloys of Ag and Pd form a complete range of solid and liquid solutions. The selected thermodynamic data for the system are based on the phase diagram presented by Massalski together with the results obtained by Karakaya and Thompson [87Kar]. A simple substitutional solution model has been used to represent the thermodynamic properties of the liquid and fcc phases. The data are valid for all compositions and temperatures, but particularly in the range 1000 – 2000 K. The present assessment [98Spe] is preferred over that of [99Gho] because the latter presents mixing enthalpies of relatively high magnitude for the liquid and solid phases which is rather surprising for a system with the given complete miscibility ranges.

Table I. Phases, structures and models.

Phase	Struktur-bericht	Prototype	Pearson symbol	Space group	SGTE name	Model
liquid					LIQUID	$(Ag,Pd)_1$
fcc	$A1$	Cu	$cF4$	$Fm\overline{3}m$	FCC_A1	$(Ag,Pd)_1$

Table IIa. Integral quantities for the liquid phase at 1850 K.

x_{Pd}	ΔG_{m} [J/mol]	ΔH_{m} [J/mol]	ΔS_{m} [J/(mol·K)]	$G_{\mathrm{m}}^{\mathrm{E}}$ [J/mol]	$S_{\mathrm{m}}^{\mathrm{E}}$ [J/(mol·K)]	ΔC_p [J/(mol·K)]
0.000	0	0	0.000	0	0.000	0.000
0.100	−6744	−1744	2.703	−1744	0.000	0.000
0.200	−10241	−2544	4.161	−2544	0.000	0.000
0.300	−12016	−2620	5.079	−2620	0.000	0.000
0.400	−12536	−2184	5.596	−2184	0.000	0.000
0.500	−12106	−1444	5.763	−1444	0.000	0.000
0.600	−10952	−600	5.596	−600	0.000	0.000
0.700	−9244	152	5.079	152	0.000	0.000
0.800	−7073	624	4.161	624	0.000	0.000
0.900	−4368	632	2.703	632	0.000	0.000
1.000	0	0	0.000	0	0.000	0.000

Reference states: Ag(liquid), Pd(liquid)

Table IIb. Partial quantities for Ag in the liquid phase at 1850 K.

x_{Ag}	ΔG_{Ag} [J/mol]	ΔH_{Ag} [J/mol]	ΔS_{Ag} [J/(mol·K)]	$G_{\mathrm{Ag}}^{\mathrm{E}}$ [J/mol]	$S_{\mathrm{Ag}}^{\mathrm{E}}$ [J/(mol·K)]	a_{Ag}	γ_{Ag}
1.000	0	0	0.000	0	0.000	1.000	1.000
0.900	−2129	−509	0.876	−509	0.000	0.871	0.967
0.800	−5172	−1740	1.855	−1740	0.000	0.714	0.893
0.700	−8751	−3265	2.966	−3265	0.000	0.566	0.809
0.600	−12529	−4672	4.247	−4672	0.000	0.443	0.738
0.500	−16231	−5569	5.763	−5569	0.000	0.348	0.696
0.400	−19674	−5580	7.619	−5580	0.000	0.278	0.696
0.300	−22868	−4349	10.010	−4349	0.000	0.226	0.754
0.200	−26292	−1536	13.382	−1536	0.000	0.181	0.905
0.100	−32239	3179	19.145	3179	0.000	0.123	1.230
0.000	$-\infty$	10100	∞	10100	0.000	0.000	1.928

Reference state: Ag(liquid)

Table IIc. Partial quantities for Pd in the liquid phase at 1850 K.

x_{Pd}	ΔG_{Pd} [J/mol]	ΔH_{Pd} [J/mol]	ΔS_{Pd} [J/(mol·K)]	$G_{\mathrm{Pd}}^{\mathrm{E}}$ [J/mol]	$S_{\mathrm{Pd}}^{\mathrm{E}}$ [J/(mol·K)]	a_{Pd}	γ_{Pd}
0.000	$-\infty$	−22900	∞	−22900	0.000	0.000	0.226
0.100	−48277	−12859	19.145	−12859	0.000	0.043	0.433
0.200	−30516	−5760	13.382	−5760	0.000	0.138	0.688
0.300	−19634	−1115	10.010	−1115	0.000	0.279	0.930
0.400	−12546	1548	7.619	1548	0.000	0.442	1.106
0.500	−7981	2681	5.763	2681	0.000	0.595	1.190
0.600	−5137	2720	4.247	2720	0.000	0.716	1.193
0.700	−3405	2081	2.966	2081	0.000	0.801	1.145
0.800	−2268	1164	1.855	1164	0.000	0.863	1.079
0.900	−1271	349	0.876	349	0.000	0.921	1.023
1.000	0	0	0.000	0	0.000	1.000	1.000

Reference state: Pd(liquid)

Ag – Pd (Silver – Palladium)

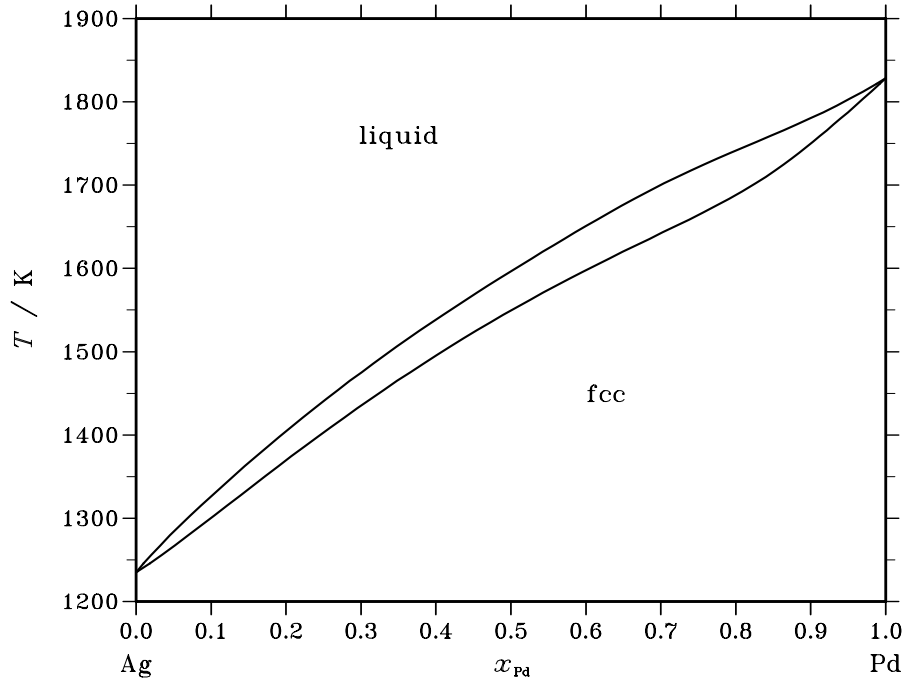

Fig. 1. Calculated phase diagram for the system Ag-Pd.

Alloys of Ag and Pd form a complete range of solid and liquid solutions. The selected thermodynamic data for the system are based on the phase diagram presented by Massalski together with the results obtained by Karakaya and Thompson [87Kar]. A simple substitutional solution model has been used to represent the thermodynamic properties of the liquid and fcc phases. The data are valid for all compositions and temperatures, but particularly in the range 1000 – 2000 K. The present assessment [98Spe] is preferred over that of [99Gho] because the latter presents mixing enthalpies of relatively high magnitude for the liquid and solid phases which is rather surprising for a system with the given complete miscibility ranges.

Table I. Phases, structures and models.

Phase	Struktur-bericht	Prototype	Pearson symbol	Space group	SGTE name	Model
liquid					LIQUID	$(Ag,Pd)_1$
fcc	$A1$	Cu	$cF4$	$Fm\overline{3}m$	FCC_A1	$(Ag,Pd)_1$

Table IIa. Integral quantities for the liquid phase at 1850 K.

x_{Pd}	ΔG_{m} [J/mol]	ΔH_{m} [J/mol]	ΔS_{m} [J/(mol·K)]	$G_{\mathrm{m}}^{\mathrm{E}}$ [J/mol]	$S_{\mathrm{m}}^{\mathrm{E}}$ [J/(mol·K)]	ΔC_p [J/(mol·K)]
0.000	0	0	0.000	0	0.000	0.000
0.100	−6744	−1744	2.703	−1744	0.000	0.000
0.200	−10241	−2544	4.161	−2544	0.000	0.000
0.300	−12016	−2620	5.079	−2620	0.000	0.000
0.400	−12536	−2184	5.596	−2184	0.000	0.000
0.500	−12106	−1444	5.763	−1444	0.000	0.000
0.600	−10952	−600	5.596	−600	0.000	0.000
0.700	−9244	152	5.079	152	0.000	0.000
0.800	−7073	624	4.161	624	0.000	0.000
0.900	−4368	632	2.703	632	0.000	0.000
1.000	0	0	0.000	0	0.000	0.000

Reference states: Ag(liquid), Pd(liquid)

Table IIb. Partial quantities for Ag in the liquid phase at 1850 K.

x_{Ag}	ΔG_{Ag} [J/mol]	ΔH_{Ag} [J/mol]	ΔS_{Ag} [J/(mol·K)]	$G_{\mathrm{Ag}}^{\mathrm{E}}$ [J/mol]	$S_{\mathrm{Ag}}^{\mathrm{E}}$ [J/(mol·K)]	a_{Ag}	γ_{Ag}
1.000	0	0	0.000	0	0.000	1.000	1.000
0.900	−2129	−509	0.876	−509	0.000	0.871	0.967
0.800	−5172	−1740	1.855	−1740	0.000	0.714	0.893
0.700	−8751	−3265	2.966	−3265	0.000	0.566	0.809
0.600	−12529	−4672	4.247	−4672	0.000	0.443	0.738
0.500	−16231	−5569	5.763	−5569	0.000	0.348	0.696
0.400	−19674	−5580	7.619	−5580	0.000	0.278	0.696
0.300	−22868	−4349	10.010	−4349	0.000	0.226	0.754
0.200	−26292	−1536	13.382	−1536	0.000	0.181	0.905
0.100	−32239	3179	19.145	3179	0.000	0.123	1.230
0.000	$-\infty$	10100	∞	10100	0.000	0.000	1.928

Reference state: Ag(liquid)

Table IIc. Partial quantities for Pd in the liquid phase at 1850 K.

x_{Pd}	ΔG_{Pd} [J/mol]	ΔH_{Pd} [J/mol]	ΔS_{Pd} [J/(mol·K)]	$G_{\mathrm{Pd}}^{\mathrm{E}}$ [J/mol]	$S_{\mathrm{Pd}}^{\mathrm{E}}$ [J/(mol·K)]	a_{Pd}	γ_{Pd}
0.000	$-\infty$	−22900	∞	−22900	0.000	0.000	0.226
0.100	−48277	−12859	19.145	−12859	0.000	0.043	0.433
0.200	−30516	−5760	13.382	−5760	0.000	0.138	0.688
0.300	−19634	−1115	10.010	−1115	0.000	0.279	0.930
0.400	−12546	1548	7.619	1548	0.000	0.442	1.106
0.500	−7981	2681	5.763	2681	0.000	0.595	1.190
0.600	−5137	2720	4.247	2720	0.000	0.716	1.193
0.700	−3405	2081	2.966	2081	0.000	0.801	1.145
0.800	−2268	1164	1.855	1164	0.000	0.863	1.079
0.900	−1271	349	0.876	349	0.000	0.921	1.023
1.000	0	0	0.000	0	0.000	1.000	1.000

Reference state: Pd(liquid)

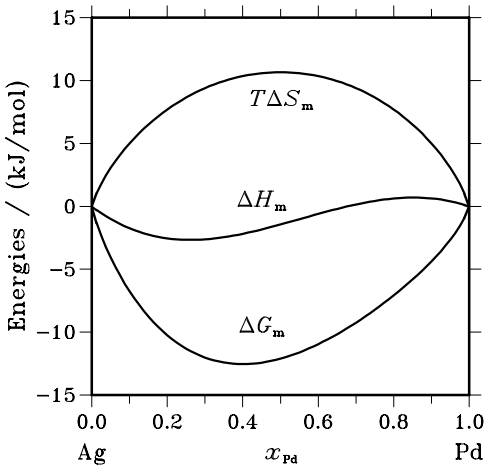

Fig. 2. Integral quantities of the liquid phase at T=1850 K.

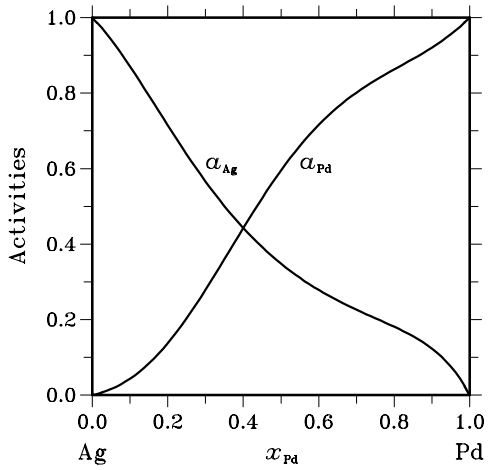

Fig. 3. Activities in the liquid phase at T=1850 K.

Table IIIa. Integral quantities for the stable phases at 1200 K.

Phase	x_{Pd}	ΔG_{m} [J/mol]	ΔH_{m} [J/mol]	ΔS_{m} [J/(mol·K)]	$G^{\mathrm{E}}_{\mathrm{m}}$ [J/mol]	$S^{\mathrm{E}}_{\mathrm{m}}$ [J/(mol·K)]	ΔC_p [J/(mol·K)]
fcc	0.000	0	0	0.000	0	0.000	0.000
	0.100	−5269	−2733	2.113	−2025	−0.590	0.000
	0.200	−8117	−4467	3.042	−3124	−1.119	0.000
	0.300	−9570	−5349	3.518	−3475	−1.561	0.000
	0.400	−9973	−5526	3.705	−3258	−1.890	0.000
	0.500	−9565	−5145	3.684	−2649	−2.080	0.000
	0.600	−8544	−4352	3.493	−1829	−2.102	0.000
	0.700	−7070	−3294	3.147	−976	−1.932	0.000
	0.800	−5260	−2119	2.618	−267	−1.543	0.000
	0.900	−3126	−972	1.795	118	−0.908	0.000
	1.000	0	0	0.000	0	0.000	0.000

Reference states: Ag(fcc), Pd(fcc)

Table IIIb. Partial quantities for Ag in the stable phases at 1200 K.

Phase	x_{Ag}	ΔG_{Ag} [J/mol]	ΔH_{Ag} [J/mol]	ΔS_{Ag} [J/(mol·K)]	$G^{\mathrm{E}}_{\mathrm{Ag}}$ [J/mol]	$S^{\mathrm{E}}_{\mathrm{Ag}}$ [J/(mol·K)]	a_{Ag}	γ_{Ag}
fcc	1.000	0	0	0.000	0	0.000	1.000	1.000
	0.900	−1544	−524	0.850	−493	−0.026	0.857	0.952
	0.800	−3960	−1899	1.717	−1733	−0.138	0.672	0.841
	0.700	−6923	−3833	2.575	−3364	−0.391	0.500	0.714
	0.600	−10126	−6032	3.411	−5029	−0.836	0.362	0.604
	0.500	−13285	−8203	4.236	−6370	−1.528	0.264	0.528
	0.400	−16172	−10051	5.101	−7029	−2.518	0.198	0.494
	0.300	−18664	−11283	6.151	−6651	−3.860	0.154	0.513
	0.200	−20936	−11606	7.775	−4878	−5.607	0.123	0.613
	0.100	−24326	−10726	11.334	−1352	−7.811	0.087	0.873
	0.000	$-\infty$	−8350	∞	4282	−10.527	0.000	1.536

Reference state: Ag(fcc)

Table IIIc. Partial quantities for Pd in the stable phases at 1200 K.

Phase	x_{Pd}	ΔG_{Pd} [J/mol]	ΔH_{Pd} [J/mol]	ΔS_{Pd} [J/(mol·K)]	G^E_{Pd} [J/mol]	S^E_{Pd} [J/(mol·K)]	a_{Pd}	γ_{Pd}
fcc	0.000	$-\infty$	−32810	∞	−25478	−6.110	0.000	0.078
	0.100	−38790	−22614	13.480	−15816	−5.665	0.020	0.205
	0.200	−24745	−14737	8.341	−8687	−5.041	0.084	0.419
	0.300	−15747	−8886	5.718	−3735	−4.293	0.206	0.688
	0.400	−9743	−4767	4.147	−601	−3.472	0.377	0.942
	0.500	−5845	−2088	3.131	1071	−2.632	0.557	1.113
	0.600	−3459	−553	2.422	1638	−1.826	0.707	1.178
	0.700	−2102	129	1.859	1457	−1.106	0.810	1.157
	0.800	−1341	253	1.328	886	−0.527	0.874	1.093
	0.900	−770	112	0.735	281	−0.141	0.926	1.029
	1.000	0	0	0.000	0	0.000	1.000	1.000

Reference state: Pd(fcc)

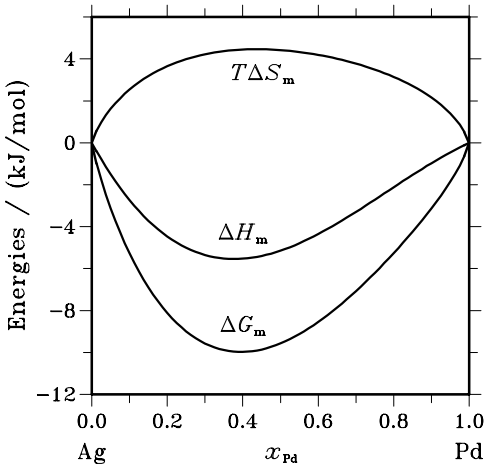

Fig. 4. Integral quantities of the stable phases at T=1200 K.

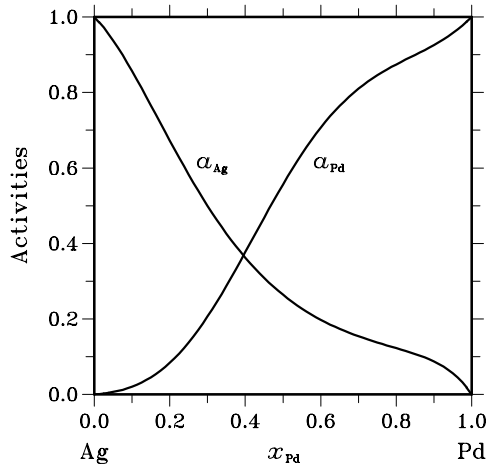

Fig. 5. Activities in the stable phases at T=1200 K.

References

[87Kar] I. Karakaya, W.T. Thompson: Bull. Alloy Phase Diagrams **9** (1988) 237–243.
[98Spe] P.J. Spencer: unpublished assessment, 1998.
[99Gho] G. Ghosh, C. Kantner, G.B. Olson: J. Phase Equilibria **20** (1999) 295–308.

Ag – Pt (Silver – Platinum)

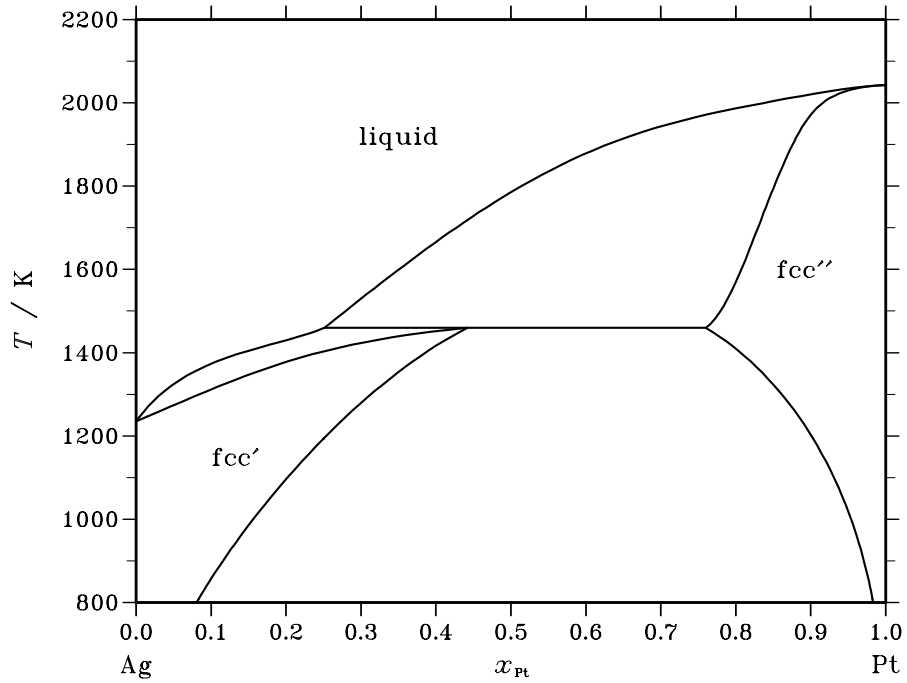

Fig. 1. Calculated phase diagram for the system Ag-Pt.

The present data for the Ag-Pt system [98Spe] are based on the somewhat incomplete phase diagram information presented by [86Mas, 87Kar]. A simple substitutional model has been used to represent the properties both of the liquid and of the fcc phase. The calculated peritectic reaction temperature and the associated liquid and (Ag) compositions agree well with experimental observation, but the (Pt) composition given by the assessment (24 at.%) is considerably higher than that chosen by Massalski (12.5 at.%). The assessment also provides a narrower solidus/liquidus gap in Ag-rich alloys than that presented in Massalski's compilation.

In a more recent experimental investigation [96Dur] the phase equilibria in the System Ag–Pt have been investigated by means of DTA. The observed temperature of the peritectic reaction (1461 ± 3 K) confirms the calculated value, however, other lines of the experimental diagram differ considerably from the calculations. In addition, X-ray and EMPA on long-time annealed samples [96Dur] revealed that the various uncertain phases which are indicated in the phase diagram of [87Kar] are not stable. Instead, it has been found [96Dur] that only one intermediate phase $Ag_{15}Pt_{17}$ is stable below 1076 K.

Table I. Phases, structures and models.

Phase	Struktur-bericht	Prototype	Pearson symbol	Space group	SGTE name	Model
liquid					LIQUID	$(Ag,Pt)_1$
fcc	$A1$	Cu	$cF4$	$Fm\overline{3}m$	FCC_A1	$(Ag,Pt)_1$

Table II. Invariant reactions.

Reaction	Type	T / K	Compositions / x_{Pt}			$\Delta_r H$ / (J/mol)
liquid + fcc$''$ $\rightleftharpoons$ fcc$'$	peritectic	1459.5	0.251	0.760	0.442	−4972

Table IIIa. Integral quantities for the liquid phase at 2100 K.

x_{Pt}	ΔG_{m} [J/mol]	ΔH_{m} [J/mol]	ΔS_{m} [J/(mol·K)]	$G_{\mathrm{m}}^{\mathrm{E}}$ [J/mol]	$S_{\mathrm{m}}^{\mathrm{E}}$ [J/(mol·K)]	ΔC_p [J/(mol·K)]
0.000	0	0	0.000	0	0.000	0.000
0.100	−3098	301	1.619	2578	−1.084	0.000
0.200	−4448	338	2.279	4289	−1.881	0.000
0.300	−5298	309	2.670	5368	−2.409	0.000
0.400	−5774	341	2.912	5977	−2.684	0.000
0.500	−5893	490	3.039	6210	−2.724	0.000
0.600	−5663	742	3.050	6088	−2.546	0.000
0.700	−5105	1010	2.912	5561	−2.167	0.000
0.800	−4227	1140	2.556	4510	−1.605	0.000
0.900	−2933	902	1.826	2744	−0.877	0.000
1.000	0	0	0.000	0	0.000	0.000

Reference states: Ag(liquid), Pt(liquid)

Table IIIb. Partial quantities for Ag in the liquid phase at 2100 K.

x_{Ag}	ΔG_{Ag} [J/mol]	ΔH_{Ag} [J/mol]	ΔS_{Ag} [J/(mol·K)]	$G_{\mathrm{Ag}}^{\mathrm{E}}$ [J/mol]	$S_{\mathrm{Ag}}^{\mathrm{E}}$ [J/(mol·K)]	a_{Ag}	γ_{Ag}
1.000	0	0	0.000	0	0.000	1.000	1.000
0.900	−1361	171	0.730	478	−0.146	0.925	1.028
0.800	−2331	384	1.293	1565	−0.563	0.875	1.094
0.700	−3328	350	1.752	2899	−1.214	0.826	1.181
0.600	−4589	−8	2.181	4330	−2.066	0.769	1.281
0.500	−6181	−554	2.679	5922	−3.084	0.702	1.404
0.400	−8049	−940	3.385	7950	−4.233	0.631	1.577
0.300	−10121	−606	4.531	10901	−5.480	0.560	1.867
0.200	−12624	1222	6.593	15478	−6.788	0.485	2.427
0.100	−17612	5530	11.020	22593	−8.125	0.365	3.647
0.000	$-\infty$	13516	∞	33371	−9.455	0.000	6.762

Reference state: Ag(liquid)

Table IIIc. Partial quantities for Pt in the liquid phase at 2100 K.

x_{Pt}	ΔG_{Pt} [J/mol]	ΔH_{Pt} [J/mol]	ΔS_{Pt} [J/(mol·K)]	$G_{\mathrm{Pt}}^{\mathrm{E}}$ [J/mol]	$S_{\mathrm{Pt}}^{\mathrm{E}}$ [J/(mol·K)]	a_{Pt}	γ_{Pt}
0.000	$-\infty$	5165	∞	31069	−12.335	0.000	5.926
0.100	−18731	1471	9.620	21474	−9.525	0.342	3.421
0.200	−12918	153	6.225	15183	−7.157	0.477	2.386
0.300	−9895	212	4.813	11127	−5.197	0.567	1.891
0.400	−7552	864	4.007	8447	−3.611	0.649	1.622
0.500	−5605	1534	3.399	6498	−2.364	0.725	1.451
0.600	−4073	1863	2.827	4846	−1.421	0.792	1.320
0.700	−2955	1703	2.218	3272	−0.747	0.844	1.206
0.800	−2128	1119	1.546	1768	−0.309	0.885	1.107
0.900	−1302	388	0.805	538	−0.072	0.928	1.031
1.000	0	0	0.000	0	0.000	1.000	1.000

Reference state: Pt(liquid)

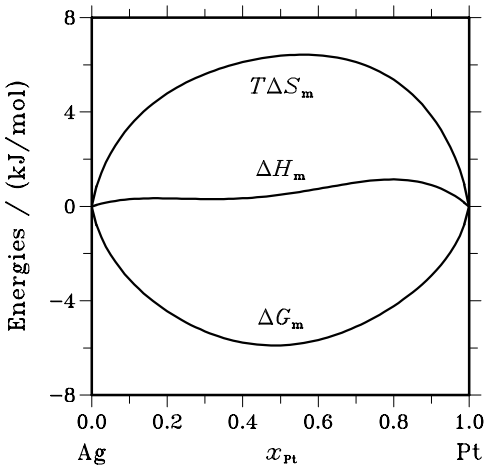

Fig. 2. Integral quantities of the liquid phase at T=2100 K.

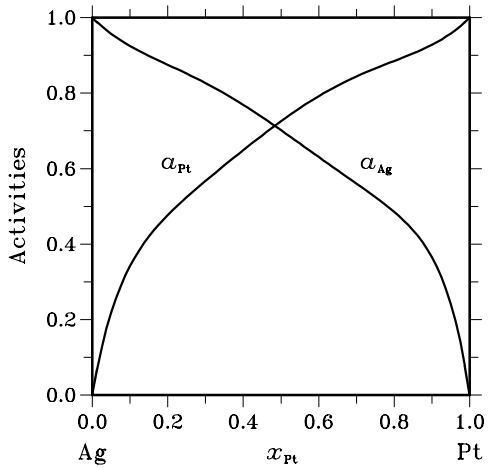

Fig. 3. Activities in the liquid phase at T=2100 K.

Table IVa. Integral quantities for the stable phases at 1200 K.

Phase	x_{Pt}	ΔG_{m} [J/mol]	ΔH_{m} [J/mol]	ΔS_{m} [J/(mol·K)]	$G^{\mathrm{E}}_{\mathrm{m}}$ [J/mol]	$S^{\mathrm{E}}_{\mathrm{m}}$ [J/(mol·K)]	ΔC_p [J/(mol·K)]
fcc′	0.000	0	0	0.000	0	0.000	0.000
	0.100	−1589	1814	2.836	1655	0.133	0.000
	0.200	−1850	3374	4.353	3143	0.193	0.000
	0.254	−1810	4087	4.914	3840	0.206	0.000
fcc″	0.901	−862	2517	2.816	2360	0.131	0.000
	1.000	0	0	0.000	0	0.000	0.000

Reference states: Ag(fcc), Pt(fcc)

Table IVb. Partial quantities for Ag in the stable phases at 1200 K.

Phase	x_{Ag}	ΔG_{Ag} [J/mol]	ΔH_{Ag} [J/mol]	ΔS_{Ag} [J/(mol·K)]	$G^{\mathrm{E}}_{\mathrm{Ag}}$ [J/mol]	$S^{\mathrm{E}}_{\mathrm{Ag}}$ [J/(mol·K)]	a_{Ag}	γ_{Ag}
fcc′	1.000	0	0	0.000	0	0.000	1.000	1.000
	0.900	−984	119	0.919	68	0.043	0.906	1.007
	0.800	−1831	543	1.979	395	0.123	0.832	1.040
	0.746	−2181	932	2.595	737	0.163	0.804	1.077
fcc″	0.099	−2181	22016	20.165	20889	0.940	0.804	8.114
	0.000	$-\infty$	29299	∞	27129	1.809	0.000	15.165

Reference state: Ag(fcc)

Table IVc. Partial quantities for Pt in the stable phases at 1200 K.

Phase	x_{Pt}	ΔG_{Pt} [J/mol]	ΔH_{Pt} [J/mol]	ΔS_{Pt} [J/(mol·K)]	$G^{\mathrm{E}}_{\mathrm{Pt}}$ [J/mol]	$S^{\mathrm{E}}_{\mathrm{Pt}}$ [J/(mol·K)]	a_{Pt}	γ_{Pt}
fcc′	0.000	$-\infty$	19252	∞	17058	1.828	0.000	5.527
	0.100	−7036	17070	20.088	15938	0.943	0.494	4.940
	0.200	−1926	14696	13.851	14132	0.470	0.824	4.122
	0.254	−717	13371	11.741	12971	0.333	0.931	3.669
fcc″	0.901	−717	373	0.909	323	0.042	0.931	1.033
	1.000	0	0	0.000	0	0.000	1.000	1.000

Reference state: Pt(fcc)

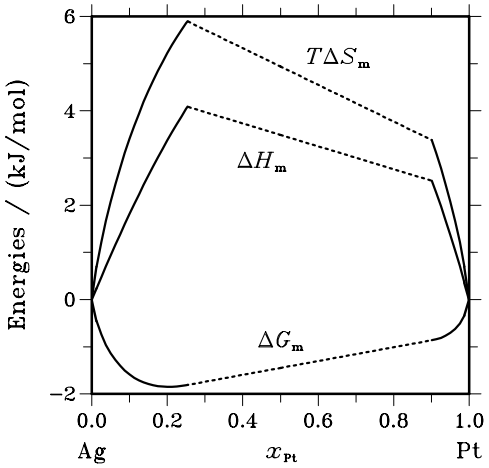

Fig. 4. Integral quantities of the stable phases at T=1200 K.

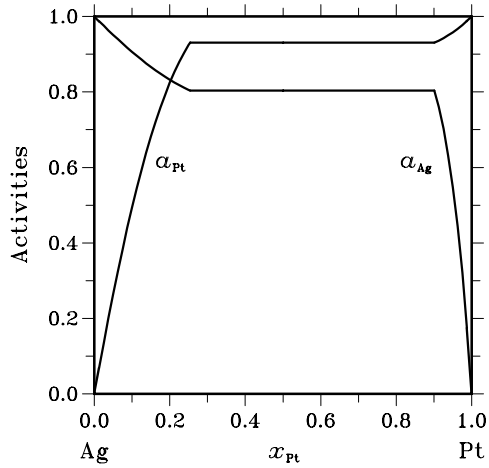

Fig. 5. Activities in the stable phases at T=1200 K.

References

[86Mas] T.B. Massalski (ed.): Binary Alloy Phase Diagrams, ASM, Metals Park, Ohio, 1986.
[87Kar] I. Karakaya, W.T. Thompson: Bull. Alloy Phase Diagrams **8** (1987) 334–340.
[96Dur] Ph. Durussel, P. Feschotte: J. Alloys Comp. **239** (1996) 226–230.
[98Spe] P.J. Spencer: unpublished assessment, 1998.

Ag – Rh (Silver – Rhodium)

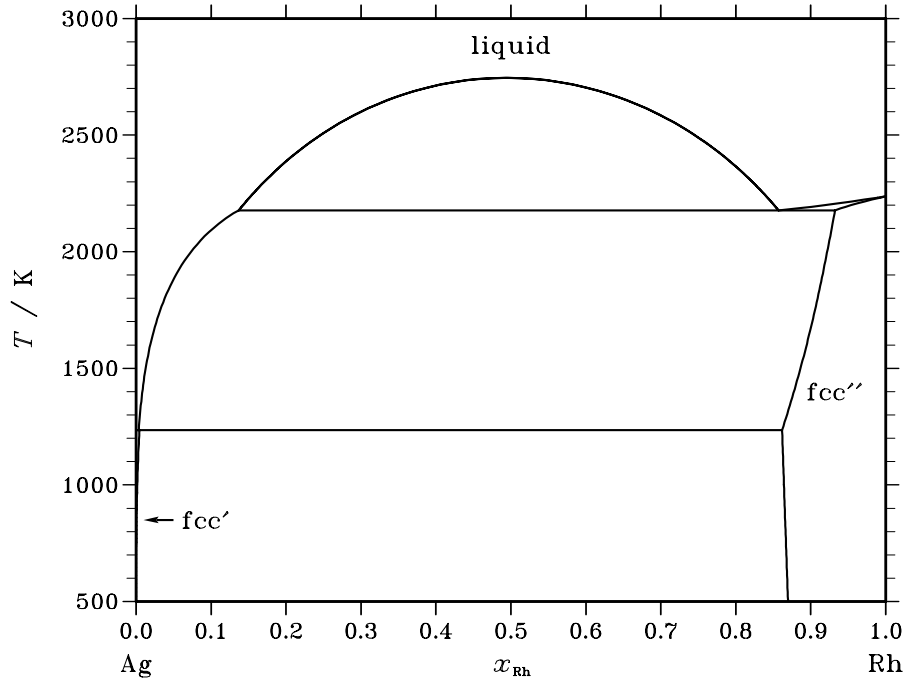

Fig. 1. Calculated phase diagram for the system Ag-Rh.

No experimental thermodynamic data for this system are available and phase diagram information is also very scarce. The suggested diagram presented by [86Kar], in which only a composition for the Rh-rich eutectic is shown as having any reliability, is clearly uncertain, but has nevertheless been used as basis for the present assessment. The assumption of an ideal mixing entropy for the liquid phase has been made here and while the main features of the system are reproduced by the present thermodynamic description, the data presented below should only be viewed as approximate values.

Table I. Phases, structures and models.

Phase	Struktur-bericht	Prototype	Pearson symbol	Space group	SGTE name	Model
liquid					LIQUID	$(Ag,Rh)_1$
fcc	$A1$	Cu	$cF4$	$Fm\overline{3}m$	FCC_A1	$(Ag,Rh)_1$

Table II. Invariant reactions.

Reaction	Type	T / K	Compositions / x_{Rh}			$\Delta_{\mathrm{r}}H$ / (J/mol)
liquid $\rightleftharpoons$ liquid′ + liquid′′	critical	2745.1	0.494	0.494	0.494	0
liquid′ $\rightleftharpoons$ liquid′′ + fcc′′	monotectic	2176.8	0.857	0.137	0.932	−28724
liquid′ + fcc′ $\rightleftharpoons$ fcc′′	peritectic	1235.8	0.004	0.862	0.004	−11285

Table IIIa. Integral quantities for the liquid phase at 2800 K.

x_{Rh}	ΔG_{m} [J/mol]	ΔH_{m} [J/mol]	ΔS_{m} [J/(mol·K)]	$G_{\mathrm{m}}^{\mathrm{E}}$ [J/mol]	$S_{\mathrm{m}}^{\mathrm{E}}$ [J/(mol·K)]	ΔC_p [J/(mol·K)]
0.000	0	0	0.000	0	0.000	0.000
0.100	−3434	4134	2.703	4134	0.000	0.000
0.200	−4312	7338	4.161	7338	0.000	0.000
0.300	−4605	9616	5.079	9616	0.000	0.000
0.400	−4695	10973	5.596	10973	0.000	0.000
0.500	−4724	11413	5.763	11413	0.000	0.000
0.600	−4729	10939	5.596	10939	0.000	0.000
0.700	−4664	9557	5.079	9557	0.000	0.000
0.800	−4379	7270	4.161	7270	0.000	0.000
0.900	−3485	4083	2.703	4083	0.000	0.000
1.000	0	0	0.000	0	0.000	0.000

Reference states: Ag(liquid), Rh(liquid)

Table IIIb. Partial quantities for Ag in the liquid phase at 2800 K.

x_{Ag}	ΔG_{Ag} [J/mol]	ΔH_{Ag} [J/mol]	ΔS_{Ag} [J/(mol·K)]	$G_{\mathrm{Ag}}^{\mathrm{E}}$ [J/mol]	$S_{\mathrm{Ag}}^{\mathrm{E}}$ [J/(mol·K)]	a_{Ag}	γ_{Ag}
1.000	0	0	0.000	0	0.000	1.000	1.000
0.900	−1987	466	0.876	466	0.000	0.918	1.020
0.800	−3338	1857	1.855	1857	0.000	0.866	1.083
0.700	−4138	4165	2.966	4165	0.000	0.837	1.196
0.600	−4510	7382	4.247	7382	0.000	0.824	1.373
0.500	−4637	11500	5.763	11500	0.000	0.819	1.639
0.400	−4822	16510	7.619	16510	0.000	0.813	2.032
0.300	−5626	22403	10.010	22403	0.000	0.785	2.618
0.200	−8298	29171	13.382	29171	0.000	0.700	3.501
0.100	−16799	36806	19.145	36806	0.000	0.486	4.860
0.000	$-\infty$	45300	∞	45300	0.000	0.000	6.999

Reference state: Ag(liquid)

Table IIIc. Partial quantities for Rh in the liquid phase at 2800 K.

x_{Rh}	ΔG_{Rh} [J/mol]	ΔH_{Rh} [J/mol]	ΔS_{Rh} [J/(mol·K)]	$G_{\mathrm{Rh}}^{\mathrm{E}}$ [J/mol]	$S_{\mathrm{Rh}}^{\mathrm{E}}$ [J/(mol·K)]	a_{Rh}	γ_{Rh}
0.000	$-\infty$	46000	∞	46000	0.000	0.000	7.213
0.100	−16459	37147	19.145	37147	0.000	0.493	4.931
0.200	−8208	29261	13.382	29261	0.000	0.703	3.514
0.300	−5695	22334	10.010	22334	0.000	0.783	2.610
0.400	−4973	16358	7.619	16358	0.000	0.808	2.019
0.500	−4812	11325	5.763	11325	0.000	0.813	1.627
0.600	−4667	7226	4.247	7226	0.000	0.818	1.364
0.700	−4252	4052	2.966	4052	0.000	0.833	1.190
0.800	−3400	1795	1.855	1795	0.000	0.864	1.080
0.900	−2005	447	0.876	447	0.000	0.917	1.019
1.000	0	0	0.000	0	0.000	1.000	1.000

Reference state: Rh(liquid)

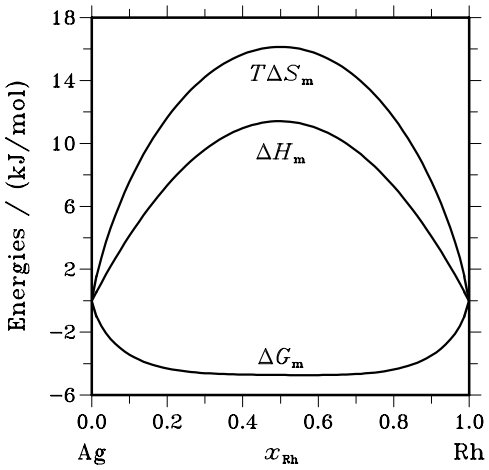

Fig. 2. Integral quantities of the liquid phase at T=2800 K.

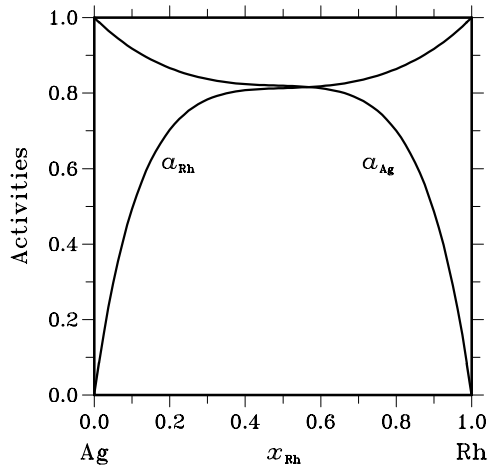

Fig. 3. Activities in the liquid phase at T=2800 K.

References

[86Kar] I. Karakaya, W.T. Thompson: Bull. Alloy Phase Diagrams **7** (1986) 362–365.

Ag – Ru (Silver – Ruthenium)

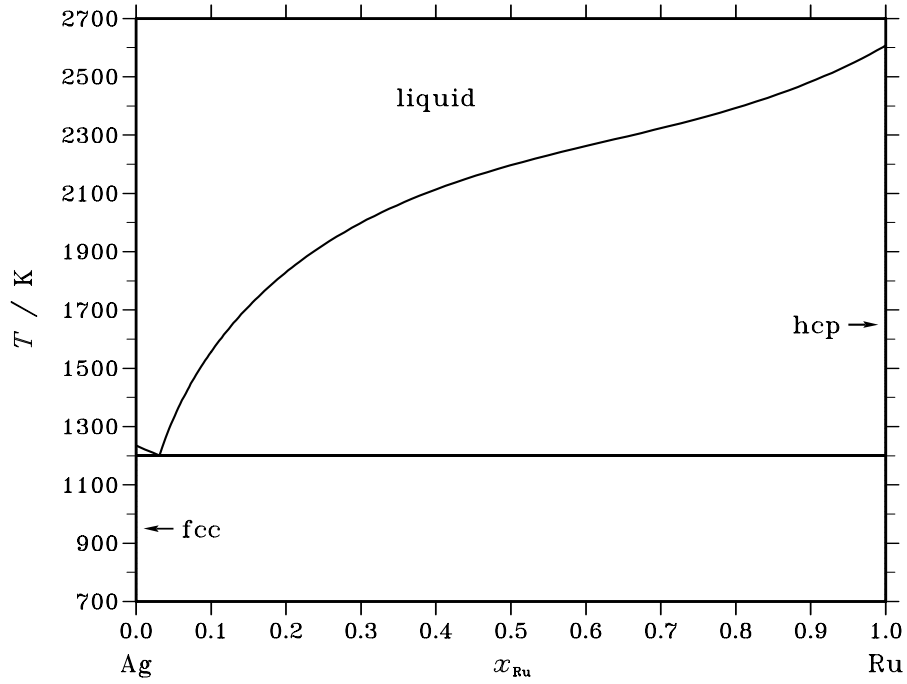

Fig. 1. Calculated phase diagram for the system Ag-Ru.

The available experimental information for this system is very scarce, being limited to the uncertain and restricted phase diagram proposed by [86Kar]. The present assessment, which makes the assumption of an ideal entropy of mixing for the liquid phase, allows the Ag-rich eutectic to be reproduced reasonably well. The thermodynamic parameters obtained for the liquid phase result in a simple eutectic behaviour for the system, rather than the liquid immiscibility suggested by [86Kar].

Table I. Phases, structures and models.

Phase	Struktur-bericht	Prototype	Pearson symbol	Space group	SGTE name	Model
liquid					LIQUID	$(Ag,Ru)_1$
fcc	$A1$	Cu	$cF4$	$Fm\overline{3}m$	FCC_A1	$(Ag,Ru)_1$
hcp	$A3$	Mg	$hP2$	$P6_3/mmc$	HCP_A3	$(Ag,Ru)_1$

Table II. Invariant reactions.

Reaction	Type	T / K	Compositions / x_{Ru}			$\Delta_r H$ / (J/mol)
liquid $\rightleftharpoons$ fcc + hcp	eutectic	1201.4	0.031	0.000	1.000	−12325

Table IIIa. Integral quantities for the liquid phase at 2700 K.

x_{Ru}	ΔG_{m} [J/mol]	ΔH_{m} [J/mol]	ΔS_{m} [J/(mol·K)]	$G_{\mathrm{m}}^{\mathrm{E}}$ [J/mol]	$S_{\mathrm{m}}^{\mathrm{E}}$ [J/(mol·K)]	ΔC_p [J/(mol·K)]
0.000	0	0	0.000	0	0.000	0.000
0.100	−5609	1689	2.703	1689	0.000	0.000
0.200	−8086	3147	4.161	3147	0.000	0.000
0.300	−9394	4320	5.079	4320	0.000	0.000
0.400	−9956	5153	5.596	5153	0.000	0.000
0.500	−9968	5593	5.763	5593	0.000	0.000
0.600	−9524	5585	5.596	5585	0.000	0.000
0.700	−8638	5076	5.079	5076	0.000	0.000
0.800	−7222	4011	4.161	4011	0.000	0.000
0.900	−4961	2337	2.703	2337	0.000	0.000
1.000	0	0	0.000	0	0.000	0.000

Reference states: Ag(liquid), Ru(liquid)

Table IIIb. Partial quantities for Ag in the liquid phase at 2700 K.

x_{Ag}	ΔG_{Ag} [J/mol]	ΔH_{Ag} [J/mol]	ΔS_{Ag} [J/(mol·K)]	$G_{\mathrm{Ag}}^{\mathrm{E}}$ [J/mol]	$S_{\mathrm{Ag}}^{\mathrm{E}}$ [J/(mol·K)]	a_{Ag}	γ_{Ag}
1.000	0	0	0.000	0	0.000	1.000	1.000
0.900	−2259	107	0.876	107	0.000	0.904	1.005
0.800	−4511	499	1.855	499	0.000	0.818	1.022
0.700	−6723	1284	2.966	1284	0.000	0.741	1.059
0.600	−8896	2571	4.247	2571	0.000	0.673	1.121
0.500	−11093	4468	5.763	4468	0.000	0.610	1.220
0.400	−13489	7081	7.619	7081	0.000	0.548	1.371
0.300	−16508	10520	10.010	10520	0.000	0.479	1.598
0.200	−21238	14893	13.382	14893	0.000	0.388	1.941
0.100	−31384	20307	19.145	20307	0.000	0.247	2.471
0.000	$-\infty$	26870	∞	26870	0.000	0.000	3.310

Reference state: Ag(liquid)

Table IIIc. Partial quantities for Ru in the liquid phase at 2700 K.

x_{Ru}	ΔG_{Ru} [J/mol]	ΔH_{Ru} [J/mol]	ΔS_{Ru} [J/(mol·K)]	$G_{\mathrm{Ru}}^{\mathrm{E}}$ [J/mol]	$S_{\mathrm{Ru}}^{\mathrm{E}}$ [J/(mol·K)]	a_{Ru}	γ_{Ru}
0.000	$-\infty$	17870	∞	17870	0.000	0.000	2.217
0.100	−35758	15933	19.145	15933	0.000	0.203	2.033
0.200	−22390	13741	13.382	13741	0.000	0.369	1.844
0.300	−15626	11402	10.010	11402	0.000	0.499	1.662
0.400	−11545	9025	7.619	9025	0.000	0.598	1.495
0.500	−8843	6718	5.763	6718	0.000	0.674	1.349
0.600	−6880	4587	4.247	4587	0.000	0.736	1.227
0.700	−5265	2742	2.966	2742	0.000	0.791	1.130
0.800	−3719	1291	1.855	1291	0.000	0.847	1.059
0.900	−2025	341	0.876	341	0.000	0.914	1.015
1.000	0	0	0.000	0	0.000	1.000	1.000

Reference state: Ru(liquid)

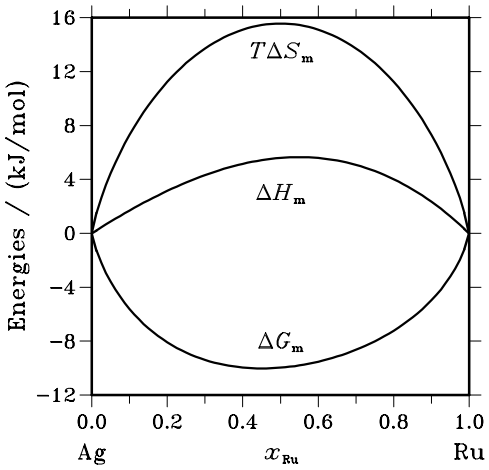

Fig. 2. Integral quantities of the liquid phase at T=2700 K.

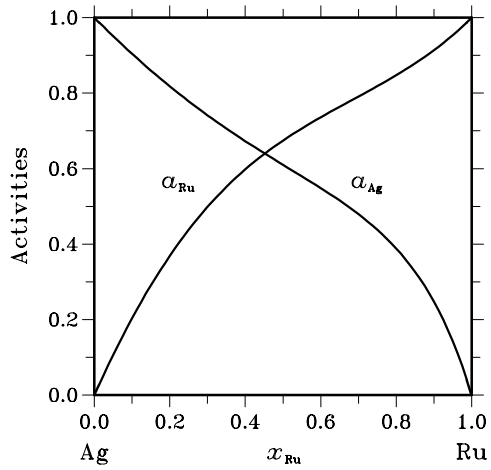

Fig. 3. Activities in the liquid phase at T=2700 K.

References

[86Kar] I. Karakaya, W.T. Thompson: Bull. Alloy Phase Diagrams **7** (1986) 365–368.

Ag – Sb (Silver – Antimony)

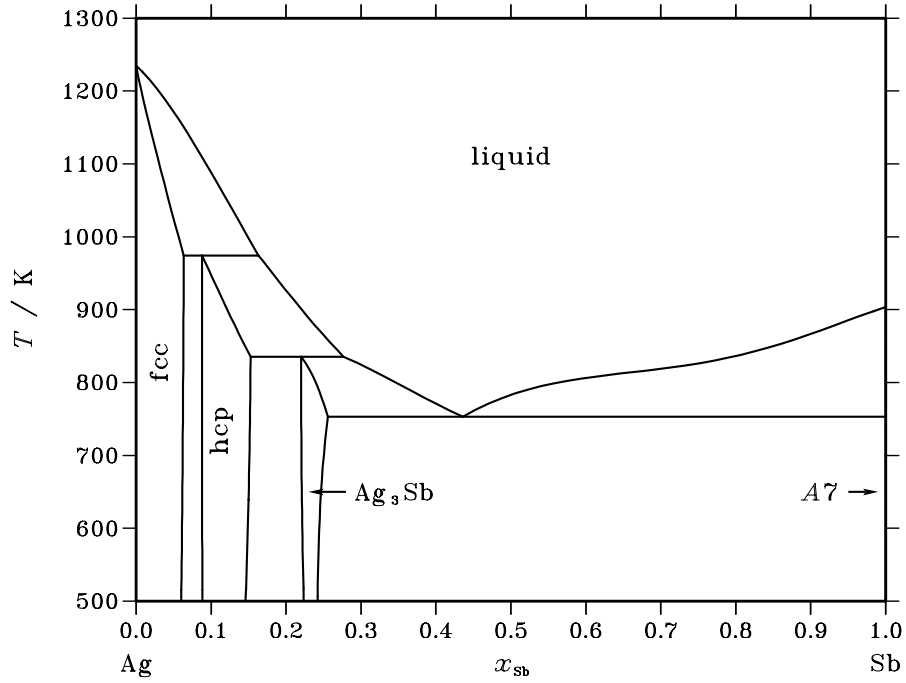

Fig. 1. Calculated phase diagram for the system Ag-Sb.

While the lead-tin system is a basic building block for a range of commonly used solders there has been a growing requirement for the development of alternative materials which are more environmentally sound and provide fewer potential health problems. Tin based solders containing elements such as Ag, Bi, Sb and Zn are candidate replacements and therefore a detailed understanding of the thermodynamics and phase equilibria in the Ag-Sb system is required. The selected assessment to be included in the SGTE database is by Oh et al. [96Oh] and is compatible with the SGTE data for the pure elements [91Din] and has shown to be successful already in the modelling of multicomponent systems.
The system is characterised by a continuous solution of the elements in the liquid phase, limited solubility of Sb in the Ag based solid solution, a region of stability for a disordered hexagonal solid solution on the Ag side of the system and an intermetallic compound Ag_3Sb (isostructural with Ag_3Sn) which exists over a range of homogeneity. Solubility of Ag in the rhombohedral structure of Sb is small. The Ag_3Sb phase was modelled as a two sublattice phase allowing a significant range of homogeneity to either side of the stoichiometric composition. There have been extensive measurements of both thermodynamic properties and the phase diagram for the system. The experimental data show some scatter but the critically assessed data are in good agreement with those considered to be most reliable. There have been comprehensive measurements of the enthalpies of mixing and activities of both components in the liquid and solid phases.

Table I. Phases, structures and models.

Phase	Struktur-bericht	Prototype	Pearson symbol	Space group	SGTE name	Model
liquid					LIQUID	$(Ag,Sb)_1$
fcc	$A1$	Cu	$cF4$	$Fm\overline{3}m$	FCC_A1	$(Ag,Sb)_1$
hcp	$A3$	Mg	$hP2$	$P6_3/mmc$	HCP_A3	$(Ag,Sb)_1$
Ag_3Sb	$L6_0$	$CuTi_3$	$tP4$	$P4/mmm$	L60_AG3SB	$(Ag,Sb)_3(Ag,Sb)_1$
$A7$	$A7$	αAs	$hR2$	$R\overline{3}m$	RHOMBO_A7	Sb_1

Table II. Invariant reactions.

Reaction	Type	T / K	Compositions / x_{Sb}			$\Delta_{\mathrm{r}}H$ / (J/mol)
fcc + liquid ⇌ hcp	peritectic	974.4	0.064	0.163	0.088	−2515
hcp + liquid ⇌ Ag_3Sb	peritectic	835.5	0.153	0.277	0.220	−6071
liquid ⇌ Ag_3Sb + $A7$	eutectic	753.2	0.436	0.256	1.000	−13852

Table IIIa. Integral quantities for the liquid phase at 1300 K.

x_{Sb}	ΔG_{m} [J/mol]	ΔH_{m} [J/mol]	ΔS_{m} [J/(mol·K)]	$G^{\mathrm{E}}_{\mathrm{m}}$ [J/mol]	$S^{\mathrm{E}}_{\mathrm{m}}$ [J/(mol·K)]	ΔC_p [J/(mol·K)]
0.000	0	0	0.000	0	0.000	0.000
0.100	−6292	−2062	3.253	−2778	0.551	0.000
0.200	−9448	−2583	5.281	−4039	1.120	0.000
0.300	−10899	−2143	6.735	−4296	1.656	0.000
0.400	−11235	−1224	7.701	−3960	2.105	0.000
0.500	−10836	−205	8.177	−3344	2.414	0.000
0.600	−9933	630	8.126	−2659	2.530	0.000
0.700	−8621	1101	7.478	−2019	2.399	0.000
0.800	−6845	1124	6.130	−1436	1.970	0.000
0.900	−4339	718	3.890	−826	1.188	0.000
1.000	0	0	0.000	0	0.000	0.000

Reference states: Ag(liquid), Sb(liquid)

Table IIIb. Partial quantities for Ag in the liquid phase at 1300 K.

x_{Ag}	ΔG_{Ag} [J/mol]	ΔH_{Ag} [J/mol]	ΔS_{Ag} [J/(mol·K)]	$G^{\mathrm{E}}_{\mathrm{Ag}}$ [J/mol]	$S^{\mathrm{E}}_{\mathrm{Ag}}$ [J/(mol·K)]	a_{Ag}	γ_{Ag}
1.000	0	0	0.000	0	0.000	1.000	1.000
0.900	−1991	−876	0.858	−852	−0.018	0.832	0.924
0.800	−5087	−2679	1.852	−2675	−0.003	0.625	0.781
0.700	−8451	−4398	3.118	−4596	0.152	0.458	0.654
0.600	−11562	−5320	4.801	−6041	0.554	0.343	0.572
0.500	−14225	−5033	7.071	−6733	1.308	0.268	0.536
0.400	−16601	−3420	10.139	−6697	2.521	0.215	0.538
0.300	−19268	−667	14.308	−6255	4.298	0.168	0.561
0.200	−23423	2743	20.128	−6027	6.746	0.115	0.573
0.100	−31824	6028	29.116	−6935	9.971	0.053	0.526
0.000	$-\infty$	8106	∞	−10198	14.080	0.000	0.389

Reference state: Ag(liquid)

Table IIIc. Partial quantities for Sb in the liquid phase at 1300 K.

x_{Sb}	ΔG_{Sb} [J/mol]	ΔH_{Sb} [J/mol]	ΔS_{Sb} [J/(mol·K)]	G^E_{Sb} [J/mol]	S^E_{Sb} [J/(mol·K)]	a_{Sb}	γ_{Sb}
0.000	$-\infty$	−30512	∞	−37314	5.232	0.000	0.032
0.100	−45002	−12741	24.816	−20114	5.671	0.016	0.156
0.200	−26894	−2200	18.995	−9498	5.614	0.083	0.415
0.300	−16611	3117	15.175	−3597	5.165	0.215	0.717
0.400	−10744	4921	12.050	−840	4.432	0.370	0.925
0.500	−7446	4622	9.283	46	3.520	0.502	1.004
0.600	−5488	3330	6.783	33	2.536	0.602	1.003
0.700	−4059	1858	4.551	−203	1.586	0.687	0.981
0.800	−2701	720	2.631	−289	0.776	0.779	0.974
0.900	−1285	128	1.088	−147	0.212	0.888	0.987
1.000	0	0	0.000	0	0.000	1.000	1.000

Reference state: Sb(liquid)

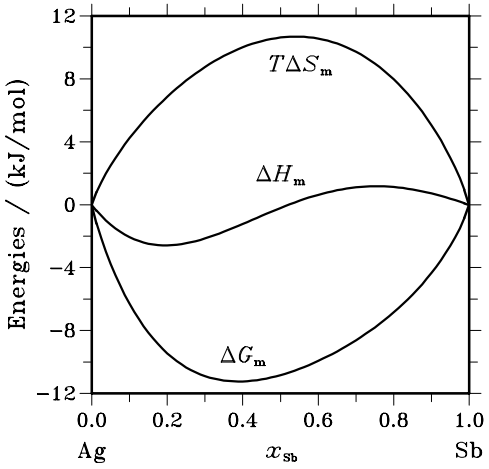

Fig. 2. Integral quantities of the liquid phase at T=1300 K.

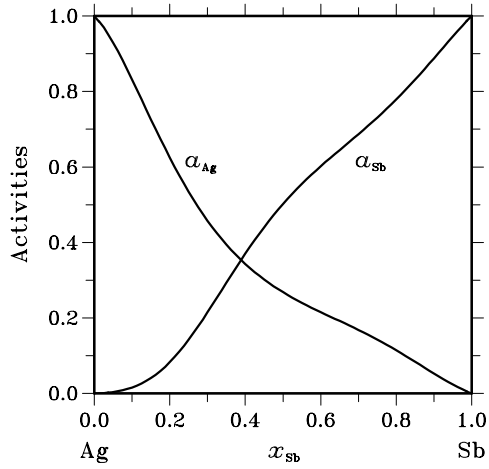

Fig. 3. Activities in the liquid phase at T=1300 K.

References

[96Oh] C.-S. Oh, J.-H. Shim, B.-J. Lee, D.N. Lee: J. Alloys Comp. **238** (1996) 155–166.

Ag – Si (Silver – Silicon)

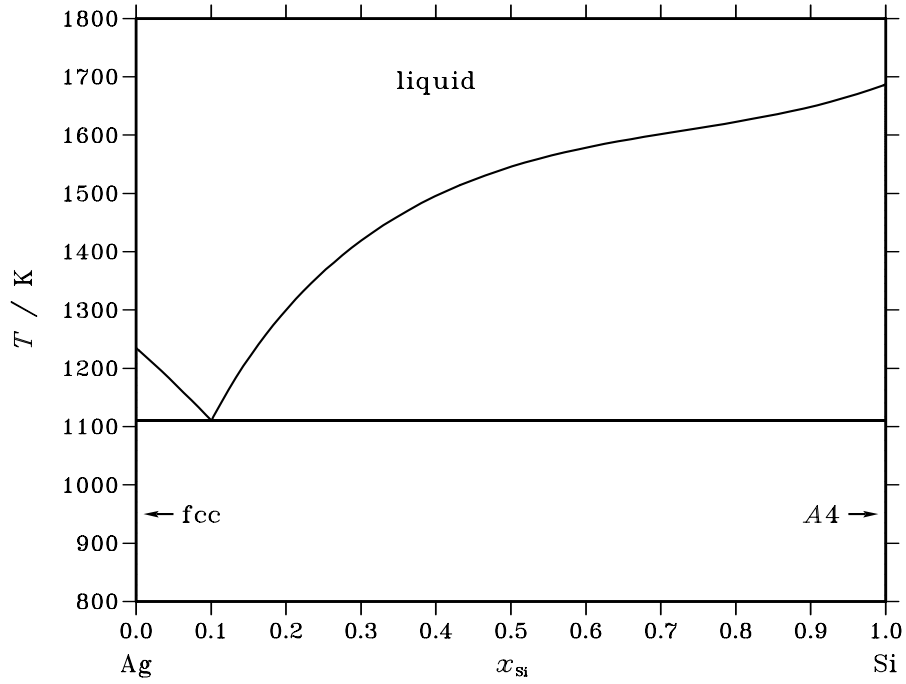

Fig. 1. Calculated phase diagram for the system Ag-Si.

The Ag-Si system has been critically assessed by Chevalier [88Che]. The phase diagram is rather simple and of eutectic type. It shows a complete mutual solubility in the liquid state, no reported solid solubility of silicon in the silver rich terminal solid solution, and a negligible solid solubility of silver in pure silicon. There are no compounds in the system and the liquid is modelled with a simple substitutional model. Solid Si is modelled as a stoichiometric phase.

The calculated liquidus is in good agreement with experimental data determined by thermal and metallographic studies [08Arr, 48Haj, 57Got, 63Hag, 75Pre]. The enthalpy of mixing in the liquid phase has been calculated by Hassam et al. [83Has] from their own calorimetric measurements. Their results are very different from those of Robinson and Tarby [71Rob] from partial pressure measurements, but in good agreement with the EMF results of Sakao and Elliott [74Sak].

The calculated chemical potentials of the elements in the liquid phase are in good agreement with the selected values of Hultgren et al. [73Hul]. The silver potential agrees with EMF measurements [70Ver, 74Sak], but it deviates substantially from older results [65OKe, 68Tup]. The activity coefficient of silicon was determined by equilibrating molten silver and silicon nitride at 1673 K in nitrogen + hydrogen gas mixtures and from the solubility data by Turkdogan and Grieveson [63Tur].

Table I. Phases, structures and models.

Phase	Struktur-bericht	Prototype	Pearson symbol	Space group	SGTE name	Model
liquid					LIQUID	$(Ag,Si)_1$
fcc	$A1$	Cu	$cF4$	$Fm\overline{3}m$	FCC_A1	Ag_1
$A4$	$A4$	C(diamond)	$cF8$	$Fd\overline{3}m$	DIAMOND_A4	Si_1

Table II. Invariant reactions.

Reaction	Type	T / K	Compositions / x_{Si}			$\Delta_{\mathrm{r}}H$ / (J/mol)
liquid $\rightleftharpoons$ fcc + $A4$	eutectic	1110.4	0.100	0.000	1.000	−14957

Table IIIa. Integral quantities for the liquid phase at 1700 K.

x_{Si}	ΔG_{m} [J/mol]	ΔH_{m} [J/mol]	ΔS_{m} [J/(mol·K)]	$G_{\mathrm{m}}^{\mathrm{E}}$ [J/mol]	$S_{\mathrm{m}}^{\mathrm{E}}$ [J/(mol·K)]	ΔC_p [J/(mol·K)]
0.000	0	0	0.000	0	0.000	0.000
0.100	−4121	−162	2.329	474	−0.374	0.000
0.200	−6006	226	3.666	1067	−0.495	0.000
0.300	−6938	971	4.653	1696	−0.426	0.000
0.400	−7237	1881	5.364	2276	−0.232	0.000
0.500	−7075	2763	5.787	2723	0.024	0.000
0.600	−6561	3424	5.874	2951	0.278	0.000
0.700	−5756	3671	5.545	2878	0.466	0.000
0.800	−4655	3311	4.686	2418	0.525	0.000
0.900	−3108	2151	3.094	1487	0.391	0.000
1.000	0	0	0.000	0	0.000	0.000

Reference states: Ag(liquid), Si(liquid)

Table IIIb. Partial quantities for Ag in the liquid phase at 1700 K.

x_{Ag}	ΔG_{Ag} [J/mol]	ΔH_{Ag} [J/mol]	ΔS_{Ag} [J/(mol·K)]	$G_{\mathrm{Ag}}^{\mathrm{E}}$ [J/mol]	$S_{\mathrm{Ag}}^{\mathrm{E}}$ [J/(mol·K)]	a_{Ag}	γ_{Ag}
1.000	0	0	0.000	0	0.000	1.000	1.000
0.900	−1563	−307	0.739	−74	−0.137	0.895	0.995
0.800	−3338	−972	1.392	−184	−0.464	0.790	0.987
0.700	−5201	−1608	2.114	−160	−0.852	0.692	0.989
0.600	−7054	−1831	3.073	166	−1.175	0.607	1.012
0.500	−8834	−1254	4.459	964	−1.304	0.535	1.071
0.400	−10551	508	6.505	2401	−1.113	0.474	1.185
0.300	−12371	3841	9.536	4647	−0.474	0.417	1.389
0.200	−14879	9130	14.123	7870	0.741	0.349	1.745
0.100	−20306	16760	21.804	12241	2.659	0.238	2.377
0.000	$-\infty$	27118	∞	17926	5.407	0.000	3.555

Reference state: Ag(liquid)

Table IIIc. Partial quantities for Si in the liquid phase at 1700 K.

x_{Si}	ΔG_{Si} [J/mol]	ΔH_{Si} [J/mol]	ΔS_{Si} [J/(mol·K)]	G^E_{Si} [J/mol]	S^E_{Si} [J/(mol·K)]	a_{Si}	γ_{Si}
0.000	$-\infty$	−5014	∞	3855	−5.217	0.000	1.314
0.100	−27145	1144	16.640	5402	−2.505	0.147	1.465
0.200	−16680	5017	12.763	6069	−0.619	0.307	1.536
0.300	−10992	6990	10.578	6026	0.567	0.459	1.532
0.400	−7511	7449	8.800	5440	1.182	0.588	1.469
0.500	−5316	6780	7.115	4482	1.352	0.687	1.373
0.600	−3902	5367	5.452	3318	1.205	0.759	1.265
0.700	−2922	3597	3.835	2120	0.869	0.813	1.162
0.800	−2099	1856	2.327	1055	0.471	0.862	1.077
0.900	−1197	528	1.015	292	0.139	0.919	1.021
1.000	0	0	0.000	0	0.000	1.000	1.000

Reference state: Si(liquid)

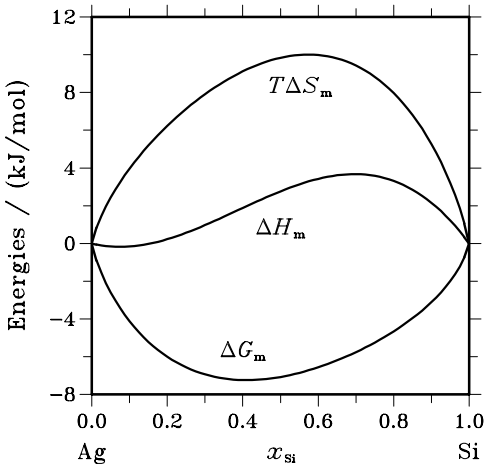

Fig. 2. Integral quantities of the liquid phase at T=1700 K.

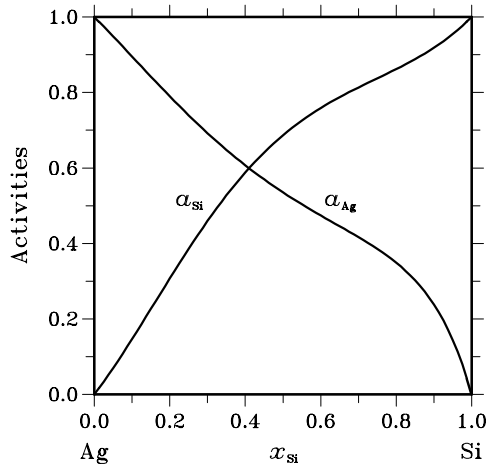

Fig. 3. Activities in the liquid phase at T=1700 K.

References

[08Arr] G. Arrivaut: Z. Anorg. Chem. **60** (1908) 436.
[48Haj] O. Hajicek: Hutn. Listy **3** (1948) 265–270.
[57Got] V. Gottardi: Met. Ital. **49** (1957) 721–724.
[63Hag] J.P. Hager: Trans. AIME **227** (1963) 1000–1002.
[63Tuk] E.T. Turkdogan, P. Grieveson: Trans. AIME **227** (1963) 1143–1146.
[65OKe] T.J. O'Keefe: Univ. Missouri, No. 65-9133, 1965.
[68Tup] R.H. Tupkary: Ind. J. Technol. **6** (1968) 132–135.
[70Ver] A. Vermande, I. Ansara, P. Desre: Rev. Int. Hautes Temp. Réfract. **7** (1970) 39–43.
[71Rob] V.S. Robinson, S.K. Tarby: Met. Trans. **2** (1971) 1347–1352.
[73Hul] R. Hultgren, P.D. Desai, D.T. Hawkins, M. Gleiser, K.K. Kelley: "Selected Values of the Thermodynamic Properties of Binary Alloys", American Society for Metals, Metals Park, Ohio, 1973.
[74Sak] H. Sakao, J.F. Elliott: Met. Trans. **5** (1974) 2063–2067.
[75Pre] B. Predel, H. Bankstahl: J. Less-Common Met. **43** (1975) 191–203.
[83Has] S. Hassam, M. Gaune-Escard, J.P. Bros: Ber. Bunsenges. Phys. Chem. **87** (1983) 785–792.
[88Che] P.-Y. Chevalier: Thermochim. Acta, **130** (1988) 33–41.

Ag – Sn (Silver – Tin)

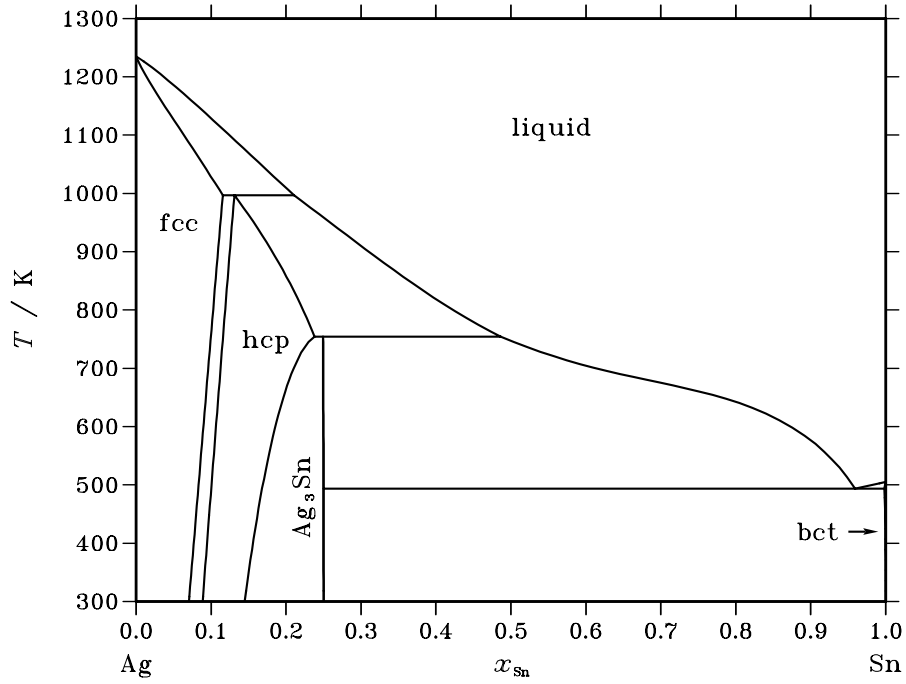

Fig. 1. Calculated phase diagram for the system Ag-Sn.

While the lead-tin system is a basic building block for a range of commonly used solders there has been a growing requirement for the development of alternative materials which are more environmentally sound and provide fewer potential health problems. Tin based solders containing elements such as Ag, Bi, Sb and Zn are candidate replacements and therefore a detailed understanding of the thermodynamics and phase equilibria in the Ag-Sn system is required. A number of good quality assessments has been carried out on the Ag-Sn system [87Kar, 96Oh, 88Che, 94Kat]. The one by Oh et al. [96Oh] was selected to be included in the SGTE database because of its basic compatibility with the SGTE data for the pure elements [91Din] and its successful use already in the modelling of multicomponent systems. A modification of the data for the fcc phase has been made [99Din] for compatibility with the latest SGTE data for the elements.
The system is characterised by a continuous solution of the elements in the liquid phase, limited solubility of Sn in the Ag based solid solution, a region of stability for a disordered hexagonal solid solution on the Ag side of the system and an intermetallic compound Ag_3Sn which exists over a narrow range of homogeneity. Solubility of Ag in the body centred tetragonal structure of Sn is small. The Ag_3Sn phase was modelled as a two sublattice phase allowing a small range of homogeneity to composition richer in Ag than the stoichiometric composition. There have been extensive measurements of both thermodynamic properties and the phase diagram and the assessed data are in very good agreement throughout. There have been comprehensive measurements of the enthalpies of mixing and activities of both components in the liquid. Experimental thermodynamic properties for the solid phases are rather more limited.

Table I. Phases, structures and models.

Phase	Struktur-bericht	Prototype	Pearson symbol	Space group	SGTE name	Model
liquid					LIQUID	$(Ag,Sn)_1$
fcc	$A1$	Cu	$cF4$	$Fm\overline{3}m$	FCC_A1	$(Ag,Sn)_1$
hcp	$A3$	Mg	$hP2$	$P6_3/mmc$	HCP_A3	$(Ag,Sn)_1$
Ag_3Sn	$L6_0$	$CuTi_3$	$tP4$	$P4/mmm$	AG3M	$Ag_3(Ag,Sn)_1$
bct	$A5$	βSn	$tI4$	$I4_1/amd$	BCT_A5	$(Ag,Sn)_1$

Table II. Invariant reactions.

Reaction	Type	T / K	Compositions / x_{Sn}			$\Delta_r H$ / (J/mol)
fcc + liquid $\rightleftharpoons$ hcp	peritectic	996.8	0.116	0.211	0.131	−1919
hcp + liquid $\rightleftharpoons$ Ag_3Sn	peritectic	754.3	0.238	0.486	0.250	−1880
liquid $\rightleftharpoons$ Ag_3Sn + bct	eutectic	493.7	0.959	0.250	0.998	−7525

Table IIIa. Integral quantities for the liquid phase at 1250 K.

x_{Sn}	ΔG_m [J/mol]	ΔH_m [J/mol]	ΔS_m [J/(mol·K)]	G_m^E [J/mol]	S_m^E [J/(mol·K)]	ΔC_p [J/(mol·K)]
0.000	0	0	0.000	0	0.000	0.000
0.100	−5629	−1986	2.915	−2251	0.212	0.000
0.200	−8530	−2725	4.643	−3329	0.483	0.000
0.300	−9948	−2633	5.852	−3599	0.773	0.000
0.400	−10356	−2058	6.639	−3362	1.043	0.000
0.500	−10056	−1287	7.016	−2852	1.253	0.000
0.600	−9238	−541	6.958	−2243	1.362	0.000
0.700	−7991	22	6.410	−1642	1.331	0.000
0.800	−6293	308	5.281	−1093	1.120	0.000
0.900	−3952	289	3.393	−573	0.690	0.000
1.000	0	0	0.000	0	0.000	0.000

Reference states: Ag(liquid), Sn(liquid)

Table IIIb. Partial quantities for Ag in the liquid phase at 1250 K.

x_{Ag}	ΔG_{Ag} [J/mol]	ΔH_{Ag} [J/mol]	ΔS_{Ag} [J/(mol·K)]	G^E_{Ag} [J/mol]	S^E_{Ag} [J/(mol·K)]	a_{Ag}	γ_{Ag}
1.000	0	0	0.000	0	0.000	1.000	1.000
0.900	−1747	−698	0.840	−652	−0.036	0.845	0.939
0.800	−4411	−2206	1.764	−2091	−0.092	0.654	0.818
0.700	−7391	−3793	2.879	−3684	−0.087	0.491	0.702
0.600	−10300	−4919	4.305	−4991	0.058	0.371	0.619
0.500	−12968	−5237	6.186	−5764	0.422	0.287	0.574
0.400	−15473	−4591	8.705	−5949	1.086	0.226	0.564
0.300	−18197	−3022	12.140	−5684	2.130	0.174	0.579
0.200	−22025	−758	17.013	−5298	3.632	0.120	0.601
0.100	−29245	1776	24.817	−5314	5.672	0.060	0.600
0.000	−∞	3965	∞	−6449	8.331	0.000	0.538

Reference state: Ag(liquid)

Table IIIc. Partial quantities for Sn in the liquid phase at 1250 K.

x_{Sn}	ΔG_{Sn} [J/mol]	ΔH_{Sn} [J/mol]	ΔS_{Sn} [J/(mol·K)]	G^E_{Sn} [J/mol]	S^E_{Sn} [J/(mol·K)]	a_{Sn}	γ_{Sn}
0.000	−∞	−27634	∞	−29745	1.689	0.000	0.057
0.100	−40567	−13581	21.589	−16636	2.444	0.020	0.202
0.200	−25007	−4803	16.163	−8280	2.782	0.090	0.451
0.300	−15914	75	12.791	−3401	2.780	0.216	0.721
0.400	−10440	2234	10.139	−917	2.521	0.366	0.916
0.500	−7144	2663	7.846	60	2.083	0.503	1.006
0.600	−5082	2159	5.793	227	1.546	0.613	1.022
0.700	−3617	1326	3.954	90	0.989	0.706	1.009
0.800	−2360	575	2.348	−41	0.493	0.797	0.996
0.900	−1142	124	1.012	−47	0.136	0.896	0.996
1.000	0	0	0.000	0	0.000	1.000	1.000

Reference state: Sn(liquid)

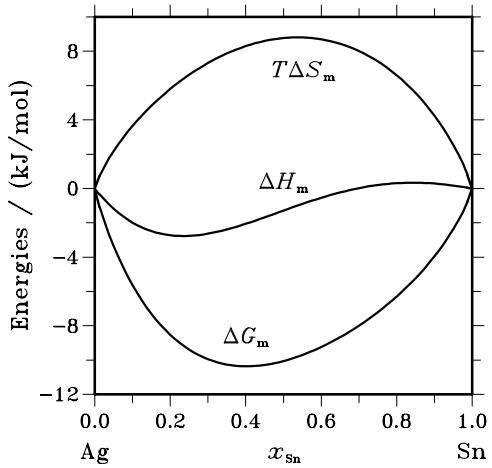

Fig. 2. Integral quantities of the liquid phase at T=1250 K.

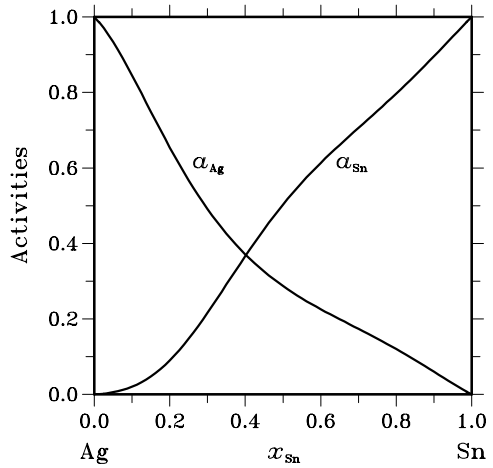

Fig. 3. Activities in the liquid phase at T=1250 K.

Table IV. Standard reaction quantities at 298.15 K for the compounds per mole of atoms.

Compound	x_{Sn}	$\Delta_{\mathrm{f}}G^{\circ}$ / (J/mol)	$\Delta_{\mathrm{f}}H^{\circ}$ / (J/mol)	$\Delta_{\mathrm{f}}S^{\circ}$ / (J/(mol·K))	$\Delta_{\mathrm{f}}C_P^{\circ}$ / (J/(mol·K))
Ag_3Sn	0.250	−4636	−3826	2.718	−0.561

References

[87Kar] I. Karakaya, W.T. Thompson: Bull. Alloy Phase Diagrams **8** (1987) 340–347.
[88Che] P.-Y. Chevalier: Thermochim. Acta **136** (1988) 45–54.
[94Kat] U.R. Kattner, W.J. Boettinger: J. Electron. Mater. **23** (1994) 603–610.
[96Oh] C.-S. Oh, J.-H. Shim, B.-J. Lee, D.N. Lee: J. Alloys Comp. **23** (1996) 155–166.
[99Din] A.T. Dinsdale: unpublished work, 1999.

Ag – Ti (Silver – Titanium)

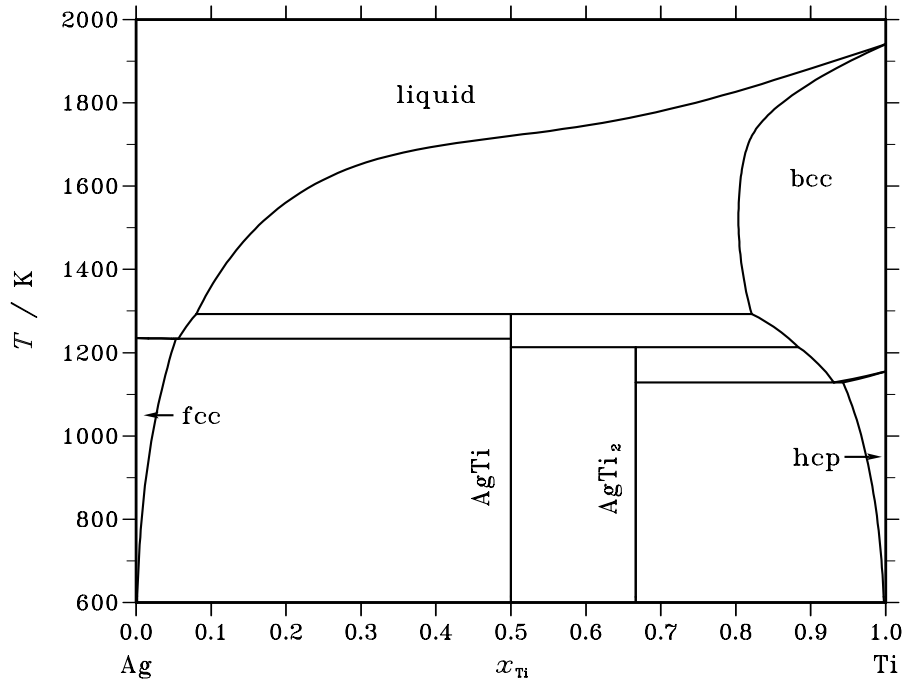

Fig. 1. Calculated phase diagram for the system Ag-Ti.

The phase diagram of the Ag-Ti system has been reviewed by [87Mur] and is characterised by two compound phases (AgTi and $AgTi_2$), which have been modelled here as stoichiometric, and by a rather extensive bcc (βTi) solid solution range, treated in the present assessment as a substitutional solution. The invariant reactions of the system are reproduced rather well by the present thermodynamic description. Activities and mixing enthalpies for the liquid phase show large positive deviations from ideality which reflect the tendency to immiscibility suggested by the rather flat liquidus.

Table I. Phases, structures and models.

Phase	Struktur-bericht	Prototype	Pearson symbol	Space group	SGTE name	Model
liquid					LIQUID	$(Ag,Ti)_1$
fcc	$A1$	Cu	$cF4$	$Fm\overline{3}m$	FCC_A1	$(Ag,Ti)_1$
AgTi	$B11$	γCuTi	$tP4$	$P4/nmm$	B11	Ag_1Ti_1
$AgTi_2$	$C11_b$	$MoSi_2$	$tI6$	$I4/mmm$	C11B	Ag_1Ti_2
hcp	$A3$	Mg	$hP2$	$P6_3/mmc$	HCP_A3	$(Ag,Ti)_1$
bcc	$A2$	W	$cI2$	$Im\overline{3}m$	BCC_A2	$(Ag,Ti)_1$

Table II. Invariant reactions.

Reaction	Type	T / K	Compositions / x_{Ti}			$\Delta_r H$ / (J/mol)
liquid + bcc $\rightleftharpoons$ AgTi	peritectic	1293.1	0.080	0.821	0.500	−11199
liquid $\rightleftharpoons$ fcc + AgTi	eutectic	1233.1	0.056	0.053	0.500	−11258
AgTi + bcc $\rightleftharpoons$ $AgTi_2$	peritectoid	1213.3	0.500	0.883	0.667	−3194
bcc $\rightleftharpoons$ $AgTi_2$ + hcp	eutectoid	1128.2	0.931	0.667	0.943	−4425

Table IIIa. Integral quantities for the liquid phase at 2000 K.

x_{Ti}	ΔG_{m} [J/mol]	ΔH_{m} [J/mol]	ΔS_{m} [J/(mol·K)]	$G_{\mathrm{m}}^{\mathrm{E}}$ [J/mol]	$S_{\mathrm{m}}^{\mathrm{E}}$ [J/(mol·K)]	ΔC_p [J/(mol·K)]
0.000	0	0	0.000	0	0.000	0.000
0.100	−3081	2403	2.742	2325	0.039	0.000
0.200	−4200	4260	4.230	4121	0.070	0.000
0.300	−4764	5577	5.170	5394	0.091	0.000
0.400	−5044	6356	5.700	6147	0.104	0.000
0.500	−5141	6602	5.872	6385	0.109	0.000
0.600	−5079	6321	5.700	6112	0.104	0.000
0.700	−4825	5516	5.170	5333	0.091	0.000
0.800	−4270	4191	4.230	4052	0.070	0.000
0.900	−3133	2351	2.742	2272	0.039	0.000
1.000	0	0	0.000	0	0.000	0.000

Reference states: Ag(liquid), Ti(liquid)

Table IIIb. Partial quantities for Ag in the liquid phase at 2000 K.

x_{Ag}	ΔG_{Ag} [J/mol]	ΔH_{Ag} [J/mol]	ΔS_{Ag} [J/(mol·K)]	$G_{\mathrm{Ag}}^{\mathrm{E}}$ [J/mol]	$S_{\mathrm{Ag}}^{\mathrm{E}}$ [J/(mol·K)]	a_{Ag}	γ_{Ag}
1.000	0	0	0.000	0	0.000	1.000	1.000
0.900	−1487	274	0.880	265	0.004	0.914	1.016
0.800	−2657	1088	1.873	1054	0.017	0.852	1.065
0.700	−3574	2436	3.005	2357	0.039	0.807	1.152
0.600	−4327	4307	4.317	4168	0.070	0.771	1.285
0.500	−5051	6693	5.872	6476	0.109	0.738	1.476
0.400	−5964	9586	7.775	9273	0.157	0.699	1.747
0.300	−7471	12976	10.224	12550	0.213	0.638	2.127
0.200	−10464	16856	13.660	16299	0.278	0.533	2.665
0.100	−17779	21216	19.497	20511	0.352	0.343	3.433
0.000	$-\infty$	26047	∞	25177	0.435	0.000	4.545

Reference state: Ag(liquid)

Table IIIc. Partial quantities for Ti in the liquid phase at 2000 K.

x_{Ti}	ΔG_{Ti} [J/mol]	ΔH_{Ti} [J/mol]	ΔS_{Ti} [J/(mol·K)]	$G_{\mathrm{Ti}}^{\mathrm{E}}$ [J/mol]	$S_{\mathrm{Ti}}^{\mathrm{E}}$ [J/(mol·K)]	a_{Ti}	γ_{Ti}
0.000	$-\infty$	26773	∞	25903	0.435	0.000	4.748
0.100	−17426	21569	19.497	20864	0.352	0.351	3.507
0.200	−10371	16949	13.660	16392	0.278	0.536	2.680
0.300	−7542	12905	10.224	12479	0.213	0.635	2.118
0.400	−6121	9429	7.775	9116	0.157	0.692	1.730
0.500	−5232	6512	5.872	6294	0.109	0.730	1.460
0.600	−4489	4144	4.317	4005	0.070	0.763	1.272
0.700	−3691	2318	3.005	2240	0.039	0.801	1.144
0.800	−2721	1024	1.873	990	0.017	0.849	1.061
0.900	−1506	255	0.880	246	0.004	0.913	1.015
1.000	0	0	0.000	0	0.000	1.000	1.000

Reference state: Ti(liquid)

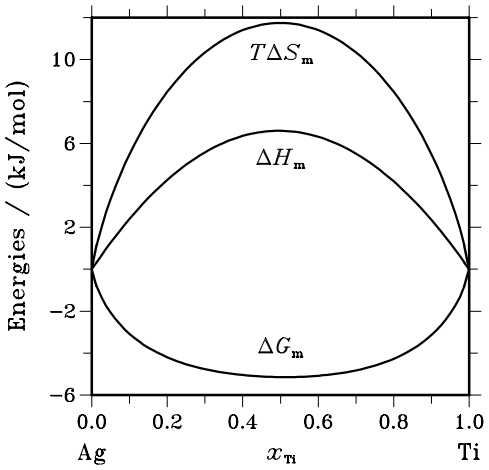

Fig. 2. Integral quantities of the liquid phase at T=2000 K.

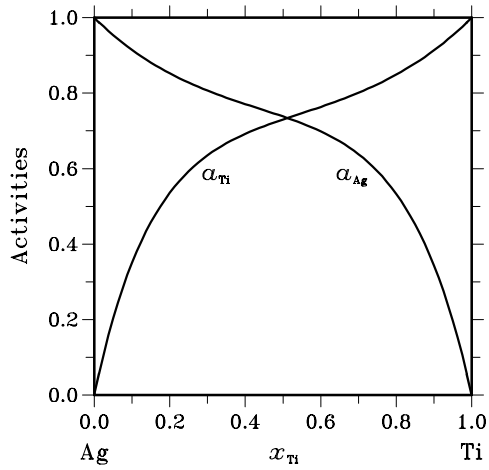

Fig. 3. Activities in the liquid phase at T=2000 K.

Table IV. Standard reaction quantities at 298.15 K for the compounds per mole of atoms.

Compound	x_{Ti}	$\Delta_f G^\circ$ / (J/mol)	$\Delta_f H^\circ$ / (J/mol)	$\Delta_f S^\circ$ / (J/(mol·K))	$\Delta_f C_P^\circ$ / (J/(mol·K))
Ag_1Ti_1	0.500	−1517	−1502	0.050	0.000
Ag_1Ti_2	0.667	−1365	−1345	0.067	0.000

References

[87Mur] J.L. Murray, K.J. Bhansali: Bull. Alloy Phase Diagrams **4** (1983) 178–183.

Ag – Tl (Silver – Thallium)

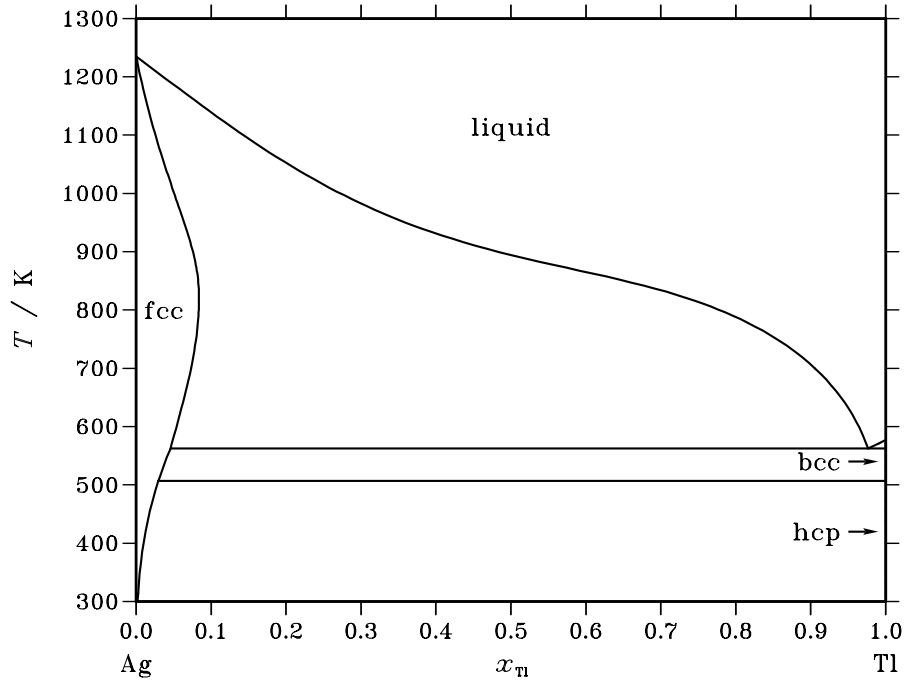

Fig. 1. Calculated phase diagram for the system Ag-Tl.

A review of experimental phase equilibrium data and thermodynamic measurements have been presented by [89Bar]. The recommended thermodynamic description [98Luk] is an update of that of Zimmermann et al. [76Zim], in order to make it compatible with the SGTE unary data.
The Ag-Tl system is a simple nearly degenerate eutectic system. The (Ag) fcc solid solution has a retrograde solidus with a maximum solubility of about 8 at.% Tl. The solubility of Ag in solid Tl has not been determined and it is assumed to be very low. The hcp and bcc phases are modelled as pure Tl. The fcc and liquid phases are described by the substitutional model. The enthalpy of mixing of Ag-Tl liquid alloys has been measured calorimetrically. The activity of Tl in liquid solutions has been obtained by EMF and by vapour pressure measurements. Recent measurements of activities of Tl in liquid Ag-Tl [83Kam] are in good agreement with the measurements used in [76Zim]. The calculated thermodynamic properties and the phase diagram are in good agreement with experimental data.

Table I. Phases, structures and models.

Phase	Struktur-bericht	Prototype	Pearson symbol	Space group	SGTE name	Model
liquid					LIQUID	$(Ag,Tl)_1$
fcc	$A1$	Cu	$cF4$	$Fm\overline{3}m$	FCC_A1	$(Ag,Tl)_1$
bcc	$A2$	W	$cI2$	$Im\overline{3}m$	BCC_A2	Tl_1
hcp	$A3$	Mg	$hP2$	$P6_3/mmc$	HCP_A3	Tl_1

Table II. Invariant reactions.

Reaction	Type	T / K	Compositions / x_{Tl}			$\Delta_{\mathrm{r}}H$ / (J/mol)
liquid ⇌ fcc + bcc	eutectic	562.4	0.976	0.046	1.000	−4734
fcc + bcc ⇌ hcp	degenerate	507.0	0.030	1.000	1.000	−360

Table IIIa. Integral quantities for the liquid phase at 1300 K.

x_{Tl}	ΔG_{m} [J/mol]	ΔH_{m} [J/mol]	ΔS_{m} [J/(mol·K)]	$G^{\mathrm{E}}_{\mathrm{m}}$ [J/mol]	$S^{\mathrm{E}}_{\mathrm{m}}$ [J/(mol·K)]	ΔC_p [J/(mol·K)]
0.000	0	0	0.000	0	0.000	0.000
0.100	−3300	1164	3.434	213	0.732	0.000
0.200	−4916	2213	5.484	492	1.323	0.000
0.300	−5839	3075	6.857	764	1.778	0.000
0.400	−6302	3692	7.688	972	2.092	0.000
0.500	−6413	4012	8.019	1079	2.256	0.000
0.600	−6209	3993	7.848	1065	2.252	0.000
0.700	−5676	3602	7.137	927	2.058	0.000
0.800	−4730	2814	5.803	678	1.643	0.000
0.900	−3161	1616	3.674	353	0.971	0.000
1.000	0	0	0.000	0	0.000	0.000

Reference states: Ag(liquid), Tl(liquid)

Table IIIb. Partial quantities for Ag in the liquid phase at 1300 K.

x_{Ag}	ΔG_{Ag} [J/mol]	ΔH_{Ag} [J/mol]	ΔS_{Ag} [J/(mol·K)]	$G^{\mathrm{E}}_{\mathrm{Ag}}$ [J/mol]	$S^{\mathrm{E}}_{\mathrm{Ag}}$ [J/(mol·K)]	a_{Ag}	γ_{Ag}
1.000	0	0	0.000	0	0.000	1.000	1.000
0.900	−1185	46	0.947	−46	0.071	0.896	0.996
0.800	−2491	280	2.132	−79	0.277	0.794	0.993
0.700	−3834	828	3.587	21	0.621	0.701	1.002
0.600	−5200	1787	5.375	322	1.128	0.618	1.030
0.500	−6655	3229	7.603	837	1.840	0.540	1.081
0.400	−8375	5195	10.439	1530	2.820	0.461	1.152
0.300	−10706	7704	14.162	2308	4.151	0.371	1.238
0.200	−14369	10744	19.317	3028	5.936	0.265	1.323
0.100	−21395	14277	27.440	3493	8.295	0.138	1.382
0.000	−∞	18238	∞	3456	11.371	0.000	1.377

Reference state: Ag(liquid)

Table IIIc. Partial quantities for Tl in the liquid phase at 1300 K.

x_{Tl}	ΔG_{Tl} [J/mol]	ΔH_{Tl} [J/mol]	ΔS_{Tl} [J/(mol·K)]	G^E_{Tl} [J/mol]	S^E_{Tl} [J/(mol·K)]	a_{Tl}	γ_{Tl}
0.000	$-\infty$	11972	∞	1519	8.041	0.000	1.151
0.100	−22336	11232	25.821	2552	6.676	0.127	1.266
0.200	−14617	9942	18.891	2780	5.509	0.259	1.293
0.300	−10516	8318	14.488	2497	4.478	0.378	1.260
0.400	−7956	6549	11.158	1948	3.539	0.479	1.197
0.500	−6171	4795	8.435	1322	2.672	0.565	1.130
0.600	−4766	3191	6.121	755	1.873	0.643	1.072
0.700	−3521	1843	4.126	335	1.160	0.722	1.031
0.800	−2321	832	2.425	91	0.570	0.807	1.008
0.900	−1135	209	1.034	4	0.158	0.900	1.000
1.000	0	0	0.000	0	0.000	1.000	1.000

Reference state: Tl(liquid)

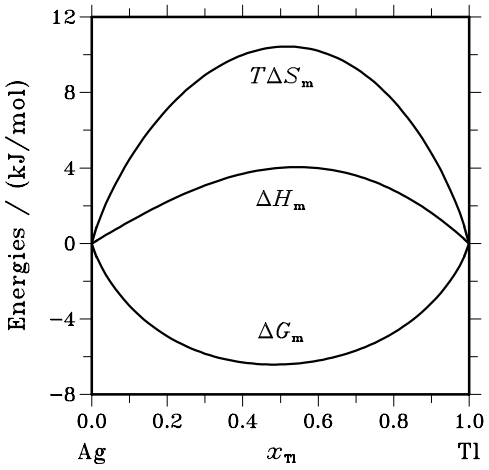

Fig. 2. Integral quantities of the liquid phase at T=1300 K.

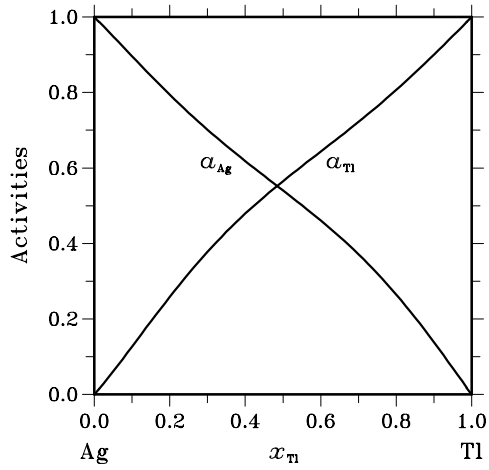

Fig. 3. Activities in the liquid phase at T=1300 K.

References

[76Zim] B. Zimmermann, E.-Th. Henig, H.L. Lukas: Z. Metallkd. **67** (1976) 815–820.
[83Kam] K. Kameda, Y. Yoshida, S. Sakairi: J. Jpn. Inst. Met. **47** (1983) 406–412.
[89Bar] M.R. Baren: Bull. Alloy Phase Diagrams **10** (1989) 641–643.
[98Luk] H.L. Lukas: unpublished optimization 1998.

Ag – Zn (Silver – Zinc)

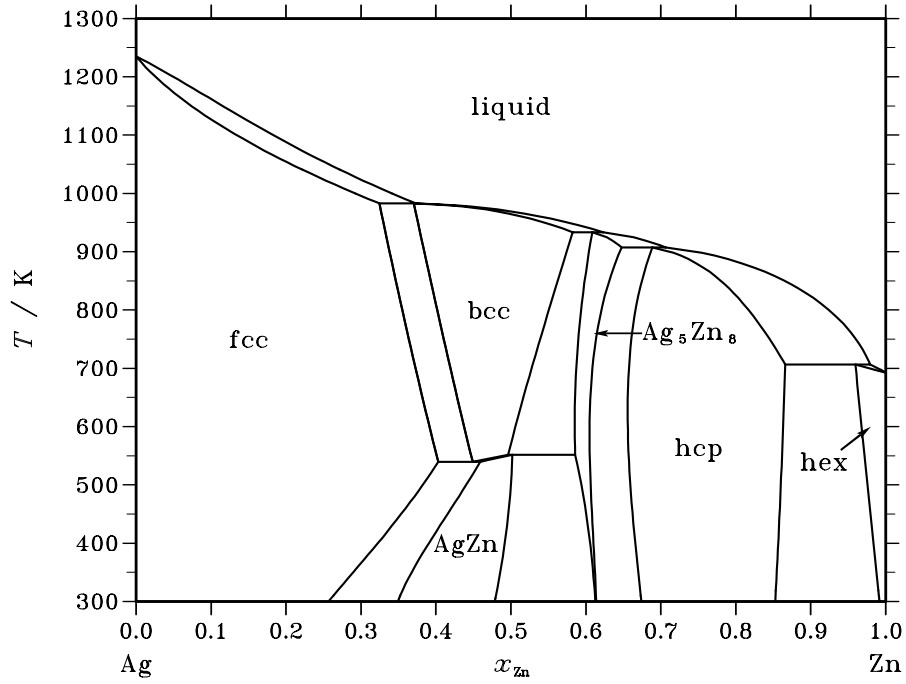

Fig. 1. Calculated phase diagram for the system Ag-Zn.

This system has many similarities with the more well known Cu-Zn system. Pure Ag is stable as fcc and pure Zn has a modified hexagonal structure, here denoted hex-Zn, with a different c/a ratio compared to normal hcp. There is a complete solubility in the liquid phase and a series of peritectic transformations with the intermediate phases. The solubility of Zn in fcc-Ag is large but only a few percent of Ag in hex-Zn. Three intermediate phases are in equilibrium with the liquid, from the Ag side these are bcc, Ag_5Zn_8 and hcp. In contrast with the Cu-Zn phase the bcc phase does not transform to an ordered $B2$ at lower temperatures but a hexagonal phase, AgZn, appears instead.
The system is important for solders. There are a lot of experimental data and the assessment reproduces these well. There are several assessments, the one selected is [98Gom].

Table I. Phases, structures and models.

Phase	Struktur-bericht	Prototype	Pearson symbol	Space group	SGTE name	Model
liquid					LIQUID	$(Ag,Zn)_1$
fcc	$A1$	Cu	$cF4$	$Fm\overline{3}m$	FCC_A1	$(Ag,Zn)_1$
bcc	$A2$	W	$cI2$	$Im\overline{3}m$	BCC_A2	$(Ag,Zn)_1$
AgZn	...	...	$hP*$	...	AGZN_Z	$Zn_1(Ag,Zn)_2$
Ag_5Zn_8	$D8_2$	Cu_5Zn_8	$cI52$	$I\overline{4}3m$	D82	$(Ag,Zn)_2Ag_2(Ag,Zn)_3(Ag,Zn)_6$
hcp	$A3$	Mg	$hP2$	$P6_3/mmc$	HCP_A3	$(Ag,Zn)_1$
hex	$A3$	Mg	$hP2$	$P6_3/mmc$	HCP_ZN	$(Ag,Zn)_1$

Table II. Invariant reactions.

Reaction	Type	T / K	Compositions / x_{Zn}			$\Delta_{\mathrm{r}}H$ / (J/mol)
fcc + liquid ⇌ bcc	peritectic	982.7	0.324	0.373	0.370	−6610
bcc + liquid ⇌ Ag_5Zn_8	peritectic	933.5	0.582	0.623	0.608	−4766
Ag_5Zn_8 + liquid ⇌ hcp	peritectic	907.4	0.648	0.706	0.694	−6762
hcp + liquid ⇌ hex	peritectic	705.6	0.904	0.981	0.962	−5429
bcc + Ag_5Zn_8 ⇌ AgZn	peritectoid	551.9	0.496	0.586	0.502	−1750
bcc ⇌ fcc + AgZn	eutectoid	539.4	0.449	0.403	0.459	−1159

Table IIIa. Integral quantities for the liquid phase at 1300 K.

x_{Zn}	ΔG_{m} [J/mol]	ΔH_{m} [J/mol]	ΔS_{m} [J/(mol·K)]	$G^{\mathrm{E}}_{\mathrm{m}}$ [J/mol]	$S^{\mathrm{E}}_{\mathrm{m}}$ [J/(mol·K)]	ΔC_p [J/(mol·K)]
0.000	0	0	0.000	0	0.000	0.000
0.100	−5684	−2880	2.157	−2170	−0.546	0.000
0.200	−9090	−4944	3.189	−3681	−0.971	0.000
0.300	−11204	−6258	3.804	−4601	−1.275	0.000
0.400	−12269	−6888	4.139	−4994	−1.457	0.000
0.500	−12419	−6900	4.246	−4927	−1.518	0.000
0.600	−11741	−6360	4.139	−4466	−1.457	0.000
0.700	−10280	−5334	3.804	−3677	−1.275	0.000
0.800	−8034	−3888	3.189	−2625	−0.971	0.000
0.900	−4892	−2088	2.157	−1378	−0.546	0.000
1.000	0	0	0.000	0	0.000	0.000

Reference states: Ag(liquid), Zn(liquid)

Table IIIb. Partial quantities for Ag in the liquid phase at 1300 K.

x_{Ag}	ΔG_{Ag} [J/mol]	ΔH_{Ag} [J/mol]	ΔS_{Ag} [J/(mol·K)]	$G^{\mathrm{E}}_{\mathrm{Ag}}$ [J/mol]	$S^{\mathrm{E}}_{\mathrm{Ag}}$ [J/(mol·K)]	a_{Ag}	γ_{Ag}
1.000	0	0	0.000	0	0.000	1.000	1.000
0.900	−1479	−419	0.815	−340	−0.061	0.872	0.969
0.800	−3684	−1588	1.613	−1272	−0.243	0.711	0.889
0.700	−6520	−3375	2.419	−2665	−0.546	0.547	0.782
0.600	−9907	−5648	3.276	−4385	−0.971	0.400	0.666
0.500	−13794	−8275	4.246	−6302	−1.518	0.279	0.558
0.400	−18187	−11124	5.433	−8283	−2.185	0.186	0.465
0.300	−23210	−14063	7.036	−10196	−2.974	0.117	0.389
0.200	−29306	−16960	9.497	−11910	−3.885	0.066	0.332
0.100	−38180	−19683	14.228	−13291	−4.917	0.029	0.292
0.000	$-\infty$	−22100	∞	−14209	−6.070	0.000	0.269

Reference state: Ag(liquid)

Table IIIc. Partial quantities for Zn in the liquid phase at 1300 K.

x_{Zn}	ΔG_{Zn} [J/mol]	ΔH_{Zn} [J/mol]	ΔS_{Zn} [J/(mol·K)]	G^E_{Zn} [J/mol]	S^E_{Zn} [J/(mol·K)]	a_{Zn}	γ_{Zn}
0.000	$-\infty$	−33100	∞	−25209	−6.070	0.000	0.097
0.100	−43526	−25029	14.228	−18637	−4.917	0.018	0.178
0.200	−30714	−18368	9.497	−13318	−3.885	0.058	0.292
0.300	−22132	−12985	7.036	−9118	−2.974	0.129	0.430
0.400	−15811	−8748	5.433	−5907	−2.185	0.232	0.579
0.500	−11044	−5525	4.246	−3552	−1.518	0.360	0.720
0.600	−7443	−3184	3.276	−1921	−0.971	0.502	0.837
0.700	−4738	−1593	2.419	−883	−0.546	0.645	0.922
0.800	−2716	−620	1.613	−304	−0.243	0.778	0.972
0.900	−1193	−133	0.815	−54	−0.061	0.896	0.995
1.000	0	0	0.000	0	0.000	1.000	1.000

Reference state: Zn(liquid)

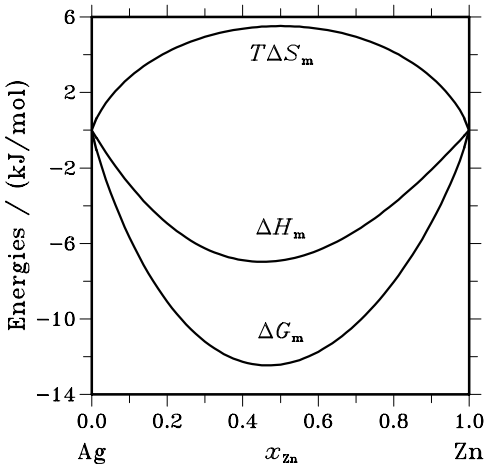

Fig. 2. Integral quantities of the liquid phase at T=1300 K.

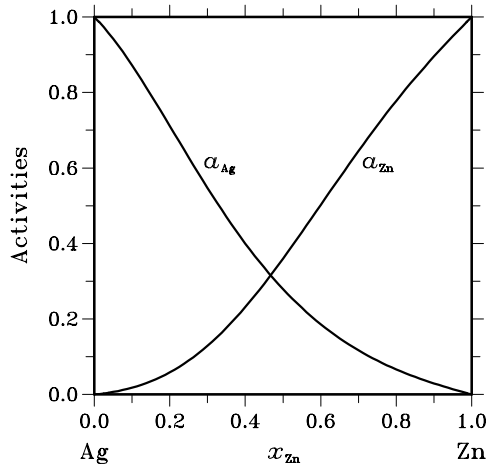

Fig. 3. Activities in the liquid phase at T=1300 K.

Table IVa. Integral quantities for the stable phases at 600 K.

Phase	x_{Zn}	ΔG_{m} [J/mol]	ΔH_{m} [J/mol]	ΔS_{m} [J/(mol·K)]	$G_{\mathrm{m}}^{\mathrm{E}}$ [J/mol]	$S_{\mathrm{m}}^{\mathrm{E}}$ [J/(mol·K)]	ΔC_p [J/(mol·K)]
fcc	0.000	0	0	0.000	0	0.000	0.000
	0.100	−3586	−1919	2.778	−1964	0.075	0.000
	0.200	−5943	−3345	4.329	−3446	0.168	0.000
	0.300	−7495	−4279	5.359	−4447	0.280	0.000
	0.391	−8280	−4702	5.963	−4941	0.397	0.000
bcc	0.438	−8530	−4447	6.804	−5111	1.106	0.000
	0.500	−8712	−4542	6.951	−5254	1.188	0.000
	0.506	−8713	−4538	6.959	−5256	1.197	0.000
Ag_5Zn_8	0.585	−8711	−5248	5.772	−8048	4.668	0.982
	0.600	−8692	−5361	5.552	−8175	4.689	1.457
	0.605	−8677	−5382	5.491	−8200	4.696	1.643
hcp	0.656	−8483	−5584	4.831	−5271	−0.522	0.000
	0.700	−8203	−5677	4.210	−5156	−0.869	0.000
	0.800	−6628	−4822	3.011	−4132	−1.150	0.000
	0.863	−4834	−3349	2.474	−2843	−0.844	0.000
hex	0.968	−1276	−573	1.173	−567	−0.010	0.000
	1.000	0	0	0.000	0	0.000	0.000

Reference states: Ag(fcc), Zn(hex)

Table IVb. Partial quantities for Ag in the stable phases at 600 K.

Phase	x_{Ag}	ΔG_{Ag} [J/mol]	ΔH_{Ag} [J/mol]	ΔS_{Ag} [J/(mol·K)]	$G_{\mathrm{Ag}}^{\mathrm{E}}$ [J/mol]	$S_{\mathrm{Ag}}^{\mathrm{E}}$ [J/(mol·K)]	a_{Ag}	γ_{Ag}
fcc	1.000	0	0	0.000	0	0.000	1.000	1.000
	0.900	−766	−246	0.867	−241	−0.009	0.858	0.953
	0.800	−2076	−985	1.819	−963	−0.036	0.660	0.824
	0.700	−3946	−2216	2.884	−2167	−0.082	0.453	0.648
	0.609	−6163	−3770	3.988	−3686	−0.139	0.291	0.478
bcc	0.562	−6163	−2935	5.381	−3292	0.596	0.291	0.517
	0.500	−8487	−4755	6.221	−5030	0.458	0.182	0.365
	0.494	−8726	−4942	6.307	−5208	0.443	0.174	0.352
Ag_5Zn_8	0.415	−8726	116	14.737	−2172	3.813	0.174	0.647
	0.400	−10309	−2143	13.610	−4431	3.813	0.127	0.411
	0.395	−10975	−3654	12.201	−5941	3.813	0.111	0.304
hcp	0.344	−10975	−2408	14.277	−5653	5.408	0.111	0.322
	0.300	−14489	−6246	13.738	−8483	3.728	0.055	0.183
	0.200	−25103	−18490	11.021	−17074	−2.361	0.007	0.033
	0.137	−34180	−29108	8.454	−24257	−8.085	0.001	0.008
hex	0.032	−34180	−17216	28.274	−17036	−0.300	0.001	0.033
	0.000	$-\infty$	−18400	∞	−18220	−0.300	0.000	0.026

Reference state: Ag(fcc)

Table IVc. Partial quantities for Zn in the stable phases at 600 K.

Phase	x_{Zn}	ΔG_{Zn} [J/mol]	ΔH_{Zn} [J/mol]	ΔS_{Zn} [J/(mol·K)]	G^E_{Zn} [J/mol]	S^E_{Zn} [J/(mol·K)]	a_{Zn}	γ_{Zn}
fcc	0.000	$-\infty$	−21650	∞	−22046	0.660	0.000	0.012
	0.100	−28959	−16972	19.977	−17472	0.833	0.003	0.030
	0.200	−21408	−12787	14.369	−13379	0.987	0.014	0.068
	0.300	−15775	−9094	11.134	−9768	1.124	0.042	0.141
	0.391	−11572	−6152	9.034	−6891	1.233	0.098	0.251
bcc	0.438	−11572	−6392	8.633	−7448	1.761	0.098	0.225
	0.500	−8937	−4328	7.681	−5479	1.918	0.167	0.333
	0.506	−8701	−4144	7.595	−5303	1.932	0.175	0.345
Ag_5Zn_8	0.585	−8701	−9051	−0.584	−12215	5.273	0.175	0.086
	0.600	−7614	−7507	0.179	−10671	5.273	0.217	0.118
	0.605	−7175	−6511	1.108	−9675	5.273	0.237	0.144
hcp	0.656	−7175	−7251	−0.126	−5071	−3.633	0.237	0.362
	0.700	−5509	−5433	0.127	−3729	−2.839	0.331	0.474
	0.800	−2010	−1405	1.008	−896	−0.847	0.668	0.836
	0.863	−182	734	1.527	551	0.303	0.964	1.117
hex	0.968	−182	−19	0.272	−19	0.000	0.964	0.996
	1.000	0	0	0.000	0	0.000	1.000	1.000

Reference state: Zn(hex)

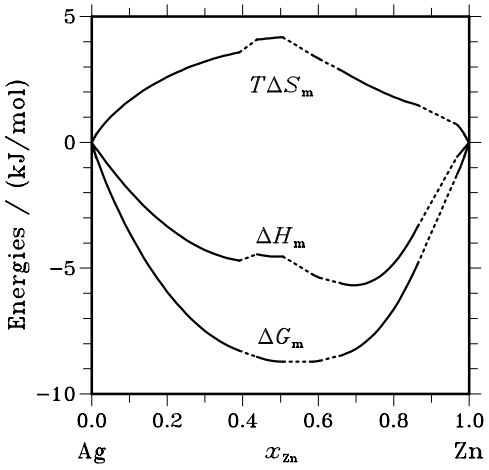

Fig. 4. Integral quantities of the stable phases at T=600 K.

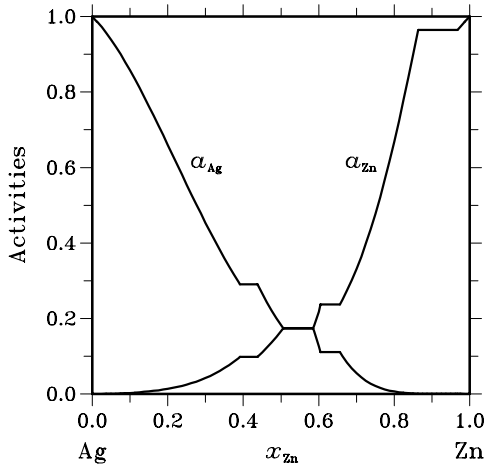

Fig. 5. Activities in the stable phases at T=600 K.

References

[98Gom] T. Gomez-Acebo: Calphad **22** (1998) 203–220.

Ag – Zr (Silver – Zirconium)

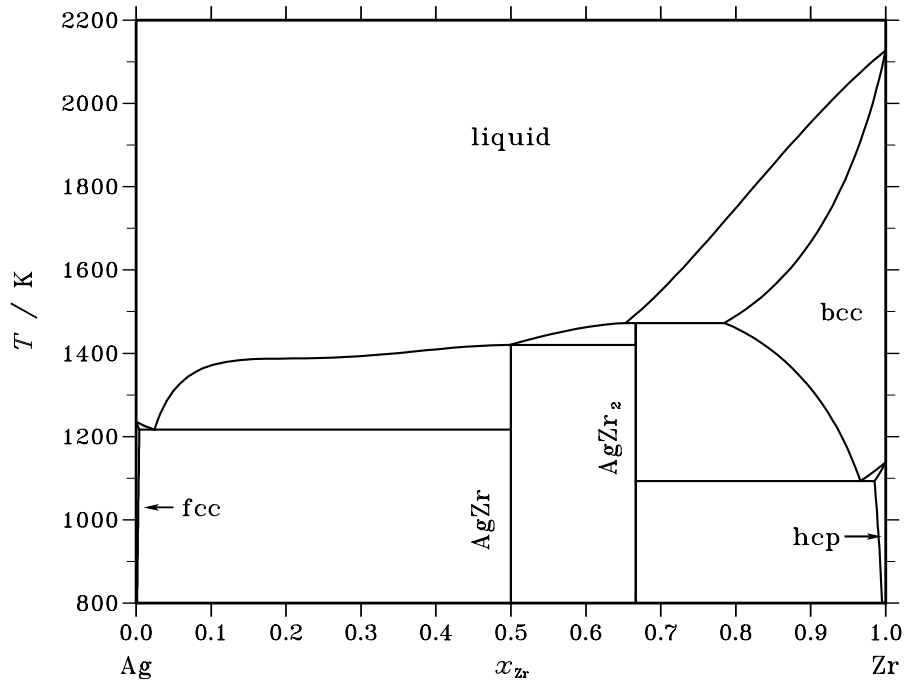

Fig. 1. Calculated phase diagram for the system Ag-Zr.

Karakaya and Thompson [92Kar] have reviewed available experimental information for the system and, due to scarcity of data, presented a phase diagram which is incomplete and not well-defined. The available phase boundaries have nevertheless been used as basis for the present thermodynamic assessment. The calculated invariant reactions give reasonable agreement with the proposed diagram. The nearly flat liquidus in the Ag-rich region of the system and the compound phases present on moving towards Zr-rich compositions are reflected by the asymmetric behaviour of the calculated enthalpies of mixing and activity values for liquid alloys.

Table I. Phases, structures and models.

Phase	Struktur-bericht	Prototype	Pearson symbol	Space group	SGTE name	Model
liquid					LIQUID	$(Ag,Zr)_1$
fcc	$A1$	Cu	$cF4$	$Fm\overline{3}m$	FCC_A1	$(Ag,Zr)_1$
AgZr	$B11$	γCuTi	$tP4$	$P4/nmm$	B11	Ag_1Zr_1
$AgZr_2$	$C11_b$	$MoSi_2$	$tI6$	$I4/mmm$	C11B	Ag_1Zr_2
hcp	$A3$	Mg	$hP2$	$P6_3/mmc$	HCP_A3	$(Ag,Zr)_1$
bcc	$A2$	W	$cI2$	$Im\overline{3}m$	BCC_A2	$(Ag,Zr)_1$

Table II. Invariant reactions.

Reaction	Type	T / K	Compositions / x_{Zr}			$\Delta_r H$ / (J/mol)
liquid + bcc $\rightleftharpoons$ $AgZr_2$	peritectic	1472.6	0.653	0.785	0.667	−22600
liquid + $AgZr_2$ $\rightleftharpoons$ AgZr	peritectic	1420.2	0.498	0.667	0.500	−21727
liquid $\rightleftharpoons$ fcc + AgZr	eutectic	1216.5	0.024	0.004	0.500	−12175
bcc $\rightleftharpoons$ $AgZr_2$ + hcp	eutectoid	1093.0	0.966	0.667	0.985	−5185

Table IIIa. Integral quantities for the liquid phase at 2200 K.

x_{Zr}	ΔG_m [J/mol]	ΔH_m [J/mol]	ΔS_m [J/(mol·K)]	G_m^E [J/mol]	S_m^E [J/(mol·K)]	ΔC_p [J/(mol·K)]
0.000	0	0	0.000	0	0.000	0.000
0.100	−4447	1558	2.730	1499	0.027	0.000
0.200	−7126	2090	4.189	2028	0.028	0.000
0.300	−9317	1884	5.091	1857	0.012	0.000
0.400	−11072	1207	5.581	1239	−0.015	0.000
0.500	−12271	309	5.718	408	−0.045	0.000
0.600	−12730	−577	5.524	−419	−0.072	0.000
0.700	−12218	−1237	4.991	−1044	−0.088	0.000
0.800	−10441	−1477	4.075	−1288	−0.086	0.000
0.900	−6934	−1118	2.644	−988	−0.059	0.000
1.000	0	0	0.000	0	0.000	0.000

Reference states: Ag(liquid), Zr(liquid)

Table IIIb. Partial quantities for Ag in the liquid phase at 2200 K.

x_{Ag}	ΔG_{Ag} [J/mol]	ΔH_{Ag} [J/mol]	ΔS_{Ag} [J/(mol·K)]	G_{Ag}^E [J/mol]	S_{Ag}^E [J/(mol·K)]	a_{Ag}	γ_{Ag}
1.000	0	0	0.000	0	0.000	1.000	1.000
0.900	−1396	562	0.890	532	0.014	0.927	1.029
0.800	−2325	1856	1.900	1757	0.045	0.881	1.101
0.700	−3362	3338	3.046	3162	0.080	0.832	1.189
0.600	−5058	4516	4.352	4286	0.104	0.758	1.264
0.500	−7953	4954	5.867	4726	0.104	0.647	1.295
0.400	−12633	4268	7.682	4128	0.064	0.501	1.253
0.300	−19826	2131	9.981	2197	−0.030	0.338	1.128
0.200	−30750	−1731	13.191	−1311	−0.191	0.186	0.931
0.100	−48701	−7538	18.710	−6582	−0.435	0.070	0.698
0.000	$-\infty$	−15455	∞	−13751	−0.775	0.000	0.472

Reference state: Ag(liquid)

Table IIIc. Partial quantities for Zr in the liquid phase at 2200 K.

x_{Zr}	ΔG_{Zr} [J/mol]	ΔH_{Zr} [J/mol]	ΔS_{Zr} [J/(mol·K)]	G_{Zr}^E [J/mol]	S_{Zr}^E [J/(mol·K)]	a_{Zr}	γ_{Zr}
0.000	$-\infty$	21701	∞	20788	0.415	0.000	3.116
0.100	−31915	10520	19.288	10204	0.143	0.175	1.747
0.200	−26329	3025	13.343	3110	−0.039	0.237	1.185
0.300	−23211	−1510	9.864	−1188	−0.146	0.281	0.937
0.400	−20093	−3758	7.425	−3333	−0.193	0.333	0.833
0.500	−16588	−4335	5.570	−3909	−0.194	0.404	0.808
0.600	−12794	−3807	4.085	−3450	−0.162	0.497	0.828
0.700	−8958	−2681	2.853	−2434	−0.113	0.613	0.875
0.800	−5364	−1413	1.796	−1282	−0.060	0.746	0.932
0.900	−2294	−404	0.859	−366	−0.017	0.882	0.980
1.000	0	0	0.000	0	0.000	1.000	1.000

Reference state: Zr(liquid)

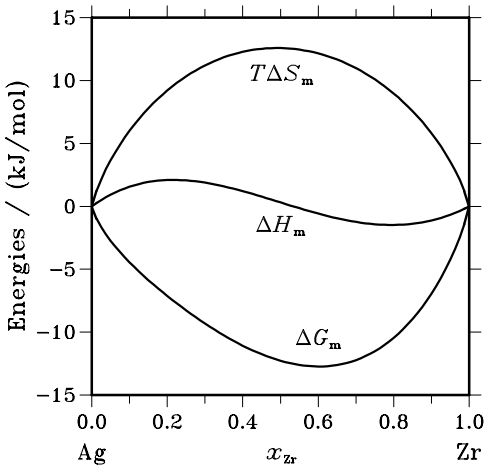

Fig. 2. Integral quantities of the liquid phase at T=2200 K.

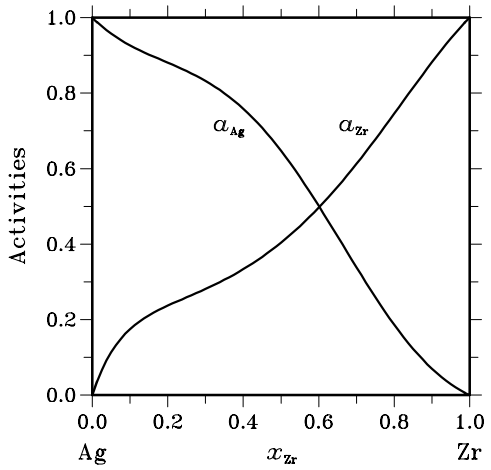

Fig. 3. Activities in the liquid phase at T=2200 K.

Table IV. Standard reaction quantities at 298.15 K for the compounds per mole of atoms.

Compound	x_{Zr}	$\Delta_f G^\circ$ / (J/mol)	$\Delta_f H^\circ$ / (J/mol)	$\Delta_f S^\circ$ / (J/(mol·K))	$\Delta_f C_P^\circ$ / (J/(mol·K))
Ag_1Zr_1	0.500	−6733	−6917	−0.619	0.000
Ag_1Zr_2	0.667	−8402	−8941	−1.809	0.000

References

[92Kar] I. Karakaya, W.T. Thompson: Bull. Alloy Phase Diagrams **13** (1992) 143–146.

Al – As (Aluminium – Arsenic)

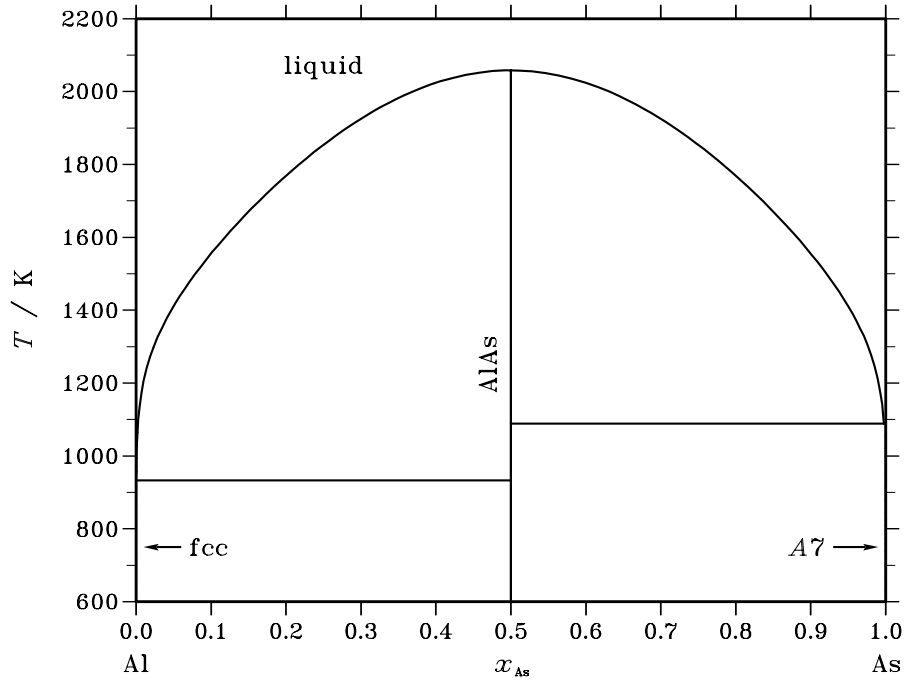

Fig. 1. Calculated phase diagram for the system Al-As (constrained system).

The ability of group III-V compound semiconductors to form miscible substitutional solutions with each other results in materials with a wide range of electrical and optical properties.
The Al-As system has one intermediate phase, AlAs, which is isotypic with ZnS (sphalerite). The melting temperature of AlAs was derived from the analysis of the ternary AlAs-GaAs system [84Ans]. The regular solution interaction parameter of the liquid phase was determined from the analysis of the ternary Al-Ga-As system [84Ans]. Figure 1 shows the phase diagram at constrained pressure sufficient to maintain As in the condensed state [94Ans]. Figure 2 represents the calculated equilibrium phase diagram at (0.1 MPa). Figure 3 shows the partial pressures of several species in the gas phase along the calculated liquidus line of Figure 1.

Table I. Phases, structures and models.

Phase	Struktur-bericht	Prototype	Pearson symbol	Space group	SGTE name	Model
liquid					LIQUID	$(Al,As)_1$
fcc	$A1$	Cu	$cF4$	$Fm\overline{3}m$	FCC_A1	$(Al,As)_1$
AlAs	$B3$	ZnS	$cF8$	$F\overline{4}3m$	B3_ZINCBLENDE	Al_1As_1
$A7$	$A7$	αAs	$hR2$	$R\overline{3}m$	RHOMBOHEDRAL_A7	As_1

Table II. Invariant reactions.

Reaction	Type	T / K	Compositions / x_{As}			$\Delta_r H$ / (J/mol)
liquid $\rightleftharpoons$ AlAs	congruent	2058.2	0.500	0.500		−72104
liquid $\rightleftharpoons$ AlAs + $A7$	eutectic	1089.0	0.998	0.500	1.000	−24662
liquid $\rightleftharpoons$ fcc + AlAs	eutectic	933.3	0.000	0.000	0.500	−10735

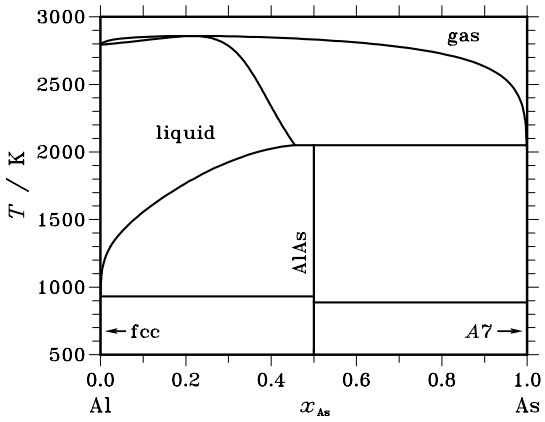

Fig. 2. Calculated phase diagram at 0.1 MPa.

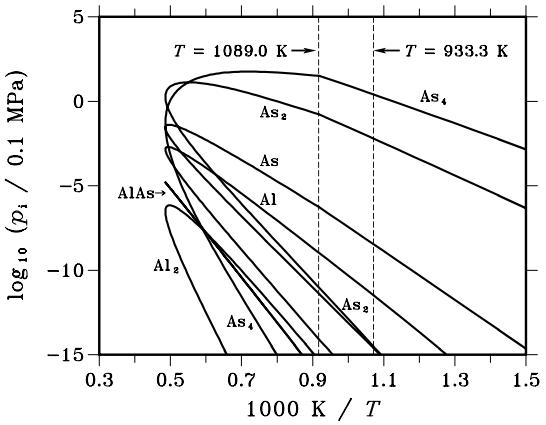

Fig. 3. Calculated partial pressures of gaseous species in the phase equilibria of the constrained system.

Table IIIa. Integral quantities for the liquid phase at 2100 K.

x_{As}	ΔG_m [J/mol]	ΔH_m [J/mol]	ΔS_m [J/(mol·K)]	G_m^E [J/mol]	S_m^E [J/(mol·K)]	ΔC_p [J/(mol·K)]
0.000	0	0	0.000	0	0.000	0.000
0.100	−13545	−1412	5.778	−7869	3.075	0.000
0.200	−22727	−2511	9.627	−13990	5.466	0.000
0.300	−29027	−3296	12.253	−18361	7.174	0.000
0.400	−32736	−3766	13.795	−20985	8.199	0.000
0.500	−33962	−3923	14.304	−21859	8.541	0.000
0.600	−32736	−3766	13.795	−20985	8.199	0.000
0.700	−29027	−3296	12.253	−18361	7.174	0.000
0.800	−22727	−2511	9.627	−13990	5.466	0.000
0.900	−13545	−1412	5.778	−7869	3.075	0.000
1.000	0	0	0.000	0	0.000	0.000

Reference states: Al(liquid), As(liquid)

Table IIIb. Partial quantities for Al in the liquid phase at 2100 K.

x_{Al}	ΔG_{Al} [J/mol]	ΔH_{Al} [J/mol]	ΔS_{Al} [J/(mol·K)]	G_{Al}^E [J/mol]	S_{Al}^E [J/(mol·K)]	a_{Al}	γ_{Al}
1.000	0	0	0.000	0	0.000	1.000	1.000
0.900	−2714	−157	1.218	−874	0.342	0.856	0.951
0.800	−7394	−628	3.222	−3497	1.367	0.655	0.818
0.700	−14097	−1412	6.040	−7869	3.075	0.446	0.637
0.600	−22909	−2511	9.713	−13990	5.466	0.269	0.449
0.500	−33962	−3923	14.304	−21859	8.541	0.143	0.286
0.400	−47476	−5649	19.917	−31477	12.299	0.066	0.165
0.300	−63865	−7690	26.750	−42843	16.740	0.026	0.086
0.200	−84060	−10044	35.246	−55959	21.864	0.008	0.041
0.100	−111027	−12711	46.817	−70823	27.672	0.002	0.017
0.000	$-\infty$	−15693	∞	−87435	34.163	0.000	0.007

Reference state: Al(liquid)

Table IIIc. Partial quantities for As in the liquid phase at 2100 K.

x_{As}	ΔG_{As} [J/mol]	ΔH_{As} [J/mol]	ΔS_{As} [J/(mol·K)]	$G^{\mathrm{E}}_{\mathrm{As}}$ [J/mol]	$S^{\mathrm{E}}_{\mathrm{As}}$ [J/(mol·K)]	a_{As}	γ_{As}
0.000	$-\infty$	−15693	∞	−87435	34.163	0.000	0.007
0.100	−111027	−12711	46.817	−70823	27.672	0.002	0.017
0.200	−84060	−10044	35.246	−55959	21.864	0.008	0.041
0.300	−63865	−7690	26.750	−42843	16.740	0.026	0.086
0.400	−47476	−5649	19.917	−31477	12.299	0.066	0.165
0.500	−33962	−3923	14.304	−21859	8.541	0.143	0.286
0.600	−22909	−2511	9.713	−13990	5.466	0.269	0.449
0.700	−14097	−1412	6.040	−7869	3.075	0.446	0.637
0.800	−7394	−628	3.222	−3497	1.367	0.655	0.818
0.900	−2714	−157	1.218	−874	0.342	0.856	0.951
1.000	0	0	0.000	0	0.000	1.000	1.000

Reference state: As(liquid)

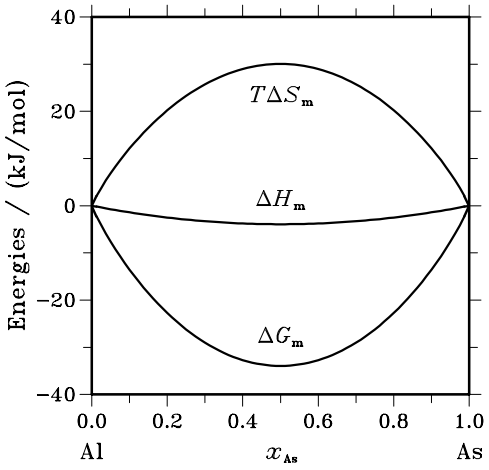

Fig. 4. Integral quantities of the liquid phase at T=2100 K.

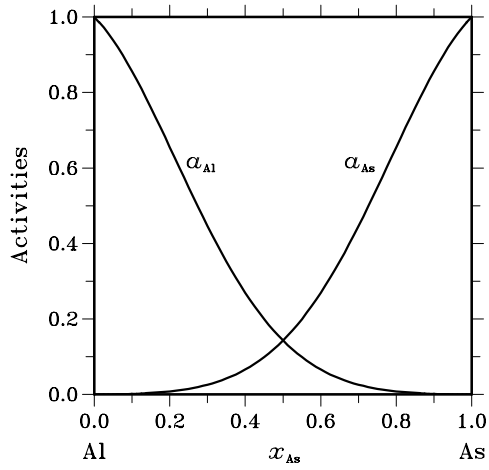

Fig. 5. Activities in the liquid phase at T=2100 K.

Table IV. Standard reaction quantities at 298.15 K for the compounds per mole of atoms.

Compound	x_{As}	$\Delta_{\mathrm{f}}G^{\circ}$ / (J/mol)	$\Delta_{\mathrm{f}}H^{\circ}$ / (J/mol)	$\Delta_{\mathrm{f}}S^{\circ}$ / (J/(mol·K))	$\Delta_{\mathrm{f}}C^{\circ}_{P}$ / (J/(mol·K))
Al_1As_1	0.500	−57405	−58565	−3.890	0.000

References

[84Ans] I. Ansara, D. Dutartre: Calphad **8** (1984) 323–342.

[94Ans] I. Ansara, C. Chatillon, H.L. Lukas, T. Nishizawa, H. Ohtani, K. Ishida, M. Hillert, B. Sundman, B.B. Argent, A. Watson, T.G. Chart, T. Anderson: Calphad **18** (1994) 177–222.

Al – Au (Aluminium – Gold)

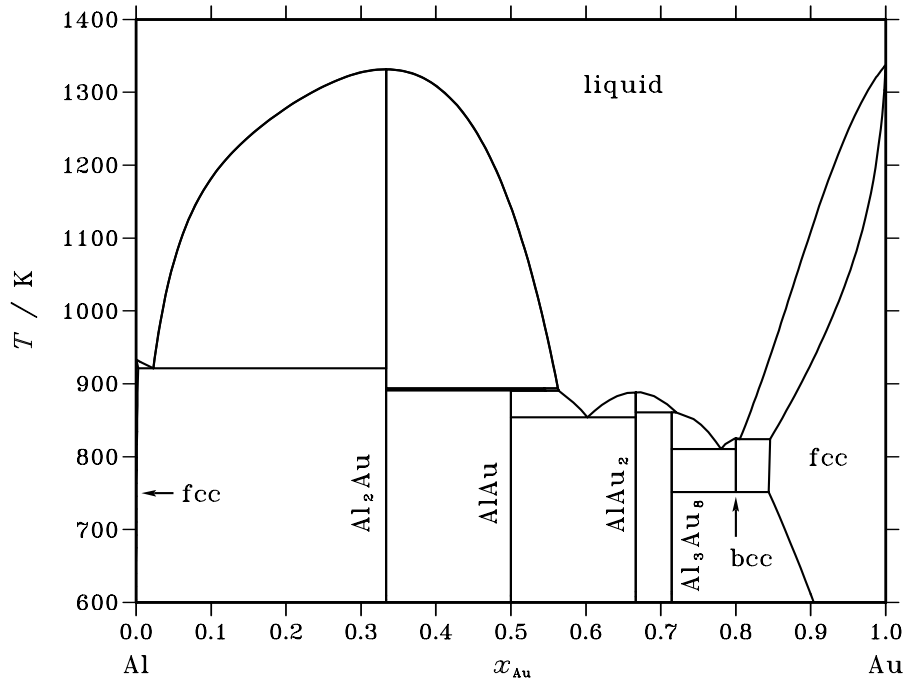

Fig. 1. Calculated phase diagram for the system Al-Au.

The phase diagram of the Al-Au system is dominated by the formation of an array of intermetallic phases some of which exhibit a range of homogeneity. The most prominent of these phases is Al_2Au which melts congruently at 1333 K. Below 923 K this phase is in equilibrium with the Al rich terminal solid solution phase which has a maximum solubility of Au of 0.06 at.%. For Au rich compositions there is a wide range of stability for the liquid phase. The maximum solubility of Al in fcc Au is 16 at.%. On the whole the experimental data for the phase diagram of the system are consistent. The experimental thermodynamic properties of the system have mainly been concerned with the liquid phase (enthalpies of mixing, emf studies and Knudsen cell mass spectrometry) and the intermetallic phases (enthalpies of formation). There are discrepancies and inconsistencies between the measurements which seem difficult to resolve. The assessed data for the system were taken from the assessment of Murray et al. [87Mur] modified by Dinsdale [98Din] to be compatible with the SGTE element data.

Table I. Phases, structures and models.

Phase	Struktur-bericht	Prototype	Pearson symbol	Space group	SGTE name	Model
liquid					LIQUID	$(Al,Au)_1$
fcc	$A1$	Cu	$cF4$	$Fm\bar{3}m$	FCC_A1	$(Al,Au)_1$
Al_2Au	$C1$	CaF_2	$cF12$	$Fm\bar{3}m$	C1_AL2AU	Al_2Au_1
AlAu	$B31$	MnP	$mP28$	$P2_1/m$	B31_ALAU	Al_1Au_1
$\gamma AlAu_2$	$C11_b$	$MoSi_2$	$tI6$	$I4/mmm$	ALAU2	Al_1Au_2
Al_2Au_5	···	···	hR^*	···	AL2AU5	Al_2Au_5
bcc	$A2$	W	$cI2$	$Im\bar{3}m$	ALAU4	Al_1Au_4
$AlAu_4$	···	···	$cP20$	$P2_13$	ALAU4	Al_1Au_4

Table II. Invariant reactions.

Reaction	Type	T / K	Compositions / x_{Au}			$\Delta_r H$ / (J/mol)
liquid ⇌ Al_2Au	congruent	1331.8	0.333	0.333		−12893
liquid ⇌ fcc + Al_2Au	eutectic	921.2	0.023	0.003	0.333	−10569
Al_2Au +liquid ⇌ AlAu	peritectic	890.9	0.333	0.563	0.500	−13739
liquid ⇌ $AlAu_2$	congruent	888.7	0.667	0.667		−11717
$AlAu_2$ + liquid ⇌ Al_2Au_5	peritectic	860.8	0.667	0.720	0.714	−9357
liquid ⇌ AlAu + $AlAu_2$	eutectic	853.9	0.602	0.500	0.667	−12655
liquid ⇌ $AlAu_4$	congruent	825.3	0.786	0.786		−3206
liquid ⇌ $AlAu_4$ + fcc	eutectic	824.2	0.805	0.800	0.846	−3311
liquid ⇌ Al_2Au_5 + $AlAu_4$	eutectic	810.4	0.780	0.714	0.800	−4692
$AlAu_4$ ⇌ Al_2Au_5 + fcc	eutectoid	751.5	0.800	0.714	0.844	−2676

Table IIIa. Integral quantities for the liquid phase at 1400 K.

x_{Au}	ΔG_{m} [J/mol]	ΔH_{m} [J/mol]	ΔS_{m} [J/(mol·K)]	$G^{\mathrm{E}}_{\mathrm{m}}$ [J/mol]	$S^{\mathrm{E}}_{\mathrm{m}}$ [J/(mol·K)]	ΔC_p [J/(mol·K)]
0.000	0	0	0.000	0	0.000	0.000
0.100	−5592	−7011	−1.014	−1808	−3.717	0.000
0.200	−10133	−13559	−2.447	−4308	−6.608	0.000
0.300	−14200	−19232	−3.594	−7090	−8.673	0.000
0.400	−17577	−23620	−4.316	−9743	−9.912	0.000
0.500	−19927	−26313	−4.562	−11858	−10.325	0.000
0.600	−20859	−26901	−4.316	−13025	−9.912	0.000
0.700	−19943	−24974	−3.594	−12833	−8.673	0.000
0.800	−16696	−20122	−2.447	−10871	−6.608	0.000
0.900	−10514	−11934	−1.014	−6730	−3.717	0.000
1.000	0	0	0.000	0	0.000	0.000

Reference states: Al(liquid), Au(liquid)

Table IIIb. Partial quantities for Al in the liquid phase at 1400 K.

x_{Al}	ΔG_{Al} [J/mol]	ΔH_{Al} [J/mol]	ΔS_{Al} [J/(mol·K)]	$G^{\mathrm{E}}_{\mathrm{Al}}$ [J/mol]	$S^{\mathrm{E}}_{\mathrm{Al}}$ [J/(mol·K)]	a_{Al}	γ_{Al}
1.000	0	0	0.000	0	0.000	1.000	1.000
0.900	−812	−164	0.463	414	−0.413	0.933	1.036
0.800	−1487	−1202	0.203	1111	−1.652	0.880	1.100
0.700	−2883	−3935	−0.751	1269	−3.717	0.781	1.115
0.600	−5878	−9183	−2.361	68	−6.608	0.604	1.006
0.500	−11381	−17767	−4.562	−3312	−10.325	0.376	0.752
0.400	−20358	−30507	−7.249	−9692	−14.868	0.174	0.435
0.300	−33907	−48224	−10.226	−19892	−20.236	0.054	0.181
0.200	−53467	−71737	−13.050	−34733	−26.431	0.010	0.051
0.100	−81837	−101868	−14.307	−55035	−33.452	0.001	0.009
0.000	$-\infty$	−139436	∞	−81617	−41.299	0.000	0.001

Reference state: Al(liquid)

Table IIIc. Partial quantities for Au in the liquid phase at 1400 K.

x_{Au}	ΔG_{Au} [J/mol]	ΔH_{Au} [J/mol]	ΔS_{Au} [J/(mol·K)]	$G^{\mathrm{E}}_{\mathrm{Au}}$ [J/mol]	$S^{\mathrm{E}}_{\mathrm{Au}}$ [J/(mol·K)]	a_{Au}	γ_{Au}
0.000	$-\infty$	−71068	∞	−13249	−41.299	0.000	0.320
0.100	−48610	−68641	−14.307	−21808	−33.452	0.015	0.154
0.200	−44716	−62986	−13.050	−25982	−26.431	0.021	0.107
0.300	−40607	−54924	−10.226	−26592	−20.236	0.031	0.102
0.400	−35126	−45275	−7.249	−24460	−14.868	0.049	0.122
0.500	−28473	−34859	−4.562	−20404	−10.325	0.087	0.173
0.600	−21193	−24498	−2.361	−15247	−6.608	0.162	0.270
0.700	−13959	−15011	−0.751	−9807	−3.717	0.301	0.431
0.800	−7503	−7218	0.203	−4906	−1.652	0.525	0.656
0.900	−2590	−1941	0.463	−1363	−0.413	0.801	0.889
1.000	0	0	0.000	0	0.000	1.000	1.000

Reference state: Au(liquid)

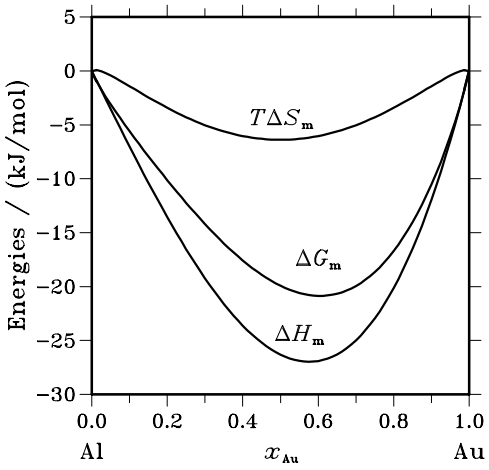

Fig. 2. Integral quantities of the liquid phase at T=1400 K.

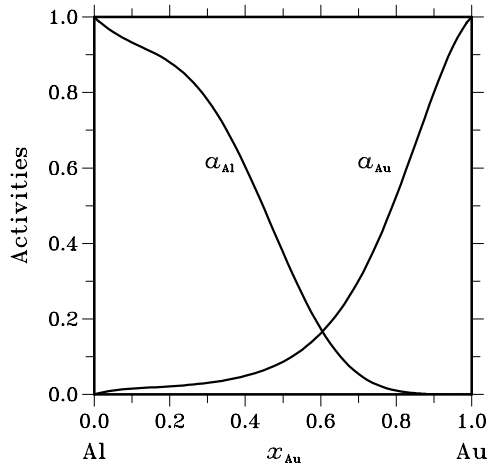

Fig. 3. Activities in the liquid phase at T=1400 K.

Table IV. Standard reaction quantities at 298.15 K for the compounds per mole of atoms.

Compound	x_{Au}	$\Delta_{\mathrm{f}}G^{\circ}$ / (J/mol)	$\Delta_{\mathrm{f}}H^{\circ}$ / (J/mol)	$\Delta_{\mathrm{f}}S^{\circ}$ / (J/(mol·K))	$\Delta_{\mathrm{f}}C^{\circ}_{P}$ / (J/(mol·K))
Al_2Au_1	0.333	−21471	−22229	−2.543	−0.002
Al_1Au_1	0.500	−27275	−30786	−11.774	−0.001
Al_1Au_2	0.667	−23555	−25602	−6.865	−0.001
Al_2Au_5	0.714	−21273	−22968	−5.685	−0.001
Al_1Au_4	0.800	−12142	−11085	3.545	0.000

References

[87Mur] J.L. Murray, H. Okamoto, T.B. Massalski: Bull. Alloy Phase Diagrams **8** (1987) 20–30.
[98Din] A.T. Dinsdale, unpublished work, 1998.

Al – B (Aluminium – Boron)

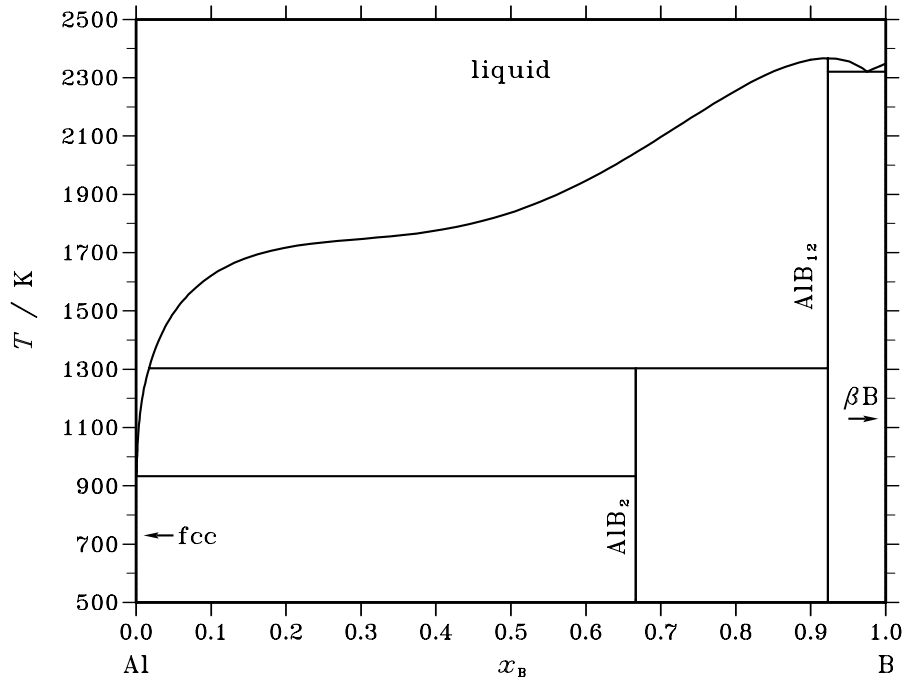

Fig. 1. Calculated phase diagram for the system Al-B.

The Al–B system is of interest because B is added in combination with Ti to Al-alloys in order to promote grain refinement, precipitation hardening and mechanical reinforcement. Besides this application the AlB_{12} phase is a promising compound for high temperature thermoelectric applications and aircraft protection.
Out of several thermodynamic assessments [84Kau, 94Dus, 99Cam, 01Luk] the description of [01Luk] is recommended here. It is based on calorimetric data and on measurements of the liquidus. The phase diagram presented by [67Ser] contradicts the phase rule as there is no two-phase field between AlB_{12} and B in [67Ser]. Later it has been concluded by [94Dus] that the phases $\beta-AlB_{12}$ and AlB_{10}, considered to be stable by [67Ser], are stabilised by impurities. The stability of the Al_2B_3 phase is also questionable. Only two stable compounds are considered by [01Luk]: AlB_2 and AlB_{12}. The most contradictory point is the melting characteristics of AlB_{12}. According to [67Ser] the AlB_{12} phase melts incongruently at 2348 K and the B phase can dissolve about 4 at.% of Al. The incongruent melting of AlB_{12} has been confirmed experimentally [94Dus], but according to the evaluation of [90Car] and calculations of [01Luk] AlB_{12} melts congruently. There is a big difference of ~80 K between the experimental temperatures of peritectic melting of AlB_2 reported by [94Dus] and [00Hal]. The data of [94Dus] are preferred by [01Luk], because the samples of [00Hal] contained Fe impurities. Enthalpies of formation have been determined calorimetrically for the compounds AlB_2 [67Dom] and AlB_{12} [67Dom, 95Mes]. The calculated enthalpies of [01Luk] closely match the calorimetric data of [95Mes]. According to the thermodynamic description of [99Cam] the incongruent melting temperature of AlB_2 is 75 K lower than obtained by [94Dus] and contradicts the calorimetric data of [67Dom, 95Mes]. The solubility of B in fcc-Al has been found to be only about 0.0055 at.%.
Both compounds and solid B are treated by [01Luk] as stoichiometric phases. The liquid is described as a substitutional solution and the solution of boron in fcc-Al is treated as an interstitial solution, analogous to B–Ni and similar systems.

Table I. Phases, structures and models.

Phase	Struktur-bericht	Prototype	Pearson symbol	Space group	SGTE name	Model
liquid					LIQUID	$(Al,B)_1$
fcc	$A1$	Cu	$cF4$	$Fm\overline{3}m$	FCC_A1	$Al_1(B,\Box)_1$
AlB_2	$C32$	AlB_2	$hP3$	$P6/mmm$	ALB2	Al_1B_2
AlB_{12}	$\cdots$	αAlB_{12}	$tP216$	$P4_12_12$	ALB12_ALPHA	Al_1B_{12}
βB	$\cdots$	βB	$hR105$	$R\overline{3}m$	BETA_RHOMBO_B	$B_{93}B_{12}$

Table II. Invariant reactions.

Reaction	Type	T / K	Compositions / x_B			$\Delta_r H$ / (J/mol)
liquid $\rightleftharpoons$ AlB_{12}	congruent	2367.1	0.923	0.923		−56029
liquid $\rightleftharpoons$ AlB_{12} + βB	eutectic	2320.3	0.975	0.923	1.000	−51877
liquid + AlB_{12} $\rightleftharpoons$ AlB_2	peritectic	1303.1	0.017	0.923	0.667	−6442
liquid $\rightleftharpoons$ fcc + AlB_2	eutectic	933.1	0.001	0.000	0.667	−10752

Table IIIa. Integral quantities for the liquid phase at 2500 K.

x_B	ΔG_m [J/mol]	ΔH_m [J/mol]	ΔS_m [J/(mol·K)]	G_m^E [J/mol]	S_m^E [J/(mol·K)]	ΔC_p [J/(mol·K)]
0.000	0	0	0.000	0	0.000	0.000
0.100	−6438	1469	3.163	319	0.460	0.000
0.200	−10275	2172	4.979	126	0.818	0.000
0.300	−13329	2053	6.153	−631	1.074	0.000
0.400	−15871	1187	6.823	−1881	1.227	0.000
0.500	−17836	−232	7.041	−3428	1.278	0.000
0.600	−18939	−1881	6.823	−4949	1.227	0.000
0.700	−18698	−3316	6.153	−6000	1.074	0.000
0.800	−16412	−3965	4.979	−6010	0.818	0.000
0.900	−11041	−3133	3.163	−4284	0.460	0.000
1.000	0	0	0.000	0	0.000	0.000

Reference states: Al(liquid), B(liquid)

Table IIIb. Partial quantities for Al in the liquid phase at 2500 K.

x_{Al}	ΔG_{Al} [J/mol]	ΔH_{Al} [J/mol]	ΔS_{Al} [J/(mol·K)]	G^E_{Al} [J/mol]	S^E_{Al} [J/(mol·K)]	a_{Al}	γ_{Al}
1.000	0	0	0.000	0	0.000	1.000	1.000
0.900	−1953	364	0.927	237	0.051	0.910	1.011
0.800	−3559	1591	2.060	1079	0.205	0.843	1.053
0.700	−4967	3598	3.426	2447	0.460	0.787	1.125
0.600	−6733	5930	5.065	3885	0.818	0.723	1.206
0.500	−9845	7759	7.041	4563	1.278	0.623	1.245
0.400	−15769	7879	9.459	3278	1.841	0.468	1.171
0.300	−26575	4715	12.516	−1549	2.505	0.278	0.928
0.200	−45322	−3687	16.654	−11868	3.272	0.113	0.565
0.100	−77868	−19652	23.287	−30006	4.142	0.024	0.236
0.000	−∞	−45881	∞	−58664	5.113	0.000	0.059

Reference state: Al(liquid)

Table IIIc. Partial quantities for B in the liquid phase at 2500 K.

x_B	ΔG_B [J/mol]	ΔH_B [J/mol]	ΔS_B [J/(mol·K)]	G^E_B [J/mol]	S^E_B [J/(mol·K)]	a_B	γ_B
0.000	−∞	18042	∞	5259	5.113	0.000	1.288
0.100	−46802	11415	23.287	1060	4.142	0.105	1.052
0.200	−37140	4495	16.654	−3686	3.272	0.168	0.838
0.300	−32839	−1550	12.516	−7813	2.505	0.206	0.687
0.400	−29576	−5928	9.459	−10530	1.841	0.241	0.603
0.500	−25826	−8222	7.041	−11418	1.278	0.289	0.577
0.600	−21052	−8389	5.065	−10434	0.818	0.363	0.605
0.700	−15322	−6758	3.426	−7908	0.460	0.478	0.684
0.800	−9184	−4035	2.060	−4546	0.205	0.643	0.804
0.900	−3615	−1298	0.927	−1425	0.051	0.840	0.934
1.000	0	0	0.000	0	0.000	1.000	1.000

Reference state: B(liquid)

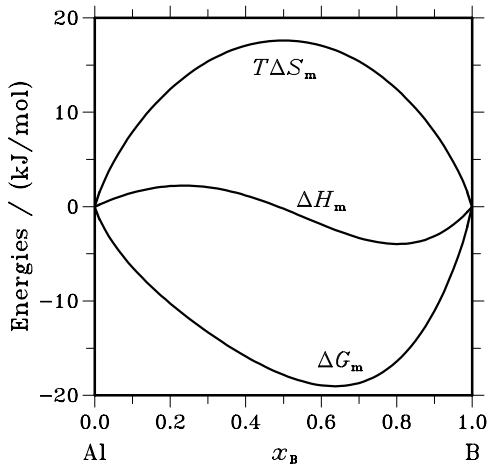

Fig. 2. Integral quantities of the liquid phase at T=2500 K.

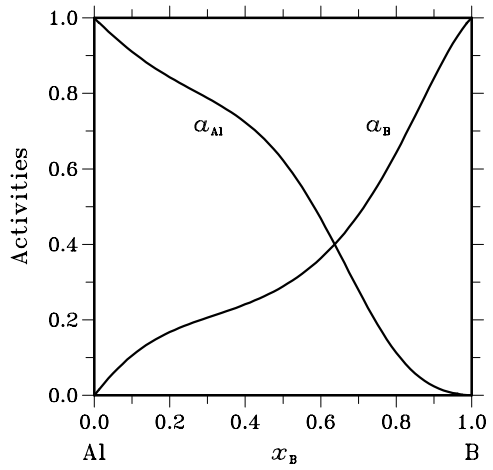

Fig. 3. Activities in the liquid phase at T=2500 K.

Table IV. Standard reaction quantities at 298.15 K for the compounds per mole of atoms.

Compound	x_{B}	$\Delta_{\mathrm{f}}G^{\circ}$ / (J/mol)	$\Delta_{\mathrm{f}}H^{\circ}$ / (J/mol)	$\Delta_{\mathrm{f}}S^{\circ}$ / (J/(mol·K))	$\Delta_{\mathrm{f}}C_P^{\circ}$ / (J/(mol·K))
Al_1B_2	0.667	−10920	−11456	−1.800	0.000
Al_1B_{12}	0.923	−11384	−11517	−0.445	0.000

References

[67Dom] E.S. Domalsky, G.T. Armstrong: J. Res. Natl. Bur. Stand. A, Phys. Chem. **71** (1967) 307–315.
[67Ser] V.T. Serebryansky, V.Z. Epel'baum, G.S. Zhdanov: Russ. J. Inorg. Chem. **12** (1967) 543–552.
[84Kau] L. Kaufman, B. Uhrenius, D. Birnie, K. Taylor: Calphad **8** (1984) 25–66.
[90Car] O.N. Carlson: Bull. Alloy Phase Diagrams **11** (1990) 560–566.
[94Dus] H. Duschanek, P. Rogl: J. Phase Equilibria **15** (1994) 543–552.
[95Mes] S.W. Meschel, O.J. Kleppa: J. Alloys Comp. **227** (1995) 93–96.
[99Cam] C.E. Campbell, U.R. Kattner: J. Phase Equilibria **20** (1999) 485–491.
[00Hal] A. Hall, J. Economy: J. Phase Equilibria **20** (2000) 63–69.
[01Luk] H.L. Lukas: unpublished assessment, 2001.

Al – Bi (Aluminium – Bismuth)

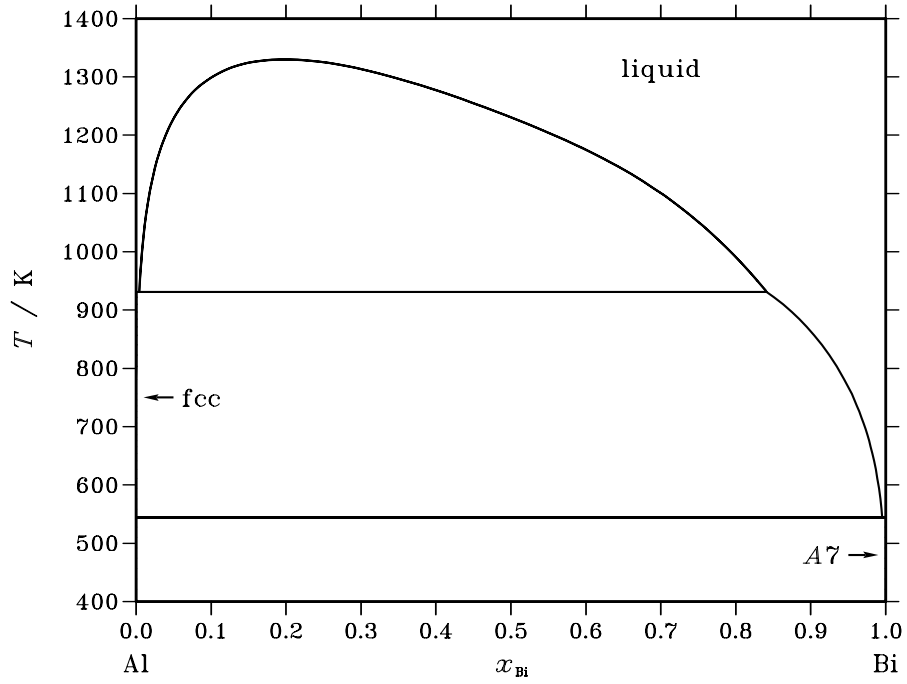

Fig. 1. Calculated phase diagram for the system Al-Bi.

The Al-Bi system is a very simple system showing a wide range of immiscibility in the liquid phase up to 1310 K where the miscibility gap closes at a composition approximately 20 at.% Bi. It has potential importance as a key subsystem for bearing alloys and automotive applications. The selected data for the Al-Bi system are from the critical assessment of McAlister [84McA]. Terminal solid solutions are very limited. The miscibility gap has been studied extensively between the monotectic temperature of 931 K and the upper consolute temperature, and the solubility of Al in the liquid at temperatures below the monotectic and the eutectic at about 543 K. The limited experimental thermodynamic studies have concerned the enthalpies of mixing and the partial Gibbs energies of Al. The assessed data are in very good agreement with all the experimental data for the system with the exception of the upper consolute temperature which is calculated to be 1330 K.

Table I. Phases, structures and models.

Phase	Struktur-bericht	Prototype	Pearson symbol	Space group	SGTE name	Model
liquid					LIQUID	$(Al,Bi)_1$
fcc	$A1$	Cu	$cF4$	$Fm\bar{3}m$	FCC_A1	$(Al,Bi)_1$
$A7$	$A7$	αAs	$hR2$	$R\bar{3}m$	RHOMBOHEDRAL_A7	Bi_1

Table II. Invariant reactions.

Reaction	Type	T / K	Compositions / x_{Bi}			$\Delta_r H$ / (J/mol)
liquid $\rightleftharpoons$ liquid′ + liquid″	critical	1329.9	0.198	0.198	0.198	0
liquid′ $\rightleftharpoons$ fcc + liquid″	monotectic	931.3	0.004	0.001	0.841	−10891
liquid $\rightleftharpoons$ fcc + $A7$	eutectic	543.5	0.995	0.000	1.000	−11404

Table IIIa. Integral quantities for the liquid phase at 1400 K.

x_{Bi}	ΔG_{m} [J/mol]	ΔH_{m} [J/mol]	ΔS_{m} [J/(mol·K)]	$G_{\mathrm{m}}^{\mathrm{E}}$ [J/mol]	$S_{\mathrm{m}}^{\mathrm{E}}$ [J/(mol·K)]	ΔC_p [J/(mol·K)]
0.000	0	0	0.000	0	0.000	0.000
0.100	−1298	4618	4.226	2486	1.523	0.000
0.200	−1816	6579	5.996	4009	1.835	0.000
0.300	−2238	7024	6.616	4873	1.537	0.000
0.400	−2588	6717	6.646	5246	1.050	0.000
0.500	−2860	6103	6.402	5208	0.639	0.000
0.600	−3051	5379	6.022	4783	0.426	0.000
0.700	−3131	4551	5.487	3980	0.408	0.000
0.800	−2991	3500	4.637	2834	0.476	0.000
0.900	−2343	2044	3.133	1441	0.431	0.000
1.000	0	0	0.000	0	0.000	0.000

Reference states: Al(liquid), Bi(liquid)

Table IIIb. Partial quantities for Al in the liquid phase at 1400 K.

x_{Al}	ΔG_{Al} [J/mol]	ΔH_{Al} [J/mol]	ΔS_{Al} [J/(mol·K)]	$G_{\mathrm{Al}}^{\mathrm{E}}$ [J/mol]	$S_{\mathrm{Al}}^{\mathrm{E}}$ [J/(mol·K)]	a_{Al}	γ_{Al}
1.000	0	0	0.000	0	0.000	1.000	1.000
0.900	−682	1553	1.597	544	0.721	0.943	1.048
0.800	−899	4485	3.846	1698	1.991	0.926	1.157
0.700	−1076	7114	5.850	3076	2.885	0.912	1.302
0.600	−1342	8765	7.219	4605	2.972	0.891	1.485
0.500	−1694	9520	8.010	6375	2.247	0.865	1.729
0.400	−2185	9965	8.678	8481	1.060	0.829	2.072
0.300	−3146	10937	10.059	10869	0.049	0.763	2.544
0.200	−5558	13271	13.450	13177	0.068	0.620	3.102
0.100	−12218	17551	21.264	14585	2.119	0.350	3.501
0.000	$-\infty$	23852	∞	13656	7.283	0.000	3.232

Reference state: Al(liquid)

Table IIIc. Partial quantities for Bi in the liquid phase at 1400 K.

x_{Bi}	ΔG_{Bi} [J/mol]	ΔH_{Bi} [J/mol]	ΔS_{Bi} [J/(mol·K)]	$G_{\mathrm{Bi}}^{\mathrm{E}}$ [J/mol]	$S_{\mathrm{Bi}}^{\mathrm{E}}$ [J/(mol·K)]	a_{Bi}	γ_{Bi}
0.000	$-\infty$	64336	∞	31077	23.757	0.000	14.436
0.100	−6844	32200	27.888	19959	8.743	0.555	5.555
0.200	−5481	14953	14.596	13253	1.214	0.624	3.122
0.300	−4948	6815	8.402	9066	−1.608	0.654	2.179
0.400	−4457	3644	5.786	6209	−1.832	0.682	1.705
0.500	−4027	2686	4.795	4041	−0.968	0.708	1.415
0.600	−3629	2322	4.251	2317	0.003	0.732	1.220
0.700	−3124	1815	3.528	1028	0.562	0.765	1.092
0.800	−2349	1058	2.433	248	0.578	0.817	1.022
0.900	−1246	321	1.119	−19	0.243	0.898	0.998
1.000	0	0	0.000	0	0.000	1.000	1.000

Reference state: Bi(liquid)

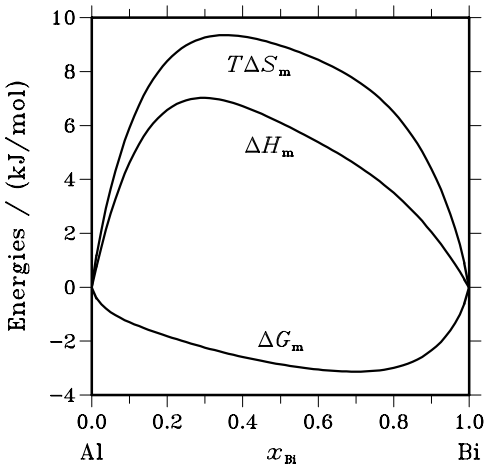

Fig. 2. Integral quantities of the liquid phase at T=1400 K.

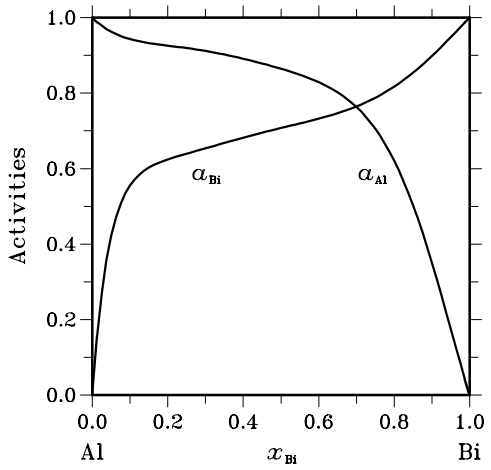

Fig. 3. Activities in the liquid phase at T=1400 K.

References

[84McA] A.J. McAlister: Bull. Alloy Phase Diagrams **5** (1984) 247–250.

Al – C (Aluminium – Carbon)

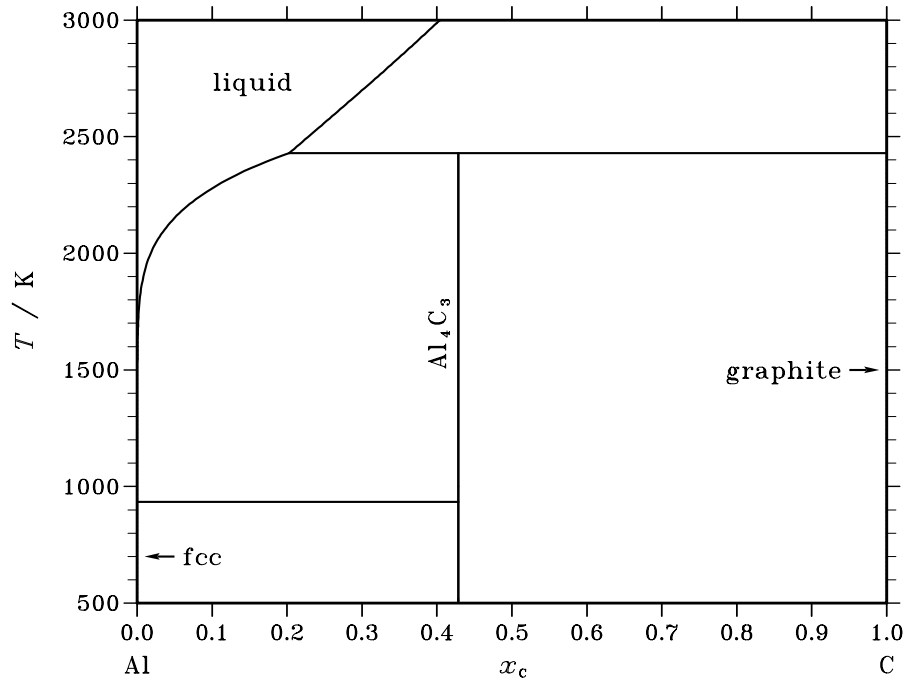

Fig. 1. Calculated phase diagram for the system Al-C.

The Al-C system is a part of the Al-C-O system which is important for modelling the carbothermic reduction of alumina. A critical review of the experimental phase equilibrium data in the system Al-C has been given by [91Sch]. The phase diagram has been re-evaluated by [92Oka]. The only stable compound in the system is Al_4C_3. According to experimental determinations it melts incongruently forming liquid and graphite. However, in the literature there are conflicting data for the temperature of this peritectic reaction. The melting point of Al_4C_3 evaluated by Massalski contradicts several experimental determinations. The thermodynamic dataset established by [94Gro, 95Gro] is recommended here. It is based on the experimentally determined solubility of carbon in the liquid phase, temperature data for the peritectic equilibrium and different kinds of data for Al_4C_3: calorimetric measurements of the enthalpy of formation, enthalpy increments measured by drop-solution calorimetry and enthalpy of decomposition into graphite and gaseous Al obtained by vapour pressure mass spectrometry.

The solubility of carbon in liquid aluminium is restricted by the decomposition of the liquid phase to graphite and gas [91Sch]. The upper limits for the stability of the liquid under normal pressure are a temperature of 2570 K and a carbon content of 25 at.% according to [94Gro]. In the thermodynamic dataset of [95Gro] the liquid phase is described by a substitutional model. The solid solubility of carbon in aluminium is very low (0.04-0.08 at.% [92Oka]) and the fcc phase is described by a sublattice model in [95Gro]. Al_4C_3 is treated as a stoichiometric compound in [95Gro].

Table I. Phases, structures and models.

Phase	Struktur-bericht	Prototype	Pearson symbol	Space group	SGTE name	Model
liquid					LIQUID	$(Al,C)_1$
fcc	$A1$	Cu	$cF4$	$Fm\overline{3}m$	FCC_A1	$Al_1(C,\square)_1$
Al_4C_3	$D7_1$	Al_4C_3	$hR7$	$R\overline{3}m$	D71_AL4C3	Al_4C_3
graphite	$A9$	C(graphite)	$hP4$	$P6_3/mmc$	GRAPHITE_A9	C_1

Table II. Invariant reactions.

Reaction	Type	T / K	Compositions / x_C			$\Delta_r H$ / (J/mol)
liquid + graphite $\rightleftharpoons$ Al_4C_3	peritectic	2428.9	0.203	1.000	0.429	−62895
liquid $\rightleftharpoons$ fcc + Al_4C_3	eutectic	933.5	0.000	0.000	0.429	−10711

Table IIIa. Integral quantities for the liquid phase at 2500 K.

x_C	ΔG_m [J/mol]	ΔH_m [J/mol]	ΔS_m [J/(mol·K)]	G_m^E [J/mol]	S_m^E [J/(mol·K)]	ΔC_p [J/(mol·K)]
0.000	0	0	0.000	0	0.000	0.000
0.025	−2063	3930	2.397	367	1.425	0.000
0.050	−3340	7809	4.460	787	2.809	0.000
0.075	−4278	11637	6.366	1259	4.151	0.000
0.100	−4973	15414	8.155	1784	5.452	0.000
0.125	−5469	19140	9.844	2362	6.711	0.000
0.150	−5794	22815	11.444	2993	7.929	0.000
0.175	−5963	26439	12.961	3676	9.105	0.000
0.200	−5989	30012	14.400	4412	10.240	0.000
0.225	−5882	33533	15.766	5201	11.333	0.000
0.228	−5857	34013	15.948	5313	11.480	0.000

Reference states: Al(liquid), C(graphite)

Table IIIb. Partial quantities for Al in the liquid phase at 2500 K.

x_{Al}	ΔG_{Al} [J/mol]	ΔH_{Al} [J/mol]	ΔS_{Al} [J/(mol·K)]	G_{Al}^E [J/mol]	S_{Al}^E [J/(mol·K)]	a_{Al}	γ_{Al}
1.000	0	0	0.000	0	0.000	1.000	1.000
0.975	−553	26	0.231	−26	0.021	0.974	0.999
0.950	−1172	102	0.510	−105	0.083	0.945	0.995
0.925	−1858	230	0.835	−237	0.187	0.915	0.989
0.900	−2612	409	1.208	−422	0.332	0.882	0.980
0.875	−3434	638	1.629	−659	0.519	0.848	0.969
0.850	−4327	919	2.099	−949	0.747	0.812	0.955
0.825	−5290	1251	2.617	−1291	1.017	0.775	0.940
0.800	−6325	1634	3.184	−1687	1.328	0.738	0.922
0.775	−7433	2069	3.801	−2135	1.681	0.699	0.902
0.772	−7591	2132	3.889	−2200	1.733	0.694	0.900

Reference state: Al(liquid)

Table IIIc. Partial quantities for C in the liquid phase at 2500 K.

x_C	ΔG_C [J/mol]	ΔH_C [J/mol]	ΔS_C [J/(mol·K)]	G_C^E [J/mol]	S_C^E [J/(mol·K)]	a_C	γ_C
0.000	$-\infty$	158230	∞	13627	57.841	0.000	1.926
0.025	−60969	156212	86.873	15709	56.202	0.053	2.129
0.050	−44532	154246	79.511	17738	54.603	0.117	2.347
0.075	−34128	152331	74.583	19715	53.047	0.194	2.582
0.100	−26224	150466	70.676	21638	51.531	0.283	2.832
0.125	−19714	148653	67.347	23510	50.057	0.387	3.099
0.150	−14106	146891	64.399	25328	48.625	0.507	3.382
0.175	−9136	145180	61.726	27094	47.234	0.644	3.682
0.200	−4647	143520	59.267	28807	45.885	0.800	3.998
0.225	−539	141911	56.980	30467	44.578	0.974	4.331
0.228	0	141694	56.678	30691	44.401	1.000	4.378

Reference state: C(graphite)

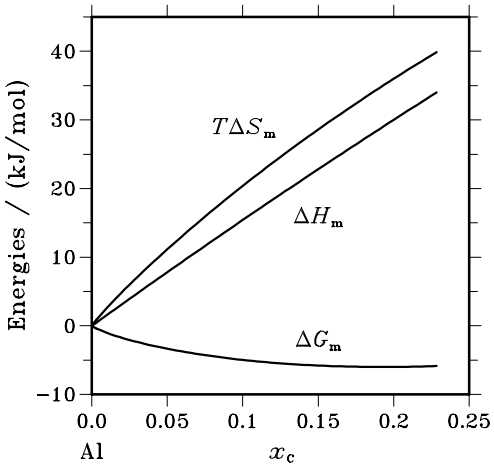

Fig. 2. Integral quantities of the liquid phase at T=2500 K.

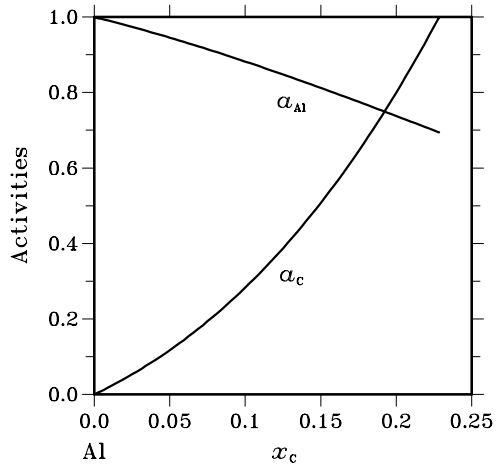

Fig. 3. Activities in the liquid phase at T=2500 K.

Table IV. Standard reaction quantities at 298.15 K for the compounds per mole of atoms.

Compound	x_C	$\Delta_f G^\circ$ / (J/mol)	$\Delta_f H^\circ$ / (J/mol)	$\Delta_f S^\circ$ / (J/(mol·K))	$\Delta_f C_P^\circ$ / (J/(mol·K))
Al_4C_3	0.429	−29633	−31481	−6.199	−1.385

References

[91Sch] J.C. Schuster: J. Phase Equilibria **12** (1991) 546–549.
[92Oka] H. Okamoto: J. Phase Equilibria **13** (1992) 97–98.
[94Gro] J. Gröbner: Ph.D. Thesis, Stuttgart University, 1994.
[95Gro] J. Gröbner, H.L. Lukas, F. Aldinger: J. Alloys Comp. **220** (1995) 8–14.

Al – Ca (Aluminium – Calcium)

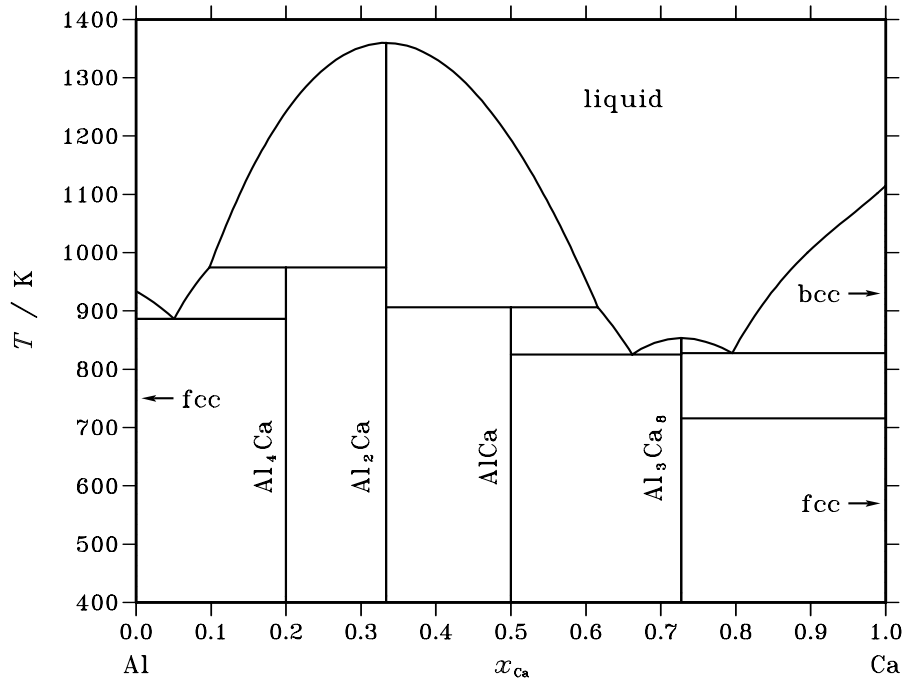

Fig. 1. Calculated phase diagram for the system Al-Ca.

This system has no solubility in the terminal phases and four intermetallic compounds with limited solubility, all modelled without any solubility. The Al_2Ca is a Laves phase and melts congruently whereas Al_4Ca is formed peritectically.
Al and Ca easily react with oxygen and this binary system is mainly interesting as part of a database where Al and Ca are used as alloying elements in other metals or slags. In a previous assessment, [93Ang], only two compounds were included but in a more recent assessment, [01Kev1, 01Kev2] two new phases were detected in the system, Al_3Ca_8 which melts congruently and AlCa which forms peritectically.

Table I. Phases, structures and models.

Phase	Struktur-bericht	Prototype	Pearson symbol	Space group	SGTE name	Model
liquid					LIQUID	$(Al,Ca)_1$
fcc	$A1$	Cu	$cF4$	$Fm\overline{3}m$	FCC_A1	$(Al,Ca)_1$
Al_4Ca	$D1_3$	Al_4Ba	$tI10$	$I4/mmm$	D13_AL4CA	Al_4Ca_1
Al_2Ca	$C15$	Cu_2Mg	$cF24$	$Fd\overline{3}m$	C15_AL2M1	Al_2Ca_1
AlCa	···	···	$mC*$	$C2/m$	ALCA	Al_1Ca_1
Al_3Ca_8	···	Ca_8In_3	$aP22$	$P\overline{1}$	AL3CA8	Al_3Ca_8
bcc	$A2$	W	$cI2$	$Im\overline{3}m$	BCC_A2	$(Al,Ca)_1$

Table II. Invariant reactions.

Reaction	Type	T / K	Compositions / x_{Ca}			$\Delta_{\mathrm{r}}H$ / (J/mol)
liquid $\rightleftharpoons$ Al_2Ca	congruent	1359.8	0.333	0.333		−19143
liquid + Al_2Ca $\rightleftharpoons$ Al_4Ca	peritectic	974.5	0.098	0.333	0.200	−9535
Al_2Ca + liquid $\rightleftharpoons$ AlCa	peritectic	906.4	0.333	0.616	0.500	−5127
liquid $\rightleftharpoons$ fcc + Al_4Ca	eutectic	886.2	0.051	0.000	0.200	−11703
liquid $\rightleftharpoons$ Al_3Ca_8	congruent	853.5	0.727	0.727		−8751
liquid $\rightleftharpoons$ Al_3Ca_8 + bcc	eutectic	827.6	0.795	0.727	1.000	−8378
liquid $\rightleftharpoons$ AlCa + Al_3Ca_8	eutectic	825.2	0.662	0.500	0.727	−8769
bcc $\rightleftharpoons$ Al_3Ca_8 + fcc	degenerate	716.0	1.000	0.727	1.000	−929

Table IIIa. Integral quantities for the liquid phase at 1400 K.

x_{Ca}	ΔG_{m} [J/mol]	ΔH_{m} [J/mol]	ΔS_{m} [J/(mol·K)]	$G^{\mathrm{E}}_{\mathrm{m}}$ [J/mol]	$S^{\mathrm{E}}_{\mathrm{m}}$ [J/(mol·K)]	ΔC_p [J/(mol·K)]
0.000	0	0	0.000	0	0.000	0.000
0.100	−8516	−8260	0.183	−4732	−2.520	0.000
0.200	−14212	−14659	−0.319	−8387	−4.480	0.000
0.300	−17951	−19072	−0.801	−10840	−5.880	0.000
0.400	−19877	−21451	−1.124	−12043	−6.720	0.000
0.500	−20094	−21825	−1.237	−12025	−7.000	0.000
0.600	−18725	−20299	−1.124	−10891	−6.720	0.000
0.700	−15935	−17056	−0.801	−8824	−5.880	0.000
0.800	−11908	−12355	−0.319	−6083	−4.480	0.000
0.900	−6788	−6532	0.183	−3004	−2.520	0.000
1.000	0	0	0.000	0	0.000	0.000

Reference states: Al(liquid), Ca(liquid)

Table IIIb. Partial quantities for Al in the liquid phase at 1400 K.

x_{Al}	ΔG_{Al} [J/mol]	ΔH_{Al} [J/mol]	ΔS_{Al} [J/(mol·K)]	$G^{\mathrm{E}}_{\mathrm{Al}}$ [J/mol]	$S^{\mathrm{E}}_{\mathrm{Al}}$ [J/(mol·K)]	a_{Al}	γ_{Al}
1.000	0	0	0.000	0	0.000	1.000	1.000
0.900	−1738	−903	0.596	−511	−0.280	0.861	0.957
0.800	−4848	−3818	0.735	−2250	−1.120	0.659	0.824
0.700	−9503	−8879	0.446	−5351	−2.520	0.442	0.631
0.600	−15665	−15990	−0.233	−9718	−4.480	0.260	0.434
0.500	−23094	−24825	−1.237	−15025	−7.000	0.138	0.275
0.400	−31380	−34826	−2.461	−20714	−10.080	0.067	0.169
0.300	−40014	−45207	−3.710	−25999	−13.720	0.032	0.107
0.200	−48597	−54950	−4.538	−29862	−17.920	0.015	0.077
0.100	−57858	−62807	−3.535	−31055	−22.680	0.007	0.069
0.000	$-\infty$	−67300	∞	−28100	−28.000	0.000	0.089

Reference state: Al(liquid)

Table IIIc. Partial quantities for Ca in the liquid phase at 1400 K.

x_{Ca}	ΔG_{Ca} [J/mol]	ΔH_{Ca} [J/mol]	ΔS_{Ca} [J/(mol·K)]	G^{E}_{Ca} [J/mol]	S^{E}_{Ca} [J/(mol·K)]	a_{Ca}	γ_{Ca}
0.000	$-\infty$	−91300	∞	−52100	−28.000	0.000	0.011
0.100	−69522	−74471	−3.535	−42719	−22.680	0.003	0.025
0.200	−51669	−58022	−4.538	−32934	−17.920	0.012	0.059
0.300	−37662	−42855	−3.710	−23647	−13.720	0.039	0.131
0.400	−26196	−29642	−2.461	−15530	−10.080	0.105	0.263
0.500	−17094	−18825	−1.237	−9025	−7.000	0.230	0.461
0.600	−10289	−10614	−0.233	−4342	−4.480	0.413	0.689
0.700	−5615	−4991	0.446	−1463	−2.520	0.617	0.882
0.800	−2736	−1706	0.735	−138	−1.120	0.791	0.988
0.900	−1114	−279	0.596	113	−0.280	0.909	1.010
1.000	0	0	0.000	0	0.000	1.000	1.000

Reference state: Ca(liquid)

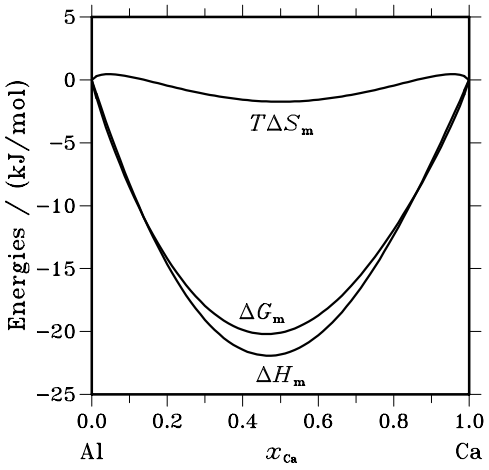

Fig. 2. Integral quantities of the liquid phase at T=1400 K.

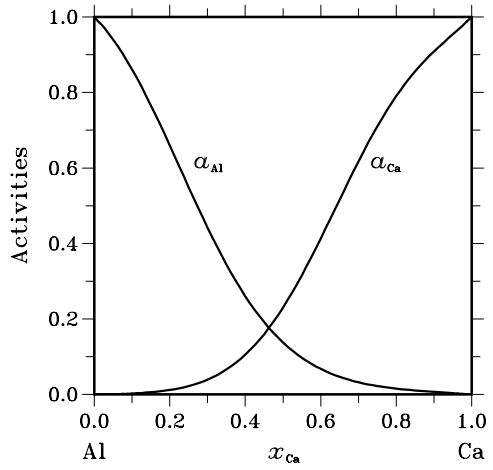

Fig. 3. Activities in the liquid phase at T=1400 K.

Table IV. Standard reaction quantities at 298.15 K for the compounds per mole of atoms.

Compound	x_{Ca}	$\Delta_f G^\circ$ / (J/mol)	$\Delta_f H^\circ$ / (J/mol)	$\Delta_f S^\circ$ / (J/(mol·K))	$\Delta_f C^\circ_P$ / (J/(mol·K))
Al_4Ca_1	0.200	−19363	−21000	−5.492	0.000
Al_2Ca_1	0.333	−28203	−29700	−5.020	0.000
Al_1Ca_1	0.500	−22160	−22800	−2.148	0.000
Al_3Ca_8	0.727	−13860	−14000	−0.470	0.000

References

[93Ang] C. Anglezio, C. Servant, I. Ansara: J. Chem. Phys. PCB **90** (1993) 339–407.
[01Kev1] D. Kevorkov, R. Schmid-Fetzer: Z. Metallkd. **92** (2001) 946–952.
[01Kev2] D. Kevorkov, R. Schmid-Fetzer, A. Pisch, F. Hodaj, C. Colinet: Z. Metallkd. **92** (2001) 953–958.

Al – Ce (Aluminium – Cerium)

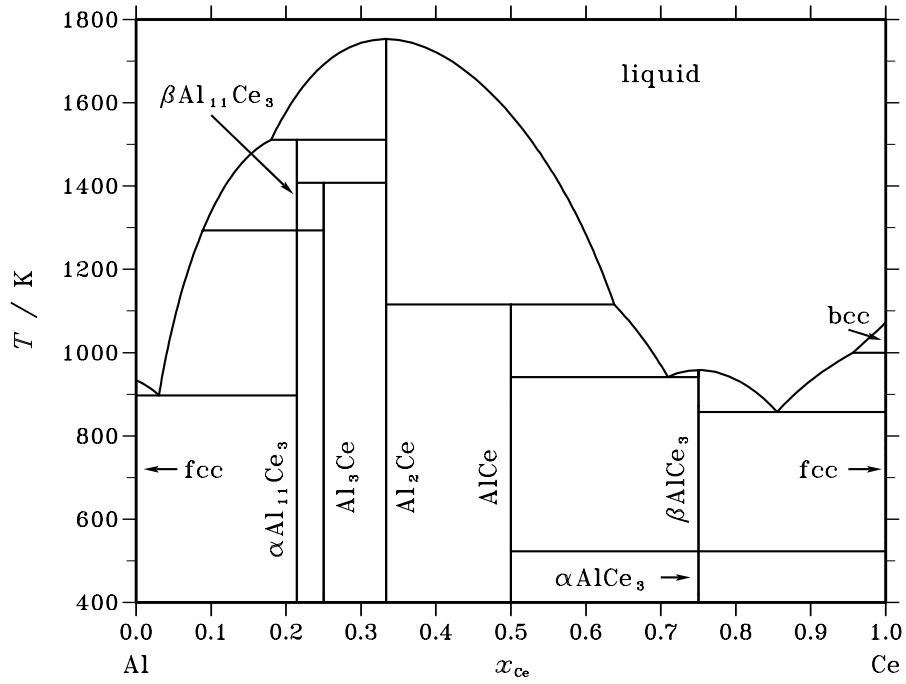

Fig. 1. Calculated phase diagram for the system Al-Ce.

The Al-Ce system is one of a number of rare earth system of interest for its potential for forming metallic glasses [93Bar]. The data for the Al-Ce system were critically assessed by Cacciamani et al. [98Ans]. The phase diagram information on the system has been reviewed by Saccone et al. [96Sac] and Gschneidner and Calderwood [88Gsc] and appears to be well understood. The system is characterised by intermetallic compounds at five compositions, solid-solid phase transformations have been reported for two of these compositions. Solid solution in pure Ce and Al is very low. Two of the compounds Al_2Ce and $AlCe_3$ melt congruently while the other three melt by peritectic reaction. The thermodynamics of the system have been studied by direct reaction calorimetry.

Table I. Phases, structures and models.

Phase	Struktur-bericht	Prototype	Pearson symbol	Space group	SGTE name	Model
liquid					LIQUID	$(Al,Ce)_1$
fcc	$A1$	Cu	$cF4$	$Fm\overline{3}m$	FCC_A1	$(Al,Ce)_1$
$\alpha Al_{11}Ce_3$	···	$\alpha Al_{11}La_3$	$oI28$	$Immm$	AL11M3	$Al_{11}Ce_3$
$\beta Al_{11}Ce_3$	$D1_3$	Al_4Ba	$tI10$	$I4/mmm$	D13_AL11M3	$Al_{11}Ce_3$
Al_3Ce	$D0_{19}$	Ni_3Sn	$hP8$	$P6_3/mmc$	D019_AL3M1	Al_3Ce_1
Al_2Ce	$C15$	Cu_2Mg	$cF24$	$Fd\overline{3}m$	C15_AL2M1	Al_2Ce_1
AlCe	···	AlCe	$oC16$	$Cmcm$	AL1M1	Al_1Ce_1
$\alpha AlCe_3$	$D0_{19}$	Ni_3Sn	$hP8$	$P6_3/mmc$	D019_AL1M3	Al_1Ce_3
$\beta AlCe_3$	$L1_2$	$AuCu_3$	$cP4$	$Pm\overline{3}m$	L12_AL1M3	Al_1Ce_3
bcc	$A2$	W	$cI2$	$Im\overline{3}m$	BCC_A2	$(Al,Ce)_1$

Table II. Invariant reactions.

Reaction	Type	T / K	Compositions / x_{Ce}			$\Delta_r H$ / (J/mol)
liquid ⇌ Al_2Ce	congruent	1752.8	0.333	0.333		−26274
liquid + Al_2Ce ⇌ $\beta Al_{11}Ce_3$	peritectic	1510.7	0.180	0.333	0.214	−15932
$\beta Al_{11}Ce_3$ + Al_2Ce ⇌ Al_3Ce	peritectoid	1408.0	0.214	0.333	0.250	−344
$\beta Al_{11}Ce_3$ ⇌ $\alpha Al_{11}Ce_3$	polymorphic	1293.0	0.214	0.214		−504
Al_2Ce + liquid ⇌ AlCe	peritectic	1115.2	0.333	0.638	0.500	−8594
liquid + bcc ⇌ fcc	peritectic	1000.0	0.956	1.000	1.000	−2992
liquid ⇌ $\beta AlCe_3$	congruent	958.3	0.750	0.750		−6646
liquid ⇌ AlCe + $\beta AlCe_3$	eutectic	941.1	0.709	0.500	0.750	−6873
liquid ⇌ fcc + $\alpha Al_{11}Ce_3$	eutectic	897.0	0.031	0.000	0.214	−10406
liquid ⇌ $\beta AlCe_3$ + fcc	eutectic	857.5	0.855	0.750	1.000	−6048
$\beta AlCe_3$ ⇌ $\alpha AlCe_3$	polymorphic	523.1	0.750	0.750		−999

Table IIIa. Integral quantities for the liquid phase at 1800 K.

x_{Ce}	ΔG_m [J/mol]	ΔH_m [J/mol]	ΔS_m [J/(mol·K)]	G_m^E [J/mol]	S_m^E [J/(mol·K)]	ΔC_p [J/(mol·K)]
0.000	0	0	0.000	0	0.000	0.000
0.100	−11453	−15622	−2.316	−6588	−5.019	1.202
0.200	−18134	−26788	−4.808	−10645	−8.969	1.930
0.300	−21713	−33869	−6.753	−12571	−11.832	2.264
0.400	−22839	−37232	−7.996	−12767	−13.592	2.278
0.500	−22005	−37246	−8.467	−11631	−14.231	2.052
0.600	−19638	−34281	−8.135	−9565	−13.731	1.661
0.700	−16112	−28705	−6.996	−6969	−12.075	1.183
0.800	−11732	−20887	−5.086	−4243	−9.247	0.696
0.900	−6652	−11196	−2.524	−1786	−5.227	0.276
1.000	0	0	0.000	0	0.000	0.000

Reference states: Al(liquid), Ce(liquid)

Table IIIb. Partial quantities for Al in the liquid phase at 1800 K.

x_{Al}	ΔG_{Al} [J/mol]	ΔH_{Al} [J/mol]	ΔS_{Al} [J/(mol·K)]	G_{Al}^E [J/mol]	S_{Al}^E [J/(mol·K)]	a_{Al}	γ_{Al}
1.000	0	0	0.000	0	0.000	1.000	1.000
0.900	−2909	−2289	0.344	−1332	−0.532	0.823	0.915
0.800	−8135	−8664	−0.294	−4795	−2.149	0.581	0.726
0.700	−14927	−18388	−1.923	−9589	−4.888	0.369	0.527
0.600	−22558	−30723	−4.536	−14913	−8.783	0.222	0.369
0.500	−30341	−44930	−8.105	−19967	−13.868	0.132	0.263
0.400	−37665	−60274	−12.561	−23951	−20.179	0.081	0.202
0.300	−44084	−76015	−17.740	−26065	−27.750	0.053	0.175
0.200	−49595	−91417	−23.234	−25508	−36.616	0.036	0.182
0.100	−55941	−105741	−27.667	−21480	−46.812	0.024	0.238
0.000	−∞	−118250	∞	−13181	−58.371	0.000	0.414

Reference state: Al(liquid)

Table IIIc. Partial quantities for Ce in the liquid phase at 1800 K.

x_{Ce}	ΔG_{Ce} [J/mol]	ΔH_{Ce} [J/mol]	ΔS_{Ce} [J/(mol·K)]	G^{E}_{Ce} [J/mol]	S^{E}_{Ce} [J/(mol·K)]	a_{Ce}	γ_{Ce}
0.000	$-\infty$	−179721	∞	−79869	−55.473	0.000	0.005
0.100	−88351	−135616	−26.258	−53890	−45.403	0.003	0.027
0.200	−58131	−99285	−22.863	−34044	−36.245	0.021	0.103
0.300	−37548	−69991	−18.024	−19530	−28.034	0.081	0.271
0.400	−23260	−46996	−13.187	−9547	−20.805	0.211	0.528
0.500	−13669	−29562	−8.830	−3295	−14.593	0.401	0.802
0.600	−7620	−16953	−5.185	25	−9.432	0.601	1.002
0.700	−4124	−8430	−2.392	1214	−5.358	0.759	1.085
0.800	−2266	−3255	−0.549	1073	−2.404	0.859	1.074
0.900	−1175	−691	0.269	402	−0.607	0.924	1.027
1.000	0	0	0.000	0	0.000	1.000	1.000

Reference state: Ce(liquid)

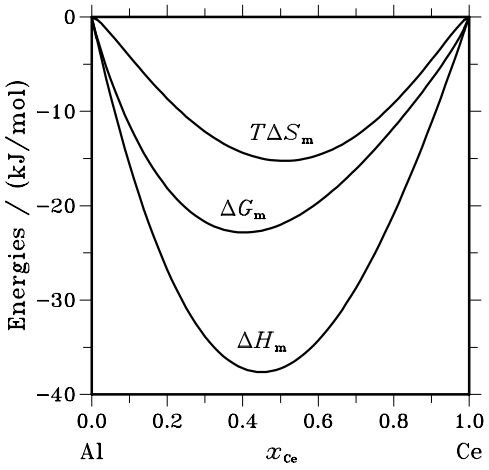

Fig. 2. Integral quantities of the liquid phase at T=1800 K.

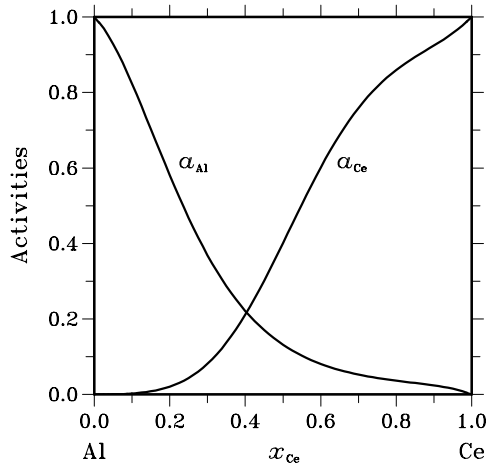

Fig. 3. Activities in the liquid phase at T=1800 K.

Table IV. Standard reaction quantities at 298.15 K for the compounds per mole of atoms.

Compound	x_{Ce}	$\Delta_f G^\circ$ / (J/mol)	$\Delta_f H^\circ$ / (J/mol)	$\Delta_f S^\circ$ / (J/(mol·K))	$\Delta_f C^\circ_P$ / (J/(mol·K))
$\alpha Al_{11}Ce_3$	0.214	−37455	−40182	−9.149	0.000
$\beta Al_{11}Ce_3$	0.214	−37067	−39678	−8.759	0.000
Al_3Ce_1	0.250	−40798	−43803	−10.080	0.000
Al_2Ce_1	0.333	−48600	−52281	−12.345	0.000
Al_1Ce_1	0.500	−41989	−45920	−13.186	0.000
αAl_1Ce_3	0.750	−23024	−25188	−7.256	0.000
βAl_1Ce_3	0.750	−22595	−24189	−5.346	0.000

References

[88Gsc] K.A. Gschneidner Jr., F.W. Calderwood: Bull. Alloy Phase Diagrams, **9** (1988) 669–672.
[93Bar] M. Baricco, L. Battezzati, G. Borzone, G. Cacciamani: J. Chim. Phys. **90** (1993) 261–268.
[96Sac] A. Saccone, A.M. Cardinale, St. Delfino, R. Ferro: Z. Metallkd. **87** (1996) 82–87.
[98Ans] I. Ansara, A.T. Dinsdale, M.H. Rand (eds.): COST 507, "Thermochemical database for light metal alloys", Vol. 2, EUR 18499, 1998, 20–22.

Al – Co (Aluminium – Cobalt)

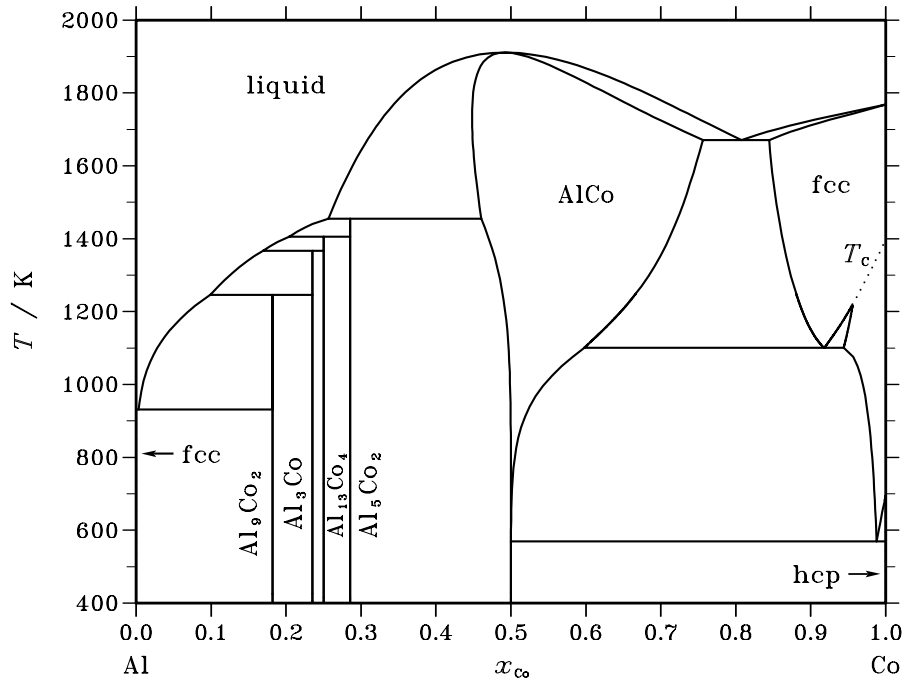

Fig. 1. Calculated phase diagram for the system Al-Co.

The Co rich side of this system is of high interest for superalloys. The $B2$ phase has been studied for the development of alloys for high-temperature applications. The Al rich side is of interest for Al alloys where the strengthening can be enhanced by the precipitation of Al_9Co_2. Finally, the ability of systems based on this binary to generate quasicrystals on the Al rich side has also generated many recent studies. Thus the phase diagram and the thermodynamic properties of this system have been widely studied. Nevertheless, some uncertainties still remain on the Al-rich side of the phase diagram; several forms of the $Al_{13}Co_4$ have been identified but the different range of stability reported show some disagreements. The thermodynamic description by Dupin and Ansara [98Dup] is based on the critical assessment of all the available experimental data for the system. The four compounds Al_9Co_2, $Al_{13}Co_4$, Al_3Co, and Al_5Co are modelled as stoichiometric. The large homogeneity range of the $B2$ compound, AlCo, is described with the compound energy formalism. The solubility of Al in fcc-Co is large and changes rapidly around the magnetic transition. The description of the magnetism of the fcc solution leads to a miscibility gap between ferro- and para-magnetic fcc-Co which has not been experimentally studied.

Table I. Phases, structures and models.

Phase	Struktur-bericht	Prototype	Pearson symbol	Space group	SGTE name	Model
liquid					LIQUID	$(Al,Co)_1$
fcc	$A1$	Cu	$cF4$	$Fm\bar{3}m$	FCC_L12	$(Al,Co)_1$
Al_9Co_2	···	···	$mP22$	$P2_1/c$	AL9CO2	Al_9Co_2
$Al_{13}Co_4$	···	···	$mC93$	C_m	AL13CO4	$Al_{13}Co_4$
Al_3Co	···	···	···	···	AL3CO	Al_3Co_1
Al_5Co_2	$D8_{11}$	Al_5Mn_2	$hP28$	$P6_3/mmc$	D811_AL5CO2	Al_5Co_2
AlCo	$B2$	CsCl	$cP2$	$Pm3m$	BCC_B2	$(Al,Co)_1(Co,\Box)_1$
hcp	$A3$	Mg	$hP2$	$P6_3/mmc$	HCP_A3	$(Al,Co)_1$

Table II. Invariant reactions.

Reaction	Type	T / K	Compositions / x_{Co}			$\Delta_{\mathrm{r}}H$ / (J/mol)
liquid ⇌ AlCo	congruent	1910.9	0.492	0.492		−25510
liquid ⇌ AlCo + fcc	eutectic	1670.6	0.808	0.756	0.845	−15183
liquid + AlCo ⇌ Al_5Co_2	peritectic	1454.6	0.256	0.460	0.286	−22443
liquid + Al_5Co_2 ⇌ Al_3Co	peritectic	1405.0	0.204	0.286	0.250	−9567
liquid + Al_3Co ⇌ $Al_{13}Co_4$	peritectic	1366.7	0.169	0.250	0.235	−3893
liquid + $Al_{13}Co_4$ ⇌ Al_9Co_2	peritectic	1245.6	0.099	0.235	0.182	−8655
fcc ⇌ fcc′ + fcc″	critical	1220.4	0.956	0.956	0.956	0
fcc ⇌ AlCo + fcc′	monotectoid	1100.4	0.918	0.598	0.944	−2260
liquid ⇌ fcc + Al_9Co_2	eutectic	931.3	0.003	0.000	0.182	−10854
fcc ⇌ AlCo + hcp	eutectoid	569.1	0.988	0.500	1.000	−467

Table IIIa. Integral quantities for the liquid phase at 2000 K.

x_{Co}	ΔG_{m} [J/mol]	ΔH_{m} [J/mol]	ΔS_{m} [J/(mol·K)]	$G^{\mathrm{E}}_{\mathrm{m}}$ [J/mol]	$S^{\mathrm{E}}_{\mathrm{m}}$ [J/(mol·K)]	ΔC_p [J/(mol·K)]
0.000	0	0	0.000	0	0.000	0.000
0.100	−11232	−14972	−1.870	−5826	−4.573	0.000
0.200	−19284	−27309	−4.013	−10963	−8.173	0.000
0.300	−25053	−35495	−5.221	−14895	−10.300	0.000
0.400	−28484	−39014	−5.265	−17293	−10.861	0.000
0.500	−29514	−38118	−4.302	−17988	−10.065	0.000
0.600	−28160	−33586	−2.713	−16968	−8.309	0.000
0.700	−24516	−26493	−0.989	−14358	−6.068	0.000
0.800	−18726	−17968	0.379	−10404	−3.782	0.000
0.900	−10873	−8960	0.957	−5467	−1.746	0.000
1.000	0	0	0.000	0	0.000	0.000

Reference states: Al(liquid), Co(liquid)

Table IIIb. Partial quantities for Al in the liquid phase at 2000 K.

x_{Al}	ΔG_{Al} [J/mol]	ΔH_{Al} [J/mol]	ΔS_{Al} [J/(mol·K)]	$G^{\mathrm{E}}_{\mathrm{Al}}$ [J/mol]	$S^{\mathrm{E}}_{\mathrm{Al}}$ [J/(mol·K)]	a_{Al}	γ_{Al}
1.000	0	0	0.000	0	0.000	1.000	1.000
0.900	−1996	−969	0.514	−244	−0.362	0.887	0.985
0.800	−5464	−6463	−0.499	−1754	−2.355	0.720	0.900
0.700	−11208	−17896	−3.344	−5277	−6.309	0.510	0.728
0.600	−19544	−34145	−7.301	−11049	−11.548	0.309	0.515
0.500	−30374	−52499	−11.063	−18847	−16.826	0.161	0.322
0.400	−43286	−69608	−13.161	−28049	−20.779	0.074	0.185
0.300	−57709	−82423	−12.357	−37688	−22.368	0.031	0.104
0.200	−73274	−89151	−7.938	−46511	−21.320	0.012	0.061
0.100	−91323	−90195	0.564	−53034	−18.580	0.004	0.041
0.000	−∞	−89104	∞	−55598	−16.753	0.000	0.035

Reference state: Al(liquid)

Table IIIc. Partial quantities for Co in the liquid phase at 2000 K.

x_{Co}	ΔG_{Co} [J/mol]	ΔH_{Co} [J/mol]	ΔS_{Co} [J/(mol·K)]	G^{E}_{Co} [J/mol]	S^{E}_{Co} [J/(mol·K)]	a_{Co}	γ_{Co}
0.000	$-\infty$	−154849	∞	−59526	−47.661	0.000	0.028
0.100	−94359	−140999	−23.320	−56069	−42.465	0.003	0.034
0.200	−74561	−110695	−18.067	−47798	−31.448	0.011	0.056
0.300	−57359	−76560	−9.601	−37338	−19.611	0.032	0.106
0.400	−41895	−46318	−2.212	−26658	−9.830	0.081	0.201
0.500	−28655	−23736	2.460	−17129	−3.303	0.178	0.357
0.600	−18076	−9572	4.252	−9581	0.005	0.337	0.562
0.700	−10290	−2523	3.883	−4359	0.918	0.539	0.769
0.800	−5088	−173	2.458	−1378	0.603	0.736	0.920
0.900	−1934	66	1.000	−182	0.124	0.890	0.989
1.000	0	0	0.000	0	0.000	1.000	1.000

Reference state: Co(liquid)

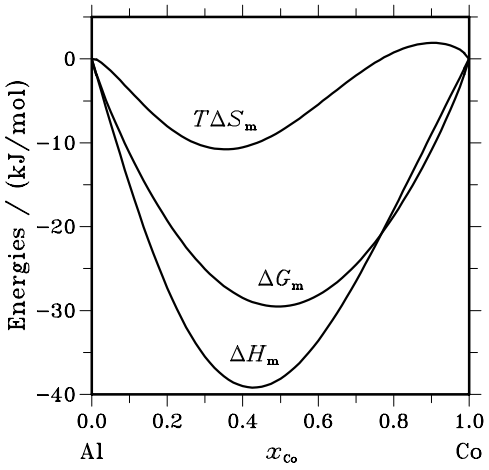

Fig. 2. Integral quantities of the liquid phase at T=2000 K.

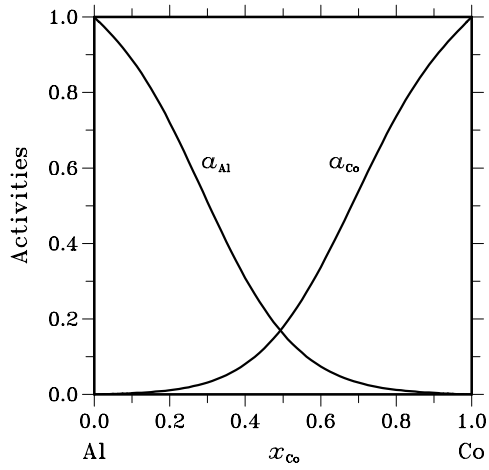

Fig. 3. Activities in the liquid phase at T=2000 K.

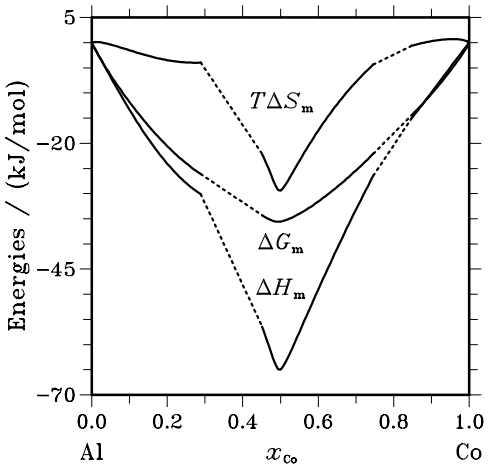

Fig. 4. Integral quantities of the stable phases at T=1600 K.

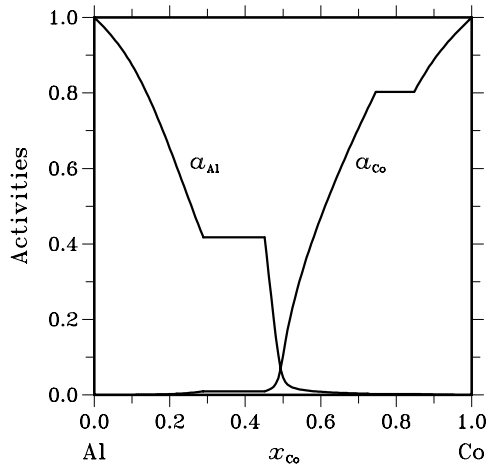

Fig. 5. Activities in the stable phases at T=1600 K.

Table IVa. Integral quantities for the stable phases at 1600 K.

Phase	x_{Co}	ΔG_{m} [J/mol]	ΔH_{m} [J/mol]	ΔS_{m} [J/(mol·K)]	$G_{\mathrm{m}}^{\mathrm{E}}$ [J/mol]	$S_{\mathrm{m}}^{\mathrm{E}}$ [J/(mol·K)]	ΔC_p [J/(mol·K)]
liquid	0.000	0	0	0.000	0	0.000	0.000
	0.050	−6467	−6861	−0.246	−3826	−1.897	−0.091
	0.100	−11826	−13345	−0.949	−7502	−3.652	−0.182
	0.150	−16524	−19150	−1.641	−10901	−5.156	−0.273
	0.200	−20581	−24055	−2.171	−13924	−6.332	−0.364
	0.250	−23974	−27906	−2.458	−16493	−7.133	−0.455
	0.289	−26133	−30107	−2.484	−18137	−7.482	−0.525
AlCo	0.452	−34320	−56482	−13.851	−31210	−15.795	−1.008
	0.500	−35547	−64949	−18.376	−34359	−19.119	15.319
	0.550	−34009	−57518	−14.693	−31480	−16.274	6.434
	0.600	−31586	−49066	−10.925	−28006	−13.163	3.603
	0.650	−28678	−40921	−7.652	−24416	−10.316	2.149
	0.700	−25390	−33182	−4.870	−20746	−7.772	1.202
	0.746	−22045	−26405	−2.725	−17288	−5.698	0.556
fcc	0.848	−14407	−15021	−0.384	−8728	−3.933	−2.461
	0.850	−14226	−14792	−0.354	−8603	−3.869	−2.454
	0.900	−10180	−9899	0.176	−5855	−2.527	−2.170
	0.950	−5595	−4898	0.435	−2954	−1.215	−1.474
	1.000	0	0	0.000	0	0.000	0.000

Reference states: Al(liquid), Co(fcc)

Table IVb. Partial quantities for Al in the stable phases at 1600 K.

Phase	x_{Al}	ΔG_{Al} [J/mol]	ΔH_{Al} [J/mol]	ΔS_{Al} [J/(mol·K)]	$G_{\mathrm{Al}}^{\mathrm{E}}$ [J/mol]	$S_{\mathrm{Al}}^{\mathrm{E}}$ [J/(mol·K)]	a_{Al}	γ_{Al}
liquid	1.000	0	0	0.000	0	0.000	1.000	1.000
	0.950	−734	−132	0.377	−52	−0.050	0.946	0.996
	0.900	−1790	−969	0.514	−389	−0.362	0.874	0.971
	0.850	−3385	−2991	0.246	−1223	−1.105	0.775	0.912
	0.800	−5664	−6463	−0.499	−2695	−2.355	0.653	0.817
	0.750	−8709	−11459	−1.719	−4882	−4.111	0.520	0.693
	0.711	−11615	−16332	−2.948	−7082	−5.782	0.418	0.587
AlCo	0.548	−11615	39552	31.979	6645	20.567	0.418	1.648
	0.500	−41083	−88188	−29.441	−43608	−27.862	0.046	0.038
	0.450	−57198	−151065	−58.667	−68657	−51.505	0.014	0.006
	0.400	−63886	−148994	−53.192	−70512	−49.051	0.008	0.005
	0.350	−69079	−144255	−46.985	−71633	−45.389	0.006	0.005
	0.300	−73857	−138559	−40.439	−72637	−41.202	0.004	0.004
	0.254	−78287	−132715	−34.018	−73560	−36.972	0.003	0.004
fcc	0.152	−78287	−95784	−10.935	−53259	−26.578	0.003	0.018
	0.150	−78699	−96020	−10.826	−53461	−26.599	0.003	0.018
	0.100	−87616	−99532	−7.448	−56985	−26.593	0.001	0.014
	0.050	−98761	−99629	−0.543	−58908	−25.451	0.001	0.012
	0.000	$-\infty$	−95457	∞	−58933	−22.828	0.000	0.012

Reference state: Al(liquid)

Table IVc. Partial quantities for Co in the stable phases at 1600 K.

Phase	x_{Co}	ΔG_{Co} [J/mol]	ΔH_{Co} [J/mol]	ΔS_{Co} [J/(mol·K)]	G^{E}_{Co} [J/mol]	S^{E}_{Co} [J/(mol·K)]	a_{Co}	γ_{Co}
liquid	0.000	$-\infty$	−138578	∞	−77051	−38.454	0.000	0.003
	0.050	−115383	−134716	−12.083	−75530	−36.991	0.000	0.003
	0.100	−102147	−124728	−14.113	−71516	−33.258	0.000	0.005
	0.150	−90980	−110718	−12.336	−65743	−28.110	0.001	0.007
	0.200	−80249	−94424	−8.859	−58838	−22.241	0.002	0.012
	0.250	−69770	−77249	−4.674	−51328	−16.201	0.005	0.021
	0.289	−61892	−64037	−1.341	−45367	−11.669	0.010	0.033
AlCo	0.452	−61892	−173096	−69.503	−77177	−59.949	0.010	0.003
	0.500	−30011	−41709	−7.312	−25111	−10.375	0.105	0.151
	0.550	−15036	19022	21.286	−1062	12.552	0.323	0.923
	0.600	−10052	17553	17.253	332	10.763	0.470	1.025
	0.650	−6924	14720	13.527	1008	8.570	0.594	1.079
	0.700	−4619	11980	10.374	1493	6.555	0.707	1.119
	0.746	−2922	9744	7.916	1847	4.936	0.803	1.149
fcc	0.848	−2922	−500	1.513	−722	0.139	0.803	0.947
	0.850	−2848	−458	1.494	−686	0.143	0.807	0.950
	0.900	−1576	61	1.023	−174	0.147	0.888	0.987
	0.950	−691	87	0.487	−9	0.060	0.949	0.999
	1.000	0	0	0.000	0	0.000	1.000	1.000

Reference state: Co(fcc)

Table V. Standard reaction quantities at 298.15 K for the compounds per mole of atoms.

Compound	x_{Co}	$\Delta_f G^\circ$ / (J/mol)	$\Delta_f H^\circ$ / (J/mol)	$\Delta_f S^\circ$ / (J/(mol·K))	$\Delta_f C^\circ_P$ / (J/(mol·K))
Al_9Co_2	0.182	−31639	−34069	−8.151	−0.026
$Al_{13}Co_4$	0.235	−37370	−39863	−8.363	−0.034
Al_3Co_1	0.250	−38907	−41492	−8.670	−0.036
Al_5Co_2	0.286	−42560	−45437	−9.648	−0.041
Al_1Co_1	0.500	−55194	−58479	−11.019	−0.072

References

[98Dup] N. Dupin, I. Ansara: Rev. Métall. **9** (1998) 1121–1129.

Al – Cr (Aluminium – Chromium)

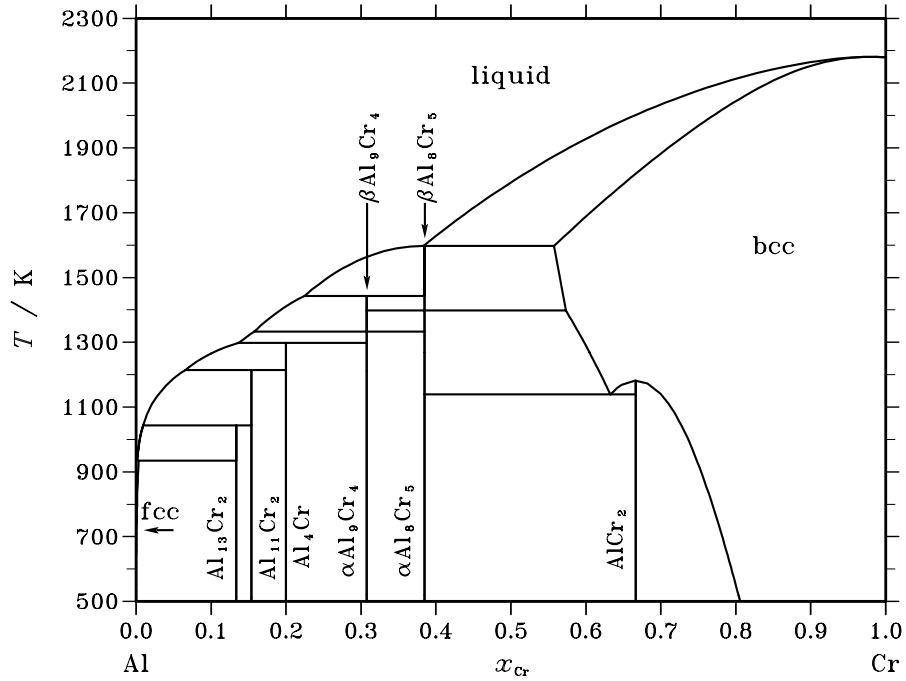

Fig. 1. Calculated phase diagram for the system Al-Cr.

There is only a small solubility of Cr in fcc Al while Al is very stable in bcc Cr. Many intermetallic phases form precipitate on cooling from the liquid. Some of these have a significant solubility range but they have all been modelled as stoichiometric compounds. They form a series of peritectic reactions with the liquid except the $AlCr_2$ compound which forms from the bcc Cr phase. Some of the intermediate phases have transformations at lower temperatures. Both Al and Cr are important alloying elements in nickel based superalloys but also in steels and other metals.
There is a limited amount of experimental data, mainly in the Al rich side. The assessment has been done by N. Saunders and the parameters are reported in COST 507 [98Ans]. To date, the assessment has not been published separately.

Table I. Phases, structures and models.

Phase	Struktur-bericht	Prototype	Pearson symbol	Space group	SGTE name	Model
liquid					LIQUID	$(Al,Cr)_1$
fcc	$A1$	Cu	$cF4$	$Fm\overline{3}m$	FCC_A1	$(Al,Cr)_1$
$Al_{13}Cr_2$	···	$Al_{45}V_7$	$mC104$	$C2/m$	AL13CR2	$Al_{13}Cr_2$
$Al_{11}Cr_2$	···	Al_5Cr	$mP48$	$P2$	AL11CR2	$Al_{10}Al_1Cr_2$
Al_4Cr	···	Al_4Cr	$mP180$	$P2/m$	AL4CR	Al_4Cr_1
αAl_9Cr_4	···	Al_9Cr_4	$cI52$	$I\overline{4}3m$	AL9CR4_L	Al_9Cr_4
βAl_9Cr_4	···	···	···	···	AL9CR4_H	Al_9Cr_4
αAl_8Cr_5	$D8_{10}$	Al_8Cr_5	$hR26$	$R\overline{3}m$	AL8CR5_L	Al_8Cr_5
βAl_8Cr_5	···	···	···	···	AL8CR5_H	Al_8Cr_5
$AlCr_2$	$C11_b$	$MoSi_2$	$tI6$	$I4/mmm$	ALCR2	Al_1Cr_2
bcc	$A2$	W	$cI2$	$Im\overline{3}m$	BCC_A2	$(Al,Cr)_1$

Table II. Invariant reactions.

Reaction	Type	T / K	Compositions / x_{Cr}			$\Delta_{\mathrm{r}}H$ / (J/mol)
liquid + bcc $\rightleftharpoons \beta Al_8Cr_5$	peritectic	1597.0	0.383	0.558	0.385	−19408
liquid + $\beta Al_8Cr_5 \rightleftharpoons \beta Al_9Cr_4$	peritectic	1443.1	0.225	0.385	0.308	−8029
$\beta Al_8Cr_5 \rightleftharpoons \alpha Al_8Cr_5$	polymorphic	1398.0	0.385	0.385		−6291
$\beta Al_9Cr_4 \rightleftharpoons \alpha Al_9Cr_4$	polymorphic	1333.0	0.308	0.308		−7409
liquid + $\alpha Al_9Cr_4 \rightleftharpoons Al_4Cr$	peritectic	1298.1	0.137	0.308	0.200	−16291
liquid + $Al_4Cr \rightleftharpoons Al_{11}Cr_2$	peritectic	1214.6	0.066	0.200	0.154	−4929
bcc $\rightleftharpoons AlCr_2$	congruent	1181.5	0.667	0.667		−2061
bcc $\rightleftharpoons \alpha Al_8Cr_5$ + $AlCr_2$	eutectoid	1139.3	0.633	0.385	0.667	−2656
liquid + $Al_{11}Cr_2 \rightleftharpoons Al_{13}Cr_2$	peritectic	1042.9	0.009	0.154	0.133	−1509
liquid + $Al_{13}Cr_2 \rightleftharpoons$ fcc	peritectic	934.8	0.002	0.133	0.003	−10473

Table IIIa. Integral quantities for the liquid phase at 2200 K.

x_{Cr}	ΔG_{m} [J/mol]	ΔH_{m} [J/mol]	ΔS_{m} [J/(mol·K)]	$G^{\mathrm{E}}_{\mathrm{m}}$ [J/mol]	$S^{\mathrm{E}}_{\mathrm{m}}$ [J/(mol·K)]	ΔC_p [J/(mol·K)]
0.000	0	0	0.000	0	0.000	0.000
0.100	−9348	−3402	2.703	−3402	0.000	0.000
0.200	−14849	−5696	4.161	−5696	0.000	0.000
0.300	−18188	−7014	5.079	−7014	0.000	0.000
0.400	−19799	−7488	5.596	−7488	0.000	0.000
0.500	−19929	−7250	5.763	−7250	0.000	0.000
0.600	−18743	−6432	5.596	−6432	0.000	0.000
0.700	−16340	−5166	5.079	−5166	0.000	0.000
0.800	−12737	−3584	4.161	−3584	0.000	0.000
0.900	−7764	−1818	2.703	−1818	0.000	0.000
1.000	0	0	0.000	0	0.000	0.000

Reference states: Al(liquid), Cr(liquid)

Table IIIb. Partial quantities for Al in the liquid phase at 2200 K.

x_{Al}	ΔG_{Al} [J/mol]	ΔH_{Al} [J/mol]	ΔS_{Al} [J/(mol·K)]	$G^{\mathrm{E}}_{\mathrm{Al}}$ [J/mol]	$S^{\mathrm{E}}_{\mathrm{Al}}$ [J/(mol·K)]	a_{Al}	γ_{Al}
1.000	0	0	0.000	0	0.000	1.000	1.000
0.900	−2503	−576	0.876	−576	0.000	0.872	0.969
0.800	−6210	−2128	1.855	−2128	0.000	0.712	0.890
0.700	−10916	−4392	2.966	−4392	0.000	0.551	0.787
0.600	−16448	−7104	4.247	−7104	0.000	0.407	0.678
0.500	−22679	−10000	5.763	−10000	0.000	0.289	0.579
0.400	−29577	−12816	7.619	−12816	0.000	0.199	0.496
0.300	−37311	−15288	10.010	−15288	0.000	0.130	0.434
0.200	−46592	−17152	13.382	−17152	0.000	0.078	0.392
0.100	−60263	−18144	19.145	−18144	0.000	0.037	0.371
0.000	$-\infty$	−18000	∞	−18000	0.000	0.000	0.374

Reference state: Al(liquid)

Table IIIc. Partial quantities for Cr in the liquid phase at 2200 K.

x_{Cr}	ΔG_{Cr} [J/mol]	ΔH_{Cr} [J/mol]	ΔS_{Cr} [J/(mol·K)]	G^E_{Cr} [J/mol]	S^E_{Cr} [J/(mol·K)]	a_{Cr}	γ_{Cr}
0.000	$-\infty$	−40000	∞	−40000	0.000	0.000	0.112
0.100	−70955	−28836	19.145	−28836	0.000	0.021	0.207
0.200	−49408	−19968	13.382	−19968	0.000	0.067	0.336
0.300	−35155	−13132	10.010	−13132	0.000	0.146	0.488
0.400	−24825	−8064	7.619	−8064	0.000	0.257	0.643
0.500	−17179	−4500	5.763	−4500	0.000	0.391	0.782
0.600	−11520	−2176	4.247	−2176	0.000	0.533	0.888
0.700	−7352	−828	2.966	−828	0.000	0.669	0.956
0.800	−4274	−192	1.855	−192	0.000	0.792	0.990
0.900	−1931	−4	0.876	−4	0.000	0.900	1.000
1.000	0	0	0.000	0	0.000	1.000	1.000

Reference state: Cr(liquid)

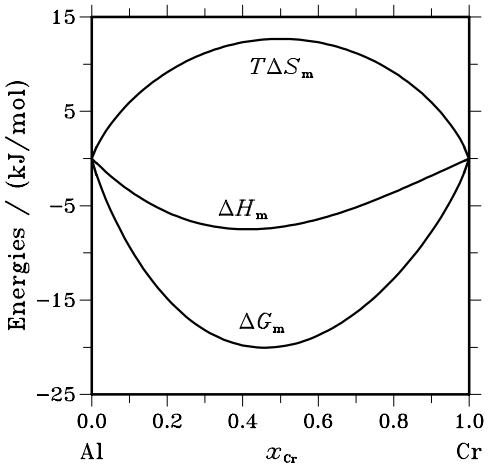

Fig. 2. Integral quantities of the liquid phase at T=2200 K.

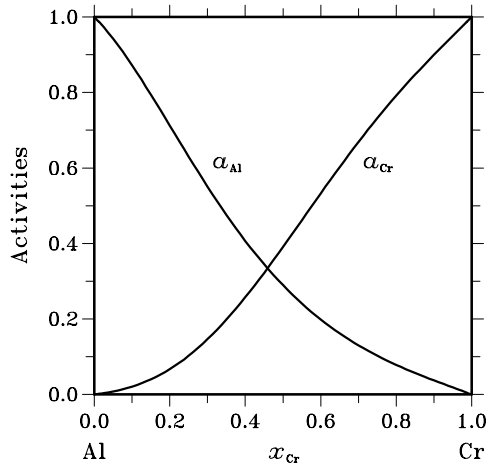

Fig. 3. Activities in the liquid phase at T=2200 K.

Table IVa. Integral quantities for the stable phases at 1600 K.

Phase	x_{Cr}	ΔG_m [J/mol]	ΔH_m [J/mol]	ΔS_m [J/(mol·K)]	G^E_m [J/mol]	S^E_m [J/(mol·K)]	ΔC_p [J/(mol·K)]
liquid	0.000	0	0	0.000	0	0.000	0.000
	0.100	−7114	−1006	3.817	−2789	1.114	−0.167
	0.200	−11127	−905	6.389	−4470	2.228	−0.335
	0.300	−13301	173	8.421	−5175	3.342	−0.502
	0.385	−13971	1753	9.827	−5106	4.287	−0.644
bcc	0.559	−14349	−13712	0.399	−5221	−5.307	0.004
	0.600	−14327	−13337	0.619	−5374	−4.977	0.004
	0.700	−13324	−11649	1.046	−5197	−4.033	0.003
	0.800	−10900	−8864	1.272	−4243	−2.888	0.002
	0.900	−6835	−4981	1.159	−2510	−1.544	0.001
	1.000	0	0	0.000	0	0.000	0.000

Reference states: Al(liquid), Cr(bcc)

Table IVb. Partial quantities for Al in the stable phases at 1600 K.

Phase	x_{Al}	ΔG_{Al} [J/mol]	ΔH_{Al} [J/mol]	ΔS_{Al} [J/(mol·K)]	G^{E}_{Al} [J/mol]	S^{E}_{Al} [J/(mol·K)]	a_{Al}	γ_{Al}
liquid	1.000	0	0	0.000	0	0.000	1.000	1.000
	0.900	−1978	−576	0.876	−576	0.000	0.862	0.958
	0.800	−5097	−2128	1.855	−2128	0.000	0.682	0.852
	0.700	−9137	−4392	2.966	−4392	0.000	0.503	0.719
	0.615	−13134	−6672	4.039	−6672	0.000	0.373	0.606
bcc	0.441	−13134	−17551	−2.760	−2245	−9.566	0.373	0.845
	0.400	−16288	−20165	−2.423	−4098	−10.042	0.294	0.735
	0.300	−25172	−27302	−1.332	−9155	−11.342	0.151	0.502
	0.200	−36401	−35537	0.540	−14990	−12.842	0.065	0.324
	0.100	−52235	−44870	4.603	−21603	−14.542	0.020	0.197
	0.000	−∞	−55301	∞	−28994	−16.442	0.000	0.113

Reference state: Al(liquid)

Table IVc. Partial quantities for Cr in the stable phases at 1600 K.

Phase	x_{Cr}	ΔG_{Cr} [J/mol]	ΔH_{Cr} [J/mol]	ΔS_{Cr} [J/(mol·K)]	G^{E}_{Cr} [J/mol]	S^{E}_{Cr} [J/(mol·K)]	a_{Cr}	γ_{Cr}
liquid	0.000	−∞	−16043	∞	−33869	11.141	0.000	0.078
	0.100	−53336	−4879	30.286	−22705	11.141	0.018	0.181
	0.200	−35247	3989	24.523	−13837	11.141	0.071	0.353
	0.300	−23017	10825	21.152	−7001	11.141	0.177	0.591
	0.385	−15308	15224	19.083	−2602	11.141	0.316	0.822
bcc	0.559	−15308	−10682	2.892	−7569	−1.946	0.316	0.566
	0.600	−13020	−8784	2.647	−6224	−1.600	0.376	0.626
	0.700	−8246	−4941	2.066	−3501	−0.900	0.538	0.769
	0.800	−4525	−2196	1.455	−1556	−0.400	0.712	0.890
	0.900	−1791	−549	0.776	−389	−0.100	0.874	0.971
	1.000	0	0	0.000	0	0.000	1.000	1.000

Reference state: Cr(bcc)

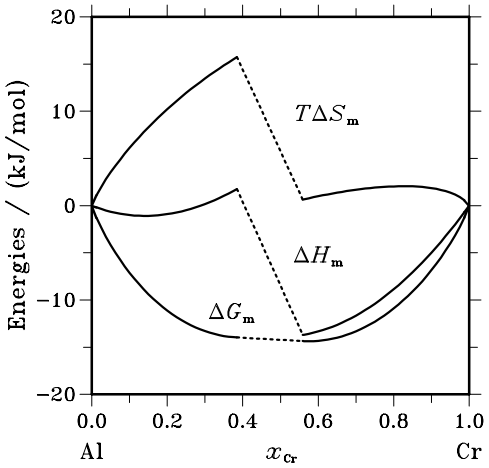

Fig. 4. Integral quantities of the stable phases at T=1600 K.

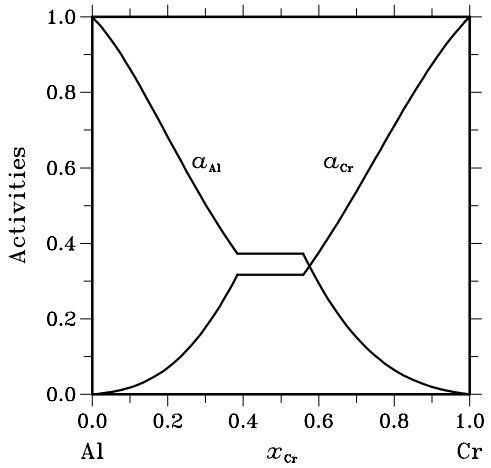

Fig. 5. Activities in the stable phases at T=1600 K.

Table V. Standard reaction quantities at 298.15 K for the compounds per mole of atoms.

Compound	x_{Cr}	$\Delta_{\mathrm{f}}G^{\circ}$ / (J/mol)	$\Delta_{\mathrm{f}}H^{\circ}$ / (J/mol)	$\Delta_{\mathrm{f}}S^{\circ}$ / (J/(mol·K))	$\Delta_{\mathrm{f}}C_P^{\circ}$ / (J/(mol·K))
$Al_{13}Cr_2$	0.133	−11186	−11626	−1.476	−0.020
$Al_{11}Cr_2$	0.154	−12908	−13499	−1.981	−0.023
Al_4Cr_1	0.200	−16669	−17803	−3.805	−0.029
αAl_9Cr_4	0.308	−17380	−17747	−1.230	−0.045
βAl_9Cr_4	0.308	−11628	−10338	4.328	−0.045
αAl_8Cr_5	0.385	−17654	−17651	0.010	−0.056
βAl_8Cr_5	0.385	−12705	−11360	4.510	−0.056
Al_1Cr_2	0.666	−11772	−10894	2.948	−0.098

References

[98Ans] I. Ansara, A.T. Dinsdale, M.H. Rand (eds.): COST 507, "Thermochemical database for light metal alloys", Vol. 2, EUR 18499, 1998, 23–27.

Al – Cu (Aluminium – Copper)

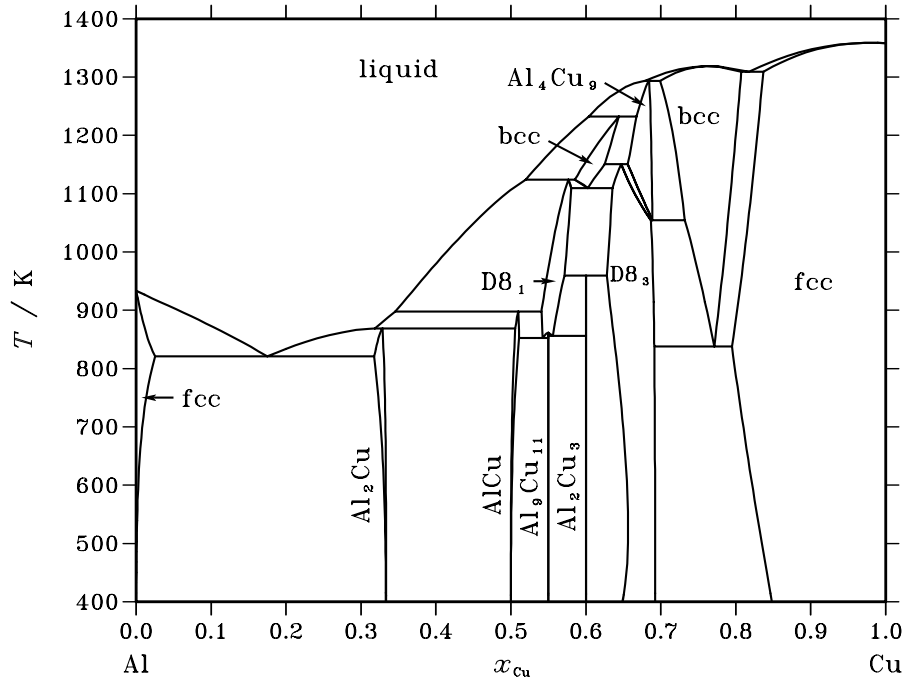

Fig. 1. Calculated phase diagram for the system Al-Cu.

The data for the Al-Cu system are taken from the critical assessment of Saunders [98Sau]. The phase diagram for this system is now well established and is characterised by a number of intermetallic phases many of which exist over appreciable ranges of homogeneity. The calculated phase diagram is similar to that recommended in the reviews by Murray [85Mur] and Raynor [44Ray]. There have been many studies of the thermodynamic properties of the system which are in reasonable agreement except for the measurements of the enthalpy of mixing in the liquid phase. The assessment of Saunders favoured the experimental results for the liquid phase of Sandakov et al. [71San] and Heyer [89Hey] over those of Itagaki and Yazawa [75ita], Kawakami [30Kaw] and Oelsen and Middel [37Oel]. There is generally good agreement between calculated and experimental data throughout the system.

Table I. Phases, structures and models.

Phase	Struktur-bericht	Prototype	Pearson symbol	Space group	SGTE name	Model
liquid					LIQUID	$(Al,Cu)_1$
fcc	$A1$	Cu	$cF4$	$Fm\overline{3}m$	FCC_A1	$(Al,Cu)_1$
Al_2Cu	$C16$	Al_2Cu	$tI12$	$I4/mcm$	C16_AL2CU	$Al_2(Al,Cu)_1$
AlCu	···	···	$mC20$	$C2/m$	ALCU_ETA	$(Al,Cu)_1Cu_1$
Al_9Cu_{11}	···	···	$hP42$	$P6/mmm$	ALCU_ZETA	Al_9Cu_{11}
$D8_1$	$D8_1$	NiAs	$hP4$	$P6_3/mmc$	D81_ALCU	$(Al,Cu)_1Cu_1$
bcc	$A2$	W	$cI2$	$Im\overline{3}m$	BCC_A2	$(Al,Cu)_1$
Al_2Cu_3	···	···	hR^*	$R\overline{3}m$	ALCU_DELTA	Al_2Cu_3
Al_4Cu_9	···	···	···	···	GAMMA_H	$Al_4(Al,Cu)_1Cu_8$
$D8_3$	$D8_3$	Al_4Cu_9	$cP52$	$P\overline{4}3m$	D83_GAMMA	$Al_4(Al,Cu)_1Cu_8$

Table II. Invariant reactions.

Reaction	Type	T / K	Compositions / x_{Cu}			$\Delta_{\mathrm{r}}H$ / (J/mol)
liquid ⇌ bcc	congruent	1318.8	0.765	0.765		−9939
liquid ⇌ bcc + fcc	eutectic	1309.3	0.818	0.807	0.837	−10449
liquid + bcc ⇌ Al_4Cu_9	peritectic	1293.4	0.679	0.699	0.684	−8074
liquid + Al_4Cu_9 ⇌ bcc	peritectic	1232.4	0.604	0.667	0.644	−1974
bcc + Al_4Cu_9 ⇌ $D8_3$	peritectoid	1150.5	0.625	0.656	0.647	−2400
liquid + bcc ⇌ $D8_1$	peritectic	1124.1	0.520	0.585	0.577	−5425
bcc ⇌ $D8_1$ + $D8_3$	eutectoid	1109.3	0.602	0.580	0.635	−4190
Al_4Cu_9 ⇌ $D8_3$ + bcc	eutectoid	1054.2	0.689	0.687	0.732	−1811
$D8_1$ + $D8_3$ ⇌ Al_2Cu_3	peritectoid	959.7	0.572	0.628	0.600	−2836
liquid + $D8_1$ ⇌ AlCu	peritectic	898.1	0.346	0.541	0.510	−4239
liquid + AlCu ⇌ Al_2Cu	peritectic	869.0	0.319	0.506	0.329	−14313
$D8_1$ ⇌ Al_9Cu_{11}	congruent	861.3	0.550	0.550		−2513
$D8_1$ ⇌ Al_9Cu_{11} + Al_2Cu_3	eutectoid	855.8	0.556	0.550	0.600	−2674
$D8_1$ ⇌ AlCu + Al_9Cu_{11}	eutectoid	852.4	0.543	0.511	0.550	−2210
bcc ⇌ $D8_3$ + fcc	eutectoid	837.9	0.771	0.691	0.795	−1210
liquid ⇌ fcc + Al_2Cu	eutectic	820.7	0.175	0.025	0.318	−12719

Table IIIa. Integral quantities for the liquid phase at 1400 K.

x_{Cu}	ΔG_{m} [J/mol]	ΔH_{m} [J/mol]	ΔS_{m} [J/(mol·K)]	$G_{\mathrm{m}}^{\mathrm{E}}$ [J/mol]	$S_{\mathrm{m}}^{\mathrm{E}}$ [J/(mol·K)]	ΔC_p [J/(mol·K)]
0.000	0	0	0.000	0	0.000	0.000
0.100	−7402	−3796	2.576	−3618	−0.127	−0.720
0.200	−12806	−7673	3.667	−6982	−0.494	−0.960
0.300	−17042	−11330	4.080	−9931	−0.999	−0.840
0.400	−20116	−14442	4.053	−12282	−1.543	−0.480
0.500	−21889	−16656	3.738	−13821	−2.025	0.000
0.600	−22142	−17591	3.251	−14307	−2.345	0.480
0.700	−20587	−16840	2.676	−13476	−2.403	0.840
0.800	−16858	−13970	2.062	−11033	−2.098	0.960
0.900	−10441	−8520	1.372	−6656	−1.331	0.720
1.000	0	0	0.000	0	0.000	0.000

Reference states: Al(liquid), Cu(liquid)

Table IIIb. Partial quantities for Al in the liquid phase at 1400 K.

x_{Al}	ΔG_{Al} [J/mol]	ΔH_{Al} [J/mol]	ΔS_{Al} [J/(mol·K)]	G^E_{Al} [J/mol]	S^E_{Al} [J/(mol·K)]	a_{Al}	γ_{Al}
1.000	0	0	0.000	0	0.000	1.000	1.000
0.900	−1330	88	1.012	−103	0.136	0.892	0.991
0.800	−3208	−35	2.267	−611	0.411	0.759	0.949
0.700	−6033	−1006	3.591	−1881	0.625	0.596	0.851
0.600	−10299	−3546	4.823	−4353	0.576	0.413	0.688
0.500	−16614	−8456	5.828	−8546	0.064	0.240	0.480
0.400	−25727	−16616	6.508	−15061	−1.111	0.110	0.274
0.300	−38594	−28990	6.860	−24580	−3.150	0.036	0.121
0.200	−56600	−46621	7.128	−37865	−6.254	0.008	0.039
0.100	−82564	−70634	8.522	−55762	−10.623	0.001	0.008
0.000	$-\infty$	−102234	∞	−79193	−16.458	0.000	0.001

Reference state: Al(liquid)

Table IIIc. Partial quantities for Cu in the liquid phase at 1400 K.

x_{Cu}	ΔG_{Cu} [J/mol]	ΔH_{Cu} [J/mol]	ΔS_{Cu} [J/(mol·K)]	G^E_{Cu} [J/mol]	S^E_{Cu} [J/(mol·K)]	a_{Cu}	γ_{Cu}
0.000	$-\infty$	−36634	∞	−36995	0.258	0.000	0.042
0.100	−62056	−38752	16.646	−35253	−2.499	0.005	0.048
0.200	−51198	−38224	9.267	−32464	−4.114	0.012	0.061
0.300	−42730	−35418	5.222	−28715	−4.788	0.025	0.085
0.400	−34841	−30785	2.897	−24176	−4.721	0.050	0.125
0.500	−27164	−24856	1.649	−19095	−4.114	0.097	0.194
0.600	−19752	−18241	1.079	−13805	−3.168	0.183	0.305
0.700	−12869	−11634	0.883	−8717	−2.083	0.331	0.473
0.800	−6922	−5808	0.796	−4324	−1.059	0.552	0.690
0.900	−2427	−1618	0.578	−1200	−0.298	0.812	0.902
1.000	0	0	0.000	0	0.000	1.000	1.000

Reference state: Cu(liquid)

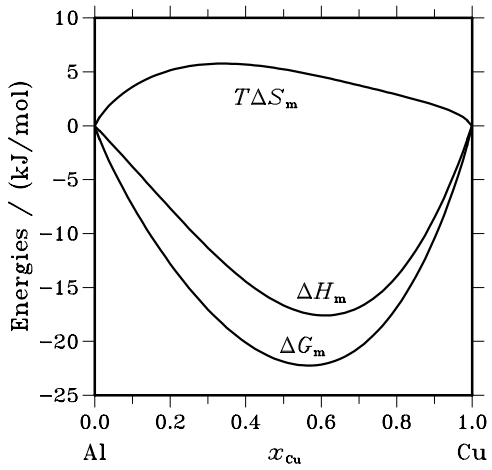

Fig. 2. Integral quantities of the liquid phase at T=1400 K.

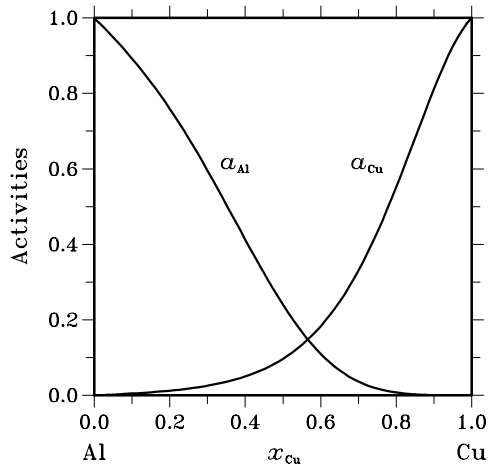

Fig. 3. Activities in the liquid phase at T=1400 K.

Table IV. Standard reaction quantities at 298.15 K for the compounds per mole of atoms.

Compound	x_{Cu}	$\Delta_{\mathrm{f}}G^{\circ}$ / (J/mol)	$\Delta_{\mathrm{f}}H^{\circ}$ / (J/mol)	$\Delta_{\mathrm{f}}S^{\circ}$ / (J/(mol·K))	$\Delta_{\mathrm{f}}C_P^{\circ}$ / (J/(mol·K))
Al_2Cu	0.333	−15131	−15802	−2.245	0.000
AlCu	0.500	−19812	−20280	−1.570	0.000
Al_9Cu_{11}	0.550	−20732	−21000	−0.900	0.000
Al_2Cu_3	0.600	−21161	−21340	−0.600	0.000

References

[30Kaw] M. Kawakami: Sci. Rep. Res. Inst. Tohoku Univ., Sendai, **19** (1930) 521–549.
[37Oel] W. Oelsen, W. Middel: Mitt. K.W.I. Eisenforsch. Düsseldorf, **19** (1937) 1–26.
[44Ray] G.V. Raynor: Annotated Equilibrium Diagram Series No. 4, 5 pp, Inst. Met, London, 1944.
[71San] V.M. Sandakov, Yu.O. Esin, P.V. Gel'd, V.D. Shantarin: Zh. Fiz. Khim. **45** (1971) 2030-2032.
[75Ita] K. Itagaki, A. Yazawa: Trans. Jpn. Inst. Met. **16** (1975) 679–686.
[85Mur] J.L. Murray: Int. Met. Rev. **30** (1985) 211–233.
[89Hey] E. Heyer: unpublished work, Univ. Wien, 1989.
[98Sau] N. Saunders in: I. Ansara, A.T. Dinsdale, M.H. Rand (eds.): COST 507, "Thermochemical database for light metal alloys", Vol. 2, EUR 18499, 1998, 28–33.

Al – Fe (Aluminium – Iron)

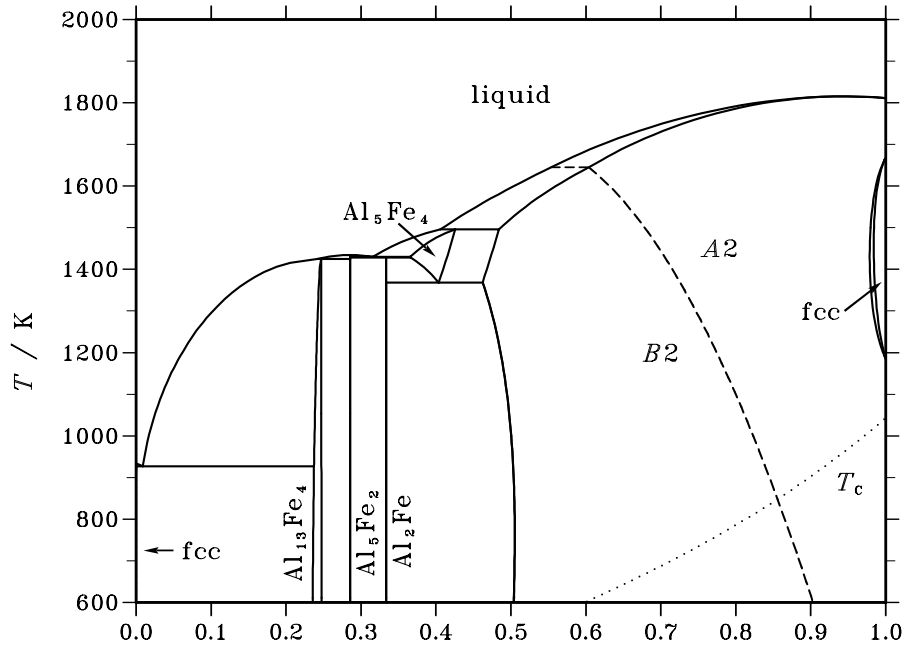

Fig. 1. Calculated phase diagram for the system Al-Fe.

There is a large solubility of Al in bcc-Fe while Fe is only slightly soluble in fcc-Al. A number of intermediate phases are formed in contact with the liquid. The bcc phase has also several ordering transformations to $B2$ and $D0_3$. These are second order at high temperature but first order at low temperature where there is an interaction also with the ferromagnetic transition in bcc-Fe. The solubility of Al in fcc-Fe is very small and a characteristic "gamma-loop" is formed.
Fe is a frequent and important impurity in Al alloys and the solubility is so low that it is important to control by alloying what kind of intermediate phase is formed. Some of these are less harmful. Al as alloying element in Fe is gaining interest but it is difficult to have high concentrations as Al easily oxidises when added to the liquid steel. Al improves the corrosion resistance but the ordering transformations at low temperatures tend to decrease the mechanical strength of these materials. The region with ordering transformations at low temperature and low Al content has attracted considerable scientific interest both experimentally and for modelling chemical and magnetic ordering.
Many experimental data are available although some of these are quite old. The selected assessment of the system has been given by [93Sei].

Table I. Phases, structures and models.

Phase	Struktur-bericht	Prototype	Pearson symbol	Space group	SGTE name	Model
liquid					LIQUID	$(Al,Fe)_1$
fcc	$A1$	Cu	$cF4$	$Fm\overline{3}m$	FCC_A1	$(Al,Fe)_1$
$Al_{13}Fe_4$	···	···	$mC102$	$C2/m$	AL13FE4	$Al_{32}Fe_{12}(Al,\square)_7$
Al_5Fe_2	$D8_{11}$	Al_5Mn_2	$hP28$	$P6_3/mmc$	AL5FE2	Al_5Fe_2
Al_2Fe	···	Al_2Fe	$aP18$	$P1$	AL2FE	Al_2Fe_1
Al_5Fe_4	···	···	$cI16$?	···	AL5FE4	$(Al,Fe)_1$
$A2$	$A2$	W	$cI2$	$Im\overline{3}m$	BCC_A2	$(Al,Fe)_1$
$B2$	$B2$	CsCl	$cP2$	$Pm\overline{3}m$	BCC_B2	$(Al,Fe)_1(Al,Fe)_1$

Table II. Invariant reactions.

Reaction	Type	T / K	Compositions / x_{Fe}			$\Delta_r H$ / (J/mol)
liquid + AlFe $\rightleftharpoons$ Al_5Fe_4	peritectic	1495.5	0.406	0.484	0.426	−8327
liquid $\rightleftharpoons$ Al_5Fe_2	congruent	1434.6	0.286	0.286		−24401
liquid $\rightleftharpoons$ Al_5Fe_2 + Al_5Fe_4	eutectic	1430.0	0.316	0.286	0.366	−19438
Al_5Fe_2 + Al_5Fe_4 $\rightleftharpoons$ Al_2Fe	peritectoid	1428.2	0.286	0.366	0.333	−6239
liquid + Al_5Fe_2 $\rightleftharpoons$ $Al_{13}Fe_4$	peritectic	1424.4	0.242	0.286	0.247	−21699
Al_5Fe_4 $\rightleftharpoons$ Al_2Fe + $B2$	eutectoid	1368.2	0.404	0.333	0.462	−7178
liquid $\rightleftharpoons$ fcc + $Al_{13}Fe_4$	eutectic	927.1	0.009	0.000	0.237	−11015

Table IIIa. Integral quantities for the liquid phase at 1900 K.

x_{Fe}	ΔG_m [J/mol]	ΔH_m [J/mol]	ΔS_m [J/(mol·K)]	G_m^E [J/mol]	S_m^E [J/(mol·K)]	ΔC_p [J/(mol·K)]
0.000	0	0	0.000	0	0.000	0.000
0.100	−9364	−8679	0.360	−4228	−2.343	0.000
0.200	−15542	−15254	0.152	−7637	−4.009	0.000
0.300	−19830	−19788	0.022	−10179	−5.057	0.000
0.400	−22441	−22346	0.050	−11809	−5.545	0.000
0.500	−23432	−22994	0.230	−12482	−5.533	0.000
0.600	−22785	−21801	0.518	−12153	−5.078	0.000
0.700	−20432	−18835	0.841	−10782	−4.238	0.000
0.800	−16231	−14165	1.087	−8326	−3.073	0.000
0.900	−9880	−7862	1.062	−4745	−1.641	0.000
1.000	0	0	0.000	0	0.000	0.000

Reference states: Al(liquid), Fe(liquid)

Table IIIb. Partial quantities for Al in the liquid phase at 1900 K.

x_{Al}	ΔG_{Al} [J/mol]	ΔH_{Al} [J/mol]	ΔS_{Al} [J/(mol·K)]	G^E_{Al} [J/mol]	S^E_{Al} [J/(mol·K)]	a_{Al}	γ_{Al}
1.000	0	0	0.000	0	0.000	1.000	1.000
0.900	−2066	−1063	0.528	−402	−0.348	0.877	0.975
0.800	−5196	−4167	0.541	−1670	−1.314	0.720	0.900
0.700	−9533	−9183	0.184	−3898	−2.781	0.547	0.781
0.600	−15245	−15977	−0.385	−7175	−4.633	0.381	0.635
0.500	−22535	−24412	−0.988	−11585	−6.751	0.240	0.480
0.400	−31687	−34349	−1.401	−17211	−9.020	0.135	0.336
0.300	−43152	−45644	−1.311	−24132	−11.322	0.065	0.217
0.200	−57847	−58148	−0.159	−32422	−13.540	0.026	0.128
0.100	−78527	−71713	3.587	−42152	−15.558	0.007	0.069
0.000	−∞	−86182	∞	−53391	−17.259	0.000	0.034

Reference state: Al(liquid)

Table IIIc. Partial quantities for Fe in the liquid phase at 1900 K.

x_{Fe}	ΔG_{Fe} [J/mol]	ΔH_{Fe} [J/mol]	ΔS_{Fe} [J/(mol·K)]	G^E_{Fe} [J/mol]	S^E_{Fe} [J/(mol·K)]	a_{Fe}	γ_{Fe}
0.000	−∞	−97527	∞	−46219	−27.004	0.000	0.054
0.100	−75042	−77226	−1.150	−38667	−20.295	0.009	0.086
0.200	−56929	−59600	−1.406	−31504	−14.788	0.027	0.136
0.300	−43855	−44532	−0.356	−24835	−10.367	0.062	0.208
0.400	−33236	−31899	0.704	−18761	−6.915	0.122	0.305
0.500	−24328	−21576	1.449	−13378	−4.315	0.214	0.429
0.600	−16851	−13435	1.798	−8781	−2.450	0.344	0.574
0.700	−10695	−7345	1.763	−5060	−1.202	0.508	0.726
0.800	−5827	−3169	1.399	−2302	−0.456	0.692	0.864
0.900	−2253	−768	0.781	−588	−0.095	0.867	0.963
1.000	0	0	0.000	0	0.000	1.000	1.000

Reference state: Fe(liquid)

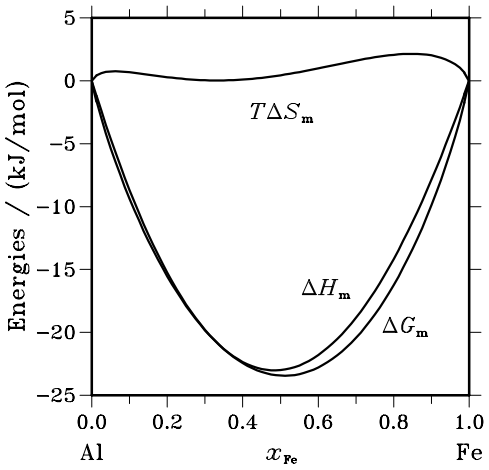

Fig. 2. Integral quantities of the liquid phase at T=1900 K.

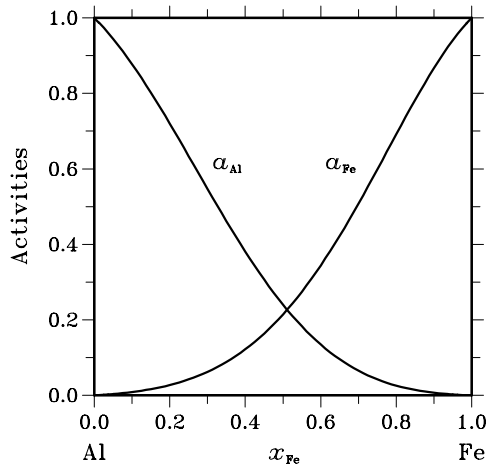

Fig. 3. Activities in the liquid phase at T=1900 K.

Table IVa. Integral quantities for the stable phases at 900 K.

Phase	x_{Fe}	ΔG_{m} [J/mol]	ΔH_{m} [J/mol]	ΔS_{m} [J/(mol·K)]	$G_{\mathrm{m}}^{\mathrm{E}}$ [J/mol]	$S_{\mathrm{m}}^{\mathrm{E}}$ [J/(mol·K)]	ΔC_p [J/(mol·K)]
fcc	0.000	0	0	0.000	0	0.000	0.000
	0.000	−18	−8	0.011	−6	−0.002	−0.002
$Al_{13}Fe_4$	0.237	−23988	−29271	−5.870	−23745	−6.141	−3.186
	0.247	−24603	−29610	−5.563	−23931	−6.309	−3.322
Al_5Fe_2	0.286	−25981	−30815	−5.371			−3.840
Al_2Fe	0.333	−26638	−30554	−4.351			−4.480
$A2$, $B2$	0.504	−27384	−29037	−1.836	−26476	−2.846	−2.838
	0.600	−26194	−26389	−0.217	−24072	−2.575	−5.315
	0.700	−22655	−21398	1.397	−19768	−1.811	−4.992
	0.800	−17214	−14685	2.810	−14020	−0.739	−2.323
	0.900	−9924	−7523	2.668	−7491	−0.035	13.207
	1.000	0	0	0.000	0	0.000	0.000

Reference states: Al(fcc), Fe($A2$)

Table IVb. Partial quantities for Al in the stable phases at 900 K.

Phase	x_{Al}	ΔG_{Al} [J/mol]	ΔH_{Al} [J/mol]	ΔS_{Al} [J/(mol·K)]	$G_{\mathrm{Al}}^{\mathrm{E}}$ [J/mol]	$S_{\mathrm{Al}}^{\mathrm{E}}$ [J/(mol·K)]	a_{Al}	γ_{Al}
fcc	1.000	0	0	0.000	0	0.000	1.000	1.000
	1.000	−1	0	0.001	0	0.000	1.000	1.000
$Al_{13}Fe_4$	0.763	−1	−21332	−23.700	−19710	−1.801	1.000	0.072
	0.753	−15764	−21332	−6.187	−19245	−2.319	0.122	0.076
Al_5Fe_2	0.714	−15764	−21880	−6.796			0.122	
	0.714	−22037	−32382	−11.494			0.053	
Al_2Fe	0.667	−22037	−32382	−11.494			0.053	
	0.667	−25178	−33523	−9.272			0.035	
$A2$, $B2$	0.496	−25178	−28636	−3.841	−37379	9.715	0.035	0.007
	0.400	−41232	−50726	−10.549	−45071	−6.284	0.004	0.002
	0.300	−54302	−62658	−9.284	−53140	−10.576	0.001	0.001
	0.200	−67918	−74338	−7.133	−60930	−14.898	0.000	0.000
	0.100	−85536	−59319	29.130	−68305	9.985	0.000	0.000
	0.000	$-\infty$	−90978	∞	−82355	−9.581	0.000	0.000

Reference state: Al(fcc)

Table IVc. Partial quantities for Fe in the stable phases at 900 K.

Phase	x_{Fe}	ΔG_{Fe} [J/mol]	ΔH_{Fe} [J/mol]	ΔS_{Fe} [J/(mol·K)]	G^E_{Fe} [J/mol]	S^E_{Fe} [J/(mol·K)]	a_{Fe}	γ_{Fe}
fcc	0.000	$-\infty$	−49409	∞	−36108	−14.779	0.000	0.008
	0.000	−101187	−49405	57.537	−36110	−14.771	0.000	0.008
$Al_{13}Fe_4$	0.237	−101182	−54823	51.510	−36727	−20.107	0.000	0.007
	0.247	−51523	−54823	−3.666	−38205	−18.464	0.001	0.006
Al_5Fe_2	0.286	−51523	−53152	−1.810			0.001	
	0.286	−35840	−26897	9.937			0.008	
Al_2Fe	0.333	−35840	−26897	9.937			0.008	
	0.333	−29558	−24615	5.492			0.019	
$A2$, $B2$	0.504	−29558	−29432	0.140	−15730	−15.225	0.019	0.122
	0.600	−16169	−10165	6.672	−10073	−0.102	0.115	0.260
	0.700	−9092	−3715	5.975	−5466	1.946	0.297	0.482
	0.800	−4538	228	5.295	−2292	2.801	0.545	0.736
	0.900	−1522	−1768	−0.272	−734	−1.148	0.816	0.907
	1.000	0	0	0.000	0	0.000	1.000	1.000

Reference state: Fe($A2$)

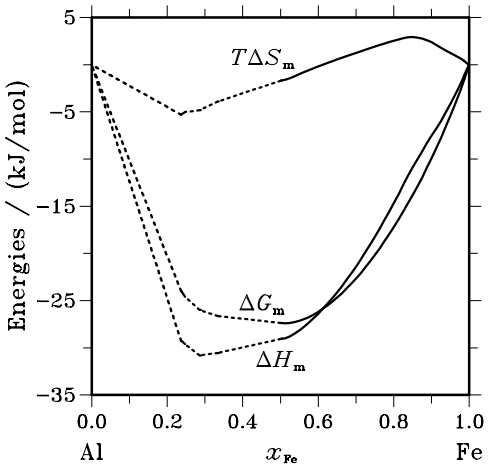

Fig. 4. Integral quantities of the stable phases at T=900 K.

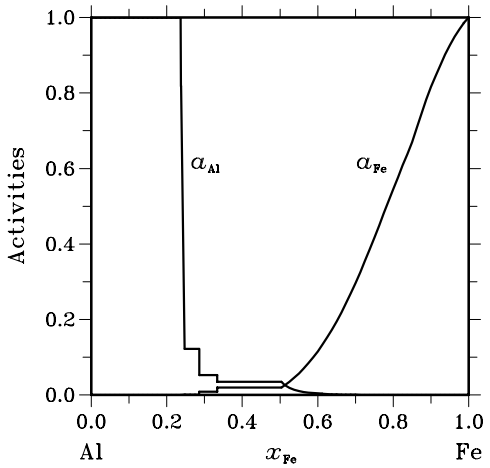

Fig. 5. Activities in the stable phases at T=900 K.

Table V. Standard reaction quantities at 298.15 K for the compounds per mole of atoms.

Compound	x_{Fe}	$\Delta_f G^\circ$ / (J/mol)	$\Delta_f H^\circ$ / (J/mol)	$\Delta_f S^\circ$ / (J/(mol·K))	$\Delta_f C^\circ_P$ / (J/(mol·K))
Al_5Fe_2	0.286	−28769	−30040	−4.261	−0.119
Al_2Fe_1	0.333	−28738	−29649	−3.055	−0.139

References

[93Sei] M. Seiersten: Sintef report STF28F93051 (1993); and in: I. Ansara, A.T. Dinsdale, M.H. Rand (eds.): COST 507, "Thermochemical database for light metal alloys", Vol. 2, EUR 18499, 1998, 34–39.

Al – Ga (Aluminium – Gallium)

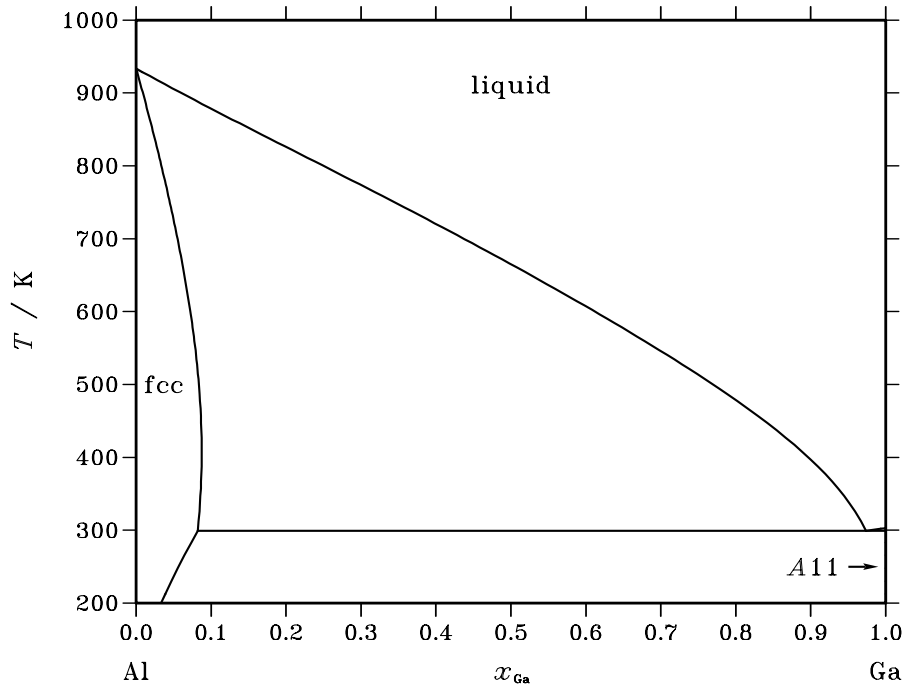

Fig. 1. Calculated phase diagram for the system Al-Ga.

An understanding of the phase diagram and thermodynamics of the Al-Ga system is important in order to model III-V semiconductor systems. The phase diagram is very simple showing moderate solubility (maximum of approximately 9 at.%) of Ga in solid Al and very low solubility of Al in solid Ga. There is eutectic slightly below the melting point of Ga with the liquid composition containing approximately 3 at.% Al. The liquidus surface has been studied by a number of researchers and the agreement is generally very good particularly for Al rich compositions. There is a fair amount of uncertainty about the extent of the solid solution of Ga in Al. The thermodynamic data for the system have been studied by direct reaction calorimetry, micro-calorimetry and emf method. The critically assessed data for this system adopted by SGTE is by Watson [92Wat] who obtained a thermodynamic dataset in good agreement with all the experimental information. Other critical assessments have been carried out by Ansara et al. [78Ans], Murray [83Mur], Sharma and Srivastava [92Sha] and Jayaganthan and Hajra [96Jay].

Table I. Phases, structures and models.

Phase	Struktur-bericht	Prototype	Pearson symbol	Space group	SGTE name	Model
liquid					LIQUID	$(Al,Ga)_1$
fcc	$A1$	Cu	$cF4$	$Fm\overline{3}m$	FCC_A1	$(Al,Ga)_1$
$A11$	$A11$	αGa	$oC8$	$Cmca$	ORTHORHOMBIC_A11	Ga_1

Table II. Invariant reactions.

Reaction	Type	T / K	Compositions / x_{Ga}			$\Delta_r H$ / (J/mol)
liquid $\rightleftharpoons$ fcc + $A11$	eutectic	299.4	0.974	0.082	1.000	−5767

Table IIIa. Integral quantities for the liquid phase at 1000 K.

x_{Ga}	ΔG_{m} [J/mol]	ΔH_{m} [J/mol]	ΔS_{m} [J/(mol·K)]	$G_{\mathrm{m}}^{\mathrm{E}}$ [J/mol]	$S_{\mathrm{m}}^{\mathrm{E}}$ [J/(mol·K)]	ΔC_p [J/(mol·K)]
0.000	0	0	0.000	0	0.000	0.000
0.100	−2671	303	2.975	32	0.272	0.000
0.200	−4138	503	4.641	23	0.480	0.000
0.300	−5088	618	5.705	−9	0.626	0.000
0.400	−5644	663	6.307	−48	0.711	0.000
0.500	−5846	653	6.500	−83	0.736	0.000
0.600	−5701	597	6.298	−105	0.702	0.000
0.700	−5188	501	5.690	−109	0.611	0.000
0.800	−4253	370	4.623	−92	0.462	0.000
0.900	−2758	204	2.961	−55	0.258	0.000
1.000	0	0	0.000	0	0.000	0.000

Reference states: Al(liquid), Ga(liquid)

Table IIIb. Partial quantities for Al in the liquid phase at 1000 K.

x_{Al}	ΔG_{Al} [J/mol]	ΔH_{Al} [J/mol]	ΔS_{Al} [J/(mol·K)]	$G_{\mathrm{Al}}^{\mathrm{E}}$ [J/mol]	$S_{\mathrm{Al}}^{\mathrm{E}}$ [J/(mol·K)]	a_{Al}	γ_{Al}
1.000	0	0	0.000	0	0.000	1.000	1.000
0.900	−853	55	0.908	24	0.032	0.903	1.003
0.800	−1787	195	1.981	69	0.126	0.807	1.008
0.700	−2862	384	3.246	104	0.280	0.709	1.013
0.600	−4139	600	4.739	108	0.492	0.608	1.013
0.500	−5696	826	6.523	67	0.760	0.504	1.008
0.400	−7641	1058	8.699	−22	1.080	0.399	0.997
0.300	−10165	1298	11.463	−154	1.452	0.294	0.982
0.200	−13696	1559	15.255	−314	1.873	0.193	0.963
0.100	−19622	1863	21.486	−478	2.341	0.094	0.944
0.000	$-\infty$	2240	∞	−612	2.853	0.000	0.929

Reference state: Al(liquid)

Table IIIc. Partial quantities for Ga in the liquid phase at 1000 K.

x_{Ga}	ΔG_{Ga} [J/mol]	ΔH_{Ga} [J/mol]	ΔS_{Ga} [J/(mol·K)]	$G_{\mathrm{Ga}}^{\mathrm{E}}$ [J/mol]	$S_{\mathrm{Ga}}^{\mathrm{E}}$ [J/(mol·K)]	a_{Ga}	γ_{Ga}
0.000	$-\infty$	3625	∞	587	3.038	0.000	1.073
0.100	−19040	2536	21.576	105	2.431	0.101	1.013
0.200	−13542	1737	15.279	−160	1.897	0.196	0.981
0.300	−10282	1163	11.445	−272	1.434	0.290	0.968
0.400	−7900	759	8.659	−281	1.040	0.387	0.967
0.500	−5996	480	6.476	−233	0.713	0.486	0.972
0.600	−4408	290	4.698	−161	0.450	0.589	0.981
0.700	−3056	160	3.216	−90	0.250	0.692	0.989
0.800	−1892	73	1.965	−37	0.110	0.796	0.996
0.900	−884	19	0.903	−8	0.027	0.899	0.999
1.000	0	0	0.000	0	0.000	1.000	1.000

Reference state: Ga(liquid)

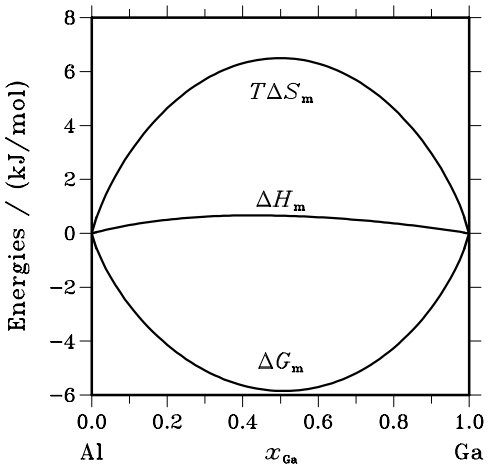

Fig. 2. Integral quantities of the liquid phase at T=1000 K.

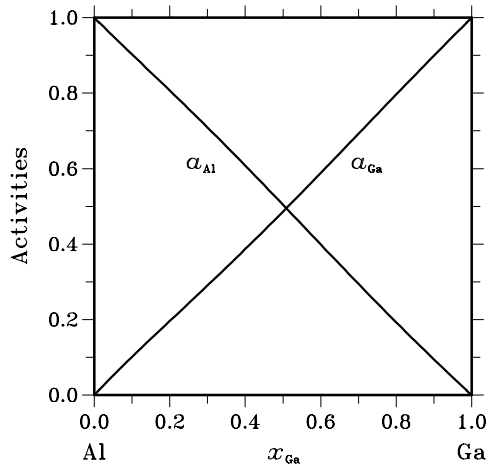

Fig. 3. Activities in the liquid phase at T=1000 K.

References

[78Ans] I. Ansara, J.-P. Bros, C. Girard: Calphad **2** (1978) 187–196.
[83Mur] J. Murray: Bull. Alloy Phase Diagrams **4** (1983) 183–190.
[92Wat] A. Watson: Calphad **16** (1992) 207–217.
[92Sha] R.C. Sharma, M. Srivastava: Calphad **16** (1992) 387–408.
[96Jay] R. Jayaganthan, J.P. Hajra: Mater. Sci. Eng. B, **B28** (1996) 96–102.

Al – Ge (Aluminium – Germanium)

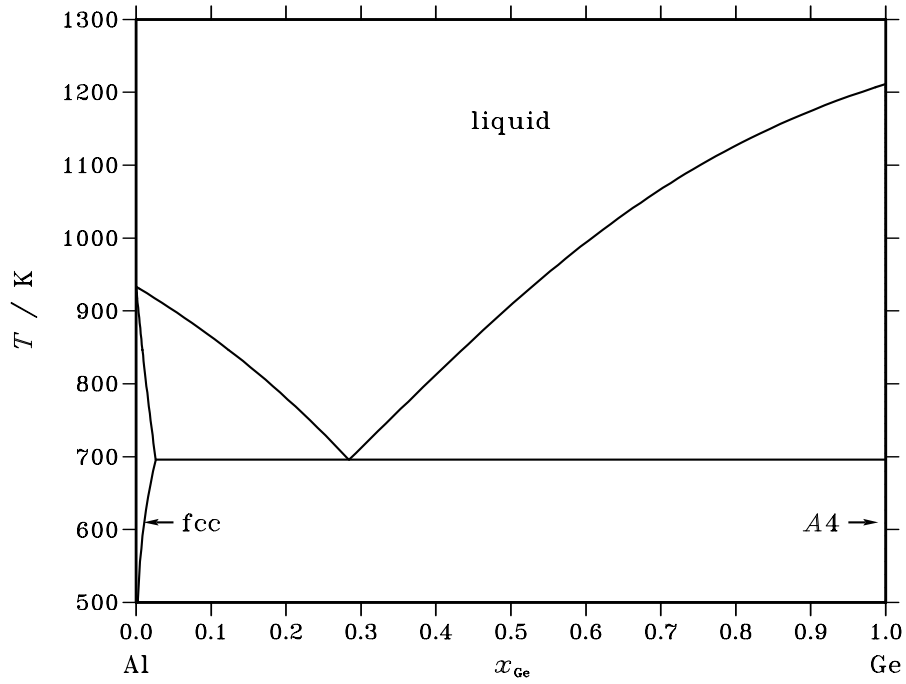

Fig. 1. Calculated phase diagram for the system Al-Ge.

The Al-Ge system is of some interest because of superconducting and semiconducting metastable phases which can form readily in the system. It is characterised by a simple phase diagram with a eutectic at about 696 K. The solubility of Ge in the aluminium based solid solution is about 2.5 at.%. The solubility of Al in solid Ge (diamond structure) is about 1.3 at.% although this has not been modelled in the selected dataset. This dataset is based upon the critical assessment of data of Ansara et al. [79Ans] but modified to accommodate the adopted data for the pure elements [91Din]. Other critical assessments of data include those of McAlister and Murray [85McA] and Srikanth et al. [96Sri] but use different data for the elements. The phase diagram is fairly well characterised by experimental results which are in good agreement with the critically assessed data. Various studies have been carried out on the thermodynamic properties of the liquid, the enthalpies of formation and partial Gibbs energies of aluminium.

Table I. Phases, structures and models.

Phase	Struktur-bericht	Prototype	Pearson symbol	Space group	SGTE name	Model
liquid					LIQUID	$(Al,Ge)_1$
fcc	$A1$	Cu	$cF4$	$Fm\overline{3}m$	FCC_A1	$(Al,Ge)_1$
$A4$	$A4$	C(diamond)	$cF8$	$Fd\overline{3}m$	DIAMOND_A4	Ge_1

Table II. Invariant reactions.

Reaction	Type	T / K	Compositions / x_{Ge}			$\Delta_r H$ / (J/mol)
liquid $\rightleftharpoons$ fcc + $A4$	eutectic	691.9	0.280	0.005	1.000	−15661

Table IIIa. Integral quantities for the liquid phase at 1273 K.

x_{Ge}	ΔG_m [J/mol]	ΔH_m [J/mol]	ΔS_m [J/(mol·K)]	G_m^E [J/mol]	S_m^E [J/(mol·K)]	ΔC_p [J/(mol·K)]
0.000	0	0	0.000	0	0.000	0.000
0.100	−5000	−938	3.191	−1559	0.488	0.000
0.200	−8127	−1858	4.925	−2830	0.764	0.000
0.300	−10231	−2612	5.985	−3765	0.906	0.000
0.400	−11454	−3096	6.566	−4331	0.970	0.000
0.500	−11845	−3250	6.752	−4508	0.988	0.000
0.600	−11418	−3056	6.569	−4295	0.973	0.000
0.700	−10168	−2542	5.991	−3702	0.912	0.000
0.800	−8055	−1778	4.931	−2758	0.770	0.000
0.900	−4946	−878	3.196	−1505	0.493	0.000
1.000	0	0	0.000	0	0.000	0.000

Reference states: Al(liquid), Ge(liquid)

Table IIIb. Partial quantities for Al in the liquid phase at 1273 K.

x_{Al}	ΔG_{Al} [J/mol]	ΔH_{Al} [J/mol]	ΔS_{Al} [J/(mol·K)]	G_{Al}^E [J/mol]	S_{Al}^E [J/(mol·K)]	a_{Al}	γ_{Al}
1.000	0	0	0.000	0	0.000	1.000	1.000
0.900	−1250	19	0.997	−134	0.121	0.889	0.987
0.800	−2972	−142	2.223	−610	0.368	0.755	0.944
0.700	−5277	−713	3.585	−1502	0.619	0.607	0.868
0.600	−8245	−1795	5.067	−2838	0.819	0.459	0.765
0.500	−11939	−3355	6.743	−4602	0.980	0.324	0.647
0.400	−16431	−5229	8.799	−6732	1.181	0.212	0.529
0.300	−21864	−7125	11.578	−9121	1.568	0.127	0.422
0.200	−28650	−8616	15.737	−11615	2.356	0.067	0.334
0.100	−38387	−9147	22.969	−14015	3.824	0.027	0.266
0.000	$-\infty$	−8030	∞	−16079	6.323	0.000	0.219

Reference state: Al(liquid)

Table IIIc. Partial quantities for Ge in the liquid phase at 1273 K.

x_{Ge}	ΔG_{Ge} [J/mol]	ΔH_{Ge} [J/mol]	ΔS_{Ge} [J/(mol·K)]	G_{Ge}^E [J/mol]	S_{Ge}^E [J/(mol·K)]	a_{Ge}	γ_{Ge}
0.000	$-\infty$	−8866	∞	−16829	6.255	0.000	0.204
0.100	−38752	−9553	22.937	−14380	3.792	0.026	0.257
0.200	−28746	−8723	15.729	−11711	2.347	0.066	0.331
0.300	−21791	−7043	11.585	−9047	1.575	0.128	0.425
0.400	−16269	−5049	8.814	−6570	1.195	0.215	0.538
0.500	−11751	−3146	6.760	−4415	0.997	0.329	0.659
0.600	−8077	−1608	5.082	−2670	0.834	0.466	0.777
0.700	−5155	−578	3.596	−1380	0.630	0.614	0.878
0.800	−2906	−68	2.229	−544	0.374	0.760	0.950
0.900	−1230	41	0.999	−115	0.123	0.890	0.989
1.000	0	0	0.000	0	0.000	1.000	1.000

Reference state: Ge(liquid)

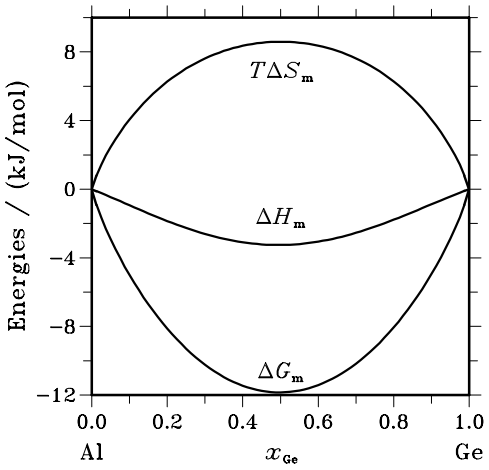

Fig. 2. Integral quantities of the liquid phase at T=1273 K.

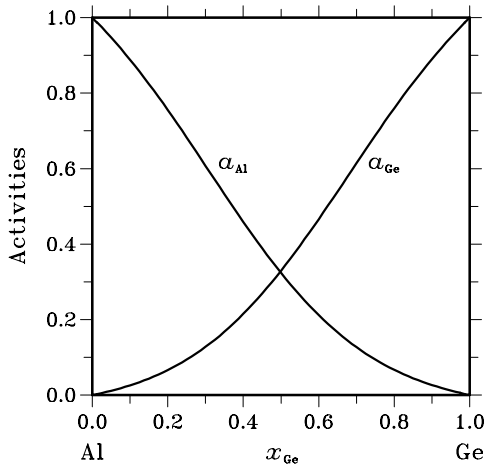

Fig. 3. Activities in the liquid phase at T=1273 K.

References

[79Ans] I. Ansara, J.P. Bros, M. Gambino: Calphad **3** (1979) 225–233.
[85McA] A.J. McAlister, J.L. Murray: Bull. Alloy Phase Diagrams **6** (1985) 111–113.
[96Sri] S. Srikanth, D. Sanyal, P. Ramachandrarao: Calphad **20** (1996) 321–332.

Al – In (Aluminium – Indium)

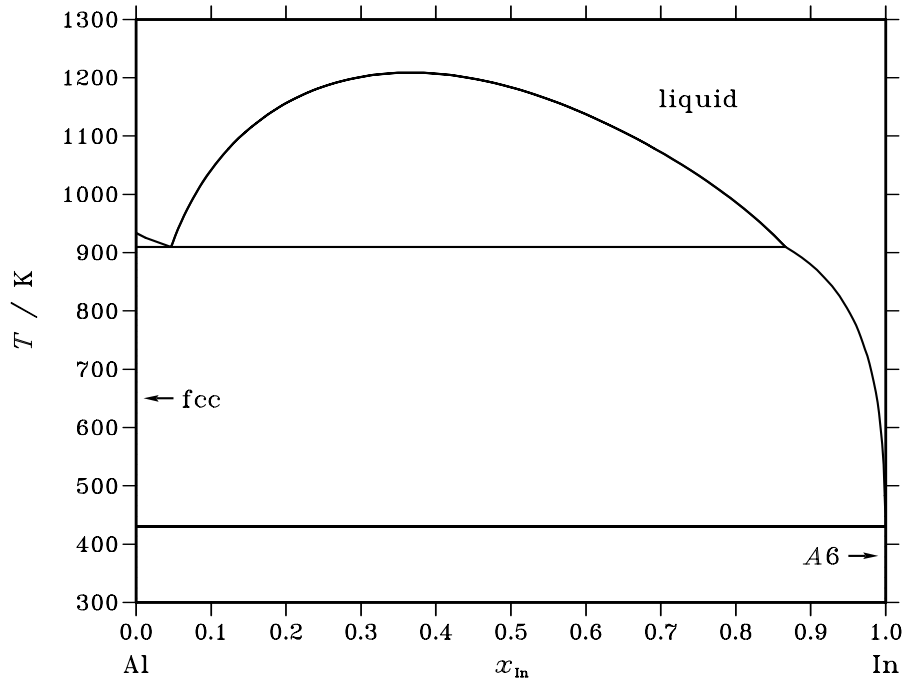

Fig. 1. Calculated phase diagram for the system Al-In.

An understanding of the phase diagram and thermodynamics of the Al-In system is important in order to model III-V semiconductor systems. The phase diagram for the system is dominated by a miscibility gap in the liquid phase with the upper critical point (approx. 1173 K) biased towards Al rich compositions. The monotectic occurs at about 910 K, over 20 K below the melting point of Al, with the Al rich liquid composition containing approximately 5 at.% In. There is considerable uncertainty in the detailed shape of the miscibility gap with experimental results showing scatter of up to 80 K. There is also uncertainty on the liquidus phase boundary close to Al. There appears to be no solubility in the pure crystalline elements. Experimental thermodynamic studies in the system have been concerned with enthalpies of mixing and partial Gibbs energies of Al derived from emf studies. There is disagreement between the studies of the experimental enthalpies of mixing. The phase diagram and thermodynamic data for the system have been reviewed by Murray [83Mur] who also obtained a set of thermodynamic coefficients for the liquid phase. The dataset adopted by SGTE were derived by Coughanowr [89Cou] reported by Ansara et al. [94Ans]. Other critical assessments have been reported by Ansara et al. [78Ans] and Sharma and Srivastava [92Sha].

Table I. Phases, structures and models.

Phase	Struktur-bericht	Prototype	Pearson symbol	Space group	SGTE name	Model
liquid					LIQUID	$(Al,In)_1$
fcc	$A1$	Cu	$cF4$	$Fm\overline{3}m$	FCC_A1	Al_1
$A6$	$A6$	In	$tI2$	$I4/mmm$	TETRAGONAL_A6	In_1

Table II. Invariant reactions.

Reaction	Type	T / K	Compositions / x_{In}			$\Delta_{\mathrm{r}}H$ / (J/mol)
liquid $\rightleftharpoons$ liquid′ + liquid″	critical	1208.4	0.366	0.366	0.366	0
liquid′ $\rightleftharpoons$ fcc + liquid″	monotectic	909.7	0.047	0.000	0.866	−11348
liquid″ $\rightleftharpoons$ fcc + $A6$	degenerated	429.6	1.000	0.000	1.000	−3296

Table IIIa. Integral quantities for the liquid phase at 1300 K.

x_{In}	ΔG_{m} [J/mol]	ΔH_{m} [J/mol]	ΔS_{m} [J/(mol·K)]	$G^{\mathrm{E}}_{\mathrm{m}}$ [J/mol]	$S^{\mathrm{E}}_{\mathrm{m}}$ [J/(mol·K)]	ΔC_p [J/(mol·K)]
0.000	0	0	0.000	0	0.000	0.000
0.100	−1415	2506	3.016	2099	0.313	0.000
0.200	−1811	4087	4.537	3598	0.376	0.000
0.300	−2034	4972	5.389	4569	0.310	0.000
0.400	−2202	5340	5.801	5073	0.205	0.000
0.500	−2336	5315	5.885	5157	0.122	0.000
0.600	−2421	4970	5.685	4854	0.090	0.000
0.700	−2417	4325	5.187	4185	0.108	0.000
0.800	−2249	3348	4.305	3159	0.145	0.000
0.900	−1743	1952	2.842	1770	0.140	0.000
1.000	0	0	0.000	0	0.000	0.000

Reference states: Al(liquid), In(liquid)

Table IIIb. Partial quantities for Al in the liquid phase at 1300 K.

x_{Al}	ΔG_{Al} [J/mol]	ΔH_{Al} [J/mol]	ΔS_{Al} [J/(mol·K)]	$G^{\mathrm{E}}_{\mathrm{Al}}$ [J/mol]	$S^{\mathrm{E}}_{\mathrm{Al}}$ [J/(mol·K)]	a_{Al}	γ_{Al}
1.000	0	0	0.000	0	0.000	1.000	1.000
0.900	−825	506	1.024	314	0.148	0.926	1.029
0.800	−1262	1689	2.270	1150	0.415	0.890	1.112
0.700	−1472	3168	3.570	2383	0.604	0.873	1.247
0.600	−1597	4720	4.859	3925	0.612	0.863	1.438
0.500	−1765	6277	6.186	5727	0.423	0.849	1.699
0.400	−2123	7933	7.735	7781	0.117	0.822	2.054
0.300	−2896	9935	9.871	10117	−0.140	0.765	2.550
0.200	−4592	12693	13.296	12804	−0.086	0.654	3.269
0.100	−8938	16769	19.775	15950	0.630	0.437	4.374
0.000	−∞	22889	∞	19704	2.450	0.000	6.190

Reference state: Al(liquid)

Table IIIc. Partial quantities for In in the liquid phase at 1300 K.

x_{In}	ΔG_{In} [J/mol]	ΔH_{In} [J/mol]	ΔS_{In} [J/(mol·K)]	$G^{\mathrm{E}}_{\mathrm{In}}$ [J/mol]	$S^{\mathrm{E}}_{\mathrm{In}}$ [J/(mol·K)]	a_{In}	γ_{In}
0.000	$-\infty$	30589	∞	24270	4.861	0.000	9.444
0.100	−6719	20512	20.947	18169	1.802	0.537	5.371
0.200	−4008	13678	13.605	13388	0.223	0.690	3.451
0.300	−3344	9181	9.634	9670	−0.376	0.734	2.446
0.400	−3109	6269	7.214	6795	−0.404	0.750	1.875
0.500	−2906	4352	5.584	4586	−0.180	0.764	1.528
0.600	−2619	2995	4.319	2902	0.071	0.785	1.308
0.700	−2212	1921	3.179	1643	0.214	0.815	1.164
0.800	−1664	1011	2.058	748	0.202	0.857	1.072
0.900	−944	305	0.961	195	0.085	0.916	1.018
1.000	0	0	0.000	0	0.000	1.000	1.000

Reference state: In(liquid)

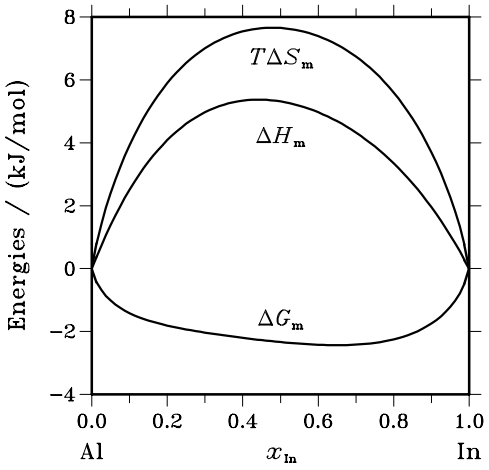

Fig. 2. Integral quantities of the liquid phase at T=1300 K.

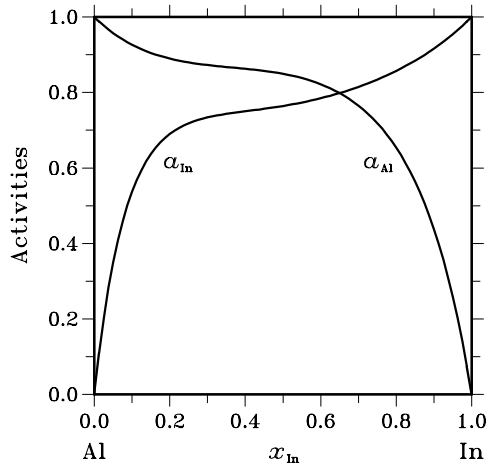

Fig. 3. Activities in the liquid phase at T=1300 K.

References

[78Ans] I. Ansara, J.P. Bros, C. Girard: Calphad **2** (1978) 2, 187–196.
[83Mur] J.L. Murray: Bull. Alloy Phase Diagrams **4** (1983) 271–278.
[89Cou] C.A. Coughanowr: Ph. D. Thesis, University of Florida 1989.
[92Sha] R.C. Sharma, M. Srivastava: Calphad **16** (1992) 409-426.
[94Ans] I. Ansara, C. Chatillon, H.L. Lukas, T. Nishizawa, H. Ohtani, K. Ishida, M. Hillert, B. Sundman, B.B. Argent, A. Watson, T.G. Chart, T. Anderson: Calphad **18** (1994) 177–222.

Al – Li (Aluminium – Lithium)

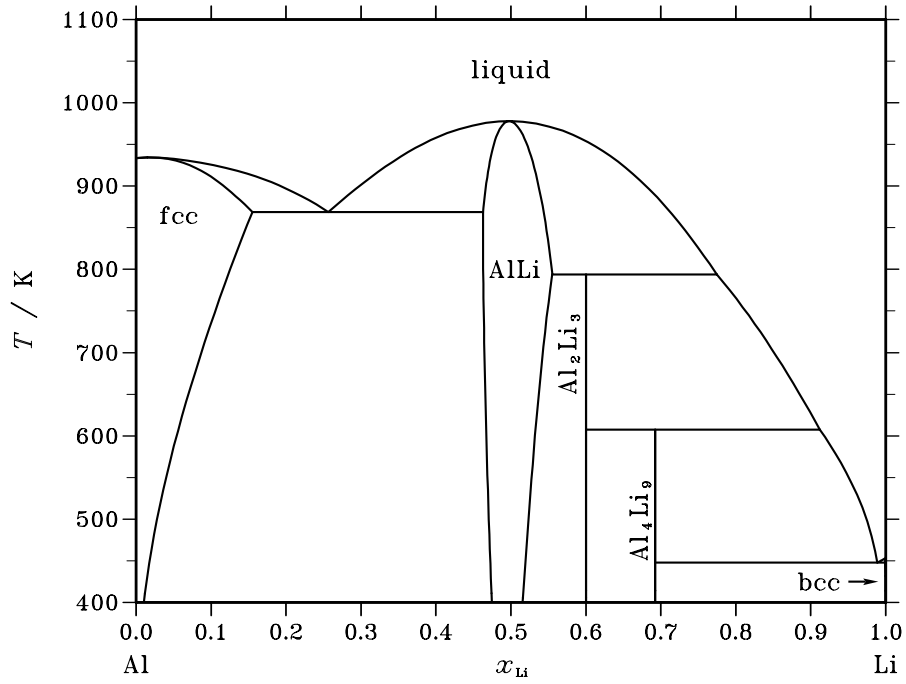

Fig. 1. Calculated phase diagram for the system Al-Li.

The addition of lithium to aluminium alloys results in an increase of the strength and Young's modulus while the density of the metal decreases. These features are particularly attractive for the application of Al-Li alloys in the aircraft industry.

Critical evaluations of the Al-Li system and overviews on experimental investigations are given by several authors [77Sab, 82McA, 89Sau]. The recommended assessment [89Sau] which is reproduced in [98Sau] is based on a fit of phase equilibria across the whole composition and temperature range of the phase diagram, including the liquidus and solidus lines, the invariant equilibria and the stability range of the fcc-phase and the non-stoichiometric AlLi-phase. The other intermetallic phases, Al_2Li_3 and Al_4Li_9, are assumed to be stoichiometric compounds. In addition, the optimisation includes a fit of lithium activities in molten and solid alloys, as well as the heat of mixing in the liquid. For Al_4Li_9, a high-temperature modification has been reported [76Myl], but no thermodynamic data are available, therefore, this compound is modelled as a single phase.

Table I. Phases, structures and models.

Phase	Struktur-bericht	Prototype	Pearson symbol	Space group	SGTE name	Model
liquid					LIQUID	$(Al,Li)_1$
fcc	$A1$	Cu	$cF4$	$Fm\overline{3}m$	FCC_A1	$(Al,Li)_1$
AlLi	$B32$	NaTl	$cF16$	$Fd\overline{3}m$	B32_ALLI	$(Al,Li)_1(Li,\Box)_1$
Al_2Li_3	···	Ga_2Te_3	$hR15$	$R\overline{3}m$	AL2LI3	Al_2Li_3
Al_4Li_9	···	Al_4Li_9	$mC26$	$C2/m$	AL4LI9	Al_4Li_9
bcc	$A2$	W	$cI2$	$Im\overline{3}m$	BCC_A2	$(Al,Li)_1$

Table II. Invariant reactions.

Reaction	Type	T / K	Compositions / x_{Li}			$\Delta_{\mathrm{r}}H$ / (J/mol)
liquid ⇌ AlLi	congruent	977.5	0.500	0.500		−15652
liquid ⇌ fcc + AlLi	eutectic	868.8	0.256	0.155	0.463	−11004
AlLi + liquid ⇌ Al_2Li_3	peritectic	793.6	0.555	0.775	0.600	−2894
Al_2Li_3 + liquid ⇌ Al_4Li_9	peritectic	607.6	0.600	0.912	0.692	−1801
liquid ⇌ Al_4Li_9 + bcc	eutectic	447.9	0.989	0.692	0.999	−3178

Table IIIa. Integral quantities for the liquid phase at 1000 K.

x_{Li}	ΔG_{m} [J/mol]	ΔH_{m} [J/mol]	ΔS_{m} [J/(mol·K)]	$G^{\mathrm{E}}_{\mathrm{m}}$ [J/mol]	$S^{\mathrm{E}}_{\mathrm{m}}$ [J/(mol·K)]	ΔC_p [J/(mol·K)]
0.000	0	0	0.000	0	0.000	0.000
0.100	−3884	−2111	1.774	−1181	−0.929	0.000
0.200	−6676	−4773	1.903	−2515	−2.257	0.000
0.300	−8823	−7344	1.479	−3744	−3.600	0.000
0.400	−10262	−9328	0.934	−4666	−4.662	0.000
0.500	−10898	−10375	0.523	−5135	−5.240	0.000
0.600	−10664	−10287	0.377	−5068	−5.219	0.000
0.700	−9522	−9017	0.505	−4443	−4.574	0.000
0.800	−7465	−6675	0.790	−3305	−3.371	0.000
0.900	−4466	−3528	0.939	−1763	−1.764	0.000
1.000	0	0	0.000	0	0.000	0.000

Reference states: Al(liquid), Li(liquid)

Table IIIb. Partial quantities for Al in the liquid phase at 1000 K.

x_{Al}	ΔG_{Al} [J/mol]	ΔH_{Al} [J/mol]	ΔS_{Al} [J/(mol·K)]	$G^{\mathrm{E}}_{\mathrm{Al}}$ [J/mol]	$S^{\mathrm{E}}_{\mathrm{Al}}$ [J/(mol·K)]	a_{Al}	γ_{Al}
1.000	0	0	0.000	0	0.000	1.000	1.000
0.900	−752	395	1.147	124	0.271	0.914	1.015
0.800	−1731	651	2.382	124	0.526	0.812	1.015
0.700	−3398	−300	3.098	−432	0.132	0.665	0.949
0.600	−6055	−3083	2.972	−1808	−1.275	0.483	0.805
0.500	−9848	−7875	1.973	−4085	−3.790	0.306	0.612
0.400	−14772	−14391	0.381	−7154	−7.237	0.169	0.423
0.300	−20715	−21876	−1.160	−10705	−11.171	0.083	0.276
0.200	−27601	−29096	−1.495	−14220	−14.876	0.036	0.181
0.100	−36104	−34327	1.777	−16959	−17.368	0.013	0.130
0.000	$-\infty$	−35348	∞	−17956	−17.392	0.000	0.115

Reference state: Al(liquid)

Table IIIc. Partial quantities for Li in the liquid phase at 1000 K.

x_{Li}	ΔG_{Li} [J/mol]	ΔH_{Li} [J/mol]	ΔS_{Li} [J/(mol·K)]	G^E_{Li} [J/mol]	S^E_{Li} [J/(mol·K)]	a_{Li}	γ_{Li}
0.000	$-\infty$	−15848	∞	−10056	−5.792	0.000	0.298
0.100	−32073	−24659	7.414	−12929	−11.731	0.021	0.211
0.200	−26457	−26467	−0.010	−13075	−13.392	0.042	0.208
0.300	−21484	−23781	−2.297	−11473	−12.308	0.075	0.252
0.400	−16571	−18695	−2.124	−8952	−9.743	0.136	0.341
0.500	−11948	−12875	−0.927	−6185	−6.690	0.238	0.475
0.600	−7925	−7551	0.374	−3677	−3.873	0.386	0.643
0.700	−4725	−3507	1.219	−1760	−1.747	0.566	0.809
0.800	−2431	−1070	1.361	−576	−0.494	0.746	0.933
0.900	−951	−105	0.845	−75	−0.031	0.892	0.991
1.000	0	0	0.000	0	0.000	1.000	1.000

Reference state: Li(liquid)

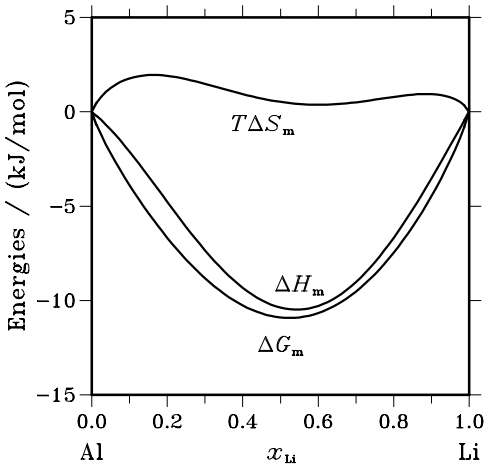

Fig. 2. Integral quantities of the liquid phase at T=1000 K.

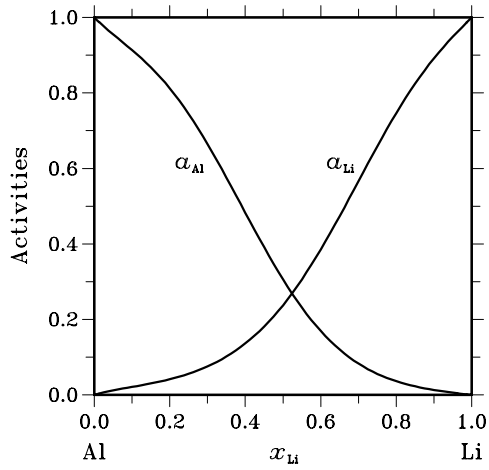

Fig. 3. Activities in the liquid phase at T=1000 K.

Table IV. Standard reaction quantities at 298.15 K for the compounds per mole of atoms.

Compound	x_{Li}	$\Delta_f G^\circ$ / (J/mol)	$\Delta_f H^\circ$ / (J/mol)	$\Delta_f S^\circ$ / (J/(mol·K))	$\Delta_f C^\circ_P$ / (J/(mol·K))
Al_2Li_3	0.600	−15973	−17928	−6.558	0.000
Al_4Li_9	0.692	−12695	−14250	−5.215	0.000

References

[76Myl] K.M. Myles, F.C. Mrazek, J.A. Smaga, J.L. Settle, Proc. Symp. and Workshop on Adv. Battery Res. and Design, U.S. ERDA Report ANL-76-8, B50-B73, 1976.

[77Sab] M.-L. Saboungi, C.C. Hsu: Calphad **1** (1977) 237–251.

[82McA] A.J. McAlister: Bull. Alloy Phase Diagrams **3** (1982) 177–183.

[89Sau] N. Saunders: Z. Metallkd. **80** (1989) 894–903.

[98Sau] N. Saunders in: I. Ansara, A.T. Dinsdale, M.H. Rand (eds.): COST 507, "Thermochemical database for light metal alloys", Vol. 2, EUR 18499, 1998, 40–43.

Al – Mg (Aluminium – Magnesium)

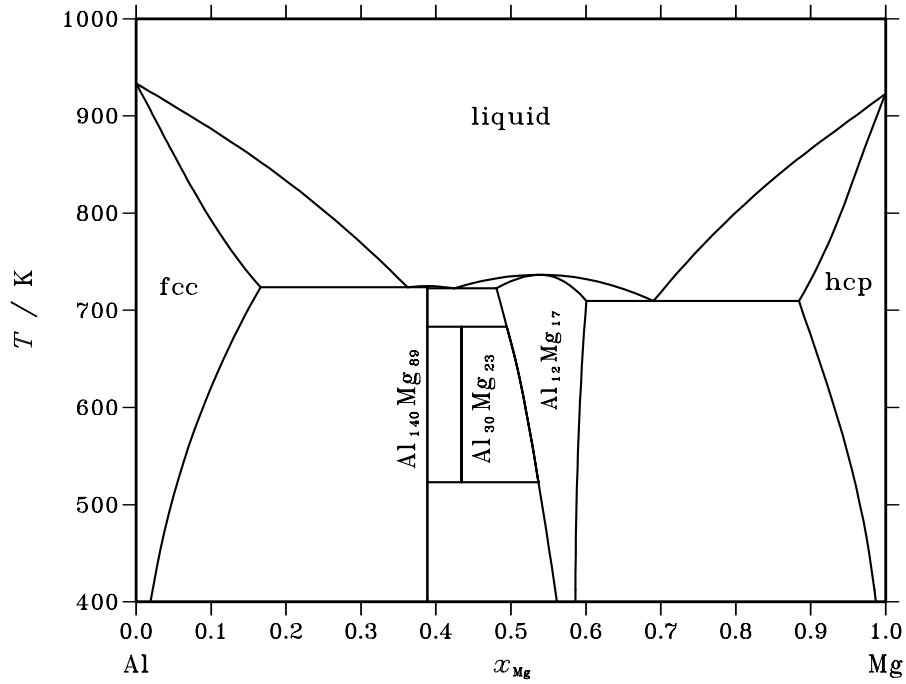

Fig. 1. Calculated phase diagram for the system Al-Mg.

The Al-Mg system is one of the key systems for aluminium light alloys with high strength, which are extensively used for aircraft construction and for other industrial applications. For successful development of new materials and improvement of existing aluminium and magnesium alloys the phase diagram and thermodynamic data are crucial. The thermodynamic parameters for the Al-Mg system were assessed by [82Mur, 90Sau, 94Cha, 98Lia]. The thermodynamic description of [90Sau] was corrected by [98Lia] taking into account new experimental results and it is accepted by SGTE. According to [98Lia] the ζ-phase included by [90Sau] is metastable. The assessment is based on the experimental phase equilibria and the measurements of thermodynamic values. The thermodynamic properties of the liquid were experimentally obtained from calorimetric measurements, partial pressure data and from EMF data. The thermodynamic data for the solid phases were obtained from DTA measurements and from EMF measurements.
The system is characterised by complete solubility in the liquid state and a limited solubility of Al in solid Mg and vice versa. The fcc-Al, hcp-Mg and liquid phases are described in [90Sau] as substitutional solutions. According to experimental data (see [82Mur]) the phase $Al_{140}Mg_{89}$ and $Al_{30}Mg_{23}$ have narrow homogeneity ranges and they are treated as stoichiometric compounds [98Lia]. The $Al_{12}Mg_{17}$-phase has a remarkable homogeneity range and is described using a sublattice model. The optimised thermodynamic parameters reproduce well the phase diagram and the thermodynamic data.

Table I. Phases, structures and models.

Phase	Struktur-bericht	Prototype	Pearson symbol	Space group	SGTE name	Model
liquid					LIQUID	$(Al,Mg)_1$
fcc	$A1$	Cu	$cF4$	$Fm\overline{3}m$	FCC_A1	$(Al,Mg)_1$
$Al_{140}Mg_{89}$	$\cdots$	Al_3Mg_2	$cF1832$	$Fd\overline{3}m$	ALMG_B	$Mg_{89}Al_{140}$
$Al_{30}Mg_{23}$	$\cdots$	CoCrMo	$hR53$	$R3$	ALMG_EPS	$Mg_{23}Al_{30}$
$Al_{12}Mg_{17}$	$A12$	αMn	$cI58$	$I\overline{4}3m$	A12_ALMG	$Mg_5(Al,Mg)_{12}(Al,Mg)_{12}$
hcp	$A3$	Mg	$hP2$	$P6_3/mmc$	HCP_A3	$(Al,Mg)_1$

Table II. Invariant reactions.

Reaction	Type	T / K	Compositions / x_{Mg}			$\Delta_r H$ / (J/mol)
liquid $\rightleftharpoons$ $Al_{12}Mg_{17}$	congruent	736.6	0.538	0.538		−7147
liquid $\rightleftharpoons$ $Al_{140}Mg_{89}$	congruent	724.8	0.389	0.389		−8252
liquid $\rightleftharpoons$ fcc + $Al_{140}Mg_{89}$	eutectic	723.6	0.362	0.166	0.389	−8158
liquid $\rightleftharpoons$ $Al_{140}Mg_{89}$ + $Al_{12}Mg_{17}$	eutectic	722.7	0.424	0.389	0.480	−7723
liquid $\rightleftharpoons$ $Al_{12}Mg_{17}$ + hcp	eutectic	709.4	0.690	0.601	0.884	−6543
$Al_{140}Mg_{89}$ + $Al_{12}Mg_{17}$ $\rightleftharpoons$ $Al_{30}Mg_{23}$	peritectoid	682.9	0.389	0.494	0.434	−175
$Al_{30}Mg_{23}$ $\rightleftharpoons$ $Al_{140}Mg_{89}$ + $Al_{12}Mg_{17}$	eutectoid	523.2	0.434	0.389	0.536	−103

Table IIIa. Integral quantities for the liquid phase at 1000 K.

x_{Mg}	ΔG_m [J/mol]	ΔH_m [J/mol]	ΔS_m [J/(mol·K)]	G_m^E [J/mol]	S_m^E [J/(mol·K)]	ΔC_p [J/(mol·K)]
0.000	0	0	0.000	0	0.000	0.000
0.100	−2976	−828	2.148	−273	−0.555	0.000
0.200	−4701	−1623	3.078	−540	−1.083	0.000
0.300	−5826	−2294	3.532	−747	−1.547	0.000
0.400	−6454	−2770	3.684	−858	−1.912	0.000
0.500	−6622	−3000	3.622	−859	−2.141	0.000
0.600	−6348	−2952	3.396	−752	−2.200	0.000
0.700	−5640	−2612	3.028	−561	−2.051	0.000
0.800	−4489	−1987	2.502	−328	−1.659	0.000
0.900	−2817	−1101	1.716	−114	−0.987	0.000
1.000	0	0	0.000	0	0.000	0.000

Reference states: Al(liquid), Mg(liquid)

Table IIIb. Partial quantities for Al in the liquid phase at 1000 K.

x_{Al}	ΔG_{Al} [J/mol]	ΔH_{Al} [J/mol]	ΔS_{Al} [J/(mol·K)]	G^E_{Al} [J/mol]	S^E_{Al} [J/(mol·K)]	a_{Al}	γ_{Al}
1.000	0	0	0.000	0	0.000	1.000	1.000
0.900	−869	0	0.868	7	−0.008	0.901	1.001
0.800	−1908	−131	1.777	−52	−0.079	0.795	0.994
0.700	−3223	−543	2.681	−258	−0.285	0.679	0.969
0.600	−4878	−1329	3.549	−631	−0.699	0.556	0.927
0.500	−6898	−2527	4.372	−1135	−1.391	0.436	0.872
0.400	−9295	−4113	5.183	−1677	−2.436	0.327	0.817
0.300	−12115	−6008	6.107	−2105	−3.903	0.233	0.776
0.200	−15592	−8076	7.515	−2210	−5.866	0.153	0.767
0.100	−20871	−10122	10.748	−1726	−8.396	0.081	0.813
0.000	−∞	−11894	∞	−328	−11.566	0.000	0.961

Reference state: Al(liquid)

Table IIIc. Partial quantities for Mg in the liquid phase at 1000 K.

x_{Mg}	ΔG_{Mg} [J/mol]	ΔH_{Mg} [J/mol]	ΔS_{Mg} [J/(mol·K)]	G^E_{Mg} [J/mol]	S^E_{Mg} [J/(mol·K)]	a_{Mg}	γ_{Mg}
0.000	−∞	−8106	∞	−2540	−5.566	0.000	0.737
0.100	−21946	−8281	13.664	−2801	−5.480	0.071	0.714
0.200	−15875	−7591	8.283	−2493	−5.098	0.148	0.741
0.300	−11898	−6379	5.519	−1888	−4.491	0.239	0.797
0.400	−8817	−4931	3.887	−1199	−3.732	0.346	0.866
0.500	−6345	−3474	2.872	−582	−2.891	0.466	0.932
0.600	−4383	−2178	2.205	−135	−2.043	0.590	0.984
0.700	−2865	−1156	1.709	101	−1.257	0.709	1.012
0.800	−1713	−464	1.249	142	−0.607	0.814	1.017
0.900	−811	−99	0.712	65	−0.164	0.907	1.008
1.000	0	0	0.000	0	0.000	1.000	1.000

Reference state: Mg(liquid)

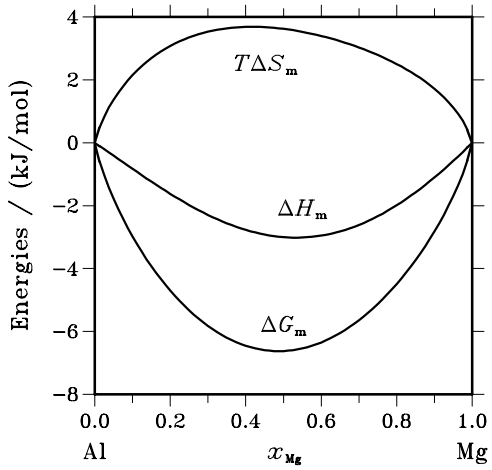

Fig. 2. Integral quantities of the liquid phase at T=1000 K.

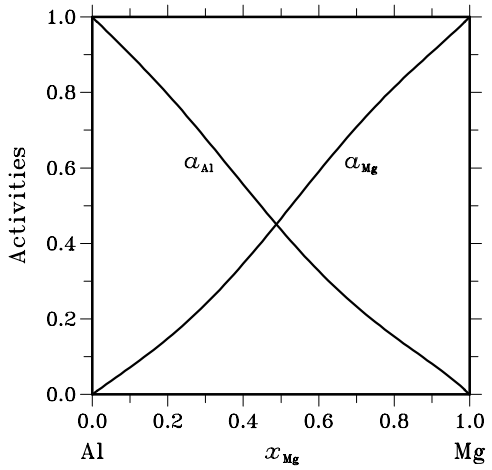

Fig. 3. Activities in the liquid phase at T=1000 K.

Table IV. Standard reaction quantities at 298.15 K for the compounds per mole of atoms.

Compound	x_{Mg}	$\Delta_{\mathrm{f}}G^{\circ}$ / (J/mol)	$\Delta_{\mathrm{f}}H^{\circ}$ / (J/mol)	$\Delta_{\mathrm{f}}S^{\circ}$ / (J/(mol·K))	$\Delta_{\mathrm{f}}C_P^{\circ}$ / (J/(mol·K))
$Al_{140}Mg_{89}$	0.389	−1955	−1075	2.950	0.000
$Al_{30}Mg_{23}$	0.434	−1966	−992	3.268	0.000

References

[82Mur] J.L. Murray: Bull. Alloy Phase Diagrams **3** (1982) 60–74.
[90Sau] N. Saunders: Calphad **14** (1990) 61–70.
[94Cha] P. Chartrand, A.D. Pelton: J. Phase Equilibria **15** (1994) 591–605.
[98Lia] P. Liang, H.-L. Su, P. Donnadieu, M.G. Harmelin, A. Quivy, P. Ochin, G. Effenberg, H.J. Seifert, H.L. Lukas, F. Aldinger: Z. Metallkd. **89** (1998) 536–540.

Al – Mn (Aluminium – Manganese)

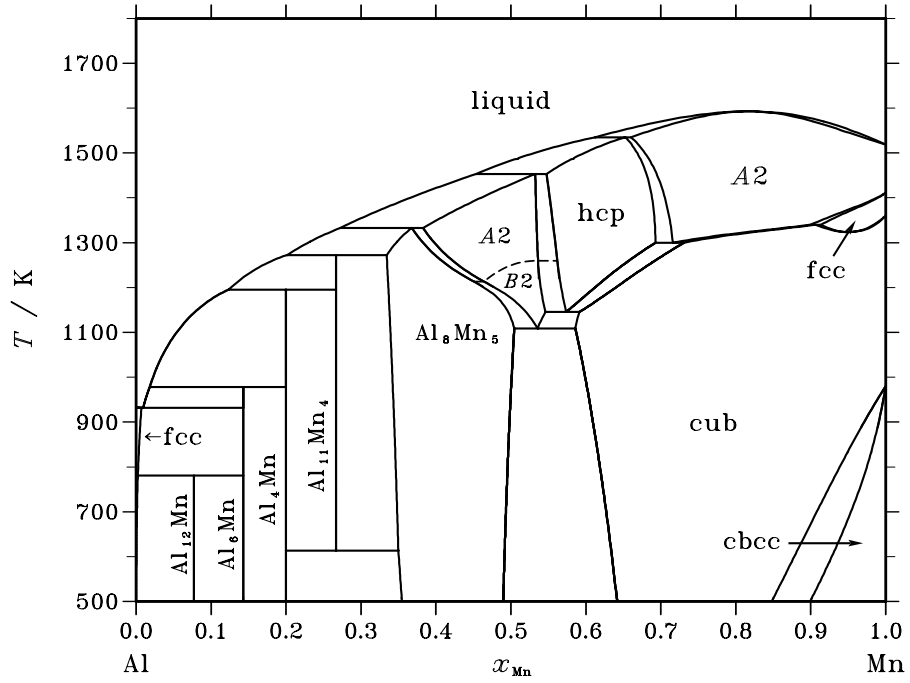

Fig. 1. Calculated phase diagram for the system Al-Mn.

There is a high solubility of Al in the Mn phases but very small solubility of Mn in fcc-Al. Several intermediate phases are formed in contact with the liquid. Recently one of the intermediate phases was identified as bcc and an order/disorder transformation to $B2$ detected. All invariant reactions with the liquid are peritectic. Some of the intermediate phases have transformations at lower temperatures.
Mn is an important alloying element in Al alloys. It is mainly added to control the type of intermediate phase formed with Fe which is an unavoidable impurity. The Al-Mn system is also important for permanent magnets and shape memory materials.
From the major thermodynamic evaluations and assessments of the Al–Mn system in the literature [87McA, 92Jan, 99Liu], the most recent is recommended here.

Table I. Phases, structures and models.

Phase	Struktur-bericht	Prototype	Pearson symbol	Space group	SGTE name	Model
liquid					LIQUID	$(Al,Mn)_1$
fcc	$A1$	Cu	$cF4$	$Fm\overline{3}m$	FCC_A1	$(Al,Mn)_1$
$Al_{12}Mn$	···	···	$cI27$	$Im\overline{3}$	AL12MN	$Al_{12}Mn_1$
Al_6Mn	$D2_h$	Al_6Mn	$oC28$	$Cmcm$	D2H_AL6MN	Al_6Mn_1
Al_4Mn	···	···	$hP574$	$P6_3/mmc$	AL4MN	Al_4Mn_1
$Al_{11}Mn_4$	···	···	$aP30$	$P\overline{1}$	AL11MN4	$Al_{11}Mn_4$
Al_8Mn_5	$D8_{10}$	Al_8Cr_5	$hR26$	$R3m$	D810_AL8MN5	$Al_{12}Mn_4(Al,Mn)_{10}$
$A2$	$A2$	W	$cI2$	$Im\overline{3}m$	BCC_A2	$(Al,Mn)_1$
$B2$	$B2$	CsCl	$cP2$	$Pm3m$	BCC_B2	$(Al,Mn)_1(Al,Mn)_1$
hcp	$A3$	Mg	$hP2$	$P6_3/mmc$	HCP_A3	$(Al,Mn)_1$
cbcc	$A12$	αMn	$cI58$	$I\overline{4}3m$	CBCC_A12	$(Al,Mn)_1$
cub	$A13$	βMn	$cP20$	$P4_132$	CUB_A13	$(Al,Mn)_1$

Table II. Invariant reactions.

Reaction	Type	T / K	Compositions / x_{Mn}			$\Delta_r H$ / (J/mol)
liquid $\rightleftharpoons$ $A2$	congruent	1592.7	0.818	0.818		−12320
liquid + $A2$ $\rightleftharpoons$ hcp	peritectic	1535.1	0.613	0.660	0.653	−3925
liquid + hcp $\rightleftharpoons$ $A2$	peritectic	1453.4	0.454	0.547	0.533	−3591
$A2$ + fcc $\rightleftharpoons$ cub	peritectoid	1340.0	0.899	0.913	0.906	−5528
liquid + $A2$ $\rightleftharpoons$ Al_8Mn_5	peritectic	1332.8	0.272	0.383	0.368	−4449
fcc $\rightleftharpoons$ cub	congruent	1323.5	0.950	0.950		−2487
$A2$ $\rightleftharpoons$ hcp + cub	eutectoid	1299.7	0.716	0.693	0.731	−5056
liquid + Al_8Mn_5 $\rightleftharpoons$ $Al_{11}Mn_4$	peritectic	1272.4	0.201	0.334	0.267	−10691
liquid + $Al_{11}Mn_4$ $\rightleftharpoons$ Al_4Mn	peritectic	1195.4	0.123	0.267	0.200	−10690
hcp $\rightleftharpoons$ $B2$ + cub	eutectoid	1145.4	0.574	0.546	0.591	−2408
$B2$ $\rightleftharpoons$ Al_8Mn_5 + cub	eutectoid	1108.6	0.536	0.504	0.586	−2047
liquid + Al_4Mn $\rightleftharpoons$ Al_6Mn	peritectic	978.1	0.018	0.200	0.143	−3463
liquid $\rightleftharpoons$ fcc + Al_6Mn	eutectic	931.4	0.010	0.007	0.143	−10765
fcc + Al_6Mn $\rightleftharpoons$ $Al_{12}Mn$	peritectoid	781.0	0.002	0.143	0.077	−111
$Al_{11}Mn_4$ $\rightleftharpoons$ Al_4Mn + Al_8Mn_5	eutectoid	613.1	0.267	0.200	0.350	−477
Al_6Mn $\rightleftharpoons$ $Al_{12}Mn$ + Al_4Mn	eutectoid	403.1	0.143	0.077	0.200	−104

Table IIIa. Integral quantities for the liquid phase at 1600 K.

x_{Mn}	ΔG_{m} [J/mol]	ΔH_{m} [J/mol]	ΔS_{m} [J/(mol·K)]	$G_{\mathrm{m}}^{\mathrm{E}}$ [J/mol]	$S_{\mathrm{m}}^{\mathrm{E}}$ [J/(mol·K)]	ΔC_p [J/(mol·K)]
0.000	0	0	0.000	0	0.000	0.000
0.100	−6439	−6648	−0.131	−2114	−2.834	0.000
0.200	−10338	−11461	−0.702	−3681	−4.862	0.000
0.300	−12900	−14616	−1.072	−4774	−6.151	0.000
0.400	−14394	−16268	−1.171	−5440	−6.767	0.000
0.500	−14925	−16544	−1.012	−5704	−6.775	0.000
0.600	−14515	−15547	−0.645	−5562	−6.240	0.000
0.700	−13113	−13355	−0.151	−4986	−5.230	0.000
0.800	−10581	−10019	0.351	−3924	−3.809	0.000
0.900	−6621	−5567	0.659	−2297	−2.044	0.000
1.000	0	0	0.000	0	0.000	0.000

Reference states: Al(liquid), Mn(liquid)

Table IIIb. Partial quantities for Al in the liquid phase at 1600 K.

x_{Al}	ΔG_{Al} [J/mol]	ΔH_{Al} [J/mol]	ΔS_{Al} [J/(mol·K)]	G^E_{Al} [J/mol]	S^E_{Al} [J/(mol·K)]	a_{Al}	γ_{Al}
1.000	0	0	0.000	0	0.000	1.000	1.000
0.900	−1690	−950	0.462	−288	−0.414	0.881	0.979
0.800	−4011	−3548	0.289	−1042	−1.567	0.740	0.925
0.700	−6897	−7476	−0.362	−2153	−3.327	0.595	0.851
0.600	−10382	−12489	−1.317	−3587	−5.564	0.458	0.764
0.500	−14609	−18421	−2.382	−5388	−8.146	0.333	0.667
0.400	−19864	−25179	−3.322	−7675	−10.940	0.225	0.562
0.300	−26659	−32747	−3.805	−10642	−13.816	0.135	0.449
0.200	−35972	−41188	−3.260	−14561	−16.641	0.067	0.335
0.100	−50411	−50636	−0.140	−19780	−19.285	0.023	0.226
0.000	−∞	−61304	∞	−26720	−21.615	0.000	0.134

Reference state: Al(liquid)

Table IIIc. Partial quantities for Mn in the liquid phase at 1600 K.

x_{Mn}	ΔG_{Mn} [J/mol]	ΔH_{Mn} [J/mol]	ΔS_{Mn} [J/(mol·K)]	G^E_{Mn} [J/mol]	S^E_{Mn} [J/(mol·K)]	a_{Mn}	γ_{Mn}
0.000	−∞	−76322	∞	−24190	−32.582	0.000	0.162
0.100	−49182	−57934	−5.470	−18550	−24.615	0.025	0.248
0.200	−35648	−43110	−4.663	−14238	−18.045	0.069	0.343
0.300	−26907	−31276	−2.731	−10890	−12.741	0.132	0.441
0.400	−20411	−21935	−0.953	−8221	−8.571	0.216	0.539
0.500	−15241	−14666	0.359	−6020	−5.404	0.318	0.636
0.600	−10949	−9125	1.140	−4153	−3.107	0.439	0.732
0.700	−7307	−5043	1.415	−2562	−1.551	0.577	0.825
0.800	−4233	−2227	1.254	−1265	−0.601	0.727	0.909
0.900	−1756	−559	0.748	−354	−0.128	0.876	0.974
1.000	0	0	0.000	0	0.000	1.000	1.000

Reference state: Mn(liquid)

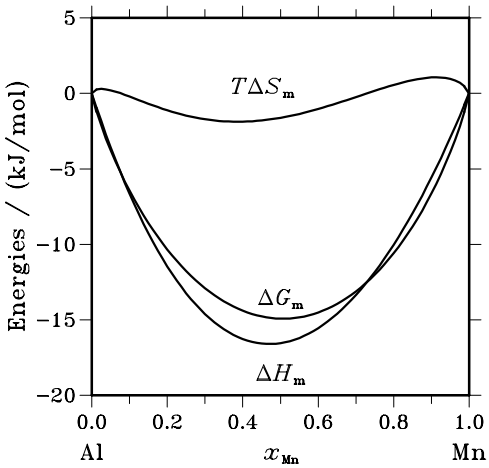

Fig. 2. Integral quantities of the liquid phase at T=1600 K.

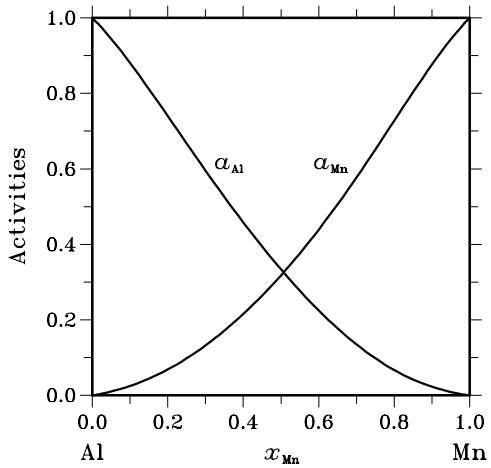

Fig. 3. Activities in the liquid phase at T=1600 K.

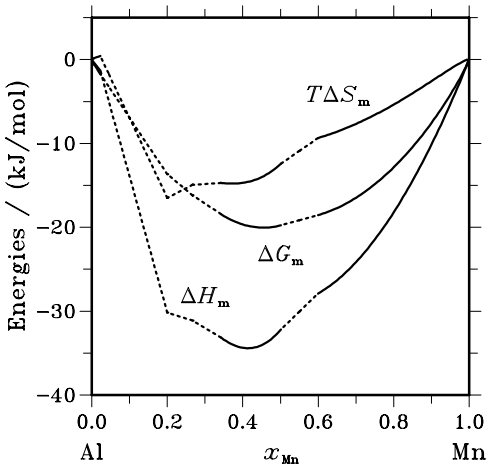

Fig. 4. Integral quantities of the stable phases at T=1000 K.

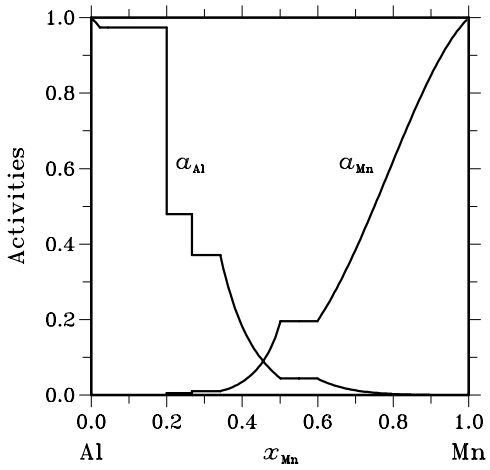

Fig. 5. Activities in the stable phases at T=1000 K.

Table IVa. Integral quantities for the stable phases at 1000 K.

Phase	x_{Mn}	ΔG_m [J/mol]	ΔH_m [J/mol]	ΔS_m [J/(mol·K)]	G_m^E [J/mol]	S_m^E [J/(mol·K)]	ΔC_p [J/(mol·K)]
liquid	0.000	0	0	0.000	0	0.000	0.000
	0.023	−1733	−1315	0.418	−837	−0.478	0.040
Al_4Mn	0.200	−13661	−30159	−16.497			1.208
$Al_{11}Mn_4$	0.267	−16177	−31116	−14.939			1.241
Al_8Mn_5	0.342	−18412	−33125	−14.713	−16197	−16.928	1.279
	0.350	−18644	−33388	−14.744	−16428	−16.960	1.283
	0.400	−19664	−34361	−14.697	−17574	−16.787	1.308
	0.450	−20036	−34056	−14.020	−18311	−15.744	1.333
	0.500	−19779	−32236	−12.457	−18740	−13.496	1.358
	0.501	−19768	−32185	−12.417	−18746	−13.439	1.359
cub	0.599	−18548	−27910	−9.362	−12949	−14.961	0.444
	0.600	−18536	−27885	−9.349	−12940	−14.945	0.443
	0.650	−17706	−26299	−8.593	−12323	−13.976	0.388
	0.700	−16481	−24151	−7.670	−11402	−12.749	0.332
	0.750	−14860	−21451	−6.591	−10185	−11.266	0.277
	0.800	−12843	−18209	−5.366	−8682	−9.527	0.221
	0.850	−10417	−14433	−4.015	−6903	−7.530	0.166
	0.900	−7559	−10133	−2.574	−4856	−5.277	0.111
	0.950	−4203	−5319	−1.116	−2552	−2.767	0.055
	1.000	0	0	0.000	0	0.000	0.000

Reference states: Al(liquid), Mn(cub)

Table IVb. Partial quantities for Al in the stable phases at 1000 K.

Phase	x_{Al}	ΔG_{Al} [J/mol]	ΔH_{Al} [J/mol]	ΔS_{Al} [J/(mol·K)]	G^{E}_{Al} [J/mol]	S^{E}_{Al} [J/(mol·K)]	a_{Al}	γ_{Al}
liquid	1.000	0	0	0.000	0	0.000	1.000	1.000
	0.977	−219	−51	0.168	−29	−0.022	0.974	0.997
Al_4Mn	0.800	−219	2347	2.565			0.974	
	0.800	−6113	−27287	−21.174			0.479	
$Al_{11}Mn_8$	0.733	−6113	−27287	−21.174			0.479	
	0.733	−8252	−23993	−15.741			0.371	
Al_8Mn_5	0.658	−8252	−21508	−13.255	−6163	−15.344	0.371	0.477
	0.650	−9076	−22657	−13.581	−6744	−15.913	0.336	0.444
	0.600	−14177	−31373	−17.196	−10174	−21.199	0.182	0.294
	0.550	−19460	−43260	−23.800	−13215	−30.046	0.096	0.204
	0.500	−25842	−58793	−32.951	−15668	−43.125	0.045	0.152
	0.499	−25999	−59131	−33.132	−15708	−43.423	0.044	0.151
cub	0.401	−25999	−43380	−17.381	−18401	−24.979	0.044	0.109
	0.400	−26092	−43513	−17.421	−18474	−25.039	0.043	0.108
	0.350	−31071	−50591	−19.520	−22342	−28.248	0.024	0.068
	0.300	−36403	−58107	−21.704	−26392	−31.715	0.013	0.042
	0.250	−42132	−66044	−23.911	−30606	−35.438	0.006	0.025
	0.200	−48346	−74381	−26.035	−34964	−39.417	0.003	0.015
	0.150	−55222	−83101	−27.880	−39448	−43.654	0.001	0.009
	0.100	−63183	−92185	−29.002	−44038	−48.147	0.001	0.005
	0.050	−73625	−101613	−27.988	−48717	−52.897	0.000	0.003
	0.000	$-\infty$	−111367	∞	−53464	−57.903	0.000	0.002

Reference state: Al(liquid)

Table IVc. Partial quantities for Mn in the stable phases at 1000 K.

Phase	x_{Mn}	ΔG_{Mn} [J/mol]	ΔH_{Mn} [J/mol]	ΔS_{Mn} [J/(mol·K)]	$G^{\mathrm{E}}_{\mathrm{Mn}}$ [J/mol]	$S^{\mathrm{E}}_{\mathrm{Mn}}$ [J/(mol·K)]	a_{Mn}	γ_{Mn}
liquid	0.000	$-\infty$	−60658	∞	−38459	−22.198	0.000	0.010
	0.023	−67432	−56171	11.261	−35897	−20.274	0.000	0.013
Al_4Mn	0.200	−67432	−160181	−92.749			0.000	
	0.200	−43854	−41647	2.207			0.005	
$Al_{11}Mn_4$	0.267	−43854	−41647	2.207			0.005	
	0.267	−37971	−50704	−12.733			0.010	
Al_8Mn_5	0.342	−37971	−55489	−17.518	−35511	−19.978	0.010	0.014
	0.350	−36413	−53317	−16.904	−34414	−18.903	0.013	0.016
	0.400	−27894	−38843	−10.949	−28675	−10.168	0.035	0.032
	0.450	−20740	−22806	−2.066	−24541	1.735	0.083	0.052
	0.500	−13717	−5680	8.038	−21812	16.132	0.192	0.073
	0.501	−13560	−5342	8.218	−21772	16.430	0.196	0.073
cub	0.599	−13560	−17555	−3.995	−9299	−8.256	0.196	0.327
	0.600	−13498	−17467	−3.969	−9251	−8.216	0.197	0.329
	0.650	−10510	−13219	−2.709	−6928	−6.290	0.283	0.435
	0.700	−7943	−9599	−1.656	−4977	−4.622	0.385	0.550
	0.750	−5770	−6587	−0.817	−3378	−3.209	0.500	0.666
	0.800	−3967	−4165	−0.199	−2111	−2.054	0.621	0.776
	0.850	−2511	−2315	0.196	−1159	−1.155	0.739	0.870
	0.900	−1379	−1016	0.363	−503	−0.513	0.847	0.941
	0.950	−549	−251	0.298	−123	−0.128	0.936	0.985
	1.000	0	0	0.000	0	0.000	1.000	1.000

Reference state: Mn(cub)

Table V. Standard reaction quantities at 298.15 K for the compounds per mole of atoms.

Compound	x_{Mn}	$\Delta_{\mathrm{f}}G^\circ$ / (J/mol)	$\Delta_{\mathrm{f}}H^\circ$ / (J/mol)	$\Delta_{\mathrm{f}}S^\circ$ / (J/(mol·K))	$\Delta_{\mathrm{f}}C^\circ_P$ / (J/(mol·K))
$Al_{12}Mn_1$	0.077	−7404	−8174	−2.583	0.000
Al_6Mn_1	0.143	−13673	−15064	−4.665	−0.001
Al_4Mn_1	0.200	−19157	−21230	−6.952	−0.001
$Al_{11}Mn_4$	0.267	−20957	−22746	−6.000	−0.001

References

[87McA] A.J. McAlister, J.L. Murray: Bull. Alloy Phase Diagrams **8** (1987) 438–447.

[92Jan] A. Jansson: Metall. Trans. **23A** (1992) 2953–2962.

[99Liu] X.J. Liu, I. Ohnuma, R. Kainuma, K. Ishida: J. Phase Equilibria **20** (1999) 45–56.

Al – Mo (Aluminium – Molybdenum)

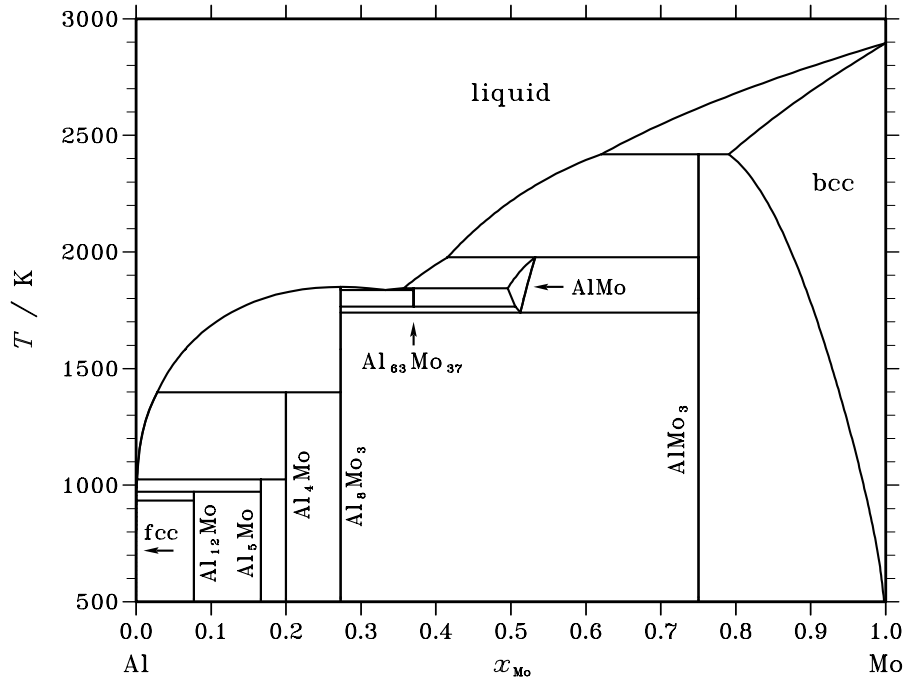

Fig. 1. Calculated phase diagram for the system Al-Mo.

The system is well known in the Al-rich end and there are several Al-rich compounds, the first is $Al_{12}Mo$. At higher Mo content the system is only estimated and the intermetallic phases are treated as stoichiometric as there is little or no experimental information.
The system is of interest for Mo as addition to Al alloys. It is possible to form an icosahedral phase in the Al-rich side. This is not included in the modelling where all phases are treated as compounds except the fcc-Al and bcc-Mo and the liquid which are all treated as substitutional regular solutions. The AlMo phase is modelled as an ordered $B2$ phase. The accepted dataset has been critically evaluated by [98Sau].

Table I. Phases, structures and models.

Phase	Struktur-bericht	Prototype	Pearson symbol	Space group	SGTE name	Model
liquid					LIQUID	$(Al,Mo)_1$
fcc	$A1$	Cu	$cF4$	$Fm\overline{3}m$	FCC_A1	$(Al,Mo)_1$
$Al_{12}Mo$	···	$Al_{12}W$	$cI26$	$Im\overline{3}$	AL12MO	$Al_{12}Mo_1$
Al_5Mo	···	Al_5W	$hP12$	$P6_3$	AL5MO	Al_5Mo_1
Al_4Mo	···	Al_4W	$mC30$	Cm	AL4MO	Al_4Mo_1
Al_8Mo_3	···	Al_8Mo_3	$mC22$	$C2/m$	AL8MO3	Al_8Mo_3
$Al_{63}Mo_{37}$	···	···	···	···	AL63MO37	$Al_{63}Mo_{37}$
AlMo	$B2$	CsCl	$cP2$	$Pm3m$	BCC_B2	$(Al,Mo)_1(Al,Mo)_1$
$AlMo_3$	$A15$	Cr_3Si	$cP8$	$Pm\overline{3}n$	CUB_A15	Al_1Mo_3
bcc	$A2$	W	$cI2$	$Im\overline{3}m$	BCC_A2	$(Al,Mo)_1$

Table II. Invariant reactions.

Reaction	Type	T / K	Compositions / x_{Mo}			$\Delta_{\mathrm{r}}H$ / (J/mol)
liquid + bcc $\rightleftharpoons$ $AlMo_3$	peritectic	2418.9	0.621	0.791	0.750	−11577
liquid + $AlMo_3$ $\rightleftharpoons$ AlMo	peritectic	1976.9	0.415	0.750	0.533	−7021
liquid $\rightleftharpoons$ Al_8Mo_3	congruent	1850.6	0.273	0.273		−35294
liquid + AlMo $\rightleftharpoons$ $Al_{63}Mo_{37}$	peritectic	1844.4	0.357	0.496	0.370	−19157
liquid $\rightleftharpoons$ Al_8Mo_3 + $Al_{63}Mo_{37}$	eutectic	1836.4	0.333	0.273	0.370	−25902
$Al_{63}Mo_{37}$ $\rightleftharpoons$ Al_8Mo_3 + AlMo	eutectoid	1765.6	0.370	0.273	0.506	−5422
AlMo $\rightleftharpoons$ Al_8Mo_3 + $AlMo_3$	eutectoid	1739.8	0.513	0.273	0.750	−13770
liquid + Al_8Mo_3 $\rightleftharpoons$ Al_4Mo	peritectic	1397.7	0.028	0.273	0.200	−3624
liquid + Al_4Mo $\rightleftharpoons$ Al_5Mo	peritectic	1025.2	0.001	0.200	0.167	−2041
liquid + Al_5Mo $\rightleftharpoons$ $Al_{12}Mo$	peritectic	971.6	0.001	0.167	0.077	−5767
liquid + $Al_{12}Mo$ $\rightleftharpoons$ fcc	peritectic	933.8	0.000	0.077	0.001	−10607
Al_4Mo $\rightleftharpoons$ Al_5Mo + Al_8Mo_3	eutectoid	332.1	0.200	0.167	0.273	−169

Table IIIa. Integral quantities for the liquid phase at 2900 K.

x_{Mo}	ΔG_{m} [J/mol]	ΔH_{m} [J/mol]	ΔS_{m} [J/(mol·K)]	$G^{\mathrm{E}}_{\mathrm{m}}$ [J/mol]	$S^{\mathrm{E}}_{\mathrm{m}}$ [J/(mol·K)]	ΔC_p [J/(mol·K)]
0.000	0	0	0.000	0	0.000	0.000
0.100	−7468	−10080	−0.901	370	−3.604	0.000
0.200	−11512	−17440	−2.044	554	−6.205	0.000
0.300	−14140	−22260	−2.800	590	−7.879	0.000
0.400	−15711	−24720	−3.107	517	−8.702	0.000
0.500	−16338	−25000	−2.987	375	−8.750	0.000
0.600	−16025	−23280	−2.502	203	−8.098	0.000
0.700	−14689	−19740	−1.742	40	−6.821	0.000
0.800	−12140	−14560	−0.835	−74	−4.995	0.000
0.900	−7939	−7920	0.007	−100	−2.696	0.000
1.000	0	0	0.000	0	0.000	0.000

Reference states: Al(liquid), Mo(liquid)

Table IIIb. Partial quantities for Al in the liquid phase at 2900 K.

x_{Al}	ΔG_{Al} [J/mol]	ΔH_{Al} [J/mol]	ΔS_{Al} [J/(mol·K)]	$G^{\mathrm{E}}_{\mathrm{Al}}$ [J/mol]	$S^{\mathrm{E}}_{\mathrm{Al}}$ [J/(mol·K)]	a_{Al}	γ_{Al}
1.000	0	0	0.000	0	0.000	1.000	1.000
0.900	−2440	−1390	0.362	100	−0.514	0.904	1.004
0.800	−5033	−5320	−0.099	348	−1.954	0.812	1.015
0.700	−7935	−11430	−1.205	665	−4.171	0.720	1.028
0.600	−11345	−19360	−2.764	972	−7.011	0.625	1.041
0.500	−15521	−28750	−4.562	1193	−10.325	0.525	1.051
0.400	−20847	−39240	−6.342	1246	−13.961	0.421	1.053
0.300	−27975	−50470	−7.757	1055	−17.767	0.313	1.045
0.200	−38266	−62080	−8.212	541	−21.594	0.205	1.023
0.100	−55894	−73710	−6.143	−374	−25.288	0.098	0.985
0.000	$-\infty$	−85000	∞	−1770	−28.700	0.000	0.929

Reference state: Al(liquid)

Table IIIc. Partial quantities for Mo in the liquid phase at 2900 K.

x_{Mo}	ΔG_{Mo} [J/mol]	ΔH_{Mo} [J/mol]	ΔS_{Mo} [J/(mol·K)]	$G^{\mathrm{E}}_{\mathrm{Mo}}$ [J/mol]	$S^{\mathrm{E}}_{\mathrm{Mo}}$ [J/(mol·K)]	a_{Mo}	γ_{Mo}
0.000	$-\infty$	−115000	∞	4770	−41.300	0.000	1.219
0.100	−52716	−88290	−12.267	2804	−31.412	0.112	1.123
0.200	−37428	−65920	−9.825	1379	−23.206	0.212	1.059
0.300	−28616	−47530	−6.522	415	−16.533	0.305	1.017
0.400	−22260	−32760	−3.621	−166	−11.239	0.397	0.993
0.500	−17156	−21250	−1.412	−443	−7.175	0.491	0.982
0.600	−12810	−12640	0.058	−492	−4.189	0.588	0.980
0.700	−8995	−6570	0.836	−395	−2.129	0.689	0.984
0.800	−5608	−2680	1.010	−228	−0.846	0.792	0.991
0.900	−2610	−610	0.690	−70	−0.186	0.897	0.997
1.000	0	0	0.000	0	0.000	1.000	1.000

Reference state: Mo(liquid)

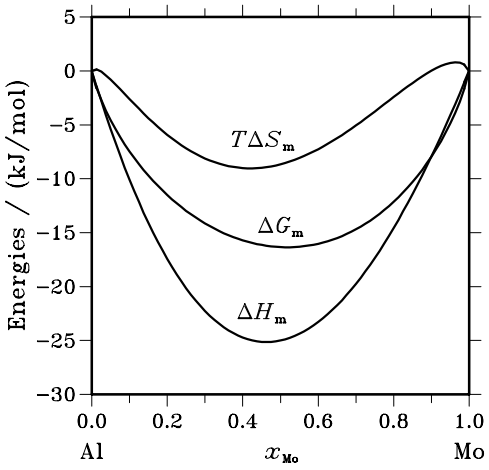

Fig. 2. Integral quantities of the liquid phase at T=2900 K.

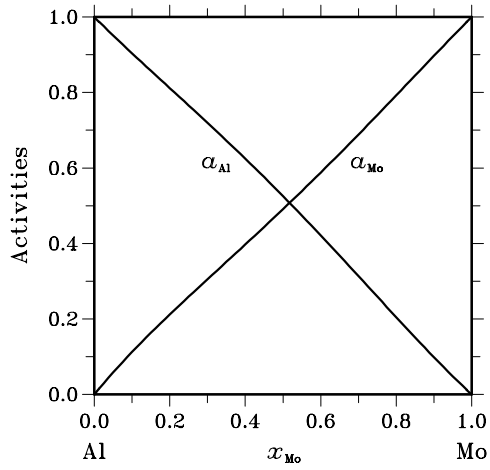

Fig. 3. Activities in the liquid phase at T=2900 K.

Table IV. Standard reaction quantities at 298.15 K for the compounds per mole of atoms.

Compound	x_{Mo}	$\Delta_{\mathrm{f}}G^{\circ}$ / (J/mol)	$\Delta_{\mathrm{f}}H^{\circ}$ / (J/mol)	$\Delta_{\mathrm{f}}S^{\circ}$ / (J/(mol·K))	$\Delta_{\mathrm{f}}C^{\circ}_{P}$ / (J/(mol·K))
$Al_{12}Mo_1$	0.083	−10081	−10700	−2.075	0.000
Al_5Mo_1	0.167	−21685	−23184	−5.026	0.000
Al_4Mo_1	0.200	−25744	−27514	−5.938	0.000
Al_8Mo_3	0.273	−34653	−37500	−9.550	0.000
$Al_{63}Mo_{37}$	0.370	−22182	−22681	−1.672	0.000
Al_1Mo_3	0.750	−20826	−22183	−4.553	0.447

References

[98Sau] N. Saunders in: I. Ansara, A.T. Dinsdale, M.H. Rand (eds.): COST 507, "Thermochemical database for light metal alloys", Vol. 2, EUR 18499, 1998, 59–64.

Al – N (Aluminium – Nitrogen)

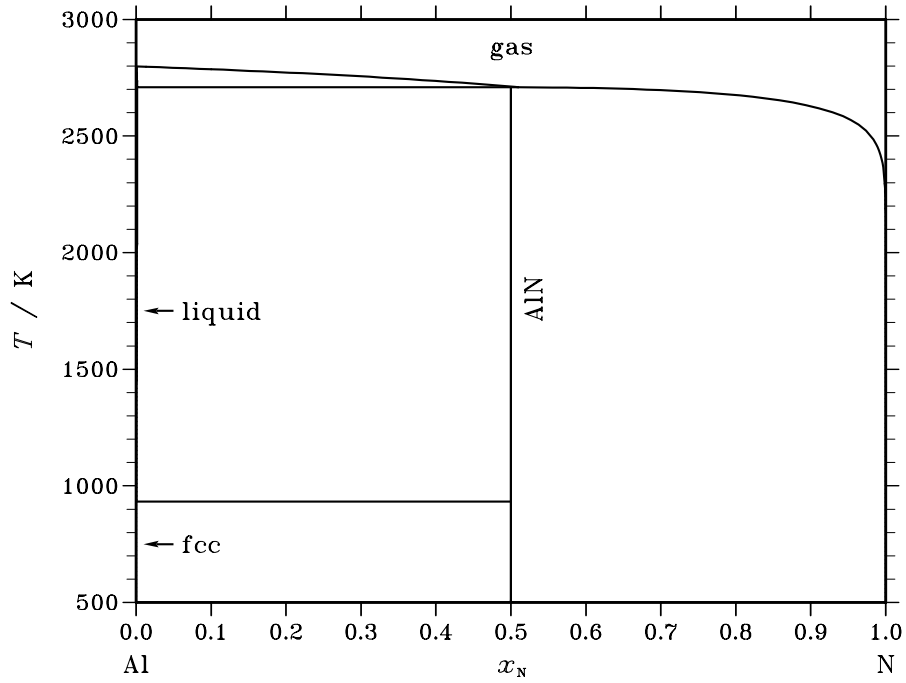

Fig. 1. Calculated phase diagram for the system Al-N.

The Si-Al-O-N system and its sub-systems are of considerable technical importance for silicon nitride and oxynitride ceramics. The thermodynamic description of [98Luk] is recommended for the Al-N system. This optimisation is based on experimental data reviewed by [71Stu] and [86Wri]. The data recommended in [71Stu] on the heat capacity and the entropy have been measured by adiabatic and drop calorimetry. The enthalpy of formation of AlN is based on calorimetric data and dissociation pressure measurements. More recent data on the enthalpy of formation of AlN derived from alkali borate solution calorimetry [97Nav, 99Lia] are in a good agreement with the value recommended by [71Stu]. The melting temperature of AlN has not been measured due to sublimation under normal pressure. The reported melting temperatures are in the range from 2423 K to 3123 K [86Wri]. This author recommends 2800 K to be the most credible melting temperature, because it has been determined under high pressure of N_2 in order to retard evaporation. Liquid Al is stable only at very low partial pressures of N_2 [86Wri]. The solubility of nitrogen in molten aluminium has been determined by several authors and it is discussed in [86Wri]. In spite of high uncertainties in the experimental data of [26Iwa], these results are recommended by [86Wri] and they are used in the assessment of [98Luk]. The solubility of nitrogen in solid aluminium is very low and no credible measurements have been reported. The liquid phase is described by a substitutional model. The sublattice model is applied to the fcc phase, and AlN is treated as a stoichiometric compound. The gas phase is considered to consist of the species Al, Al_2, N, N_2 and N_3.

Table I. Phases, structures and models.

Phase	Struktur-bericht	Prototype	Pearson symbol	Space group	SGTE name	Model
liquid					LIQUID	$(Al,N)_1$
fcc	$A1$	Cu	$cF4$	$Fm\overline{3}m$	FCC_A1	$Al_1(N,\Box)_1$
AlN	$B4$	ZnS(Wurtzite)	$hP4$	$P6_3mc$	ALN	Al_1N_1

Table II. Invariant reactions.

Reaction	Type	T / K	Compositions / x_N			$\Delta_r H$ / (J/mol)
liquid + gas ⇌ AlN	gas-peritectic	2707.1	0.002	0.505	0.500	−307637
liquid ⇌ fcc + AlN	degenerate	933.3	0.000	0.000	0.500	−10712

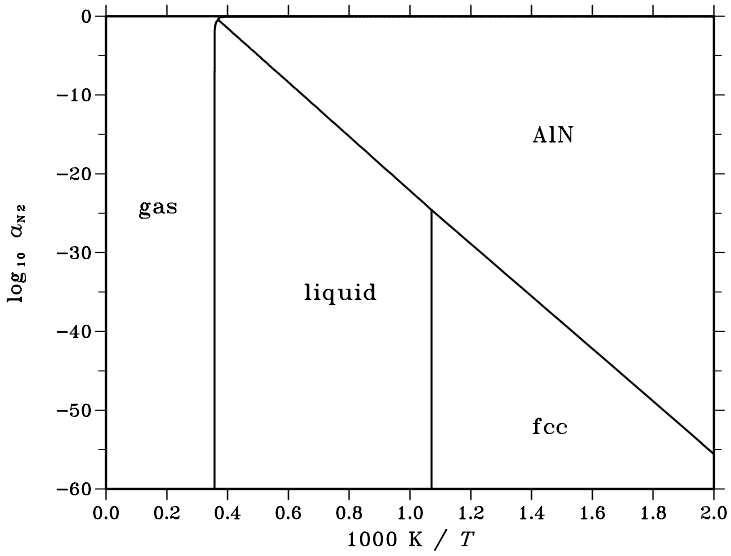

Fig. 2. Calculated temperature-activity phase diagram. Reference state: N(gas, 0.1 MPa).

Table III. Standard reaction quantities at 298.15 K for the compounds per mole of atoms.

Compound	x_N	$\Delta_f G°$ / (J/mol)	$\Delta_f H°$ / (J/mol)	$\Delta_f S°$ / (J/(mol·K))	$\Delta_f C_P°$ / (J/(mol·K))
Al_1N_1	0.500	−143503	−158990	−51.945	−5.264

References

[26Iwa] K. Iwase: Sci. Rep. Tohoku Imp. Univ., Ser. 1, **15** (1926) 534–566.
[71Stu] D.R. Stull, H. Prophet: "JANAF Thermochemical Tables", 2nd ed., NSRDS-NBS37, USGPO, Washington, DC, 1971.
[86Wri] H.A. Wriedt: Bull. Alloy Phase Diagrams **7** (1986) 329–333.
[97Nav] A. Navrotsky, S.H. Risbud, J. Liang, V.J. Leppert: J. Phys. Chem. **B101** (1997) 9433–9435.
[98Luk] H.L. Lukas in: I. Ansara, A.T. Dinsdale, M.H. Rand (eds.): COST 507, "Thermochemical database for light metal alloys", Vol. 2, EUR 18499, 1998, 65–68.
[99Lia] J. Liang, A. Navrotsky, V.J. Leppert, M. Pashkowitz, S.H. Risbud: J. Mater. Res. **14** (1999) 4630–4636.

Al – Nb (Aluminium – Niobium)

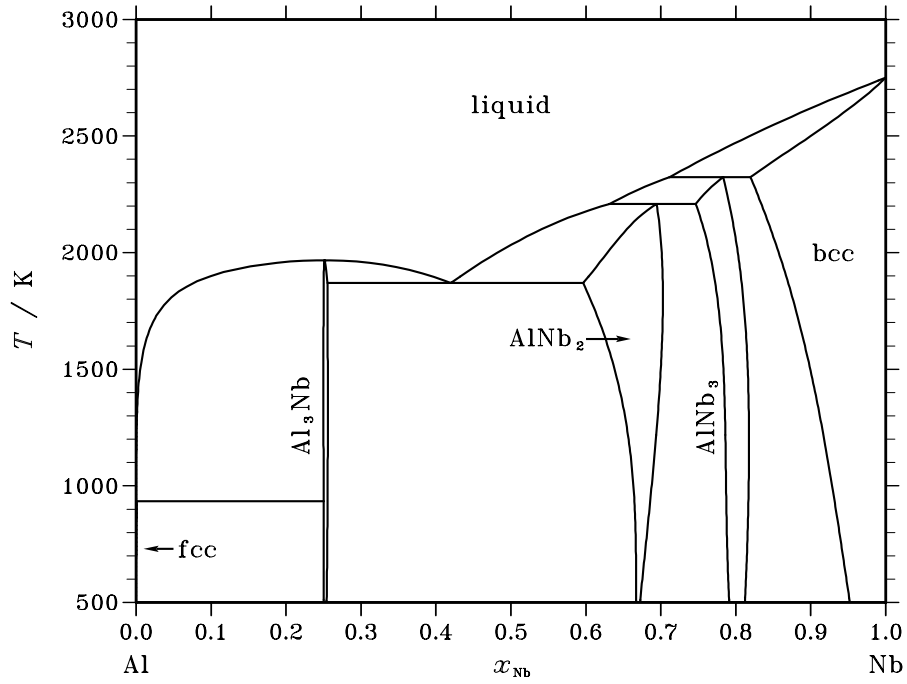

Fig. 1. Calculated phase diagram for the system Al-Nb.

Aluminium and Niobium are both important alloying elements for high temperature alloys, such as superalloys. The intermetallic $AlNb_3$ phase is also of interest because of its superconducting properties.
The experimental data reported for this system scatter significantly, for example the congruent melting temperature of Al_3Nb reported by several investigations ranges from 1878 K to 2023 K. The most consistent phase diagram can be constructed from the data reported by [80Jor] and [76Yer]. The majority of thermodynamic assessments of this system are based on these data. The recommended assessment of [97Ser] reproduces these data well, including liquidus and solidus data, phase boundary data for $AlNb_2$, $AlNb_3$ and bcc-Nb and the melting point of Al_3Nb, and the enthalpy of formation data of the intermediate compounds reported by [93Mes]. However, the description of the liquid phase results in the formation of an inverse miscibility gap at temperatures above 4284 K, and the description of this system should, therefore, not be used for calculations at temperatures above 4000 K.

Table I. Phases, structures and models.

Phase	Struktur-bericht	Prototype	Pearson symbol	Space group	SGTE name	Model
liquid					LIQUID	$(Al,Nb)_1$
fcc	$A1$	Cu	$cF4$	$Fm\overline{3}m$	FCC_A1	$(Al,Nb)_1$
Al_3Nb	$D0_{22}$	Al_3Ti	$tI8$	$I4/mmm$	NBAL3	$(Al,Nb)_1(Al,Nb)_3$
$AlNb_2$	$D8_b$	σCrFe	$tP30$	$P4_2/mnm$	NB2AL	$(Al,Nb)_8(Al,Nb)_5Nb_2$
$AlNb_3$	$A15$	Cr_3Si	$cP8$	$Pm\overline{3}n$	A15_NB3AL	$(Al,Nb)_3(Al,Nb)_1$
bcc	$A2$	W	$cI2$	$Im\overline{3}m$	BCC_A2	$(Al,Nb)_1$

Table II. Invariant reactions.

Reaction	Type	T / K	Compositions / x_{Nb}			$\Delta_{\mathrm{r}}H$ / (J/mol)
liquid + bcc $\rightleftharpoons$ $AlNb_3$	peritectic	2324.0	0.712	0.820	0.783	−9687
liquid + $AlNb_3$ $\rightleftharpoons$ $AlNb_2$	peritectic	2208.9	0.632	0.746	0.694	−13316
liquid $\rightleftharpoons$ Al_3Nb	congruent	1967.5	0.251	0.251		−38805
liquid $\rightleftharpoons$ Al_3Nb + $AlNb_2$	eutectic	1869.5	0.419	0.255	0.596	−29078
liquid + Al_3Nb $\rightleftharpoons$ fcc	peritectic	934.2	0.000	0.250	0.001	−10629

Table IIIa. Integral quantities for the liquid phase at 2800 K.

x_{Nb}	ΔG_{m} [J/mol]	ΔH_{m} [J/mol]	ΔS_{m} [J/(mol·K)]	$G^{\mathrm{E}}_{\mathrm{m}}$ [J/mol]	$S^{\mathrm{E}}_{\mathrm{m}}$ [J/(mol·K)]	ΔC_p [J/(mol·K)]
0.000	0	0	0.000	0	0.000	0.000
0.100	−6640	−7867	−0.438	928	−3.141	0.000
0.200	−11230	−13937	−0.967	420	−5.127	0.000
0.300	−15085	−18027	−1.051	−864	−6.130	0.000
0.400	−18044	−20071	−0.724	−2376	−6.320	0.000
0.500	−19821	−20118	−0.106	−3684	−5.869	0.000
0.600	−20138	−18326	0.647	−4470	−4.949	0.000
0.700	−18750	−14973	1.349	−4528	−3.730	0.000
0.800	−15418	−10447	1.776	−3768	−2.385	0.000
0.900	−9781	−5250	1.618	−2213	−1.085	0.000
1.000	0	0	0.000	0	0.000	0.000

Reference states: Al(liquid), Nb(liquid)

Table IIIb. Partial quantities for Al in the liquid phase at 2800 K.

x_{Al}	ΔG_{Al} [J/mol]	ΔH_{Al} [J/mol]	ΔS_{Al} [J/(mol·K)]	$G^{\mathrm{E}}_{\mathrm{Al}}$ [J/mol]	$S^{\mathrm{E}}_{\mathrm{Al}}$ [J/(mol·K)]	a_{Al}	γ_{Al}
1.000	0	0	0.000	0	0.000	1.000	1.000
0.900	−1615	−860	0.270	838	−0.606	0.933	1.037
0.800	−2782	−3736	−0.341	2412	−2.196	0.887	1.109
0.700	−4729	−8820	−1.461	3575	−4.427	0.816	1.166
0.600	−8377	−15959	−2.708	3516	−6.955	0.698	1.163
0.500	−14368	−24662	−3.676	1769	−9.439	0.539	1.079
0.400	−23122	−34092	−3.918	−1790	−11.536	0.370	0.926
0.300	−34974	−43073	−2.892	−6944	−12.903	0.223	0.742
0.200	−50604	−50086	0.185	−13135	−13.196	0.114	0.569
0.100	−73068	−53271	7.070	−19462	−12.075	0.043	0.433
0.000	$-\infty$	−50426	∞	−24683	−9.194	0.000	0.346

Reference state: Al(liquid)

Table IIIc. Partial quantities for Nb in the liquid phase at 2800 K.

x_{Nb}	ΔG_{Nb} [J/mol]	ΔH_{Nb} [J/mol]	ΔS_{Nb} [J/(mol·K)]	G^E_{Nb} [J/mol]	S^E_{Nb} [J/(mol·K)]	a_{Nb}	γ_{Nb}
0.000	$-\infty$	−86778	∞	18944	−37.758	0.000	2.256
0.100	−51865	−70938	−6.812	1740	−25.957	0.108	1.078
0.200	−45020	−54739	−3.471	−7551	−16.853	0.145	0.723
0.300	−39249	−39510	−0.093	−11220	−10.104	0.185	0.618
0.400	−32545	−26239	2.252	−11213	−5.366	0.247	0.618
0.500	−25275	−15573	3.465	−9138	−2.299	0.338	0.675
0.600	−18149	−7816	3.690	−6257	−0.557	0.459	0.764
0.700	−11797	−2931	3.166	−3493	0.201	0.602	0.861
0.800	−6622	−537	2.173	−1427	0.318	0.752	0.941
0.900	−2750	86	1.013	−297	0.137	0.889	0.987
1.000	0	0	0.000	0	0.000	1.000	1.000

Reference state: Nb(liquid)

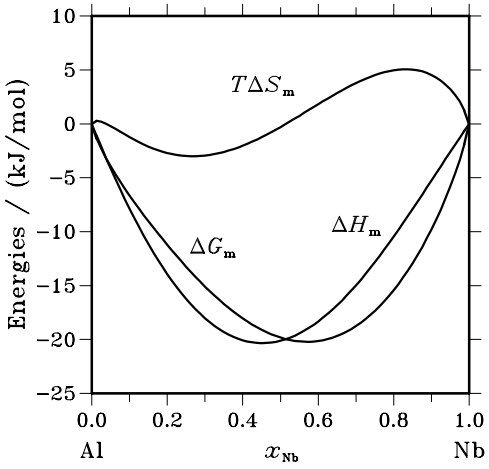

Fig. 2. Integral quantities of the liquid phase at T=2800 K.

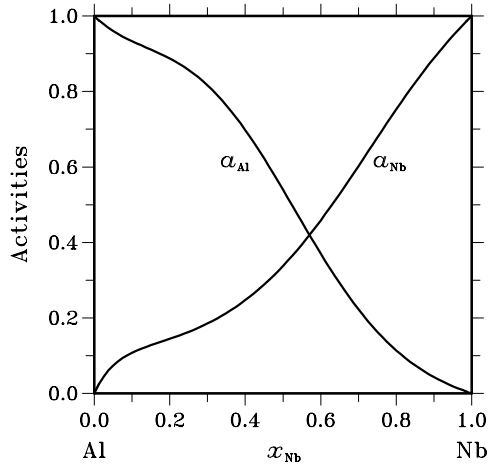

Fig. 3. Activities in the liquid phase at T=2800 K.

References

[76Yer] V.N. Yeremenko, Ya.V. Natazon, V.I. Dybkov: J. Less-Common Met. **50** (1976) 29–48.
[80Jor] J.L. Jorda, R. Flükiger, J. Müller: J. Less-Common Met. **75** (1980) 227–239.
[93Mes] S.V. Meschel, O.J. Kleppa: J. Alloys Comp. **191** (1993) 111–116.
[97Ser] C. Servant, I. Ansara: J. Chim. Phys. **94** (1997) 869–888.

Al – Nd (Aluminium – Neodymium)

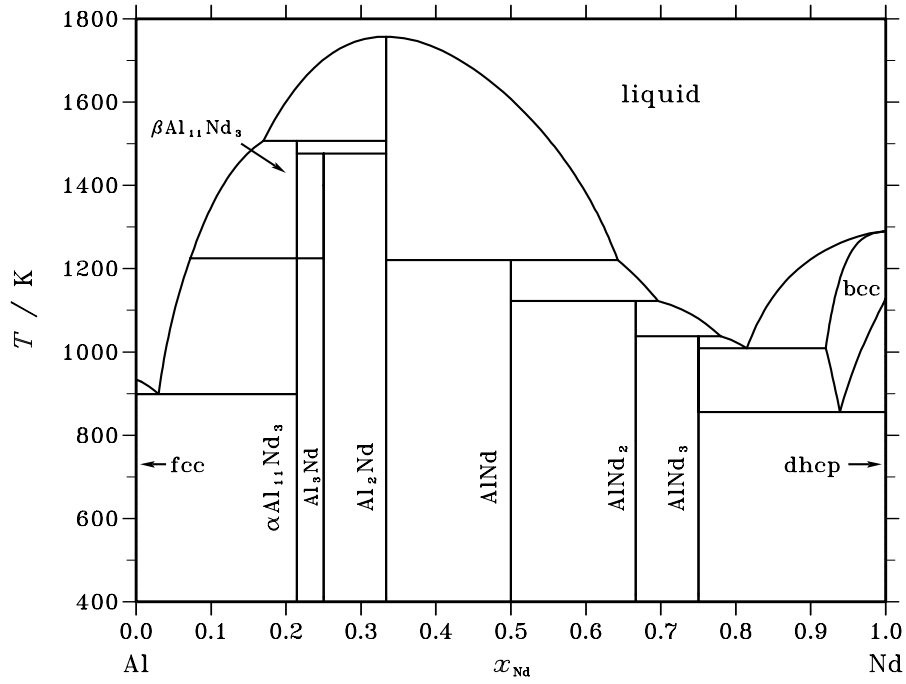

Fig. 1. Calculated phase diagram for the system Al-Nd.

The Al-Nd system is one of a number of rare earth systems of interest for its potential for forming metallic glasses [93Bar] with the possibilities for the development of high strength materials. The phase diagram for the system is dominated by the appearance of a number of intermetallic compounds which, with the exception of Al_2Nd, melt peritectically. There appears to be very little solubility of Nd in solid Al. However, the solubility of Al in both crystalline phases of Nd is appreciable - perhaps 10% Al in the high temperature bcc phase and 2% Al in the low temperature dhcp phase. The liquid phase boundaries in equilibrium with the compound phases seem to be fairly well defined. Thermodynamic studies have concerned the enthalpies of formation and heat capacities of the compounds, enthalpies of mixing in the liquid, emf and vapour pressure measurements. The data for the system have been reviewed by Clavaguera and Du [96Cla] who also provided a full critical assessment of thermodynamic and phase diagram data for the system. A similar evaluation has also been undertaken by Wang [96Wan]. The dataset adopted by SGTE was an updated version of that provided by Cacciamani et al. [91Cac], published in the COST 507 final report [98Ans]. A particular advantage of the data of [91Cac] over those of [96Cla, 96Wan] is that it models the solubility of Al in the high temperature solid phase of Nd.

Table I. Phases, structures and models.

Phase	Struktur-bericht	Prototype	Pearson symbol	Space group	SGTE name	Model
liquid					LIQUID	$(Al,Nd)_1$
fcc	$A1$	Cu	$cF4$	$Fm\overline{3}m$	FCC_A1	$(Al,Nd)_1$
$\alpha Al_{11}Nd_3$	$\cdots$	$\alpha Al_{11}La_3$	$oI28$	$Immm$	AL11M3	$Al_{11}Nd_3$
$\beta Al_{11}Nd_3$	$D1_3$	Al_4Ba	$tI10$	$I4/mmm$	D13_AL11M3	$Al_{11}Nd_3$
Al_3Nd	$D0_{19}$	Ni_3Sn	$hP8$	$P6_3/mmc$	D019_AL3M1	Al_3Nd_1
Al_2Nd	$C15$	Cu_2Mg	$cF24$	$Fd\overline{3}m$	C15_AL2M1	Al_2Nd_1
AlNd	$\cdots$	AlCe	$oC16$	$Cmcm$	AL1M1	Al_1Nd_1
$AlNd_2$	$C23$	Co_2Si	$oP12$	$Pnma$	C23_ALND2	Al_1Nd_2
$AlNd_3$	$D0_{19}$	Ni_3Sn	$hP8$	$P6_3/mmc$	D019_ALM3	Al_1Nd_3
bcc	$A2$	W	$cI2$	$Im\overline{3}m$	BCC_A2	$(Al,Nd)_1$
dhcp	$A3'$	αLa	$hP4$	$P6_3/mmc$	DHCP_A3	Nd_1

Table II. Invariant reactions.

Reaction	Type	T / K	Compositions / x_{Nd}			$\Delta_r H$ / (J/mol)
liquid $\rightleftharpoons$ Al_2Nd	congruent	1757.1	0.333	0.333		−29461
liquid + Al_2Nd $\rightleftharpoons$ $\beta Al_{11}Nd_3$	peritectic	1506.6	0.170	0.333	0.214	−14274
$\beta Al_{11}Nd_3$ + Al_2Nd $\rightleftharpoons$ Al_3Nd	peritectoid	1475.8	0.214	0.333	0.250	−3060
$\beta Al_{11}Nd_3$ $\rightleftharpoons$ $\alpha Al_{11}Nd_3$	polymorphic	1224.7	0.214	0.214		−1538
Al_2Nd + liquid $\rightleftharpoons$ AlNd	peritectic	1220.3	0.333	0.643	0.500	−11500
AlNd + liquid $\rightleftharpoons$ $AlNd_2$	peritectic	1122.2	0.500	0.696	0.667	−8761
$AlNd_2$ + liquid $\rightleftharpoons$ $AlNd_3$	peritectic	1037.9	0.667	0.780	0.750	−5087
liquid $\rightleftharpoons$ $AlNd_3$ + bcc	eutectic	1008.9	0.815	0.750	0.920	−5234
liquid $\rightleftharpoons$ fcc + $\alpha Al_{11}Nd_3$	eutectic	898.6	0.030	0.000	0.214	−10081
bcc $\rightleftharpoons$ $AlNd_3$ + dhcp	eutectoid	855.3	0.939	0.750	1.000	−2555

Table IIIa. Integral quantities for the liquid phase at 1800 K.

x_{Nd}	ΔG_m [J/mol]	ΔH_m [J/mol]	ΔS_m [J/(mol·K)]	G_m^E [J/mol]	S_m^E [J/(mol·K)]	ΔC_p [J/(mol·K)]
0.000	0	0	0.000	0	0.000	0.000
0.100	−11284	−13592	−1.282	−6419	−3.985	2.662
0.200	−17525	−24128	−3.668	−10036	−7.829	4.088
0.300	−20509	−31622	−6.174	−11367	−11.253	4.519
0.400	−20999	−36086	−8.382	−10927	−13.977	4.198
0.500	−19606	−37535	−9.960	−9232	−15.723	3.365
0.600	−16872	−35981	−10.616	−6800	−16.212	2.263
0.700	−13286	−31437	−10.084	−4144	−15.163	1.134
0.800	−9271	−23917	−8.137	−1782	−12.297	0.219
0.900	−5093	−13433	−4.633	−228	−7.336	−0.239
1.000	0	0	0.000	0	0.000	0.000

Reference states: Al(liquid), Nd(liquid)

Table IIIb. Partial quantities for Al in the liquid phase at 1800 K.

x_{Al}	ΔG_{Al} [J/mol]	ΔH_{Al} [J/mol]	ΔS_{Al} [J/(mol·K)]	G^E_{Al} [J/mol]	S^E_{Al} [J/(mol·K)]	a_{Al}	γ_{Al}
1.000	0	0	0.000	0	0.000	1.000	1.000
0.900	−3064	−1530	0.852	−1487	−0.024	0.815	0.905
0.800	−8600	−6102	1.388	−5261	−0.468	0.563	0.704
0.700	−15627	−13691	1.076	−10289	−1.890	0.352	0.503
0.600	−23184	−24269	−0.602	−15539	−4.850	0.212	0.354
0.500	−30354	−37810	−4.142	−19981	−9.905	0.132	0.263
0.400	−36294	−54287	−9.996	−22581	−17.615	0.088	0.221
0.300	−40328	−73676	−18.527	−22309	−28.537	0.068	0.225
0.200	−42219	−95948	−29.849	−18132	−43.231	0.060	0.298
0.100	−43480	−121078	−43.110	−9019	−62.255	0.055	0.547
0.000	−∞	−149039	∞	6063	−86.168	0.000	1.499

Reference state: Al(liquid)

Table IIIc. Partial quantities for Nd in the liquid phase at 1800 K.

x_{Nd}	ΔG_{Nd} [J/mol]	ΔH_{Nd} [J/mol]	ΔS_{Nd} [J/(mol·K)]	G^E_{Nd} [J/mol]	S^E_{Nd} [J/(mol·K)]	a_{Nd}	γ_{Nd}
0.000	−∞	−151238	∞	−79922	−39.620	0.000	0.005
0.100	−85268	−122147	−20.488	−50808	−39.633	0.003	0.034
0.200	−53225	−96229	−23.891	−29138	−37.273	0.029	0.143
0.300	−31901	−73460	−23.088	−13882	−33.099	0.119	0.396
0.400	−17722	−53812	−20.050	−4008	−27.669	0.306	0.765
0.500	−8858	−37260	−15.779	1516	−21.542	0.553	1.107
0.600	−3924	−23776	−11.029	3722	−15.276	0.769	1.282
0.700	−1697	−13334	−6.465	3641	−9.431	0.893	1.275
0.800	−1033	−5909	−2.709	2306	−4.564	0.933	1.167
0.900	−828	−1473	−0.358	749	−1.234	0.946	1.051
1.000	0	0	0.000	0	0.000	1.000	1.000

Reference state: Nd(liquid)

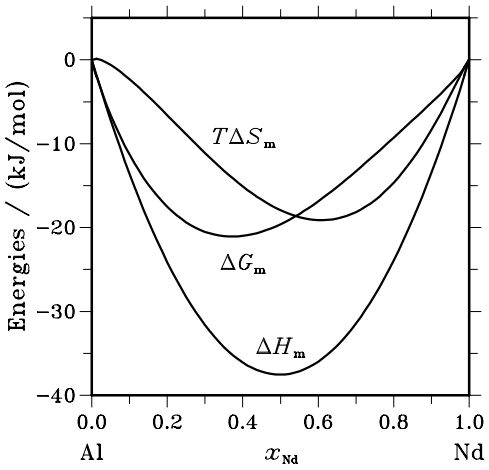

Fig. 2. Integral quantities of the liquid phase at T=1800 K.

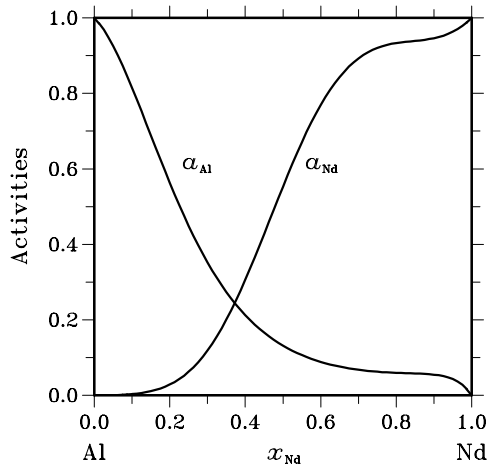

Fig. 3. Activities in the liquid phase at T=1800 K.

Table IV. Standard reaction quantities at 298.15 K for the compounds per mole of atoms.

Compound	x_{Nd}	$\Delta_{\mathrm{f}}G^{\circ}$ / (J/mol)	$\Delta_{\mathrm{f}}H^{\circ}$ / (J/mol)	$\Delta_{\mathrm{f}}S^{\circ}$ / (J/(mol·K))	$\Delta_{\mathrm{f}}C_P^{\circ}$ / (J/(mol·K))
$\alpha Al_{11}Nd_3$	0.214	−36350	−39165	−9.440	0.000
$\beta Al_{11}Nd_3$	0.214	−35187	−37627	−8.184	0.000
Al_3Nd_1	0.250	−41732	−45292	−11.940	0.000
Al_2Nd_1	0.333	−48867	−52978	−13.791	0.000
Al_1Nd_1	0.500	−44811	−49927	−17.161	0.000
Al_1Nd_2	0.667	−32252	−35929	−12.333	0.000
Al_1Nd_3	0.750	−24259	−26869	−8.754	0.000

References

[91Cac] G. Cacciamani, G. Borzone, R. Ferro: An. Fis. **86B** (1991) 160–162.
[93Bar] M. Baricco, L. Battezzati, G. Borzone, G. Cacciamani: J. Chim. Phys. **90** (1993) 261–268.
[96Cla] N. Clavaguera, Y. Du: J. Phase Equilibria **17** (1996) 107–111.
[96Wan] J. Wang: Calphad **20** (1996) 135–138.
[98Ans] I. Ansara, A.T. Dinsdale, M.H. Rand (eds.): COST 507, "Thermochemical database for light metal alloys", Vol. 2, EUR 18499, 1998, 75–78.

Al – Ni (Aluminium – Nickel)

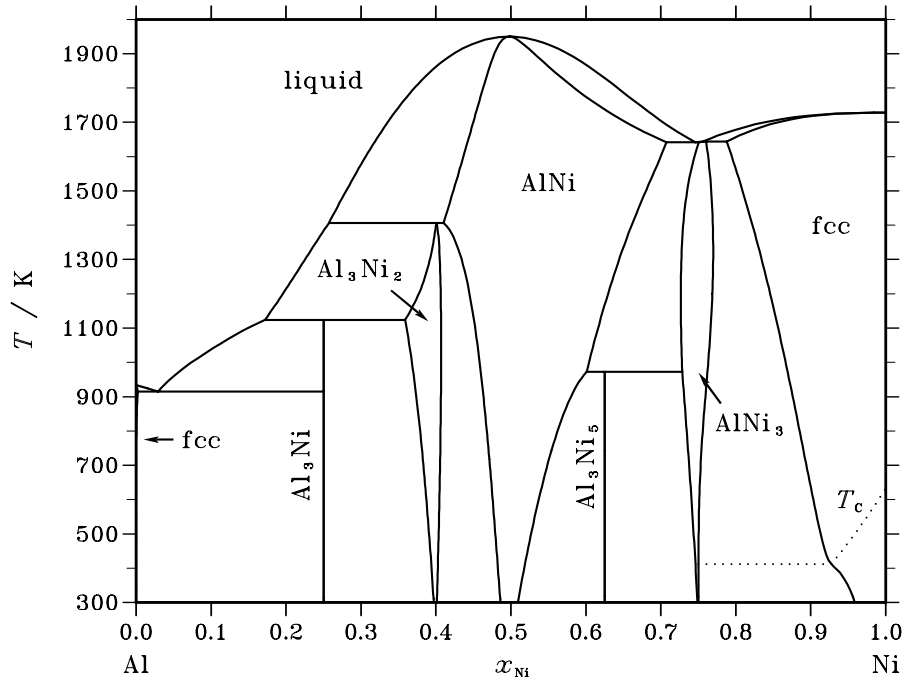

Fig. 1. Calculated phase diagram for the system Al-Ni.

This system is the foundation of all Ni-base superalloys with good high temperature properties and good corrosion resistance. The $L1_2$ ordered phase, $AlNi_3$, also known as γ', has unique mechanical properties with increasing strength at high temperature. It can also form a coherent precipitation for strengthening the alloys. The ordered $B2$ phase, AlNi is also an interesting candidate for shape memory alloys and for high temperature applications.
The Al-rich part of the system is of less practical interest. There are several assessments of this system, [97Ans] is preferred as it has been integrated into multicomponent databases and uses a consistent modelling of the ordered phases based on the Compound Energy Formalism. More theoretically based assessments using Cluster Variation Methods or Monte-Carlo techniques are available but these have not been extended to multicomponent alloys.

Table I. Phases, structures and models.

Phase	Struktur-bericht	Prototype	Pearson symbol	Space group	SGTE name	Model
liquid					LIQUID	$(Al,Ni)_1$
fcc	$A1$	Cu	$cF4$	$Fm\overline{3}m$	FCC_A1	$(Al,Ni)_1$
Al_3Ni	$D0_{11}$	Fe_3C	$oP16$	$Pnma$	D011_AL3NI1	Al_3Ni_1
Al_3Ni_2	$D5_{13}$	Al_3Ni_2	$hP5$	$P\overline{3}m1$	D513_AL3NI2	$Al_3(Al,Ni)_2(Ni,\Box)_1$
AlNi	$B2$	CsCl	$cP2$	$Pm3m$	BCC_B2	$(Al,Ni,\Box)_1(Al,Ni,\Box)_1$
Al_3Ni_5	$\cdots$	Ga_3Pt_5	$oC16$	$Cmmm$	AL3NI5	Al_3Ni_5
$AlNi_3$	$L1_2$	$AuCu_3$	$cP4$	$Pm\overline{3}m$	FCC_L12	$(Al,Ni)_3(Al,Ni)_1$

Table II. Invariant reactions.

Reaction	Type	T / K	Compositions / x_{Ni}			$\Delta_{\mathrm{r}}H$ / (J/mol)
liquid ⇌ AlNi	congruent	1950.0	0.498	0.498		−27660
fcc ⇌ liquid + $AlNi_3$	peritectic	1643.4	0.756	0.760	0.788	−16957
liquid ⇌ AlNi + $AlNi_3$	eutectic	1642.2	0.707	0.746	0.750	−19446
liquid + AlNi ⇌ Al_3Ni_2	peritectic	1406.5	0.257	0.410	0.401	−4833
liquid + Al_3Ni_2 ⇌ Al_3Ni	peritectic	1123.5	0.172	0.359	0.250	−16100
AlNi + $AlNi_3$ ⇌ Al_3Ni_5	peritectoid	972.5	0.625	0.728	0.601	−1902
liquid ⇌ fcc + Al_3Ni	eutectic	914.8	0.029	0.002	0.250	−11865

Table IIIa. Integral quantities for the liquid phase at 2000 K.

x_{Ni}	ΔG_{m} [J/mol]	ΔH_{m} [J/mol]	ΔS_{m} [J/(mol·K)]	$G^{\mathrm{E}}_{\mathrm{m}}$ [J/mol]	$S^{\mathrm{E}}_{\mathrm{m}}$ [J/(mol·K)]	ΔC_p [J/(mol·K)]
0.000	0	0	0.000	0	0.000	0.000
0.100	−15376	−15309	0.033	−9970	−2.670	0.000
0.200	−27028	−29745	−1.359	−18707	−5.519	0.000
0.300	−35573	−41680	−3.053	−25415	−8.133	0.000
0.400	−40826	−49416	−4.295	−29634	−9.891	0.000
0.500	−42646	−51777	−4.566	−31120	−10.329	0.000
0.600	−40972	−48455	−3.741	−29781	−9.337	0.000
0.700	−35817	−40086	−2.135	−25659	−7.214	0.000
0.800	−27281	−28091	−0.405	−18960	−4.566	0.000
0.900	−15539	−14245	0.647	−10133	−2.056	0.000
1.000	0	0	0.000	0	0.000	0.000

Reference states: Al(liquid), Ni(liquid)

Table IIIb. Partial quantities for Al in the liquid phase at 2000 K.

x_{Al}	ΔG_{Al} [J/mol]	ΔH_{Al} [J/mol]	ΔS_{Al} [J/(mol·K)]	$G^{\mathrm{E}}_{\mathrm{Al}}$ [J/mol]	$S^{\mathrm{E}}_{\mathrm{Al}}$ [J/(mol·K)]	a_{Al}	γ_{Al}
1.000	0	0	0.000	0	0.000	1.000	1.000
0.900	−2201	−210	0.996	−449	0.120	0.876	0.973
0.800	−6772	−2772	2.000	−3062	0.145	0.665	0.832
0.700	−14788	−11410	1.689	−8857	−1.276	0.411	0.587
0.600	−26613	−28698	−1.043	−18119	−5.290	0.202	0.336
0.500	−42257	−54324	−6.033	−30731	−11.797	0.079	0.158
0.400	−61514	−84616	−11.551	−46277	−19.170	0.025	0.062
0.300	−83913	−113349	−14.718	−63892	−24.729	0.006	0.021
0.200	−108634	−133824	−12.595	−81870	−25.977	0.001	0.007
0.100	−135324	−142213	−3.444	−97034	−22.589	0.000	0.003
0.000	$-\infty$	−142186	∞	−103853	−19.166	0.000	0.002

Reference state: Al(liquid)

Table IIIc. Partial quantities for Ni in the liquid phase at 2000 K.

x_{Ni}	ΔG_{Ni} [J/mol]	ΔH_{Ni} [J/mol]	ΔS_{Ni} [J/(mol·K)]	G^E_{Ni} [J/mol]	S^E_{Ni} [J/(mol·K)]	a_{Ni}	γ_{Ni}
0.000	$-\infty$	−153827	∞	−102074	−25.876	0.000	0.002
0.100	−133949	−151208	−8.630	−95659	−27.774	0.000	0.003
0.200	−108051	−137638	−14.794	−81287	−28.176	0.002	0.008
0.300	−84071	−112311	−14.120	−64050	−24.130	0.006	0.021
0.400	−62144	−80492	−9.174	−46907	−16.792	0.024	0.060
0.500	−43035	−49231	−3.098	−31509	−8.861	0.075	0.150
0.600	−27278	−24347	1.465	−18784	−2.782	0.194	0.323
0.700	−15204	−8688	3.258	−9273	0.293	0.401	0.573
0.800	−6943	−1658	2.642	−3232	0.787	0.659	0.823
0.900	−2229	−26	1.101	−477	0.225	0.875	0.972
1.000	0	0	0.000	0	0.000	1.000	1.000

Reference state: Ni(liquid)

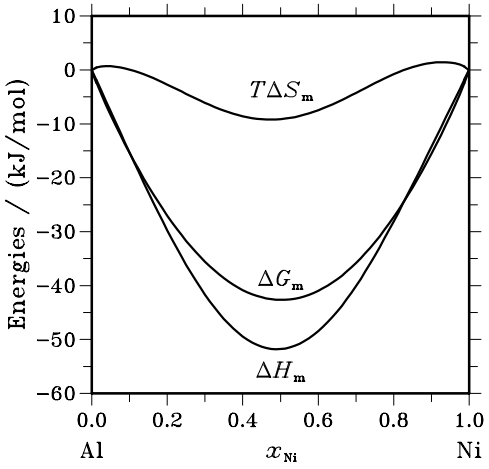

Fig. 2. Integral quantities of the liquid phase at T=2000 K.

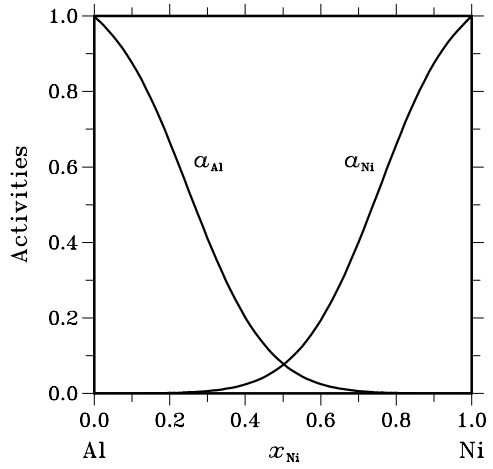

Fig. 3. Activities in the liquid phase at T=2000 K.

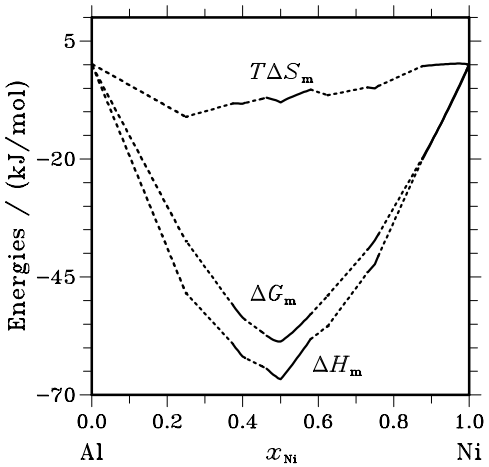

Fig. 4. Integral quantities of the stable phases at T=900 K.

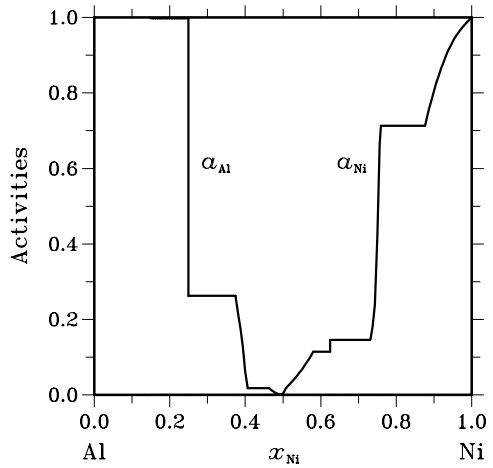

Fig. 5. Activities in the stable phases at T=900 K.

Table IVa. Integral quantities for the stable phases at 900 K.

Phase	x_{Ni}	ΔG_{m} [J/mol]	ΔH_{m} [J/mol]	ΔS_{m} [J/(mol·K)]	$G_{\mathrm{m}}^{\mathrm{E}}$ [J/mol]	$S_{\mathrm{m}}^{\mathrm{E}}$ [J/(mol·K)]	ΔC_p [J/(mol·K)]
fcc	0.000	0	0	0.000	0	0.000	0.000
	0.002	−292	−160	0.146	−190	0.034	−0.001
Al_3Ni	0.250	−37409	−48455	−12.274			−0.129
Al_3Ni_2	0.374	−50984	−59212	−9.142	−50366	−9.829	−0.113
	0.400	−53609	−61876	−9.186	−53476	−9.334	0.097
	0.407	−54067	−62172	−9.006	−53794	−9.309	−0.167
AlNi	0.463	−57428	−64431	−7.781	−55936	−9.439	−0.235
	0.500	−58679	−66692	−8.903	−58619	−8.970	0.094
	0.550	−55369	−61542	−6.858	−54150	−8.213	−0.254
	0.580	−52872	−58158	−5.872	−51224	−7.704	−0.281
Al_3Ni_5	0.625	−48955	−55436	−7.201			−0.323
$AlNi_3$	0.731	−39196	−43997	−5.334	−38529	−6.075	−0.303
	0.750	−37233	−42260	−5.586	−37132	−5.698	0.444
	0.759	−35976	−40492	−5.017	−35658	−5.371	−0.105
fcc	0.876	−19777	−20075	−0.331	−16971	−3.449	−0.443
	0.900	−16330	−16459	−0.143	−13897	−2.846	−0.443
	0.950	−8593	−8416	0.196	−7107	−1.455	−0.375
	1.000	0	0	0.000	0	0.000	0.000

Reference states: Al(fcc), Ni(fcc)

Table IVb. Partial quantities for Al in the stable phases at 900 K.

Phase	x_{Al}	ΔG_{Al} [J/mol]	ΔH_{Al} [J/mol]	ΔS_{Al} [J/(mol·K)]	G^{E}_{Al} [J/mol]	S^{E}_{Al} [J/(mol·K)]	a_{Al}	γ_{Al}
fcc	1.000	0	0	0.000	0	0.000	1.000	1.000
	0.998	−14	0	0.016	0	0.000	0.998	1.000
Al_3Ni	0.750	−14	201	0.239			0.998	
	0.750	−10004	−26738	−18.594			0.263	
Al_3Ni_2	0.626	−10004	−17855	−8.724	−3401	−16.060	0.263	0.635
	0.600	−20719	−31929	−12.456	−18535	−14.882	0.063	0.084
	0.593	−30009	−49269	−21.400	−41229	−8.932	0.018	0.004
AlNi	0.537	−30009	−27646	2.626	−17407	−11.377	0.018	0.098
	0.500	−74536	−92064	−19.476	−76334	−17.478	0.000	0.000
	0.450	−98361	−121570	−25.789	−106153	−17.131	0.000	0.000
	0.420	−103521	−125157	−24.039	−109047	−17.899	0.000	0.000
Al_3Ni_5	0.375	−103521	−93351	11.300			0.000	
	0.375	−106499	−122887	−18.209			0.000	
$AlNi_3$	0.269	−106499	−102835	4.072	−86034	−18.668	0.000	0.000
	0.250	−129762	−153175	−26.014	−128175	−27.777	0.000	0.000
	0.241	−141542	−187863	−51.467	−159338	−31.694	0.000	0.000
fcc	0.124	−141542	−147877	−7.039	−125926	−24.390	0.000	0.000
	0.100	−148728	−155215	−7.209	−131497	−26.354	0.000	0.000
	0.050	−162552	−166313	−4.179	−140135	−29.087	0.000	0.000
	0.000	$-\infty$	−168417	∞	−143031	−28.207	0.000	0.000

Reference state: Al(fcc)

Table IVc. Partial quantities for Ni in the stable phases at 900 K.

Phase	x_{Ni}	ΔG_{Ni} [J/mol]	ΔH_{Ni} [J/mol]	ΔS_{Ni} [J/(mol·K)]	$G^{\mathrm{E}}_{\mathrm{Ni}}$ [J/mol]	$S^{\mathrm{E}}_{\mathrm{Ni}}$ [J/(mol·K)]	a_{Ni}	γ_{Ni}
fcc	0.000	$-\infty$	−86162	∞	−102711	18.389	0.000	0.000
	0.002	−149593	−86200	70.437	−102529	18.144	0.000	0.000
Al_3Ni	0.250	−149593	−194423	−49.812			0.000	
	0.250	−119624	−113604	6.689			0.000	
Al_3Ni_2	0.374	−119624	−128484	−9.844	−129032	0.609	0.000	0.000
	0.400	−102945	−106797	−4.280	−105887	−1.012	0.000	0.000
	0.407	−89181	−81006	9.084	−72133	−9.858	0.000	0.000
AlNi	0.463	−89181	−107031	−19.834	−100557	−7.194	0.000	0.000
	0.500	−42823	−41320	1.670	−40904	−0.462	0.003	0.004
	0.550	−20195	−12428	8.630	−11602	−0.917	0.067	0.212
	0.580	−16215	−9667	7.276	−9374	−0.325	0.115	0.286
Al_3Ni_5	0.625	−16215	−32686	−18.301			0.115	
	0.625	−14429	−14965	−0.596			0.145	
$AlNi_3$	0.731	−14429	−22344	−8.795	−21047	−1.441	0.145	0.060
	0.750	−6390	−5289	1.224	−6784	1.662	0.426	0.404
	0.759	−2527	6203	9.701	3531	2.969	0.713	1.603
fcc	0.876	−2527	−1970	0.619	−1536	−0.483	0.713	0.814
	0.900	−1619	−1041	0.642	−831	−0.234	0.805	0.895
	0.950	−490	−106	0.426	−106	0.000	0.937	0.986
	1.000	0	0	0.000	0	0.000	1.000	1.000

Reference state: Ni(fcc)

Table V. Standard reaction quantities at 298.15 K for the compounds per mole of atoms.

Compound	x_{Ni}	$\Delta_{\mathrm{f}}G^{\circ}$ / (J/mol)	$\Delta_{\mathrm{f}}H^{\circ}$ / (J/mol)	$\Delta_{\mathrm{f}}S^{\circ}$ / (J/(mol·K))	$\Delta_{\mathrm{f}}C^{\circ}_{P}$ / (J/(mol·K))
Al_3Ni_1	0.250	−44598	−48024	−11.492	−0.191
Al_3Ni_2	0.400	−58870	−61274	−8.063	−0.301
Al_1Ni_1	0.500	−63672	−65880	−7.405	−0.382
Al_3Ni_5	0.625	−52794	−54358	−5.248	−0.478
Al_1Ni_3	0.750	−40064	−41069	−3.372	−0.562

References

[97Ans] I. Ansara, N. Dupin, H.L. Lukas, B. Sundman: J. Alloys Comp. **247** (1997) 20–30.

Al – O (Aluminium – Oxygen)

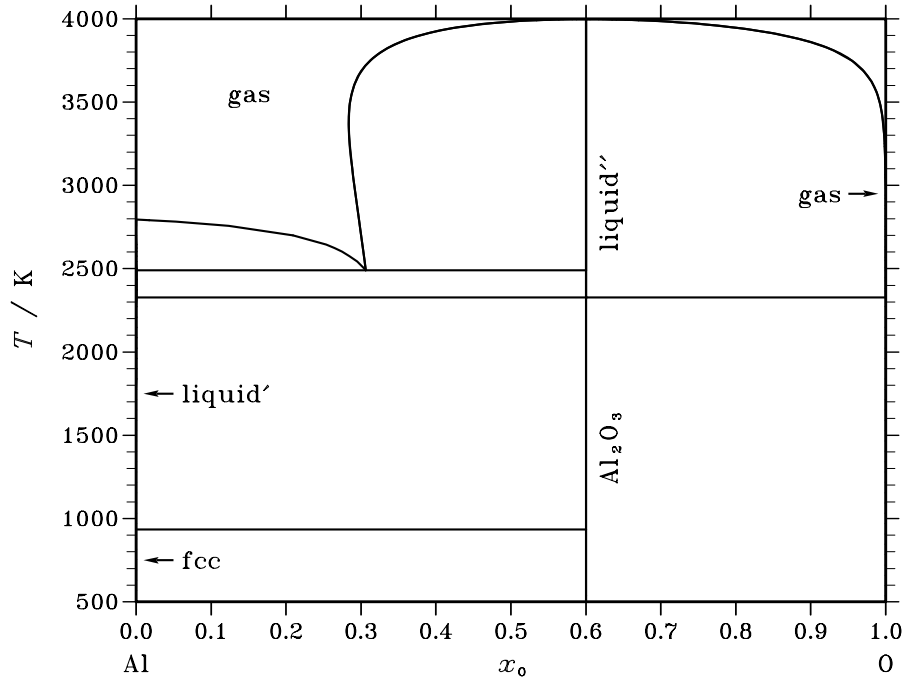

Fig. 1. Calculated phase diagram for the system Al-O.

The Al-O system is part of many industrially important systems, ranging from the aluminium production to ceramics. The compound Al_2O_3 is a major constituent of many slag systems and ceramic systems. A critical review of experimental studies in the Al-O system is given by [85Wri]. The thermodynamic description of this system is presented by [93Hal] based on a previous assessment of [92Tay]. The only stable compound in the system is corundum, α-Al_2O_3. It is essentially a stoichiometric compound with a congruent melting point of 2327 K [85Wri]. The solubility of oxygen in the metallic melt and the solubility of aluminium in liquid Al_2O_3 are very low and their measurement is difficult [85Wri]. Liquid Al exists only at very low oxygen partial pressures and the experimental data on oxygen solubilities in liquid Al are contradictory [85Wri]. The oxygen solubility in liquid Al presented by [92Tay] is derived from correlations between the enthalpy and entropy of solution of oxygen in other liquid metals. The data for the liquid phase given by [92Tay] have been re-evaluated by [93Hal] assuming that oxygen dissolves as $AlO_{3/2}$ in the melt yielding the same oxygen solubility as in [92Tay]. The solubility of Al in Al_2O_3 is much lower than given in [92Tay], however, due to a lack of experimental data no optimisation has been done. According to both datasets [92Tay, 93Hal] oxide and metallic liquids react forming a gas phase at 2490 K. The boiling points of Al and Al_2O_3 are calculated to be 2791 and 4000 K, respectively.

Metallic and oxide liquid are described as a single phase exhibiting a very wide miscibility gap. This phase is described by a two-sublattice ionic model with Al^{3+}-species on the cation sublattice and O^{2-}, vacancies and $AlO_{3/2}$ on the anion sublattice. The gas phase is assumed to consist of the species Al, AlO, AlO_2, Al_2O, Al_2O_2, O, O_2 and O_3. Al_2O_3 is treated as a stoichiometric phase.

Table I. Phases, structures and models.

Phase	Struktur-bericht	Prototype	Pearson symbol	Space group	SGTE name	Model
liquid					IONIC_LIQ	$Al_p^{3+}(O^{2-},AlO_{3/2},\Box)_3$
fcc	$A1$	Cu	$cF4$	$Fm\overline{3}m$	FCC_A1	$(Al,O)_1$
Al_2O_3	$D5_1$	αAl_2O_3	$hR10$	$R\overline{3}c$	CORUNDUM_D51	$Al_2^{3+}O_3^{2-}$

Table II. Invariant reactions.

Reaction	Type	T / K	Compositions / x_O			$\Delta_r H$ / (J/mol)
gas $\rightleftharpoons$ liquid″	congruent	4000.0	0.600	0.600		−360973
gas $\rightleftharpoons$ liquid′ + liquid″	gas-eutectic	2490.2	0.306	0.001	0.600	−123298
liquid″ $\rightleftharpoons$ Al_2O_3	congruent	2327.0	0.600	0.600		−22217
liquid′ $\rightleftharpoons$ fcc + Al_2O_3	eutectoid	933.5	0.000	0.000	0.600	−10711

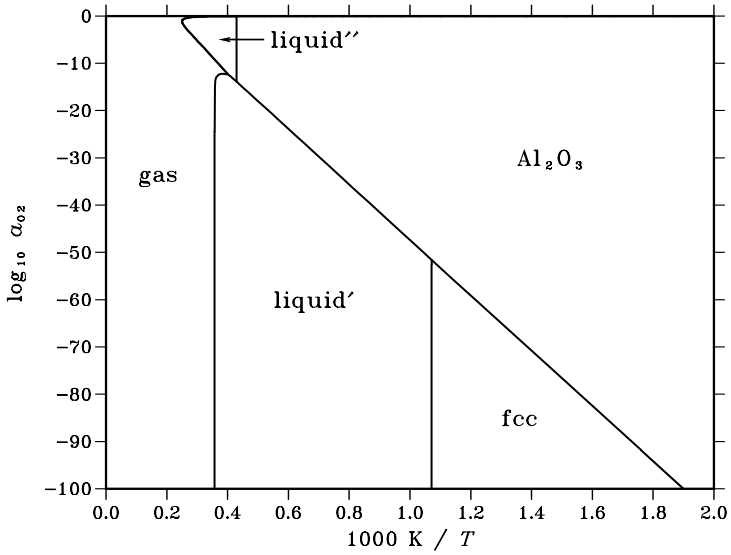

Fig. 2. Calculated temperature-activity phase diagram. Reference state: O(gas, 0.1 MPa).

Table III. Standard reaction quantities at 298.15 K for the compounds per mole of atoms.

Compound	x_O	$\Delta_f G^\circ$ / (J/mol)	$\Delta_f H^\circ$ / (J/mol)	$\Delta_f S^\circ$ / (J/(mol·K))	$\Delta_f C_P^\circ$ / (J/(mol·K))
Al_2O_3	0.600	−316461	−335138	−62.643	−2.727

References

[85Wri] H.A. Wriedt: Bull. Alloy Phase Diagrams **6** (1985) 548–553.
[92Tay] J.R. Taylor, A.T. Dinsdale, M. Hillert, M. Selleby: Calphad **16** (1992) 173–179.
[93Hal] B. Hallstedt: J. Phase Equilibria **14** (1993) 662–675.

Al – P (Aluminium – Phosphorus)

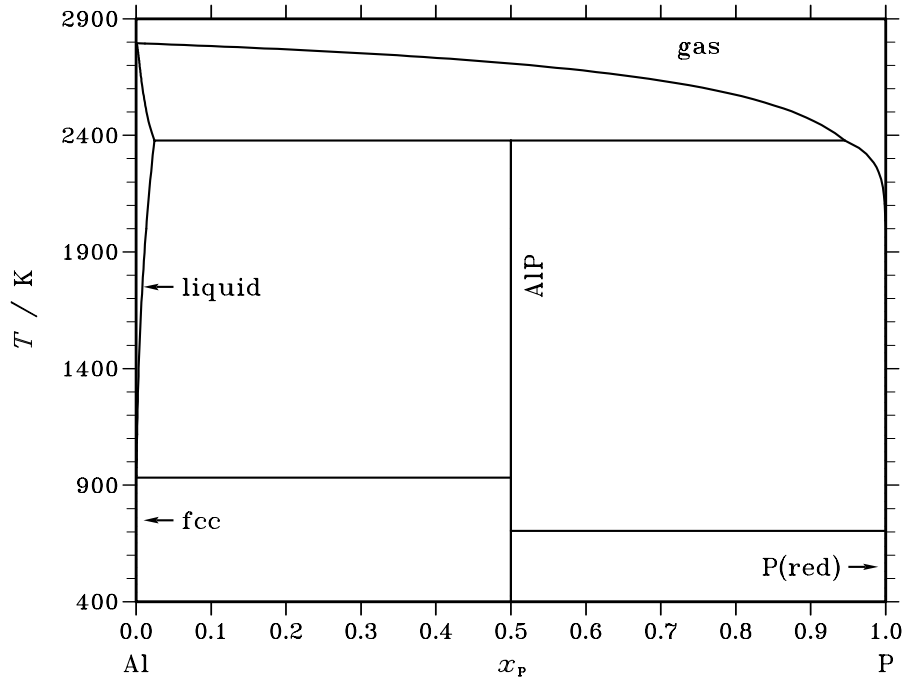

Fig. 1. Calculated phase diagram for the system Al-P.

The Al-P system belongs to the group of III-V semiconductor compounds which are important materials for opto-electronic devices. The Al-P system is characterised by a single very highly melting compound AlP which is isoelectronic to diamond-type Si.
A review of experimental data was presented in [85McA]. There are several thermodynamic assessments [81Kau, 94Ans, 01Luk]. The selected assessment for the SGTE database [01Luk] is composed of the descriptions for the AlP compound and the gas species in the SGTE substance database [99SGTE] and a single linearly temperature dependent Redlich-Kister excess term for the liquid to reproduce the measured solubilities [69Bee] of AlP in liquid Al. For the pure elements the SGTE data [91Din] are used. An earlier assessment [94Ans] includes an additional experimental value, the melting temperature of AlP [74Pev], but contains a description of AlP with physically impossible negative heat capacity. The selected description of the liquid is valid only for high Al concentrations. To generate a description covering both, this dilute range and molten AlP, needs more experimental information. The model for the gas phase contains the species Al, AlP, AlP_2, Al_2, P, P_2, P_3, and P_4. The liquid phase is described by the substitutional model. AlP and fcc-Al are treated as stoichiometric phases.

Table I. Phases, structures and models.

Phase	Struktur-bericht	Prototype	Pearson symbol	Space group	SGTE name	Model
liquid					LIQUID	$(Al,P)_1$
fcc	$A1$	Cu	$cF4$	$Fm\overline{3}m$	FCC_A1	Al_1
AlP	$B3$	ZnS	$cF8$	$F\overline{4}3m$	B3_ZINCBLENDE	Al_1P_1
P(red)	···	···	···	···	RED_P	P_1
αP	···	αP	$c*^*$	···	WHITE_P	P_1

Table II. Invariant reactions.

Reaction	Type	T / K	Compositions / x_P			$\Delta_r H$ / (J/mol)
liquid + gas ⇌ AlP	gas-peritectic	2377.5	0.024	0.945	0.500	−130556
liquid ⇌ fcc + AlP	eutectic	933.2	0.000	0.000	0.500	−10723
AlP + gas ⇌ P(red)	degenerate	704.3	0.500	1.000	1.000	−29925

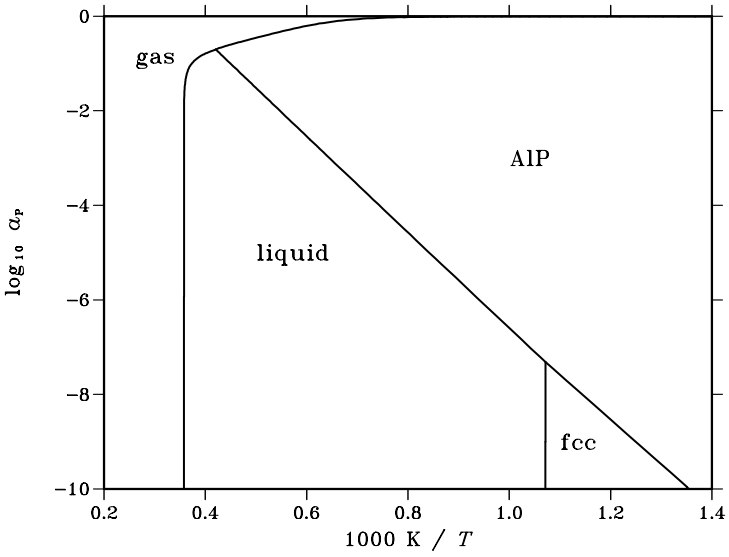

Fig. 2. Calculated temperature-activity phase diagram. Reference state: P(gas, 0.1 MPa).

Table III. Standard reaction quantities at 298.15 K for the compounds per mole of atoms.

Compound	x_P	$\Delta_f G^\circ$ / (J/mol)	$\Delta_f H^\circ$ / (J/mol)	$\Delta_f S^\circ$ / (J/(mol·K))	$\Delta_f C_P^\circ$ / (J/(mol·K))
Al_1P_1	0.500	−78919	−82215	−11.055	−3.040

References

[69Bee] S.Z. Beer: J. Electrochem. Soc. **116** (1969) 263–265.
[74Pev] S.O. Peviak, A.V. Sandulova: Izv. Akad. Nauk SSSR, Neorg. Mater. **10** (1974) 146–147.
[81Kau] L. Kaufman, J. Nell, K. Taylor, F. Hayes: Calphad **5** (1981) 185–215.
[85McA] A.J. McAlister: Bull. Alloy Phase Diagrams **6** (1985) 222–224.
[94Ans] I. Ansara, C. Chatillon, H.L. Lukas, T. Nishizawa, H. Ohtani, K. Ishida, M. Hillert, B. Sundman, B.B. Argent, A. Watson, T.G. Chart, T. Anderson: Calphad **18** (1994) 177–222.
[99SGTE] Scientific Group Thermodata Europe: "Thermodynamic Properties of Inorganic Materials compiled by SGTE", Landolt-Börnstein New Series IV/19A1, Springer Verlag, Berlin Heidelberg, 1999.
[01Luk] H.L. Lukas: unpublished optimization 2001.

Al – Pb (Aluminium – Lead)

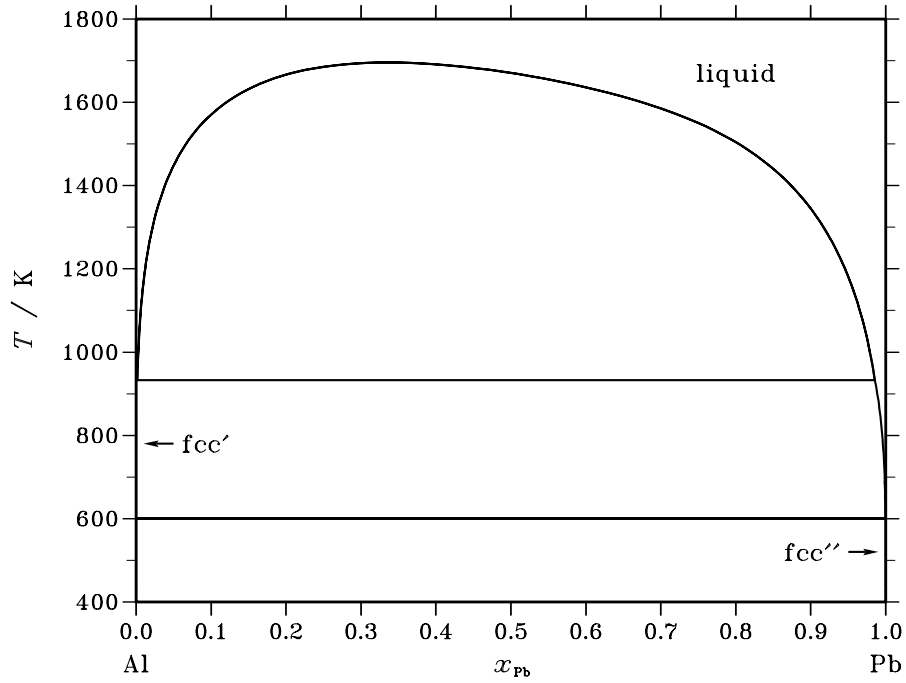

Fig. 1. Calculated phase diagram for the system Al-Pb.

The Al-Pb system is a very simple system showing a wide range of immiscibility in the liquid phase up to 1695 K where the miscibility gap closes at a composition approximately 34 at.% Pb. It has potential importance as a key subsystem for bearing alloys and automotive applications. The selected data for the Al-Pb system are from the critical assessment of Yu et al. [96Yu]. The system had also been assessed by Ansara [86Ans]. The assessment of Yu et al. is preferred being based on more recent experimental data. Although Al and Pb crystallise in the same structure terminal solid solutions are very limited. The miscibility gap has been studied extensively between the monotectic temperature of 932 K and the upper consolute temperature, and the solubility of Al in the liquid at temperatures below the monotectic and the eutectic at about 600 K. The limited experimental thermodynamic studies have concerned the enthalpies of mixing and the partial Gibbs energies of both Al and Pb. The assessed data are in very good agreement with all the experimental data for the system.

Table I. Phases, structures and models.

Phase	Struktur-bericht	Prototype	Pearson symbol	Space group	SGTE name	Model
liquid					LIQUID	$(Al,Pb)_1$
fcc	$A1$	Cu	$cF4$	$Fm\overline{3}m$	FCC_A1	$(Al,Pb)_1$

Table II. Invariant reactions.

Reaction	Type	T / K	Compositions / x_{Pb}			$\Delta_r H$ / (J/mol)
liquid $\rightleftharpoons$ liquid′ + liquid″	critical	1695.2	0.336	0.336	0.336	0
liquid′ $\rightleftharpoons$ fcc′ + liquid″	monotectic	932.4	0.002	0.000	0.986	−10800
liquid″ $\rightleftharpoons$ fcc′ + fcc″	eutectic	600.4	1.000	0.000	1.000	−4791

Table IIIa. Integral quantities for the liquid phase at 1700 K.

x_{Pb}	ΔG_{m} [J/mol]	ΔH_{m} [J/mol]	ΔS_{m} [J/(mol·K)]	$G_{\mathrm{m}}^{\mathrm{E}}$ [J/mol]	$S_{\mathrm{m}}^{\mathrm{E}}$ [J/(mol·K)]	ΔC_p [J/(mol·K)]
0.000	0	0	0.000	0	0.000	0.000
0.100	−1495	5625	4.188	3100	1.485	0.000
0.200	−1819	9326	6.556	5254	2.395	0.000
0.300	−2017	11436	7.913	6617	2.834	0.000
0.400	−2200	12241	8.495	7313	2.899	0.000
0.500	−2370	11983	8.443	7427	2.680	0.000
0.600	−2497	10858	7.856	7015	2.260	0.000
0.700	−2537	9015	6.796	6097	1.717	0.000
0.800	−2414	6559	5.279	4659	1.118	0.000
0.900	−1941	3550	3.230	2653	0.527	0.000
1.000	0	0	0.000	0	0.000	0.000

Reference states: Al(liquid), Pb(liquid)

Table IIIb. Partial quantities for Al in the liquid phase at 1700 K.

x_{Al}	ΔG_{Al} [J/mol]	ΔH_{Al} [J/mol]	ΔS_{Al} [J/(mol·K)]	$G_{\mathrm{Al}}^{\mathrm{E}}$ [J/mol]	$S_{\mathrm{Al}}^{\mathrm{E}}$ [J/(mol·K)]	a_{Al}	γ_{Al}
1.000	0	0	0.000	0	0.000	1.000	1.000
0.900	−988	1021	1.182	501	0.306	0.933	1.036
0.800	−1372	3618	2.935	1782	1.080	0.907	1.134
0.700	−1461	7194	5.091	3581	2.126	0.902	1.288
0.600	−1480	11291	7.513	5740	3.265	0.901	1.501
0.500	−1596	15585	10.106	8202	4.343	0.893	1.786
0.400	−1942	19890	12.842	11010	5.224	0.872	2.179
0.300	−2708	24156	15.802	14310	5.792	0.826	2.752
0.200	−4401	28469	19.336	18348	5.954	0.732	3.662
0.100	−9075	33054	24.781	23471	5.637	0.526	5.262
0.000	$-\infty$	38269	∞	30130	4.787	0.000	8.429

Reference state: Al(liquid)

Table IIIc. Partial quantities for Pb in the liquid phase at 1700 K.

x_{Pb}	ΔG_{Pb} [J/mol]	ΔH_{Pb} [J/mol]	ΔS_{Pb} [J/(mol·K)]	$G_{\mathrm{Pb}}^{\mathrm{E}}$ [J/mol]	$S_{\mathrm{Pb}}^{\mathrm{E}}$ [J/(mol·K)]	a_{Pb}	γ_{Pb}
0.000	$-\infty$	67083	∞	36325	18.093	0.000	13.065
0.100	−6064	47057	31.248	26482	12.103	0.651	6.511
0.200	−3608	32157	21.039	19141	7.657	0.775	3.873
0.300	−3315	21332	14.498	13703	4.488	0.791	2.636
0.400	−3280	13666	9.968	9672	2.350	0.793	1.982
0.500	−3144	8382	6.780	6653	1.017	0.801	1.601
0.600	−2868	4837	4.532	4352	0.285	0.816	1.361
0.700	−2464	2526	2.936	2577	−0.030	0.840	1.200
0.800	−1917	1082	1.764	1237	−0.091	0.873	1.091
0.900	−1149	272	0.836	340	−0.040	0.922	1.024
1.000	0	0	0.000	0	0.000	1.000	1.000

Reference state: Pb(liquid)

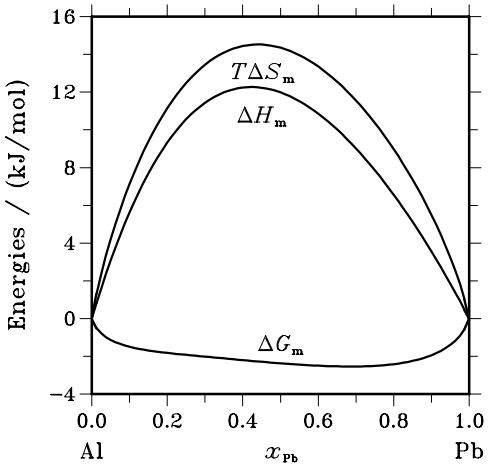

Fig. 2. Integral quantities of the liquid phase at T=1700 K.

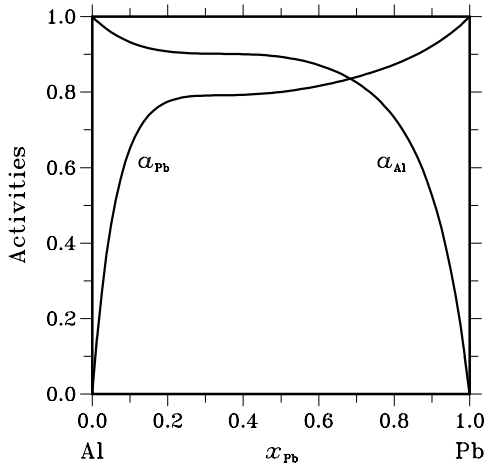

Fig. 3. Activities in the liquid phase at T=1700 K.

References

[84McA] A.J. McAlister: Bull. Alloy Phase Diagrams **5** (1984) 69–73.
[96Yu] S.K. Yu, F. Sommer, B. Predel: Z. Metallkd. **87** (1996) 574–580.

Al – Sb (Aluminium – Antimony)

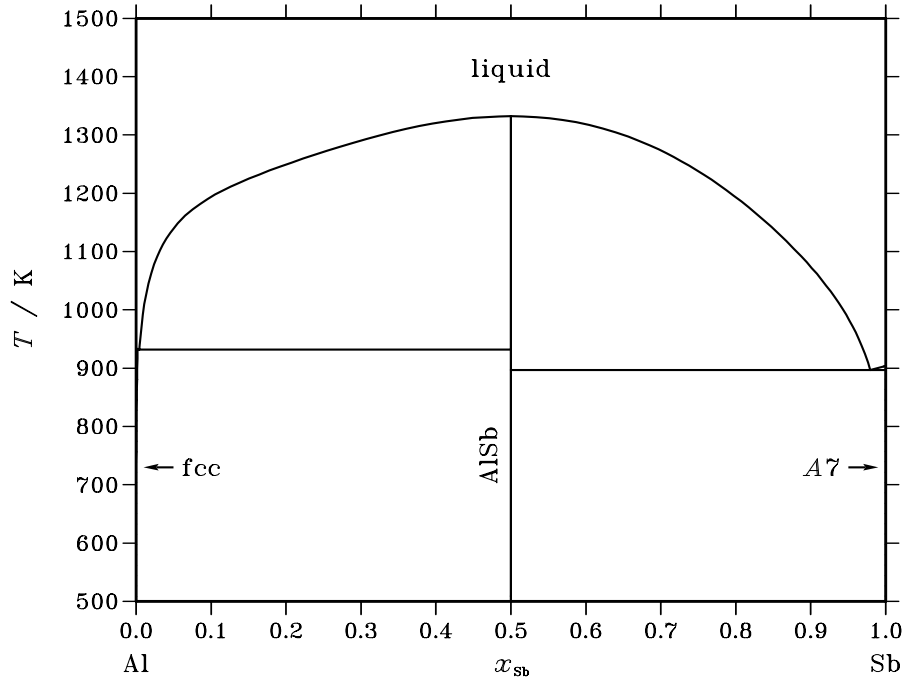

Fig. 1. Calculated phase diagram for the system Al-Sb (constrained system).

The ability of group III-V compound semiconductors to form miscible substitutional solutions with each other results in materials with a wide range of electrical and optical properties.
The Al-Sb system is a simple system with one intermediate phase, AlSb, which is isotypic with ZnS (sphalerite). None of the solid phases reveals significant homogeneity ranges. Several thermodynamic assessments of this system are published in the literature. Since the liquid phase in this system reveals an ordering tendency the associate model was used for its description in some of these assessments. The recommended assessment of [90Cou] used the associate as well as the Redlich-Kister model for the description of the liquid phase. However, for the construction of multicomponent databases the more general character of the Redlich-Kister model description is preferable. The assessment of [90Cou] is based on liquidus temperature, enthalpy of mixing of the liquid, enthalpy content of AlSb and partial Gibbs energy data.

Table I. Phases, structures and models.

Phase	Struktur-bericht	Prototype	Pearson symbol	Space group	SGTE name	Model
liquid					LIQUID	$(Al,Sb)_1$
fcc	$A1$	Cu	$cF4$	$Fm\overline{3}m$	FCC_A1	Al_1
AlSb	$B3$	ZnS	$cF8$	$F\overline{4}3m$	B3_ZINCBLENDE	Al_1Sb_1
$A7$	$A7$	αAs	$hR2$	$R\overline{3}m$	RHOMBOHEDRAL_A7	Sb_1

Table II. Invariant reactions.

Reaction	Type	T / K	Compositions / x_{Sb}			$\Delta_r H$ / (J/mol)
liquid $\rightleftharpoons$ AlSb	congruent	1332.1	0.500	0.500		−40419
liquid $\rightleftharpoons$ fcc + AlSb	eutectic	932.1	0.004	0.002	0.500	−10842
liquid $\rightleftharpoons$ AlSb + $A7$	eutectic	896.9	0.979	0.500	1.000	−20526

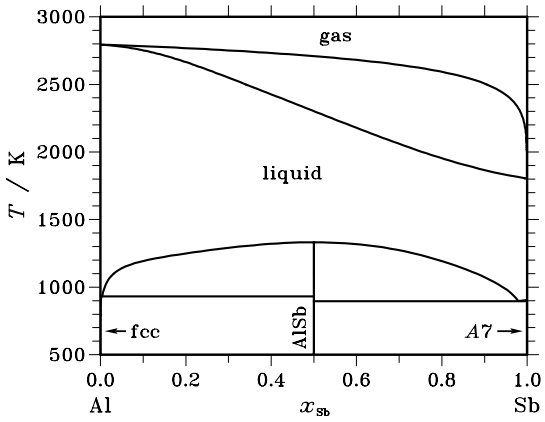

Fig. 2. Calculated phase diagram at 0.1 MPa.

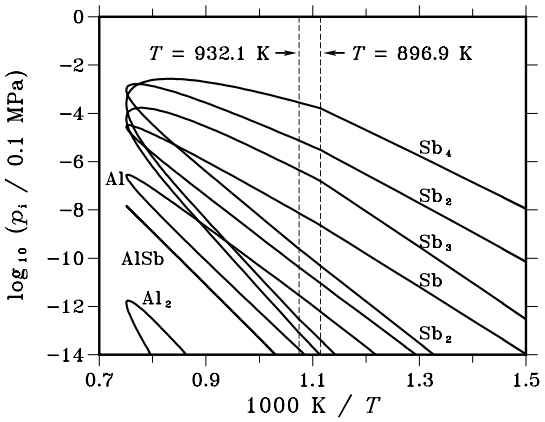

Fig. 3. Calculated partial pressures of gaseous species in the phase equilibria of the constrained system.

Table IIIa. Integral quantities for the liquid phase at 1400 K.

x_{Sb}	ΔG_m [J/mol]	ΔH_m [J/mol]	ΔS_m [J/(mol·K)]	G_m^E [J/mol]	S_m^E [J/(mol·K)]	ΔC_p [J/(mol·K)]
0.000	0	0	0.000	0	0.000	0.000
0.100	−4043	485	3.234	−259	0.531	2.041
0.200	−6723	−89	4.739	−898	0.578	3.628
0.300	−8802	−1077	5.518	−1691	0.439	4.762
0.400	−10279	−1997	5.915	−2445	0.319	5.443
0.500	−11072	−2537	6.097	−3004	0.334	5.669
0.600	−11084	−2543	6.101	−3250	0.505	5.443
0.700	−10212	−2032	5.843	−3101	0.764	4.762
0.800	−8335	−1181	5.110	−2510	0.949	3.628
0.900	−5251	−334	3.512	−1467	0.809	2.041
1.000	0	0	0.000	0	0.000	0.000

Reference states: Al(liquid), Sb(liquid)

Table IIIb. Partial quantities for Al in the liquid phase at 1400 K.

x_{Al}	ΔG_{Al} [J/mol]	ΔH_{Al} [J/mol]	ΔS_{Al} [J/(mol·K)]	G_{Al}^E [J/mol]	S_{Al}^E [J/(mol·K)]	a_{Al}	γ_{Al}
1.000	0	0	0.000	0	0.000	1.000	1.000
0.900	−995	650	1.175	232	0.299	0.918	1.020
0.800	−1994	1659	2.609	604	0.754	0.843	1.053
0.700	−3437	1985	3.872	715	0.907	0.744	1.063
0.600	−5673	1078	4.822	273	0.575	0.614	1.024
0.500	−8974	−1115	5.614	−906	−0.149	0.463	0.925
0.400	−13561	−4154	6.719	−2895	−0.899	0.312	0.780
0.300	−19674	−7105	8.978	−5660	−1.032	0.184	0.615
0.200	−27790	−8539	13.750	−9056	0.369	0.092	0.459
0.100	−39632	−6534	23.641	−12829	4.496	0.033	0.332
0.000	$-\infty$	1326	∞	−16617	12.816	0.000	0.240

Reference state: Al(liquid)

Table IIIc. Partial quantities for Sb in the liquid phase at 1400 K.

x_{Sb}	ΔG_{Sb} [J/mol]	ΔH_{Sb} [J/mol]	ΔS_{Sb} [J/(mol·K)]	$G^{\mathrm{E}}_{\mathrm{Sb}}$ [J/mol]	$S^{\mathrm{E}}_{\mathrm{Sb}}$ [J/(mol·K)]	a_{Sb}	γ_{Sb}
0.000	$-\infty$	12698	∞	168	8.950	0.000	1.015
0.100	−31474	−1008	21.762	−4671	2.617	0.067	0.669
0.200	−25641	−7084	13.256	−6907	−0.126	0.110	0.552
0.300	−21319	−8219	9.357	−7305	−0.653	0.160	0.534
0.400	−17187	−6610	7.554	−6521	−0.064	0.228	0.571
0.500	−13171	−3958	6.580	−5102	0.817	0.323	0.645
0.600	−9433	−1469	5.688	−3487	1.441	0.445	0.741
0.700	−6156	142	4.499	−2004	1.533	0.589	0.842
0.800	−3471	659	2.950	−873	1.094	0.742	0.928
0.900	−1431	355	1.276	−205	0.400	0.884	0.983
1.000	0	0	0.000	0	0.000	1.000	1.000

Reference state: Sb(liquid)

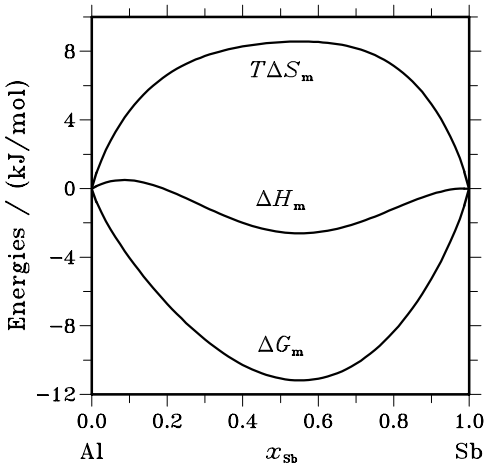

Fig. 4. Integral quantities of the liquid phase at T=1400 K.

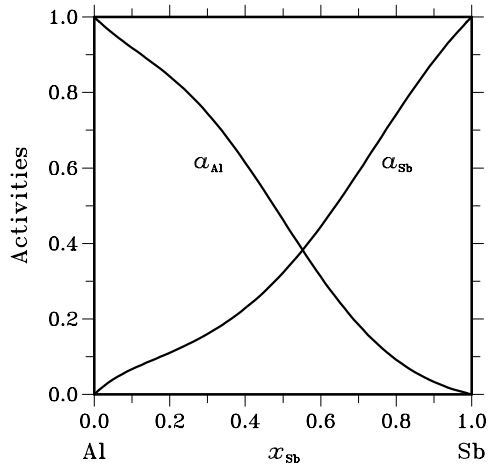

Fig. 5. Activities in the liquid phase at T=1400 K.

Table IV. Standard reaction quantities at 298.15 K for the compounds per mole of atoms.

Compound	x_{Sb}	$\Delta_{\mathrm{f}}G^{\circ}$ / (J/mol)	$\Delta_{\mathrm{f}}H^{\circ}$ / (J/mol)	$\Delta_{\mathrm{f}}S^{\circ}$ / (J/(mol·K))	$\Delta_{\mathrm{f}}C^{\circ}_{P}$ / (J/(mol·K))
$\mathrm{Al_1Sb_1}$	0.500	−23409	−24477	−3.582	−0.770

References

[90Cou] C.A. Coughanowr, U.R. Kattner, T.J. Anderson: Calphad **14** (1990) 193–202.

Al – Si (Aluminium – Silicon)

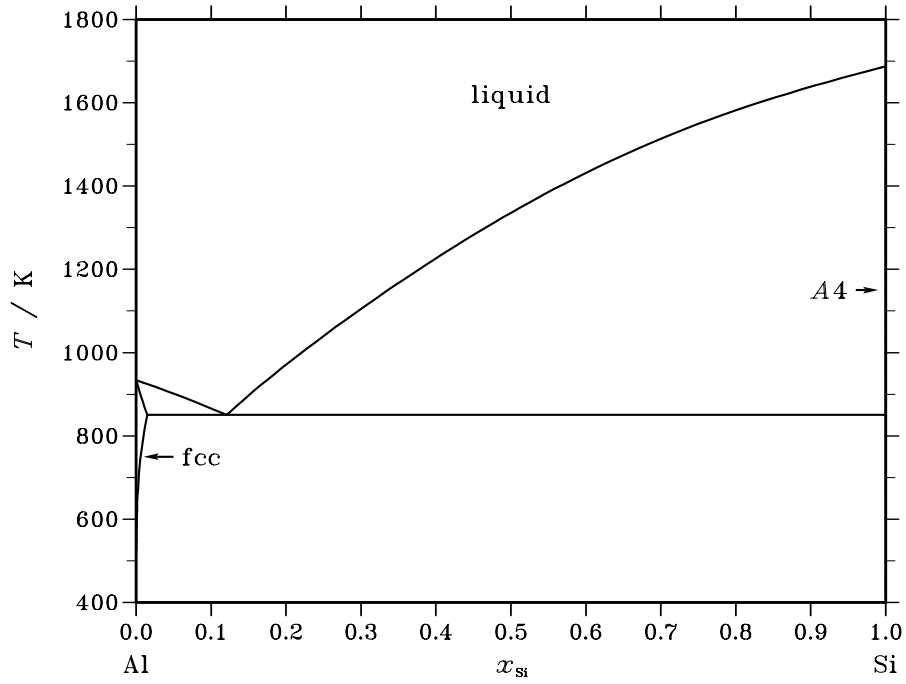

Fig. 1. Calculated phase diagram for the system Al-Si.

Al-Si alloys are the basis of technologically important aluminium castings. Small additions of Na and Mg vastly improve the properties of binary alloys. The thermodynamic parameters of the Al-Si system have been optimised in several works [80Doe, 86Mey, 92Cha, 97Feu]. The new dilatometric determination of the solvus temperature for alloys containing 0.84 mass-% Si by [97Feu] is taken into account in addition to the experimental data used by previous assessments. The assessment of [97Feu] is recommended here because more experimental data are taken into account, but the difference between calculations based on data of [97Feu] and others is quite small.

The phase diagram of the Al-Si systems is a eutectic phase diagram with fcc solid solution. The experimental phase equilibrium data and thermodynamic measurements mentioned below are used in the optimisation. Partial Gibbs energy values of the melt are derived from EMF data and vapour pressure measurements. The calorimetric data for the Al-Si liquid are the enthalpy content, the heat capacity and the enthalpy of mixing. The maximal solid solubility of silicon in aluminium is determined to be 1.5 at.% at 850 K. The solubility of aluminium in silicon is as low as 0.016 at.%. The liquid and the fcc phases are described by a substitutional model and solid Si is treated as a stoichiometric phase.

Table I. Phases, structures and models.

Phase	Struktur-bericht	Prototype	Pearson symbol	Space group	SGTE name	Model
liquid					LIQUID	$(Al,Si)_1$
fcc	$A1$	Cu	$cF4$	$Fm\overline{3}m$	FCC_A1	$(Al,Si)_1$
$A4$	$A4$	C(diamond)	$cF8$	$Fd\overline{3}m$	DIAMOND_A4	Si_1

Table II. Invariant reactions.

Reaction	Type	T / K	Compositions / x_{Si}			$\Delta_r H$ / (J/mol)
liquid $\rightleftharpoons$ fcc + $A4$	eutectic	850.1	0.121	0.015	1.000	−13675

Table IIIa. Integral quantities for the liquid phase at 1700 K.

x_{Si}	ΔG_m [J/mol]	ΔH_m [J/mol]	ΔS_m [J/(mol·K)]	G_m^E [J/mol]	S_m^E [J/(mol·K)]	ΔC_p [J/(mol·K)]
0.000	0	0	0.000	0	0.000	0.000
0.100	−5762	−1144	2.716	−1167	0.013	0.000
0.200	−9210	−2023	4.227	−2137	0.067	0.000
0.300	−11483	−2602	5.224	−2848	0.145	0.000
0.400	−12775	−2869	5.827	−3262	0.231	0.000
0.500	−13157	−2835	6.072	−3359	0.308	0.000
0.600	−12658	−2530	5.957	−3145	0.361	0.000
0.700	−11278	−2009	5.452	−2643	0.373	0.000
0.800	−8976	−1345	4.489	−1903	0.328	0.000
0.900	−5586	−636	2.912	−991	0.209	0.000
1.000	0	0	0.000	0	0.000	0.000

Reference states: Al(liquid), Si(liquid)

Table IIIb. Partial quantities for Al in the liquid phase at 1700 K.

x_{Al}	ΔG_{Al} [J/mol]	ΔH_{Al} [J/mol]	ΔS_{Al} [J/(mol·K)]	G_{Al}^E [J/mol]	S_{Al}^E [J/(mol·K)]	a_{Al}	γ_{Al}
1.000	0	0	0.000	0	0.000	1.000	1.000
0.900	−1576	−125	0.853	−86	−0.023	0.895	0.994
0.800	−3592	−558	1.785	−438	−0.070	0.776	0.969
0.700	−6187	−1332	2.856	−1146	−0.109	0.645	0.922
0.600	−9455	−2417	4.140	−2235	−0.107	0.512	0.854
0.500	−13462	−3718	5.732	−3664	−0.031	0.386	0.772
0.400	−18281	−5073	7.769	−5329	0.150	0.274	0.686
0.300	−24077	−6258	10.482	−7059	0.471	0.182	0.607
0.200	−31367	−6980	14.345	−8618	0.964	0.109	0.544
0.100	−42251	−6882	20.805	−9705	1.660	0.050	0.503
0.000	−∞	−5544	∞	−9953	2.594	0.000	0.495

Reference state: Al(liquid)

Table IIIc. Partial quantities for Si in the liquid phase at 1700 K.

x_{Si}	ΔG_{Si} [J/mol]	ΔH_{Si} [J/mol]	ΔS_{Si} [J/(mol·K)]	G^E_{Si} [J/mol]	S^E_{Si} [J/(mol·K)]	a_{Si}	γ_{Si}
0.000	$-\infty$	−12606	∞	−12392	−0.126	0.000	0.416
0.100	−43436	−10314	19.483	−10890	0.339	0.046	0.463
0.200	−31679	−7884	13.997	−8930	0.616	0.106	0.532
0.300	−23838	−5566	10.748	−6820	0.738	0.185	0.617
0.400	−17754	−3548	8.356	−4803	0.738	0.285	0.712
0.500	−12852	−1952	6.412	−3055	0.648	0.403	0.806
0.600	−8909	−835	4.749	−1689	0.502	0.532	0.887
0.700	−5792	−188	3.297	−751	0.331	0.664	0.948
0.800	−3378	64	2.024	−224	0.169	0.787	0.984
0.900	−1512	58	0.924	−23	0.048	0.899	0.998
1.000	0	0	0.000	0	0.000	1.000	1.000

Reference state: Si(liquid)

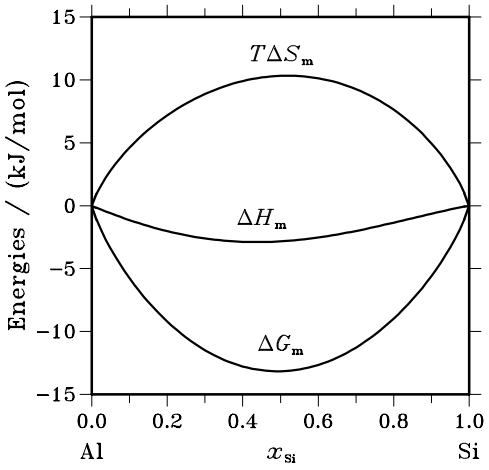

Fig. 2. Integral quantities of the liquid phase at T=1700 K.

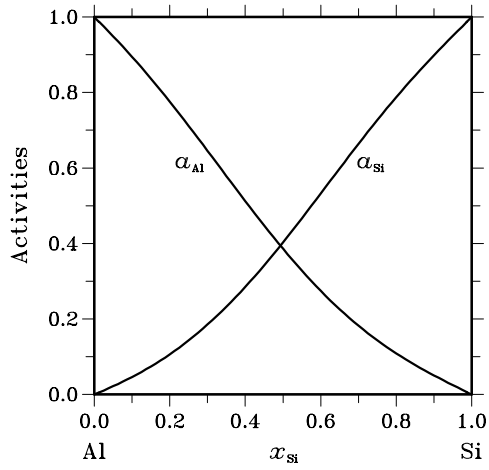

Fig. 3. Activities in the liquid phase at T=1700 K.

References

[80Doe] P. Dörner, E.T. Henig, H. Krieg, H.L. Lukas, G. Petzow: Calphad **4** (1980) 241–254.
[86Mey] S. an Mey, K. Hack: Z. Metallkd. **77** (1986) 454–459.
[92Cha] N. Chakraborti, H.L. Lukas: Calphad **16** (1992) 79–86.
[97Feu] H. Feufel, T. Gödecke, H.L. Lukas, F. Sommer: J. Alloys Comp. **247** (1997) 31–42.

Al – Ta (Aluminium – Tantalum)

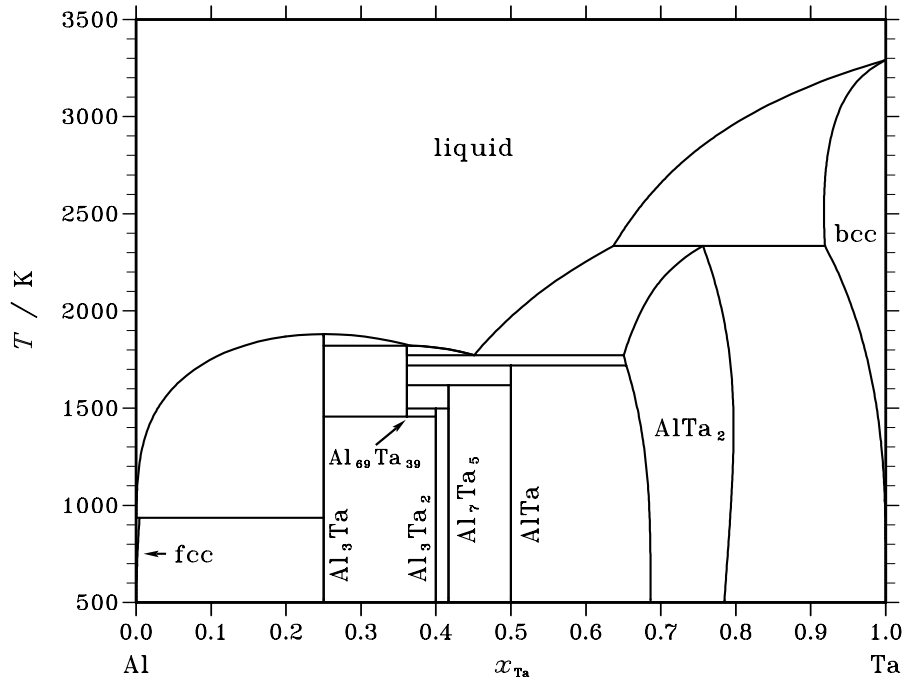

Fig. 1. Calculated phase diagram for the system Al-Ta.

Aluminum and Tantalum are both important alloying elements for high temperature alloys, such as superalloys.

Three different versions of the phase diagram have been published as result of different experimental investigations [85Sch, 90Sub, 95Mah]. Common to all phase diagram versions are the Al_3Ta and $AlTa_2$ phases in addition to the liquid and two terminal solid solution phases. It is also common that the $AlTa_2$ phase forms peritectically from the liquid and bcc-Ta at temperatures between 2273 K and 2373 K. The Al_3Ta phase is shown to form either peritectically or congruently at temperatures between 1823 K and 1903 K. The number and stoichiometries of the phases reported for the composition regime between Al_3Ta and $AlTa_2$ differs between these experimental investigations.

Several assessments are based on these different versions of the phase diagram. The assessment of [96Du] is preferred since it is based on the most comprehensive dataset available for this system. This dataset includes phase diagram, enthalpy and partial Gibbs energy data. The assessment reproduces the phase diagram of [95Mah]. The description of the liquid phase results in the formation of an inverse miscibility gap at temperatures above 5667 K, and the description of this system should, therefore, not be used for calculations at temperatures above 5400 K.

Table I. Phases, structures and models.

Phase	Struktur-bericht	Prototype	Pearson symbol	Space group	SGTE name	Model
liquid					LIQUID	$(Al,Ta)_1$
fcc	$A1$	Cu	$cF4$	$Fm\overline{3}m$	FCC_A1	$(Al,Ta)_1$
Al_3Ta	$D0_{22}$	Al_3Ti	$tI8$	$I4/mmm$	D022_AL3TA1	Al_3Ta_1
$Al_{69}Ta_{39}$	···	···	$cF432$	$F\overline{4}3m$	AL69TA39	$Al_{69}Ta_{39}$
Al_3Ta_2	···	···	$cF*$	···	AL3TA2	Al_3Ta_2
Al_7Ta_5	···	···	$hP*$	···	AL7TA5	Al_7Ta_5
AlTa	···	···	$mP*$	···	ALTA	Al_1Ta_1
$AlTa_2$	$D8_b$	σCrFe	$tP30$	$P4_2/mnm$	SIGMA10_D8B	$(Al,Ta)_5Ta_2(Al,Ta)_8$
bcc	$A2$	W	$cI2$	$Im\overline{3}m$	BCC_A2	$(Al,Ta)_1$

Table II. Invariant reactions.

Reaction	Type	T / K	Compositions / x_{Ta}			$\Delta_r H$ / (J/mol)
liquid + bcc $\rightleftharpoons$ $AlTa_2$	peritectic	2334.2	0.637	0.919	0.756	−11534
liquid $\rightleftharpoons$ Al_3Ta	congruent	1881.2	0.250	0.250		−27120
Al_3Ta + liquid $\rightleftharpoons$ $Al_{69}Ta_{39}$	peritectic	1820.8	0.250	0.367	0.361	−18237
liquid $\rightleftharpoons$ $Al_{69}Ta_{39}$ + $AlTa_2$	eutectic	1772.5	0.451	0.361	0.651	−16104
$Al_{69}Ta_{39}$ + $AlTa_2$ $\rightleftharpoons$ $AlTa_2$	peritectoid	1718.9	0.361	0.654	0.500	−1688
$Al_{69}Ta_{39}$ + $AlTa_2$ $\rightleftharpoons$ Al_7Ta_5	peritectoid	1618.4	0.361	0.500	0.417	−1104
$Al_{69}Ta_{39}$ + Al_7Ta_5 $\rightleftharpoons$ Al_3Ta_2	peritectoid	1498.7	0.361	0.417	0.400	−559
$Al_{69}Ta_{39}$ $\rightleftharpoons$ Al_3Ta + Al_3Ta_2	eutectoid	1456.1	0.361	0.250	0.400	−1871
liquid + Al_3Ta $\rightleftharpoons$ fcc	peritectic	936.5	0.000	0.250	0.005	−10402

Table IIIa. Integral quantities for the liquid phase at 3300 K.

x_{Ta}	ΔG_m [J/mol]	ΔH_m [J/mol]	ΔS_m [J/(mol·K)]	G_m^E [J/mol]	S_m^E [J/(mol·K)]	ΔC_p [J/(mol·K)]
0.000	0	0	0.000	0	0.000	0.000
0.100	−8803	−6331	0.749	117	−1.954	0.000
0.200	−13316	−11957	0.412	414	−3.749	0.000
0.300	−15946	−16614	−0.202	815	−5.281	0.000
0.400	−17225	−20038	−0.853	1242	−6.448	0.000
0.500	−17402	−21969	−1.384	1616	−7.147	0.000
0.600	−16604	−22141	−1.678	1862	−7.274	0.000
0.700	−14860	−20294	−1.647	1901	−6.726	0.000
0.800	−12075	−16163	−1.239	1655	−5.399	0.000
0.900	−7872	−9486	−0.489	1047	−3.192	0.000
1.000	0	0	0.000	0	0.000	0.000

Reference states: Al(liquid), Ta(liquid)

Table IIIb. Partial quantities for Al in the liquid phase at 3300 K.

x_{Al}	ΔG_{Al} [J/mol]	ΔH_{Al} [J/mol]	ΔS_{Al} [J/(mol·K)]	G^E_{Al} [J/mol]	S^E_{Al} [J/(mol·K)]	a_{Al}	γ_{Al}
1.000	0	0	0.000	0	0.000	1.000	1.000
0.900	−2994	−309	0.814	−103	−0.062	0.897	0.996
0.800	−6433	−1587	1.468	−310	−0.387	0.791	0.989
0.700	−10251	−4360	1.785	−465	−1.180	0.688	0.983
0.600	−14429	−9153	1.599	−413	−2.648	0.591	0.985
0.500	−19018	−16492	0.765	1	−4.998	0.500	1.000
0.400	−24209	−26903	−0.816	932	−8.435	0.414	1.035
0.300	−30500	−40912	−3.155	2535	−13.166	0.329	1.097
0.200	−39194	−59044	−6.015	4965	−19.397	0.240	1.198
0.100	−54800	−81825	−8.189	8378	−27.334	0.136	1.357
0.000	−∞	−109781	∞	12928	−37.185	0.000	1.602

Reference state: Al(liquid)

Table IIIc. Partial quantities for Ta in the liquid phase at 3300 K.

x_{Ta}	ΔG_{Ta} [J/mol]	ΔH_{Ta} [J/mol]	ΔS_{Ta} [J/(mol·K)]	G^E_{Ta} [J/mol]	S^E_{Ta} [J/(mol·K)]	a_{Ta}	γ_{Ta}
0.000	−∞	−65968	∞	3	−19.991	0.000	1.000
0.100	−61082	−60532	0.167	2097	−18.978	0.108	1.079
0.200	−40849	−53436	−3.814	3311	−17.196	0.226	1.128
0.300	−29233	−45205	−4.840	3801	−14.851	0.345	1.149
0.400	−21418	−36367	−4.530	3723	−12.149	0.458	1.145
0.500	−15787	−27445	−3.533	3232	−9.296	0.563	1.125
0.600	−11534	−18967	−2.252	2482	−6.500	0.657	1.095
0.700	−8158	−11458	−1.000	1629	−3.966	0.743	1.061
0.800	−5295	−5443	−0.045	827	−1.900	0.824	1.031
0.900	−2658	−1448	0.367	233	−0.509	0.908	1.009
1.000	0	0	0.000	0	0.000	1.000	1.000

Reference state: Ta(liquid)

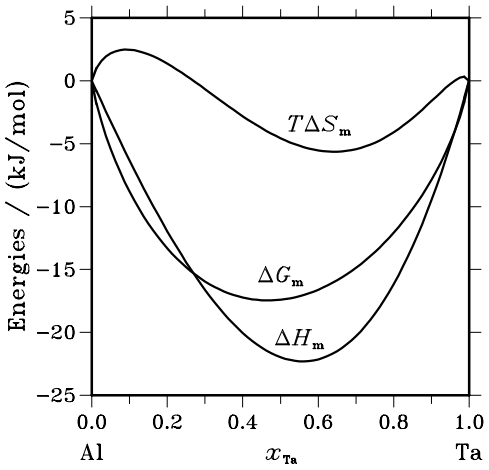

Fig. 2. Integral quantities of the liquid phase at T=3300 K.

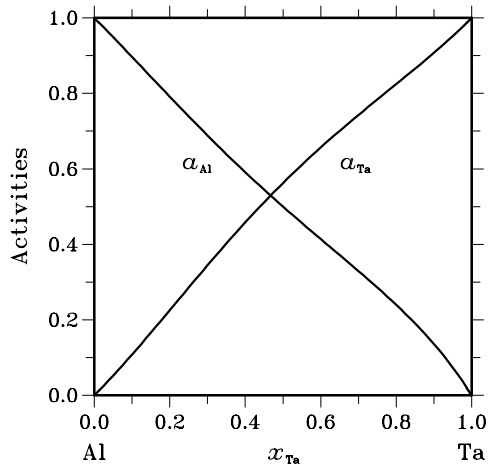

Fig. 3. Activities in the liquid phase at T=3300 K.

Table IV. Standard reaction quantities at 298.15 K for the compounds per mole of atoms.

Compound	x_{Ta}	$\Delta_{\mathrm{f}}G^{\circ}$ / (J/mol)	$\Delta_{\mathrm{f}}H^{\circ}$ / (J/mol)	$\Delta_{\mathrm{f}}S^{\circ}$ / (J/(mol·K))	$\Delta_{\mathrm{f}}C_P^{\circ}$ / (J/(mol·K))
Al_3Ta_1	0.250	−24824	−25916	−3.663	0.000
$Al_{69}Ta_{39}$	0.361	−20234	−20532	−1.000	0.000
Al_3Ta_2	0.400	−20636	−21173	−1.802	0.000
Al_7Ta_5	0.417	−20168	−20649	−1.613	0.000
Al_1Ta_1	0.500	−17817	−18064	−0.827	0.000

References

[85Sch] J.C. Schuster: Z. Metallkd. **76** (1985) 724–727.
[90Sub] P.R. Subramanian, D.B. Miracle, S. Mazdiyasni: Metall. Trans. **21A** (1990) 539–545.
[95Mah] S. Mahne, B. Harbrecht, F. Krumeich: J. Alloys Comp. **218** (1995) 177–182.
[96Du] Y. Du, R. Schmid-Fetzer: J. Phase Equilibria **17** (1996) 311–324.

Al – Ti (Aluminium – Titanium)

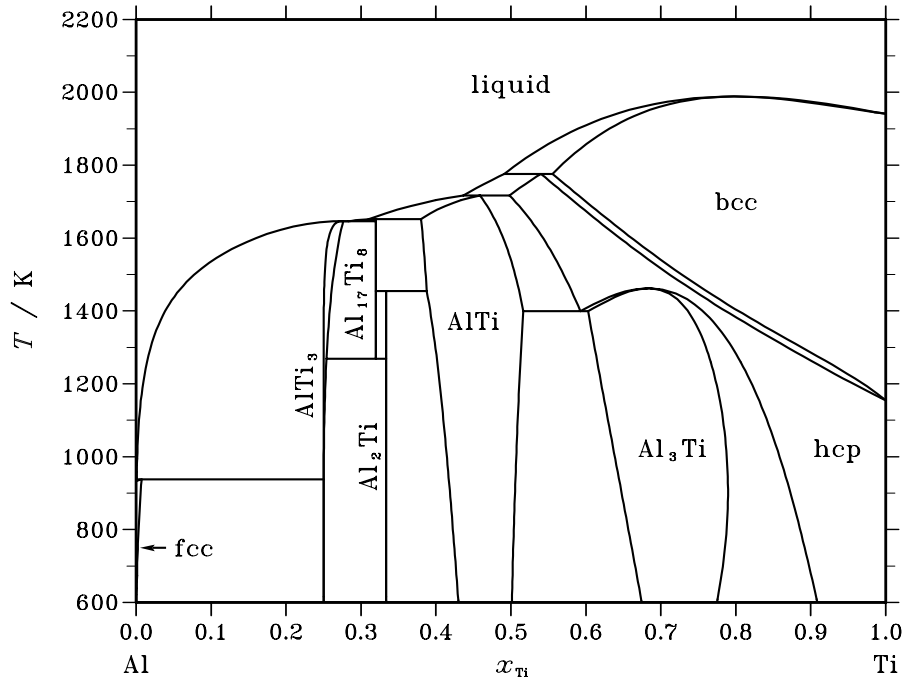

Fig. 1. Calculated phase diagram for the system Al-Ti.

This system is of great interest for high temperature applications and for good corrosion resistance. The ordered $L1_0$ phase, AlTi, has good mechanical properties. The hcp/bcc transition in Ti is moved to higher temperatures by Al and the shape of this two-phase region has been studied by many authors. The ordering in the hcp phase at lower temperature, forming a $D0_{19}$ structure is very close to this two-phase region and recently it has been confirmed that $B2$ ordering of the bcc phase is also stable [94Kai]. But this transformation has not been included in the present diagram which is from [98Sau] with small modifications. The modelling is based on CEF but the ordered phases are modelled separately from the disordered parent phases. A full assessment of the whole phase diagram with consistent modelling of the order/disorder transformations is in progress.

Table I. Phases, structures and models.

Phase	Struktur-bericht	Prototype	Pearson symbol	Space group	SGTE name	Model
liquid					LIQUID	$(Al,Ti)_1$
fcc	$A1$	Cu	$cF4$	$Fm\overline{3}m$	FCC_A1	$(Al,Ti)_1$
Al_3Ti	$D0_{22}$	Al_3Ti	$tI8$	$I4/mmm$	D022_AL3M1	$(Al,Ti)_3Ti_1$
$Al_{11}Ti_5$	···	···	···	···	AL11TI5	$Al_{17}Ti_8$
Al_2Ti	···	···	$tI24$	$I4_1/amd$	AL2TI	Al_2Ti_1
AlTi	$L1_0$	AuCu	$tP2$	$P4/mmm$	L10_ALTI	$(Al,Ti)_1(Al,Ti)_1$
$AlTi_3$	$D0_{19}$	Ni_3Sn	$hP8$	$P6_3/mmc$	D019_AL1M3	$(Al,Ti)_3(Al,Ti)_1$
bcc	$A2$	W	$cI2$	$Im\overline{3}m$	BCC_A2	$(Al,Ti)_1$
hcp	$A3$	Mg	$hP2$	$P6_3/mmc$	HCP_A3	$(Al,Ti)_1$

Table II. Invariant reactions.

Reaction	Type	T / K	Compositions / x_{Ti}			$\Delta_r H$ / (J/mol)
liquid ⇌ bcc	congruent	1988.5	0.799	0.799		−15738
liquid + bcc ⇌ hcp	peritectic	1775.9	0.491	0.555	0.540	−6380
liquid + hcp ⇌ AlTi	peritectic	1716.6	0.436	0.498	0.459	−16846
liquid + AlTi ⇌ $Al_{11}Ti_5$	peritectic	1651.9	0.311	0.380	0.320	−23232
liquid ⇌ Al_3Ti	congruent	1646.2	0.274	0.274		−24885
liquid ⇌ Al_3Ti + $Al_{11}Ti_5$	eutectic	1645.9	0.283	0.276	0.320	−24944
hcp ⇌ $AlTi_3$	congruent	1462.5	0.684	0.684		−3259
$Al_{11}Ti_5$ + AlTi ⇌ Al_2Ti	peritectoid	1454.4	0.320	0.388	0.333	−1607
hcp ⇌ AlTi + $AlTi_3$	eutectoid	1399.3	0.593	0.516	0.603	−3207
$Al_{11}Ti_5$ ⇌ Al_3Ti + Al_2Ti	eutectoid	1269.1	0.320	0.254	0.333	−897
liquid + Al_3Ti ⇌ fcc	peritectic	938.0	0.001	0.250	0.007	−10180

Table IIIa. Integral quantities for the liquid phase at 2000 K.

x_{Ti}	ΔG_{m} [J/mol]	ΔH_{m} [J/mol]	ΔS_{m} [J/(mol·K)]	$G_{\mathrm{m}}^{\mathrm{E}}$ [J/mol]	$S_{\mathrm{m}}^{\mathrm{E}}$ [J/(mol·K)]	ΔC_p [J/(mol·K)]
0.000	0	0	0.000	0	0.000	0.000
0.100	−7156	−9311	−1.077	−1751	−3.780	0.000
0.200	−12233	−17032	−2.399	−3912	−6.560	0.000
0.300	−16091	−22733	−3.321	−5933	−8.400	0.000
0.400	−18596	−26124	−3.764	−7404	−9.360	0.000
0.500	−19589	−27063	−3.737	−8063	−9.500	0.000
0.600	−18980	−25548	−3.284	−7788	−8.880	0.000
0.700	−16763	−21725	−2.481	−6605	−7.560	0.000
0.800	−13001	−15880	−1.439	−4680	−5.600	0.000
0.900	−7732	−8447	−0.357	−2327	−3.060	0.000
1.000	0	0	0.000	0	0.000	0.000

Reference states: Al(liquid), Ti(liquid)

Table IIIb. Partial quantities for Al in the liquid phase at 2000 K.

x_{Al}	ΔG_{Al} [J/mol]	ΔH_{Al} [J/mol]	ΔS_{Al} [J/(mol·K)]	$G_{\mathrm{Al}}^{\mathrm{E}}$ [J/mol]	$S_{\mathrm{Al}}^{\mathrm{E}}$ [J/(mol·K)]	a_{Al}	γ_{Al}
1.000	0	0	0.000	0	0.000	1.000	1.000
0.900	−1443	−711	0.366	310	−0.510	0.917	1.019
0.800	−3281	−3490	−0.105	430	−1.960	0.821	1.026
0.700	−6458	−8987	−1.264	−527	−4.230	0.678	0.969
0.600	−11511	−17416	−2.953	−3016	−7.200	0.500	0.834
0.500	−18589	−28563	−4.987	−7063	−10.750	0.327	0.654
0.400	−27495	−41778	−7.141	−12258	−14.760	0.191	0.478
0.300	−37783	−55983	−9.100	−17763	−19.110	0.103	0.344
0.200	−49067	−69664	−10.298	−22304	−23.680	0.052	0.262
0.100	−62468	−80879	−9.205	−24179	−28.350	0.023	0.234
0.000	$-\infty$	−87250	∞	−21250	−33.000	0.000	0.279

Reference state: Al(liquid)

Table IIIc. Partial quantities for Ti in the liquid phase at 2000 K.

x_{Ti}	ΔG_{Ti} [J/mol]	ΔH_{Ti} [J/mol]	ΔS_{Ti} [J/(mol·K)]	$G^{\mathrm{E}}_{\mathrm{Ti}}$ [J/mol]	$S^{\mathrm{E}}_{\mathrm{Ti}}$ [J/(mol·K)]	a_{Ti}	γ_{Ti}
0.000	$-\infty$	−99250	∞	−13250	−43.000	0.000	0.451
0.100	−58580	−86711	−14.065	−20291	−33.210	0.030	0.295
0.200	−48043	−71200	−11.578	−21280	−24.960	0.056	0.278
0.300	−38567	−54807	−8.120	−18547	−18.130	0.098	0.328
0.400	−29223	−39186	−4.981	−13986	−12.600	0.173	0.431
0.500	−20589	−25563	−2.487	−9063	−8.250	0.290	0.580
0.600	−13303	−14728	−0.713	−4808	−4.960	0.449	0.749
0.700	−7754	−7043	0.356	−1823	−2.610	0.627	0.896
0.800	−3985	−2434	0.775	−274	−1.080	0.787	0.984
0.900	−1651	−399	0.626	102	−0.250	0.906	1.006
1.000	0	0	0.000	0	0.000	1.000	1.000

Reference state: Ti(liquid)

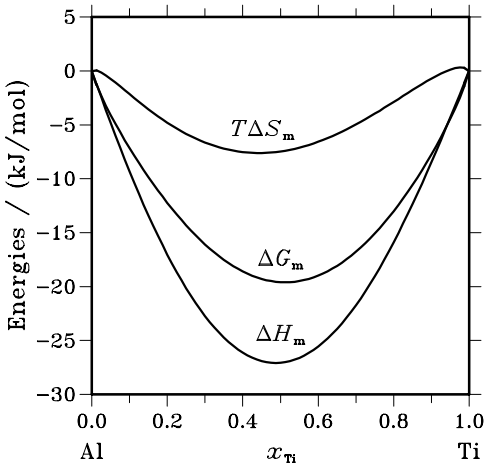

Fig. 2. Integral quantities of the liquid phase at T=2000 K.

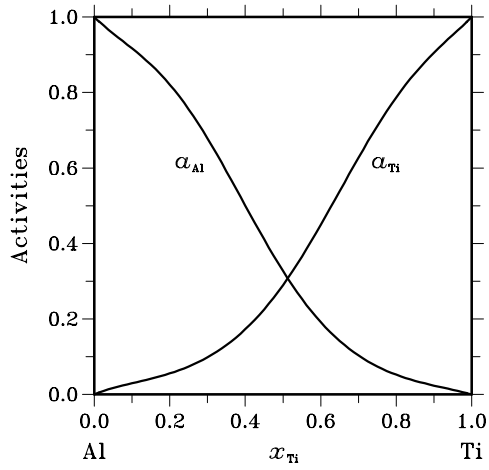

Fig. 3. Activities in the liquid phase at T=2000 K.

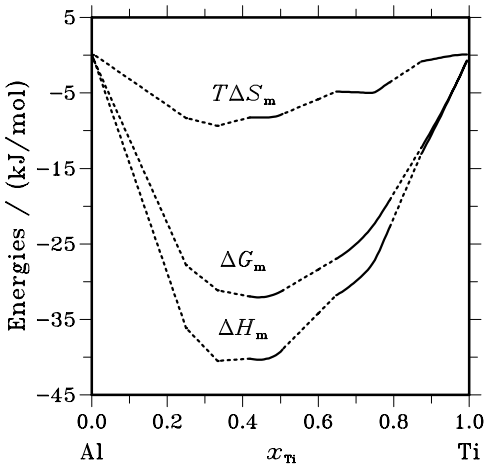

Fig. 4. Integral quantities of the stable phases at T=900 K.

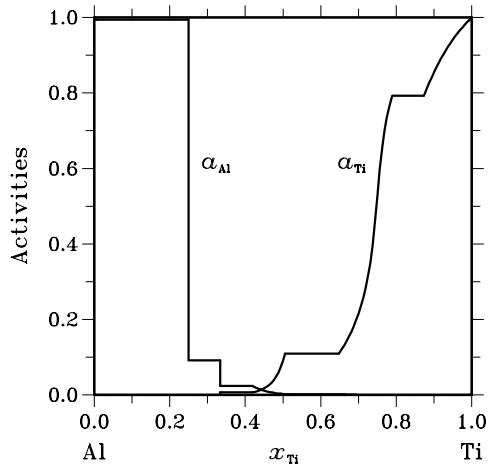

Fig. 5. Activities in the stable phases at T=900 K.

Table IVa. Integral quantities for the stable phases at 900 K.

Phase	x_{Ti}	ΔG_{m} [J/mol]	ΔH_{m} [J/mol]	ΔS_{m} [J/(mol·K)]	$G_{\mathrm{m}}^{\mathrm{E}}$ [J/mol]	$S_{\mathrm{m}}^{\mathrm{E}}$ [J/(mol·K)]	ΔC_p [J/(mol·K)]
fcc	0.000	0	0	0.000	0	0.000	0.000
	0.006	−711	−645	0.073	−437	−0.232	0.000
Al_3Ti	0.250	−27818	−36148	−9.256	−27818	−9.256	0.000
	0.250	−27824	−36143	−9.244	−27814	−9.254	0.000
Al_2Ti	0.333	−31140	−40500	−10.400			0.000
AlTi	0.419	−31958	−40196	−9.153	−30266	−11.033	0.293
	0.450	−32056	−40316	−9.178	−30760	−10.618	0.667
	0.500	−31330	−39259	−8.810	−30592	−9.630	2.408
	0.505	−31178	−38971	−8.659	−30411	−9.511	2.333
$AlTi_3$	0.648	−26967	−31795	−5.364	−24726	−7.855	0.068
	0.650	−26898	−31729	−5.367	−24689	−7.822	0.072
	0.700	−25029	−29937	−5.454	−23632	−7.006	0.243
	0.750	−22239	−27123	−5.427	−21764	−5.955	1.883
	0.790	−19156	−22737	−3.979	−18256	−4.978	0.674
hcp	0.873	−12253	−13091	−0.931	−9404	−4.096	0.000
	0.900	−9949	−10513	−0.627	−7516	−3.330	0.000
	0.950	−5325	−5426	−0.112	−3840	−1.762	0.000
	1.000	0	0	0.000	0	0.000	0.000

Reference states: Al(fcc), Ti(hcp)

Table IVb. Partial quantities for Al in the stable phases at 900 K.

Phase	x_{Al}	ΔG_{Al} [J/mol]	ΔH_{Al} [J/mol]	ΔS_{Al} [J/(mol·K)]	$G_{\mathrm{Al}}^{\mathrm{E}}$ [J/mol]	$S_{\mathrm{Al}}^{\mathrm{E}}$ [J/(mol·K)]	a_{Al}	γ_{Al}
fcc	1.000	0	0	0.000	0	0.000	1.000	1.000
	0.994	−45	−2	0.049	0	−0.001	0.994	1.000
Al_3Ti	0.750	−45	−45197	−50.169	−34060	−12.375	0.994	0.011
	0.750	−17853	−45199	−30.384	−34062	−12.375	0.092	0.011
Al_2Ti	0.667	−17854	−23046	−5.769			0.092	
	0.667	−27947	−41689	−15.270			0.024	
AlTi	0.581	−27947	−35387	−8.266	−21498	−15.432	0.024	0.057
	0.550	−33554	−42045	−9.434	−26023	−17.802	0.011	0.031
	0.500	−44768	−63980	−21.346	−45306	−20.749	0.003	0.002
	0.495	−46130	−68068	−24.375	−49432	−20.706	0.002	0.001
$AlTi_3$	0.352	−46130	−50182	−4.502	−35017	−16.850	0.002	0.009
	0.350	−46536	−50585	−4.499	−35299	−16.984	0.002	0.009
	0.300	−56625	−59964	−3.710	−41956	−20.009	0.001	0.004
	0.250	−74579	−94605	−22.251	−73097	−23.898	0.000	0.001
	0.210	−84482	−114156	−32.971	−92093	−24.514	0.000	0.000
hcp	0.127	−84482	−94171	−10.765	−69042	−27.921	0.000	0.000
	0.100	−88902	−98483	−10.645	−71672	−29.790	0.000	0.000
	0.050	−97954	−105594	−8.489	−75536	−33.398	0.000	0.000
	0.000	$-\infty$	−111269	∞	−77789	−37.200	0.000	0.000

Reference state: Al(fcc)

Table IVc. Partial quantities for Ti in the stable phases at 900 K.

Phase	x_{Ti}	ΔG_{Ti} [J/mol]	ΔH_{Ti} [J/mol]	ΔS_{Ti} [J/(mol·K)]	$G^{\mathrm{E}}_{\mathrm{Ti}}$ [J/mol]	$S^{\mathrm{E}}_{\mathrm{Ti}}$ [J/(mol·K)]	a_{Ti}	γ_{Ti}
fcc	0.000	$-\infty$	−107970	∞	−72960	−38.900	0.000	0.000
	0.006	−111134	−107429	4.117	−72838	−38.434	0.000	0.000
Al_3Ti	0.250	−111134	−9000	113.483	−9090	0.100	0.000	0.000
	0.250	−57714	−8995	54.133	−9085	0.100	0.000	0.297
Al_2Ti	0.333	−57711	−75408	−19.663			0.000	
	0.333	−37527	−38122	−0.661			0.007	
AlTi	0.419	−37527	−46873	−10.385	−42440	−4.925	0.007	0.003
	0.450	−30224	−38203	−8.865	−36548	−1.838	0.018	0.008
	0.500	−17891	−14538	3.725	−15878	1.489	0.092	0.120
	0.505	−16544	−10493	6.723	−11795	1.446	0.110	0.207
$AlTi_3$	0.648	−16544	−21794	−5.833	−19129	−2.961	0.110	0.078
	0.650	−16324	−21576	−5.835	−18976	−2.889	0.113	0.079
	0.700	−11487	−17068	−6.201	−15779	−1.433	0.215	0.121
	0.750	−4792	−4629	0.181	−4653	0.026	0.527	0.537
	0.790	−1742	1633	3.750	1426	0.229	0.792	1.210
hcp	0.873	−1742	−1292	0.500	−725	−0.629	0.792	0.908
	0.900	−1176	−739	0.486	−388	−0.390	0.855	0.950
	0.950	−450	−154	0.329	−66	−0.098	0.942	0.991
	1.000	0	0	0.000	0	0.000	1.000	1.000

Reference state: Ti(hcp)

Table V. Standard reaction quantities at 298.15 K for the compounds per mole of atoms.

Compound	x_{Ti}	$\Delta_{\mathrm{f}}G^{\circ}$ / (J/mol)	$\Delta_{\mathrm{f}}H^{\circ}$ / (J/mol)	$\Delta_{\mathrm{f}}S^{\circ}$ / (J/(mol·K))	$\Delta_{\mathrm{f}}C^{\circ}_{P}$ / (J/(mol·K))
Al_3Ti	0.250	−33388	−36148	−9.256	0.000
$Al_{17}Ti_8$	0.320	−36026	−38845	−9.456	0.000
Al_2Ti_1	0.333	−37399	−40500	−10.400	0.000
AlTi	0.500	−36960	−39822	−9.599	0.011
$AlTi_3$	0.750	−25740	−27520	−5.970	0.003

References

[94Kai] R. Kainuma, M. Palm, G. Inden: Intermetallics **2** (1994) 321–332.

[98Sau] N. Saunders in: I. Ansara, A.T. Dinsdale, M.H. Rand (eds.): COST 507, "Thermochemical database for light metal alloys", Vol. 2, EUR 18499, 1998, 89–94.

Al – V (Aluminium – Vanadium)

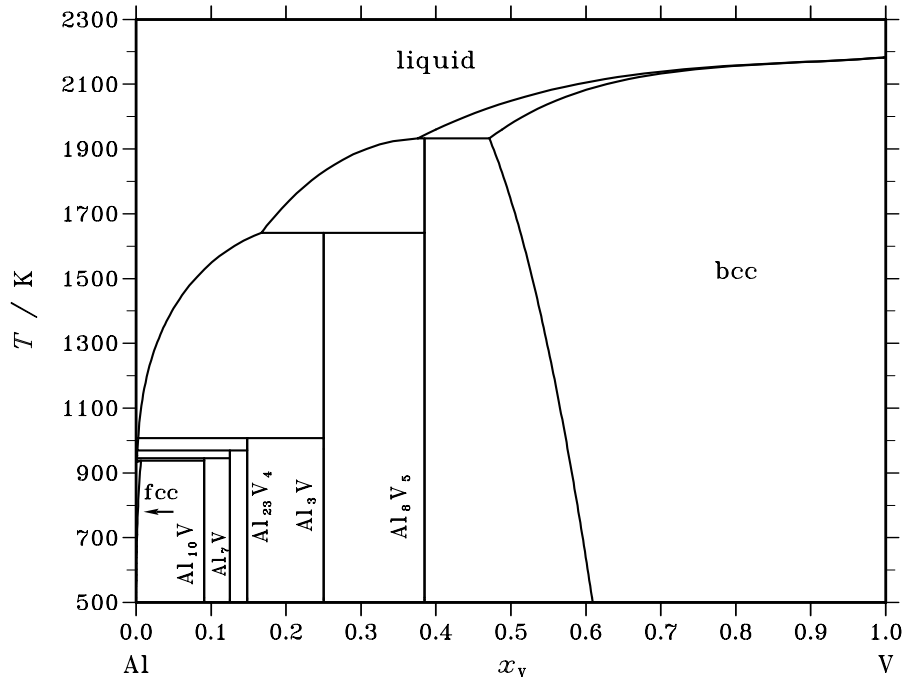

Fig. 1. Calculated phase diagram for the system Al-V.

An understanding of the Al-V system is necessary since it is an important sub- system in the commercial aerospace alloy Ti6Al4V and because vanadium is often added to aluminium alloys as a grain refiner. The basic phase diagram for the system is fairly well characterised, although the details of the liquidus surface on the aluminium rich side of the system remain unclear. The system is characterised by a continuous range of solutions in the liquid phase, substantial solubility of aluminium in bcc-V up to 50 at.% Al maximum at 1933 K, limited solubility of vanadium in fcc-Al with a maximum solubility of 0.3 at.% V and a variety of aluminium vanadium intermetallic compounds all of which melt peritectically.
The thermodynamic properties of the intermetallic phases have been studied by direct reaction calorimetry. More recently the enthalpies of mixing in the liquid phase have been measured for Al rich compositions. Partial Gibbs energies of Al in the bcc solid solution range have been studied by emf and by an isopiestic technique.
The phase diagram and thermodynamic data for this systems have been critically assessed by Lee and Lee [86Lee], Murray [89Mur] and Saunders [98Sau]. The data of Saunders have been adopted by SGTE and COST507 as a basis for the calculation of multicomponent phase equilibria.

Table I. Phases, structures and models.

Phase	Struktur-bericht	Prototype	Pearson symbol	Space group	SGTE name	Model
liquid					LIQUID	$(Al,V)_1$
fcc	$A1$	Cu	$cF4$	$Fm\overline{3}m$	FCC_A1	$(Al,V)_1$
$Al_{10}V$	$\cdots$	$\cdots$	$cF176$	$Fd\overline{3}m$	AL10V	$Al_{10}V_1$
Al_7V	$\cdots$	$Al_{45}V_7$	$mC104$	$C2/m$	AL7V	Al_7V_1
$Al_{23}V_4$	$\cdots$	$Al_{23}V_4$	$hP54$	$P6_3/mmc$	AL23V4	$Al_{23}V_4$
Al_3V	$D0_{22}$	Al_3Ti	$tI8$	$I4/mmm$	D022_AL3M1	$(Al,V)_3V_1$
Al_8V_5	$D8_2$	Cu_5Zn_8	$cI52$	$I\overline{4}3m$	D82_AL8V5	Al_8V_5
bcc	$A2$	W	$cI2$	$Im\overline{3}m$	BCC_A2	$(Al,V)_1$

Table II. Invariant reactions.

Reaction	Type	T / K	Compositions / x_V			$\Delta_r H$ / (J/mol)
liquid + bcc $\rightleftharpoons$ Al_8V_5	peritectic	1932.7	0.376	0.471	0.385	−22479
liquid + Al_8V_5 $\rightleftharpoons$ Al_3V	peritectic	1640.8	0.167	0.385	0.250	−19772
liquid + Al_3V $\rightleftharpoons$ $Al_{23}V_4$	peritectic	1007.3	0.003	0.250	0.148	−4918
liquid + $Al_{23}V_4$ $\rightleftharpoons$ Al_7V	peritectic	969.0	0.002	0.148	0.125	−1836
liquid + Al_7V $\rightleftharpoons$ $Al_{10}V$	peritectic	945.2	0.001	0.125	0.091	−3173
liquid + $Al_{10}V$ $\rightleftharpoons$ fcc	peritectic	937.6	0.001	0.091	0.006	−9815

Table IIIa. Integral quantities for the liquid phase at 2200 K.

x_V	ΔG_m [J/mol]	ΔH_m [J/mol]	ΔS_m [J/(mol·K)]	G_m^E [J/mol]	S_m^E [J/(mol·K)]	ΔC_p [J/(mol·K)]
0.000	0	0	0.000	0	0.000	0.000
0.100	−8542	−5645	1.317	−2596	−1.386	0.000
0.200	−13852	−9556	1.953	−4698	−2.208	0.000
0.300	−17450	−11912	2.517	−6276	−2.562	0.000
0.400	−19608	−12894	3.052	−7297	−2.544	0.000
0.500	−20410	−12681	3.513	−7731	−2.250	0.000
0.600	−19858	−11454	3.820	−7547	−1.776	0.000
0.700	−17887	−9392	3.861	−6713	−1.218	0.000
0.800	−14351	−6676	3.489	−5198	−0.672	0.000
0.900	−8917	−3485	2.469	−2970	−0.234	0.000
1.000	0	0	0.000	0	0.000	0.000

Reference states: Al(liquid), V(liquid)

Table IIIb. Partial quantities for Al in the liquid phase at 2200 K.

x_{Al}	ΔG_{Al} [J/mol]	ΔH_{Al} [J/mol]	ΔS_{Al} [J/(mol·K)]	G^E_{Al} [J/mol]	S^E_{Al} [J/(mol·K)]	a_{Al}	γ_{Al}
1.000	0	0	0.000	0	0.000	1.000	1.000
0.900	−2169	−897	0.578	−242	−0.298	0.888	0.987
0.800	−5090	−3349	0.791	−1008	−1.064	0.757	0.946
0.700	−8886	−6995	0.860	−2362	−2.106	0.615	0.879
0.600	−13710	−11476	1.015	−4366	−3.232	0.473	0.788
0.500	−19760	−16431	1.513	−7081	−4.250	0.340	0.679
0.400	−27332	−21501	2.651	−10571	−4.968	0.224	0.561
0.300	−36921	−26325	4.816	−14899	−5.194	0.133	0.443
0.200	−49565	−30544	8.646	−20125	−4.736	0.067	0.333
0.100	−68432	−33797	15.743	−26313	−3.402	0.024	0.237
0.000	−∞	−35725	∞	−33525	−1.000	0.000	0.160

Reference state: Al(liquid)

Table IIIc. Partial quantities for V in the liquid phase at 2200 K.

x_V	ΔG_V [J/mol]	ΔH_V [J/mol]	ΔS_V [J/(mol·K)]	G^E_V [J/mol]	S^E_V [J/(mol·K)]	a_V	γ_V
0.000	−∞	−65725	∞	−28325	−17.000	0.000	0.213
0.100	−65904	−48377	7.967	−23786	−11.178	0.027	0.272
0.200	−48899	−34384	6.598	−19459	−6.784	0.069	0.345
0.300	−37431	−23385	6.384	−15408	−3.626	0.129	0.431
0.400	−28455	−15021	6.107	−11695	−1.512	0.211	0.528
0.500	−21060	−8931	5.513	−8381	−0.250	0.316	0.632
0.600	−14874	−4756	4.599	−5530	0.352	0.443	0.739
0.700	−9729	−2135	3.452	−3204	0.486	0.588	0.839
0.800	−5548	−709	2.199	−1466	0.344	0.738	0.923
0.900	−2304	−117	0.994	−377	0.118	0.882	0.980
1.000	0	0	0.000	0	0.000	1.000	1.000

Reference state: V(liquid)

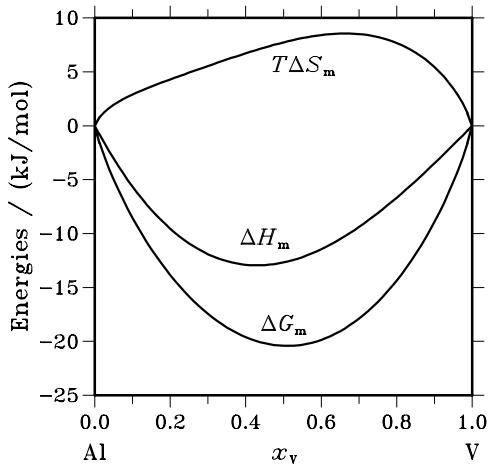

Fig. 2. Integral quantities of the liquid phase at T=2200 K.

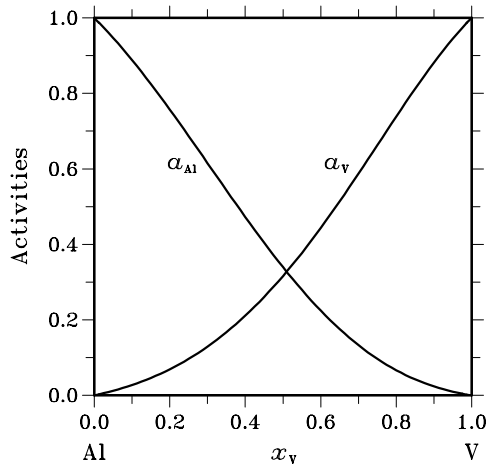

Fig. 3. Activities in the liquid phase at T=2200 K.

Table IV. Standard reaction quantities at 298.15 K for the compounds per mole of atoms.

Compound	x_{V}	$\Delta_{\mathrm{f}}G^{\circ}$ / (J/mol)	$\Delta_{\mathrm{f}}H^{\circ}$ / (J/mol)	$\Delta_{\mathrm{f}}S^{\circ}$ / (J/(mol·K))	$\Delta_{\mathrm{f}}C_P^{\circ}$ / (J/(mol·K))
$Al_{10}V_1$	0.091	−9598	−10111	−1.719	0.000
Al_7V_1	0.125	−12974	−13600	−2.100	0.000
$Al_{23}V_4$	0.148	−15236	−15950	−2.395	0.000
Al_8V_5	0.385	−22938	−22640	1.000	0.000

References

[86Lee] S.K. Lee, D.N. Lee: J. Korean Inst. Met. **24** (1986) 1290–1301.

[89Mur] J.L. Murray, in: "Phase diagrams of binary vanadium alloys", J.F. Smith (ed.), ASM International, 1989, pp. 6–12.

[98Sau] N. Saunders, in: I. Ansara, A.T. Dinsdale, M.H. Rand (eds.): COST 507, "Thermochemical database for light metal alloys", Vol. 2, EUR 18499, 1998, pp. 95–98.

Al – W (Aluminium – Tungsten)

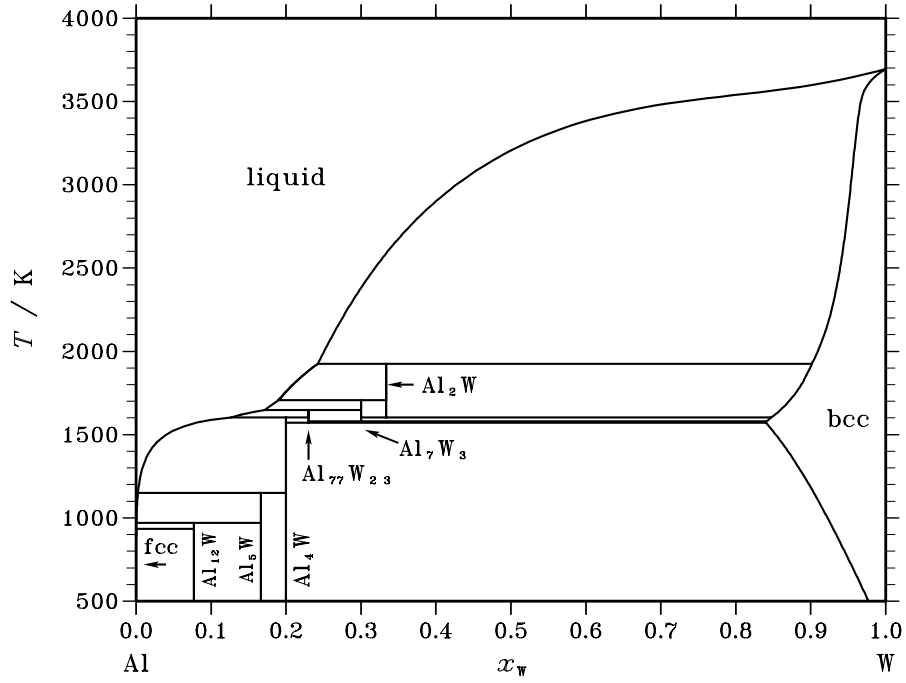

Fig. 1. Calculated phase diagram for the system Al-W.

An understanding of the Al-W system is necessary since it is an important component system in potential high temperature aerospace TiAl alloys.

The experimental information on the phase diagram for this system is somewhat sparse. The phase diagram is characterised by a continuous series of solutions in the liquid phase, significant solubility of Al in bcc-W with a maximum of about 15 at.% at 1600 K, low solubility of W in fcc-Al up to a maximum of approximately 0.02 close to the melting temperature of Al. There are several intermetallic compounds in the system, all of which appear to melt peritectically. The three intermetallic phases richest in W are stable over a relatively narrow temperature range decomposing on cooling by eutectoid reaction. There appear to be no experimental thermodynamic information available.

The thermodynamic and phase diagram data for the system have been critically assessed by Kaufman and Nesor [78Kau] and more recently by Saunders [98Sau]. The data of Saunders have been adopted by SGTE and COST 507 as a basis for the calculation of multicomponent phase equilibria.

Table I. Phases, structures and models.

Phase	Struktur-bericht	Prototype	Pearson symbol	Space group	SGTE name	Model
liquid					LIQUID	$(Al,W)_1$
fcc	$A1$	Cu	$cF4$	$Fm\overline{3}m$	FCC_A1	$(Al,W)_1$
$Al_{12}W$	···	$Al_{12}W$	$cI26$	$Im3$	AL12W	$Al_{12}W_1$
Al_5W	···	Al_5Mo	$hP12$	$P6_3$	AL5W	Al_5W_1
Al_4W	···	Al_4W	$mC30$	Cm	AL4W	Al_4W_1
$Al_{77}W_{23}$	···	···	···	···	AL77W23	$Al_{77}W_{23}$
Al_7W_3	···	···	···	···	AL7W3	Al_7W_3
Al_2W	···	···	···	···	AL2W	Al_2W_1
bcc	$A2$	W	$cI2$	$Im\overline{3}m$	BCC_A2	$(Al,W)_1$

Table II. Invariant reactions.

Reaction	Type	T / K	Compositions / x_W			$\Delta_r H$ / (J/mol)
liquid + bcc $\rightleftharpoons$ Al_2W	peritectic	1925.7	0.243	0.901	0.333	−2689
liquid + Al_2W $\rightleftharpoons$ Al_7W_3	peritectic	1706.8	0.190	0.333	0.300	−1973
liquid + Al_7W_3 $\rightleftharpoons$ $Al_{77}W_{23}$	peritectic	1648.2	0.172	0.300	0.230	−8167
liquid + $Al_{77}W_{23}$ $\rightleftharpoons$ Al_4W	peritectic	1604.1	0.127	0.230	0.200	−12758
Al_2W $\rightleftharpoons$ Al_7W_3 + bcc	eutectoid	1602.6	0.333	0.300	0.847	−1318
Al_7W_3 $\rightleftharpoons$ $Al_{77}W_{23}$ + bcc	eutectoid	1580.0	0.300	0.230	0.841	−5272
$Al_{77}W_{23}$ $\rightleftharpoons$ Al_4W + bcc	eutectoid	1571.0	0.230	0.200	0.840	−9120
liquid + Al_4W $\rightleftharpoons$ Al_5W	peritectic	1149.6	0.002	0.200	0.167	−1951
liquid + Al_5W $\rightleftharpoons$ $Al_{12}W$	peritectic	969.5	0.000	0.167	0.077	−6053
liquid + $Al_{12}W$ $\rightleftharpoons$ fcc	peritectic	933.6	0.000	0.077	0.000	−10676

Table IIIa. Integral quantities for the liquid phase at 3700 K.

x_W	ΔG_m [J/mol]	ΔH_m [J/mol]	ΔS_m [J/(mol·K)]	G_m^E [J/mol]	S_m^E [J/(mol·K)]	ΔC_p [J/(mol·K)]
0.000	0	0	0.000	0	0.000	0.000
0.100	−3782	−5436	−0.447	6219	−3.150	0.000
0.200	−5010	−10336	−1.439	10384	−5.600	0.000
0.300	−5793	−14196	−2.271	12999	−7.350	0.000
0.400	−6280	−16656	−2.804	14424	−8.400	0.000
0.500	−6449	−17500	−2.987	14875	−8.750	0.000
0.600	−6280	−16656	−2.804	14424	−8.400	0.000
0.700	−5793	−14196	−2.271	12999	−7.350	0.000
0.800	−5010	−10336	−1.439	10384	−5.600	0.000
0.900	−3782	−5436	−0.447	6219	−3.150	0.000
1.000	0	0	0.000	0	0.000	0.000

Reference states: Al(liquid), W(liquid)

Table IIIb. Partial quantities for Al in the liquid phase at 3700 K.

x_{Al}	ΔG_{Al} [J/mol]	ΔH_{Al} [J/mol]	ΔS_{Al} [J/(mol·K)]	G_{Al}^E [J/mol]	S_{Al}^E [J/(mol·K)]	a_{Al}	γ_{Al}
1.000	0	0	0.000	0	0.000	1.000	1.000
0.900	−2118	−172	0.526	1123	−0.350	0.933	1.037
0.800	−3117	−1432	0.455	3748	−1.400	0.904	1.130
0.700	−3890	−4572	−0.184	7083	−3.150	0.881	1.259
0.600	−4947	−9952	−1.353	10768	−5.600	0.851	1.419
0.500	−6449	−17500	−2.987	14875	−8.750	0.811	1.622
0.400	−8280	−26712	−4.981	19908	−12.600	0.764	1.910
0.300	−10236	−36652	−7.140	26803	−17.150	0.717	2.390
0.200	−12584	−45952	−9.018	36928	−22.400	0.664	3.321
0.100	−18753	−52812	−9.205	52083	−28.350	0.544	5.436
0.000	$-\infty$	−55000	∞	74500	−35.000	0.000	11.265

Reference state: Al(liquid)

Table IIIc. Partial quantities for W in the liquid phase at 3700 K.

x_W	ΔG_W [J/mol]	ΔH_W [J/mol]	ΔS_W [J/(mol·K)]	G_W^E [J/mol]	S_W^E [J/(mol·K)]	a_W	γ_W
0.000	$-\infty$	−55000	∞	74500	−35.000	0.000	11.265
0.100	−18753	−52812	−9.205	52083	−28.350	0.544	5.436
0.200	−12584	−45952	−9.018	36928	−22.400	0.664	3.321
0.300	−10236	−36652	−7.140	26803	−17.150	0.717	2.390
0.400	−8280	−26712	−4.981	19908	−12.600	0.764	1.910
0.500	−6449	−17500	−2.987	14875	−8.750	0.811	1.622
0.600	−4947	−9952	−1.353	10768	−5.600	0.851	1.419
0.700	−3890	−4572	−0.184	7083	−3.150	0.881	1.259
0.800	−3117	−1432	0.455	3748	−1.400	0.904	1.130
0.900	−2118	−172	0.526	1123	−0.350	0.933	1.037
1.000	0	0	0.000	0	0.000	1.000	1.000

Reference state: W(liquid)

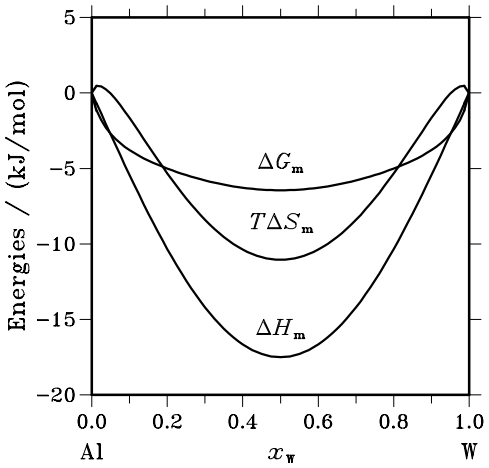

Fig. 2. Integral quantities of the liquid phase at T=3700 K.

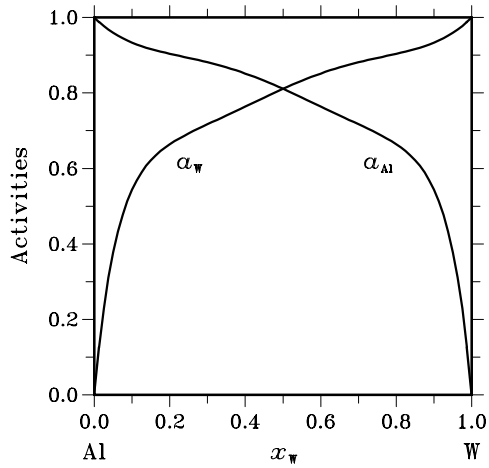

Fig. 3. Activities in the liquid phase at T=3700 K.

Table IV. Standard reaction quantities at 298.15 K for the compounds per mole of atoms.

Compound	x_W	$\Delta_f G^\circ$ / (J/mol)	$\Delta_f H^\circ$ / (J/mol)	$\Delta_f S^\circ$ / (J/(mol·K))	$\Delta_f C_P^\circ$ / (J/(mol·K))
$Al_{12}W_1$	0.077	−4582	−4800	−0.730	0.000
Al_5W_1	0.167	−9324	−9741	−1.400	0.000
Al_4W_1	0.200	−10920	−11500	−1.946	0.000
$Al_{77}W_{23}$	0.230	−3086	−1893	4.000	0.000
Al_7W_3	0.300	1383	3470	7.000	0.000
Al_2W_1	0.333	2288	4512	7.460	0.000

References

[78Kau] L. Kaufman, H. Nesor: Calphad **2** (1978) 325–348.

[98Sau] N. Saunders, in: I. Ansara, A.T. Dinsdale, M.H. Rand (eds.): "Thermochemical database for light metal alloys", Vol. 2, EUR 18499, 1998, pp.95–98.

Al – Y (Aluminium – Yttrium)

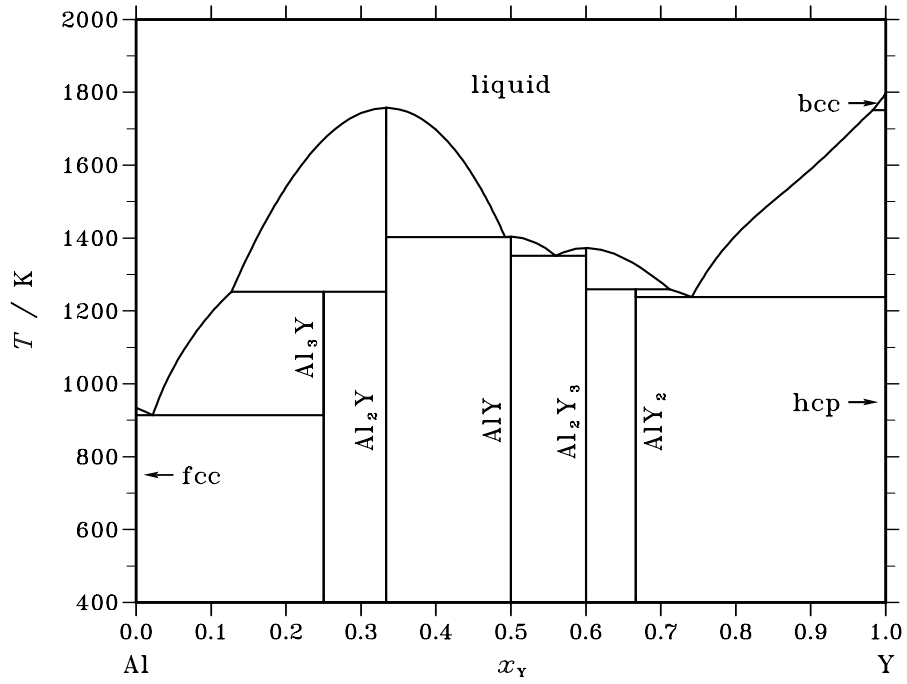

Fig. 1. Calculated phase diagram for the system Al-Y.

Yttrium is an important additive to refine the macro- and micro- structure of aluminium and its alloys resulting in an increase of hardness and strength but with little change of ductility. The thermodynamic parameters of the Al-Y system have been assessed by [89Ran] based on the phase diagram, calorimetric measurements of enthalpies of formation of Al_3Y and Al_2Y, enthalpies of mixing in the liquid phase, the chemical potential of Y derived from EMF measurements, and the chemical potential of Al obtained from vapour pressure data. [95Gro] re-assessed the thermodynamic parameters taking into account new calorimetric data on the enthalpy of formation of Al_2Y and Al_2Y_3. The thermodynamic dataset of [95Gro] has been accepted here. More recent calorimetric measurements for Al_2Y, Al_3Y, and Al_2Y_3 reported by [97Tim] are in good agreement with calculations of [95Gro].

The system is characterised by a complete miscibility in the liquid and very low (less than 0.1 mass-%) mutual solubility in the solid state. Five intermetallic compounds Al_3Y, Al_2Y, AlY, Al_2Y_3 and AlY_2 have been reported. The compound Al_3Y_5 reported by [87Ric] is most probably metastable [95Gro]. Two modifications of Al_3Y have been found by [60Sny] but only the high-temperature modification has been confirmed independently as a stable compound. The thermodynamic data are in agreement with the phase diagram and thermodynamic measurements. The experimental data for the chemical potential of Y and Al contradict the calculated values and other experimental information on the system. The liquid phase is described by a substitutional model and the intermetallic compounds are treated as stoichiometric phases. The mutual solubility of Al and Y in the solid phases is lower than 0.1 mass-%. Therefore, solid Al and Y are treated as stoichiometric phases.

Table I. Phases, structures and models.

Phase	Struktur-bericht	Prototype	Pearson symbol	Space group	SGTE name	Model
liquid					LIQUID	$(Al,Y)_1$
fcc	$A1$	Cu	$cF4$	$Fm\overline{3}m$	FCC_A1	Al_1
Al_3Y	$\cdots$	$BaPb_3$	$hR12$	$R\overline{3}m$	AL3Y	Al_3Y_1
Al_2Y	$C15$	Cu_2Mg	$cF24$	$Fd\overline{3}m$	C15_AL2Y	Al_2Y_1
AlY	$B33$	CrB	$oC8$	$Cmcm$	B33_ALY	Al_1Y_1
Al_2Y_3	$\cdots$	Al_2Zr_3	$tP20$	$P4_2/mnm$	AL2Y3	Al_2Y_3
AlY_2	$C23$	Co_2Si	$oP12$	$Pnma$	C23_ALY2	Al_1Y_2
bcc	$A2$	W	$cI2$	$Im\overline{3}m$	BCC_A2	Y_1
hcp	$A3$	Mg	$hP2$	$P6_3/mmc$	HCP_A3	Y_1

Table II. Invariant reactions.

Reaction	Type	T / K	Compositions / x_Y			$\Delta_r H$ / (J/mol)
liquid $\rightleftharpoons$ Al_2Y	congruent	1757.4	0.333	0.333		−24364
bcc $\rightleftharpoons$ liquid + hcp	degenerate	1751.1	1.000	0.983	1.000	−4886
liquid $\rightleftharpoons$ AlY	congruent	1403.9	0.500	0.500		−16280
liquid $\rightleftharpoons$ Al_2Y_3 + AlY	eutectic	1402.9	0.492	0.333	0.500	−16337
liquid $\rightleftharpoons$ Al_2Y_3	congruent	1372.9	0.600	0.600		−15827
liquid $\rightleftharpoons$ AlY + Al_2Y_3	eutectic	1351.2	0.560	0.500	0.600	−15434
Al_2Y_3 + liquid $\rightleftharpoons$ AlY_2	peritectic	1259.9	0.600	0.712	0.667	−9472
liquid + Al_2Y_3 $\rightleftharpoons$ Al_3Y_5	peritectic	1253.0	0.127	0.333	0.250	−14327
liquid $\rightleftharpoons$ AlY_2 + hcp	eutectic	1237.7	0.741	0.667	1.000	−14037
liquid $\rightleftharpoons$ fcc + Al_3Y_5	eutectic	914.1	0.022	0.000	0.250	−11441

Table IIIa. Integral quantities for the liquid phase at 1800 K.

x_Y	ΔG_m [J/mol]	ΔH_m [J/mol]	ΔS_m [J/(mol·K)]	G_m^E [J/mol]	S_m^E [J/(mol·K)]	ΔC_p [J/(mol·K)]
0.000	0	0	0.000	0	0.000	0.000
0.100	−14569	−14976	−0.226	−9704	−2.929	0.000
0.200	−25194	−27326	−1.184	−17705	−5.345	0.000
0.300	−32649	−36277	−2.015	−23507	−7.094	0.000
0.400	−36615	−40945	−2.406	−26543	−8.002	0.000
0.500	−36931	−40936	−2.225	−26557	−7.988	0.000
0.600	−33859	−36618	−1.533	−23786	−7.129	0.000
0.700	−28078	−29099	−0.567	−18936	−5.646	0.000
0.800	−20452	−19875	0.320	−12963	−3.840	0.000
0.900	−11518	−10178	0.744	−6653	−1.958	0.000
1.000	0	0	0.000	0	0.000	0.000

Reference states: Al(liquid), Y(liquid)

Table IIIb. Partial quantities for Al in the liquid phase at 1800 K.

x_{Al}	ΔG_{Al} [J/mol]	ΔH_{Al} [J/mol]	ΔS_{Al} [J/(mol·K)]	G^E_{Al} [J/mol]	S^E_{Al} [J/(mol·K)]	a_{Al}	γ_{Al}
1.000	0	0	0.000	0	0.000	1.000	1.000
0.900	−2377	−1233	0.635	−800	−0.241	0.853	0.948
0.800	−7033	−5700	0.741	−3693	−1.115	0.625	0.781
0.700	−15355	−15485	−0.072	−10017	−3.037	0.358	0.512
0.600	−28070	−31602	−1.963	−20424	−6.210	0.153	0.255
0.500	−44235	−52401	−4.537	−33861	−10.300	0.052	0.104
0.400	−61260	−73530	−6.817	−47547	−14.435	0.017	0.042
0.300	−75975	−89480	−7.503	−57957	−17.513	0.006	0.021
0.200	−86894	−96676	−5.434	−62807	−18.816	0.003	0.015
0.100	−98502	−98148	0.197	−64041	−18.948	0.001	0.014
0.000	−∞	−109760	∞	−71817	−21.080	0.000	0.008

Reference state: Al(liquid)

Table IIIc. Partial quantities for Y in the liquid phase at 1800 K.

x_Y	ΔG_Y [J/mol]	ΔH_Y [J/mol]	ΔS_Y [J/(mol·K)]	G^E_Y [J/mol]	S^E_Y [J/(mol·K)]	a_Y	γ_Y
0.000	−∞	−162299	∞	−105172	−31.737	0.000	0.001
0.100	−124299	−138661	−7.979	−89838	−27.124	0.000	0.002
0.200	−97840	−113832	−8.885	−73753	−22.267	0.001	0.007
0.300	−73002	−84792	−6.550	−54983	−16.561	0.008	0.025
0.400	−49433	−54960	−3.070	−35720	−10.689	0.037	0.092
0.500	−29627	−29471	0.087	−19254	−5.676	0.138	0.276
0.600	−15591	−12010	1.989	−7946	−2.258	0.353	0.588
0.700	−7550	−3221	2.405	−2212	−0.560	0.604	0.863
0.800	−3841	−675	1.759	−501	−0.097	0.774	0.967
0.900	−1853	−403	0.805	−276	−0.071	0.884	0.982
1.000	0	0	0.000	0	0.000	1.000	1.000

Reference state: Y(liquid)

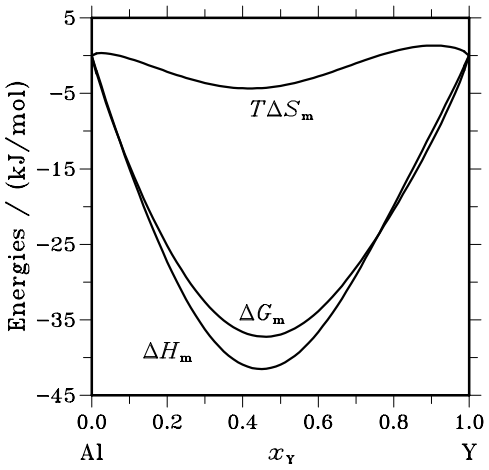

Fig. 2. Integral quantities of the liquid phase at T=1800 K.

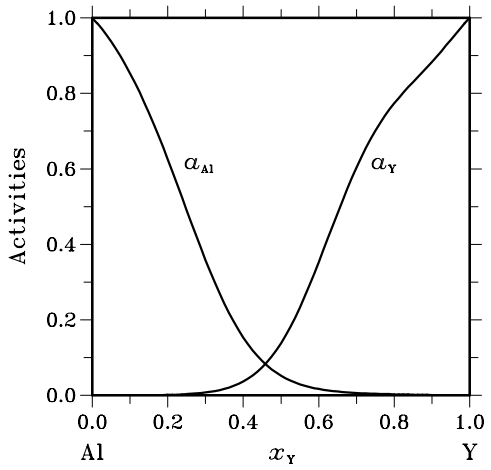

Fig. 3. Activities in the liquid phase at T=1800 K.

Table IV. Standard reaction quantities at 298.15 K for the compounds per mole of atoms.

Compound	x_{Y}	$\Delta_{\mathrm{f}}G^{\circ}$ / (J/mol)	$\Delta_{\mathrm{f}}H^{\circ}$ / (J/mol)	$\Delta_{\mathrm{f}}S^{\circ}$ / (J/(mol·K))	$\Delta_{\mathrm{f}}C_P^{\circ}$ / (J/(mol·K))
$\mathrm{Al_3Y_1}$	0.250	−44336	−47500	−10.613	0.000
$\mathrm{Al_2Y_1}$	0.333	−48736	−50400	−5.581	0.000
$\mathrm{Al_1Y_1}$	0.500	−43701	−45000	−4.358	0.000
$\mathrm{Al_2Y_3}$	0.600	−38795	−40000	−4.040	0.000
$\mathrm{Al_1Y_2}$	0.667	−33658	−35000	−4.500	0.000

References

[60Sny] R.L. Snyder: Ph.D. Thesis, Iowa State University, 1960.

[87Ric] R. Richter, Z. Altounian, J.O. Strom-Olsen, U. Koester, M. Blank-Bewersdorff: J. Mater. Sci. **22** (1987) 2983–2986.

[89Ran] Q. Ran, H.L. Lukas, G. Effenberg, G. Petzow: J. Less-Common Met. **146** (1989) 213–222.

[95Gro] J. Gröbner, H.L. Lukas, F. Aldinger: J. Alloys Comp. **220** (1995) 8–14.

[97Tim] V.S. Timofeev, A.A. Turchanin, A.A. Zubkov, I.A. Tomilin: Thermochim. Acta **299** (1997) 37–41.

Al – Zn (Aluminium – Zinc)

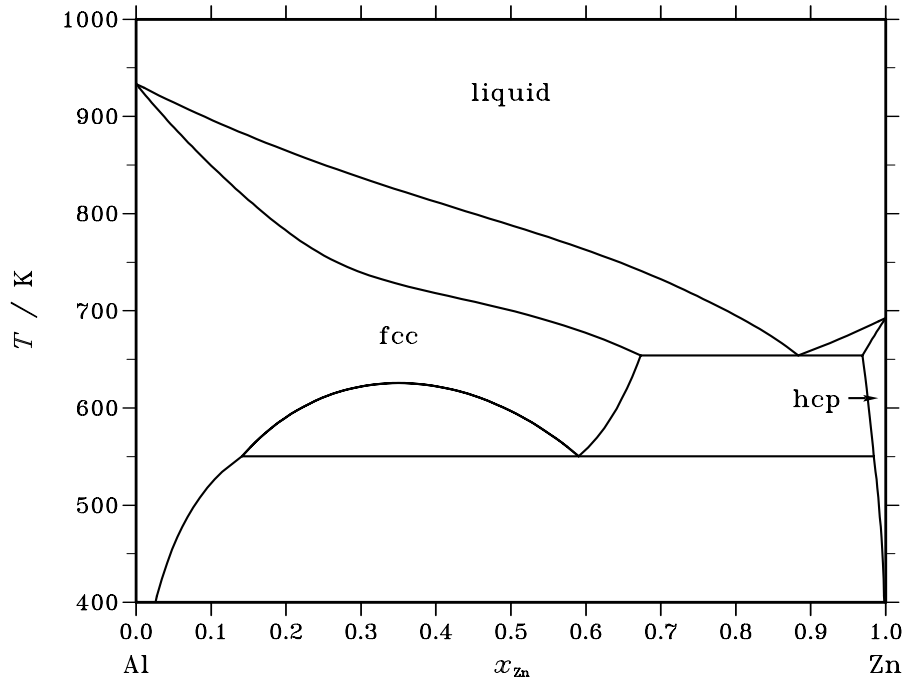

Fig. 1. Calculated phase diagram for the system Al-Zn.

The aluminium-zinc system is the basis of many technically important alloys. Medium-strength Al-Zn-Mg alloys are known for good weldability and the capability of hardening after welding. Adding Cu to these ternary alloys results in an appreciable increase of the strength.
An extensive review of experimental data on the Al-Zn system including an evaluation of the thermodynamic functions has been given by [83Mur]. The recommended assessment [93Mey] is an update of [86Mey]. The evaluation takes into account many experimental data from independent sources. The fit of the phase diagram is in very good agreement with experimental data throughout the whole composition and temperature range, except for the miscibility gap in the fcc-phase. Here, the experimental location of the critical point is around 40 at.% Zn, whereas the calculated value is 35 at.%. Accordingly, in fcc solid solutions calculated values for the enthalpy of mixing and the chemical potential of Zn differ from experimental data. In liquid alloys the corresponding calculated properties are in very good agreement with experiments.

Table I. Phases, structures and models.

Phase	Struktur-bericht	Prototype	Pearson symbol	Space group	SGTE name	Model
liquid					LIQUID	$(Al,Zn)_1$
fcc	$A1$	Cu	$cF4$	$Fm\overline{3}m$	FCC_A1	$(Al,Zn)_1$
hcp	$A3$	Mg	$hP2$	$P6_3/mmc$	HCP_ZN	$(Al,Zn)_1$

Table II. Invariant reactions.

Reaction	Type	T / K	Compositions / x_{Zn}			$\Delta_r H$ / (J/mol)
liquid $\rightleftharpoons$ fcc + hcp	eutectic	654.0	0.884	0.673	0.969	−7371
fcc $\rightleftharpoons$ fcc′ + fcc″	critical	625.2	0.350	0.350	0.350	0
fcc″ $\rightleftharpoons$ fcc′ + hcp	monotectoid	550.4	0.590	0.141	0.984	−2207

Table IIIa. Integral quantities for the liquid phase at 1000 K.

x_{Zn}	ΔG_{m} [J/mol]	ΔH_{m} [J/mol]	ΔS_{m} [J/(mol·K)]	$G_{\mathrm{m}}^{\mathrm{E}}$ [J/mol]	$S_{\mathrm{m}}^{\mathrm{E}}$ [J/(mol·K)]	ΔC_p [J/(mol·K)]
0.000	0	0	0.000	0	0.000	0.000
0.100	−2066	942	3.008	637	0.305	0.000
0.200	−3029	1674	4.703	1132	0.543	0.000
0.300	−3594	2198	5.791	1485	0.712	0.000
0.400	−3898	2512	6.410	1698	0.814	0.000
0.500	−3995	2616	6.611	1768	0.848	0.000
0.600	−3898	2512	6.410	1698	0.814	0.000
0.700	−3594	2198	5.791	1485	0.712	0.000
0.800	−3029	1674	4.703	1132	0.543	0.000
0.900	−2066	942	3.008	637	0.305	0.000
1.000	0	0	0.000	0	0.000	0.000

Reference states: Al(liquid), Zn(liquid)

Table IIIb. Partial quantities for Al in the liquid phase at 1000 K.

x_{Al}	ΔG_{Al} [J/mol]	ΔH_{Al} [J/mol]	ΔS_{Al} [J/(mol·K)]	$G_{\mathrm{Al}}^{\mathrm{E}}$ [J/mol]	$S_{\mathrm{Al}}^{\mathrm{E}}$ [J/(mol·K)]	a_{Al}	γ_{Al}
1.000	0	0	0.000	0	0.000	1.000	1.000
0.900	−805	105	0.910	71	0.034	0.908	1.009
0.800	−1572	419	1.991	283	0.136	0.828	1.035
0.700	−2329	942	3.271	637	0.305	0.756	1.080
0.600	−3116	1674	4.790	1132	0.543	0.687	1.146
0.500	−3995	2616	6.611	1768	0.848	0.618	1.237
0.400	−5072	3768	8.840	2546	1.221	0.543	1.358
0.300	−6545	5128	11.673	3466	1.662	0.455	1.517
0.200	−8855	6698	15.553	4527	2.171	0.345	1.724
0.100	−13416	8477	21.893	5729	2.748	0.199	1.992
0.000	$-\infty$	10466	∞	7073	3.393	0.000	2.341

Reference state: Al(liquid)

Table IIIc. Partial quantities for Zn in the liquid phase at 1000 K.

x_{Zn}	ΔG_{Zn} [J/mol]	ΔH_{Zn} [J/mol]	ΔS_{Zn} [J/(mol·K)]	$G_{\mathrm{Zn}}^{\mathrm{E}}$ [J/mol]	$S_{\mathrm{Zn}}^{\mathrm{E}}$ [J/(mol·K)]	a_{Zn}	γ_{Zn}
0.000	$-\infty$	10466	∞	7073	3.393	0.000	2.341
0.100	−13416	8477	21.893	5729	2.748	0.199	1.992
0.200	−8855	6698	15.553	4527	2.171	0.345	1.724
0.300	−6545	5128	11.673	3466	1.662	0.455	1.517
0.400	−5072	3768	8.840	2546	1.221	0.543	1.358
0.500	−3995	2616	6.611	1768	0.848	0.618	1.237
0.600	−3116	1674	4.790	1132	0.543	0.687	1.146
0.700	−2329	942	3.271	637	0.305	0.756	1.080
0.800	−1572	419	1.991	283	0.136	0.828	1.035
0.900	−805	105	0.910	71	0.034	0.908	1.009
1.000	0	0	0.000	0	0.000	1.000	1.000

Reference state: Zn(liquid)

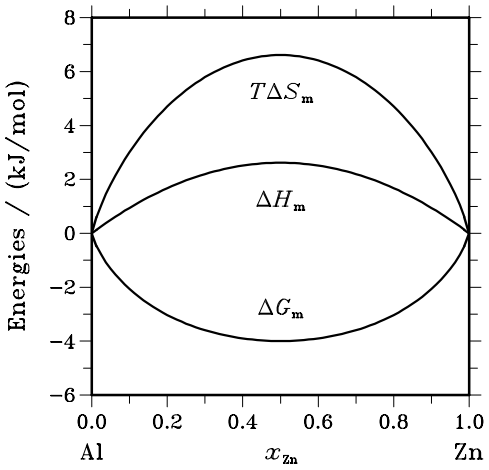

Fig. 2. Integral quantities of the liquid phase at T=1000 K.

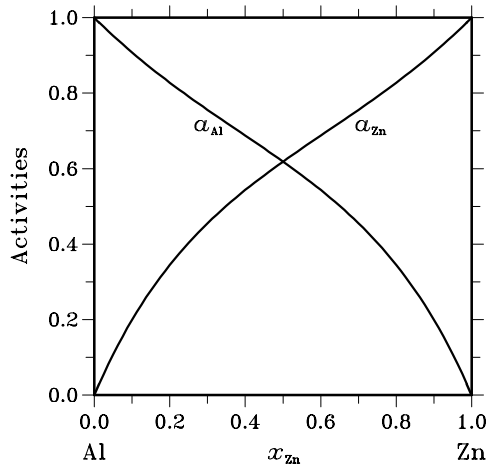

Fig. 3. Activities in the liquid phase at T=1000 K.

Table IVa. Integral quantities for the stable phases at 650 K.

Phase	x_{Zn}	ΔG_m [J/mol]	ΔH_m [J/mol]	ΔS_m [J/(mol·K)]	G^E_m [J/mol]	S^E_m [J/(mol·K)]	ΔC_p [J/(mol·K)]
fcc	0.000	0	0	0.000	0	0.000	0.000
	0.100	−671	1251	2.957	1086	0.254	0.000
	0.200	−804	2218	4.649	1901	0.488	0.000
	0.300	−846	2875	5.725	2455	0.646	0.000
	0.400	−867	3227	6.298	2770	0.702	0.000
	0.500	−870	3309	6.429	2876	0.666	0.000
	0.600	−825	3186	6.171	2812	0.576	0.000
	0.671	−734	3024	5.782	2689	0.516	0.000
hcp	0.970	−204	735	1.444	529	0.317	0.000
	1.000	0	0	0.000	0	0.000	0.000

Reference states: Al(fcc), Zn(hcp)

Table IVb. Partial quantities for Al in the stable phases at 650 K.

Phase	x_{Al}	ΔG_{Al} [J/mol]	ΔH_{Al} [J/mol]	ΔS_{Al} [J/(mol·K)]	G^E_{Al} [J/mol]	S^E_{Al} [J/(mol·K)]	a_{Al}	γ_{Al}
fcc	1.000	0	0	0.000	0	0.000	1.000	1.000
	0.900	−432	136	0.874	137	−0.002	0.923	1.026
	0.800	−669	591	1.939	537	0.083	0.884	1.104
	0.700	−764	1371	3.286	1163	0.320	0.868	1.240
	0.600	−810	2391	4.925	1951	0.677	0.861	1.435
	0.500	−937	3478	6.792	2809	1.029	0.841	1.682
	0.400	−1334	4368	8.772	3618	1.154	0.781	1.953
	0.329	−1927	4691	10.182	4084	0.934	0.700	2.129
hcp	0.030	−1927	23624	39.309	16982	10.219	0.700	23.154
	0.000	$-\infty$	25006	∞	18017	10.752	0.000	28.041

Reference state: Al(fcc)

Table IVc. Partial quantities for Zn in the stable phases at 650 K.

Phase	x_{Zn}	ΔG_{Zn} [J/mol]	ΔH_{Zn} [J/mol]	ΔS_{Zn} [J/(mol·K)]	G^E_{Zn} [J/mol]	S^E_{Zn} [J/(mol·K)]	a_{Zn}	γ_{Zn}
fcc	0.000	$-\infty$	13783	∞	12236	2.379	0.000	9.623
	0.100	−2816	11292	21.704	9628	2.559	0.594	5.939
	0.200	−1343	8725	15.489	7355	2.107	0.780	3.900
	0.300	−1037	6383	11.416	5470	1.405	0.825	2.751
	0.400	−952	4481	8.359	4000	0.740	0.838	2.096
	0.500	−802	3141	6.066	2944	0.303	0.862	1.724
	0.600	−486	2398	4.437	2275	0.190	0.914	1.523
	0.671	−150	2207	3.627	2005	0.311	0.973	1.449
hcp	0.970	−150	21	0.263	16	0.008	0.973	1.003
	1.000	0	0	0.000	0	0.000	1.000	1.000

Reference state: Zn(hcp)

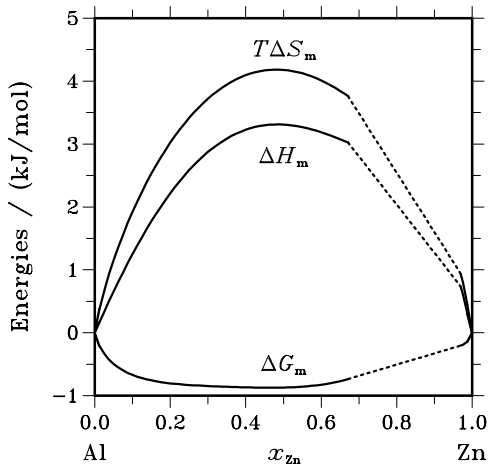

Fig. 4. Integral quantities of the stable phases at T=650 K.

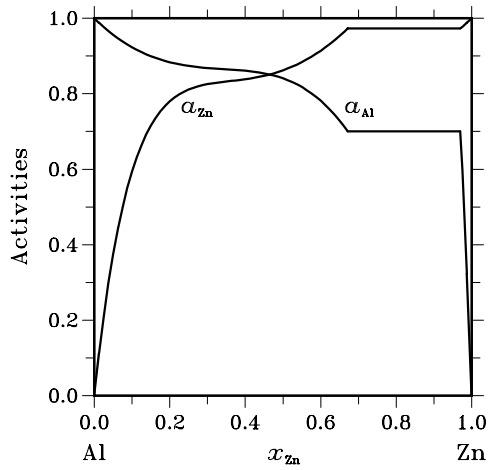

Fig. 5. Activities in the stable phases at T=650 K.

References

[83Mur] J.L. Murray: Bull. Alloy Phase Diagrams **4** (1983) 55–73.
[86Mey] S. an Mey, G. Effenberg: Z. Metallkd. **77** (1986) 449–453.
[93Mey] S. an Mey: Z. Metallkd. **84** (1993) 451–455.

Al – Zr (Aluminium – Zirconium)

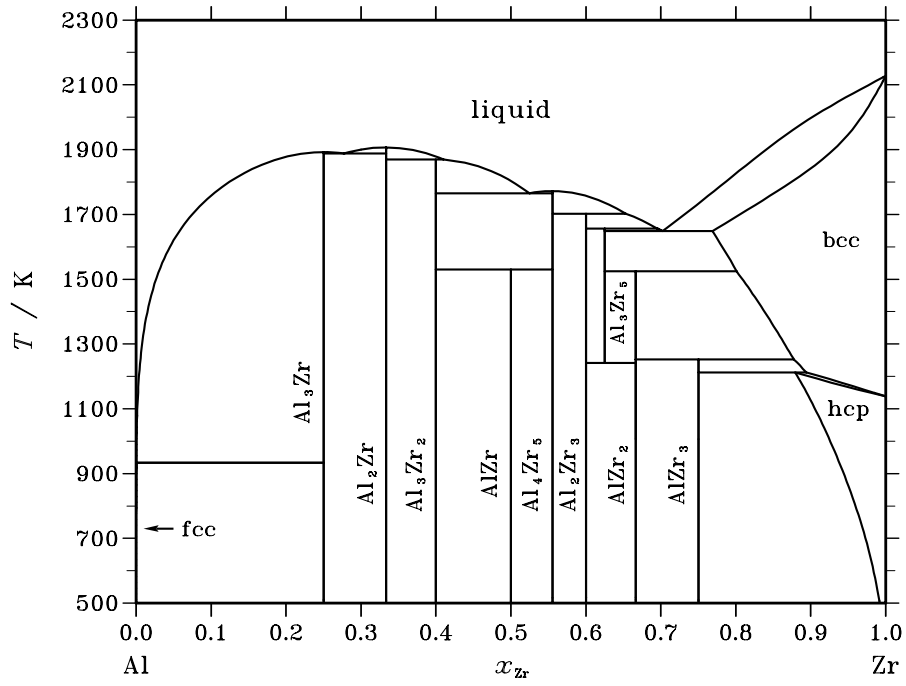

Fig. 1. Calculated phase diagram for the system Al-Zr.

Zirconium can be added in combination with Cr to Al-alloys in order to produce alloys with high specific modulus and desirable high-temperature properties. The System Al–Zr has been reviewed and critically assessed by [86Sau, 92Mur, 92Mas]. The selected dataset [98Sau] is an update of [86Sau]. The liquidus curve, the solidus curve with bcc-Zr, the phase boundaries between hcp-Zr and bcc-Zr as well as those between bcc-Zr and Zr_3Al have to be considered uncertain. According to Saunders [86Sau] the phase Zr_4Al_3 does not exist while Zr_5Al_4 is stable down to low temperatures. An internally consistent set of Gibbs energy data for the system has been derived from an optimization including phase diagram data and heats of formations of the compounds.

Table I. Phases, structures and models.

Phase	Struktur-bericht	Prototype	Pearson symbol	Space group	SGTE name	Model
liquid					LIQUID	$(Al,Zr)_1$
fcc	$A1$	Cu	$cF4$	$Fm\overline{3}m$	FCC_A1	$(Al,Zr)_1$
Al_3Zr	$D0_{23}$	Al_3Zr	$tI16$	$I4/mmm$	D022_AL3ZR	Al_3Zr_1
Al_2Zr	$C14$	$MgZn_2$	$hP12$	$P6_3/mmc$	C14_AL2ZR	Al_2Zr_1
Al_3Zr_2	···	Al_3Zr_2	$oF40$	$Fdd2$	AL3ZR2	Al_3Zr_2
AlZr	B_f	BCr	$oC8$	$Cmcm$	C23_ALZR	Al_1Zr_1
Al_4Zr_5	···	Ga_4Ti_5	$hP18$	$P6_3/mcm$	AL4ZR5	Al_4Zr_5
Al_2Zr_3	···	Al_2Zr_3	$tP20$	$P4_2/mnm$	AL2ZR3	Al_2Zr_3
Al_3Zr_5	$D8_m$	W_5Si_3	$tI32$	$I4/mcm$	D8M_AL3ZR5	Al_3Zr_5
$AlZr_2$	$B8_2$	Ni_2In	$hP6$	$P6_3/mmc$	D82_ALZR2	Al_1Zr_2
$AlZr_3$	$L1_2$	$AuCu_3$	$cP4$	$Pm\overline{3}m$	L12_ALZR3	Al_1Zr_3
bcc	$A2$	W	$cI2$	$Im\overline{3}m$	BCC_A2	$(Al,Zr)_1$
hcp	$A3$	Mg	$hP2$	$P6_3/mmc$	HCP_A3	$(Al,Zr)_1$

Table II. Invariant reactions.

Reaction	Type	T / K	Compositions / x_{Zr}			$\Delta_{\mathrm{r}}H$ / (J/mol)
liquid $\rightleftharpoons$ Al_2Zr	congruent	1906.9	0.333	0.333		−30688
liquid $\rightleftharpoons$ Al_3Zr	congruent	1892.3	0.250	0.250		−29366
liquid $\rightleftharpoons$ Al_3Zr + Al_2Zr	eutectic	1887.9	0.277	0.250	0.333	−29588
Al_2Zr + liquid $\rightleftharpoons$ Al_3Zr_2	peritectic	1869.1	0.333	0.410	0.400	−26124
liquid $\rightleftharpoons$ Al_4Zr_5	congruent	1772.5	0.556	0.556		−25170
liquid $\rightleftharpoons$ Al_3Zr_2 + Al_4Zr_5	eutectic	1765.3	0.525	0.400	0.556	−25613
Al_4Zr_5 + liquid $\rightleftharpoons$ Al_2Zr_3	peritectic	1701.8	0.556	0.653	0.600	−10704
Al_2Zr_3 + liquid $\rightleftharpoons$ Al_3Zr_5	peritectic	1655.8	0.600	0.696	0.625	−5422
liquid $\rightleftharpoons$ Al_3Zr_5 + bcc	eutectic	1648.7	0.702	0.625	0.769	−17128
Al_3Zr_2 + Al_4Zr_5 $\rightleftharpoons$ AlZr	peritectoid	1529.5	0.400	0.556	0.500	−1379
Al_3Zr_5 + bcc $\rightleftharpoons$ $AlZr_2$	peritectoid	1524.3	0.625	0.801	0.667	−2289
$AlZr_2$ + bcc $\rightleftharpoons$ $AlZr_3$	peritectoid	1252.4	0.667	0.877	0.750	−3993
Al_3Zr_5 $\rightleftharpoons$ Al_2Zr_3 + $AlZr_2$	eutectoid	1241.6	0.625	0.600	0.667	−285
$AlZr_3$ + bcc $\rightleftharpoons$ hcp	peritectoid	1212.1	0.750	0.894	0.879	−2871
liquid + Al_3Zr $\rightleftharpoons$ fcc	peritectic	933.8	0.000	0.250	0.001	−10657

Table IIIa. Integral quantities for the liquid phase at 2200 K.

x_{Zr}	ΔG_{m} [J/mol]	ΔH_{m} [J/mol]	ΔS_{m} [J/(mol·K)]	$G_{\mathrm{m}}^{\mathrm{E}}$ [J/mol]	$S_{\mathrm{m}}^{\mathrm{E}}$ [J/(mol·K)]	ΔC_p [J/(mol·K)]
0.000	0	0	0.000	0	0.000	0.000
0.100	−9197	−11063	−0.848	−3251	−3.551	0.000
0.200	−15710	−20053	−1.974	−6556	−6.135	0.000
0.300	−20535	−26561	−2.739	−9361	−7.818	0.000
0.400	−23571	−30329	−3.072	−11261	−8.667	0.000
0.500	−24679	−31250	−2.987	−12000	−8.750	0.000
0.600	−23788	−29369	−2.537	−11477	−8.133	0.000
0.700	−20914	−24881	−1.803	−9740	−6.882	0.000
0.800	−16143	−18133	−0.905	−6989	−5.065	0.000
0.900	−9521	−9623	−0.046	−3575	−2.749	0.000
1.000	0	0	0.000	0	0.000	0.000

Reference states: Al(liquid), Zr(liquid)

Table IIIb. Partial quantities for Al in the liquid phase at 2200 K.

x_{Al}	ΔG_{Al} [J/mol]	ΔH_{Al} [J/mol]	ΔS_{Al} [J/(mol·K)]	G^E_{Al} [J/mol]	S^E_{Al} [J/(mol·K)]	a_{Al}	γ_{Al}
1.000	0	0	0.000	0	0.000	1.000	1.000
0.900	−1794	−956	0.381	133	−0.495	0.907	1.007
0.800	−4367	−4444	−0.035	−285	−1.890	0.788	0.985
0.700	−8665	−11056	−1.087	−2140	−4.052	0.623	0.890
0.600	−15209	−20930	−2.600	−5865	−6.848	0.435	0.726
0.500	−24116	−33750	−4.379	−11437	−10.142	0.268	0.535
0.400	−35142	−48748	−6.185	−18381	−13.803	0.146	0.366
0.300	−47792	−64700	−7.685	−25769	−17.696	0.073	0.244
0.200	−61658	−79930	−8.305	−32218	−21.687	0.034	0.172
0.100	−78012	−92308	−6.498	−35893	−25.643	0.014	0.141
0.000	−∞	−99250	∞	−34504	−29.430	0.000	0.152

Reference state: Al(liquid)

Table IIIc. Partial quantities for Zr in the liquid phase at 2200 K.

x_{Zr}	ΔG_{Zr} [J/mol]	ΔH_{Zr} [J/mol]	ΔS_{Zr} [J/(mol·K)]	G^E_{Zr} [J/mol]	S^E_{Zr} [J/(mol·K)]	a_{Zr}	γ_{Zr}
0.000	−∞	−119250	∞	−29996	−40.570	0.000	0.194
0.100	−75821	−102028	−11.912	−33702	−31.057	0.016	0.158
0.200	−61081	−82490	−9.731	−31641	−23.113	0.035	0.177
0.300	−48234	−62740	−6.594	−26211	−16.604	0.072	0.239
0.400	−36115	−44428	−3.778	−19355	−11.397	0.139	0.347
0.500	−25243	−28750	−1.594	−12564	−7.358	0.252	0.503
0.600	−16219	−16450	−0.105	−6875	−4.352	0.412	0.687
0.700	−9395	−7816	0.718	−2871	−2.248	0.598	0.855
0.800	−4764	−2684	0.945	−682	−0.910	0.771	0.963
0.900	−1911	−436	0.671	16	−0.205	0.901	1.001
1.000	0	0	0.000	0	0.000	1.000	1.000

Reference state: Zr(liquid)

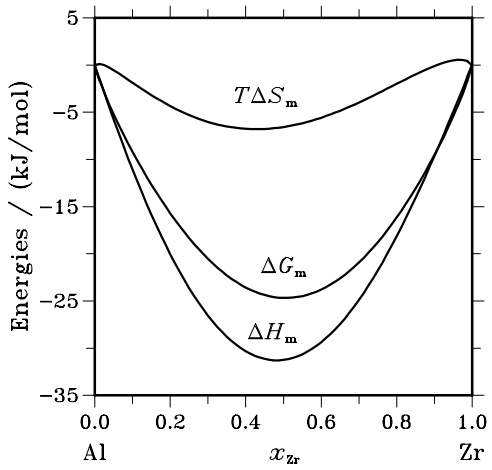

Fig. 2. Integral quantities of the liquid phase at T=2200 K.

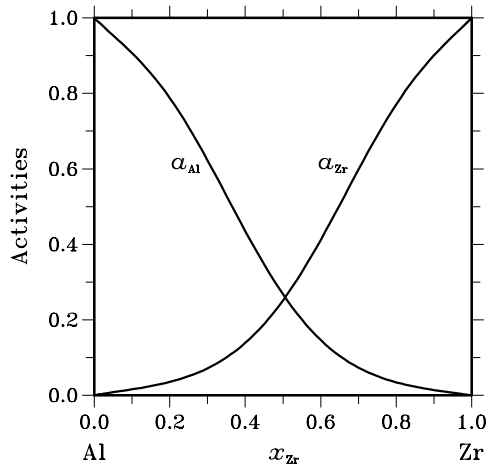

Fig. 3. Activities in the liquid phase at T=2200 K.

Table IV. Standard reaction quantities at 298.15 K for the compounds per mole of atoms.

Compound	x_{Zr}	$\Delta_{\mathrm{f}}G^{\circ}$ / (J/mol)	$\Delta_{\mathrm{f}}H^{\circ}$ / (J/mol)	$\Delta_{\mathrm{f}}S^{\circ}$ / (J/(mol·K))	$\Delta_{\mathrm{f}}C_P^{\circ}$ / (J/(mol·K))
Al_3Zr_1	0.250	−38469	−40625	−7.230	0.000
Al_2Zr_1	0.333	−43282	−45810	−8.480	0.000
Al_3Zr_2	0.400	−44310	−46940	−8.820	0.000
Al_1Zr_1	0.500	−41960	−44500	−8.519	0.000
Al_4Zr_5	0.556	−38928	−41000	−6.950	0.000
Al_2Zr_3	0.600	−36459	−38427	−6.600	0.000
Al_3Zr_5	0.625	−34432	−36248	−6.090	0.000
Al_1Zr_2	0.667	−31631	−33375	−5.851	0.000
Al_1Zr_3	0.750	−25332	−27000	−5.595	0.000

References

[86Sau] N. Saunders, V.G. Rivlin: Mater. Sci. Technol. **2** (1986) 521–527.

[92Mur] Z. Murray, A. Peruzzi, J.P. Abriata: J. Phase Equilibria **13** (1992) 277–291.

[92Mas] T.B. Massalski, Ed.: "Binary Alloy Phase Diagrams", ASM International, Materials Park, Ohio, 1992.

[98Sau] N. Saunders in: I. Ansara, A.T. Dinsdale, M.H. Rand (eds.): COST 507, "Thermochemical database for light metal alloys", Vol. 2, EUR 18499, 1998, 112–116.

As – Au (Arsenic – Gold)

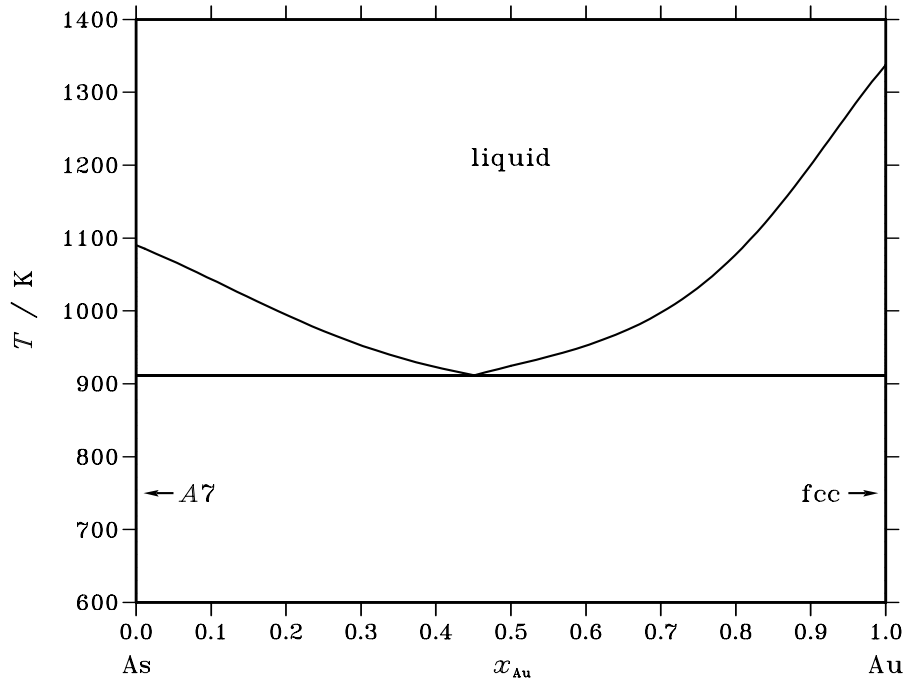

Fig. 1. Calculated phase diagram for the system As-Au.

The As-Au system is a simple eutectic with no significant solid state solubility of either component in the other. The present thermodynamic description [98Spe] gives a good representation of the reported phase diagram and indicates small positive departures from ideality of activity and enthalpy of mixing values for the liquid phase. The dataset is based on DTA data [76Gat] and on the critical assessment of [84Oka].

Table I. Phases, structures and models.

Phase	Struktur-bericht	Prototype	Pearson symbol	Space group	SGTE name	Model
liquid					LIQUID	$(As,Au)_1$
$A7$	$A7$	αAs	$hR2$	$R\overline{3}m$	RHOMBOHEDRAL_A7	As_1
fcc	$A1$	Cu	$cF4$	$Fm\overline{3}m$	FCC_A1	$(As,Au)_1$

Table II. Invariant reactions.

Reaction	Type	T / K	Compositions / x_{Au}			$\Delta_r H$ / (J/mol)
liquid $\rightleftharpoons$ A7 + fcc	eutectic	911.8	0.451	0.000	1.000	−23246

Table IIIa. Integral quantities for the liquid phase at 1400 K.

x_{Au}	ΔG_{m} [J/mol]	ΔH_{m} [J/mol]	ΔS_{m} [J/(mol·K)]	$G_{\mathrm{m}}^{\mathrm{E}}$ [J/mol]	$S_{\mathrm{m}}^{\mathrm{E}}$ [J/(mol·K)]	ΔC_p [J/(mol·K)]
0.000	0	0	0.000	0	0.000	0.000
0.100	−3851	405	3.040	−67	0.337	0.000
0.200	−5895	1361	5.183	−70	1.022	0.000
0.300	−7222	2545	6.977	−112	1.898	0.000
0.400	−8078	3681	8.399	−244	2.804	0.000
0.500	−8543	4540	9.345	−475	3.582	0.000
0.600	−8596	4942	9.669	−761	4.074	0.000
0.700	−8127	4751	9.199	−1017	4.120	0.000
0.800	−6930	3883	7.723	−1105	3.562	0.000
0.900	−4627	2296	4.945	−843	2.242	0.000
1.000	0	0	0.000	0	0.000	0.000

Reference states: As(liquid), Au(liquid)

Table IIIb. Partial quantities for As in the liquid phase at 1400 K.

x_{As}	ΔG_{As} [J/mol]	ΔH_{As} [J/mol]	ΔS_{As} [J/(mol·K)]	$G_{\mathrm{As}}^{\mathrm{E}}$ [J/mol]	$S_{\mathrm{As}}^{\mathrm{E}}$ [J/(mol·K)]	a_{As}	γ_{As}
1.000	0	0	0.000	0	0.000	1.000	1.000
0.900	−1279	−333	0.675	−52	−0.201	0.896	0.996
0.800	−2649	−879	1.264	−51	−0.591	0.796	0.996
0.700	−4017	−1061	2.112	134	−0.854	0.708	1.012
0.600	−5453	−446	3.576	493	−0.671	0.626	1.043
0.500	−7196	1257	6.038	873	0.274	0.539	1.078
0.400	−9688	4198	9.919	977	2.300	0.435	1.088
0.300	−13644	8385	15.734	371	5.724	0.310	1.032
0.200	−20260	13682	24.245	−1526	10.863	0.175	0.877
0.100	−32237	19815	37.180	−5434	18.035	0.063	0.627
0.000	$-\infty$	26365	∞	−12215	27.558	0.000	0.350

Reference state: As(liquid)

Table IIIc. Partial quantities for Au in the liquid phase at 1400 K.

x_{Au}	ΔG_{Au} [J/mol]	ΔH_{Au} [J/mol]	ΔS_{Au} [J/(mol·K)]	$G_{\mathrm{Au}}^{\mathrm{E}}$ [J/mol]	$S_{\mathrm{Au}}^{\mathrm{E}}$ [J/(mol·K)]	a_{Au}	γ_{Au}
0.000	$-\infty$	100	∞	−1437	1.098	0.000	0.884
0.100	−26999	7050	24.321	−196	5.176	0.098	0.983
0.200	−18881	10320	20.858	−146	7.476	0.197	0.987
0.300	−14700	10959	18.327	−685	8.317	0.283	0.943
0.400	−12016	9871	15.634	−1350	8.016	0.356	0.890
0.500	−9890	7823	12.653	−1822	6.889	0.428	0.855
0.600	−7867	5437	9.503	−1921	5.256	0.509	0.848
0.700	−5763	3194	6.398	−1612	3.433	0.609	0.871
0.800	−3597	1433	3.593	−1000	1.737	0.734	0.918
0.900	−1559	350	1.363	−333	0.487	0.875	0.972
1.000	0	0	0.000	0	0.000	1.000	1.000

Reference state: Au(liquid)

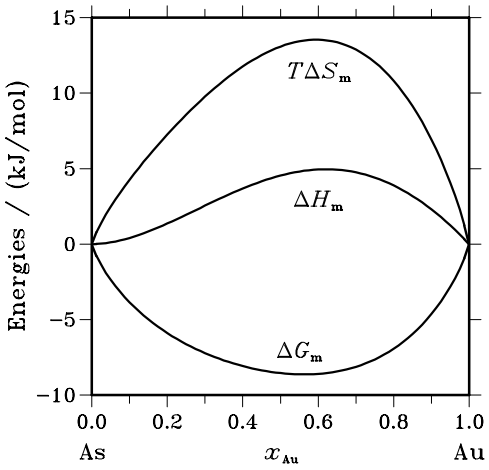

Fig. 2. Integral quantities of the liquid phase at T=1400 K.

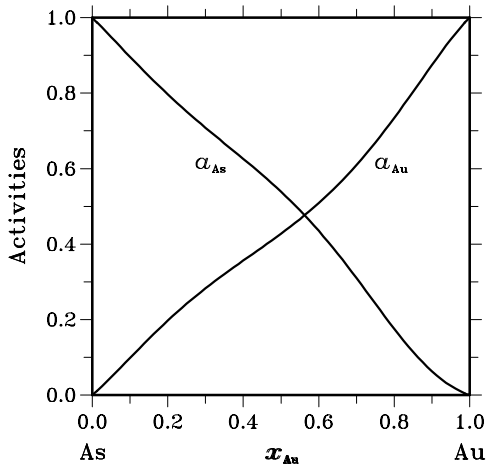

Fig. 3. Activities in the liquid phase at T=1400 K.

References

[76Gat] B. Gather, R. Blachnik: Z. Metallkd. **67** (1976) 168–169.
[84Oka] H. Okamoto, T.B. Massalski: Bull. Alloy Phase Diagrams **5** (1984) 56–59.
[98Spe] P.J. Spencer, unpublished assessment, 1998.

As – Cu (Arsenic – Copper)

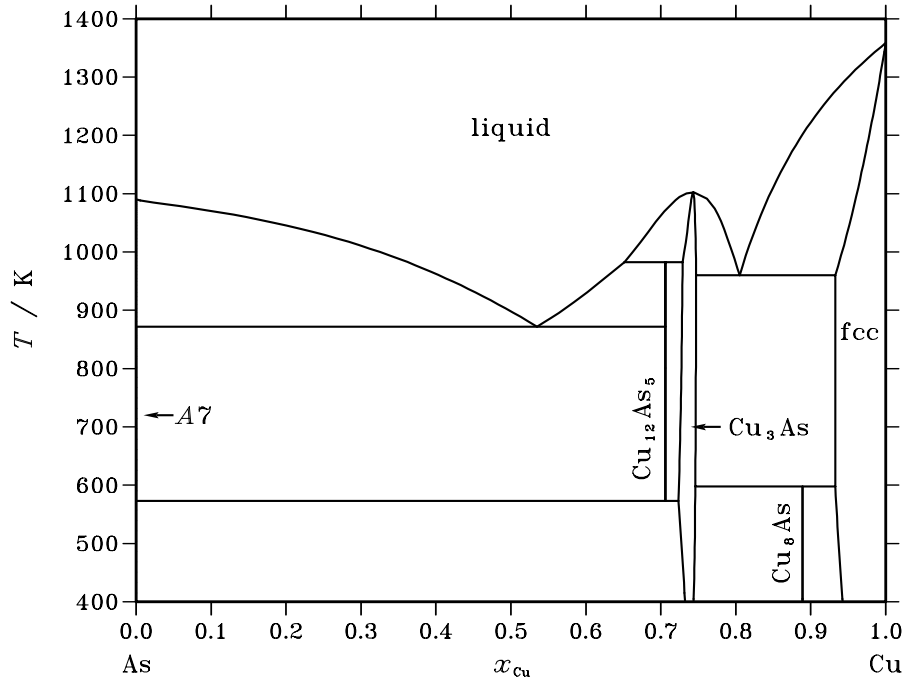

Fig. 1. Calculated phase diagram for the system As-Cu.

Arsenic is a harmful impurity in copper ores which deserves special special attention in copper smelting. The As-Cu system has been reviewed by [88Sub] and thermodynamically assessed by [91Tep, 94Pei]. The dataset of [94Pei] is recommendet here because it provides a good and consistent description of the available experimental data. The optimization includes data on the phase equilibria across the whole composition range. The liquidus in the concentration range below 50 at.% As has been determined in very many investigations. In addition, the component activies in the liquid have been optimised in the range below 40 at.% As. For the solid solution of As in fcc-Cu, the calculated partial molar Gibbs energy of As shows larger deviations from the experimental data. For the intermediate phases no other thermodynamic information have been available than the data from the phase diagram.

Table I. Phases, structures and models.

Phase	Struktur-bericht	Prototype	Pearson symbol	Space group	SGTE name	Model
liquid					IONIC_LIQ	$Cu_p^+(As,As^{3-},\square^-)_1$
$A7$	$A7$	αAs	$hR2$	$R\bar{3}m$	RHOMBO_A7	As_1
Cu_8As	$A3$	Mg	$hP2$	$P6_3/mmc$	CU8AS	As_1Cu_8
Cu_3As	$\cdots$	Cu_3As	$hP24$	$P\bar{3}c1$	CU3AS	$(Cu,\square)_3As_1$
$Cu_{12}As_5$	$D0_3$	BiF_3	$cF16$	$Fm\bar{3}m$	CU12AS5	$Cu_{12}As_5$
fcc	$A1$	Cu	$cF4$	$Fm\bar{3}m$	FCC_A1	$(As,Cu)_1$

Table II. Invariant reactions.

Reaction	Type	T / K	Compositions / x_{Cu}			$\Delta_{\mathrm{r}}H$ / (J/mol)
liquid ⇌ Cu_3As	congruent	1102.5	0.743	0.743		−6913
liquid + Cu_3As ⇌ $Cu_{12}As_5$	peritectic	982.7	0.652	0.729	0.706	−2929
liquid ⇌ Cu_3As + fcc	eutectic	960.1	0.805	0.747	0.933	−7020
liquid ⇌ $A7$ + $Cu_{12}As_5$	eutectic	872.1	0.535	0.000	0.706	−15368
Cu_3As + fcc ⇌ Cu_8As	peritectoid	597.8	0.746	0.933	0.889	−183
$Cu_{12}As_5$ ⇌ $A7$ + Cu_3As	eutectoid	573.1	0.706	0.000	0.723	−407

Table IIIa. Integral quantities for the liquid phase at 1423 K.

x_{Cu}	ΔG_{m} [J/mol]	ΔH_{m} [J/mol]	ΔS_{m} [J/(mol·K)]	$G^{\mathrm{E}}_{\mathrm{m}}$ [J/mol]	$S^{\mathrm{E}}_{\mathrm{m}}$ [J/(mol·K)]	ΔC_p [J/(mol·K)]
0.000	0	0	0.000	0	0.000	0.000
0.100	−5874	709	4.627	−2028	1.924	0.000
0.200	−10860	1326	8.564	−4940	4.404	0.000
0.300	−15288	1732	11.961	−8060	6.882	0.000
0.400	−19093	1814	14.693	−11130	9.097	0.000
0.500	−22062	1377	16.472	−13861	10.709	0.000
0.600	−23732	47	16.711	−15769	11.115	0.000
0.700	−23096	−2702	14.332	−15869	9.253	0.000
0.800	−18927	−4346	10.247	−13006	6.086	0.000
0.900	−11109	−2301	6.190	−7263	3.487	0.000
1.000	0	0	0.000	0	0.000	0.000

Reference states: As(liquid), Cu(liquid)

Table IIIb. Partial quantities for As in the liquid phase at 1423 K.

x_{As}	ΔG_{As} [J/mol]	ΔH_{As} [J/mol]	ΔS_{As} [J/(mol·K)]	$G^{\mathrm{E}}_{\mathrm{As}}$ [J/mol]	$S^{\mathrm{E}}_{\mathrm{As}}$ [J/(mol·K)]	a_{As}	γ_{As}
1.000	0	0	0.000	0	0.000	1.000	1.000
0.900	−587	23	0.430	658	−0.446	0.952	1.057
0.800	−1449	282	1.217	1190	−0.638	0.885	1.106
0.700	−2873	914	2.662	1346	−0.303	0.784	1.121
0.600	−5342	2359	5.413	701	1.166	0.637	1.061
0.500	−9919	5388	10.758	−1718	4.995	0.432	0.865
0.400	−19228	11874	21.857	−8387	14.239	0.197	0.492
0.300	−39203	20261	41.788	−24958	31.778	0.036	0.121
0.200	−67372	−12284	38.713	−48330	25.331	0.003	0.017
0.100	−95019	−23729	50.098	−67776	30.953	0.000	0.003
0.000	$-\infty$	−23843	∞	−76887	37.276	0.000	0.002

Reference state: As(liquid)

Table IIIc. Partial quantities for Cu in the liquid phase at 1423 K.

x_{Cu}	ΔG_{Cu} [J/mol]	ΔH_{Cu} [J/mol]	ΔS_{Cu} [J/(mol·K)]	$G^{\mathrm{E}}_{\mathrm{Cu}}$ [J/mol]	$S^{\mathrm{E}}_{\mathrm{Cu}}$ [J/(mol·K)]	a_{Cu}	γ_{Cu}
0.000	$-\infty$	0	∞	0	0	0.000	1.000
0.100	−53458	6960	42.459	−26215	23.314	0.011	0.109
0.200	−48504	5536	37.977	−29462	24.595	0.017	0.083
0.300	−44256	3608	33.637	−30011	23.627	0.024	0.079
0.400	−39719	1009	28.622	−28878	21.003	0.035	0.087
0.500	−34205	−2623	22.194	−26004	16.431	0.056	0.111
0.600	−26735	−7840	13.278	−20691	9.031	0.104	0.174
0.700	−16193	−12543	2.565	−11973	−0.400	0.254	0.363
0.800	−6815	−2359	3.132	−4175	1.276	0.562	0.703
0.900	−1786	331	1.489	−539	0.613	0.860	0.955
1.000	0	0	0.000	0	0.000	1.000	1.000

Reference state: Cu(liquid)

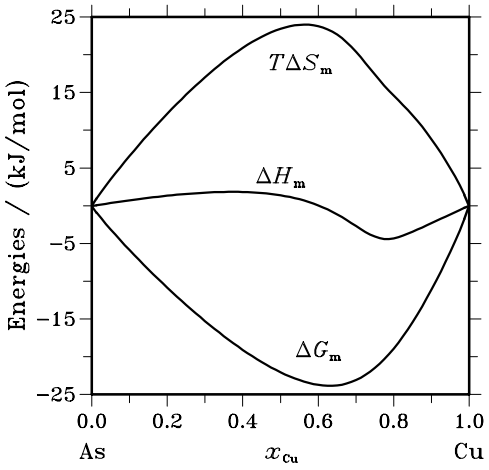

Fig. 2. Integral quantities of the liquid phase at T=1423 K.

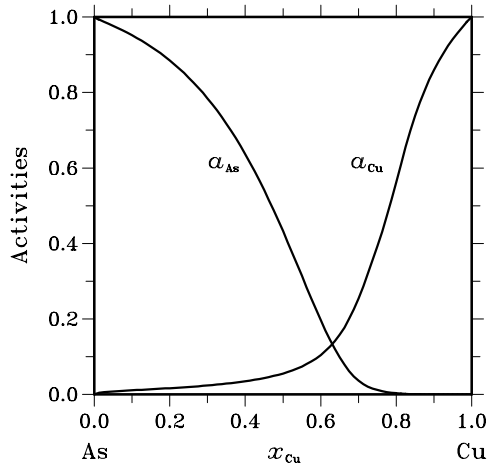

Fig. 3. Activities in the liquid phase at T=1423 K.

Table IV. Standard reaction quantities at 298.15 K for the compounds per mole of atoms.

Compound	x_{Cu}	$\Delta_{\mathrm{f}}G^{\circ}$ / (J/mol)	$\Delta_{\mathrm{f}}H^{\circ}$ / (J/mol)	$\Delta_{\mathrm{f}}S^{\circ}$ / (J/(mol·K))	$\Delta_{\mathrm{f}}C^{\circ}_{P}$ / (J/(mol·K))
$Cu_{12}As_5$	0.706	−548	5216	19.334	0.000
Cu_8As_1	0.889	−621	1864	8.336	0.000

References

[88Sub] P.R. Subramanian, D.E. Laughlin: Bull. Alloy Phase Diagrams **9** (1988) 605–618.
[91Tep] O. Teppo, P. Taskinen: Scand. J. Metall. **20** (1991) 141–148.
[94Pei] B. Pei, B. Björkman, B. Jansson, B. Sundman: Z. Metallkd. **85** (1994) 178–184.

As – Fe (Arsenic – Iron)

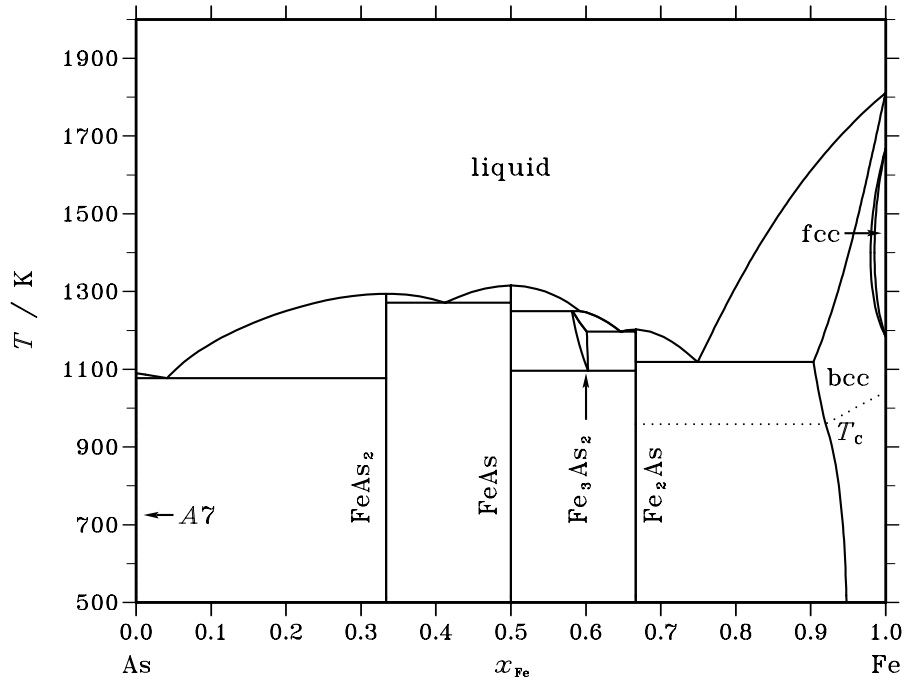

Fig. 1. Calculated phase diagram for the system As-Fe.

The system As–Fe is of interest because As is a harmful constituent in certain Fe-Cu and Fe-ores. The system As–Fe has been reviewed by [91Oka] and a thermodynamic assessment has been given by [93Pei] which is presented here. For the optimisation of the system data on the phase diagram and the activities of As and Fe in the liquid have been used. In alloys with less than 50 at.% As there is plenty of experimental information available but at higher As contents the data are very scarce. The liquid has been modelled using the ionic 2-sublattice model in order to take account of the strong non-ideal mixing behavior. For the intermetallic compounds, the calculated Gibbs energies of formation deviate considerably from the experimental data.

Table I. Phases, structures and models.

Phase	Struktur-bericht	Prototype	Pearson symbol	Space group	SGTE name	Model
liquid					IONIC_LIQ	$Fe_p^{2+}(As,As^{3-},\Box^{2-})_2$
$A7$	$A7$	αAs	$hR2$	$R\overline{3}m$	RHOMBO_A7	As_1
$FeAs_2$	$C18$	FeS_2	$oP6$	$Pnnm$	FEAS2	Fe_1As_2
FeAs	$B31$	MnP	$oP8$	$Pnma$	FEAS	Fe_1As_1
Fe_3As_2	...	...	...	...	FE3AS2	$Fe_4(As,\Box)_3$
Fe_2As	$C38$	Cu_2Sb	$tP6$	$P4/nmm$	FE2AS	Fe_2As_1
fcc	$A1$	Cu	$cF4$	$Fm\overline{3}m$	FCC_A1	$(As,Fe)_1$
bcc	$A2$	W	$cI2$	$Im\overline{3}m$	BCC_A2	$(As,Fe)_1$

Table II. Invariant reactions.

Reaction	Type	T / K	Compositions / x_{Fe}			$\Delta_{\mathrm{r}}H$ / (J/mol)
liquid ⇌ FeAs	congruent	1315.3	0.500	0.500		−22592
liquid ⇌ $FeAs_2$	congruent	1294.0	0.333	0.333		−28496
liquid ⇌ $FeAs_2$ + FeAs	eutectic	1271.4	0.412	0.333	0.500	−25203
FeAs + liquid ⇌ Fe_3As_2	peritectic	1249.9	0.500	0.592	0.582	−9031
liquid ⇌ Fe_2As	congruent	1202.5	0.667	0.667		−14773
liquid ⇌ Fe_3As_2 + Fe_2As	eutectic	1196.7	0.646	0.601	0.667	−13855
liquid ⇌ Fe_2As + bcc	eutectic	1118.5	0.749	0.667	0.904	−12981
Fe_3As_2 ⇌ FeAs + Fe_2As	eutectoid	1096.1	0.603	0.500	0.667	−4490
liquid ⇌ $A7$ + $FeAs_2$	eutectic	1077.5	0.041	0.000	0.333	−24739

Table IIIa. Integral quantities for the liquid phase at 1873 K.

x_{Fe}	ΔG_{m} [J/mol]	ΔH_{m} [J/mol]	ΔS_{m} [J/(mol·K)]	$G^{\mathrm{E}}_{\mathrm{m}}$ [J/mol]	$S^{\mathrm{E}}_{\mathrm{m}}$ [J/(mol·K)]	ΔC_p [J/(mol·K)]
0.000	0	0	0.000	0	0.000	0.000
0.100	−9682	−4720	2.649	−4619	−0.054	0.000
0.200	−17294	−9199	4.322	−9502	0.162	0.000
0.300	−23539	−13235	5.501	−14026	0.422	0.000
0.400	−28278	−16551	6.261	−17797	0.665	0.000
0.500	−31089	−18644	6.645	−20295	0.881	0.000
0.600	−31371	−18922	6.647	−20890	1.051	0.000
0.700	−28476	−16873	6.195	−18963	1.116	0.000
0.800	−22088	−12253	5.251	−14295	1.090	0.000
0.900	−12783	−6393	3.411	−7720	0.709	0.000
1.000	0	0	0.000	0	0.000	0.000

Reference states: As(liquid), Fe(liquid)

Table IIIb. Partial quantities for As in the liquid phase at 1873 K.

x_{As}	ΔG_{As} [J/mol]	ΔH_{As} [J/mol]	ΔS_{As} [J/(mol·K)]	$G^{\mathrm{E}}_{\mathrm{As}}$ [J/mol]	$S^{\mathrm{E}}_{\mathrm{As}}$ [J/(mol·K)]	a_{As}	γ_{As}
1.000	0	0	0.000	0	0.000	1.000	1.000
0.900	−1331	−20	0.700	308	−0.176	0.918	1.020
0.800	−3446	−621	1.509	28	−0.347	0.801	1.002
0.700	−6919	−2070	2.589	−1364	−0.377	0.641	0.916
0.600	−12812	−5304	4.009	−4857	−0.239	0.439	0.732
0.500	−22834	−12334	5.606	−12039	−0.157	0.231	0.462
0.400	−38518	−23435	8.053	−24248	0.434	0.084	0.211
0.300	−61298	−41352	10.649	−42548	0.639	0.020	0.065
0.200	−85649	−55797	15.938	−60585	2.556	0.004	0.020
0.100	−108723	−62078	24.904	−72865	5.759	0.001	0.009
0.000	$-\infty$	−65592	∞	−81381	8.430	0.000	0.005

Reference state: As(liquid)

Table IIIc. Partial quantities for Fe in the liquid phase at 1873 K.

x_{Fe}	ΔG_{Fe} [J/mol]	ΔH_{Fe} [J/mol]	ΔS_{Fe} [J/(mol·K)]	G^E_{Fe} [J/mol]	S^E_{Fe} [J/(mol·K)]	a_{Fe}	γ_{Fe}
0.000	$-\infty$	0	∞	0	0.000	0.000	1.000
0.100	−84834	−46462	20.487	−48976	1.342	0.004	0.043
0.200	−72687	−43533	15.565	−47623	2.184	0.009	0.047
0.300	−62319	−39399	12.237	−43570	2.227	0.018	0.061
0.400	−51476	−33410	9.645	−37207	2.027	0.037	0.092
0.500	−39345	−24954	7.683	−28550	1.920	0.080	0.160
0.600	−26606	−15910	5.711	−18651	1.463	0.181	0.302
0.700	−14410	−6376	4.289	−8855	1.324	0.396	0.566
0.800	−6197	−1213	2.661	−2722	0.806	0.672	0.840
0.900	−2122	−181	1.037	−482	0.161	0.873	0.970
1.000	0	0	0.000	0	0.000	1.000	1.000

Reference state: Fe(liquid)

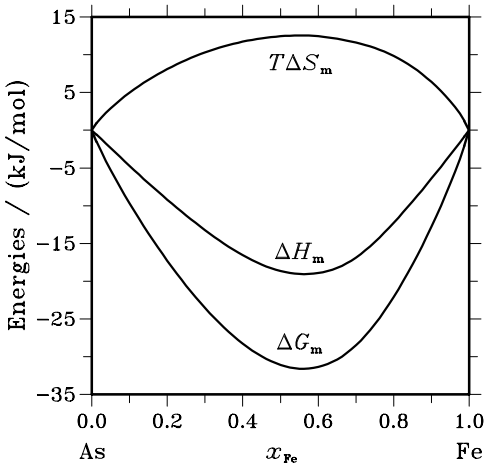

Fig. 2. Integral quantities of the liquid phase at T=1873 K.

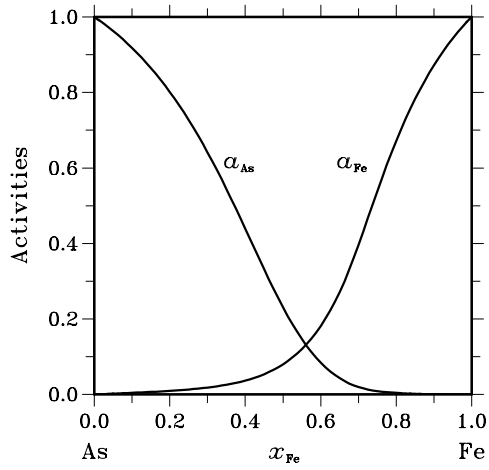

Fig. 3. Activities in the liquid phase at T=1873 K.

Table IV. Standard reaction quantities at 298.15 K for the compounds per mole of atoms.

Compound	x_{Fe}	$\Delta_f G^\circ$ / (J/mol)	$\Delta_f H^\circ$ / (J/mol)	$\Delta_f S^\circ$ / (J/(mol·K))	$\Delta_f C^\circ_P$ / (J/(mol·K))
Fe_1As_2	0.333	−21110	−19952	3.884	−0.139
Fe_1As_1	0.500	−21544	−19048	8.372	−0.209
Fe_2As_1	0.667	−14600	−11050	11.907	−0.278

References

[91Oka] H. Okamoto: J. Phase Equilibria **12** (1991) 457–461.
[94Pei] B. Pei, B. Björkman, B. Jansson, B. Sundman: Z. Metallkd. **85** (1994) 171–177.

As – Ga (Arsenic – Gallium)

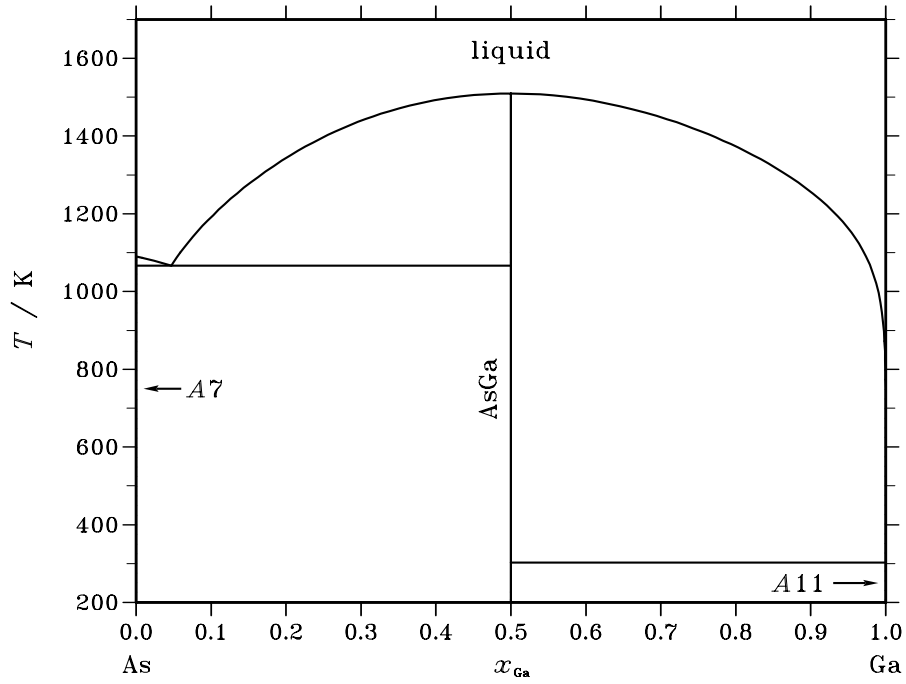

Fig. 1. Calculated phase diagram for the system As-Ga (constrained system).

The As-Ga system is one of the most important of the group of III-V semiconductor systems used in optoelectronic and high speed electronic device applications. An understanding of the phase diagram and thermochemistry of this system is essential in order to model processes for the fabrication of these devices. The phase diagram for the As-Ga system is very simple featuring a near stoichiometric compound GaAs which melts congruently at 1510 K, complete miscibility within the liquid phase and negligible solubility of Ga in rhombohedral As and of As in crystalline Ga. There is a eutectic on the As rich side of the system at 1067 K and a eutectic on the Ga rich side of the system very close to the melting point of Ga itself. The critically assessed dataset for this system is from the work of Chatillon et al. [90Cha]. The calculated phase diagram is in very good agreement with the large number of measurements of the liquidus. The thermodynamic properties of the system have been studied by Knudsen cell mass spectrometry and drop calorimetry and are reproduced well by the critically assessed data.

Table I. Phases, structures and models.

Phase	Struktur-bericht	Prototype	Pearson symbol	Space group	SGTE name	Model
liquid					LIQUID	$(As,Ga)_1$
$A7$	$A7$	αAs	$hR2$	$R\overline{3}m$	RHOMBOHEDRAL_A7	As_1
AsGa	$B3$	ZnS	$cF8$	$F\overline{4}3m$	B3_ZINCBLENDE	Ga_1As_1
$A11$	$A11$	αGa	$oC8$	$Cmca$	ORTHORHOMBIC_A11	Ga_1

Table II. Invariant reactions.

Reaction	Type	T / K	Compositions / x_{Ga}			$\Delta_{\mathrm{r}}H$ / (J/mol)
liquid ⇌ AsGa	congruent	1509.4	0.500	0.500		−53161
liquid ⇌ $A7$ + AsGa	eutectic	1066.6	0.047	0.000	0.500	−26450
liquid ⇌ AsGa + $A11$	degenerate	302.9	1.000	0.500	1.000	−5590

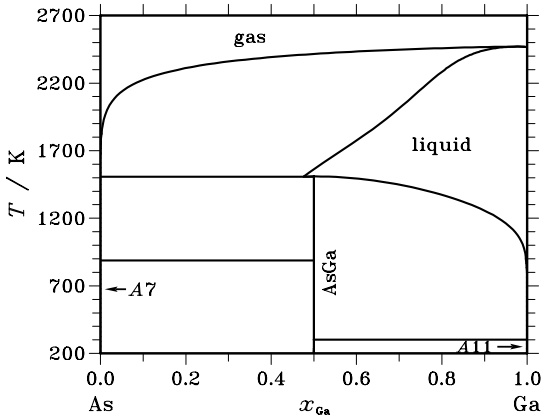

Fig. 2. Calculated phase diagram at 0.1 MPa.

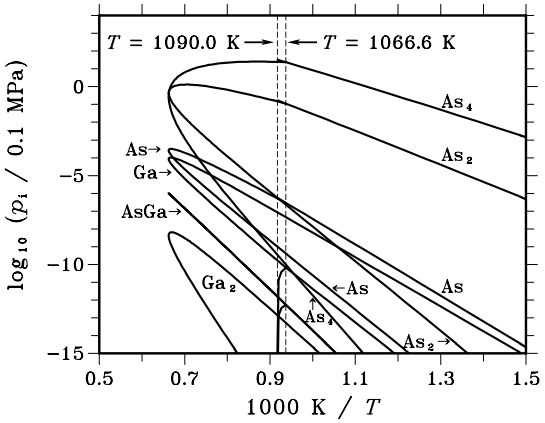

Fig. 3. Calculated partial pressures of gaseous species in the phase equilibria of the constrained system.

Table IIIa. Integral quantities for the liquid phase at 1550 K.

x_{Ga}	ΔG_{m} [J/mol]	ΔH_{m} [J/mol]	ΔS_{m} [J/(mol·K)]	$G_{\mathrm{m}}^{\mathrm{E}}$ [J/mol]	$S_{\mathrm{m}}^{\mathrm{E}}$ [J/(mol·K)]	ΔC_p [J/(mol·K)]
0.000	0	0	0.000	0	0.000	0.000
0.100	−7459	−2668	3.091	−3269	0.388	0.000
0.200	−12095	−4577	4.850	−5646	0.690	0.000
0.300	−15066	−5790	5.984	−7194	0.905	0.000
0.400	−16646	−6369	6.630	−7973	1.035	0.000
0.500	−16979	−6376	6.841	−8046	1.078	0.000
0.600	−16150	−5872	6.630	−7476	1.035	0.000
0.700	−14197	−4921	5.984	−6324	0.905	0.000
0.800	−11102	−3584	4.850	−4653	0.690	0.000
0.900	−6714	−1923	3.091	−2524	0.388	0.000
1.000	0	0	0.000	0	0.000	0.000

Reference states: As(liquid), Ga(liquid)

Table IIIb. Partial quantities for As in the liquid phase at 1550 K.

x_{As}	ΔG_{As} [J/mol]	ΔH_{As} [J/mol]	ΔS_{As} [J/(mol·K)]	G^E_{As} [J/mol]	S^E_{As} [J/(mol·K)]	a_{As}	γ_{As}
1.000	0	0	0.000	0	0.000	1.000	1.000
0.900	−1814	−390	0.919	−456	0.043	0.869	0.965
0.800	−4619	−1476	2.028	−1743	0.172	0.699	0.874
0.700	−8332	−3134	3.354	−3735	0.388	0.524	0.748
0.600	−12892	−5240	4.937	−6309	0.690	0.368	0.613
0.500	−18273	−7670	6.841	−9340	1.078	0.242	0.484
0.400	−24513	−10299	9.170	−12705	1.552	0.149	0.373
0.300	−31794	−13004	12.123	−16278	2.112	0.085	0.283
0.200	−40678	−15660	16.141	−19936	2.759	0.043	0.213
0.100	−53230	−18143	22.637	−23555	3.492	0.016	0.161
0.000	−∞	−20329	∞	−27011	4.311	0.000	0.123

Reference state: As(liquid)

Table IIIc. Partial quantities for Ga in the liquid phase at 1550 K.

x_{Ga}	ΔG_{Ga} [J/mol]	ΔH_{Ga} [J/mol]	ΔS_{Ga} [J/(mol·K)]	G^E_{Ga} [J/mol]	S^E_{Ga} [J/(mol·K)]	a_{Ga}	γ_{Ga}
0.000	−∞	−30678	∞	−37360	4.311	0.000	0.055
0.100	−58260	−23173	22.637	−28585	3.492	0.011	0.109
0.200	−42003	−16985	16.141	−21261	2.759	0.038	0.192
0.300	−30780	−11990	12.123	−15264	2.112	0.092	0.306
0.400	−22278	−8064	9.170	−10469	1.552	0.178	0.444
0.500	−15686	−5082	6.841	−6753	1.078	0.296	0.592
0.600	−10574	−2921	4.937	−3991	0.690	0.440	0.734
0.700	−6655	−1457	3.354	−2058	0.388	0.597	0.852
0.800	−3708	−565	2.028	−832	0.172	0.750	0.937
0.900	−1545	−120	0.919	−187	0.043	0.887	0.986
1.000	0	0	0.000	0	0.000	1.000	1.000

Reference state: Ga(liquid)

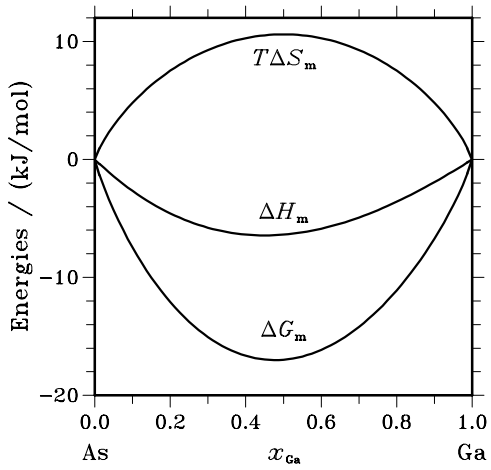

Fig. 4. Integral quantities of the liquid phase at T=1550 K.

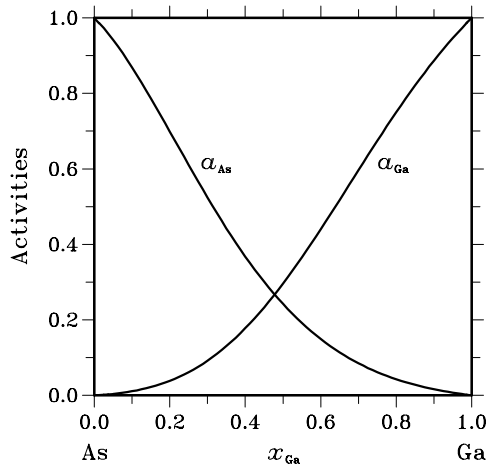

Fig. 5. Activities in the liquid phase at T=1550 K.

Table IV. Standard reaction quantities at 298.15 K for the compounds per mole of atoms.

Compound	x_{Ga}	$\Delta_{\mathrm{f}}G^{\circ}$ / (J/mol)	$\Delta_{\mathrm{f}}H^{\circ}$ / (J/mol)	$\Delta_{\mathrm{f}}S^{\circ}$ / (J/(mol·K))	$\Delta_{\mathrm{f}}C_P^{\circ}$ / (J/(mol·K))
$\mathrm{As_1Ga_1}$	0.500	−42408	−44422	−6.755	−1.969

References

[90Cha] C. Chatillon, I. Ansara, A. Watson, B.B. Argent: Calphad **14** (1990) 203–214.

As – Ge (Arsenic – Germanium)

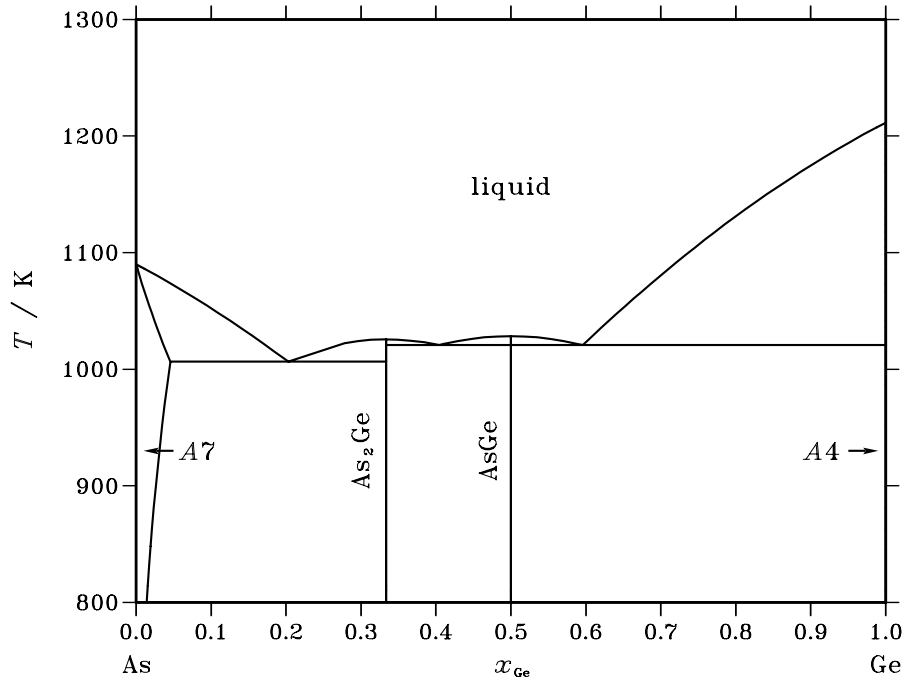

Fig. 1. Calculated phase diagram for the system As-Ge.

Data for the As-Ge system are required in order to model processes for the fabrication of optoelectronic and high speed electronic devices. An understanding of the phase diagram and thermochemistry of this system is essential for this purpose.

The As-Ge system is characterised by complete miscibility in the liquid phase, negligible solubility of As in crystalline Ge (diamond structure), two intermetallic compounds GeAs and $GeAs_2$, and a range of solid solution of Ge in rhombohedral As. According to the selected SGTE assessment GeAs melts congruently at 1028 K while $GeAs_2$ melts congruently at 1026 K. The solubility of Ge in rhombohedral As is not well defined. According to [85Uga] this reaches 12 at.% at the eutectic temperature. In the selected dataset, which was derived by Ansara and Dutartre [84Ans] this solubility has been ignored. The dataset was based on experimental liquidus temperature and heat capacities of the compound phases. The two sets of measurements of the vapour pressures in the system were in poor agreement and were not used in the analysis.

Table I. Phases, structures and models.

Phase	Struktur-bericht	Prototype	Pearson symbol	Space group	SGTE name	Model
liquid					LIQUID	$(As,Ge)_1$
$A7$	$A7$	αAs	$hR2$	$R\bar{3}m$	RHOMBOHEDRAL_A7	$(As,Ge)_1$
As_2Ge	···	···	$oP*$	$Pbam$	AS2GE	As_2Ge_1
AsGe	···	···	$mC24$	$C2/m$	ASGE	As_1Ge_1
$A4$	$A4$	C(diamond)	$cF8$	$Fd\bar{3}m$	DIAMOND_A4	Ge_1

Table II. Invariant reactions.

Reaction	Type	T / K	Compositions / x_{Ge}			$\Delta_r H$ / (J/mol)
liquid ⇌ AsGe	congruent	1028.4	0.500	0.500		−31847
liquid ⇌ As_2Ge	congruent	1025.6	0.333	0.333		−28616
liquid ⇌ As_2Ge + AsGe	eutectic	1020.7	0.405	0.333	0.500	−29952
liquid ⇌ AsGe + $A4$	eutectic	1020.7	0.596	0.500	1.000	−32520
liquid ⇌ A7 + As_2Ge	eutectic	1006.5	0.203	0.046	0.333	−26050

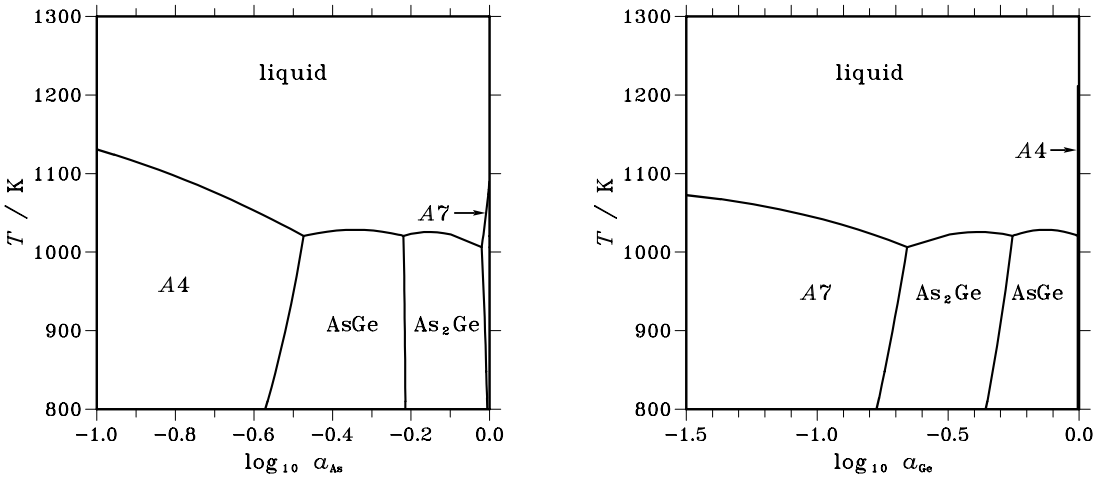

Fig. 2. Calculated temperature-activity diagrams. Reference states: As($A7$), Ge($A4$)

Table IIIa. Integral quantities for the liquid phase at 1300 K.

x_{Ge}	ΔG_m [J/mol]	ΔH_m [J/mol]	ΔS_m [J/(mol·K)]	G_m^E [J/mol]	S_m^E [J/(mol·K)]	ΔC_p [J/(mol·K)]
0.000	0	0	0.000	0	0.000	0.000
0.100	−4305	−791	2.703	−791	0.000	0.000
0.200	−6815	−1406	4.161	−1406	0.000	0.000
0.300	−8448	−1845	5.079	−1845	0.000	0.000
0.400	−9383	−2109	5.596	−2109	0.000	0.000
0.500	−9689	−2197	5.763	−2197	0.000	0.000
0.600	−9383	−2109	5.596	−2109	0.000	0.000
0.700	−8448	−1845	5.079	−1845	0.000	0.000
0.800	−6815	−1406	4.161	−1406	0.000	0.000
0.900	−4305	−791	2.703	−791	0.000	0.000
1.000	0	0	0.000	0	0.000	0.000

Reference states: As(liquid), Ge(liquid)

Table IIIb. Partial quantities for As in the liquid phase at 1300 K.

x_{As}	ΔG_{As} [J/mol]	ΔH_{As} [J/mol]	ΔS_{As} [J/(mol·K)]	G^E_{As} [J/mol]	S^E_{As} [J/(mol·K)]	a_{As}	γ_{As}
1.000	0	0	0.000	0	0.000	1.000	1.000
0.900	−1227	−88	0.876	−88	0.000	0.893	0.992
0.800	−2763	−351	1.855	−351	0.000	0.774	0.968
0.700	−4646	−791	2.966	−791	0.000	0.651	0.929
0.600	−6927	−1406	4.247	−1406	0.000	0.527	0.878
0.500	−9689	−2197	5.763	−2197	0.000	0.408	0.816
0.400	−13067	−3163	7.619	−3163	0.000	0.299	0.746
0.300	−17319	−4305	10.010	−4305	0.000	0.201	0.671
0.200	−23019	−5623	13.382	−5623	0.000	0.119	0.594
0.100	−32005	−7117	19.145	−7117	0.000	0.052	0.518
0.000	−∞	−8786	∞	−8786	0.000	0.000	0.444

Reference state: As(liquid)

Table IIIc. Partial quantities for Ge in the liquid phase at 1300 K.

x_{Ge}	ΔG_{Ge} [J/mol]	ΔH_{Ge} [J/mol]	ΔS_{Ge} [J/(mol·K)]	G^E_{Ge} [J/mol]	S^E_{Ge} [J/(mol·K)]	a_{Ge}	γ_{Ge}
0.000	−∞	−8786	∞	−8786	0.000	0.000	0.444
0.100	−32005	−7117	19.145	−7117	0.000	0.052	0.518
0.200	−23019	−5623	13.382	−5623	0.000	0.119	0.594
0.300	−17319	−4305	10.010	−4305	0.000	0.201	0.671
0.400	−13067	−3163	7.619	−3163	0.000	0.299	0.746
0.500	−9689	−2197	5.763	−2197	0.000	0.408	0.816
0.600	−6927	−1406	4.247	−1406	0.000	0.527	0.878
0.700	−4646	−791	2.966	−791	0.000	0.651	0.929
0.800	−2763	−351	1.855	−351	0.000	0.774	0.968
0.900	−1227	−88	0.876	−88	0.000	0.893	0.992
1.000	0	0	0.000	0	0.000	1.000	1.000

Reference state: Ge(liquid)

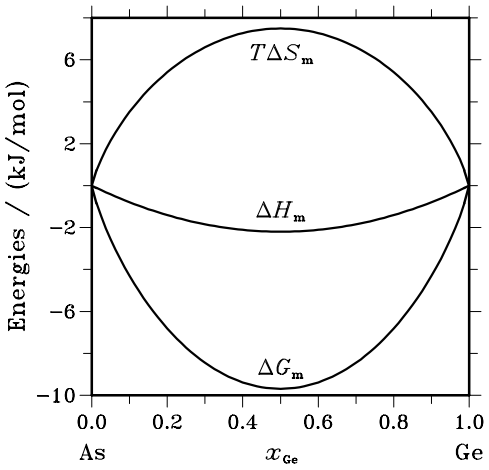

Fig. 3. Integral quantities of the liquid phase at T=1300 K.

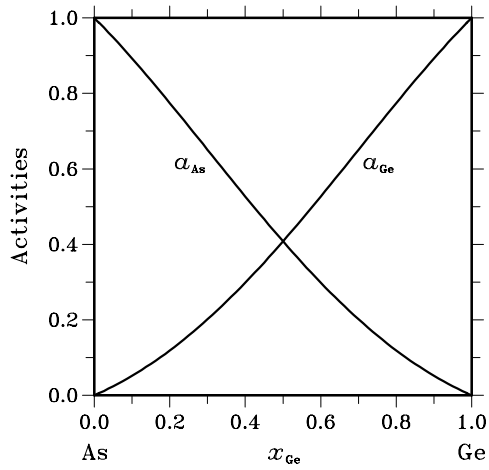

Fig. 4. Activities in the liquid phase at T=1300 K.

Table IV. Standard reaction quantities at 298.15 K for the compounds per mole of atoms.

Compound	x_{Ge}	$\Delta_{\mathrm{f}}G^{\circ}$ / (J/mol)	$\Delta_{\mathrm{f}}H^{\circ}$ / (J/mol)	$\Delta_{\mathrm{f}}S^{\circ}$ / (J/(mol·K))	$\Delta_{\mathrm{f}}C_P^{\circ}$ / (J/(mol·K))
$\mathrm{As_2Ge_1}$	0.333	−3040	−2347	2.323	−1.241
$\mathrm{As_1Ge_1}$	0.500	−4122	−4147	−0.083	1.226

References

[84Ans] I. Ansara, D. Dutartre: Calphad **8** (1984) 323–342.

[85Uga] Ya.A. Ugai, S.P. Evseeva, A.E. Popov, E.G. Goncharov, O.V. Grigor'eva: Zh. Neorg. Khim. **30** (1985) 2951–2953 (in Russian); tr.: Russ. J. Inorg. Chem. **30** (1985) 1681–1682.

As – In (Arsenic – Indium)

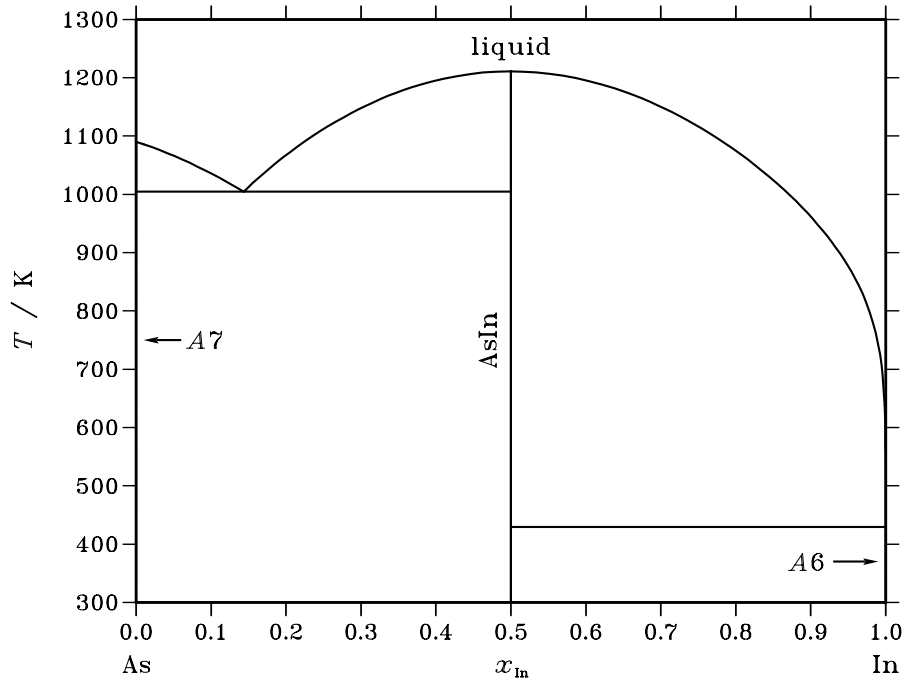

Fig. 1. Calculated phase diagram for the system As-In (constrained system).

Data for the As-In system are required in order to model processes for the fabrication of optoelectronic and high speed electronic devices based on III-V semiconductor systems. An understanding of the phase diagram and thermochemistry of this system is essential for this purpose.
The phase diagram for the As-In system is very simple featuring a near stoichiometric compound InAs which melts congruently at 1211 K, complete miscibility within the liquid phase and negligible solubility of In in rhombohedral As and of As in crystalline In. There is a eutectic on the As rich side of the system at 1005 K and a eutectic on the In rich side of the system very close to the melting point of In itself. The critically assessed dataset for this system is from the work of Chatillon et al. [90Cha]. The calculated phase diagram is in very good agreement with the large number of measurements of the liquidus. The thermodynamic properties of the system have been studied by Knudsen cell mass spectrometry, drop calorimetry and emf measurements and are reproduced well by the critically assessed data.

Table I. Phases, structures and models.

Phase	Struktur-bericht	Prototype	Pearson symbol	Space group	SGTE name	Model
liquid					LIQUID	$(As,In)_1$
$A7$	$A7$	αAs	$hR2$	$R\bar{3}m$	RHOMBOHEDRAL_A7	$(As,In)_1$
AsIn	$B3$	ZnS	$cF8$	$F\bar{4}3m$	B3_ZINCBLENDE	In_1As_1
$A6$	$A6$	In	$tI2$	$I4/mmm$	TETRAGONAL_A6	In_1

Table II. Invariant reactions.

Reaction	Type	T / K	Compositions / x_{In}			$\Delta_r H$ / (J/mol)
liquid ⇌ AsIn	congruent	1210.9	0.500	0.500		−38739
liquid ⇌ $A7$ + AsIn	eutectic	1004.7	0.143	0.000	0.500	−27768
liquid ⇌ AsIn + $A6$	degenerate	429.8	1.000	0.500	1.000	−3283

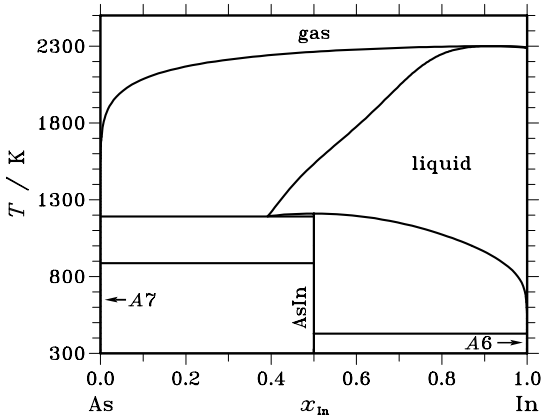

Fig. 2. Calculated phase diagram at 0.1 MPa.

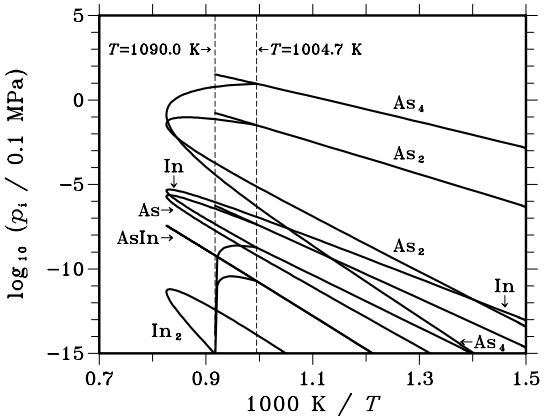

Fig. 3. Calculated partial pressures of gaseous species in the phase equilibria of the constrained system.

Table IIIa. Integral quantities for the liquid phase at 1250 K.

x_{In}	ΔG_{m} [J/mol]	ΔH_{m} [J/mol]	ΔS_{m} [J/(mol·K)]	$G_{\mathrm{m}}^{\mathrm{E}}$ [J/mol]	$S_{\mathrm{m}}^{\mathrm{E}}$ [J/(mol·K)]	ΔC_p [J/(mol·K)]
0.000	0	0	0.000	0	0.000	0.000
0.100	−6161	−1514	3.717	−2782	1.014	0.000
0.200	−10108	−2653	5.964	−4907	1.803	0.000
0.300	−12739	−3431	7.446	−6390	2.367	0.000
0.400	−14239	−3863	8.301	−7244	2.705	0.000
0.500	−14689	−3963	8.581	−7485	2.818	0.000
0.600	−14122	−3746	8.301	−7127	2.705	0.000
0.700	−12534	−3226	7.446	−6185	2.367	0.000
0.800	−9874	−2419	5.964	−4673	1.803	0.000
0.900	−5985	−1339	3.717	−2607	1.014	0.000
1.000	0	0	0.000	0	0.000	0.000

Reference states: As(liquid), In(liquid)

Table IIIb. Partial quantities for As in the liquid phase at 1250 K.

x_{As}	ΔG_{As} [J/mol]	ΔH_{As} [J/mol]	ΔS_{As} [J/(mol·K)]	G^E_{As} [J/mol]	S^E_{As} [J/(mol·K)]	a_{As}	γ_{As}
1.000	0	0	0.000	0	0.000	1.000	1.000
0.900	−1426	−190	0.989	−331	0.113	0.872	0.969
0.800	−3624	−741	2.306	−1305	0.451	0.706	0.882
0.700	−6599	−1624	3.980	−2892	1.014	0.530	0.757
0.600	−10373	−2809	6.051	−5063	1.803	0.369	0.614
0.500	−14994	−4268	8.581	−7790	2.818	0.236	0.473
0.400	−20565	−5970	11.676	−11042	4.057	0.138	0.346
0.300	−27303	−7887	15.533	−14790	5.523	0.072	0.241
0.200	−35732	−9989	20.595	−19005	7.213	0.032	0.161
0.100	−47589	−12247	28.274	−23658	9.129	0.010	0.103
0.000	−∞	−14632	∞	−28720	11.271	0.000	0.063

Reference state: As(liquid)

Table IIIc. Partial quantities for In in the liquid phase at 1250 K.

x_{In}	ΔG_{In} [J/mol]	ΔH_{In} [J/mol]	ΔS_{In} [J/(mol·K)]	G^E_{In} [J/mol]	S^E_{In} [J/(mol·K)]	a_{In}	γ_{In}
0.000	−∞	−17071	∞	−31159	11.271	0.000	0.050
0.100	−48775	−13432	28.274	−24843	9.129	0.009	0.092
0.200	−36044	−10301	20.595	−19317	7.213	0.031	0.156
0.300	−27064	−7647	15.533	−14551	5.523	0.074	0.247
0.400	−20038	−5443	11.676	−10515	4.057	0.145	0.364
0.500	−14384	−3658	8.581	−7180	2.818	0.251	0.501
0.600	−9826	−2263	6.051	−4517	1.803	0.389	0.648
0.700	−6204	−1229	3.980	−2497	1.014	0.551	0.786
0.800	−3409	−527	2.306	−1090	0.451	0.720	0.900
0.900	−1363	−127	0.989	−268	0.113	0.877	0.975
1.000	0	0	0.000	0	0.000	1.000	1.000

Reference state: In(liquid)

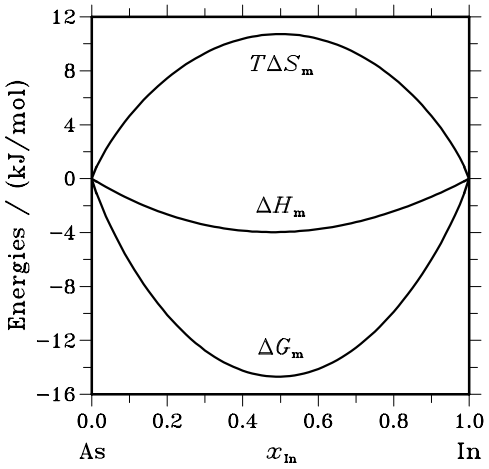

Fig. 4. Integral quantities of the liquid phase at T=1250 K.

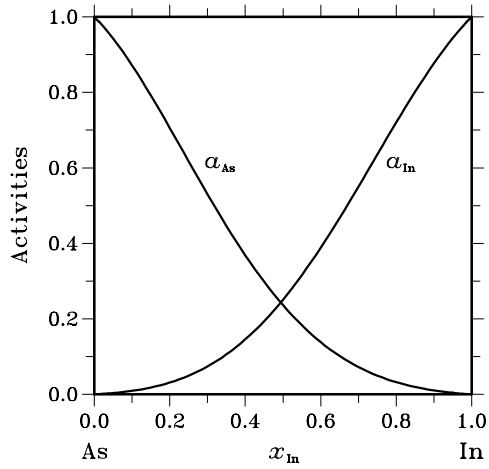

Fig. 5. Activities in the liquid phase at T=1250 K.

Table IV. Standard reaction quantities at 298.15 K for the compounds per mole of atoms.

Compound	x_{In}	$\Delta_{\mathrm{f}}G^{\circ}$ / (J/mol)	$\Delta_{\mathrm{f}}H^{\circ}$ / (J/mol)	$\Delta_{\mathrm{f}}S^{\circ}$ / (J/(mol·K))	$\Delta_{\mathrm{f}}C_P^{\circ}$ / (J/(mol·K))
$\mathrm{As_1In_1}$	0.500	−26796	−29219	−8.128	−1.706

References

[90Cha] C. Chatillon, I. Ansara, A. Watson, B.B. Argent: Calphad **14** (1990) 203–214.

As – P (Arsenic – Phosphorus)

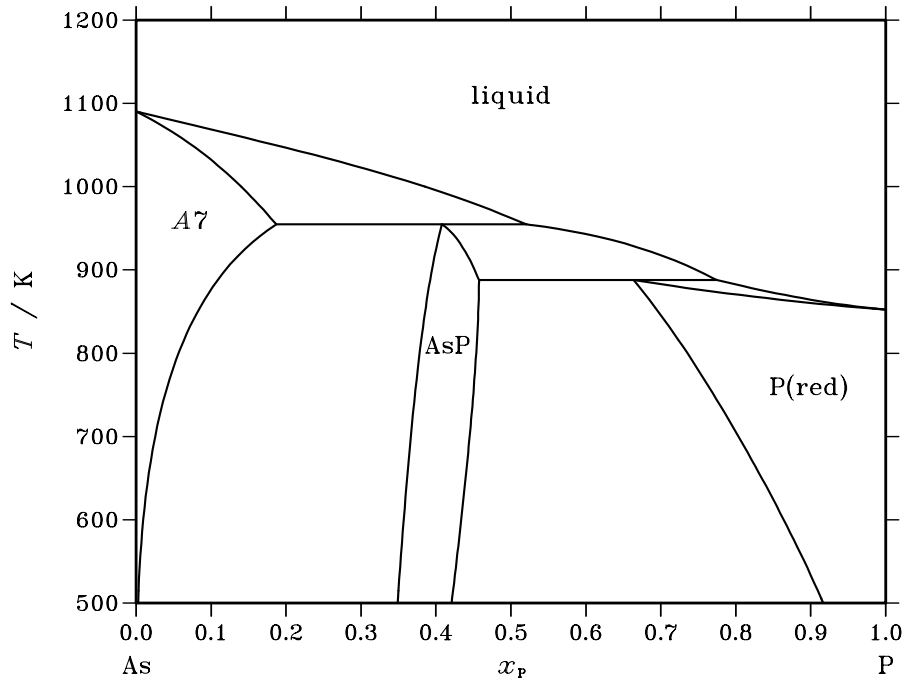

Fig. 1. Calculated phase diagram for the system As-P (constrained system).

An understanding of the thermodynamic data and equilibrium phase relationships for the As-P system is essential in order to model processes for the fabrication of optoelectronic and high speed electronic devices based on III-V semiconductor systems. The critically assessed data for the system are taken from the assessment of Ansara and Chatillon reported in [94Ans]. Earlier assessments of data were published by Kaufman et al. [81Kau] and Karakaya and Thompson [91Kar]. The phase diagram is characterised by complete mixing in the liquid phase, appreciable solubility of P in As and of As in red P and the formation of the intermediate AsP phase which itself exhibits a wide range of homogeneity. The experimental phase boundary data show considerable scatter reflecting the high vapour pressure experienced along the liquidus surface. No experimental thermodynamic data have been reported.

Table I. Phases, structures and models.

Phase	Struktur-bericht	Prototype	Pearson symbol	Space group	SGTE name	Model
liquid					LIQUID	$(As,P)_1$
$A7$	$A7$	αAs	$hR2$	$R\bar{3}m$	RHOMBOHEDRAL_A7	As_1
AsP	···	···	···	···	ASP	$(As,P)_1$
P(red)	···	···	···	···	P_RED	P_1
αP	···	αP	$c*$	···	P_WHITE	P_1

Table II. Invariant reactions.

Reaction	Type	T / K	Compositions / x_P			$\Delta_r H$ / (J/mol)
$A7$ + liquid ⇌ AsP	peritectic	954.7	0.187	0.521	0.408	−17330
AsP + liquid ⇌ P(red)	peritectic	887.7	0.457	0.775	0.664	−10382

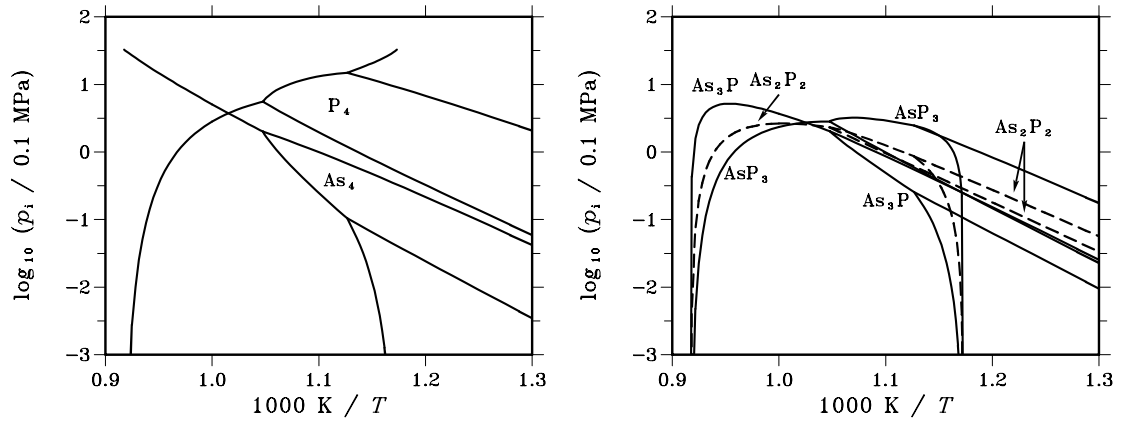

Fig. 2. Calculated partial pressures of gaseous species in the phase equilibria of the constrained system.

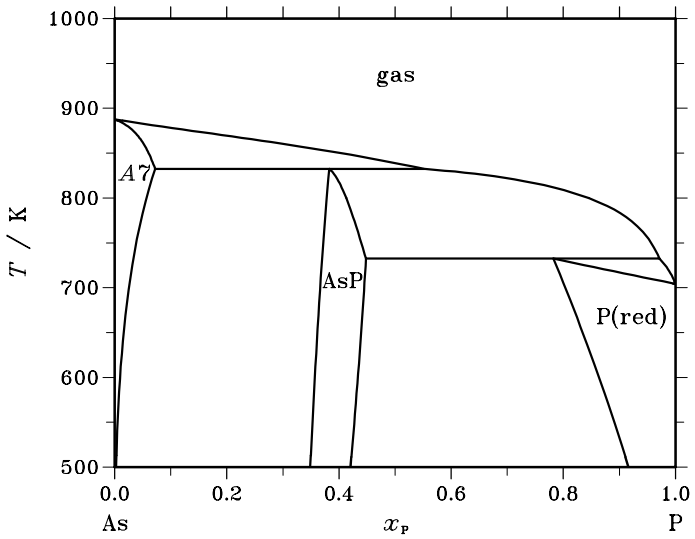

Fig. 3. Calculated phase diagram at 0.1 MPa.

Table IIIa. Integral quantities for the liquid phase at 1100 K.

x_{P}	ΔG_{m} [J/mol]	ΔH_{m} [J/mol]	ΔS_{m} [J/(mol·K)]	$G_{\mathrm{m}}^{\mathrm{E}}$ [J/mol]	$S_{\mathrm{m}}^{\mathrm{E}}$ [J/(mol·K)]	ΔC_p [J/(mol·K)]
0.000	0	0	0.000	0	0.000	0.000
0.100	−2484	490	2.703	490	0.000	0.000
0.200	−3763	813	4.161	813	0.000	0.000
0.300	−4594	993	5.079	993	0.000	0.000
0.400	−5106	1049	5.596	1049	0.000	0.000
0.500	−5336	1004	5.763	1004	0.000	0.000
0.600	−5277	878	5.596	878	0.000	0.000
0.700	−4893	693	5.079	693	0.000	0.000
0.800	−4105	471	4.161	471	0.000	0.000
0.900	−2740	233	2.703	233	0.000	0.000
1.000	0	0	0.000	0	0.000	0.000

Reference states: As(liquid), P(liquid)

Table IIIb. Partial quantities for As in the liquid phase at 1100 K.

x_{As}	ΔG_{As} [J/mol]	ΔH_{As} [J/mol]	ΔS_{As} [J/(mol·K)]	G^E_{As} [J/mol]	S^E_{As} [J/(mol·K)]	a_{As}	γ_{As}
1.000	0	0	0.000	0	0.000	1.000	1.000
0.900	−877	86	0.876	86	0.000	0.909	1.010
0.800	−1724	317	1.855	317	0.000	0.828	1.035
0.700	−2612	650	2.966	650	0.000	0.752	1.074
0.600	−3631	1041	4.247	1041	0.000	0.672	1.121
0.500	−4891	1449	5.763	1449	0.000	0.586	1.172
0.400	−6551	1830	7.619	1830	0.000	0.489	1.221
0.300	−8870	2142	10.010	2142	0.000	0.379	1.264
0.200	−12379	2341	13.382	2341	0.000	0.258	1.292
0.100	−18673	2386	19.145	2386	0.000	0.130	1.298
0.000	−∞	2234	∞	2234	0.000	0.000	1.277

Reference state: As(liquid)

Table IIIc. Partial quantities for P in the liquid phase at 1100 K.

x_P	ΔG_P [J/mol]	ΔH_P [J/mol]	ΔS_P [J/(mol·K)]	G^E_P [J/mol]	S^E_P [J/(mol·K)]	a_P	γ_P
0.000	−∞	5795	∞	5795	0.000	0.000	1.884
0.100	−16942	4117	19.145	4117	0.000	0.157	1.569
0.200	−11923	2797	13.382	2797	0.000	0.272	1.358
0.300	−9219	1793	10.010	1793	0.000	0.365	1.217
0.400	−7320	1061	7.619	1061	0.000	0.449	1.123
0.500	−5781	558	5.763	558	0.000	0.531	1.063
0.600	−4429	243	4.247	243	0.000	0.616	1.027
0.700	−3189	73	2.966	73	0.000	0.706	1.008
0.800	−2037	4	1.855	4	0.000	0.800	1.000
0.900	−970	−6	0.876	−6	0.000	0.899	0.999
1.000	0	0	0.000	0	0.000	1.000	1.000

Reference state: P(liquid)

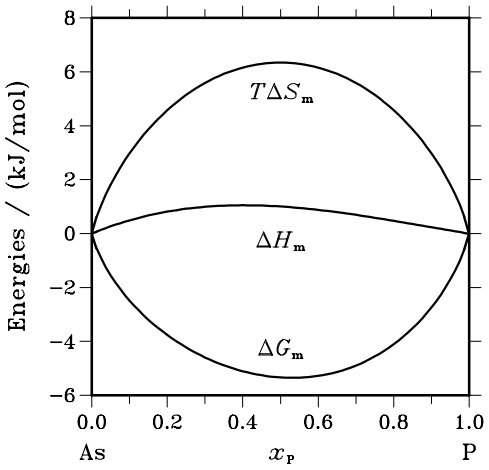

Fig. 4. Integral quantities of the liquid phase at T=1100 K.

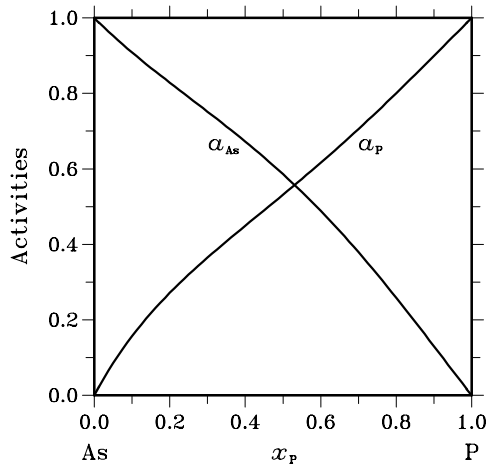

Fig. 5. Activities in the liquid phase at T=1100 K.

References

[81Kau] L. Kaufman, J. Nell, K. Taylor, F. Hayes: Calphad **5** (1981) 185–215.
[91Kar] I. Karakaya, W.T. Thompson: J. Phase Equilibria **5** (1991) 343–346.
[94Ans] I. Ansara, C. Chatillon, H.L. Lukas, T. Nishizawa, H. Ohtani, K. Ishida, M. Hillert, B. Sundman, B.B. Argent, A. Watson, T.G. Chart, T. Anderson: Calphad **18** (1994) 177–222.

As – Sb (Arsenic – Antimony)

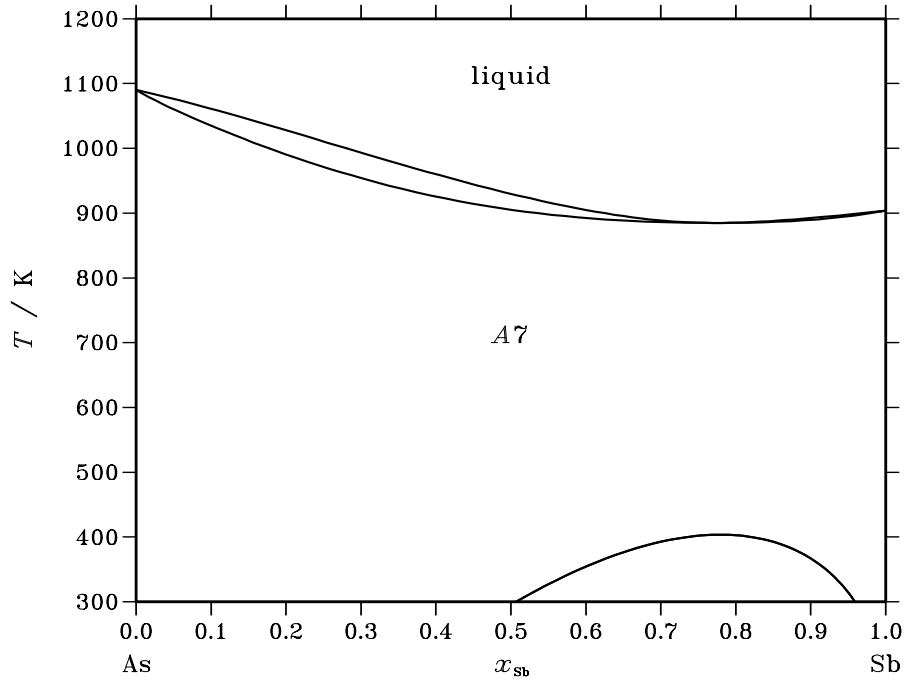

Fig. 1. Calculated phase diagram for the system As-Sb (constrained system).

Data for the AsSb system are required in order to model processes for the fabrication of optoelectronic and high speed electronic devices based on III-V semiconductor systems. An understanding of the phase diagram and thermochemistry of this system is essential for this purpose.
The As-Sb system is characterised by complete solubility between the components in the liquid and in the rhombohedral phase above 400 K. Below 400 K a miscibility gap is predicted skewed towards Sb rich compositions, based on experimentally determined positive enthalpies of mixing. The thermodynamic properties of the liquid phase have also been determined by emf and vapour pressure studies. The critically assessed data selected are from Ohtani quoted by Ansara et al. [94Ans].

Table I. Phases, structures and models.

Phase	Struktur-bericht	Prototype	Pearson symbol	Space group	SGTE name	Model
liquid					LIQUID	$(As,Sb)_1$
$A7$	$A7$	αAs	$hR2$	$R\bar{3}m$	RHOMBOHEDRAL_A7	$(As,Sb)_1$

Table II. Invariant reactions.

Reaction	Type	T / K	Compositions / x_{Sb}			$\Delta_r H$ / (J/mol)
liquid $\rightleftharpoons A7$	congruent	884.8	0.775	0.775		−17664
$A7 \rightleftharpoons A7' + A7''$	critical	403.3	0.779	0.779	0.779	0

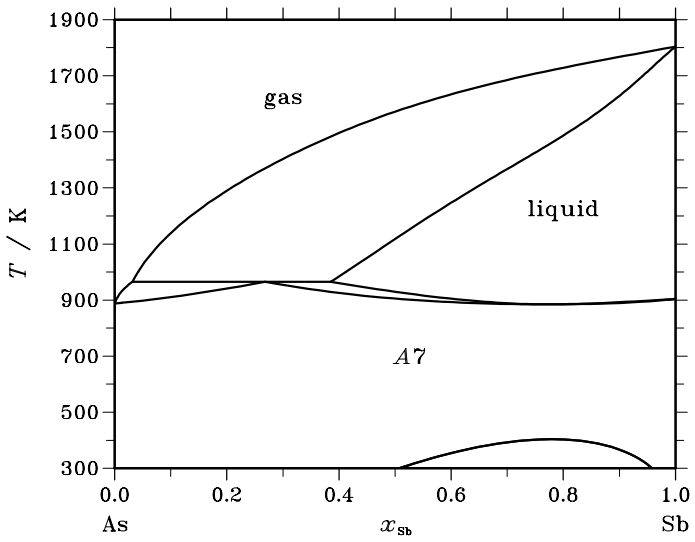

Fig. 2. Calculated phase diagram at 0.1 MPa.

Table IIIa. Integral quantities for the liquid phase at 1373 K.

x_{Sb}	ΔG_{m} [J/mol]	ΔH_{m} [J/mol]	ΔS_{m} [J/(mol·K)]	$G_{\mathrm{m}}^{\mathrm{E}}$ [J/mol]	$S_{\mathrm{m}}^{\mathrm{E}}$ [J/(mol·K)]	ΔC_p [J/(mol·K)]
0.000	0	0	0.000	0	0.000	0.000
0.100	−4428	−1819	1.900	−717	−0.803	0.000
0.200	−6827	−3073	2.734	−1114	−1.427	0.000
0.300	−8225	−3823	3.207	−1252	−1.873	0.000
0.400	−8873	−4128	3.456	−1190	−2.140	0.000
0.500	−8901	−4049	3.534	−989	−2.229	0.000
0.600	−8391	−3646	3.456	−708	−2.140	0.000
0.700	−7382	−2980	3.207	−409	−1.873	0.000
0.800	−5863	−2110	2.734	−151	−1.427	0.000
0.900	−3706	−1096	1.900	5	−0.803	0.000
1.000	0	0	0.000	0	0.000	0.000

Reference states: As(liquid), Sb(liquid)

Table IIIb. Partial quantities for As in the liquid phase at 1373 K.

x_{As}	ΔG_{As} [J/mol]	ΔH_{As} [J/mol]	ΔS_{As} [J/(mol·K)]	G^E_{As} [J/mol]	S^E_{As} [J/(mol·K)]	a_{As}	γ_{As}
1.000	0	0	0.000	0	0.000	1.000	1.000
0.900	−1373	−292	0.787	−170	−0.089	0.887	0.985
0.800	−3147	−1089	1.499	−600	−0.357	0.759	0.949
0.700	−5241	−2271	2.163	−1169	−0.803	0.632	0.903
0.600	−7588	−3716	2.821	−1757	−1.427	0.514	0.857
0.500	−10156	−5304	3.534	−2243	−2.229	0.411	0.822
0.400	−12968	−6915	4.409	−2508	−3.210	0.321	0.803
0.300	−16174	−8428	5.641	−2429	−4.369	0.242	0.808
0.200	−20262	−9724	7.675	−1889	−5.707	0.170	0.848
0.100	−27050	−10681	11.922	−764	−7.223	0.094	0.935
0.000	−∞	−11179	∞	1064	−8.917	0.000	1.098

Reference state: As(liquid)

Table IIIc. Partial quantities for Sb in the liquid phase at 1373 K.

x_{Sb}	ΔG_{Sb} [J/mol]	ΔH_{Sb} [J/mol]	ΔS_{Sb} [J/(mol·K)]	G^E_{Sb} [J/mol]	S^E_{Sb} [J/(mol·K)]	a_{Sb}	γ_{Sb}
0.000	−∞	−21215	∞	−8972	−8.917	0.000	0.456
0.100	−31928	−15558	11.922	−5642	−7.223	0.061	0.610
0.200	−21546	−11008	7.675	−3173	−5.707	0.151	0.757
0.300	−15190	−7445	5.641	−1446	−4.369	0.264	0.881
0.400	−10800	−4747	4.409	−340	−3.210	0.388	0.971
0.500	−7647	−2795	3.534	266	−2.229	0.512	1.024
0.600	−5340	−1468	2.821	491	−1.427	0.626	1.044
0.700	−3615	−645	2.163	457	−0.803	0.729	1.041
0.800	−2264	−206	1.499	283	−0.357	0.820	1.025
0.900	−1112	−32	0.787	91	−0.089	0.907	1.008
1.000	0	0	0.000	0	0.000	1.000	1.000

Reference state: Sb(liquid)

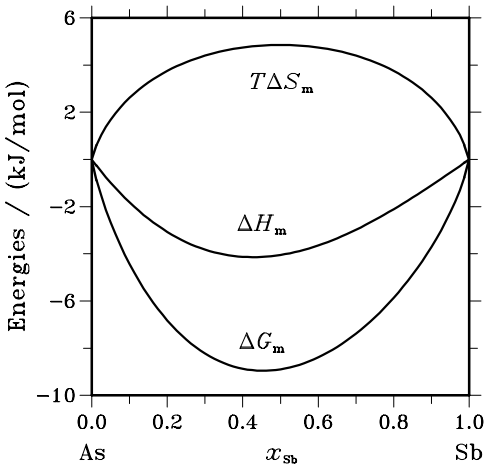

Fig. 3. Integral quantities of the liquid phase at T=1373 K.

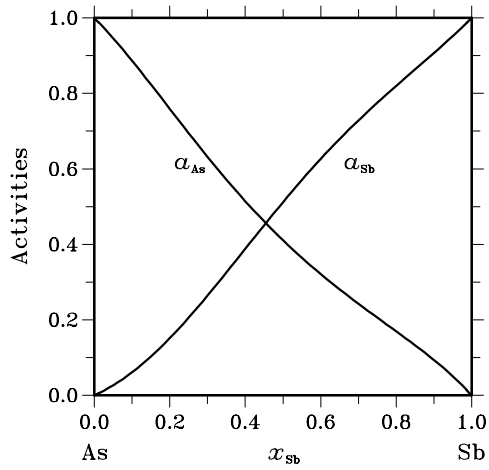

Fig. 4. Activities in the liquid phase at T=1373 K.

Table IVa. Integral quantities for the stable phases at 600 K.

Phase	x_{Sb}	ΔG_{m} [J/mol]	ΔH_{m} [J/mol]	ΔS_{m} [J/(mol·K)]	$G_{\mathrm{m}}^{\mathrm{E}}$ [J/mol]	$S_{\mathrm{m}}^{\mathrm{E}}$ [J/(mol·K)]	ΔC_p [J/(mol·K)]
$A7$	0.000	0	0	0.000	0	0.000	0.000
	0.100	−1981	−186	2.992	−359	0.289	0.000
	0.200	−2966	−161	4.675	−469	0.515	0.000
	0.300	−3441	12	5.754	−393	0.675	0.000
	0.400	−3553	268	6.368	−195	0.772	0.000
	0.500	−3396	544	6.567	62	0.804	0.000
	0.600	−3044	777	6.368	314	0.772	0.000
	0.700	−2550	902	5.754	497	0.675	0.000
	0.800	−1948	857	4.675	548	0.515	0.000
	0.900	−1218	577	2.992	404	0.289	0.000
	1.000	0	0	0.000	0	0.000	0.000

Reference states: As($A7$), Sb($A7$)

Table IVb. Partial quantities for As in the stable phases at 600 K.

Phase	x_{As}	ΔG_{As} [J/mol]	ΔH_{As} [J/mol]	ΔS_{As} [J/(mol·K)]	$G_{\mathrm{As}}^{\mathrm{E}}$ [J/mol]	$S_{\mathrm{As}}^{\mathrm{E}}$ [J/(mol·K)]	a_{As}	γ_{As}
$A7$	1.000	0	0	0.000	0	0.000	1.000	1.000
	0.900	−661	−116	0.908	−135	0.032	0.876	0.973
	0.800	−1570	−379	1.984	−457	0.129	0.730	0.913
	0.700	−2616	−663	3.255	−836	0.289	0.592	0.846
	0.600	−3696	−839	4.762	−1148	0.515	0.477	0.794
	0.500	−4721	−781	6.567	−1263	0.804	0.388	0.776
	0.400	−5627	−361	8.776	−1056	1.158	0.324	0.809
	0.300	−6405	547	11.586	−399	1.576	0.277	0.923
	0.200	−7193	2071	15.440	836	2.058	0.236	1.182
	0.100	−8711	4339	21.750	2775	2.605	0.174	1.744
	0.000	$-\infty$	7476	∞	5546	3.216	0.000	3.040

Reference state: As($A7$)

Table IVc. Partial quantities for Sb in the stable phases at 600 K.

Phase	x_{Sb}	ΔG_{Sb} [J/mol]	ΔH_{Sb} [J/mol]	ΔS_{Sb} [J/(mol·K)]	$G_{\mathrm{Sb}}^{\mathrm{E}}$ [J/mol]	$S_{\mathrm{Sb}}^{\mathrm{E}}$ [J/(mol·K)]	a_{Sb}	γ_{Sb}
$A7$	0.000	$-\infty$	−3124	∞	−5054	3.216	0.000	0.363
	0.100	−13863	−813	21.750	−2376	2.605	0.062	0.621
	0.200	−8550	714	15.440	−521	2.058	0.180	0.901
	0.300	−5366	1586	11.586	640	1.576	0.341	1.137
	0.400	−3338	1928	8.776	1234	1.158	0.512	1.281
	0.500	−2071	1869	6.567	1387	0.804	0.660	1.320
	0.600	−1322	1535	4.762	1227	0.515	0.767	1.279
	0.700	−899	1054	3.255	881	0.289	0.835	1.193
	0.800	−637	553	1.984	476	0.129	0.880	1.100
	0.900	−385	160	0.908	140	0.032	0.926	1.029
	1.000	0	0	0.000	0	0.000	1.000	1.000

Reference state: Sb($A7$)

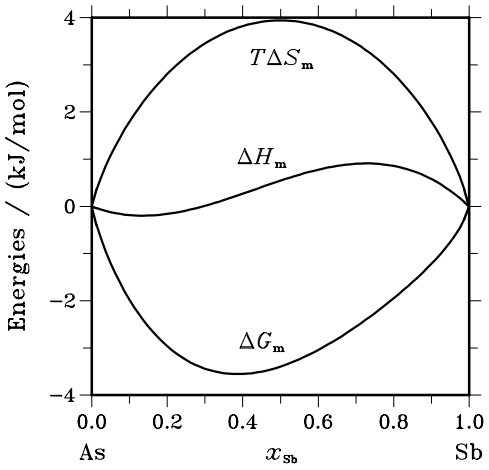

Fig. 5. Integral quantities of the stable phases at T=600 K.

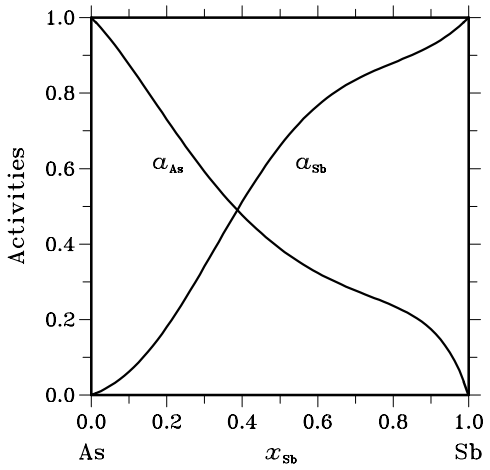

Fig. 6. Activities in the stable phases at T=600 K.

References

[94Ans] I. Ansara, C. Chatillon, H.L. Lukas, T. Nishizawa, H. Ohtani, K. Ishida, M. Hillert, B. Sundman, B.B. Argent, A. Watson, T.G. Chart, T. Anderson: Calphad **18** (1994) 177–222.

Au – Bi (Gold – Bismuth)

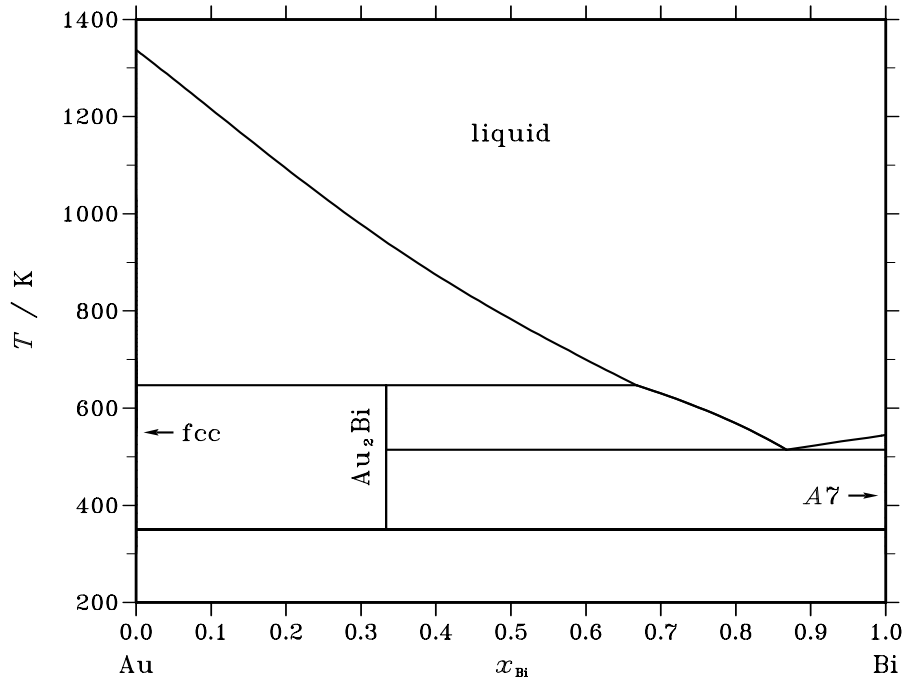

Fig. 1. Calculated phase diagram for the system Au-Bi.

According to the review of [83Oka], the phase diagram shows only one intermetallic compound, Au_2Bi, stable in a limited temperature range. From lattice parameter measurements, [35Jur] reported a very narrow range of existence for the solid phase Au_2Bi, which was described as stoichiometric. The reported enthalpy of mixing shows very small deviation from ideality. The liquid was described by a simple substitutional solution. The dataset has been derived from the critical assessment by Chevalier [88Che].

Table I. Phases, structures and models.

Phase	Struktur-bericht	Prototype	Pearson symbol	Space group	SGTE name	Model
liquid					LIQUID	$(Au,Bi)_1$
fcc	$A1$	Cu	$cF4$	$Fm\overline{3}m$	FCC_A1	$(Au,Bi)_1$
Au_2Bi	$C15$	Cu_2Mg	$cF24$	$Fd\overline{3}m$	AU2BI	Au_2Bi_1
$A7$	$A7$	αAs	$hR2$	$R\overline{3}m$	RHOMBOHEDRAL_A7	Bi_1

Table II. Invariant reactions.

Reaction	Type	T / K	Compositions / x_{Bi}			$\Delta_r H$ / (J/mol)
fcc + liquid $\rightleftharpoons$ Au_2Bi	peritectic	647.0	0.001	0.667	0.333	−4307
liquid $\rightleftharpoons$ Au_2Bi + $A7$	eutectic	514.3	0.868	0.333	1.000	−11339
Au_2Bi $\rightleftharpoons$ fcc + $A7$	eutectoid	350.0	0.333	0.000	1.000	−1645

Table IIIa. Integral quantities for the liquid phase at 1400 K.

x_{Bi}	ΔG_{m} [J/mol]	ΔH_{m} [J/mol]	ΔS_{m} [J/(mol·K)]	$G_{\mathrm{m}}^{\mathrm{E}}$ [J/mol]	$S_{\mathrm{m}}^{\mathrm{E}}$ [J/(mol·K)]	ΔC_p [J/(mol·K)]
0.000	0	0	0.000	0	0.000	0.000
0.100	−4307	−118	2.992	−522	0.289	0.000
0.200	−6755	50	4.860	−930	0.700	0.000
0.300	−8349	316	6.189	−1238	1.110	0.000
0.400	−9274	554	7.020	−1440	1.425	0.000
0.500	−9584	692	7.340	−1515	1.577	0.000
0.600	−9278	701	7.128	−1444	1.532	0.000
0.700	−8329	589	6.370	−1219	1.291	0.000
0.800	−6683	393	5.054	−858	0.893	0.000
0.900	−4201	172	3.124	−417	0.421	0.000
1.000	0	0	0.000	0	0.000	0.000

Reference states: Au(liquid), Bi(liquid)

Table IIIb. Partial quantities for Au in the liquid phase at 1400 K.

x_{Au}	ΔG_{Au} [J/mol]	ΔH_{Au} [J/mol]	ΔS_{Au} [J/(mol·K)]	$G_{\mathrm{Au}}^{\mathrm{E}}$ [J/mol]	$S_{\mathrm{Au}}^{\mathrm{E}}$ [J/(mol·K)]	a_{Au}	γ_{Au}
1.000	0	0	0.000	0	0.000	1.000	1.000
0.900	−1290	−179	0.793	−63	−0.083	0.895	0.995
0.800	−2812	−435	1.698	−215	−0.157	0.785	0.982
0.700	−4616	−490	2.947	−464	−0.019	0.673	0.961
0.600	−6817	−232	4.704	−871	0.456	0.557	0.928
0.500	−9561	319	7.057	−1492	1.294	0.440	0.880
0.400	−13002	1037	10.028	−2336	2.409	0.327	0.818
0.300	−17324	1725	13.607	−3310	3.597	0.226	0.753
0.200	−22905	2148	17.895	−4171	4.513	0.140	0.699
0.100	−31281	2056	23.812	−4478	4.667	0.068	0.681
0.000	$-\infty$	1224	∞	−3540	3.403	0.000	0.738

Reference state: Au(liquid)

Table IIIc. Partial quantities for Bi in the liquid phase at 1400 K.

x_{Bi}	ΔG_{Bi} [J/mol]	ΔH_{Bi} [J/mol]	ΔS_{Bi} [J/(mol·K)]	$G_{\mathrm{Bi}}^{\mathrm{E}}$ [J/mol]	$S_{\mathrm{Bi}}^{\mathrm{E}}$ [J/(mol·K)]	a_{Bi}	γ_{Bi}
0.000	$-\infty$	−3387	∞	−5943	1.826	0.000	0.600
0.100	−31460	434	22.782	−4657	3.637	0.067	0.670
0.200	−22524	1989	17.509	−3790	4.128	0.144	0.722
0.300	−17059	2196	13.753	−3044	3.743	0.231	0.770
0.400	−12960	1734	10.495	−2294	2.877	0.328	0.821
0.500	−9607	1066	7.623	−1538	1.860	0.438	0.876
0.600	−6795	477	5.195	−849	0.947	0.558	0.930
0.700	−4474	102	3.269	−323	0.303	0.681	0.973
0.800	−2627	−46	1.844	−30	−0.012	0.798	0.997
0.900	−1192	−37	0.825	35	−0.051	0.903	1.003
1.000	0	0	0.000	0	0.000	1.000	1.000

Reference state: Bi(liquid)

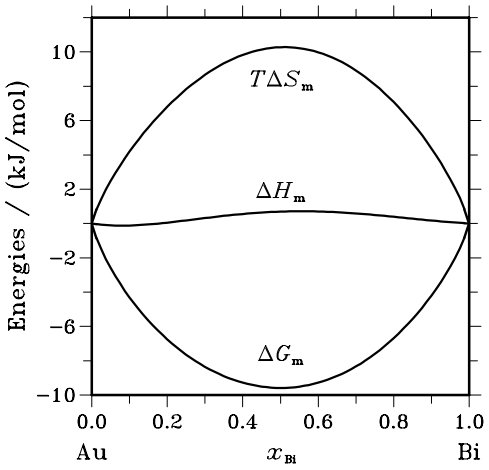

Fig. 2. Integral quantities of the liquid phase at T=1400 K.

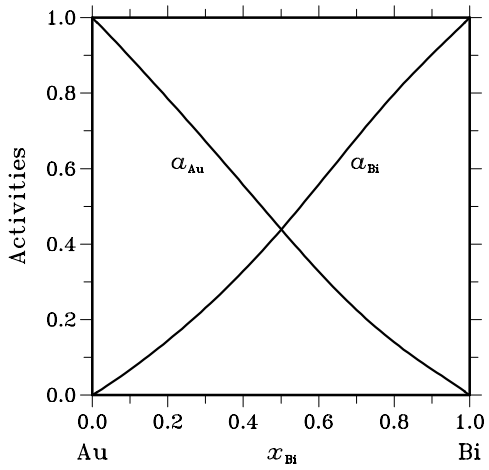

Fig. 3. Activities in the liquid phase at T=1400 K.

Table IV. Standard reaction quantities at 298.15 K for the compounds per mole of atoms.

Compound	x_{Bi}	$\Delta_f G^\circ$ / (J/mol)	$\Delta_f H^\circ$ / (J/mol)	$\Delta_f S^\circ$ / (J/(mol·K))	$\Delta_f C_P^\circ$ / (J/(mol·K))
Au_2Bi_1	0.333	240	1609	4.590	0.750

References

[35Jur] T. Jurriaanse: Z. Krist. **90** (1935) 322-329.
[83Oka] H. Okamoto, T.B. Massalski: Bull. Alloy Phase Diagrams, **4** (1983) 401–407.
[88Che] P.-Y. Chevalier: Thermochim. Acta **130** (1988) 15–24.

Au – C (Gold – Carbon)

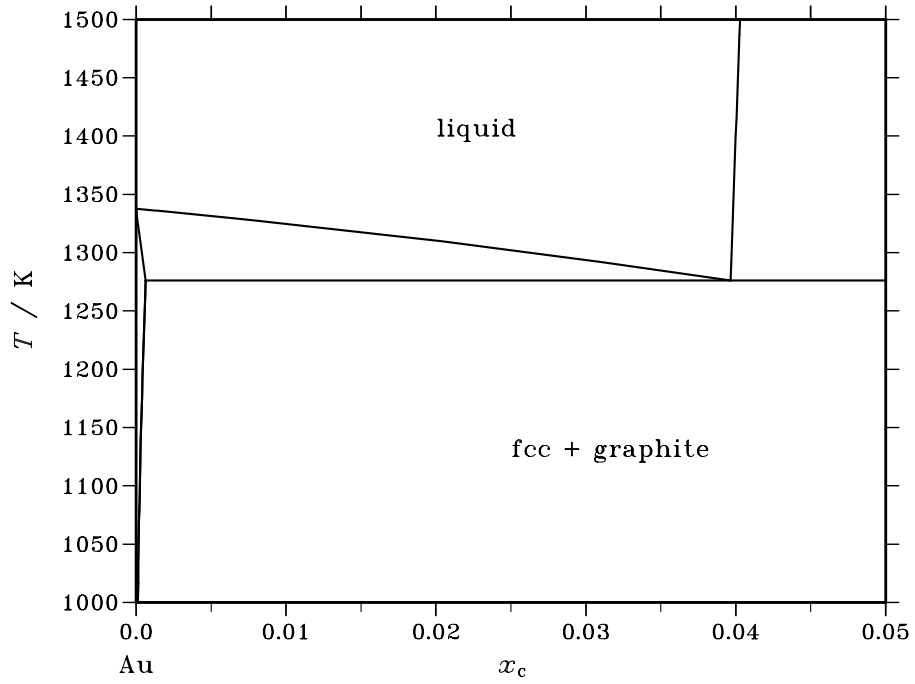

Fig. 1. Calculated partial phase diagram for the system Au-C.

The Au-C system, for which very limited experimental information is available (reviewed by [84Oka]), is presented by Massalski to a concentration of 6 at.% C only. The system displays eutectic behaviour in this range. The present thermodynamic description [98Spe] reproduces the reported behaviour satisfactorily, but should be viewed as being of only limited reliability.

References

[84Oka] H. Okamoto, T.B. Massalski: Bull. Alloy Phase Diagrams **5** (1984) 378–379.
[98Spe] P.J. Spencer, unpublished assessment, 1998.

Table I. Phases, structures and models.

Phase	Struktur-bericht	Prototype	Pearson symbol	Space group	SGTE name	Model
liquid					LIQUID	$(Au,C)_1$
fcc	$A1$	Cu	$cF4$	$Fm\overline{3}m$	FCC_A1	$Au_1(C,\Box)_1$
graphite	$A9$	C(graphite)	$hP4$	$P6_3/mmc$	GRAPHITE	C_1

Table II. Invariant reactions.

Reaction	Type	T / K	Compositions / x_C			$\Delta_r H$ / (J/mol)
liquid $\rightleftharpoons$ fcc + graphite	eutectic	1276.0	0.040	0.001	1.000	−11693

Table IIIa. Integral quantities for the liquid phase at 1400 K.

x_C	ΔG_m [J/mol]	ΔH_m [J/mol]	ΔS_m [J/(mol·K)]	G_m^E [J/mol]	S_m^E [J/(mol·K)]	ΔC_p [J/(mol·K)]
0.000	0	0	0.000	0	0.000	0.000
0.010	−334	−160	0.125	317	−0.341	0.000
0.020	−489	−266	0.159	652	−0.656	0.000
0.030	−565	−321	0.174	1003	−0.946	0.000
0.040	−584	−325	0.185	1371	−1.211	0.000

Reference states: Au(liquid), C(graphite)

Table IIIb. Partial quantities for Au in the liquid phase at 1400 K.

x_{Au}	ΔG_{Au} [J/mol]	ΔH_{Au} [J/mol]	ΔS_{Au} [J/(mol·K)]	G_{Au}^E [J/mol]	S_{Au}^E [J/(mol·K)]	a_{Au}	γ_{Au}
1.000	0	0	0.000	0	0.000	1.000	1.000
0.990	−126	−27	0.071	−9	−0.013	0.989	0.999
0.980	−269	−105	0.117	−34	−0.051	0.977	0.997
0.970	−430	−234	0.140	−76	−0.113	0.964	0.994
0.960	−608	−412	0.140	−133	−0.199	0.949	0.989

Reference state: Au(liquid)

Table IIIc. Partial quantities for C in the liquid phase at 1400 K.

x_C	ΔG_C [J/mol]	ΔH_C [J/mol]	ΔS_C [J/(mol·K)]	G_C^E [J/mol]	S_C^E [J/(mol·K)]	a_C	γ_C
0.000	$-\infty$	−18631	∞	30887	−35.370	0.000	14.203
0.010	−21017	−13337	5.486	32588	−32.804	0.164	16.438
0.020	−11285	−8174	2.222	34252	−30.305	0.379	18.964
0.030	−4938	−3141	1.283	35880	−27.872	0.654	21.810
0.040	0	1762	1.258	37470	−25.506	1.000	25.003

Reference state: C(graphite)

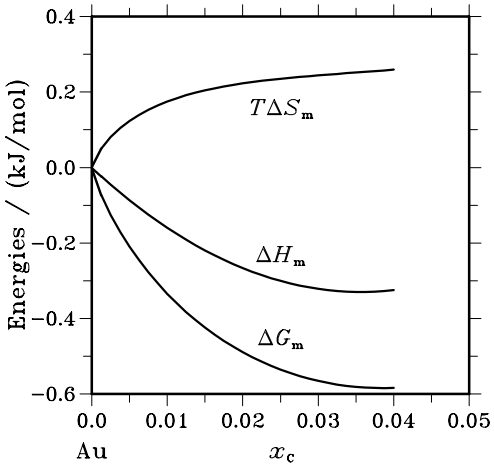

Fig. 2. Integral quantities of the liquid phase at T=1400 K.

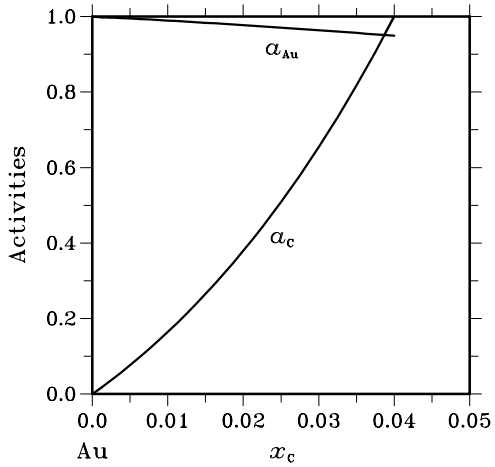

Fig. 3. Activities in the liquid phase at T=1400 K.

Au – Cr (Gold – Chromium)

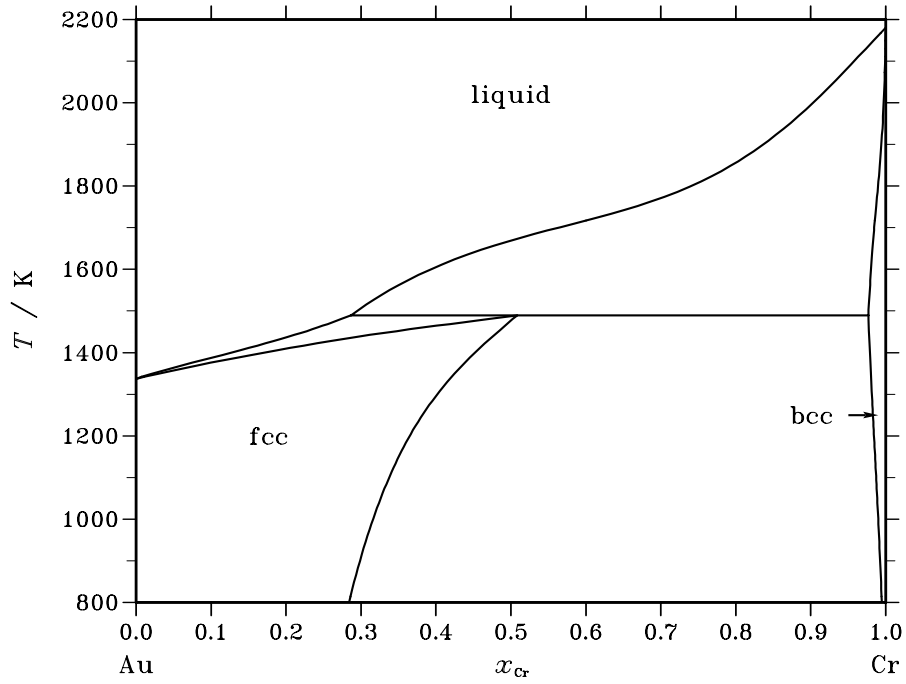

Fig. 1. Calculated phase diagram for the system Au-Cr.

Experimental phase boundary information is available for Au-rich alloys only. The phase diagram presented by Massalski is therefore indicated as being uncertain in the Cr-rich range. The present thermodynamic assessment [98Spe] reproduces the proposed diagram [85Oka] reasonably well, considering the limited information available, but omits the α' phase reported as existing at low temperatures in Au-rich alloys. The tabulated data should be regarded as of limited accuracy only.

Table I. Phases, structures and models.

Phase	Struktur-bericht	Prototype	Pearson symbol	Space group	SGTE name	Model
liquid					LIQUID	$(Au,Cr)_1$
fcc	$A1$	Cu	$cF4$	$Fm\overline{3}m$	FCC_A1	$(Au,Cr)_1$
bcc	$A2$	W	$cI2$	$Im\overline{3}m$	BCC_A2	$(Au,Cr)_1$

Table II. Invariant reactions.

Reaction	Type	T / K	Compositions / x_{Cr}			$\Delta_r H$ / (J/mol)
liquid + bcc $\rightleftharpoons$ fcc	peritectic	1489.6	0.287	0.977	0.508	−16894

Table IIIa. Integral quantities for the liquid phase at 2200 K.

x_{Cr}	ΔG_{m} [J/mol]	ΔH_{m} [J/mol]	ΔS_{m} [J/(mol·K)]	$G_{\mathrm{m}}^{\mathrm{E}}$ [J/mol]	$S_{\mathrm{m}}^{\mathrm{E}}$ [J/(mol·K)]	ΔC_p [J/(mol·K)]
0.000	0	0	0.000	0	0.000	0.000
0.100	−8357	3393	5.341	−2410	2.638	0.000
0.200	−12868	7403	9.214	−3715	5.053	0.000
0.300	−15441	11376	12.189	−4267	7.110	0.000
0.400	−16651	14739	14.268	−4340	8.672	0.000
0.500	−16808	16997	15.366	−4128	9.602	0.000
0.600	−16056	17736	15.360	−3746	9.764	0.000
0.700	−14400	16621	14.101	−3226	9.021	0.000
0.800	−11679	13397	11.398	−2526	7.238	0.000
0.900	−7465	7889	6.979	−1518	4.276	0.000
1.000	0	0	0.000	0	0.000	0.000

Reference states: Au(liquid), Cr(liquid)

Table IIIb. Partial quantities for Au in the liquid phase at 2200 K.

x_{Au}	ΔG_{Au} [J/mol]	ΔH_{Au} [J/mol]	ΔS_{Au} [J/(mol·K)]	$G_{\mathrm{Au}}^{\mathrm{E}}$ [J/mol]	$S_{\mathrm{Au}}^{\mathrm{E}}$ [J/(mol·K)]	a_{Au}	γ_{Au}
1.000	0	0	0.000	0	0.000	1.000	1.000
0.900	−2546	−424	0.964	−618	0.088	0.870	0.967
0.800	−6045	−785	2.391	−1963	0.535	0.719	0.898
0.700	−9970	105	4.580	−3446	1.614	0.580	0.828
0.600	−14065	3194	7.845	−4721	3.597	0.464	0.773
0.500	−18356	9191	12.522	−5677	6.758	0.367	0.733
0.400	−23207	18568	18.989	−6446	11.370	0.281	0.703
0.300	−29420	31555	27.716	−7397	17.706	0.200	0.667
0.200	−38578	48145	39.420	−9138	26.038	0.121	0.607
0.100	−54636	68091	55.785	−12517	36.640	0.050	0.504
0.000	$-\infty$	90906	∞	−18621	49.785	0.000	0.361

Reference state: Au(liquid)

Table IIIc. Partial quantities for Cr in the liquid phase at 2200 K.

x_{Cr}	ΔG_{Cr} [J/mol]	ΔH_{Cr} [J/mol]	ΔS_{Cr} [J/(mol·K)]	$G_{\mathrm{Cr}}^{\mathrm{E}}$ [J/mol]	$S_{\mathrm{Cr}}^{\mathrm{E}}$ [J/(mol·K)]	a_{Cr}	γ_{Cr}
0.000	$-\infty$	28465	∞	−31010	27.034	0.000	0.184
0.100	−60657	37744	44.728	−18539	25.583	0.036	0.363
0.200	−40164	40153	36.508	−10724	23.126	0.111	0.556
0.300	−28206	37675	29.946	−6183	19.935	0.214	0.713
0.400	−20531	32056	23.903	−3770	16.284	0.325	0.814
0.500	−15259	24802	18.209	−2580	12.446	0.434	0.868
0.600	−11289	17181	12.941	−1945	8.694	0.539	0.899
0.700	−7963	10220	8.265	−1439	5.300	0.647	0.924
0.800	−4954	4710	4.393	−873	2.537	0.763	0.953
0.900	−2224	1199	1.556	−296	0.680	0.886	0.984
1.000	0	0	0.000	0	0.000	1.000	1.000

Reference state: Cr(liquid)

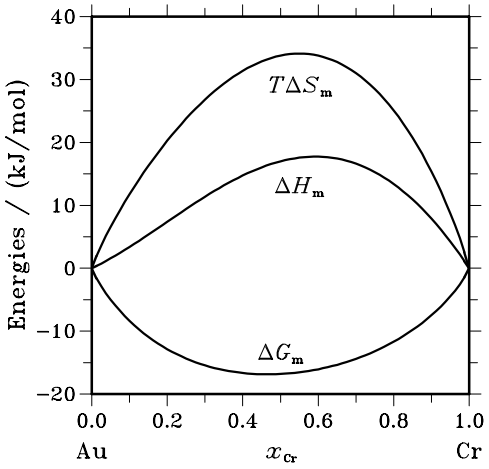

Fig. 2. Integral quantities of the liquid phase at T=2200 K.

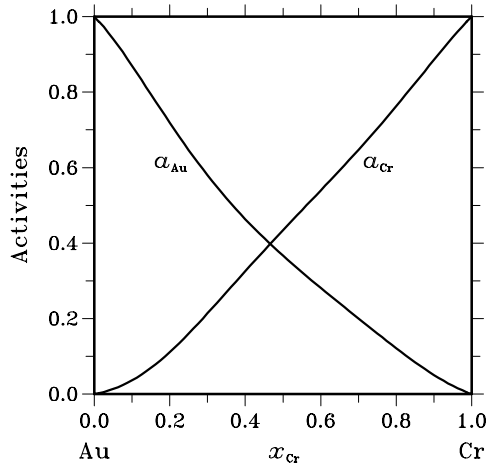

Fig. 3. Activities in the liquid phase at T=2200 K.

Table IVa. Integral quantities for the stable phases at 1300 K.

Phase	x_{Cr}	ΔG_{m} [J/mol]	ΔH_{m} [J/mol]	ΔS_{m} [J/(mol·K)]	$G^{\mathrm{E}}_{\mathrm{m}}$ [J/mol]	$S^{\mathrm{E}}_{\mathrm{m}}$ [J/(mol·K)]	ΔC_p [J/(mol·K)]
fcc	0.000	0	0	0.000	0	0.000	0.000
	0.100	−3443	−2578	0.665	71	−2.038	0.000
	0.200	−4562	−3146	1.089	847	−3.071	0.000
	0.300	−4654	−2352	1.771	1948	−3.308	0.000
	0.400	−4180	−750	2.639	3094	−2.957	0.000
	0.402	−4170	−721	2.653	3112	−2.948	0.000
bcc	0.982	−313	321	0.488	683	−0.278	0.000
	1.000	0	0	0.000	0	0.000	0.000

Reference states: Au(fcc), Cr(bcc)

Table IVb. Partial quantities for Au in the stable phases at 1300 K.

Phase	x_{Au}	ΔG_{Au} [J/mol]	ΔH_{Au} [J/mol]	ΔS_{Au} [J/(mol·K)]	$G^{\mathrm{E}}_{\mathrm{Au}}$ [J/mol]	$S^{\mathrm{E}}_{\mathrm{Au}}$ [J/(mol·K)]	a_{Au}	γ_{Au}
fcc	1.000	0	0	0.000	0	0.000	1.000	1.000
	0.900	−1563	−1122	0.339	−424	−0.537	0.865	0.962
	0.800	−3552	−3572	−0.015	−1141	−1.870	0.720	0.900
	0.700	−5394	−6197	−0.618	−1538	−3.584	0.607	0.867
	0.600	−6822	−8138	−1.013	−1300	−5.260	0.532	0.887
	0.598	−6841	−8160	−1.015	−1291	−5.284	0.531	0.887
bcc	0.018	−6841	17138	18.445	36291	−14.732	0.531	28.717
	0.000	$-\infty$	17621	∞	37556	−15.335	0.000	32.283

Reference state: Au(fcc)

Table IVc. Partial quantities for Cr in the stable phases at 1300 K.

Phase	x_{Cr}	ΔG_{Cr} [J/mol]	ΔH_{Cr} [J/mol]	ΔS_{Cr} [J/(mol·K)]	G^{E}_{Cr} [J/mol]	S^{E}_{Cr} [J/(mol·K)]	a_{Cr}	γ_{Cr}
fcc	0.000	$-\infty$	−38250	∞	−4324	−26.097	0.000	0.670
	0.100	−20363	−15685	3.598	4525	−15.546	0.152	1.520
	0.200	−8599	−1440	5.507	8797	−7.875	0.451	2.257
	0.300	−2929	6619	7.345	10085	−2.666	0.763	2.542
	0.400	−219	10332	8.116	9686	0.497	0.980	2.450
	0.402	−190	10365	8.119	9671	0.533	0.983	2.447
bcc	0.982	−190	5	0.150	12	−0.006	0.983	1.001
	1.000	−131	2	0.102	5	−0.003	0.988	1.000

Reference state: Cr(bcc)

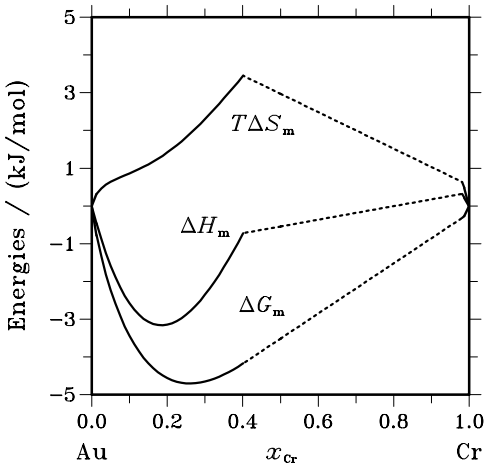

Fig. 4. Integral quantities of the stable phases at T=1300 K.

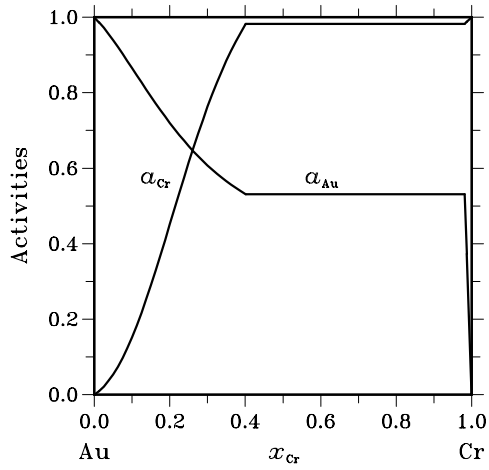

Fig. 5. Activities in the stable phases at T=1300 K.

References

[85Oka] H. Okamoto, T.B. Massalski: Bull. Alloy Phase Diagrams **6** (1985) 224–228.
[98Spe] P.J. Spencer, unpublished assessment, 1998.

Au – Cu (Gold – Copper)

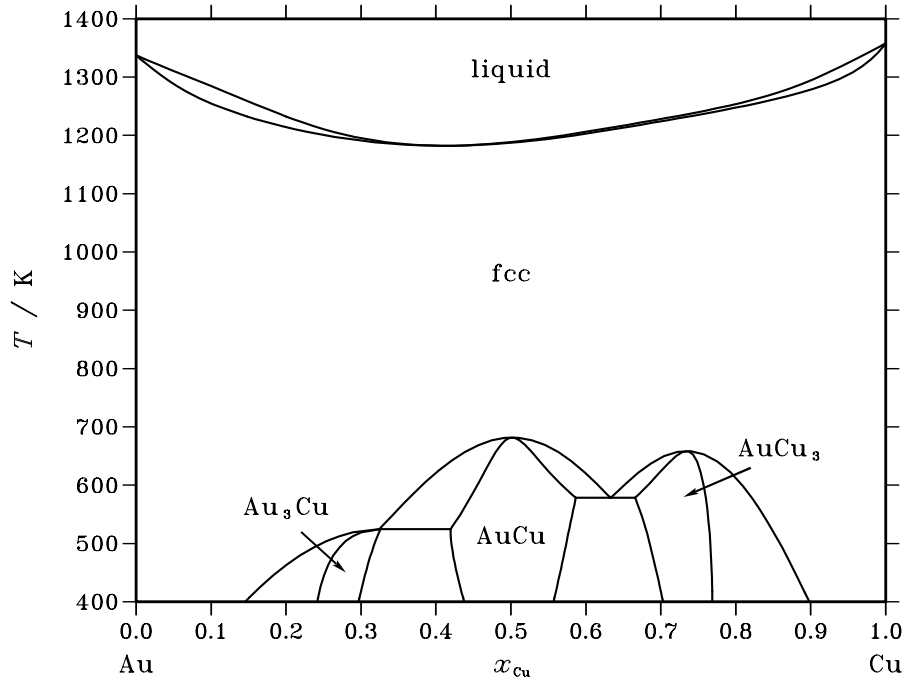

Fig. 1. Calculated phase diagram for the system Au-Cu.

Au–Cu based alloys are encountered in jewelry, gold coins and dental alloys. In addition, this system is a treasure for investigations on order/disorder phenomena in alloys. Au–Cu alloys are among the earliest systems in which order/disorder phenomena have been discovered. Since then, this system has been the subject of intense experimental and theoretical studies. A comprehensive literature survey over the thermodynamics and crystal structure data has been given by Okamoto et al. [87Oka]. The recommended thermodynamic description of the system [98Sun] provides a compromise between the models which are presently available for the Calphad-type modelling and the need to incorporate the ordering phenomena. The ordered phases with $L1_0$ and $L1_2$ structure are described by a 4-sublattice model which becomes equivalent to a simple substitutional model for the fcc-phase above the critical temperatures. The dataset has been optimised in order to provide a good fit of the phase diagram over the whole composition and temperature range. In addition, experimental mixing enthalpies as well as activities of Cu and Au in liquid and solid solutions have been taken into consideration in the optimisation.

Table I. Phases, structures and models.

Phase	Struktur-bericht	Prototype	Pearson symbol	Space group	SGTE name	Model
liquid					LIQUID	$(Au,Cu)_1$
fcc	$A1$	Cu	$cF4$	$Fm\overline{3}m$	FCC_L102	$(Au,Cu)_1$
Au_3Cu, $AuCu_3$	$L1_2$	Cu_3Au	$cP4$	$Pm\overline{3}m$	FCC_L102	$3(Au,Cu)_1$ $1(Au,Cu)_1$
AuCu	$L1_0$	AuCu	$tP4$	$P4/mmm$	FCC_L102	$2(Au,Cu)_1$ $2(Au,Cu)_1$

Table II. Invariant reactions.

Reaction	Type	T / K	Compositions / x_{Cu}			$\Delta_{\mathrm{r}}H$ / (J/mol)
liquid ⇌ fcc	congruent	1182.0	0.411	0.411		−10682
fcc ⇌ AuCu	congruent	681.8	0.502	0.502		−2591
fcc ⇌ $AuCu_3$	congruent	658.5	0.734	0.734		−1719
fcc ⇌ AuCu + $AuCu_3$	eutectoid	578.2	0.633	0.586	0.666	−1477
fcc + AuCu ⇌ Au_3Cu	peritectoid	524.7	0.325	0.419	0.326	−861

Table IIIa. Integral quantities for the liquid phase at 1400 K.

x_{Cu}	ΔG_{m} [J/mol]	ΔH_{m} [J/mol]	ΔS_{m} [J/(mol·K)]	$G^{\mathrm{E}}_{\mathrm{m}}$ [J/mol]	$S^{\mathrm{E}}_{\mathrm{m}}$ [J/(mol·K)]	ΔC_p [J/(mol·K)]
0.000	0	0	0.000	0	0.000	0.000
0.100	−5597	−1969	2.591	−1813	−0.112	0.000
0.200	−9575	−3808	4.119	−3750	−0.042	0.000
0.300	−12584	−5344	5.171	−5473	0.092	0.000
0.400	−14558	−6435	5.802	−6724	0.206	0.000
0.500	−15394	−6975	6.013	−7325	0.250	0.000
0.600	−15013	−6889	5.802	−7178	0.206	0.000
0.700	−13379	−6139	5.171	−6268	0.092	0.000
0.800	−10483	−4716	4.119	−4658	−0.042	0.000
0.900	−6278	−2650	2.591	−2494	−0.112	0.000
1.000	0	0	0.000	0	0.000	0.000

Reference states: Au(liquid), Cu(liquid)

Table IIIb. Partial quantities for Au in the liquid phase at 1400 K.

x_{Au}	ΔG_{Au} [J/mol]	ΔH_{Au} [J/mol]	ΔS_{Au} [J/(mol·K)]	$G^{\mathrm{E}}_{\mathrm{Au}}$ [J/mol]	$S^{\mathrm{E}}_{\mathrm{Au}}$ [J/(mol·K)]	a_{Au}	γ_{Au}
1.000	0	0	0.000	0	0.000	1.000	1.000
0.900	−1101	−33	0.763	126	−0.113	0.910	1.011
0.800	−2587	−381	1.576	10	−0.279	0.801	1.001
0.700	−5055	−1342	2.652	−903	−0.313	0.648	0.925
0.600	−8876	−3113	4.116	−2930	−0.131	0.466	0.777
0.500	−14211	−5793	6.013	−6143	0.250	0.295	0.590
0.400	−21039	−9375	8.331	−10373	0.713	0.164	0.410
0.300	−29225	−13756	11.049	−15211	1.039	0.081	0.271
0.200	−38737	−18730	14.290	−20003	0.909	0.036	0.179
0.100	−50657	−23991	19.048	−23855	−0.097	0.013	0.129
0.000	$-\infty$	−29130	∞	−25630	−2.500	0.000	0.111

Reference state: Au(liquid)

Table IIIc. Partial quantities for Cu in the liquid phase at 1400 K.

x_{Cu}	ΔG_{Cu} [J/mol]	ΔH_{Cu} [J/mol]	ΔS_{Cu} [J/(mol·K)]	G^E_{Cu} [J/mol]	S^E_{Cu} [J/(mol·K)]	a_{Cu}	γ_{Cu}
0.000	$-\infty$	−19670	∞	−16170	−2.500	0.000	0.249
0.100	−46060	−19393	19.048	−19257	−0.097	0.019	0.191
0.200	−37526	−17519	14.290	−18792	0.909	0.040	0.199
0.300	−30152	−14683	11.049	−16138	1.039	0.075	0.250
0.400	−23082	−11419	8.331	−12416	0.713	0.138	0.344
0.500	−16576	−8158	6.013	−8508	0.250	0.241	0.481
0.600	−10995	−5232	4.116	−5049	−0.131	0.389	0.648
0.700	−6587	−2874	2.652	−2436	−0.313	0.568	0.811
0.800	−3420	−1213	1.576	−822	−0.279	0.745	0.932
0.900	−1347	−279	0.763	−120	−0.113	0.891	0.990
1.000	0	0	0.000	0	0.000	1.000	1.000

Reference state: Cu(liquid)

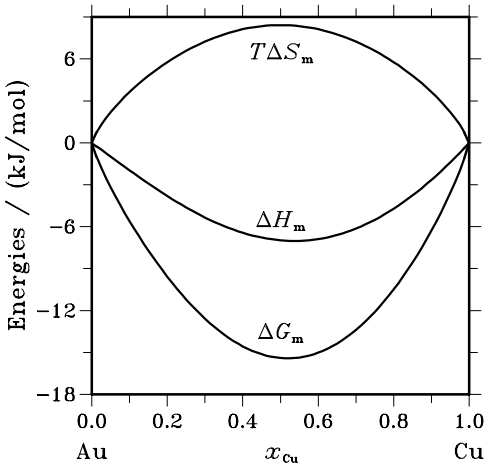

Fig. 2. Integral quantities of the liquid phase at T=1400 K.

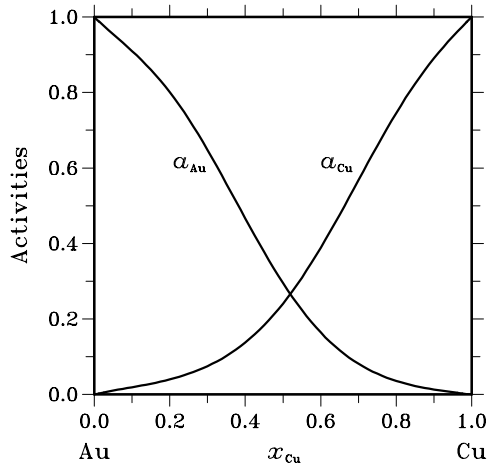

Fig. 3. Activities in the liquid phase at T=1400 K.

Table IVa. Integral quantities for the stable phases at 800 K.

Phase	x_{Cu}	ΔG_m [J/mol]	ΔH_m [J/mol]	ΔS_m [J/(mol·K)]	G^E_m [J/mol]	S^E_m [J/(mol·K)]	ΔC_p [J/(mol·K)]
fcc	0.000	0	0	0.000	0	0.000	0.000
	0.100	−3413	−1462	2.439	−1251	−0.264	0.423
	0.200	−5967	−2788	3.974	−2638	−0.187	0.751
	0.300	−7999	−3920	5.098	−3936	0.019	0.986
	0.400	−9434	−4795	5.799	−4958	0.203	1.127
	0.500	−10155	−5324	6.038	−5544	0.275	1.174
	0.600	−10042	−5402	5.799	−5565	0.203	1.127
	0.700	−9002	−4923	5.098	−4939	0.019	0.986
	0.800	−6998	−3819	3.974	−3670	−0.187	0.751
	0.900	−4067	−2116	2.439	−1904	−0.264	0.423
	1.000	0	0	0.000	0	0.000	0.000

Reference states: Au(fcc), Cu(fcc)

Table IVb. Partial quantities for Au in the stable phases at 800 K.

Phase	x_{Au}	ΔG_{Au} [J/mol]	ΔH_{Au} [J/mol]	ΔS_{Au} [J/(mol·K)]	G^E_{Au} [J/mol]	S^E_{Au} [J/(mol·K)]	a_{Au}	γ_{Au}
fcc	1.000	0	0	0.000	0	0.000	1.000	1.000
	0.900	−590	−58	0.665	111	−0.211	0.915	1.017
	0.800	−1370	−311	1.325	114	−0.531	0.814	1.017
	0.700	−2743	−872	2.339	−371	−0.627	0.662	0.946
	0.600	−5040	−1921	3.899	−1642	−0.348	0.469	0.781
	0.500	−8543	−3713	6.038	−3933	0.275	0.277	0.554
	0.400	−13429	−6510	8.649	−7334	1.031	0.133	0.332
	0.300	−19653	−10423	11.537	−11645	1.526	0.052	0.174
	0.200	−26826	−15171	14.569	−16121	1.187	0.018	0.089
	0.100	−34468	−19746	18.402	−19152	−0.743	0.006	0.056
	0.000	−∞	−22004	∞	−17843	−5.201	0.000	0.068

Reference state: Au(fcc)

Table IVc. Partial quantities for Cu in the stable phases at 800 K.

Phase	x_{Cu}	ΔG_{Cu} [J/mol]	ΔH_{Cu} [J/mol]	ΔS_{Cu} [J/(mol·K)]	G^E_{Cu} [J/mol]	S^E_{Cu} [J/(mol·K)]	a_{Cu}	γ_{Cu}
fcc	0.000	−∞	−15074	∞	−10913	−5.201	0.000	0.194
	0.100	−28820	−14098	18.402	−13504	−0.743	0.013	0.131
	0.200	−24352	−12696	14.569	−13646	1.187	0.026	0.129
	0.300	−20262	−11032	11.537	−12254	1.526	0.048	0.158
	0.400	−16025	−9106	8.649	−9930	1.031	0.090	0.225
	0.500	−11766	−6936	6.038	−7156	0.275	0.171	0.341
	0.600	−7783	−4664	3.899	−4385	−0.348	0.310	0.517
	0.700	−4437	−2566	2.339	−2065	−0.627	0.513	0.733
	0.800	−2041	−982	1.325	−557	−0.531	0.736	0.920
	0.900	−689	−157	0.665	12	−0.211	0.902	1.002
	1.000	0	0	0.000	0	0.000	1.000	1.000

Reference state: Cu(fcc)

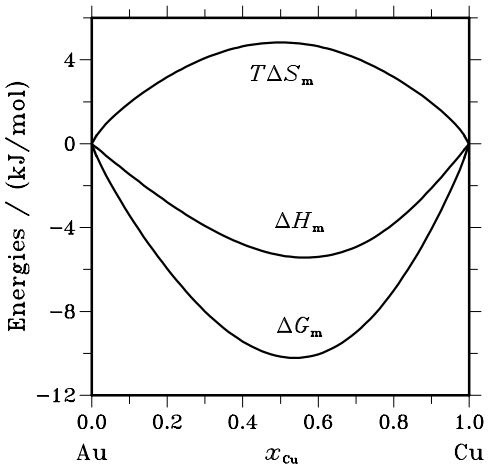

Fig. 4. Integral quantities of the stable phases at T=800 K.

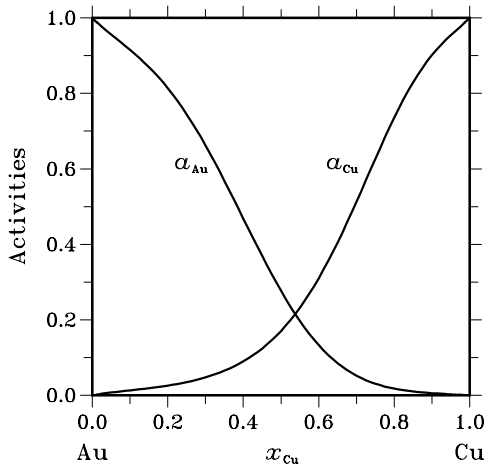

Fig. 5. Activities in the stable phases at T=800 K.

References

[87Oka] H. Okamoto, D.J. Chakrabarti, D.E. Laughlin, T.B. Massalski: Bull. Alloy Phase Diagrams **8** (1987) 454–474.

[98Sun] B. Sundman, S.G. Fries, A. Oates: Calphad **22** (1998) 335–354.

Au – Ge (Gold – Germanium)

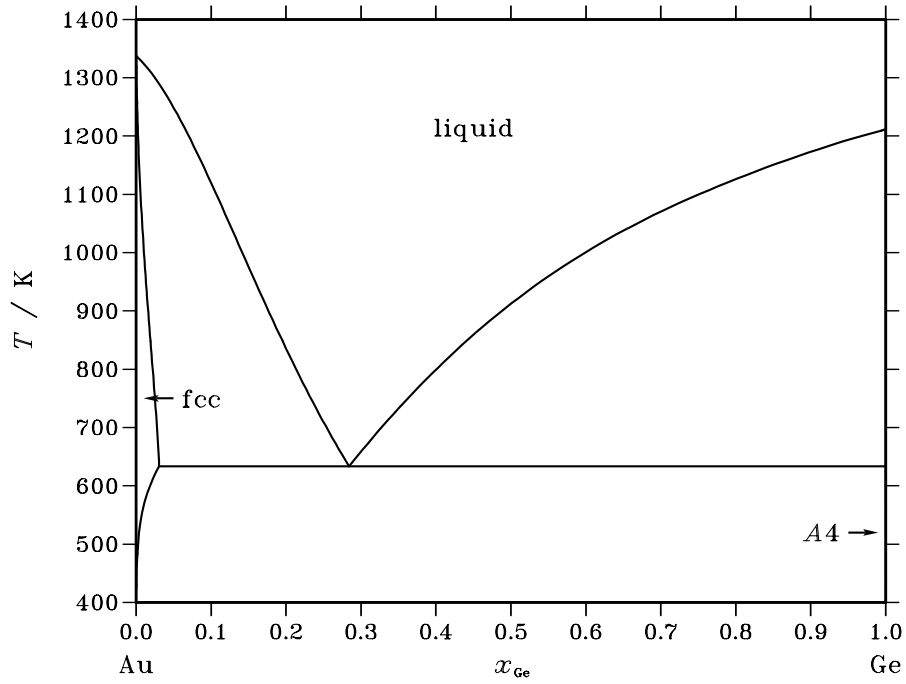

Fig. 1. Calculated phase diagram for the system Au-Ge.

This system is of interest for the electronic industry. An assessment has been provided by Chevalier [89Che]. The phase diagram is of a simple eutectic type, with a deep eutectic in the gold rich side. The solid solution of Ge in Au is going up to 3.1 at.% at the eutectic temperature, but the solubility of Au in Ge is negligible. Two types of metastable phases obtained by splat cooling have been reported for compositions of Ge in the range from 17.5 to 22.5 at.% [64Luo, 65Ana].

Table I. Phases, structures and models.

Phase	Struktur-bericht	Prototype	Pearson symbol	Space group	SGTE name	Model
liquid					LIQUID	$(Au,Ge)_1$
fcc	$A1$	Cu	$cF4$	$Fm\overline{3}m$	FCC_A1	$(Au,Ge)_1$
$A4$	$A4$	C(diamond)	$cF8$	$Fd\overline{3}m$	DIAMOND_A4	Ge_1

Table II. Invariant reactions.

Reaction	Type	T / K	Compositions / x_{Ge}			$\Delta_r H$ / (J/mol)
liquid $\rightleftharpoons$ fcc + $A4$	eutectic	633.5	0.284	0.031	1.000	−13884

Table IIIa. Integral quantities for the liquid phase at 1400 K.

x_{Ge}	ΔG_m [J/mol]	ΔH_m [J/mol]	ΔS_m [J/(mol·K)]	G_m^E [J/mol]	S_m^E [J/(mol·K)]	ΔC_p [J/(mol·K)]
0.000	0	0	0.000	0	0.000	0.000
0.100	−8951	−2714	4.455	−5167	1.752	0.000
0.200	−13992	−4032	7.114	−8167	2.954	0.000
0.300	−16648	−4576	8.623	−9537	3.544	0.000
0.400	−17560	−4690	9.193	−9726	3.597	0.000
0.500	−17163	−4515	9.035	−9095	3.271	0.000
0.600	−15749	−4070	8.342	−7914	2.746	0.000
0.700	−13478	−3327	7.250	−6367	2.171	0.000
0.800	−10370	−2293	5.770	−4545	1.609	0.000
0.900	−6236	−1082	3.681	−2452	0.979	0.000
1.000	0	0	0.000	0	0.000	0.000

Reference states: Au(liquid), Ge(liquid)

Table IIIb. Partial quantities for Au in the liquid phase at 1400 K.

x_{Au}	ΔG_{Au} [J/mol]	ΔH_{Au} [J/mol]	ΔS_{Au} [J/(mol·K)]	G_{Au}^E [J/mol]	S_{Au}^E [J/(mol·K)]	a_{Au}	γ_{Au}
1.000	0	0	0.000	0	0.000	1.000	1.000
0.900	−2407	−829	1.127	−1180	0.251	0.813	0.904
0.800	−6559	−2325	3.024	−3961	1.169	0.569	0.712
0.700	−11552	−3702	5.607	−7400	2.642	0.371	0.530
0.600	−16767	−4854	8.509	−10821	4.262	0.237	0.395
0.500	−21882	−6048	11.310	−13813	5.547	0.153	0.305
0.400	−26901	−7606	13.782	−16235	6.164	0.099	0.248
0.300	−32229	−9599	16.164	−18214	6.153	0.063	0.209
0.200	−38882	−11532	19.536	−20148	6.154	0.035	0.177
0.100	−49511	−12034	26.769	−22708	7.624	0.014	0.142
0.000	−∞	−8542	∞	−26837	13.068	0.000	0.100

Reference state: Au(liquid)

Table IIIc. Partial quantities for Ge in the liquid phase at 1400 K.

x_{Ge}	ΔG_{Ge} [J/mol]	ΔH_{Ge} [J/mol]	ΔS_{Ge} [J/(mol·K)]	G_{Ge}^E [J/mol]	S_{Ge}^E [J/(mol·K)]	a_{Ge}	γ_{Ge}
0.000	−∞	−37046	∞	−64515	19.621	0.000	0.004
0.100	−67849	−19677	34.408	−41046	15.263	0.003	0.029
0.200	−43724	−10857	23.476	−24990	10.095	0.023	0.117
0.300	−28537	−6615	15.659	−14522	5.648	0.086	0.287
0.400	−18750	−4443	10.219	−8084	2.601	0.200	0.499
0.500	−12445	−2982	6.759	−4376	0.996	0.343	0.687
0.600	−8313	−1712	4.715	−2367	0.468	0.490	0.816
0.700	−5442	−639	3.430	−1290	0.465	0.627	0.895
0.800	−3242	17	2.328	−645	0.473	0.757	0.946
0.900	−1428	134	1.116	−202	0.240	0.885	0.983
1.000	0	0	0.000	0	0.000	1.000	1.000

Reference state: Ge(liquid)

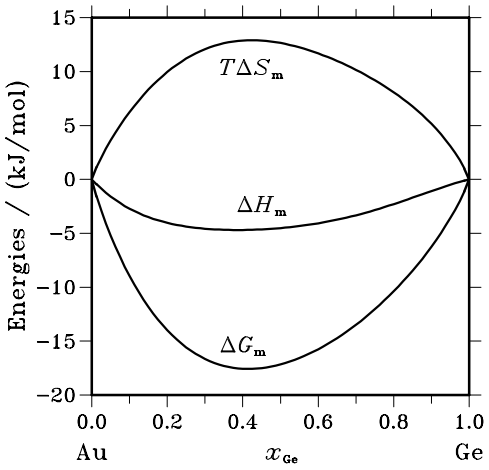

Fig. 2. Integral quantities of the liquid phase at T=1400 K.

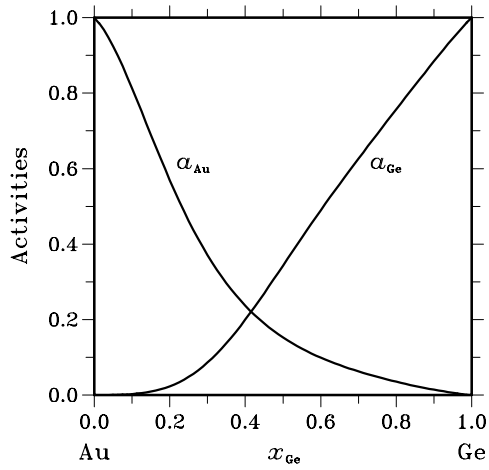

Fig. 3. Activities in the liquid phase at T=1400 K.

References

[64Luo] H.L. Luo, W. Klement jr.: CA Inst. Technol. Tech. Rept. **24** (1964) 1–6.
[65Ana] T.R. Anantharaman, H.L. Luo, W. Klement jr.: Trans. AIME **233** (1965) 2014–2017.
[89Che] P.-Y. Chevalier: Thermochim. Acta **141** (1989) 217–226.

Au – In (Gold – Indium)

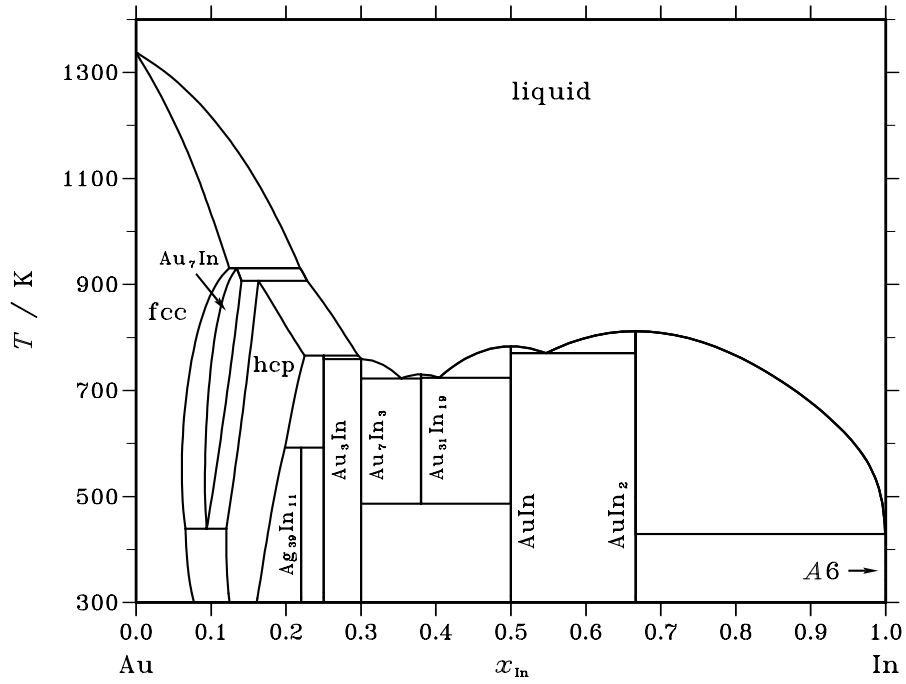

Fig. 1. Calculated phase diagram for the system Au-In.

The thermodynamic assessment of this system by [92Ans] provides good agreement with the invariant reactions indicated in the phase diagram presented by Massalski [90Mas]. In this system several intermetallic phases with narrow homogeneity range transform between high- and low-temperature modifications but due to the lack of sufficient data they have been modelled as only one phase. Therefore, the phases β/β', ϵ/ϵ' and γ/γ' are represented by the line compounds $Au_{39}In_{11}$, Au_3In and Au_7In, respectively. Similarly, the ψ phase with a broader stability range is also described as a stoichiometric compound, $Au_{31}In_{19}$. However, the thermodynamic modelling still allows the thermodynamic properties of this complex system to be described with some accuracy and allows portions of the diagram indicated by Massalski as being uncertain to be presented with greater confidence. The system displays significant negative departures from ideality.

Table I. Phases, structures and models.

Phase	Struktur-bericht	Prototype	Pearson symbol	Space group	SGTE name	Model
liquid					LIQUID	$(Au,In)_1$
fcc	$A1$	Cu	$cF4$	$Fm\overline{3}m$	FCC_A1	$(Au,In)_1$
Au_7In	$D0_{24}$ or $A3'$	Ni_3Ti or αLa	$hP16$ or $hP4$	$P6_3/mmc$	AUIN_ALPHA1	$(Au,In)_1$
hcp	$A3$	Mg	$hP2$	$P6_3/mmc$	HCP_A3	$(Au,In)_1$
$Au_{39}In_{11}$	$\cdots$	$Cu_{33}Sb$ or $Cu_{10}Sb_3$	$hP26$ or $hP*$	$P\overline{3}$	AU4IN	$Au_{39}In_{11}$
Au_3In	$D0_a$	βCu_3Ti	$oP8$	$Pmmn$	AU3IN	Au_3In_1
Au_7In_3	$\cdots$	Au_7In_3	$hP60$	$P\overline{3}$	AU7IN3	Au_7In_3
$Au_{31}In_{19}$	$D5_{13}$	Al_3Ni_2	$hP5$	$Pnma$	D513_AUIN	$Au_{31}In_{19}$
AuIn	$\cdots$	$\cdots$	$aP*$	$\cdots$	AUIN	Au_1In_1
$AuIn_2$	$C1$	CaF_2	$cF12$	$Fm\overline{3}m$	C1_AUIN2	Au_1In_2
$A6$	$A6$	In	$tI2$	$I4/mmm$	TETRAGONAL_A6	In_1

Table II. Invariant reactions.

Reaction	Type	T / K	Compositions / x_{In}			$\Delta_r H$ / (J/mol)
fcc + liquid $\rightleftharpoons$ Au_7In	peritectic	930.9	0.124	0.219	0.134	−1518
Au_7In + liquid $\rightleftharpoons$ hcp	peritectic	907.1	0.141	0.228	0.163	−1657
liquid $\rightleftharpoons$ $AuIn_2$	congruent	811.9	0.667	0.667		−18855
liquid $\rightleftharpoons$ AuIn	congruent	783.3	0.500	0.500		−9424
liquid $\rightleftharpoons$ AuIn + $AuIn_2$	eutectic	770.3	0.547	0.500	0.667	−11699
hcp + liquid $\rightleftharpoons$ Au_3In	peritectic	765.7	0.225	0.296	0.250	−2266
Au_3In + liquid $\rightleftharpoons$ Au_7In_3	peritectic	759.4	0.250	0.301	0.300	−5221
liquid $\rightleftharpoons$ $Au_{31}In_{19}$	congruent	730.6	0.380	0.380		−5188
liquid $\rightleftharpoons$ $Au_{31}In_{19}$ + AuIn	eutectic	723.9	0.404	0.380	0.500	−5808
liquid $\rightleftharpoons$ Au_7In_3 + $Au_{31}In_{19}$	eutectic	722.8	0.354	0.300	0.380	−5043
hcp + Au_3In $\rightleftharpoons$ $Au_{39}In_{11}$	peritectoid	591.9	0.199	0.250	0.220	−143
$Au_{31}In_{19}$ $\rightleftharpoons$ Au_7In_3 + AuIn	eutectoid	486.6	0.380	0.300	0.500	−813
Au_7In $\rightleftharpoons$ fcc + hcp	eutectoid	439.4	0.094	0.066	0.121	−180
liquid $\rightleftharpoons$ $AuIn_2$ + $A6$	eutectic	429.4	0.999	0.667	1.000	−3318

Table IIIa. Integral quantities for the liquid phase at 1400 K.

x_{In}	ΔG_{m} [J/mol]	ΔH_{m} [J/mol]	ΔS_{m} [J/(mol·K)]	$G_{\mathrm{m}}^{\mathrm{E}}$ [J/mol]	$S_{\mathrm{m}}^{\mathrm{E}}$ [J/(mol·K)]	ΔC_p [J/(mol·K)]
0.000	0	0	0.000	0	0.000	0.000
0.100	−8630	−7201	1.021	−4846	−1.682	1.800
0.200	−14346	−12267	1.485	−8521	−2.675	2.783
0.300	−18171	−15397	1.981	−11060	−3.098	3.105
0.400	−20333	−16794	2.528	−12499	−3.068	2.923
0.500	−20940	−16657	3.059	−12872	−2.704	2.393
0.600	−20049	−15188	3.472	−12215	−2.123	1.671
0.700	−17675	−12587	3.634	−10564	−1.445	0.915
0.800	−13779	−9055	3.375	−7954	−0.786	0.280
0.900	−8205	−4792	2.438	−4421	−0.265	−0.077
1.000	0	0	0.000	0	0.000	0.000

Reference states: Au(liquid), In(liquid)

Table IIIb. Partial quantities for Au in the liquid phase at 1400 K.

x_{Au}	ΔG_{Au} [J/mol]	ΔH_{Au} [J/mol]	ΔS_{Au} [J/(mol·K)]	$G_{\mathrm{Au}}^{\mathrm{E}}$ [J/mol]	$S_{\mathrm{Au}}^{\mathrm{E}}$ [J/(mol·K)]	a_{Au}	γ_{Au}
1.000	0	0	0.000	0	0.000	1.000	1.000
0.900	−1818	−1101	0.512	−592	−0.364	0.855	0.950
0.800	−4917	−4137	0.557	−2319	−1.299	0.655	0.819
0.700	−9264	−8707	0.398	−5112	−2.568	0.451	0.645
0.600	−14845	−14408	0.312	−8899	−3.935	0.279	0.466
0.500	−21678	−20840	0.599	−13610	−5.164	0.155	0.311
0.400	−29839	−27600	1.599	−19173	−6.019	0.077	0.193
0.300	−39532	−34288	3.746	−25518	−6.264	0.034	0.112
0.200	−51308	−40501	7.719	−32574	−5.663	0.012	0.061
0.100	−67072	−45839	15.167	−40269	−3.978	0.003	0.031
0.000	$-\infty$	−49899	∞	−48534	−0.975	0.000	0.015

Reference state: Au(liquid)

Table IIIc. Partial quantities for In in the liquid phase at 1400 K.

x_{In}	ΔG_{In} [J/mol]	ΔH_{In} [J/mol]	ΔS_{In} [J/(mol·K)]	$G_{\mathrm{In}}^{\mathrm{E}}$ [J/mol]	$S_{\mathrm{In}}^{\mathrm{E}}$ [J/(mol·K)]	a_{In}	γ_{In}
0.000	$-\infty$	−83359	∞	−54439	−20.657	0.000	0.009
0.100	−69942	−62100	5.601	−43139	−13.544	0.002	0.025
0.200	−52064	−44784	5.200	−33329	−8.182	0.011	0.057
0.300	−38954	−31009	5.675	−24939	−4.335	0.035	0.117
0.400	−28563	−20373	5.850	−17897	−1.768	0.086	0.215
0.500	−20202	−12475	5.519	−12134	−0.244	0.176	0.353
0.600	−13523	−6913	4.721	−7576	0.474	0.313	0.522
0.700	−8307	−3286	3.586	−4155	0.621	0.490	0.700
0.800	−4397	−1193	2.289	−1800	0.433	0.685	0.857
0.900	−1665	−231	1.024	−438	0.148	0.867	0.963
1.000	0	0	0.000	0	0.000	1.000	1.000

Reference state: In(liquid)

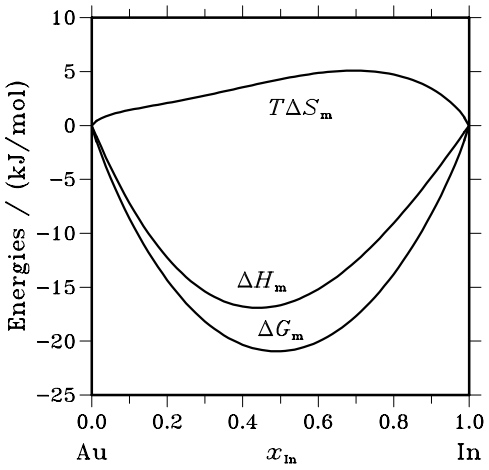

Fig. 2. Integral quantities of the liquid phase at T=1400 K.

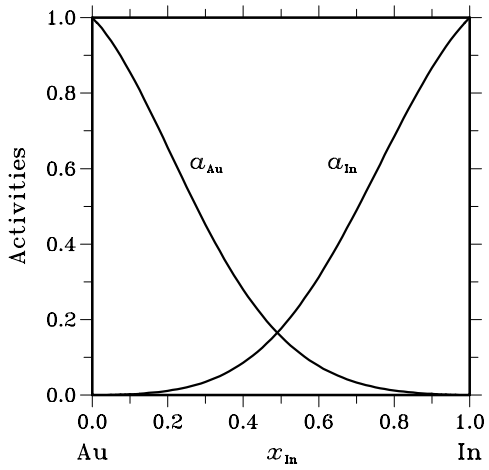

Fig. 3. Activities in the liquid phase at T=1400 K.

Table IV. Standard reaction quantities at 298.15 K for the compounds per mole of atoms.

Compound	x_{In}	$\Delta_f G^\circ$ / (J/mol)	$\Delta_f H^\circ$ / (J/mol)	$\Delta_f S^\circ$ / (J/(mol·K))	$\Delta_f C_P^\circ$ / (J/(mol·K))
$Au_{39}In_{11}$	0.220	−10472	−9762	2.380	0.000
Au_3In_1	0.250	−11700	−11055	2.166	0.000
Au_7In_3	0.300	−13513	−12936	1.937	0.000
$Au_{31}In_{19}$	0.380	−15429	−14805	2.093	0.000
Au_1In_1	0.500	−19088	−19639	−1.848	0.000
$AuIn_2$	0.667	−23148	−26731	−12.016	0.000

References

[90Mas] T.B. Massalski, H. Okamoto, P.R. Subramanian, L. Kacprzak: "Binary Alloy Phase Diagrams", 2nd ed., ASM International, Materials Park, Ohio, USA, 1990.

[92Ans] I. Ansara, J.-P. Nabot: Calphad **16** (1992) 13–18.

Au – Pb (Gold – Lead)

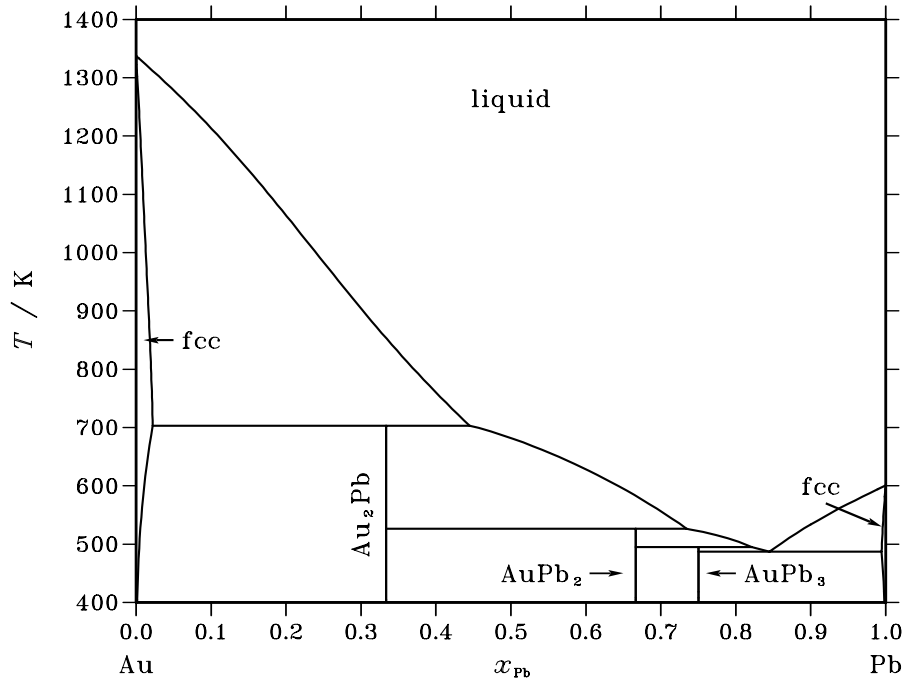

Fig. 1. Calculated phase diagram for the system Au-Pb.

The Au-Pb system is characterised by three peritectically forming compound phases, which in the thermodynamic assessment of the system by [86Nab] are modelled as being of stoichiometric composition. There is good agreement of calculated invariant reactions with those presented in the phase diagram due to Massalski.

Table I. Phases, structures and models.

Phase	Struktur-bericht	Prototype	Pearson symbol	Space group	SGTE name	Model
liquid					LIQUID	$(Au,Pb)_1$
fcc	$A1$	Cu	$cF4$	$Fm\overline{3}m$	FCC_A1	$(Au,Pb)_1$
Au_2Pb	$C15$	Cu_2Mg	$cF24$	$Fd\overline{3}m$	AU2PB	Au_2Pb_1
$AuPb_2$	$C16$	Al_2Cu	$tI12$	$I4/mcm$	AUPB2	Au_1Pb_2
$AuPb_3$	$\cdots$	αV_3S	$tI32$	$I\overline{4}2m$	AUPB3	Au_1Pb_3

Table II. Invariant reactions.

Reaction	Type	T / K	Compositions / x_{Pb}			$\Delta_r H$ / (J/mol)
fcc + liquid $\rightleftharpoons$ Au_2Pb	peritectic	703.4	0.022	0.445	0.333	−7931
Au_2Pb + liquid $\rightleftharpoons$ $AuPb_2$	peritectic	526.3	0.333	0.734	0.667	−5573
$AuPb_2$ + liquid $\rightleftharpoons$ $AuPb_3$	peritectic	495.0	0.667	0.821	0.750	−2830
liquid $\rightleftharpoons$ $AuPb_3$ + fcc	eutectic	487.0	0.845	0.750	0.994	−4969

Table IIIa. Integral quantities for the liquid phase at 1400 K.

x_{Pb}	ΔG_{m} [J/mol]	ΔH_{m} [J/mol]	ΔS_{m} [J/(mol·K)]	$G^{\mathrm{E}}_{\mathrm{m}}$ [J/mol]	$S^{\mathrm{E}}_{\mathrm{m}}$ [J/(mol·K)]	ΔC_p [J/(mol·K)]
0.000	0	0	0.000	0	0.000	0.000
0.100	−4824	−2191	1.881	−1040	−0.822	−2.454
0.200	−7720	−3184	3.239	−1895	−0.921	−3.226
0.300	−9659	−3247	4.580	−2548	−0.499	−2.742
0.400	−10817	−2646	5.836	−2983	0.240	−1.428
0.500	−11249	−1647	6.859	−3180	1.095	0.289
0.600	−10957	−515	7.458	−3123	1.863	1.983
0.700	−9905	481	7.419	−2794	2.340	3.227
0.800	−8001	1077	6.484	−2176	2.323	3.595
0.900	−5034	1005	4.314	−1250	1.611	2.662
1.000	0	0	0.000	0	0.000	0.000

Reference states: Au(liquid), Pb(liquid)

Table IIIb. Partial quantities for Au in the liquid phase at 1400 K.

x_{Au}	ΔG_{Au} [J/mol]	ΔH_{Au} [J/mol]	ΔS_{Au} [J/(mol·K)]	$G^{\mathrm{E}}_{\mathrm{Au}}$ [J/mol]	$S^{\mathrm{E}}_{\mathrm{Au}}$ [J/(mol·K)]	a_{Au}	γ_{Au}
1.000	0	0	0.000	0	0.000	1.000	1.000
0.900	−1316	−643	0.480	−89	−0.396	0.893	0.992
0.800	−2978	−2217	0.544	−380	−1.312	0.774	0.968
0.700	−5060	−4188	0.622	−908	−2.343	0.647	0.925
0.600	−7654	−6025	1.163	−1708	−3.084	0.518	0.864
0.500	−10883	−7195	2.634	−2814	−3.129	0.393	0.785
0.400	−14929	−7165	5.546	−4263	−2.073	0.277	0.693
0.300	−20104	−5402	10.501	−6090	0.491	0.178	0.593
0.200	−27063	−1375	18.349	−8329	4.967	0.098	0.489
0.100	−37818	5451	30.906	−11015	11.762	0.039	0.388
0.000	$-\infty$	15607	∞	−14185	21.280	0.000	0.296

Reference state: Au(liquid)

Table IIIc. Partial quantities for Pb in the liquid phase at 1400 K.

x_{Pb}	ΔG_{Pb} [J/mol]	ΔH_{Pb} [J/mol]	ΔS_{Pb} [J/(mol·K)]	$G^{\mathrm{E}}_{\mathrm{Pb}}$ [J/mol]	$S^{\mathrm{E}}_{\mathrm{Pb}}$ [J/(mol·K)]	a_{Pb}	γ_{Pb}
0.000	$-\infty$	−28780	∞	−11257	−12.517	0.000	0.380
0.100	−36396	−16121	14.481	−9593	−4.663	0.044	0.439
0.200	−26688	−7056	14.023	−7954	0.641	0.101	0.505
0.300	−20391	−1052	13.814	−6377	3.803	0.173	0.578
0.400	−15562	2423	12.846	−4896	5.227	0.263	0.657
0.500	−11615	3902	11.083	−3546	5.320	0.369	0.737
0.600	−8309	3918	8.734	−2363	4.486	0.490	0.816
0.700	−5534	3003	6.097	−1382	3.132	0.622	0.888
0.800	−3235	1690	3.518	−638	1.662	0.757	0.947
0.900	−1392	511	1.359	−165	0.483	0.887	0.986
1.000	0	0	0.000	0	0.000	1.000	1.000

Reference state: Pb(liquid)

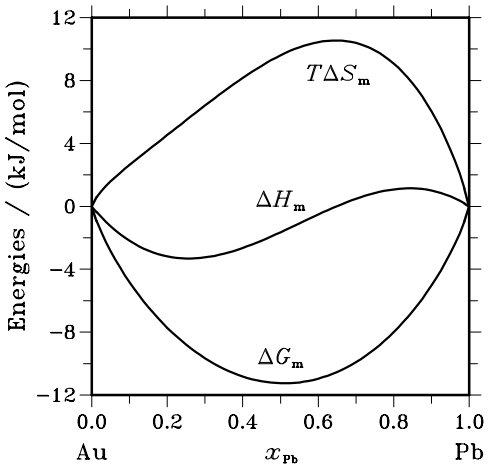

Fig. 2. Integral quantities of the liquid phase at T=1400 K.

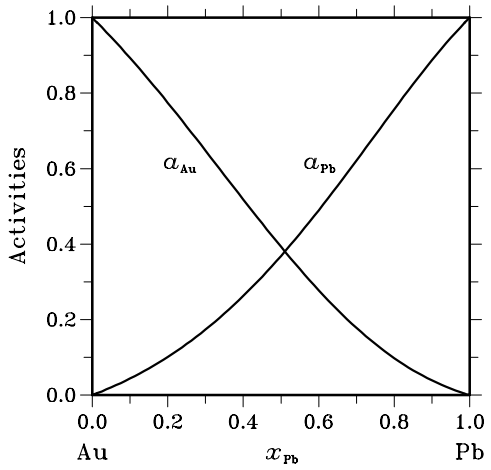

Fig. 3. Activities in the liquid phase at T=1400 K.

Table IV. Standard reaction quantities at 298.15 K for the compounds per mole of atoms.

Compound	x_{Pb}	$\Delta_f G^\circ$ / (J/mol)	$\Delta_f H^\circ$ / (J/mol)	$\Delta_f S^\circ$ / (J/(mol·K))	$\Delta_f C_P^\circ$ / (J/(mol·K))
Au_2Pb_1	0.333	−2222	−1519	2.356	−2.244
Au_1Pb_2	0.667	−2059	−2170	−0.375	0.000
Au_1Pb_3	0.750	−1597	−1656	−0.199	0.000

References

[86Nab] J.-P. Nabot: Thesis, INPG, Grenoble, 1986.

Au – Pd (Gold – Palladium)

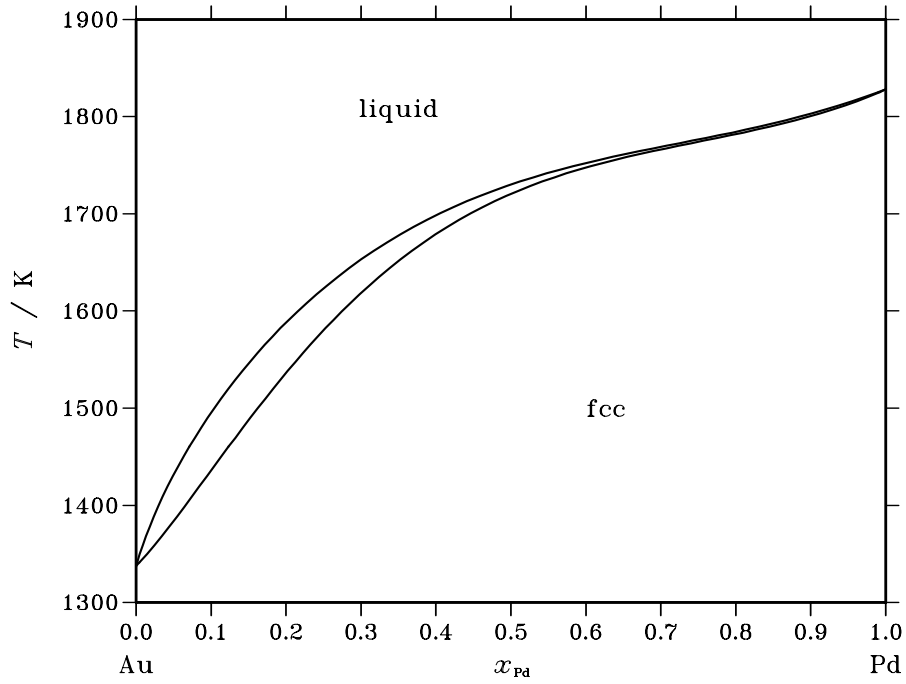

Fig. 1. Calculated phase diagram for the system Au-Pd.

The system displays a complete range of solid and liquid solutions with a narrow solidus- liquidus gap. The phase diagram and the compilation of data presented by [85Oka] have been used as basis for the present thermodynamic assessment [98Spe], but the reported ordering around the compositions Au_3Pd, AuPd and $AuPd_3$ has not been described. There is good agreement of the calculated solidus/liquidus boundaries with those in Massalski's diagram and the negative deviations from ideality in the solid phase are consistent with the reported ordering behaviour.

Table I. Phases, structures and models.

Phase	Struktur-bericht	Prototype	Pearson symbol	Space group	SGTE name	Model
liquid					LIQUID	$(Au,Pd)_1$
fcc	$A1$	Cu	$cF4$	$Fm\overline{3}m$	FCC_A1	$(Au,Pd)_1$

Table IIa. Integral quantities for the liquid phase at 2000 K.

x_{Pd}	ΔG_{m} [J/mol]	ΔH_{m} [J/mol]	ΔS_{m} [J/(mol·K)]	$G_{\mathrm{m}}^{\mathrm{E}}$ [J/mol]	$S_{\mathrm{m}}^{\mathrm{E}}$ [J/(mol·K)]	ΔC_p [J/(mol·K)]
0.000	0	0	0.000	0	0.000	0.000
0.100	−6206	−3060	1.573	−801	−1.130	0.000
0.200	−9691	−5120	2.286	−1370	−1.875	0.000
0.300	−11886	−6300	2.793	−1728	−2.286	0.000
0.400	−13086	−6720	3.183	−1894	−2.413	0.000
0.500	−13416	−6500	3.458	−1889	−2.305	0.000
0.600	−12925	−5760	3.583	−1734	−2.013	0.000
0.700	−11605	−4620	3.492	−1447	−1.587	0.000
0.800	−9370	−3200	3.085	−1049	−1.076	0.000
0.900	−5966	−1620	2.173	−560	−0.530	0.000
1.000	0	0	0.000	0	0.000	0.000

Reference states: Au(liquid), Pd(liquid)

Table IIb. Partial quantities for Au in the liquid phase at 2000 K.

x_{Au}	ΔG_{Au} [J/mol]	ΔH_{Au} [J/mol]	ΔS_{Au} [J/(mol·K)]	$G_{\mathrm{Au}}^{\mathrm{E}}$ [J/mol]	$S_{\mathrm{Au}}^{\mathrm{E}}$ [J/(mol·K)]	a_{Au}	γ_{Au}
1.000	0	0	0.000	0	0.000	1.000	1.000
0.900	−1871	−520	0.676	−119	−0.200	0.894	0.993
0.800	−4160	−1920	1.120	−450	−0.735	0.779	0.973
0.700	−6882	−3960	1.461	−951	−1.504	0.661	0.944
0.600	−10079	−6400	1.839	−1584	−2.408	0.545	0.909
0.500	−13834	−9000	2.417	−2308	−3.346	0.435	0.870
0.400	−18319	−11520	3.400	−3082	−4.219	0.332	0.831
0.300	−23888	−13720	5.084	−3867	−4.926	0.238	0.793
0.200	−31386	−15360	8.013	−4623	−5.369	0.151	0.757
0.100	−43598	−16200	13.699	−5309	−5.446	0.073	0.727
0.000	$-\infty$	−16000	∞	−5885	−5.058	0.000	0.702

Reference state: Au(liquid)

Table IIc. Partial quantities for Pd in the liquid phase at 2000 K.

x_{Pd}	ΔG_{Pd} [J/mol]	ΔH_{Pd} [J/mol]	ΔS_{Pd} [J/(mol·K)]	$G_{\mathrm{Pd}}^{\mathrm{E}}$ [J/mol]	$S_{\mathrm{Pd}}^{\mathrm{E}}$ [J/(mol·K)]	a_{Pd}	γ_{Pd}
0.000	$-\infty$	−36000	∞	−9231	−13.385	0.000	0.574
0.100	−45225	−25920	9.652	−6935	−9.493	0.066	0.659
0.200	−31814	−17920	6.947	−5051	−6.435	0.148	0.738
0.300	−23560	−11760	5.900	−3539	−4.110	0.242	0.808
0.400	−17596	−7200	5.198	−2359	−2.420	0.347	0.868
0.500	−12998	−4000	4.499	−1471	−1.264	0.458	0.915
0.600	−9329	−1920	3.704	−834	−0.543	0.571	0.951
0.700	−6340	−720	2.810	−409	−0.155	0.683	0.976
0.800	−3866	−160	1.853	−155	−0.002	0.793	0.991
0.900	−1784	0	0.892	−32	0.016	0.898	0.998
1.000	0	0	0.000	0	0.000	1.000	1.000

Reference state: Pd(liquid)

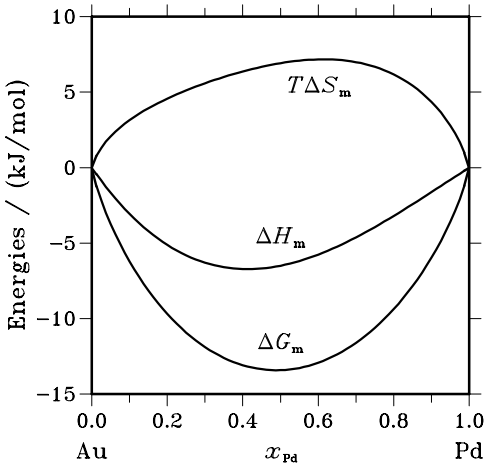

Fig. 2. Integral quantities of the liquid phase at T=2000 K.

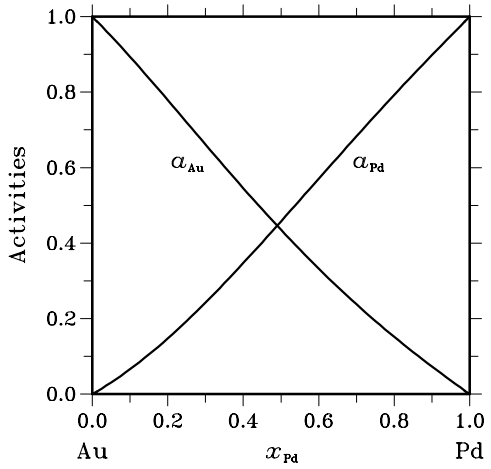

Fig. 3. Activities in the liquid phase at T=2000 K.

Table IIIa. Integral quantities for the stable phases at 1300 K.

Phase	x_{Pd}	ΔG_{m} [J/mol]	ΔH_{m} [J/mol]	ΔS_{m} [J/(mol·K)]	$G^{\mathrm{E}}_{\mathrm{m}}$ [J/mol]	$S^{\mathrm{E}}_{\mathrm{m}}$ [J/(mol·K)]	ΔC_p [J/(mol·K)]
fcc	0.000	0	0	0.000	0	0.000	0.000
	0.100	−5865	−3820	1.573	−2351	−1.130	0.000
	0.200	−9322	−6350	2.286	−3913	−1.875	0.000
	0.300	−11388	−7757	2.793	−4785	−2.286	0.000
	0.400	−12343	−8205	3.183	−5069	−2.413	0.000
	0.500	−12355	−7860	3.458	−4863	−2.305	0.000
	0.600	−11543	−6885	3.583	−4268	−2.013	0.000
	0.700	−9987	−5447	3.492	−3384	−1.587	0.000
	0.800	−7721	−3710	3.085	−2312	−1.076	0.000
	0.900	−4664	−1839	2.173	−1150	−0.530	0.000
	1.000	0	0	0.000	0	0.000	0.000

Reference states: Au(fcc), Pd(fcc)

Table IIIb. Partial quantities for Au in the stable phases at 1300 K.

Phase	x_{Au}	ΔG_{Au} [J/mol]	ΔH_{Au} [J/mol]	ΔS_{Au} [J/(mol·K)]	$G^{\mathrm{E}}_{\mathrm{Au}}$ [J/mol]	$S^{\mathrm{E}}_{\mathrm{Au}}$ [J/(mol·K)]	a_{Au}	γ_{Au}
fcc	1.000	0	0	0.000	0	0.000	1.000	1.000
	0.900	−1550	−672	0.676	−411	−0.200	0.866	0.963
	0.800	−3924	−2468	1.120	−1512	−0.735	0.696	0.869
	0.700	−6957	−5057	1.461	−3102	−1.504	0.525	0.751
	0.600	−10502	−8111	1.839	−4980	−2.408	0.378	0.631
	0.500	−14440	−11298	2.417	−6948	−3.346	0.263	0.526
	0.400	−18708	−14288	3.400	−8804	−4.219	0.177	0.443
	0.300	−23362	−16753	5.084	−10348	−4.926	0.115	0.384
	0.200	−28778	−18361	8.013	−11382	−5.369	0.070	0.349
	0.100	−36591	−18783	13.699	−11703	−5.446	0.034	0.339
	0.000	$-\infty$	−17688	∞	−11113	−5.058	0.000	0.358

Reference state: Au(fcc)

Table IIIc. Partial quantities for Pd in the stable phases at 1300 K.

Phase	x_{Pd}	ΔG_{Pd} [J/mol]	ΔH_{Pd} [J/mol]	ΔS_{Pd} [J/(mol·K)]	G^E_{Pd} [J/mol]	S^E_{Pd} [J/(mol·K)]	a_{Pd}	γ_{Pd}
fcc	0.000	$-\infty$	−45190	∞	−27790	−13.385	0.000	0.076
	0.100	−44697	−32149	9.652	−19808	−9.493	0.016	0.160
	0.200	−30913	−21881	6.947	−13516	−6.434	0.057	0.286
	0.300	−21728	−14058	5.900	−8714	−4.110	0.134	0.447
	0.400	−15105	−8348	5.198	−5201	−2.420	0.247	0.618
	0.500	−10270	−4422	4.499	−2778	−1.264	0.387	0.773
	0.600	−6766	−1950	3.704	−1244	−0.543	0.535	0.891
	0.700	−4255	−602	2.810	−400	−0.155	0.675	0.964
	0.800	−2456	−47	1.853	−44	−0.002	0.797	0.996
	0.900	−1117	43	0.892	22	0.016	0.902	1.002
	1.000	0	0	0.000	0	0.000	1.000	1.000

Reference state: Pd(fcc)

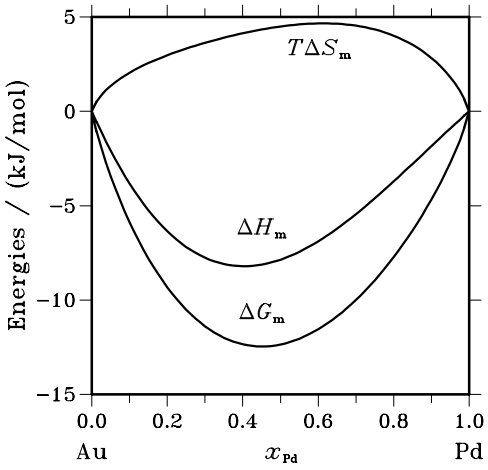

Fig. 4. Integral quantities of the stable phases at T=1300 K.

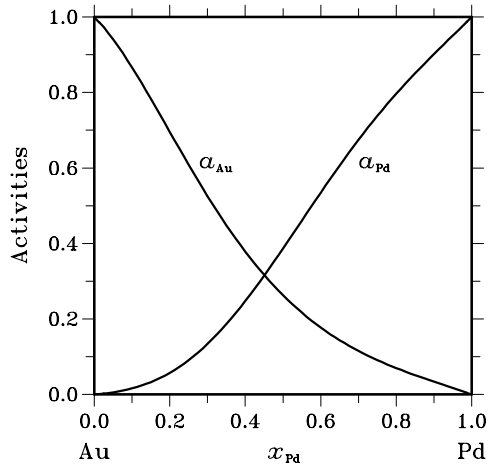

Fig. 5. Activities in the stable phases at T=1300 K.

References

[85Oka] H. Okamoto, T.B. Massalski: Bull. Alloy Phase Diagrams **6** (1985) 229–235.
[98Spe] P.J. Spencer, unpublished assessment, 1998.

Au – Rh (Gold – Rhodium)

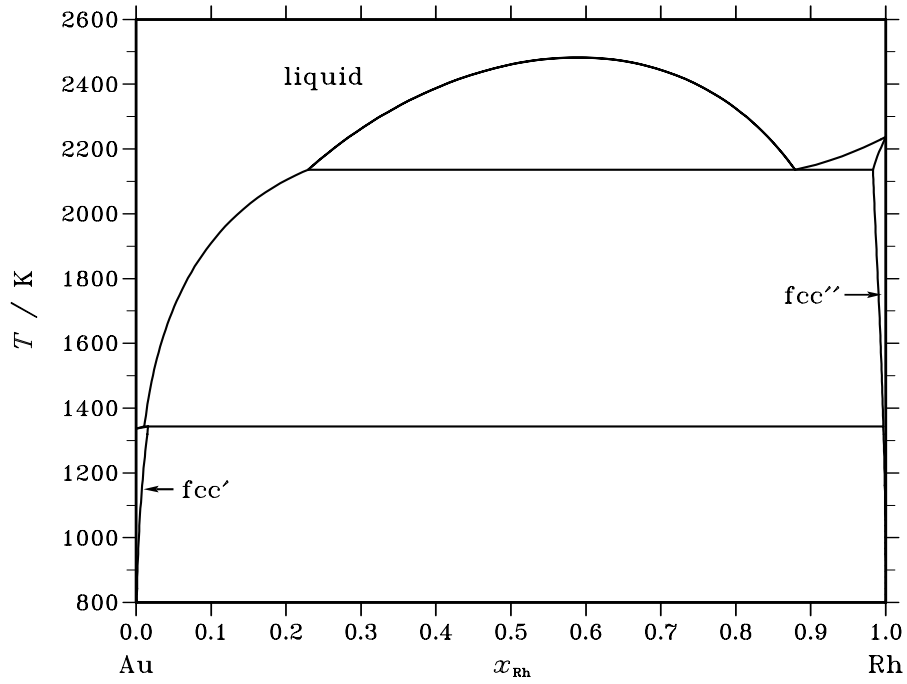

Fig. 1. Calculated phase diagram for the system Au-Rh.

Experimental information for the Au-Rh system is very scarce. Available results are incorporated in the uncertain phase diagram proposed by Okamoto and Massalski [84Oka], which indicates restricted solid solubility of the components and an extensive miscibility gap in the liquid phase. The present assessment [98Spe] results in a calculated phase diagram which reproduces all the features proposed in the diagram of [84Oka], but with a miscibility gap with a lower critical temperature.

Table I. Phases, structures and models.

Phase	Struktur-bericht	Prototype	Pearson symbol	Space group	SGTE name	Model
liquid					LIQUID	$(Au,Rh)_1$
fcc	$A1$	Cu	$cF4$	$Fm\overline{3}m$	FCC_A1	$(Au,Rh)_1$

Table II. Invariant reactions.

Reaction	Type	T / K	Compositions / x_{Rh}			$\Delta_r H$ / (J/mol)
liquid $\rightleftharpoons$ liquid′ + liquid′′	critical	2481.7	0.589	0.589	0.589	0
liquid $\rightleftharpoons$ liquid′ + fcc	monotectic	2135.7	0.879	0.229	0.983	−26586
liquid + fcc $\rightleftharpoons$ fcc′	peritectic	1343.1	0.011	0.997	0.016	−12368

Table IIIa. Integral quantities for the liquid phase at 2500 K.

x_{Rh}	ΔG_{m} [J/mol]	ΔH_{m} [J/mol]	ΔS_{m} [J/(mol·K)]	$G_{\mathrm{m}}^{\mathrm{E}}$ [J/mol]	$S_{\mathrm{m}}^{\mathrm{E}}$ [J/(mol·K)]	ΔC_p [J/(mol·K)]
0.000	0	0	0.000	0	0.000	0.000
0.100	−3559	4578	3.255	3198	0.552	0.000
0.200	−4548	8306	5.142	5854	0.981	0.000
0.300	−4794	11122	6.367	7903	1.288	0.000
0.400	−4706	12963	7.067	9284	1.472	0.000
0.500	−4475	13765	7.296	9933	1.533	0.000
0.600	−4203	13466	7.067	9787	1.472	0.000
0.700	−3914	12003	6.367	8784	1.288	0.000
0.800	−3542	9313	5.142	6860	0.981	0.000
0.900	−2804	5333	3.255	3953	0.552	0.000
1.000	0	0	0.000	0	0.000	0.000

Reference states: Au(liquid), Rh(liquid)

Table IIIb. Partial quantities for Au in the liquid phase at 2500 K.

x_{Au}	ΔG_{Au} [J/mol]	ΔH_{Au} [J/mol]	ΔS_{Au} [J/(mol·K)]	$G_{\mathrm{Au}}^{\mathrm{E}}$ [J/mol]	$S_{\mathrm{Au}}^{\mathrm{E}}$ [J/(mol·K)]	a_{Au}	γ_{Au}
1.000	0	0	0.000	0	0.000	1.000	1.000
0.900	−1929	414	0.937	261	0.061	0.911	1.013
0.800	−3510	1741	2.101	1128	0.245	0.845	1.056
0.700	−4687	4106	3.517	2727	0.552	0.798	1.140
0.600	−5435	7636	5.228	5183	0.981	0.770	1.283
0.500	−5785	12455	7.296	8623	1.533	0.757	1.514
0.400	−5875	18690	9.826	13171	2.207	0.754	1.884
0.300	−6072	26466	13.015	18954	3.004	0.747	2.489
0.200	−7356	35909	17.306	26098	3.924	0.702	3.510
0.100	−13134	47145	24.111	34728	4.967	0.532	5.316
0.000	$-\infty$	60300	∞	44971	6.132	0.000	8.701

Reference state: Au(liquid)

Table IIIc. Partial quantities for Rh in the liquid phase at 2500 K.

x_{Rh}	ΔG_{Rh} [J/mol]	ΔH_{Rh} [J/mol]	ΔS_{Rh} [J/(mol·K)]	$G_{\mathrm{Rh}}^{\mathrm{E}}$ [J/mol]	$S_{\mathrm{Rh}}^{\mathrm{E}}$ [J/(mol·K)]	a_{Rh}	γ_{Rh}
0.000	$-\infty$	49819	∞	34490	6.132	0.000	5.255
0.100	−18227	42051	24.111	29635	4.967	0.416	4.161
0.200	−8698	34567	17.306	24757	3.924	0.658	3.290
0.300	−5045	27493	13.015	19981	3.004	0.785	2.615
0.400	−3611	20953	9.826	15435	2.207	0.841	2.101
0.500	−3165	15075	7.296	11243	1.533	0.859	1.717
0.600	−3087	9983	5.228	7531	0.981	0.862	1.437
0.700	−2989	5804	3.517	4425	0.552	0.866	1.237
0.800	−2588	2664	2.101	2050	0.245	0.883	1.104
0.900	−1657	687	0.937	534	0.061	0.923	1.026
1.000	0	0	0.000	0	0.000	1.000	1.000

Reference state: Rh(liquid)

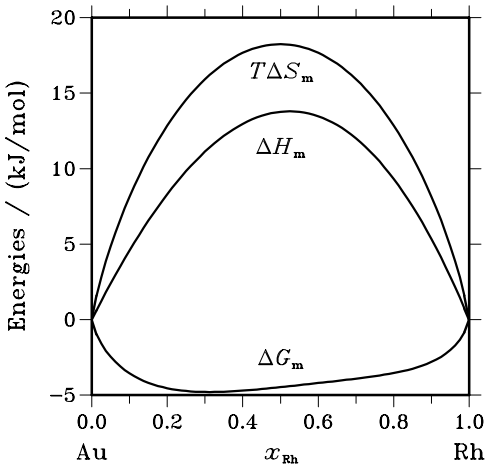

Fig. 2. Integral quantities of the liquid phase at T=2500 K.

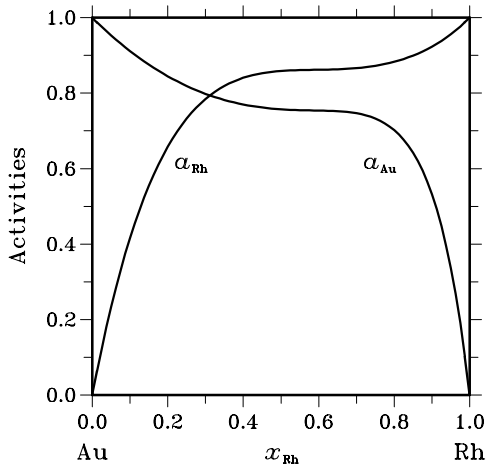

Fig. 3. Activities in the liquid phase at T=2500 K.

References

[84Oka] H. Okamoto, T.B. Massalski: Bull. Alloy Phase Diagrams **5** (1984) 384–387.
[98Spe] P.J. Spencer, unpublished assessment, 1998.

Au – Ru (Gold – Ruthenium)

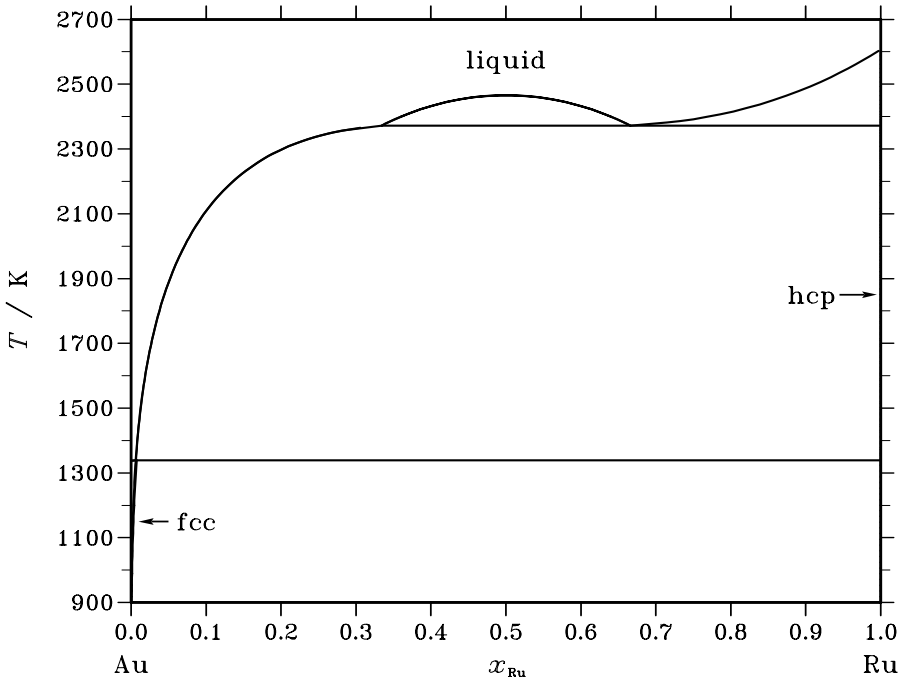

Fig. 1. Calculated phase diagram for the system Au-Ru.

There is only very limited experimental information available for the Au-Ru system. Okamoto and Massalski [84Oka] have incorporated this rather uncertain data into a proposed phase diagram which indicates very limited solubility of Ru in Au and a small miscibility gap in the liquid phase. The present assessment [98Spe] reproduces the main features of the diagram in [84Oka], but results in a miscibility gap with a smaller concentration range.

Table I. Phases, structures and models.

Phase	Struktur-bericht	Prototype	Pearson symbol	Space group	SGTE name	Model
liquid					LIQUID	$(Au,Ru)_1$
fcc	$A1$	Cu	$cF4$	$Fm\overline{3}m$	FCC_A1	$(Au,Ru)_1$
hcp	$A3$	Mg	$hP2$	$P6_3/mmc$	HCP_A3	$(Au,Ru)_1$

Table II. Invariant reactions.

Reaction	Type	T / K	Compositions / x_{Ru}			$\Delta_r H$ / (J/mol)
liquid $\rightleftharpoons$ liquid′ + liquid″	critical	2464.4	0.500	0.500	0.500	0
liquid $\rightleftharpoons$ liquid′ + hcp	monotectic	2372.4	0.666	0.334	1.000	−23352
liquid $\rightleftharpoons$ fcc + hcp	peritectic	1339.0	0.008	0.006	1.000	−12444

Table IIIa. Integral quantities for the liquid phase at 2700 K.

x_{Ru}	ΔG_{m} [J/mol]	ΔH_{m} [J/mol]	ΔS_{m} [J/(mol·K)]	$G_{\mathrm{m}}^{\mathrm{E}}$ [J/mol]	$S_{\mathrm{m}}^{\mathrm{E}}$ [J/(mol·K)]	ΔC_p [J/(mol·K)]
0.000	0	0	0.000	0	0.000	0.000
0.100	−3608	3690	2.703	3690	0.000	0.000
0.200	−4674	6560	4.161	6560	0.000	0.000
0.300	−5103	8610	5.079	8610	0.000	0.000
0.400	−5269	9840	5.596	9840	0.000	0.000
0.500	−5311	10250	5.763	10250	0.000	0.000
0.600	−5269	9840	5.596	9840	0.000	0.000
0.700	−5103	8610	5.079	8610	0.000	0.000
0.800	−4674	6560	4.161	6560	0.000	0.000
0.900	−3608	3690	2.703	3690	0.000	0.000
1.000	0	0	0.000	0	0.000	0.000

Reference states: Au(liquid), Ru(liquid)

Table IIIb. Partial quantities for Au in the liquid phase at 2700 K.

x_{Au}	ΔG_{Au} [J/mol]	ΔH_{Au} [J/mol]	ΔS_{Au} [J/(mol·K)]	$G_{\mathrm{Au}}^{\mathrm{E}}$ [J/mol]	$S_{\mathrm{Au}}^{\mathrm{E}}$ [J/(mol·K)]	a_{Au}	γ_{Au}
1.000	0	0	0.000	0	0.000	1.000	1.000
0.900	−1955	410	0.876	410	0.000	0.917	1.018
0.800	−3369	1640	1.855	1640	0.000	0.861	1.076
0.700	−4317	3690	2.966	3690	0.000	0.825	1.179
0.600	−4908	6560	4.247	6560	0.000	0.804	1.339
0.500	−5311	10250	5.763	10250	0.000	0.789	1.579
0.400	−5810	14760	7.619	14760	0.000	0.772	1.930
0.300	−6938	20090	10.010	20090	0.000	0.734	2.447
0.200	−9891	26240	13.382	26240	0.000	0.644	3.218
0.100	−18481	33210	19.145	33210	0.000	0.439	4.390
0.000	$-\infty$	41000	∞	41000	0.000	0.000	6.211

Reference state: Au(liquid)

Table IIIc. Partial quantities for Ru in the liquid phase at 2700 K.

x_{Ru}	ΔG_{Ru} [J/mol]	ΔH_{Ru} [J/mol]	ΔS_{Ru} [J/(mol·K)]	$G_{\mathrm{Ru}}^{\mathrm{E}}$ [J/mol]	$S_{\mathrm{Ru}}^{\mathrm{E}}$ [J/(mol·K)]	a_{Ru}	γ_{Ru}
0.000	$-\infty$	41000	∞	41000	0.000	0.000	6.211
0.100	−18481	33210	19.145	33210	0.000	0.439	4.390
0.200	−9891	26240	13.382	26240	0.000	0.644	3.218
0.300	−6938	20090	10.010	20090	0.000	0.734	2.447
0.400	−5810	14760	7.619	14760	0.000	0.772	1.930
0.500	−5311	10250	5.763	10250	0.000	0.789	1.579
0.600	−4908	6560	4.247	6560	0.000	0.804	1.339
0.700	−4317	3690	2.966	3690	0.000	0.825	1.179
0.800	−3369	1640	1.855	1640	0.000	0.861	1.076
0.900	−1955	410	0.876	410	0.000	0.917	1.018
1.000	0	0	0.000	0	0.000	1.000	1.000

Reference state: Ru(liquid)

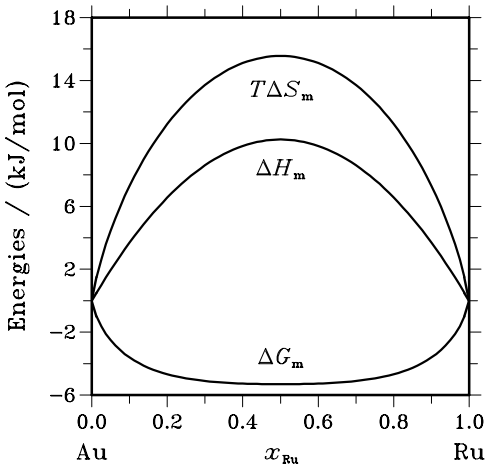

Fig. 2. Integral quantities of the liquid phase at T=2700 K.

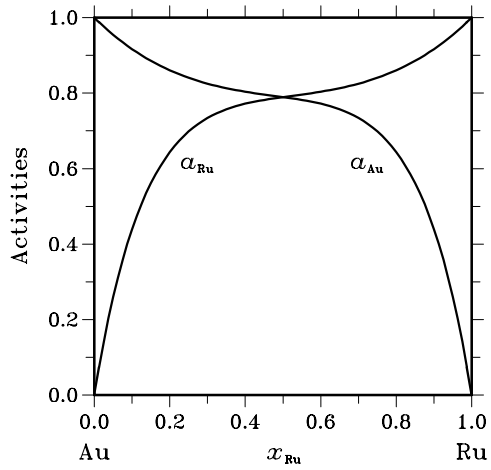

Fig. 3. Activities in the liquid phase at T=2700 K.

References

[84Oka] H. Okamoto, T.B. Massalski: Bull. Alloy Phase Diagrams **5** (1984) 388–390.
[98Spe] P.J. Spencer, unpublished assessment, 1998.

Au – Sb (Gold – Antimony)

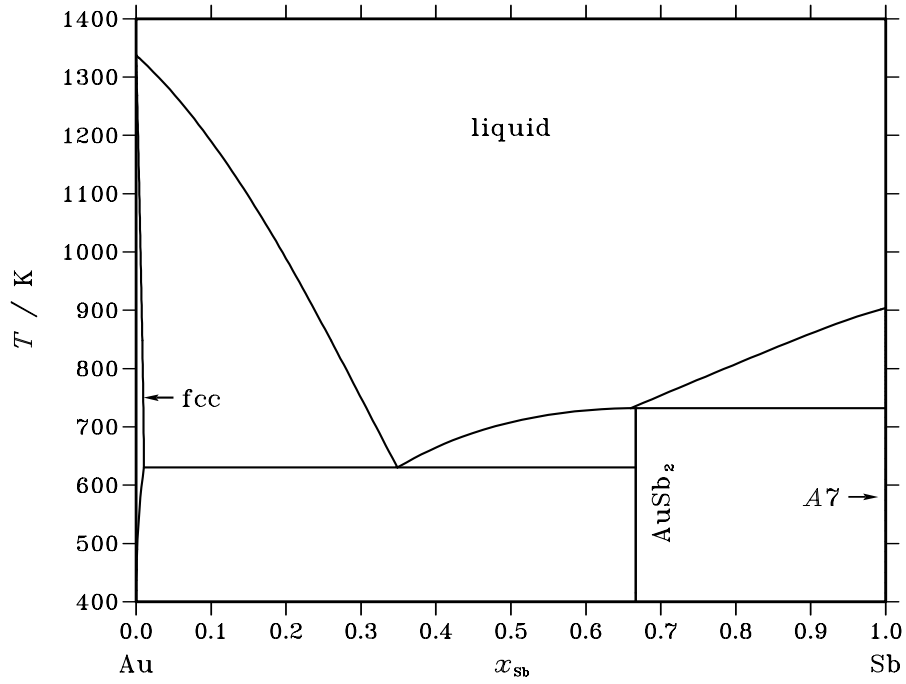

Fig. 1. Calculated phase diagram for the system Au-Sb.

The gold antimony system is of interest for solders, used in the electronic industry. The terminal gold-phase is modelled by a substitutional solution. Since there is no significant solubility of gold in antimony, this phase is treated stoichiometric. In the system, only one intermetallic phase is found, $AuSb_2$, which is described as a stoichiometric compound. The values for the invariant equilibria from the selected assessment [89Che] are in good agreement with data reported by [86Leg, 90Pri].

Table I. Phases, structures and models.

Phase	Struktur-bericht	Prototype	Pearson symbol	Space group	SGTE name	Model
liquid					LIQUID	$(Au,Sb)_1$
fcc	$A1$	Cu	$cF4$	$Fm\overline{3}m$	FCC_A1	$(Au,Sb)_1$
$AuSb_2$	$C2$	FeS_2	$cP12$	$Pa\overline{3}$	AUSB2	Au_1Sb_2
$A7$	$A7$	αAs	$hR2$	$R\overline{3}m$	RHOMBOHEDRAL_A7	Sb_1

Table II. Invariant reactions.

Reaction	Type	T / K	Compositions / x_{Sb}			$\Delta_r H$ / (J/mol)
liquid + A7 $\rightleftharpoons$ $AuSb_2$	peritectic	732.1	0.660	1.000	0.667	−20000
liquid $\rightleftharpoons$ fcc + $AuSb_2$	eutectic	630.3	0.349	0.011	0.667	−12740

Table IIIa. Integral quantities for the liquid phase at 1400 K.

x_{Sb}	ΔG_{m} [J/mol]	ΔH_{m} [J/mol]	ΔS_{m} [J/(mol·K)]	$G_{\mathrm{m}}^{\mathrm{E}}$ [J/mol]	$S_{\mathrm{m}}^{\mathrm{E}}$ [J/(mol·K)]	ΔC_p [J/(mol·K)]
0.000	0	0	0.000	0	0.000	0.000
0.100	−5784	−2993	1.993	−2000	−0.709	0.000
0.200	−9286	−4526	3.400	−3461	−0.761	0.000
0.300	−11602	−4969	4.738	−4492	−0.341	0.000
0.400	−12991	−4651	5.957	−5157	0.361	0.000
0.500	−13550	−3859	6.922	−5481	1.159	0.000
0.600	−13284	−2841	7.459	−5450	1.863	0.000
0.700	−12115	−1802	7.367	−5004	2.288	0.000
0.800	−9872	−906	6.404	−4047	2.244	0.000
0.900	−6223	−278	4.247	−2439	1.544	0.000
1.000	0	0	0.000	0	0.000	0.000

Reference states: Au(liquid), Sb(liquid)

Table IIIb. Partial quantities for Au in the liquid phase at 1400 K.

x_{Au}	ΔG_{Au} [J/mol]	ΔH_{Au} [J/mol]	ΔS_{Au} [J/(mol·K)]	$G_{\mathrm{Au}}^{\mathrm{E}}$ [J/mol]	$S_{\mathrm{Au}}^{\mathrm{E}}$ [J/(mol·K)]	a_{Au}	γ_{Au}
1.000	0	0	0.000	0	0.000	1.000	1.000
0.900	−1517	−795	0.516	−290	−0.360	0.878	0.975
0.800	−3596	−2666	0.664	−998	−1.192	0.734	0.918
0.700	−6123	−4936	0.848	−1971	−2.118	0.591	0.844
0.600	−9126	−7049	1.484	−3180	−2.763	0.457	0.761
0.500	−12787	−8573	3.010	−4718	−2.753	0.333	0.667
0.400	−17469	−9199	5.907	−6803	−1.711	0.223	0.557
0.300	−23789	−8742	10.748	−9775	0.738	0.130	0.432
0.200	−32829	−7139	18.351	−14095	4.969	0.060	0.298
0.100	−47153	−4448	30.503	−20350	11.358	0.017	0.174
0.000	$-\infty$	−855	∞	−29249	20.282	0.000	0.081

Reference state: Au(liquid)

Table IIIc. Partial quantities for Sb in the liquid phase at 1400 K.

x_{Sb}	ΔG_{Sb} [J/mol]	ΔH_{Sb} [J/mol]	ΔS_{Sb} [J/(mol·K)]	$G_{\mathrm{Sb}}^{\mathrm{E}}$ [J/mol]	$S_{\mathrm{Sb}}^{\mathrm{E}}$ [J/(mol·K)]	a_{Sb}	γ_{Sb}
0.000	$-\infty$	−38563	∞	−23146	−11.012	0.000	0.137
0.100	−44187	−22775	15.294	−17384	−3.850	0.022	0.225
0.200	−32048	−11965	14.345	−13314	0.963	0.064	0.319
0.300	−24388	−5047	13.815	−10373	3.804	0.123	0.410
0.400	−18788	−1054	12.667	−8122	5.048	0.199	0.498
0.500	−14313	854	10.834	−6244	5.070	0.292	0.585
0.600	−10493	1398	8.494	−4547	4.246	0.406	0.677
0.700	−7112	1173	5.918	−2960	2.952	0.543	0.775
0.800	−4133	652	3.418	−1535	1.562	0.701	0.876
0.900	−1675	185	1.329	−449	0.453	0.866	0.962
1.000	0	0	0.000	0	0.000	1.000	1.000

Reference state: Sb(liquid)

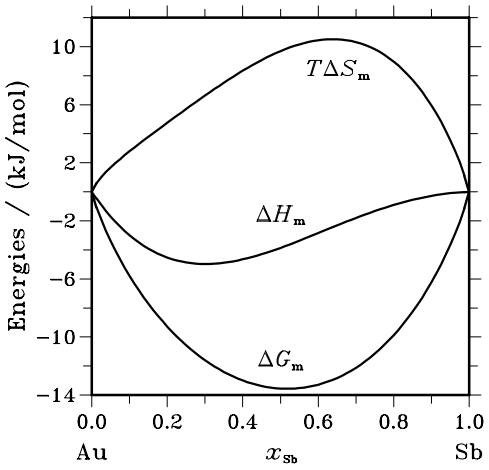

Fig. 2. Integral quantities of the liquid phase at T=1400 K.

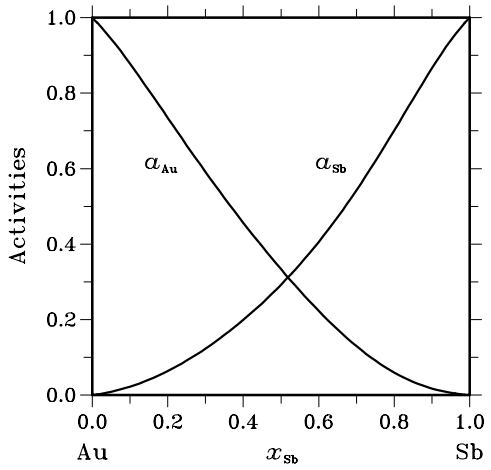

Fig. 3. Activities in the liquid phase at T=1400 K.

Table IV. Standard reaction quantities at 298.15 K for the compounds per mole of atoms.

Compound	x_{Sb}	$\Delta_f G^\circ$ / (J/mol)	$\Delta_f H^\circ$ / (J/mol)	$\Delta_f S^\circ$ / (J/(mol·K))	$\Delta_f C_P^\circ$ / (J/(mol·K))
Au_1Sb_2	0.667	−4458	−5410	−3.192	0.620

References

[86Leg] B. Legendre, Chhay Hancheng: Bull. Soc. Chim. Fr. **2** (1986) 138–144.
[89Che] P.-Y. Chevalier: Thermochim. Acta **155** (1989) 211–225.
[90Pri] A. Prince, G.V. Raynor, D.S. Evans: "Phase diagrams of ternary gold alloys", The Institute of Metals, 1990.

Au – Si (Gold – Silicon)

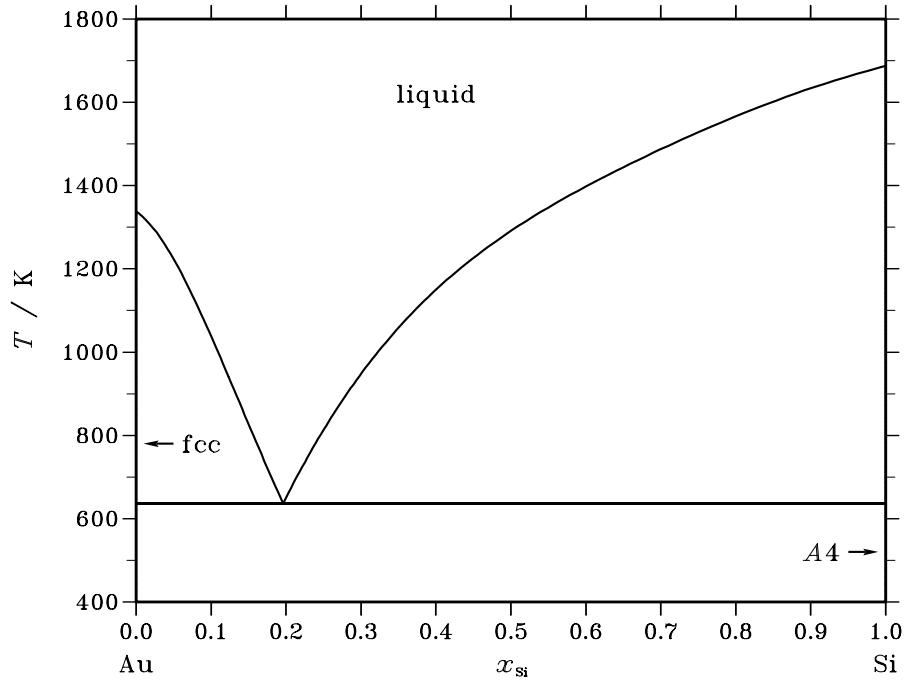

Fig. 1. Calculated phase diagram for the system Au-Si.

The Au-Si system has been critically assessed by Chevalier [89Che]. The phase diagram, reported by Okamoto and Massalski [83Oka], is a simple eutectic. It shows a complete mutual solubility in the liquid phase which is described by a simple substitutional model. The terminal solid phases are represented by practically pure elements.

The calculated liquidus is in satisfactory agreement with the experimental one determined by chemical analysis of gravity-segregated eutectic liquid [61Hea], thermal analysis [67Ger, 75Pre], equilibration of specimens at temperatures above and below the liquidus line followed by quenching into iced brine [75Ana]. The agreement between experimental and calculated data is better on the Si-rich side of the eutectic composition than on the other side.

The calculated enthalpy of mixing of the liquid phase agrees with the calorimetric results [83Has]. The calculated activities of the elements in the liquid phase are in good agreement with data from Knudsen-experiments [78Ber].

Table I. Phases, structures and models.

Phase	Struktur-bericht	Prototype	Pearson symbol	Space group	SGTE name	Model
liquid					LIQUID	$(Au,Si)_1$
fcc	$A1$	Cu	$cF4$	$Fm\overline{3}m$	FCC_A1	$(Au,Si)_1$
$A4$	$A4$	C(diamond)	$cF8$	$Fd\overline{3}m$	DIAMOND_A4	Si_1

Table II. Invariant reactions.

Reaction	Type	T / K	Compositions / x_{Si}			$\Delta_r H$ / (J/mol)
liquid $\rightleftharpoons$ fcc + $A4$	eutectic	636.7	0.196	0.000	1.000	−12665

Table IIIa. Integral quantities for the liquid phase at 1700 K.

x_{Si}	ΔG_{m} [J/mol]	ΔH_{m} [J/mol]	ΔS_{m} [J/(mol·K)]	$G_{\mathrm{m}}^{\mathrm{E}}$ [J/mol]	$S_{\mathrm{m}}^{\mathrm{E}}$ [J/(mol·K)]	ΔC_p [J/(mol·K)]
0.000	0	0	0.000	0	0.000	0.000
0.100	−12074	−5218	4.033	−7479	1.330	0.000
0.200	−18505	−7411	6.526	−11432	2.365	0.000
0.300	−21668	−7757	8.183	−13033	3.104	0.000
0.400	−22627	−7084	9.143	−13115	3.547	0.000
0.500	−22018	−5938	9.458	−12220	3.695	0.000
0.600	−20185	−4642	9.143	−10672	3.547	0.000
0.700	−17265	−3353	8.183	−8630	3.104	0.000
0.800	−13227	−2133	6.526	−6154	2.365	0.000
0.900	−7858	−1002	4.033	−3263	1.330	0.000
1.000	0	0	0.000	0	0.000	0.000

Reference states: Au(liquid), Si(liquid)

Table IIIb. Partial quantities for Au in the liquid phase at 1700 K.

x_{Au}	ΔG_{Au} [J/mol]	ΔH_{Au} [J/mol]	ΔS_{Au} [J/(mol·K)]	$G_{\mathrm{Au}}^{\mathrm{E}}$ [J/mol]	$S_{\mathrm{Au}}^{\mathrm{E}}$ [J/(mol·K)]	a_{Au}	γ_{Au}
1.000	0	0	0.000	0	0.000	1.000	1.000
0.900	−3480	−1740	1.024	−1991	0.148	0.782	0.869
0.800	−9361	−5202	2.447	−6207	0.591	0.516	0.645
0.700	−15888	−8585	4.296	−10846	1.330	0.325	0.464
0.600	−22242	−11001	6.612	−15022	2.365	0.207	0.345
0.500	−28314	−12235	9.458	−18517	3.695	0.135	0.270
0.400	−34491	−12493	12.940	−21539	5.321	0.087	0.218
0.300	−41494	−12164	17.253	−24476	7.243	0.053	0.177
0.200	−50397	−11566	22.841	−27648	9.460	0.028	0.141
0.100	−63609	−10710	31.117	−31063	11.972	0.011	0.111
0.000	$-\infty$	−9046	∞	−34173	14.781	0.000	0.089

Reference state: Au(liquid)

Table IIIc. Partial quantities for Si in the liquid phase at 1700 K.

x_{Si}	ΔG_{Si} [J/mol]	ΔH_{Si} [J/mol]	ΔS_{Si} [J/(mol·K)]	$G_{\mathrm{Si}}^{\mathrm{E}}$ [J/mol]	$S_{\mathrm{Si}}^{\mathrm{E}}$ [J/(mol·K)]	a_{Si}	γ_{Si}
0.000	$-\infty$	−72203	∞	−97331	14.781	0.000	0.001
0.100	−89416	−36516	31.117	−56870	11.972	0.002	0.018
0.200	−55077	−16247	22.841	−32328	9.460	0.020	0.102
0.300	−35154	−5824	17.253	−18136	7.243	0.083	0.277
0.400	−23205	−1208	12.940	−10254	5.321	0.194	0.484
0.500	−15721	358	9.458	−5924	3.695	0.329	0.658
0.600	−10648	593	6.612	−3427	2.365	0.471	0.785
0.700	−6881	422	4.296	−1839	1.330	0.615	0.878
0.800	−3934	225	2.447	−780	0.591	0.757	0.946
0.900	−1663	77	1.024	−174	0.148	0.889	0.988
1.000	0	0	0.000	0	0.000	1.000	1.000

Reference state: Si(liquid)

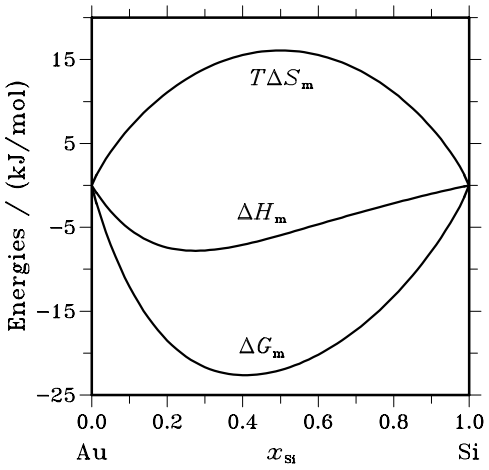

Fig. 2. Integral quantities of the liquid phase at T=1700 K.

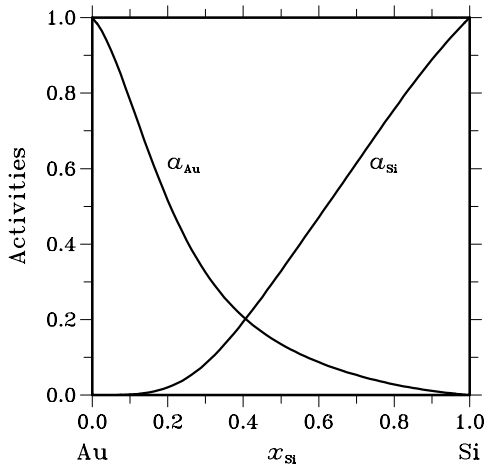

Fig. 3. Activities in the liquid phase at T=1700 K.

References

[61Hea] E.G. Heath: J. Electron. Control. **11** (1961) 13–15.
[67Ger] W. Gerlach, B. Goel: Solid State Electron. **10** (1967) 589–592.
[75Ana] R.P. Anantatmula, A.A. Johnson, S.P. Gupta, R.J. Horylev: J. Electron. Mater. **4** (1975) 445–463.
[75Pre] B. Predel, H. Bankstahl: J. Less-Common Met. **43** (1975) 191–203.
[78Ber] C. Bergman, R. Chastel, M. Gilbert, R. Castanet: High Temp. High Pressures **10** (1978) 581–589.
[83Has] S. Hassam, M. Gaune-Escard, J.P. Bros: Ber. Bunsenges. Phys. Chem. **87** (1983) 785–792.
[83Oka] H. Okamoto, T.B. Massalski: Bull. Alloy Phase Diagrams, **4** (1983) 190–198.
[89Che] P.-Y. Chevalier: Thermochim. Acta **141** (1989) 217–226; updated (1999).

Au – Te (Gold – Tellurium)

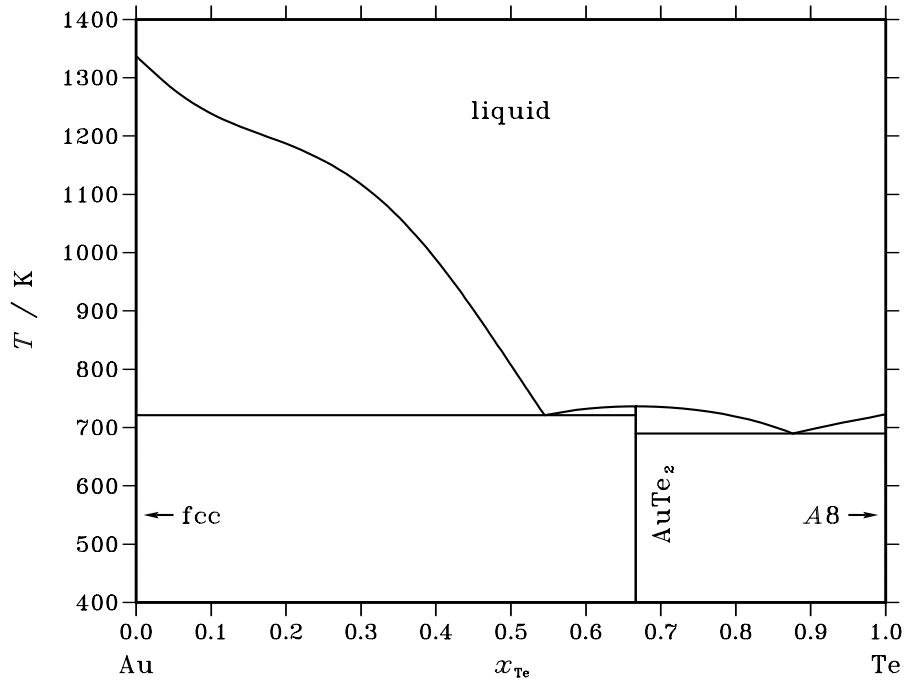

Fig. 1. Calculated phase diagram for the system Au-Te.

According to the review of [84Oka] the system shows only one intermetallic compound and no terminal solid solution. The optimisation by [94Feu] is accepted here. The shape of the liquidus [10Pel, 65Cab, 77Ber, 94Feu] depicts a tendency for de-mixing on the gold-rich side in agreement with the positive enthalpy of mixing of the melt encountered in the same composition range [77Ber]. Heat capacity measurements in good agreement were reported by [71And] and [76Ita], while another value, significantly higher than that of the others was not used in the optimisation. Starting with the whole literature data set, a significantly lower mean square of error was obtained by removing the partial vapour pressure measurements carried out at 1281 K by [75Pre] and the enthalpies of mixing measured at 1200 K by [77Ber]. These two investigations, carried out at high temperature, may be inaccurate due to evaporation problems. The same observation occurred with C_P measurements in liquid $AuTe_2$ by [76Ita] who found a small positive excess C_P value which is in complete disagreement with the evolution of the enthalpy of mixing observed for the composition $x_{Te} = 0.333$. This is not large enough to model the liquid phase with the associated solution model. The liquid was thus modelled using the general Redlich-Kister polynomial.

Table I. Phases, structures and models.

Phase	Struktur-bericht	Prototype	Pearson symbol	Space group	SGTE name	Model
liquid					LIQUID	$(Au,Te)_1$
fcc	$A1$	Cu	$cF4$	$Fm\bar{3}m$	FCC_A1	Au_1
$AuTe_2$	$C34$	$AuTe_2$	$mC6$	$C2/m$	AUTE2	Au_1Te_2
$A8$	$A8$	γSe	$hP3$	$P3_121$	HEXAGONAL_A8	Te_1

Table II. Invariant reactions.

Reaction	Type	T / K	Compositions / x_{Te}			$\Delta_{\mathrm{r}}H$ / (J/mol)
liquid ⇌ $AuTe_2$	congruent	736.7	0.667	0.667		−17313
liquid ⇌ fcc + $AuTe_2$	eutectic	721.2	0.545	0.000	0.667	−16042
liquid ⇌ $AuTe_2$ + $A8$	eutectic	690.0	0.876	0.667	1.000	−17061

Table IIIa. Integral quantities for the liquid phase at 1350 K.

x_{Te}	ΔG_{m} [J/mol]	ΔH_{m} [J/mol]	ΔS_{m} [J/(mol·K)]	$G^{\mathrm{E}}_{\mathrm{m}}$ [J/mol]	$S^{\mathrm{E}}_{\mathrm{m}}$ [J/(mol·K)]	ΔC_p [J/(mol·K)]
0.000	0	0	0.000	0	0.000	0.000
0.100	−3877	3205	5.246	−228	2.543	3.063
0.200	−6120	2851	6.645	−503	2.484	3.845
0.300	−7771	1307	6.725	−915	1.646	2.947
0.400	−8816	−435	6.209	−1262	0.613	0.968
0.500	−9109	−2054	5.226	−1329	−0.537	−1.491
0.600	−8600	−3401	3.851	−1045	−1.745	−3.831
0.700	−7399	−4231	2.347	−542	−2.732	−5.452
0.800	−5706	−4138	1.162	−90	−2.999	−5.754
0.900	−3580	−2729	0.630	69	−2.073	−4.136
1.000	0	0	0.000	0	0.000	0.000

Reference states: Au(liquid), Te(liquid)

Table IIIb. Partial quantities for Au in the liquid phase at 1350 K.

x_{Au}	ΔG_{Au} [J/mol]	ΔH_{Au} [J/mol]	ΔS_{Au} [J/(mol·K)]	$G^{\mathrm{E}}_{\mathrm{Au}}$ [J/mol]	$S^{\mathrm{E}}_{\mathrm{Au}}$ [J/(mol·K)]	a_{Au}	γ_{Au}
1.000	0	0	0.000	0	0.000	1.000	1.000
0.900	−1215	2333	2.628	−33	1.752	0.897	0.997
0.800	−2280	5254	5.581	224	3.725	0.816	1.020
0.700	−3654	6503	7.523	350	4.558	0.722	1.032
0.600	−6058	6392	9.223	−325	4.975	0.583	0.971
0.500	−9677	5500	11.242	−1896	5.479	0.422	0.845
0.400	−13914	3467	12.874	−3629	5.256	0.290	0.724
0.300	−17753	−1122	12.319	−4239	2.309	0.206	0.685
0.200	−20807	−9747	8.193	−2742	−5.189	0.157	0.783
0.100	−25691	−21878	2.825	154	−16.320	0.101	1.014
0.000	$-\infty$	−31799	∞	99	−23.628	0.000	1.009

Reference state: Au(liquid)

Table IIIc. Partial quantities for Te in the liquid phase at 1350 K.

x_{Te}	ΔG_{Te} [J/mol]	ΔH_{Te} [J/mol]	ΔS_{Te} [J/(mol·K)]	$G^{\mathrm{E}}_{\mathrm{Te}}$ [J/mol]	$S^{\mathrm{E}}_{\mathrm{Te}}$ [J/(mol·K)]	a_{Te}	γ_{Te}
0.000	$-\infty$	62993	∞	−3792	49.471	0.000	0.713
0.100	−27831	11054	28.804	−1985	9.659	0.084	0.838
0.200	−21478	−6762	10.901	−3413	−2.480	0.148	0.738
0.300	−17379	−10816	4.862	−3865	−5.149	0.213	0.709
0.400	−12953	−10675	1.688	−2668	−5.931	0.315	0.788
0.500	−8541	−9607	−0.790	−761	−6.553	0.467	0.934
0.600	−5057	−7980	−2.165	677	−6.413	0.637	1.062
0.700	−2961	−5563	−1.927	1042	−4.893	0.768	1.097
0.800	−1931	−2736	−0.596	573	−2.452	0.842	1.052
0.900	−1123	−602	0.386	60	−0.490	0.905	1.005
1.000	0	0	0.000	0	0.000	1.000	1.000

Reference state: Te(liquid)

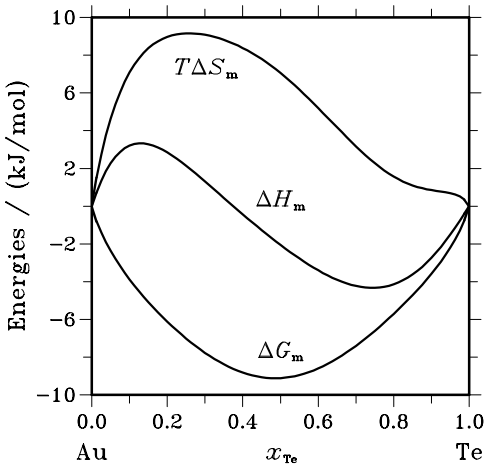

Fig. 2. Integral quantities of the liquid phase at T=1350 K.

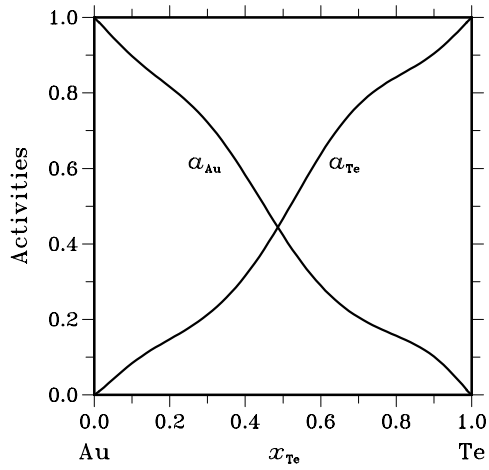

Fig. 3. Activities in the liquid phase at T=1350 K.

Table IV. Standard reaction quantities at 298.15 K for the compounds per mole of atoms.

Compound	x_{Te}	$\Delta_{\mathrm{f}}G^{\circ}$ / (J/mol)	$\Delta_{\mathrm{f}}H^{\circ}$ / (J/mol)	$\Delta_{\mathrm{f}}S^{\circ}$ / (J/(mol·K))	$\Delta_{\mathrm{f}}C^{\circ}_{P}$ / (J/(mol·K))
Au_1Te_2	0.667	−3103	−2826	0.930	−0.276

References

[10Pel] G. Pellini, E. Quercigh: Atti Accad. Naz. Lincei **19** (1910) 445–449.
[65Cab] L.J. Cabri: Economic Geology **60** (1965) 1569–1606.
[71And] R.J.L. Andon, J.F. Martin, K.C. Mills: J. Chem. Soc. A **11** (1971) 1788–1791.
[75Pre] B. Predel, J. Piehl: Z. Metallkd. **66** (1975) 33–38.
[76Ita] K. Itagaki: J. Jpn. Inst. Met. **40** (1976) 1038–1046.
[77Ber] C. Bergman, R. Castanet: Ber. Bunsenges. Phys. Chem. **81** (1977) 1000–1003.
[84Oka] H. Okamoto, T.B. Massalski: Bull. Alloy Phase Diagrams **5** (1984) 172–177.
[94Feu] Y. Feutelais, D. Mouani, J.-R. Didry, B. Legendre: J. Phase Equilibria **15** (1994) 380–385.

Au – Tl (Gold – Thallium)

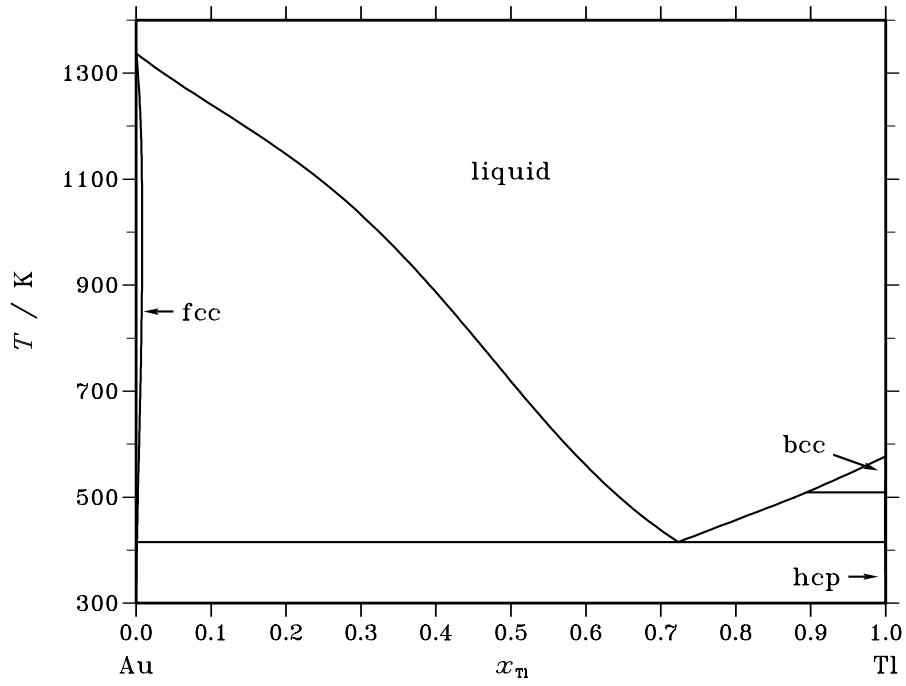

Fig. 1. Calculated phase diagram for the system Au-Tl.

The Au-Tl system has been critically assessed by Chevalier [89Che]. The phase diagram is a simple eutectic. It shows a complete mutual solubility in the liquid state, a small solubility of thallium in the gold rich terminal solid solution, fcc-Au, and a negligible solubility of gold bcc-Tl and hcp-Tl. There is no compound in the system and all the solution phases were modelled with a simple substitutional model.
The calculated liquidus is in satisfactory agreement with data obtained by thermal analysis [05Lev] and the eutectic point reported by [48Haj]. The calculated solubility of Tl in solid Au is in acceptable agreement with the measurements of Raub and Engel [46Rau]. The calculated heat of formation of Tl-rich melts shows certain deviations from the experimental results [51Kle], whereas the calculated activity of thallium is in good agreement with EMF measurements at 973 K [56Kle,76Kam] and at 1073 K [76Kam].

Table I. Phases, structures and models.

Phase	Struktur-bericht	Prototype	Pearson symbol	Space group	SGTE name	Model
liquid					LIQUID	$(Au,Tl)_1$
fcc	$A1$	Cu	$cF4$	$Fm\overline{3}m$	FCC_A1	$(Au,Tl)_1$
bcc	$A2$	W	$cI2$	$Im\overline{3}m$	BCC_A2	$(Au,Tl)_1$
hcp	$A3$	Mg	$hP2$	$P6_3/mmc$	HCP_A3	$(Au,Tl)_1$

Table II. Invariant reactions.

Reaction	Type	T / K	Compositions / x_{Tl}			$\Delta_r H$ / (J/mol)
liquid + bcc $\rightleftharpoons$ hcp	peritectic	508.8	0.894	1.000	0.999	−372
liquid $\rightleftharpoons$ fcc + hcp	eutectic	415.4	0.723	0.001	0.999	−5775

Table IIIa. Integral quantities for the liquid phase at 1400 K.

x_{Tl}	ΔG_{m} [J/mol]	ΔH_{m} [J/mol]	ΔS_{m} [J/(mol·K)]	$G_{\mathrm{m}}^{\mathrm{E}}$ [J/mol]	$S_{\mathrm{m}}^{\mathrm{E}}$ [J/(mol·K)]	ΔC_p [J/(mol·K)]
0.000	0	0	0.000	0	0.000	0.000
0.100	−3709	−1361	1.677	75	−1.026	0.000
0.200	−6005	−2135	2.764	−180	−1.396	0.000
0.300	−7757	−2428	3.807	−646	−1.272	0.000
0.400	−9042	−2348	4.782	−1208	−0.814	0.000
0.500	−9816	−2001	5.582	−1747	−0.181	0.000
0.600	−9981	−1494	6.062	−2147	0.466	0.000
0.700	−9400	−933	6.047	−2289	0.968	0.000
0.800	−7882	−427	5.325	−2057	1.165	0.000
0.900	−5117	−80	3.598	−1333	0.895	0.000
1.000	0	0	0.000	0	0.000	0.000

Reference states: Au(liquid), Tl(liquid)

Table IIIb. Partial quantities for Au in the liquid phase at 1400 K.

x_{Au}	ΔG_{Au} [J/mol]	ΔH_{Au} [J/mol]	ΔS_{Au} [J/(mol·K)]	$G_{\mathrm{Au}}^{\mathrm{E}}$ [J/mol]	$S_{\mathrm{Au}}^{\mathrm{E}}$ [J/(mol·K)]	a_{Au}	γ_{Au}
1.000	0	0	0.000	0	0.000	1.000	1.000
0.900	−1042	−311	0.522	184	−0.354	0.914	1.016
0.800	−2017	−1103	0.653	581	−1.203	0.841	1.051
0.700	−3197	−2161	0.740	955	−2.226	0.760	1.085
0.600	−4874	−3273	1.144	1072	−3.104	0.658	1.096
0.500	−7371	−4225	2.248	697	−3.515	0.531	1.062
0.400	−11070	−4803	4.477	−404	−3.142	0.386	0.966
0.300	−16481	−4793	8.348	−2467	−1.662	0.243	0.809
0.200	−24459	−3983	14.625	−5725	1.244	0.122	0.612
0.100	−37216	−2159	25.040	−10413	5.895	0.041	0.409
0.000	$-\infty$	892	∞	−16766	12.613	0.000	0.237

Reference state: Au(liquid)

Table IIIc. Partial quantities for Tl in the liquid phase at 1400 K.

x_{Tl}	ΔG_{Tl} [J/mol]	ΔH_{Tl} [J/mol]	ΔS_{Tl} [J/(mol·K)]	$G_{\mathrm{Tl}}^{\mathrm{E}}$ [J/mol]	$S_{\mathrm{Tl}}^{\mathrm{E}}$ [J/(mol·K)]	a_{Tl}	γ_{Tl}
0.000	$-\infty$	−16899	∞	2788	−14.062	0.000	1.271
0.100	−27712	−10806	12.076	−910	−7.069	0.092	0.925
0.200	−21956	−6261	11.211	−3222	−2.171	0.152	0.758
0.300	−18398	−3050	10.963	−4383	0.952	0.206	0.686
0.400	−15294	−960	10.239	−4628	2.620	0.269	0.672
0.500	−12260	223	8.917	−4192	3.153	0.349	0.698
0.600	−9255	712	7.119	−3308	2.872	0.452	0.753
0.700	−6365	721	5.061	−2213	2.095	0.579	0.827
0.800	−3737	463	3.000	−1140	1.145	0.725	0.907
0.900	−1551	151	1.216	−324	0.340	0.875	0.973
1.000	0	0	0.000	0	0.000	1.000	1.000

Reference state: Tl(liquid)

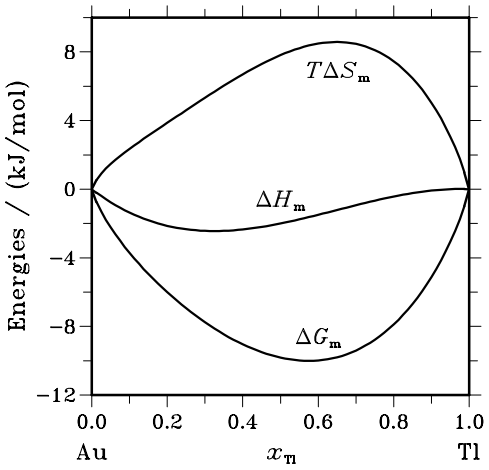

Fig. 2. Integral quantities of the liquid phase at T=1400 K.

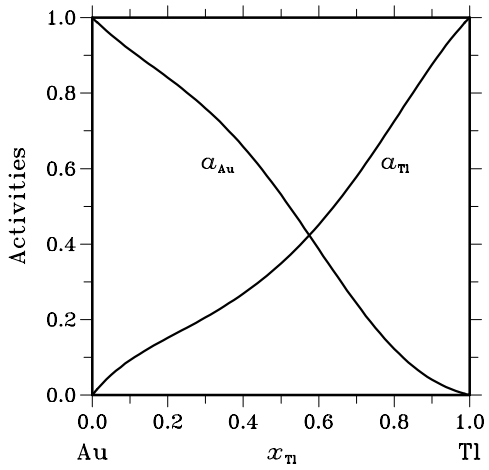

Fig. 3. Activities in the liquid phase at T=1400 K.

References

[05Lev] M. Levin: Z. Anorg. Chem. **45** (1905) 31–38.
[46Rau] E. Raub, A. Engel: Z. Metallkd. **37** (1946) 76.
[48Haj] O. Hajicek: Hutn. Listy **3** (1948) 265–270.
[51Kle] O.J. Kleppa: J. Amer. Ceram. Soc. **73** (1951) 385–390.
[56Kle] O.J. Kleppa: J. Phys. Chem. **60** (1956) 446–452.
[76Kam] K. Kameda, S. Sakairi, Y. Yoshida: Nippon Kinzoku Gakkaishi **40** (1976) 387–392.
[89Che] P.-Y. Chevalier: Thermochim. Acta **155** (1989) 211–225.